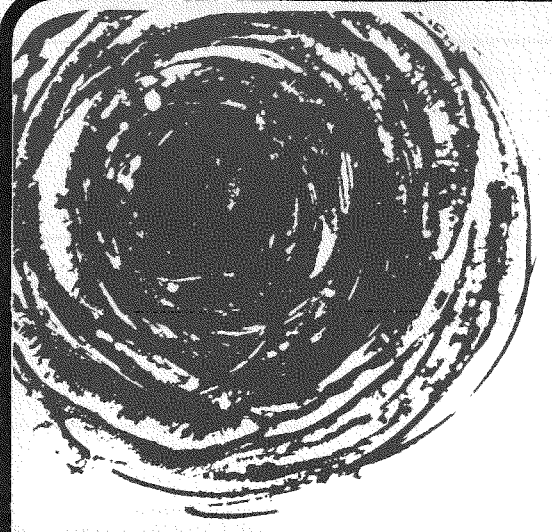


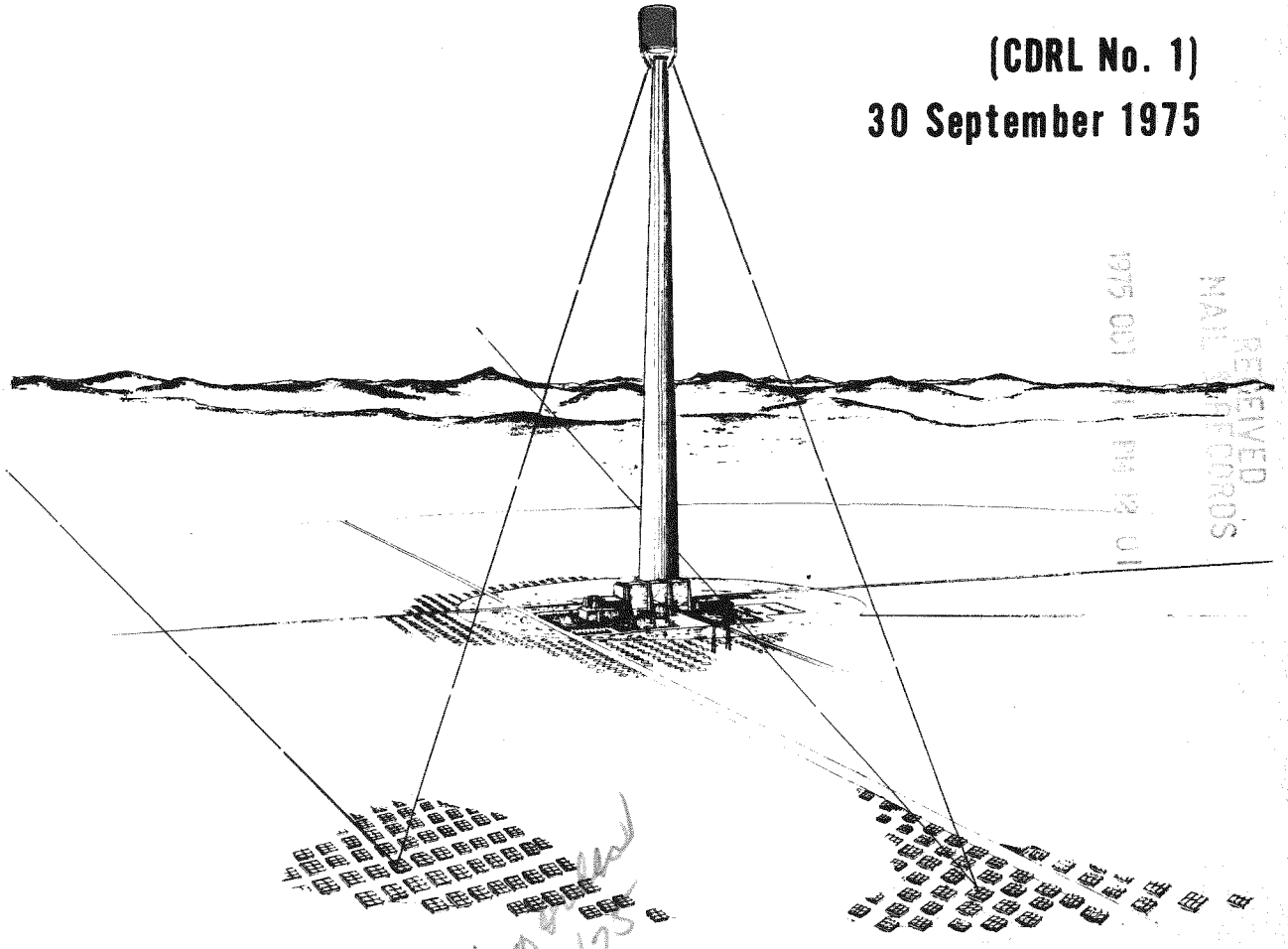
ERDA CONTRACT NO. E(04-3)-1109

MASTER SOLAR PILOT PLANT Phase I

Preliminary Design Baseline Report

(CDRL No. 1)

30 September 1975



RECEIVED
NATIONAL TECHNICAL INFORMATION SERVICE
1975 OCT 14 PM 2 0

HONEYWELL INC.

BLACK & VEATCH

F3419-DR-101

DISTRIBUTION OF THIS DOCUMENT IS UNLIMITED

DISCLAIMER

This report was prepared as an account of work sponsored by an agency of the United States Government. Neither the United States Government nor any agency thereof, nor any of their employees, makes any warranty, express or implied, or assumes any legal liability or responsibility for the accuracy, completeness, or usefulness of any information, apparatus, product, or process disclosed, or represents that its use would not infringe privately owned rights. Reference herein to any specific commercial product, process, or service by trade name, trademark, manufacturer, or otherwise does not necessarily constitute or imply its endorsement, recommendation, or favoring by the United States Government or any agency thereof. The views and opinions of authors expressed herein do not necessarily state or reflect those of the United States Government or any agency thereof.

DISCLAIMER

Portions of this document may be illegible in electronic image products. Images are produced from the best available original document.

DISCLAIMER

This book was prepared as an account of work sponsored by an agency of the United States Government. Neither the United States Government nor any agency thereof, nor any of their employees, makes any warranty, express or implied, or assumes any legal liability or responsibility for the accuracy, completeness, or usefulness of any information, apparatus, product, or process disclosed, or represents that its use would not infringe privately owned rights. Reference herein to any specific commercial product, process, or service by trade name, trademark, manufacturer, or otherwise, does not necessarily constitute or imply its endorsement, recommendation, or favoring by the United States Government or any agency thereof. The views and opinions of authors expressed herein do not necessarily state or reflect those of the United States Government or any agency thereof.

Honeywell

ERDA Control No. E(04-3)-1109

30 September 1975

SOLAR PILOT PLANT
PHASE I

Preliminary Design Baseline Report
(CDRL Item No. 1)

Systems & Research Center
2600 RIDGWAY PARKWAY,
MINNEAPOLIS, MINNESOTA 55413

40203 Printed in U.S.A. F3419-DR-101

DISTRIBUTION OF THIS DOCUMENT IS UNLIMITED

FOREWORD

This is the first submittal of the Solar Pilot Plant Preliminary Design Baseline Report per CDRL No. 1 under ERDA Contract No. E(04-3) 1109. This study report was prepared in written form which documents the oral presentation delivered concurrently. This report is submitted for review and approval by ERDA.

The baseline design delineated in this report was configured around parameters which were set on approximately September 1, 1975. Continued activity in the systems engineering area have modified slightly some of these parameters. However, in accordance with the Pilot Plant program plan, an updating of all parameters is required utilizing the results of all previous activity. Honeywell, therefore, plans to update this baseline in the Pilot Plant Preliminary Design Report CDRL No. 2.

As part of this foreword, we are including a copy of the meeting agenda which lists the principal investigator in each area and a copy of the meeting attendee's.

The appendices included with this document are numbered the same as the section which they append.

AGENDA
SOLAR PILOT PLANT PROGRAM
PRELIMINARY DESIGN BASELINE REVIEW
AND
PROGRAM REVIEW
Sept. 30, Oct. 1, 1975
Minneapolis

Tuesday-September 30, 1975		Honeywell Executive Conference Room
8:30 AM	OPENING REMARKS	Roger Schmidt
8:45 AM	PRELIMINARY DESIGN BASELINE REVIEW	
	• ERDA Remarks	ERDA
	• Introduction	Jerry Powell
	• System Tradeoffs	Jeff Hammer
	• Pilot Plant Concept	Charles Grosskreutz
12:00-1:00 PM	LUNCH	Honeywell Cafeteria
1:00 PM	PDBR CONTINUED	
	• Collector Subsystem	Ted Carr/Bob Parker
	• Receiver Subsystem	Ed McBride
	• Steam Generator	Bill Oberjohn
5:00 PM	ADJOURN	

EVENING ARRANGEMENTS - To be announced.

SOLAR PILOT PLANT PROGRAM
Meeting Attendees
Preliminary Design Baseline Review

ATTENDEES

ERDA

Sandia Livermore

Alan Skinrood
Cliff Selvage
Tom Brumeleve
Cliffort Yokomizo
Morrie Reynolds
Bob Johnson

San Francisco

Bob Hughey

Headquarters

Jim Rannels
George Kaplan

Aerospace Corporation

Jed Woolley

Honeywell - Systems and Research Center

Roger Schmidt
Jerry Powell
Jeff Hammer
Ray Stiles
Dick LeFrois
Will Berry
Gary Smith
Bob Beale
Bill Bursack
Ozzie Severson
Don Smith
Bill Harris
Ron Shoquist
H. Venkatasetty
Bob Eagle
Jack Bunnel
Herb Schoon
Jim Ramsey

Aerospace Division

Bob Snyder
Bob Younski
Bob Parker
Ted Carr
Carl Vignoli
Jim Fisher
Kay Turner

Babcock and Wilcox

George Watson
Bill Oberjohn
John Kidwell

Northern States Power

Les Weber
Gary Ashley
Booker Hoffs

Black and Veatch

John Kintigh
Charles Grosskreutz
Ron Ott
Ed McBride
Tim Sullentrop
John Harder

Blank

CONTENTS

		Page
SECTION I	INTRODUCTION	1-1
SECTION II	SYSTEMS TRADEOFFS	2-1
	Cycle Choice	2-2
	Secondary Injection Turbines	2-6
	Costs	2-12
	Optics	2-24
	Annual Rays Lost	2-30
	Rays Lost on Supports	2-32
	System Engineering	2-50
	System Effectiveness	2-50
SECTION III	PILOT PLANT CONCEPT	3-1
	Plant Layout	3-2
	Concept Overview	3-2
	Site Arrangement	3-4
	Plant Arrangement	3-6
	Major Plant Characteristics	3-8
	Subsystem Identification	3-9
	Collector Subsystem	3-9
	Receiver Subsystem	3-10
	Thermal Storage Subsystem	3-11
	Electrical Generation Subsystem	3-12
	Controls	3-14
	Subsystem Interfaces	3-16
	Collector Subsystem Interfaces	3-16
	Receiver Subsystem Interfaces	3-18
	Thermal Storage Subsystem Interfaces	3-20
	Electrical Generation Subsystem Interfaces	3-22
SECTION IV	COLLECTOR SUBSYSTEM	4-1
	Program Overview and Derivation of a Baseline Subsystem	4-2
	Establishing Appropriate Application Requirements	4-2
	Performance and Environment Drive Basic Functional Definition and Modes	4-4
	Safety and Maintenance Costs Determine Secondary Performance Characteristics	4-6
	Highlights of Solar Collector Subsystem Concept Design	4-8
	Apportionment of Tracking Errors	4-10
	Cost Sensitivities	4-12

	Baseline Subsystem Analysis and Tradeoffs	4-14
	Characterization of Heliostat Configuration	4-14
	Axis Selection Influence on Heliostat and Control System Design	4-16
	Tilt-Tilt Configuration Eliminates Energy Loss	4-18
	Axis Selection Influence on Control System Design	4-20
	Selection of Heliostat Configuration	4-22
	Analysis, Tradeoff, and Description of Heliostat Components	4-24
	Site Influence on Foundation Design	4-24
	Pointing Accuracy Governs Outer Signal Drive Selection	4-26
	Precision of the Mirror Module Drive	4-30
	Reflective Surface Properties and Contour Control	4-32
	Heliostat Installation and Alignment	4-34
	Analysis, Tradeoff, and Description of Power and Control System Components	4-36
	Introduction to System Control	4-36
	Control System Operation via Software	4-38
	Accuracy Factors in Sun Tracking	4-40
	Fundamentals of Heliostat Control	4-42
	Serial Data Bus Provides Heliostat Communication	4-44
	Motor Controller for Gimbal Devices	4-46
	Effective Heliostat Calibration	4-48
	Emergency Defocus for Boiler Protection	4-50
	Distribution and Conversion of Power	4-52
	Multiport Input/Output Services Heliostats, Plant Controller and Operator	4-54
	Summary Characterization of Concept Design	4-56
	Achieving System Availability	4-56
	Estimated Cost for Pilot Plant Scale	4-58
	Cost Effectiveness Features of the Operational Plant Scale	4-60
SECTION V	RECEIVER SUBSYSTEM	5-1
	Concept	5-2
	Tower Structure	5-4
	Type of Construction	5-4
	Dimensions	5-6
	Radiation Protection	5-8
	Tower Piping	5-10
	Steam Generator Housing	5-14
	Geometry and Materials	5-14
	Aperture Doors	5-18

	Costs	5-22
	Steam Generator	5-24
	Steam Generator Requirement	5-24
	Design Approach	5-26
	Preliminary Design Concept	5-28
	Preliminary Design Arrangement	5-30
	Steam Generator Components	5-32
	Steam Generator Specifications	5-48
	Heat Transfer Surface Layout	5-52
	Steam Generator Summary	5-58
SECTION VI	STORAGE SUBSYSTEM	6-1
	Storage Concept	6-2
	Defining the Requirements	6-2
	Baseline Design	6-4
	Storage Field Capacity	6-4
	Thermal Storage Charging Rate	6-6
	Thermal Storage Discharge Rate	6-8
	Determining the Equipment Layout	6-10
	Storage Field Heat Loss	6-12
	Main Storage Unit Cell	6-16
	Boiler Design Summary	6-18
	Superheater Design Summary	6-22
	Salt Selection	6-24
	Thermal Storage Cycle and Storage Design	6-26
	Thermal Storage Control	6-30
	Operations	6-34
SECTION VII	ELECTRICAL GENERATION SUBSYSTEM	7-1
	Concept and Requirements	7-2
	Generate Electrical Power Using Receiver Steam or Thermal Storage Unit Steam	7-2
	Performance and Operational Requirements Using Receiver Subsystem Steam	7-4
	Performance and Operational Requirements Using Storage Subsystem Steam	7-6
	Performance and Operational Requirements Using Receiver Subsystem Steam Simultaneously	7-8
	Generation Capabilities During High Summer Flux Periods	7-10
	Tradeoffs and Analysis Review	7-12
	Selection of Turbine Throttle Conditions When Using Receiver Subsystem Steam to Meet Performance, Operating and Extrapolation Requirements	7-12

Selection of a Turbine Design to Facilitate Dual Steam Source Operating Modes	7-16
Determination of Air-Cooled Condenser Capacitity for Optimum Plant Performance	7-20
Major Component Specifications and Layout	7-22
Turbine Generator	7-22
Condenser - Heat Rejection System	7-24
Turbine Area Ground Floor Layout	7-26
Turbine Area Mezzanine Floor Layout	7-28
Turbine Area Operating Floor Layout	7-30
Major Piping and Instrument System Description	7-34
High Pressure Steam Supply	7-34
Turbine Extraction Steam and Heater Drains System	7-38
Feedwater System	7-40
Condensate System	7-44
Low Pressure Steam and Heat Rejection System	7-48
Control Concept and Requirements	7-50
Objective of Plant Control	7-50
Plant Subsystem Control Coordination	7-52
Requirement for a Plant Protective System	7-54
Centralized Plant Control	7-56
Individual Subsystem Control Requirements	7-58
Plant Operating Modes	7-60
Transitions Between Steady-State Modes	7-60
Mode A - Receiver On, Storage Unit Holding, Turbine On	7-62
Mode B - Receiver On, Storage Unit Charging, Turbine Generator Driven by Receiver Steam	7-64
Mode C - Receiver On, Storage Unit Discharging, Turbine Using Both Receiver Steam and Storage Steam	7-66
Mode D - Receiver Off, Storage Unit Discharging, Turbine Driven by Storage Steam Only	7-68
Mode E - Receiver On, Storage Unit Charging, Turbine Off	7-70
Mode F - Receiver Off, Storage Unit Holding, Turbine Off	7-72

APPENDIX 2A ECONOMIC ANALYSIS ASSUMPTIONS

APPENDIX 2B SYSTEMS EFFECTIVENESS PROGRAM PLAN

APPENDIX 4A DRIVE RATE ANALYSIS

APPENDIX 4B AERODYNAMIC STUDY OF HELIOSTAT DESIGN CONCEPTS

APPENDIX 4C MATHEMATICS OF SUN TRACKING

APPENDIX 4D SOLAR COLLECTOR DETAIL SPECIFICATIONS

APPENDIX 4E HELIOSTAT DETAIL SPECIFICATIONS

APPENDIX 4F HELIOSTAT CONTROL SOFTWARE DETAIL SPECIFICATIONS

APPENDIX 4G CALIBRATION ARRAY DETAIL SPECIFICATIONS

APPENDIX 4H HELIOSTAT FOUNDATION

APPENDIX 4I OUTER GIMBAL AND DRIVE ASSEMBLY

APPENDIX 4J MIRROR MODULE ASSEMBLY

APPENDIX 6A THERMAL STORAGE SALT TRADEOFF SELECTION ANALYSIS

APPENDIX 6B MATERIALS EVALUATION FOR THERMAL ENERGY STORAGE

APPENDIX 6C STORAGE SUBSYSTEM SALT CHARACTERISTICS

APPENDIX 7A EGS SYSTEMS AND SUBSYSTEMS SPECIFICATIONS

APPENDIX 7B LEGENDS, SYMBOLS AND WIRING SCHEMATICS

ILLUSTRATIONS

Figure		Page
2-1	Estimated Plant Costs versus Pressure Ratio	2-3
2-2	Mills/kWh Annual Electric Energy and Annual Electric Energy versus Pressure Ratio	2-5
2-3	Comparison of Front End and Secondary Admission Turbines	2-7
2-4	Comparison of Front Injection and Secondary Admission Turbines on a Mills/kWh Basis versus Cycle Pressure	2-9
2-5	Total Plant Cost Utilizing Oil Storage	2-11
2-6	Cost versus Temperature Range of Oil	2-13
2-7	Comparison of Oil and Salt Storage versus Coal Backup on a Mills/kWh Basis versus Cycle Choice	2-15
2-8	Approximate Cost Breakdown for the Storage Subsystem	2-17
2-9	Cost Breakdown for the 1450 psia/950°F Cycle and Oil Storage	2-19
2-10	Cost Breakdown for the 1450 psia/950°F Cycle and Salt Storage	2-21
2-11	Cost Breakdown for the 1450 psia/950°F Cycle and Salt Storage	2-23
2-12	Net MWh(th) versus Aperture Area for 45 Percent Ground Cover Tilt-Tilt Heliostats One Milliradian Error Budget	2-25
2-13	Net MWh(th) versus Aperature Area for 45 Percent Ground Cover Tilt-Tilt Heliostats with Three Milliradian Error Budget	2-27
2-14	Tracking Error Sensitivity Study Results	2-29
2-15	Annual Rays Lost to High and Low Misses versus Aperture Area	2-31
2-16	Annual Rays Lost on Supports versus Aperture Area	2-33
2-17	Bus Bar Energy Cost versus Tower Height for 40 Percent Ground Cover	2-35

2-18	Annual Energy Absorbed versus Aperture Angle	2-37
2-19	Energy from the Field through the Year	2-39
2-20	Energy from the Field through the Year	2-40
2-21	Annual Energy from Various Field Segments	2-43
2-22	System Performance versus Ground Cover	2-45
2-23	China Lake Wind Speed versus Energy Correlation	2-47
2-24	Extra Startup and Shutdown Cycles per Year due to Weather	2-49
2-25	Systems Effectiveness Program Solar Pilot Plant Phase I	2-51
3-1	10 MW Solar Pilot Plant	3-3
3-2	10 MW Solar Pilot Plant - Site Plan	3-5
3-3	10 MW Solar Pilot Plant - Central Plant Complex	3-7
3-4	Control Coordination of Plant Subsystems	3-15
3-5	Collector Receiver Interface	3-17
3-6	Receiver Subsystem Interfaces	3-19
3-7	Thermal Storage Subsystem Interfaces	3-21
3-8	Electrical Generation Subsystem Interfaces	3-23
4-1	Performance and Environments Drive Primary Functional Definition of System and Operating Modes	4-5
4-2	Secondary Performance Characteristics of the Solar Collector Subsystem are Established by Safety and Availability Factors	4-7
4-3	Solar Collector Subsystem Fundamental Characteristics and Concept Tradeoffs	4-9
4-4	Cost Apportionment Percent of 200 Ft^2 Tilt-Tilt Heliostat Cost	4-13
4-5	Az-El Configuration	4-15
4-6	Tilt-Tilt Configuration	4-15

4-7	Gimbal Tracking Rate Limitation	4-19
4-8	Foundation	4-25
4-9	Outer Gimbal Drive Mechanism	4-27
4-10	Outer Gimbal Assembly	4-28
4-11	Stiffness	4-28
4-12	Mirror Module Drive System	4-31
4-13	Mirror Module Configuration	4-33
4-14	Heliostat Installation and Alignment	4-35
4-15	A Field of 4968 Heliostats	4-37
4-16	Real-Time Executive Control Logic	4-39
4-17	Atmospheric Refraction Increases the Sun's Altitude	4-41
4-18	Command and Control	4-43
4-19	Serial Data Bus	4-45
4-20	Motor Controller Electronics	4-47
4-21	Calibration Geometry	4-49
4-22	AC Grid Distribution System	4-53
4-23	Heliostat Power Supply	4-53
4-24	Control Panel	4-55
4-25	Solar Collector Subsystem Availability is Established by Reliability and Maintainability Features of the Design	4-57
5-1	Receiver Concept	5-3
5-2	Slipforming Arrangement	5-5
5-3	Support Tower	5-7
5-4	Radiation Shielding	5-9
5-5	Radiation Shielding	5-9

5-6	Tower Piping Expansion Loops	5-11
5-7	Tower Piping Hangars	5-12
5-8	Steam Generator Housing and Supports	5-15
5-9	Steam Generator Housing and Supports	5-16
5-10	Aperture Doors - Closed Position	5-19
5-11	Aperture Door Operating Mechanism	5-20
5-12	Program Schedule	5-27
5-13	Solar Steam Generator - Flow Schematic	5-29
5-14	Preliminary Design Arrangement	5-31
5-15	Membrane Wall	5-33
5-16	Membrane Wall Sections Assembled for Round Shape	5-35
5-17	Membrane Wall with Block Insulation and Lagging	5-36
5-18	Drum and Internals - Solar Steam Generator	5-42
5-19	Superheater Spray Attemperator	5-45
5-20	Superheater Bypass System for Solar Steam Generator	5-47
5-21	Typical Water-Steam Cycle Indicating Control Monitoring Locations and Instrumentation Required for Volatile Water Treatment	5-51
5-22	Flux Map of Pilot Plant Cavity Walls	5-53
5-23	Layout of Heat Transfer Surface	5-55
6-1	Thermal Storage Concept	6-3
6-2	Thermal Storage Field Capacity Design	6-5
6-3	Thermal Storage Charging Rate	6-7
6-4	Thermal Storage Discharge Rate	6-9
6-5	Thermal Storage Field Layout	6-11
6-6	Storage Field Construction	6-13
6-7	Temperature Drop	6-14

6-8	Main Storage Unit Cell	6-17
6-9	Boiler Design	6-19
6-10	Condenser Design	6-21
6-11	Superheater Design	6-23
6-12	Thermal Storage Cycle	6-25
6-13	Thermal Storage Operating Cycle	6-27
6-14	Thermal Storage ΔT versus Single-Admission Turbine Loading	6-28
6-15	Thermal Storage Control	6-31
6-16	Three Operating Strategies	6-35
6-17	Thermal Power Profile A	6-36
6-18	Thermal Power Profile B	6-37
7-1	Electrical Generation Subsystem	7-3
7-2	Performance Using Receiving Subsystem Steam	7-5
7-3	Performance Using Storage Subsystem Steam	7-7
7-4	Performance Using Receiver Subsystem and Storage Subsystem Steam Simultaneously	7-9
7-5	Performance with Receiver Maximum Capability Steam Flow	7-11
7-6	Comparative Cycle Heat Rates	7-13
7-7	Saturation Temperatures	7-13
7-8	Millier Diagram	7-17
7-9	Typical General Electric Single Automatic Extraction Steam Turbine	7-23
7-10	Air-Cooled Condenser	7-25
7-11	Turbine Area Plant Arrangement - Ground Floor Plan	7-27
7-12	Turbine Area Plant Arrangement - Mezzanine Floor Plan	7-29

7-13	Turbine Area Plant Arrangement - Operating Floor Plan	7-31
7-14	Turbine Area Plant Arrangement - Cross Section	7-32
7-15	High Pressure Steam Piping and Instrumentation	7-35
7-16	Extraction Steam and Heater Drains Piping and Instrumentation	7-39
7-17	Feedwater Piping and Instrumentation	7-41
7-18	Condensate Piping and Instrumentation	7-45
7-19	Low-Pressure Steam and Heat Rejection Piping and Instrumentation	7-49
7-20	Typical Daily Operation	7-51
7-21	Control Coordination of Plant Subsystems	7-53
7-22	Plant Control Room	7-57
7-23	Feedwater and Steam Temperature Controls	7-59
7-24	Mode A-Receiver On, Storage Holding, Turbine Generator On	7-63
7-25	Mode B-Receiver On, Storage Charging, Turbine Generator Driven by Receiver Steam	7-65
7-26	Mode C-Receiver On, Turbine Generator Driven by Receiver Steam and by Storage Steam	7-67
7-27	Mode D-Receiver Off, Turbine Generator Driven by Storage Steam	7-69
7-28	Mode E-Receiver On, Storage Charging, Turbine Generator Off	7-71
7-29	Mode F-Receiver Off, Storage Holding, Turbine Generator Off	7-73

TABLES

Table		Page
3-1	Major Plant Characteristics	3-8
3-2	Collector Subsystem Characteristics	3-9
3-3	Receiver Subsystem Characteristics	3-10
3-4	Thermal Storage Subsystem Characteristics	3-11
3-5	Electrical Generation Subsystem Characteristics	3-12
4-1	Solar Collector Subsystem Requirements	4-3
4-2	Collector Subsystem - Error Budget	4-11
4-3	Gimbal Order Comparison	4-23
4-4	Emergency Defocus	4-51
4-5	Estimated Cost for Pilot Plant Scale	4-58
5-1	Tower Piping Specifications	5-10
5-2	Receiver Subsystem Capital Costs	5-23
5-3	Solar Steam Generator Steam Conditions	5-25
5-4	Action Initiated by High and Low Water Level Signals	5-41
5-5	Ferrous Tube Material Specifications and Maximum Allowable Metal Temperatures Based on Oxidation Characteristics	5-49
6-1	Thermal Storage Subsystem Specific Costs and Goals	6-38
7-1	Air-Cooled Condenser Performance and Cost Comparison	7-21
7-2	High-Pressure (HP) Steam Piping Specifications	7-36
7-3	Feedwater Piping Specifications	7-42
7-4	Condensate Piping Specifications	7-46
7-5	System Protective Conditions	7-55
7-6	Solar Power Plant Steady-State Operating Modes	7-61

SECTION I
INTRODUCTION

Introduction

The Pilot Plant Design is obtained from considerations of Commercial Scale.

The 215MW(e) nameplate capacity plant is considered an upper limit for commercial-size operation due to the maximum nominal tower height of 1500 feet. A 10MW(e) net output has been judged reasonable for the first solar plant. A direct geometric scaling of mirror area with power results in baseline plant dimensions. Cycle selection, heliostat design, and storage design are constrained to be the same to ensure maximum carryover of Pilot Plant results to commercial scale.

	COMMERCIAL	PILOT PLANT
NAMEPLATE CAPACITY	215MW(e)	15MW(e)
AVE POWER (NET-4000 HRS)	172MW(e)	10MW(e)
TOWER HEIGHT	1550 FT	400 FT
FIELD OD	6540 FT	1700 FT
NUMBER OF HELIOSTATS	73,829	4968
HELIOSTAT SIZE	200 FT^2	- - -
TURBINE CYCLE (FROM RCVR)	1450/950	- - -
TURBINE CYCLE (FROM STORAGE)	575/534	- - -
STORAGE TYPE	PHASE CHANGE	- - -
STORAGE CAPACITY	?	200MWH(t)
RECEIVER	CAVITY	- - -
COOLING	DRY	- - -
LOCATION	INYOKERN	- - -

Introduction

The current baseline operates simultaneously from receiver and from storage steam.

Steam from the receiver may be fed directly to the high-pressure turbine inlet or may be passed through the charging heat exchanger of the super heater salt tank, or may be divided between these two choices. The charging steam, after exiting from the super-heat salt tank, is desuperheated and then condensed in the boiler salt tank. The condensate is returned to the low-pressure feedwater system. When the turbine is driven partially or fully from storage, feedwater is heated in the boiler salt tank; steam is drawn from the drum and passed through the superheater salt tank to obtain an additional 50°F of super heat to ensure dry steam.

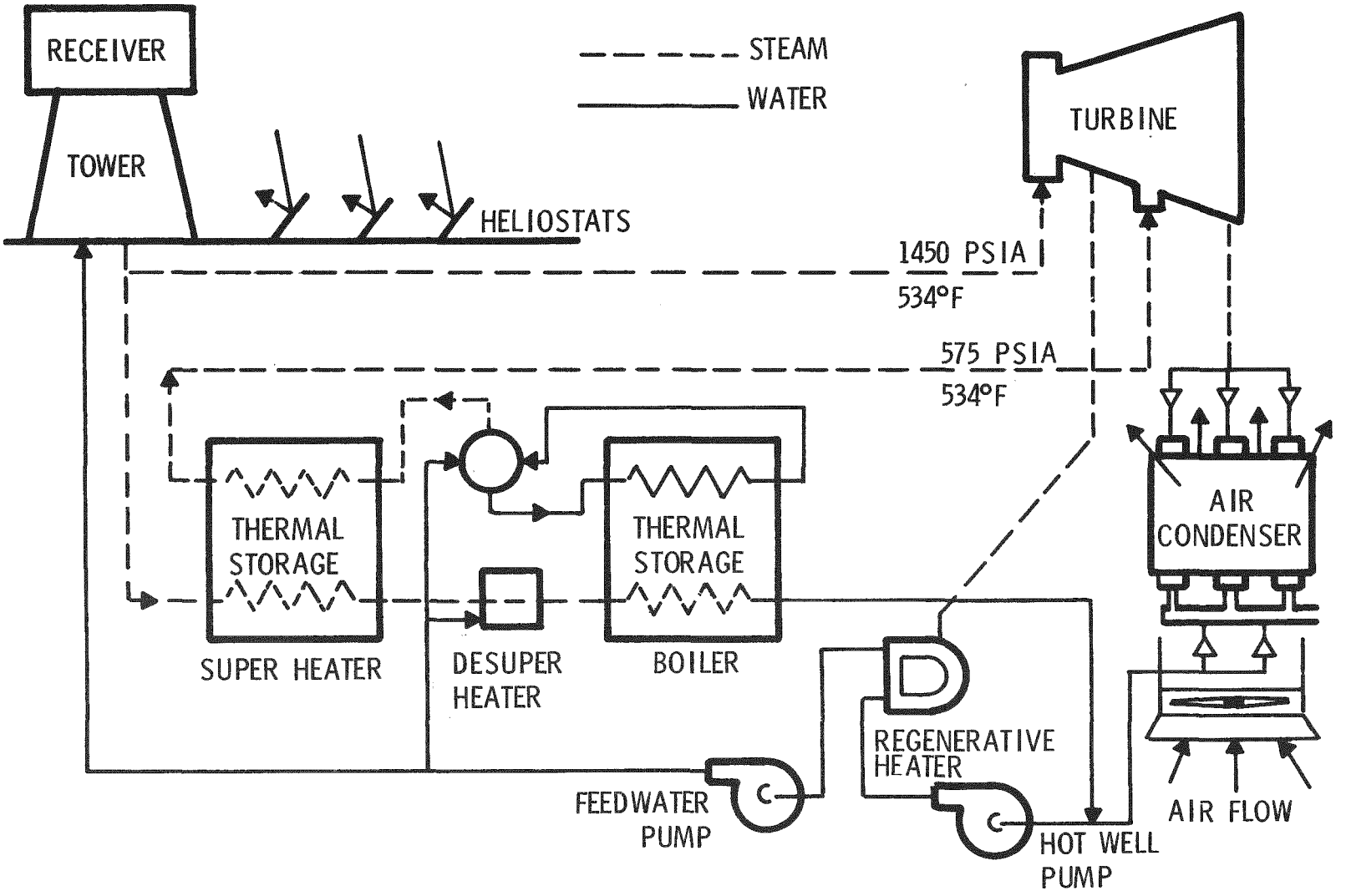


Figure 1-1. Baseline Design Schematic

Introduction

Conceptual Design has resulted in three major recommended changes to the 7/15/75 base line.

- The heliostat azimuth/elevation gimbal order has been changed to a tilt/tilt order to reduce the high torquing rate induced by the az/el rotation order.
- The 7/15/75 base line used primary turbine admission only for both receiver and storage steam. The temperature mismatch between these two sources was a problem. By injecting storage steam down stream, a better temperature/pressure match can be accomplished. This change results in admission from both sources simultaneously. In the original base line this was thought unwise due to temperature-fatigue problems with side-by-side use of two steam sources.
- The cycle choice of 1450 psi/950°F is recommended over the 7/15/75 base line of 850/950 due to higher cycle efficiency without deleterious side effects. The 575 psi/534°F storage cycle selection minimizes the total plant cost.

MAJOR CHANGES FROM 7/15/75 BASELINE

- HELIOSTAT CONFIGURATION
  - AZ-EL TO TILT-TILT GIMBAL SEQUENCE
  - 432 FT^2 TO 200 FT^2
- TURBINE CONFIGURATION
  - SECONDARY ADMISSION FOR STORAGE STEAM
  - SIMULTANEOUS OPERATION FOR RCVR/STORAGE STEAM
- CYCLE SELECTION
  - FROM 850 PSI/950°F TO 1450 PSI/950°F (FROM RCVR)
  - 575 PSI/534°F STORAGE STEAM

Introduction

The cost baseline for the commercial plant is expected to change.

The 7/15/75 commercial baseline has not been updated. The following areas however are expected to change:

- Annual energy production increase due to better design
- Heliostat price increase per better design definition
- Piping/heat exchangers - no significant change
- Turbine Generator/Heat Rejection/Pumps - up sharply due to dry cooling
- Balance of Plant - no significant change
- Storage - some reduction
- Indirect Costs - no significant change

At this time we do not forecast changes exceeding ±20 percent in energy cost.

7/15/75 COST SUMMARY FOR 215 MW PEAK
COMMERCIAL BASELINE

STORAGE CAPACITY	NONE	1/2 HR (80.5 MWH)	6 HR (677 MWH)
AVERAGE POWER (4000 HRS.)	172 MW	172 MW	TBD
ANNUAL ENERGY PRODUCTION	690 x 10^3 MWH	690 x 10^3 MWH	650 x 10^3 MWH
DIRECT COST ($1000)			
LAND	600		
HELIOSTATS ($5.74/FT^2)	84,500		
PIPING/HEAT EXCHANGER (LESS STORAGE)	1,500		
TOWER/RECEIVER	12,000		
TURBINE-GEN./HEAT REJ/PUMPS	12,200		
BALANCE OF PLANT	9,200		
STORAGE ($100/kWH)	NONE	8,000	67,000
INDIRECT COST (21%)	25,200	26,900	39,400
	145,200	154,900	227,100
UNIT CAP COST ($/KW)	844	900	TBD
CONTRIBUTION OF CAPITAL INV. TO COST (MILLS/kWH)	33.7	35.9	55.9

Introduction

The Cost of Storage and Heliostats are the largest leverage items in the Power Plant

The percentage distribution for the 7/15/75 base line illustrates that heliostats, storage and indirect costs make up approximately 85 percent of the total plant cost. Indirect costs are made up of:

- Interest during construction
- Ad valorem taxes
- Client charges
- A&E charges
- Legal and administrative fees

and to depend upon the bookkeeping approach of the procuring activity. Both storage and heliostat costs are a function of the selected design.

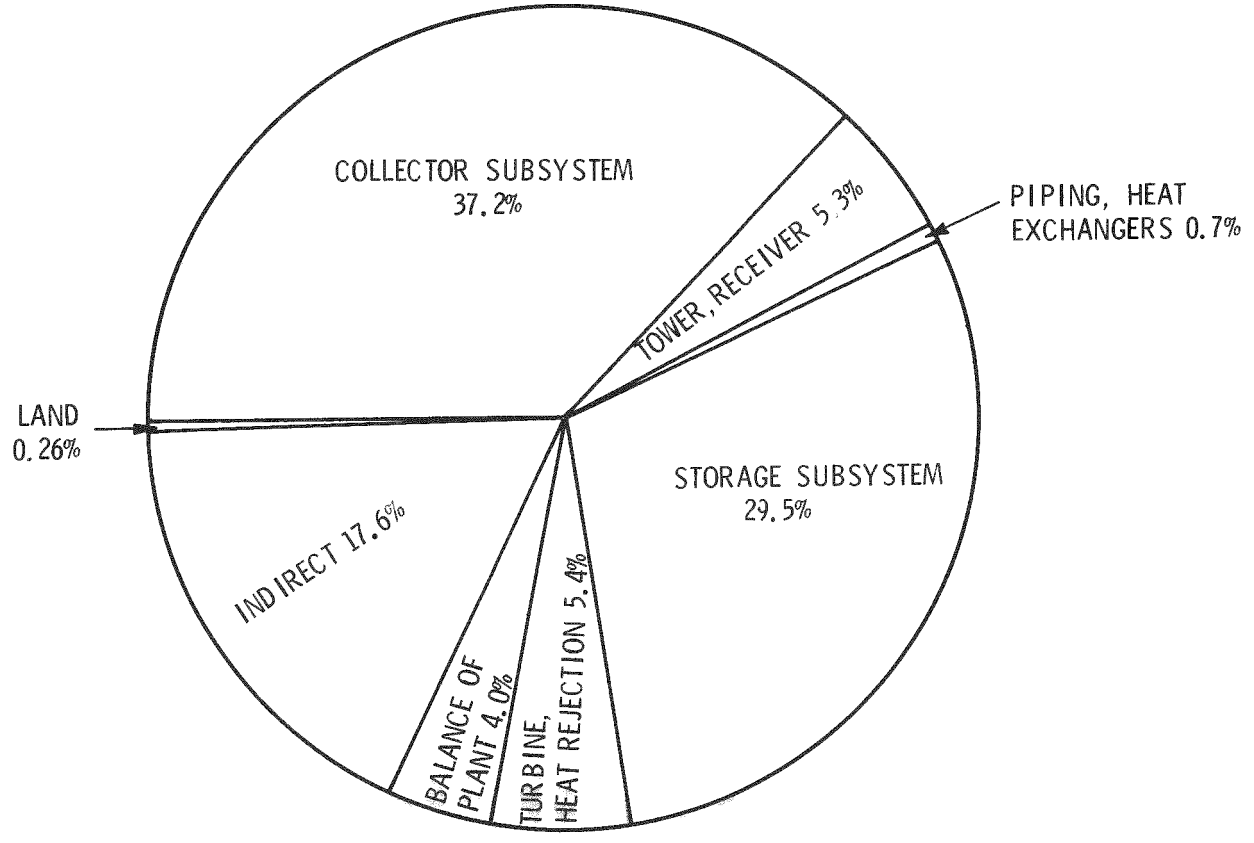


Figure 1-2. Commercial Baseline with 6 Hours Storage

Introduction

The Pilot Plant Baseline (9/30/75) reflects changes due to economy of scale.

The heliostat and storage subsystems, together with indirect expense, comprise only ~75 percent for the pilot plant. The cost for dry cooling has increased and the relative costs for turbine, receiver, tower, and balance of plant are higher at the smaller scale of 10MW(e). Storage cost estimates have been reduced from $100/KW to $75/KW.

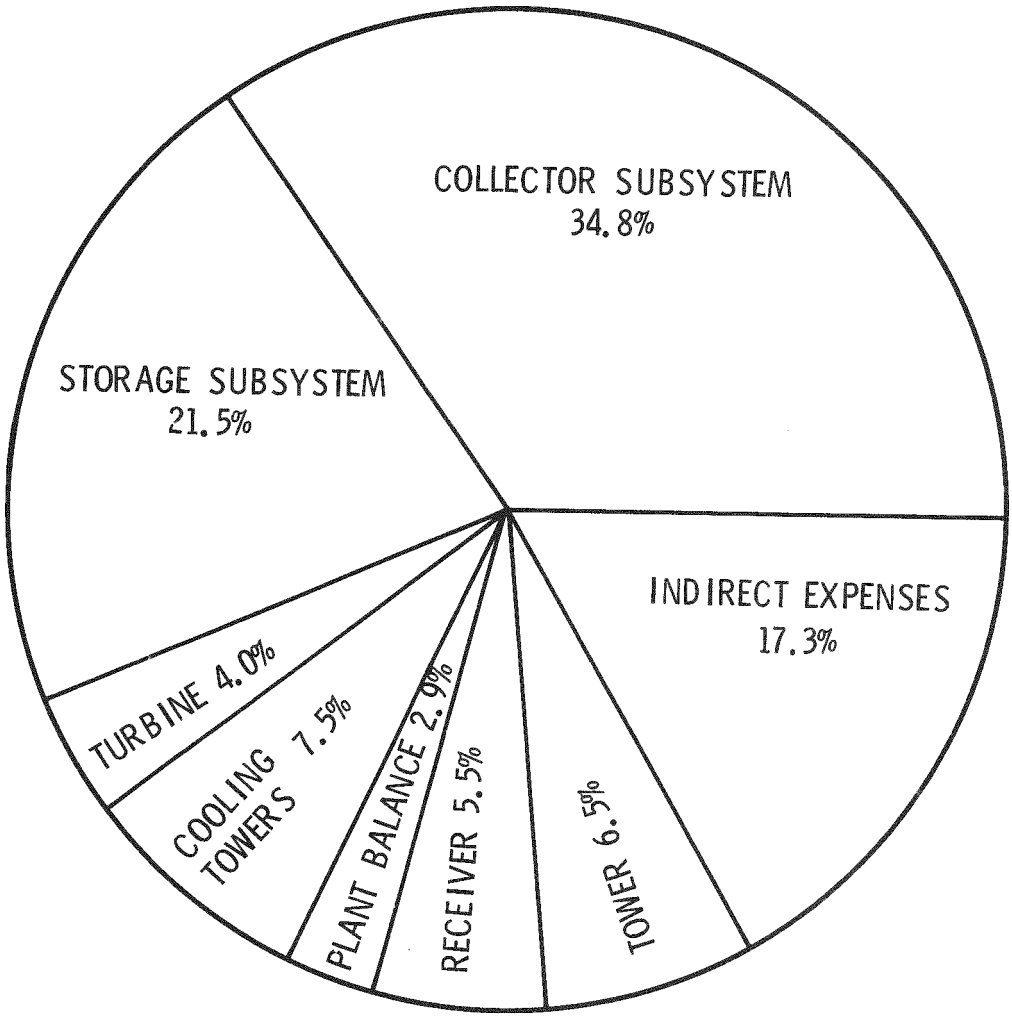


Figure 1-3. 9/30/75 Pilot Plant Baseline for 1450 Psia/950°F Cycle and Salt Storage

SECTION II
SYSTEMS TRADEOFFS

	Page
Cycle Choice	2-2
Costs	2-12
Optics	2-24
System Engineering	2-50

Systems Tradeoffs

Cycle Choice

The tradeoff between turbine/heat rejection system costs and storage costs is the key issue which sets the design.

The "turbine cost" line shows the cost of a secondary injection turbine as a function of pressure ratio. It decreases with increasing pressure ratio. The cooling tower costs, the second curve up, also decrease with increasing pressure ratio due to the higher efficiency of the turbine when running from storage steam. Storage costs, the third line up, show a minimum of its own. At lower pressure ratios, storage is expensive because of the larger capacity of storage needed due to low turbine efficiency. At higher pressure ratios, the ΔT across storage becomes small and the heat exchangers get very large. The upper line shows the summation of all the effects.

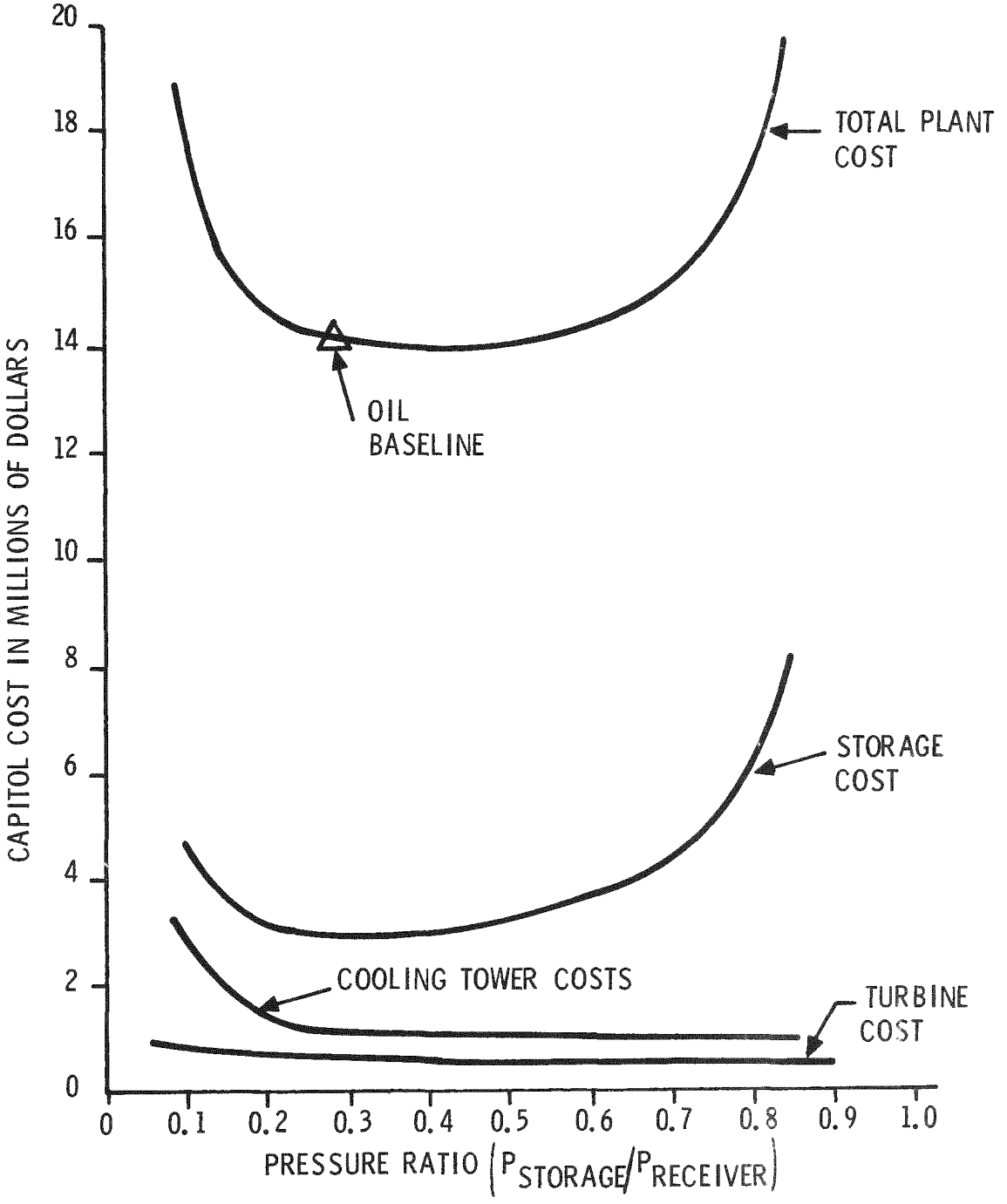


Figure 2-1. Estimated Plant Costs versus Pressure Ratio for the 1450 psia, 950°F Turbine Cycle; 50°F Superheat, 100 psia Pressure Drop When Running From Storage

Systems Tradeoffs

Cycle Choice

The loss of energy through storage (degradation) at lower pressure ratios drives the optimal design to higher pressure ratios.

The "Energy from Storage" line shows that at low pressure ratios, large amounts of energy are lost because of the low turbine efficiency at the low pressure ratio. The "directly used energy" line shows the electricity generated from steam run directly to the turbine. The "total energy line" is the sum of the storage and direct energy lines. The dark line is the mills/kWh line. The minimum of this line occurs at a slightly higher pressure ratio than the minimum of the plant cost. The magnitude of the effect of energy degradation on minimum pressure ratio depends on operational strategy.

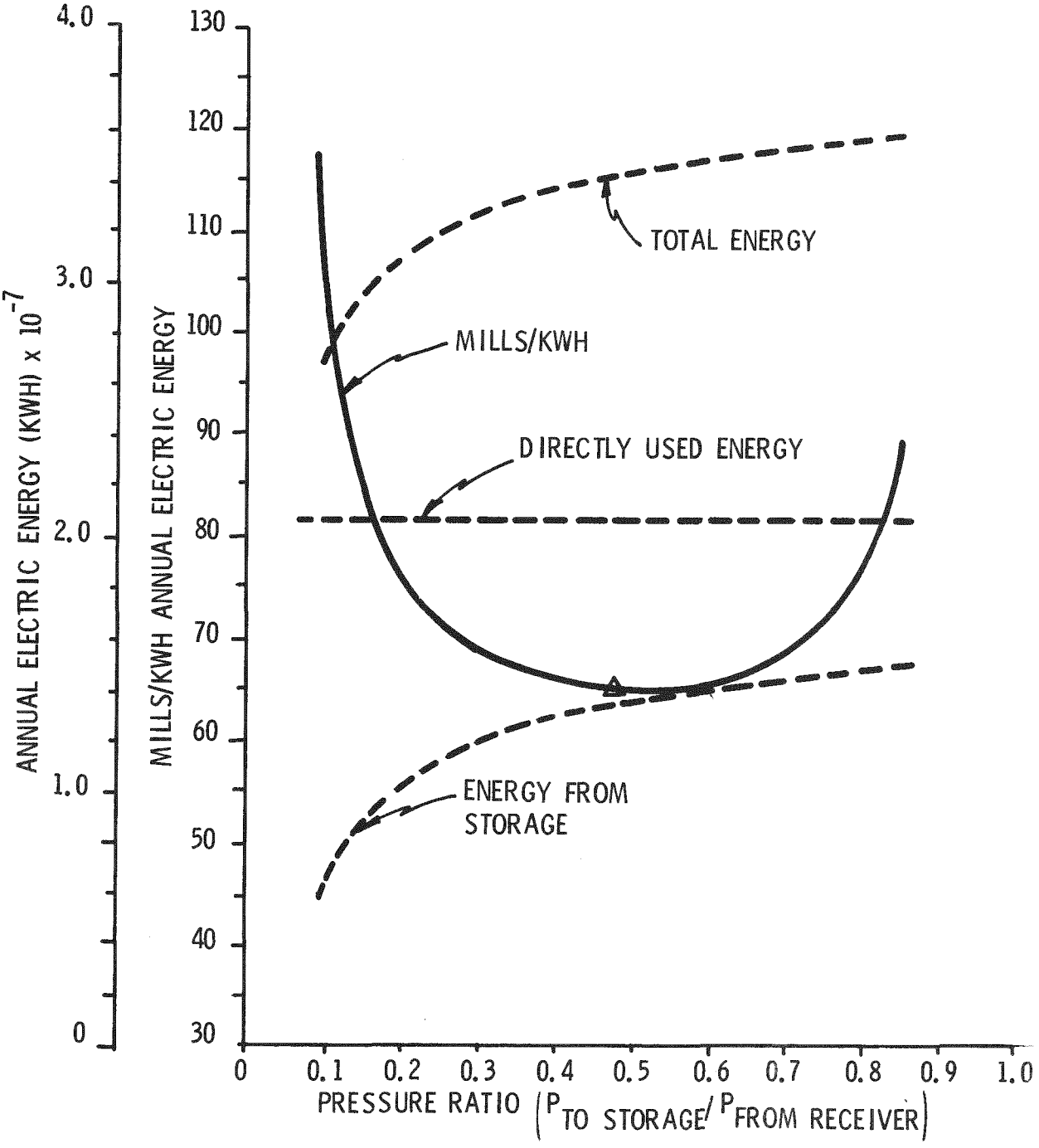


Figure 2-2. Mills/kWh Annual Electric Energy and Annual Electric Energy versus Pressure Ratio for the 1450 psia, 950°F Cycle Assuming a) 50°F Storage Superheat, b) 100 psia Storage Pressure Drop, and c) 45% of Annual Thermal Energy Run through Storage

Systems Tradeoffs

Cycle Choice

SECONDARY INJECTION TURBINES

Secondary Injection Turbines have multiple advantages over Primary Injection Turbines.

The curves in the illustration are for the 1450 psia/950°F receiver steam cycle choice. The curve labeled "front injection turbine" shows the cost in Mills/kWh versus pressure ratio (P from Storage/P from receiver) for the front injection turbine, under the conditions that the turbine must be capable of supplying 7 MW(e) when running from storage steam. The curve labeled secondary injection turbine is the same curve for the plant built using a secondary injection turbine. Not only is the secondary injection turbine cheaper at all pressure ratios, but the minimum cost point for secondary injection turbines occurs at a lower pressure ratio, giving us a larger ΔT across storage, and a larger temperature range to explore for eutectic salts.

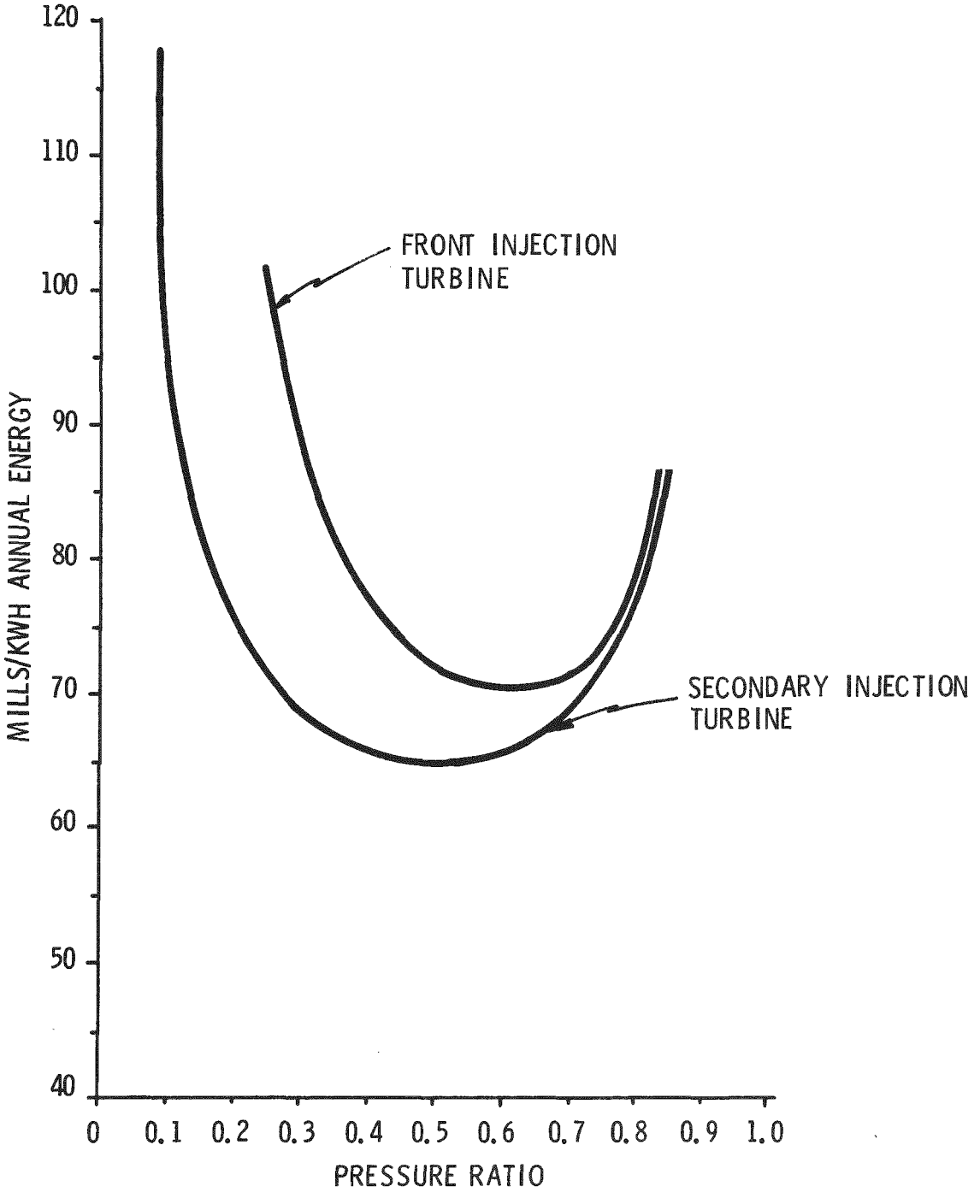


Figure 2-3. Comparison of Front End and Secondary Admission Turbines

Systems Tradeoffs

Cycle Choice

Secondary Admission Turbines are better than normal turbines at all design pressures.

The line labeled normal turbine is the locus of all the minimum coat paints (as a function of pressure ratio) for the front injection turbine. The curve labeled secondary injection turbine is the locus of minimum cost paints for the secondary injection turbine. The advantage of secondary injection over primary injection is the fact that the turbine does not need to be oversized in order to get the desired output when running from storage steam.

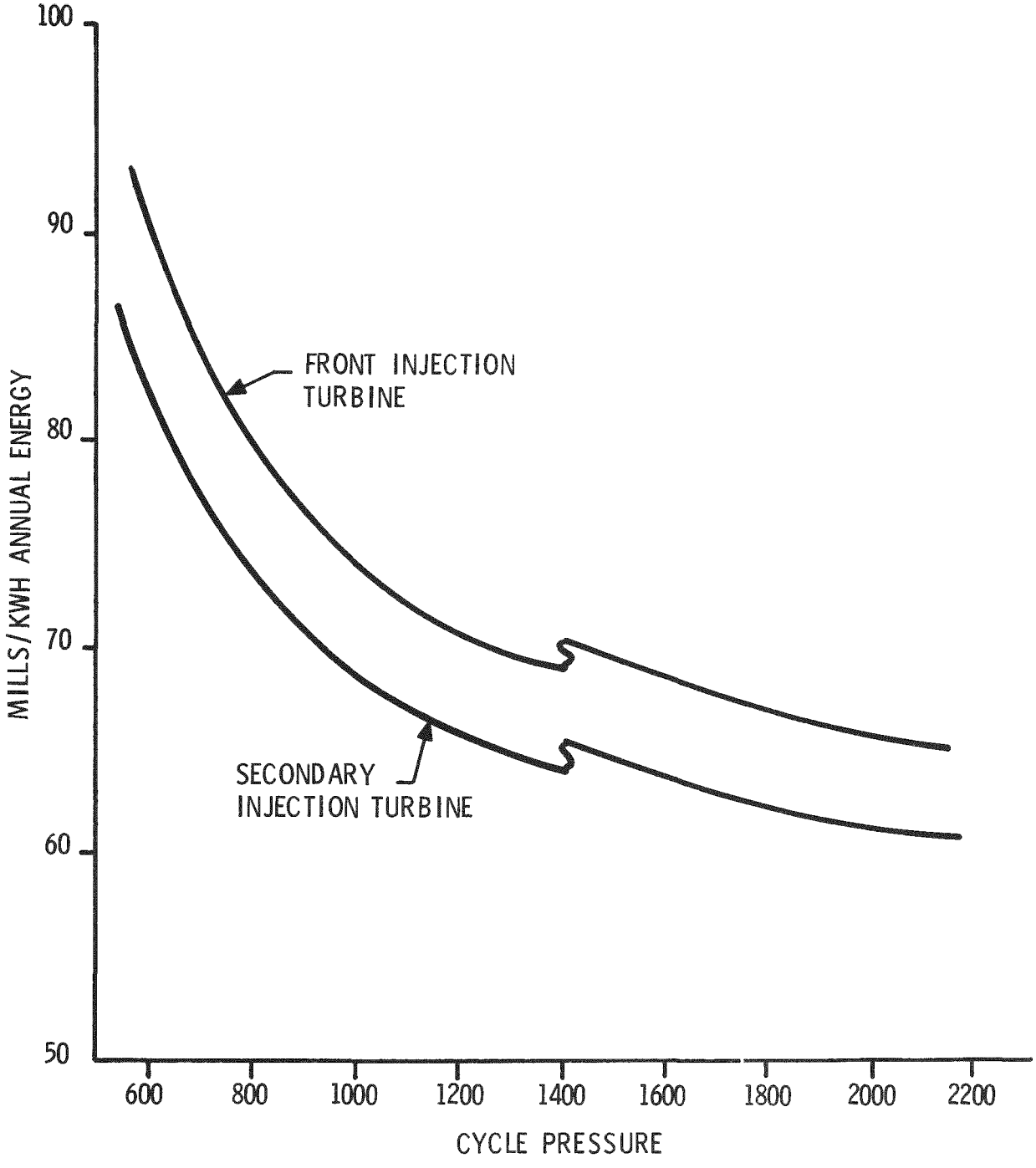


Figure 2-4. Comparison of Front Injection and Secondary Admission Turbines on a Mills/kWh Basis versus Cycle Pressure

Systems Tradeoffs

Cycle Choice

Sensible heat oil storage plant designs have a higher energy than salt storage, and show a sharp plant cost minimum as a function of pressure ratio.

The solid line is the total plant cost in millions of dollars for a plant utilizing oil storage, secondary injection turbine, and a 1450 psia/750°F receiver steam cycle. The dotted line shows the cost of electricity under these conditions (Mills/kWh). The effect of energy degradation at low pressure ratios is indicated by the fact that the optimal pressure ratio based on bus bar energy cost is higher than the optimal pressure ratio based on initial plant capital cost.

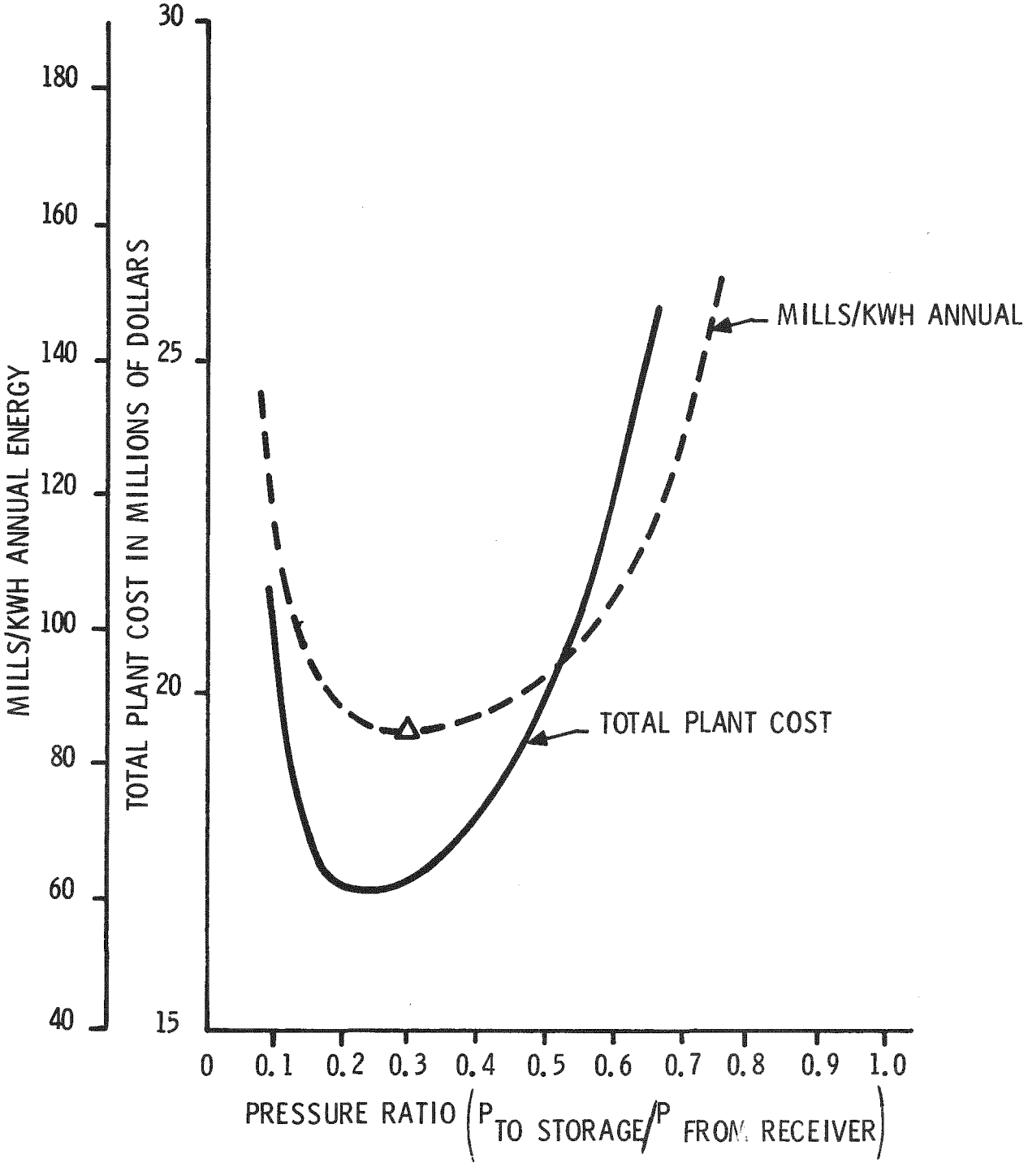


Figure 2-5. Total Plant Cost Utilizing Oil Storage

Systems Tradeoffs

Costs

The cost of oil is the overriding effect in determining the optimal temperature range for oil sensible heat storage.

The graph shown is for the optimal pressure ratio (0.279) for oil storage utilizing the 1450 psia/950°F receiver steam cycle. The lowermost curve is the heat exchanger costs which increases with increasing temperature range. The oil cost curve decreases with increasing temperature range due to reduced amount of oil needed. The total storage cost is a minimum at the higher temperature ranges as dictated by the oil cost.

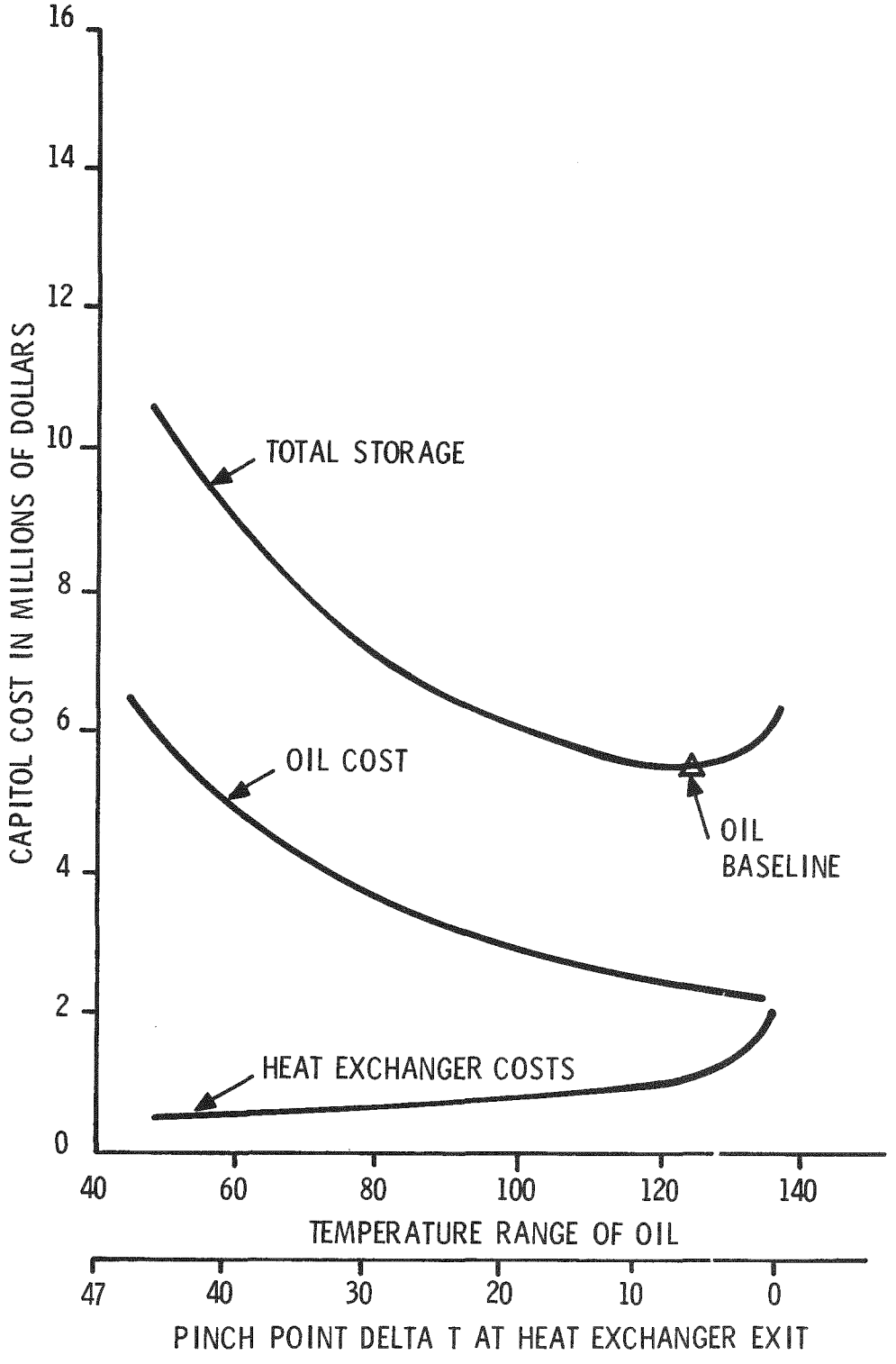


Figure 2-6. Cost versus Temperature Range of Oil for the 1450 psia, 950°F Turbine Cycle and the Optimal Storage Pressure Ratio (P_{Boiler} = 405 psia)

Systems Tradeoffs

Costs

Salt storage has a significant cost advantage over oil storage.

The Oil Storage Line is the cost in miles kWh of electricity produced by a plant utilizing oil storage and cycling 45 percent of its annual collected thermal energy through storage. The Salt Storage Line is the same line for a plant which uses salt storage. Both lines use secondary injection turbines. The bottom two lines are the costs of building the solar plant with no storage and then building a backup coal plant capable of output at the same rate as storage [7 MW(e)]. The "coal backup not used" line corresponds to the cost in miles/kW if the backup plant is built and never used. The "coal backup used" line corresponds to the cost in miles/kW(e) if the coal backup plant is run 6 hr/day (the same duration that storage is capable of). The results indicate that salt storage could be competitive with a fossil fuel backup scheme.

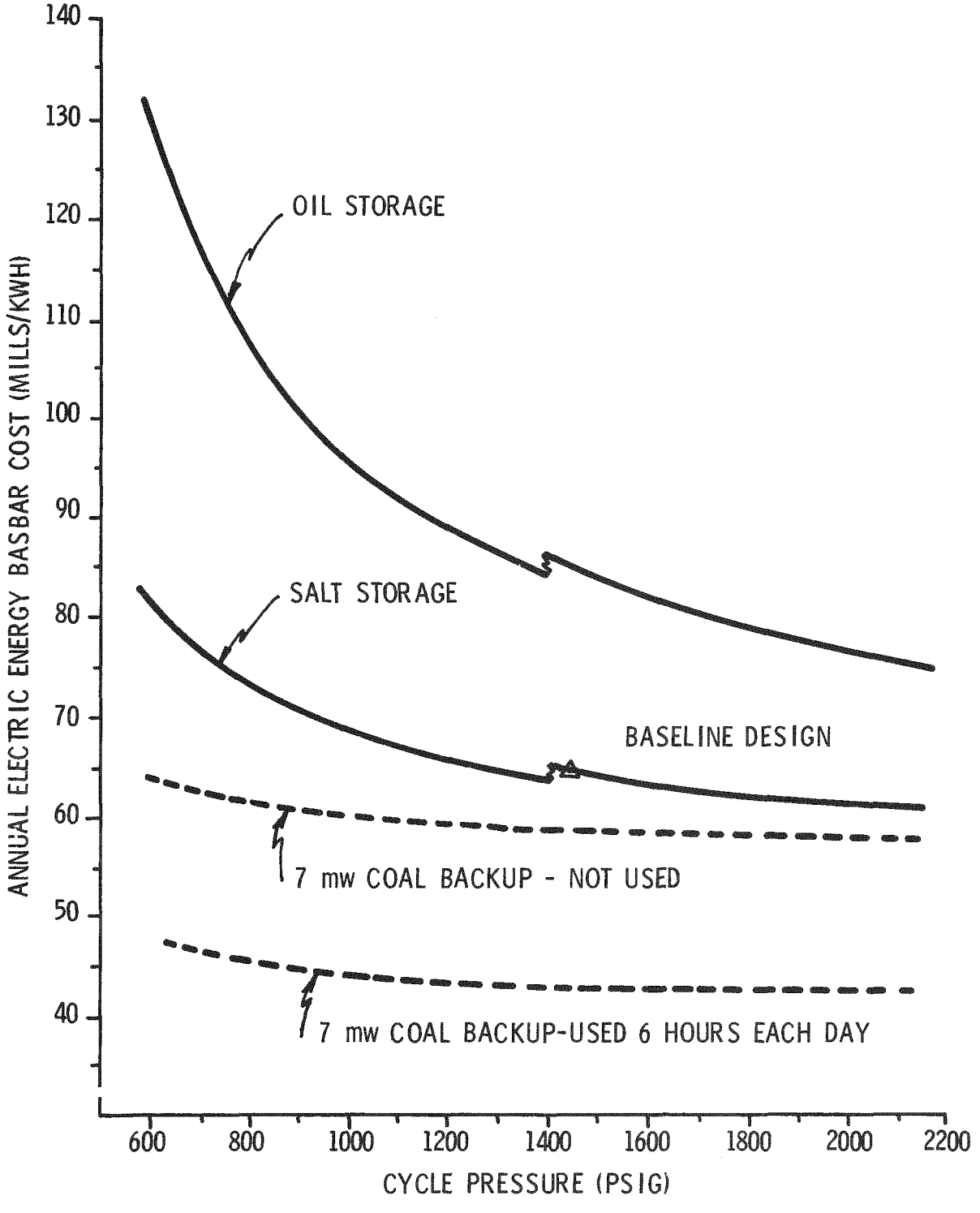


Figure 2-7. Comparison of Oil and Salt Storage versus Coal Backup on a Mills/kWh Basis versus Cycle Choice

System Tradeoffs

Costs

The major cost of salt storage is due to the heat exchangers.

This pie chart shows the cost breakdown for the storage subsystem at the design point (1450 psia /950°F Receiver Steam). Salt is assumed to cost 8¢/lb.

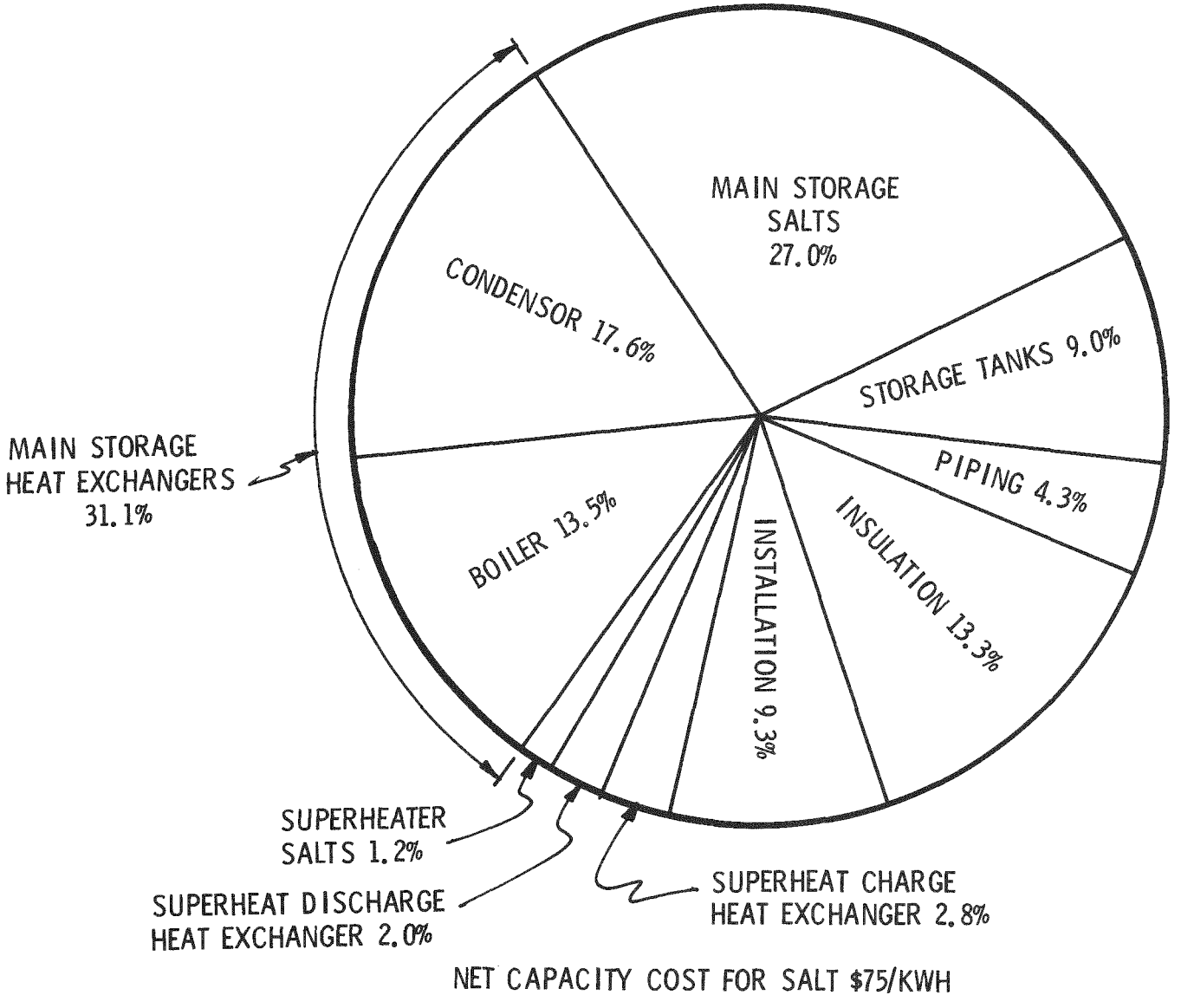


Figure 2-8. Approximate Cost Breakdown for the Storage Subsystem

Systems Tradeoffs

Costs

The major cost factor in oil storage is the oil itself.

Therminol was used as a basis for a heat exchanger fluid, with a $1.50/ gallon cost. The cost of the superheat system was not included in this analysis.

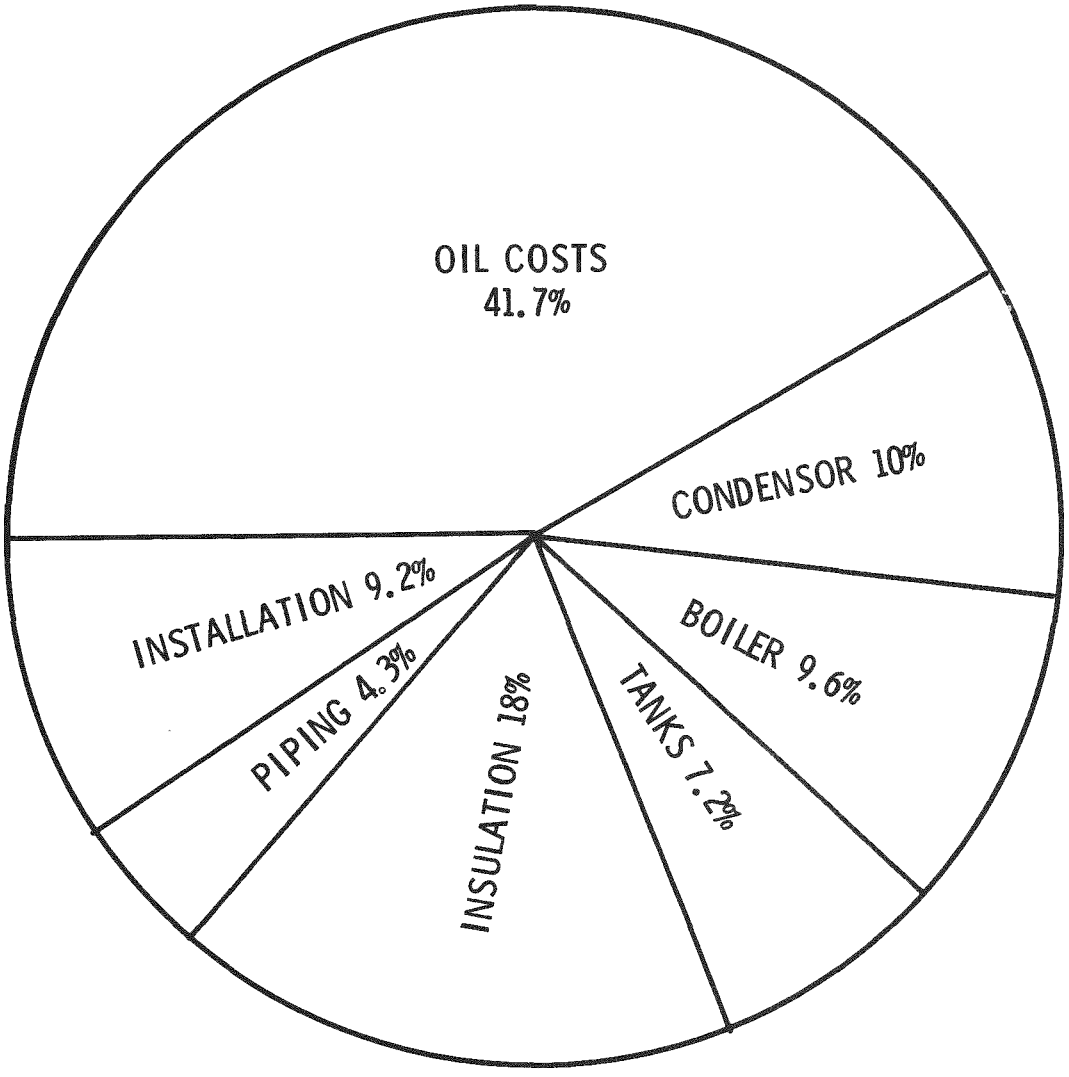


Figure 2-9. Cost Breakdown for the 1450 psia/950°F Cycle and Oil Storage

Systems Tradeoffs

Costs

The major costs of the solar plant are due to the collector subsystem and the storage cost.

The graph is based on salt storage with salt at 8¢/lb, and a collector subsystem cost of $5.75/ft^2. In addition, the cost of the dry cooling towers is a significant part of the total plant cost.

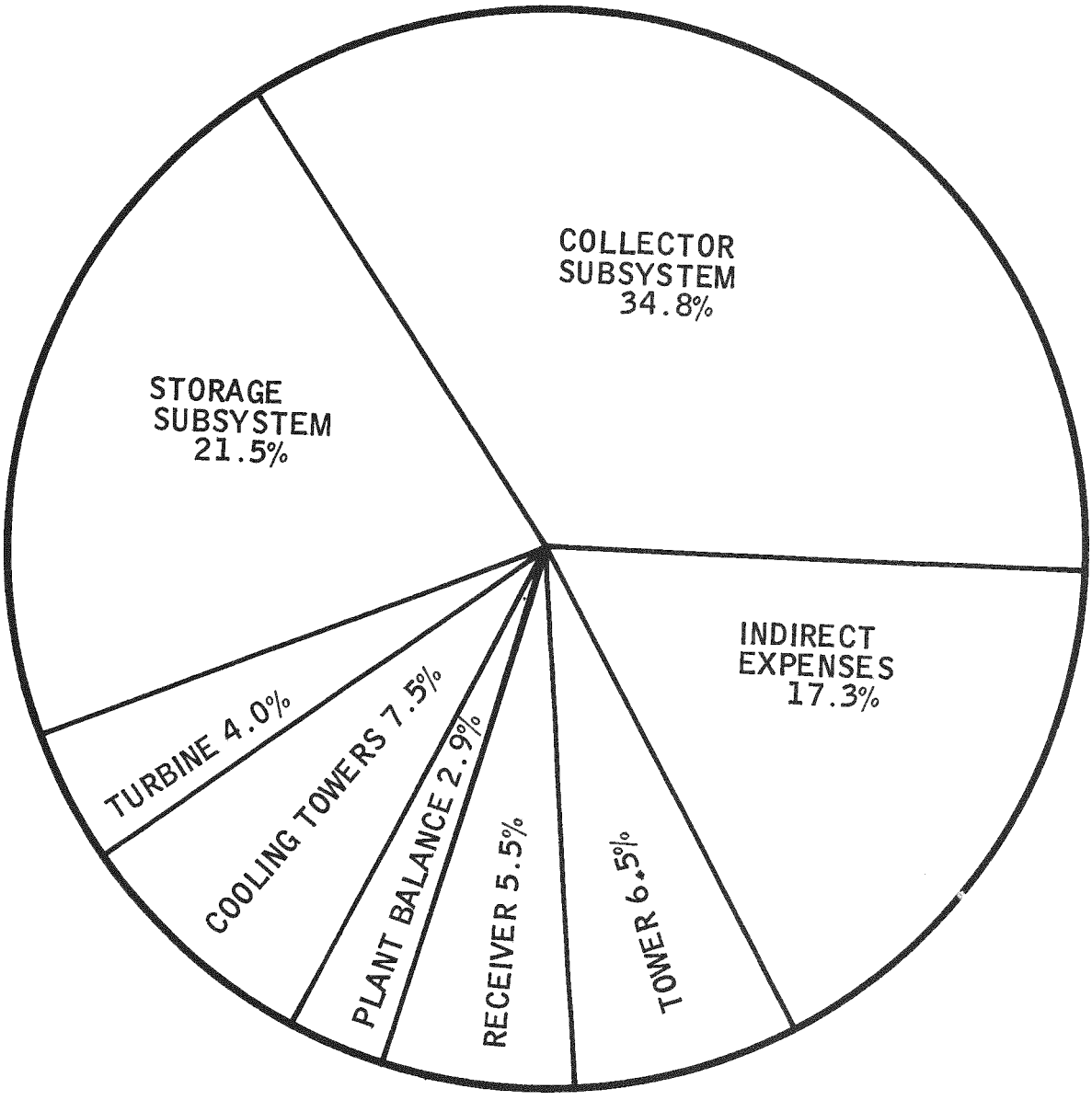


Figure 2-10. Cost Breakdown for the 1450 psia/950°F Cycle and Salt Storage

System Tradeoffs

Costs

There is no single leverage item in the total plant cost.

This pie chart is a breakdown of plant cost into major components. The chart assumes salt storage and a 1450 psia/950°F cycle.

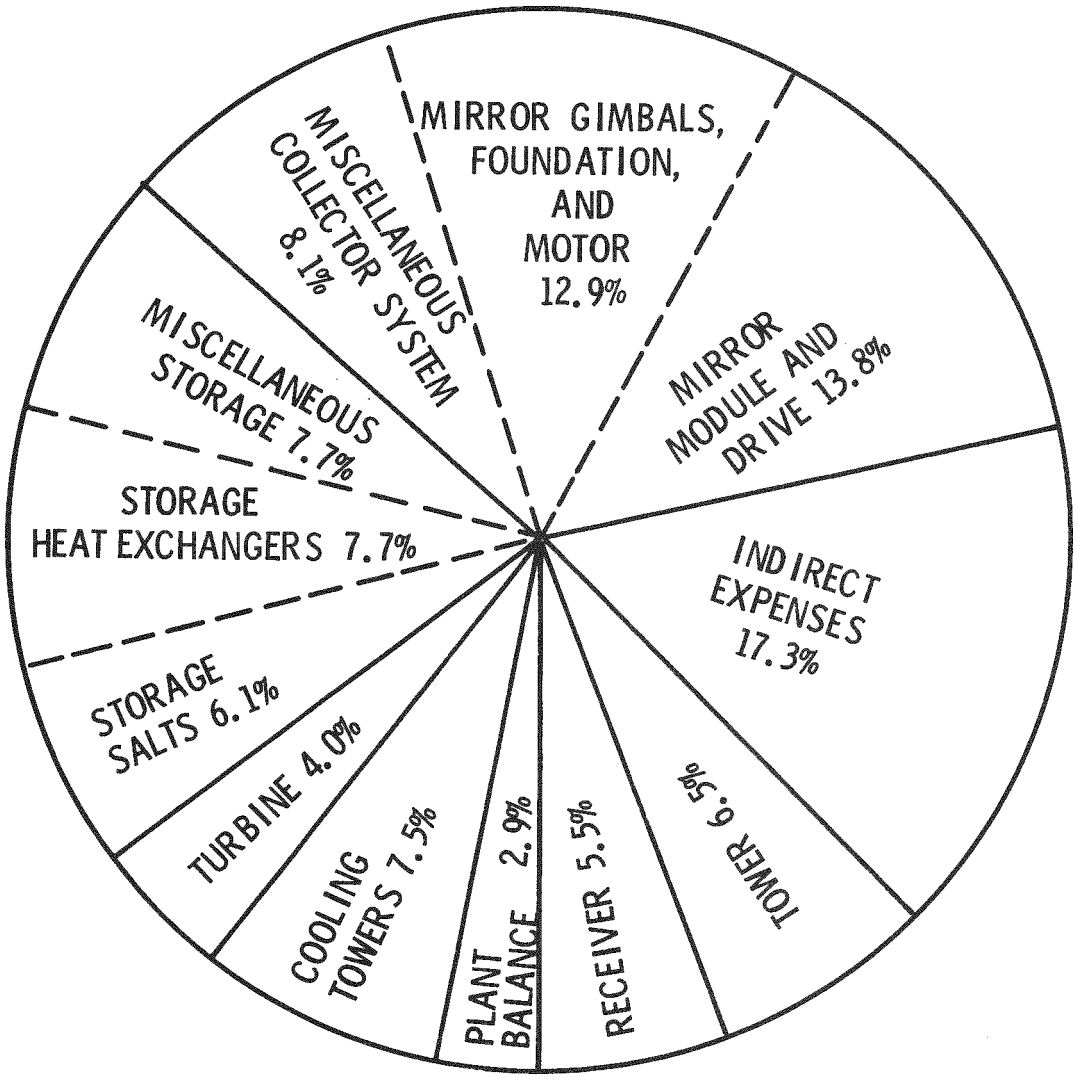


Figure 2-11. Cost Breakdown for the 1450 psia/950°F Cycle and Salt Storage

Systems Tradeoffs

Optics

The receiver strongly interacts with the field geometry to set the aperture dimensions and the net annual efficiency.

To set the aperture configuration, we ran a set of net annual energy calculations for a range of aperture configurations. The results of these Monte Carlo calculations are shown in Figure 2-12. The ordinate is net annual energy per unit heliostat area (incident annual flux minus reradiated flux), and the abscissa is aperture area. Each curve represents a constant separation distance (Sep) between the lower aperture boundary and its upper boundary. The aperture is an inverted cone fustram. Each different area is a larger or smaller-diameter cone. The cone angle was fixed as its optimal value as determined by other computer runs. Notice that for each separation (cone frustum height) there is a different optimal area (diameter). At low diameters, many rays miss the cone on either side. At large areas, (diameters), almost all rays are captured but the unnecessarily large area reradiates more energy and hence the curves roll off. The optimal aperture on this plot is clearly 100 square meters area with a 12-foot cone height (Sep=12). The plot required 30 computer runs at 110 central processor se seconds per run for a total of 3300 seconds computer time. Future aperture configuration work will require less computer time since we can make better estimates of the optimal configuration from these runs. The aperture configuration shown is for a ground cover fraction of 45 percent with a tilt-tilt-type heliostat and a 1-milliradian RMS error budget for each tracking drive axis.

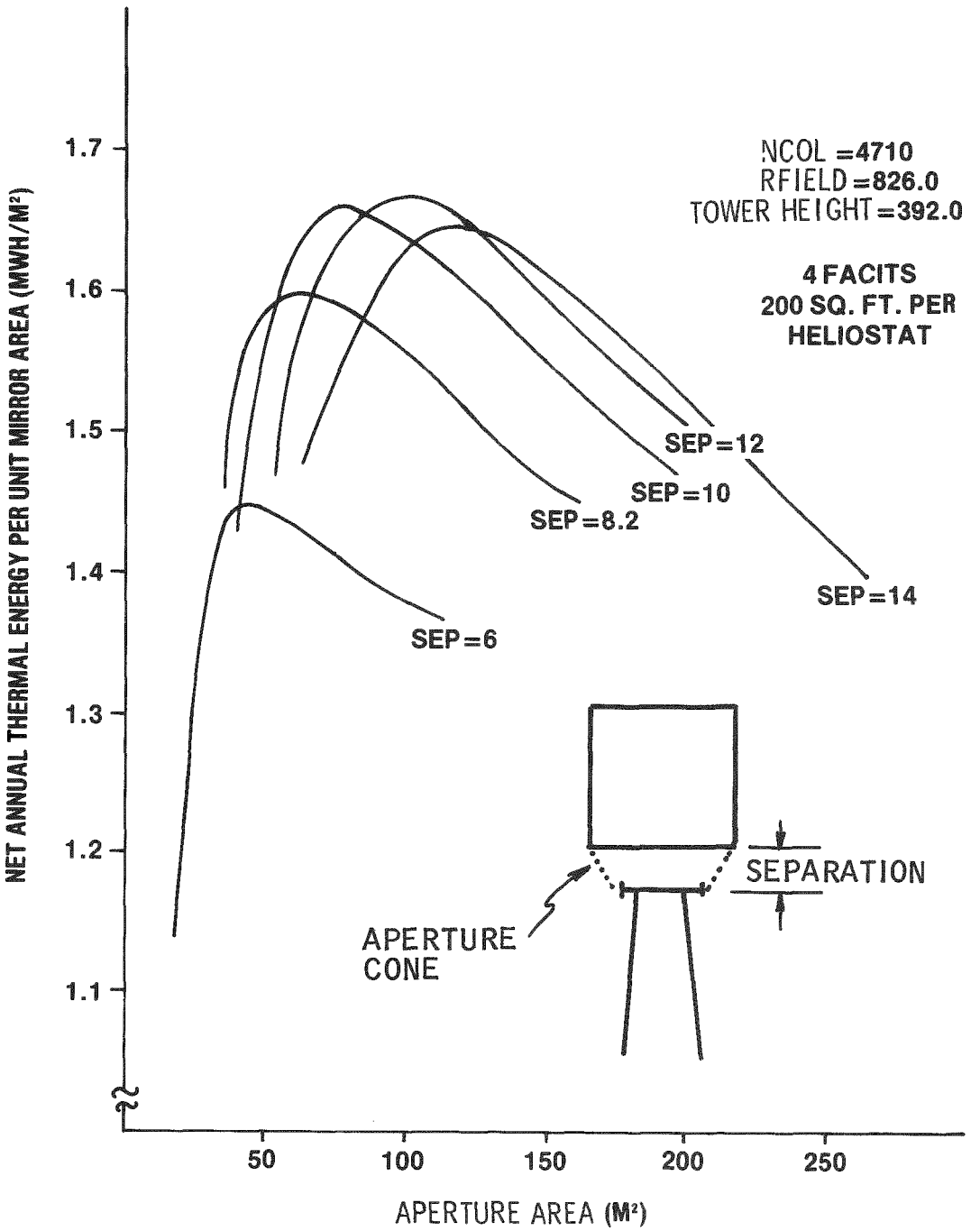


Figure 2-12. Net MWh(th) versus Aperture Area for 45 Percent Ground Cover Tilt-Tilt Heliostats One Milliradian Error Budget

Systems Tradeoffs

Optics

The relationship between tracking accuracy and system cost and performance is very strong.

To investigate the effect of an increased tracking error budget on annual energy performance, the optimal aperture configuration for a 3-milliradian tracking error tilt-tilt heliostat was determined. The plot of net annual energy per unit collector area versus aperture area is shown in Figure 2-13. In this case, the optimal receiver aperture is larger and receives less net annual energy than the 1-milliradian design.

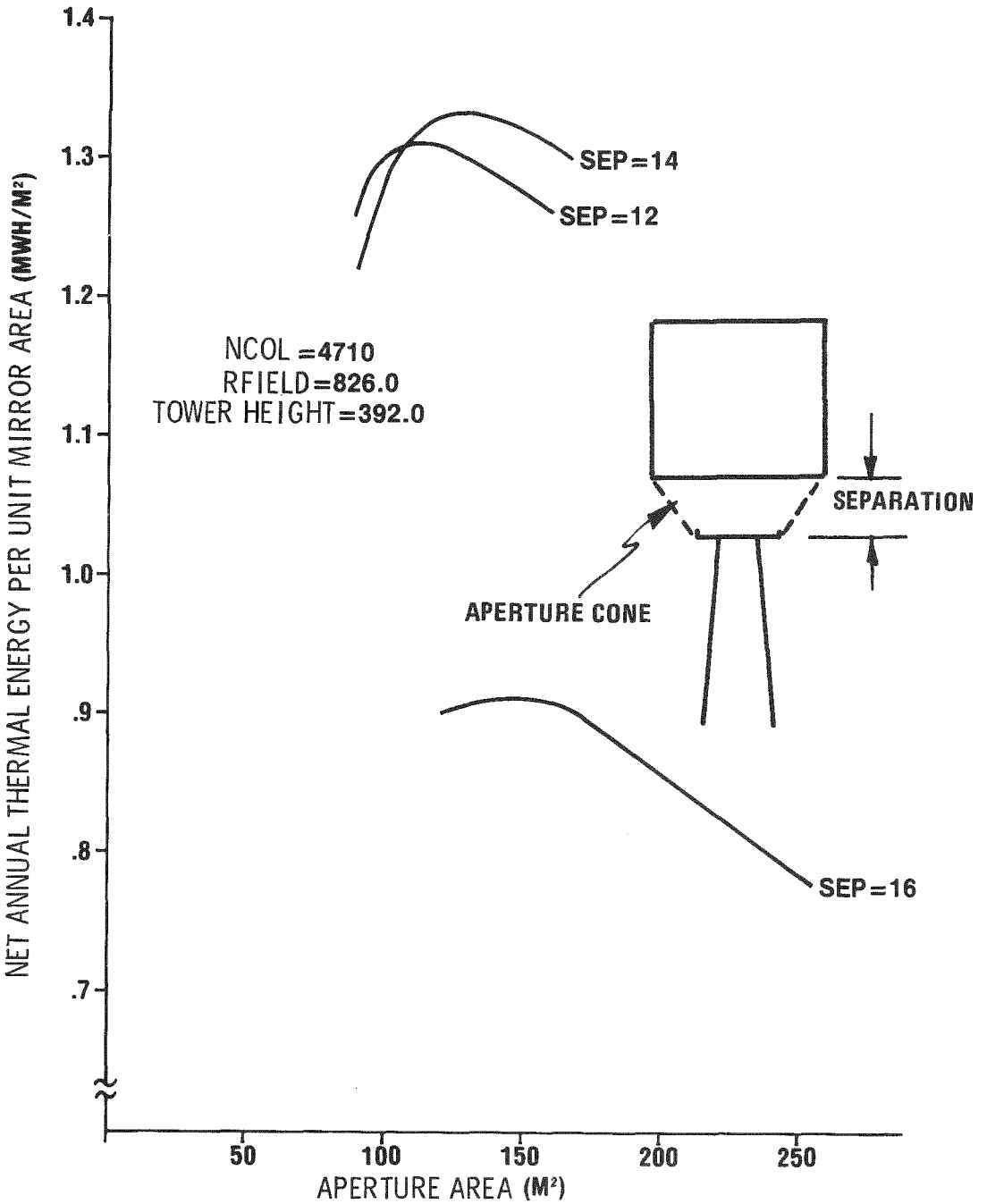


Figure 2-13. Net MWh(th) versus Aperture Area for 45 Percent Ground Cover Tilt-Tilt Heliostats with Three Milliradian Error Budget

Systems Tradeoffs

Optics

The reduced accuracy heliostat must have a lower cost than a more accurate heliostat to be cost effective.

The summary chart of Figure 2-14 shows the relative performance for 1- and 3-milliradian tracking RMS uncertainty. The outcome is that the 3-milliradian heliostat must be 20 percent cheaper to be as cost effective as the 1-milliradian design. In other words, if we can effect a 10 percent heliostat cost saving, we can economically justify a 1-milliradian increase in RMS tracking error on each tracking axis. This result is valid for a 45 percent ground cover. At lower ground cover, the cost reduction per milliradian should be greater than 10 percent.

ERROR	OPTIMAL APERATURE AREA	NET ANNUAL ENERGY PER UNIT AREA	BREAK EVEN COST
0.05° RMS	100M²	1.67 $\frac{MWH}{M^2}$	1.0
0.15° RMS	125M²	1.33 $\frac{MWH}{M^2}$	0.80

BREAK EVEN COST REDUCTION FOR TRIPLE ERROR BUDGET IS 20% REDUCTION OR 10% COST REDUCTION FOR EVERY ADDITIONAL MILLIRADIAN OF TRACKING ERROR ALLOWED.

Figure 2-14. Tracking Error Sensitivity Study Results

Systems Tradeoffs

Optics

ANNUAL RAYS LOST

The optimal receiver design does not minimize lost rays.

The adjacent figure shows the fraction of the Monte Carlo rays drawn for the annual energy calculations which miss the aperture high and low. Recall that the net annual energy optimal was sep=12 and 100 square meters aperture area.

Notice that no matter how large the aperture (diameter) is made, the rays that miss high and low cannot be reduced to zero.

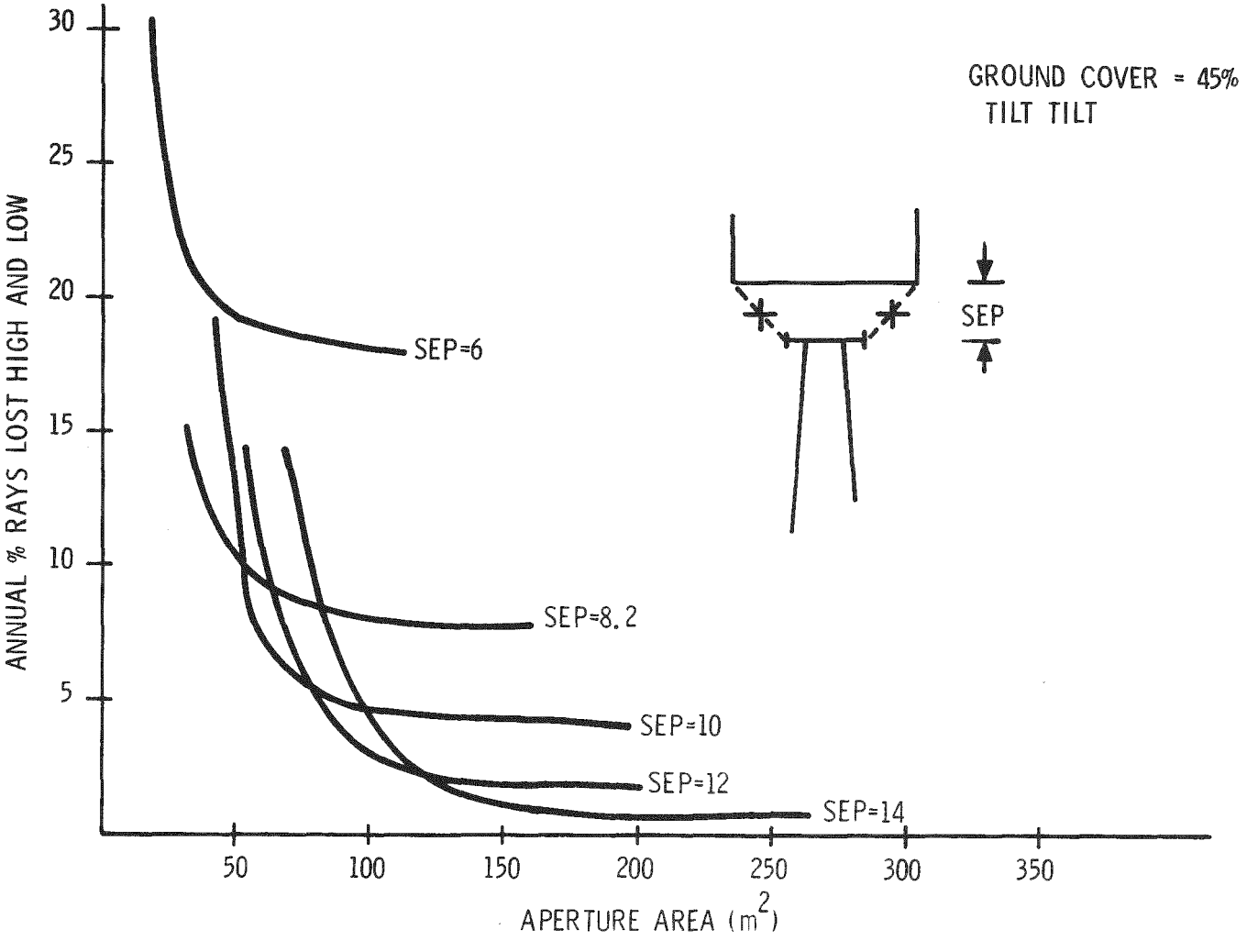


Figure 2-15. Annual Rays Lost to High and Low Misses Versus Aperture Area

Systems Tradeoffs

Optics

RAYS LOST ON SUPPORTS

The selected aim strategy is successful at keeping stray flux off of the receiver support structure (corbles).

All computer runs simulate three corbles, and aim strategy intended to keep flux from hitting them. The corbles are two feet wide and cover seven percent of the aperture area. On an annual energy basis, less than one quarter of one percent of the drawn rays accidentally hit the corbles.

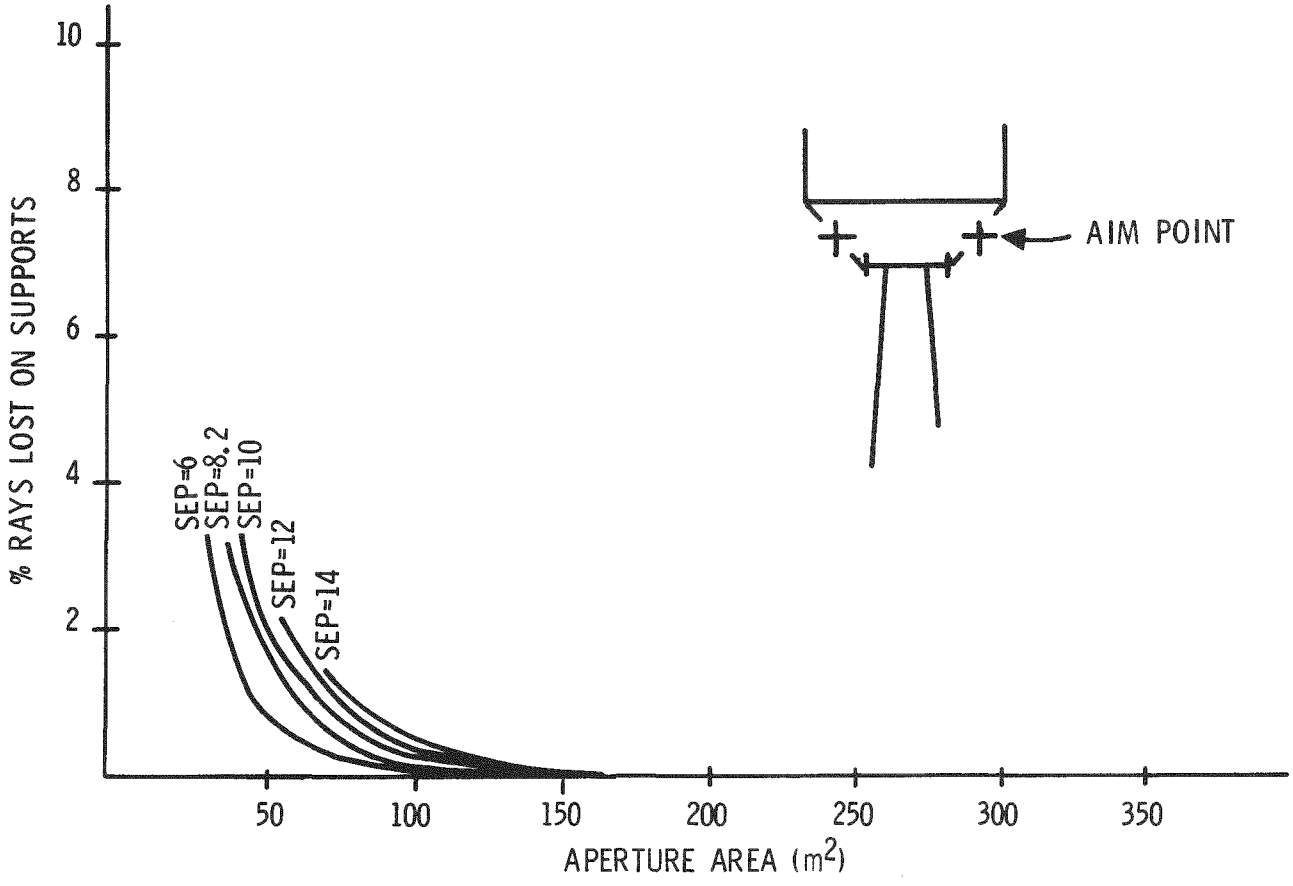


Figure 2-16. Annual Rays Lost on Supports Versus Aperture Area

Optics

There exists an optimal ratio of tower height to field radius, or rim angle; however, the optimal is relatively "flat" (insensitive) so that the tower height choice should be made to the low side of optimal to be conservative.

The adjacent figure shows the bus bar energy cost for a pilot plant scale system with 40 percent ground cover, and tilt-tilt heliostats, plotted against the tower height and/or rim angle. The inset figure defines rim angle. The baseline design is nominally a 400 foot tower while the optimal is somewhat higher. We believe that for practical fabrication, operation, and maintenance reasons, the tower should be as low as possible.

If it were possible to very accurately define the cost of all tower height-related issues, we would design at the optimal height which appears to be between 400 and 500 feet. Since the cost model is not sufficiently detailed, we have chosen 400 feet on a "knee of the curve" basis.

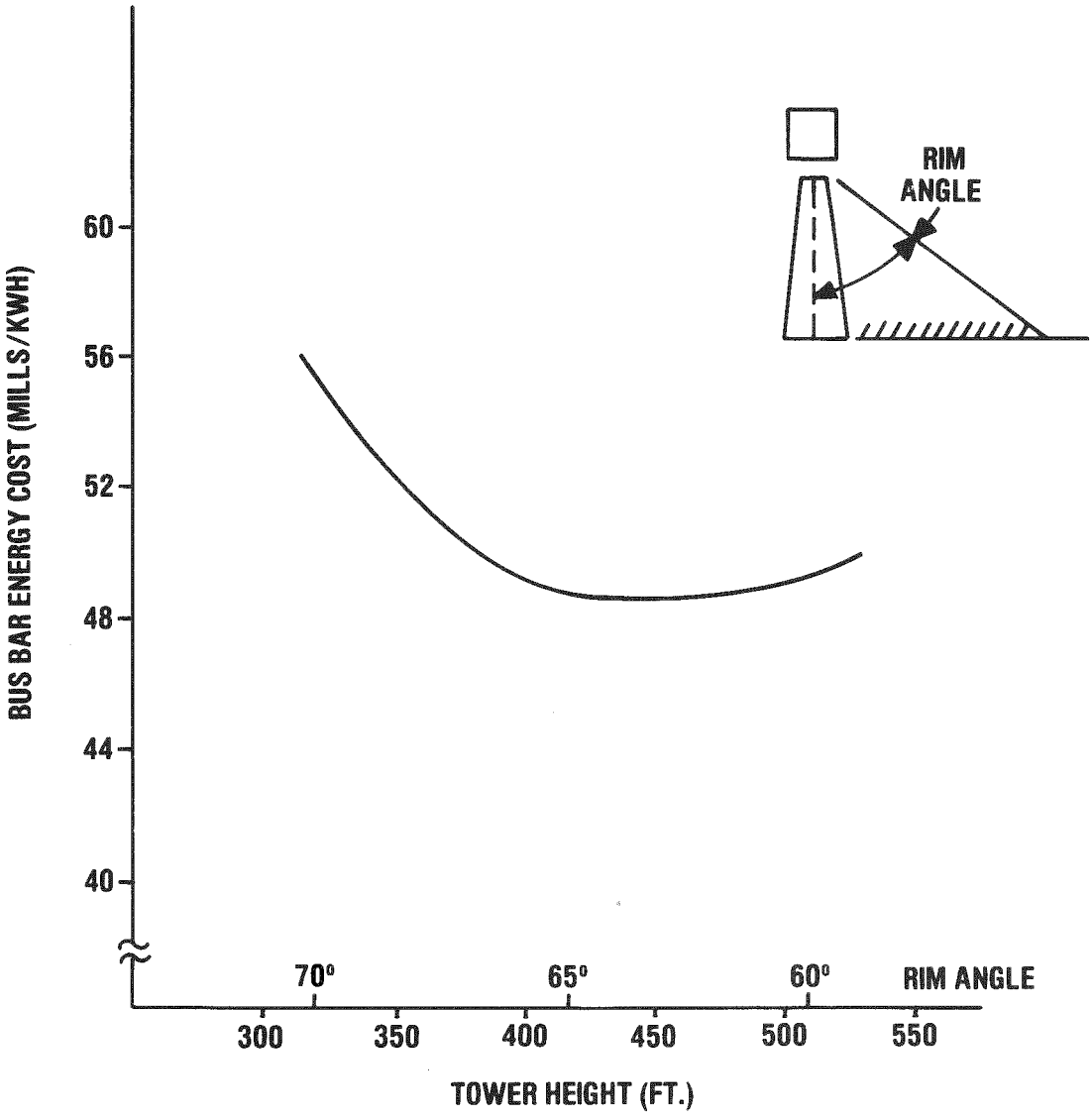


Figure 2-17. Bus Bar Energy Cost Versus Tower Height for 40% Ground Cover

Systems Tradeoffs

Optics

The angle the cavity aperture makes with the mirror field is of little consequence.

The adjacent figure illustrates the variation in yearly absorbed power as a function of the aperture opening orientation. A 60-degree value has been selected for future performance calculations although this parameter is not a serious issue in final system performance. The final value will be selected as the baseline design reaches its final form.

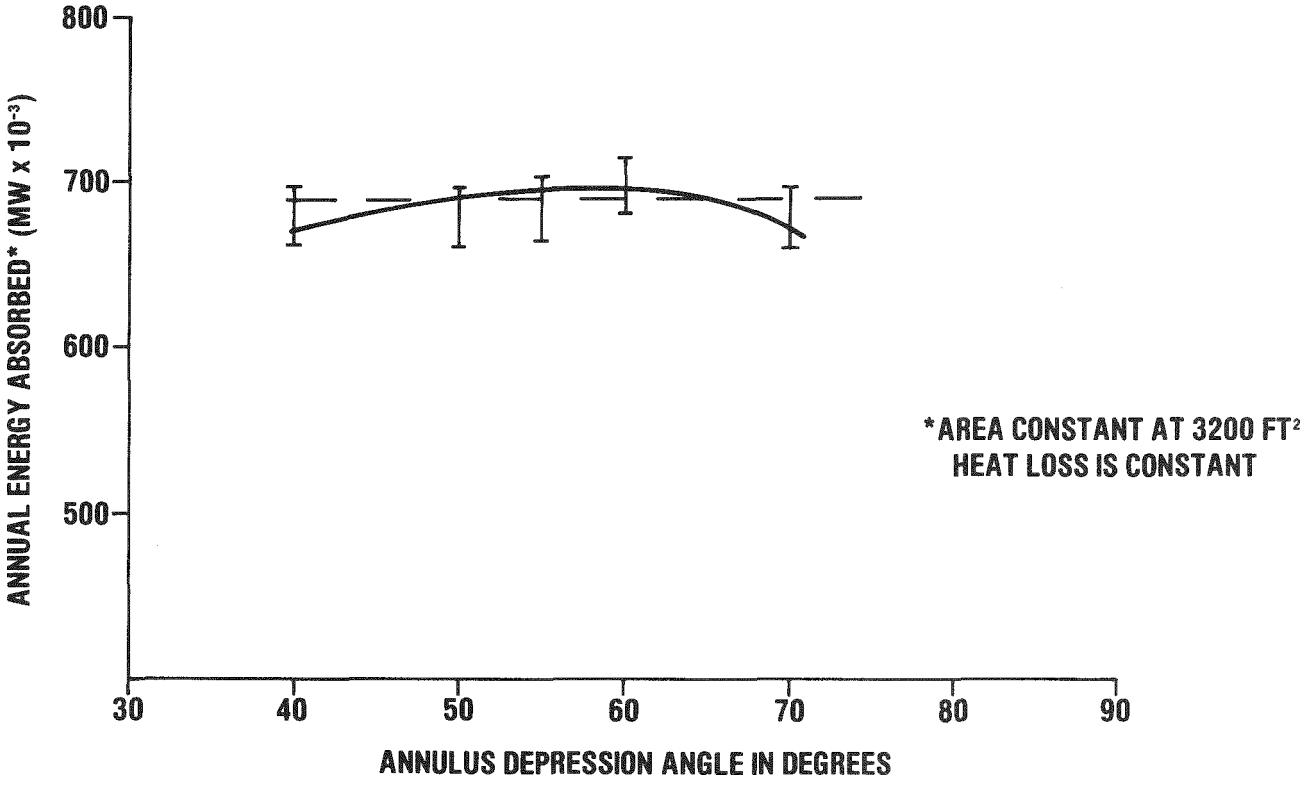


Figure 2-18. Annual Energy Absorbed Versus Aperture Angle

Systems Tradeoffs

Optics

The north heliostat field is better than the south field, but not by much.

The two adjacent figures illustrate the differences between the north and south heliostat fields at a uniform 30 percent ground cover and at Pilot Plant Scale. The upper figure compares the entire north half versus the entire south half. The lower figure compares the northern-most quarter to the southern-most quarter. The results show that the north field is substantially better performing than the south field in the winter months. As the sun moves seasonally higher in the sky, the south field markedly improves and during the summer months exceeds the north performance. These results suggest placement of the tower south of the field centroid.

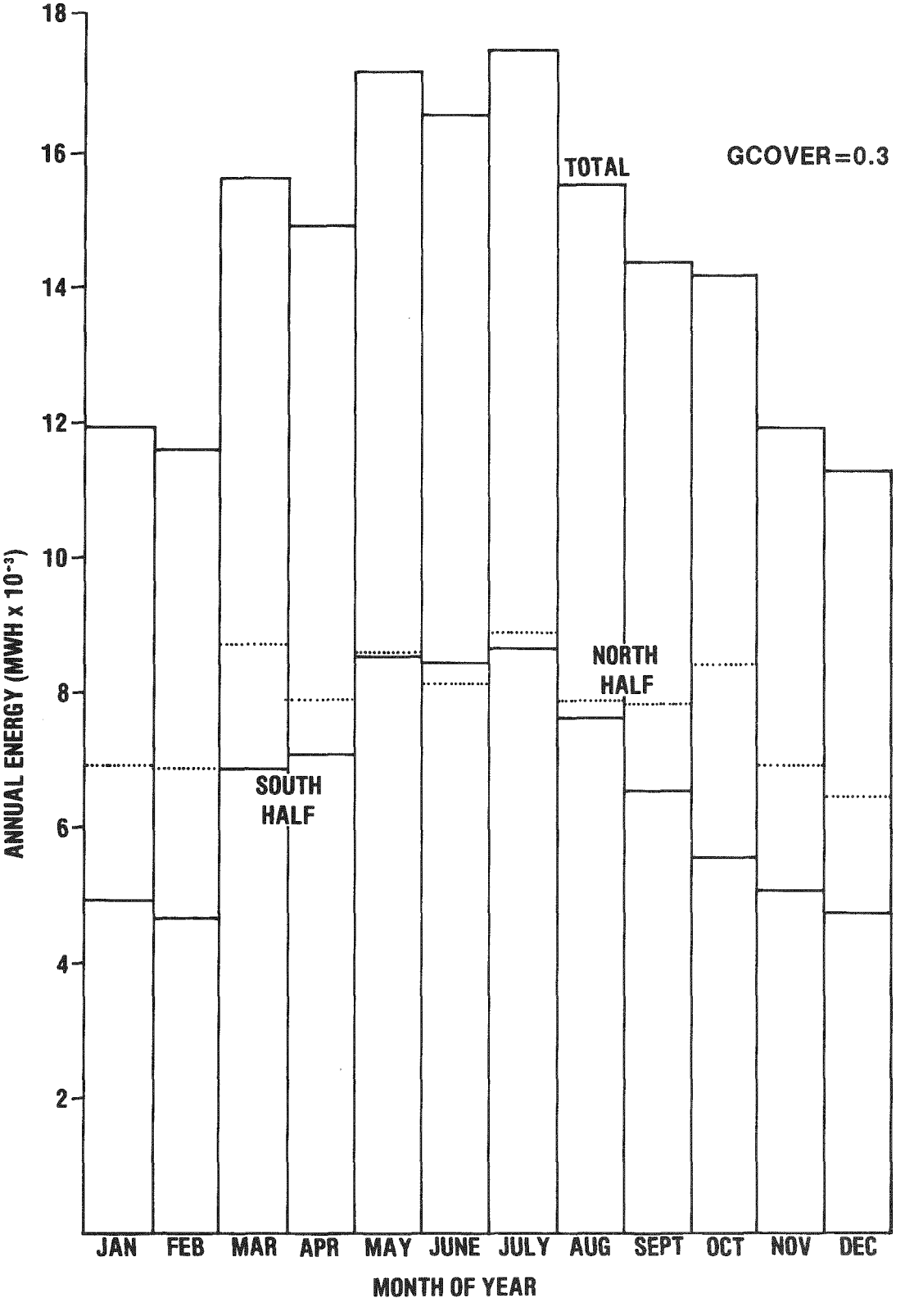


Figure 2-19. Energy From the Field Through the Year

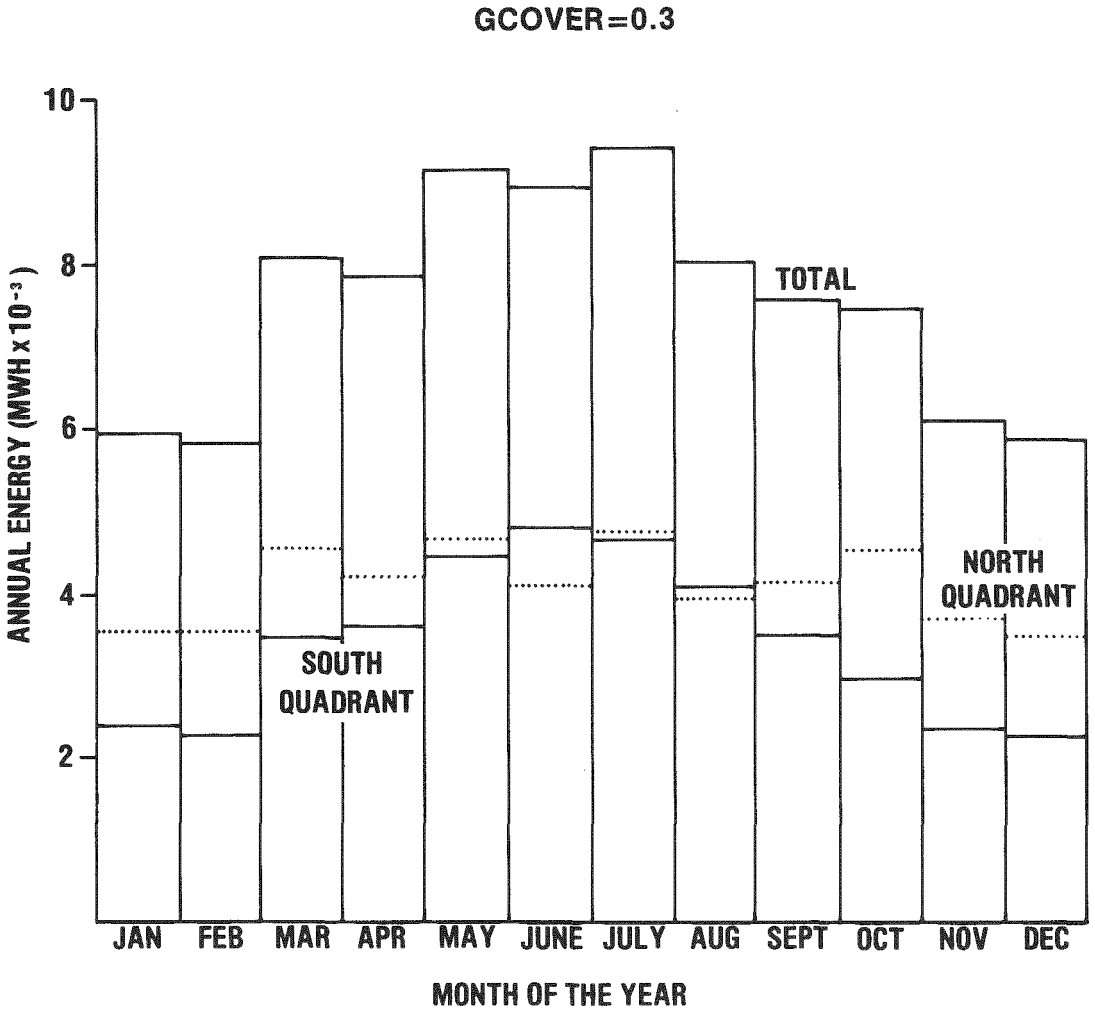


Figure 2-20. Energy From the Field Through the Year

This page intentionally left blank.

Systems Tradeoffs

Optics

Heliostat performance over the entire heliostat field is relatively uniform.

The adjacent figure illustrates the average annual power per square meter of mirror area at different locations in the field. The following conclusions may be reached:

- Near-in heliostats are worth more than more distant heliostats.
- The heliostats on the outer north edge of the field are 15 percent less effective than those at the center.
- Heliostats at the outer south edge of the field are worth significantly less and the field shape should be trimmed accordingly.
- With proper field shaping, the variation of heliostat average power over the field will probably not exceed 20 percent.
- Since the close-in south field heliostats are better than the most distant north heliostats, we know that the optional field is not north only while a smaller south field is indicated.

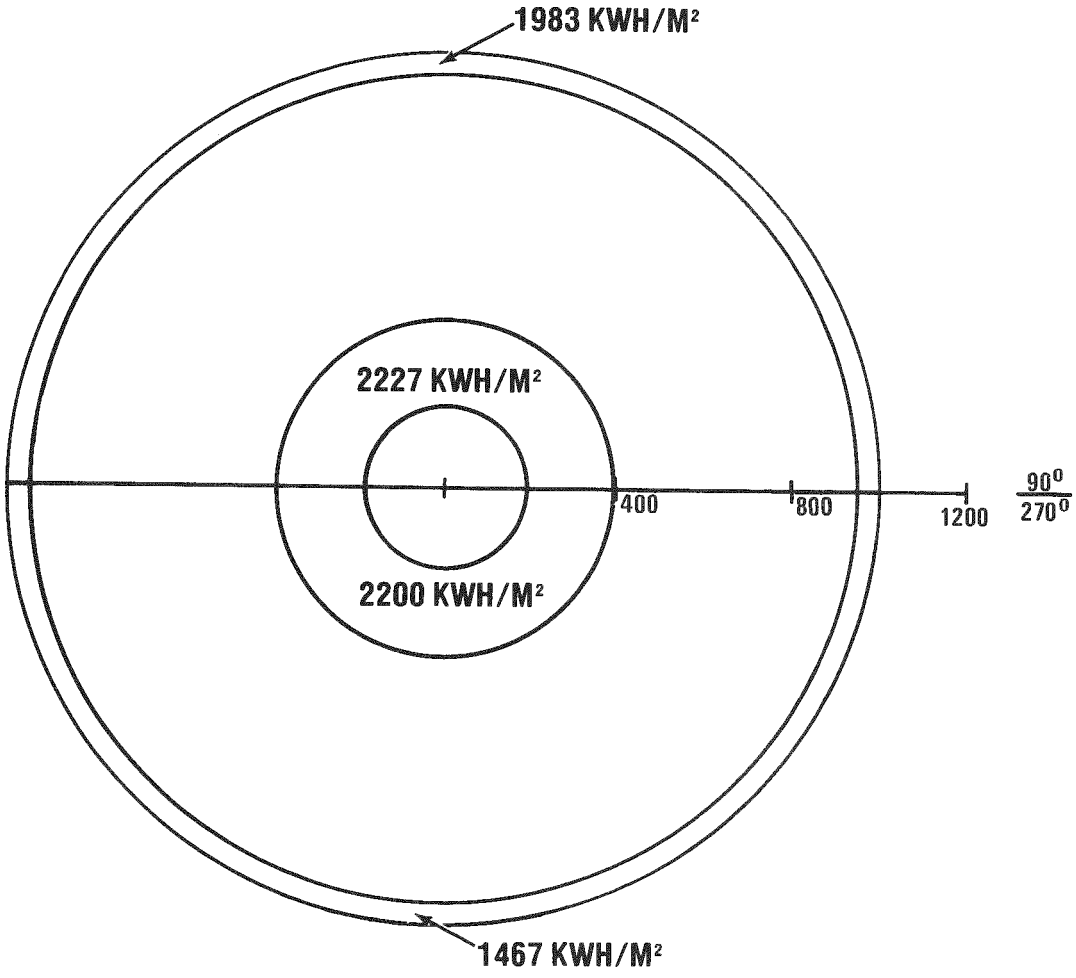


Figure 2-21. Annual Energy From Various Field Segments (Field Average = 1990 KWH/M^2)

Systems Tradeoffs

Optics

The optimal ground cover fraction for either the AZ-EL or the tilt-tilt heliostat design is 0.3.

The adjacent figures show net annual energy per unit heliostat area and bus bar energy cost as a function of design ground cover. Each ground cover requires a different field area to contain the same number of heliostats and hence yield the same nominal capacity power plant. All other dimensions, including tower height and aperture dimensions, were scaled linearly with field radius. Thus, each aperture is nearly optimal for each ground cover. The curves show that the tilt-tilt heliostat is superior to the AZ-EL heliostat at all ground cover fractions. This result proved to be misleading. Both types of heliostats shown had fixed facet spacing on the heliostat frame at each ground cover fraction. The tilt-tilt design utilized a relatively wide interfacet spacing (of its four facets) while the facets were close together on the AZ-EL frame (3 facets for AZ-EL). The reason for the close spacing on the AZ-EL frame was the relatively poor packing density of the AZ-EL design. Basically, the spacing for the AZ-EL design is such that at 45 percent ground cover the AZ-EL heliostats just miss each other as they track. Thus, 45 percent was the maximum ground cover fraction for the AZ-EL design we used. The tilt-tilt design could be used all the way out to 60 percent ground cover. Since the optimal ground cover fraction came out much lower than 45 percent, we were able to significantly increase the facet spacing for the AZ-EL design. This increase improved the performance of the AZ-EL design so that it is superior to the tilt-tilt design. We also increased the facet spacing for the tilt-tilt design, but its performance showed no significant improvement. The reason for this is the AZ-EL design shades and blocks itself from facet to facet, while shading and blocking from heliostat plays almost no role in setting performance. The tilt-tilt configuration is just the inverse of this. The shading and blocking for the tilt-tilt design is almost entirely from heliostat to heliostat and much less from facet to facet on a given heliostat. The data shown represents a two step optimization procedure. First, the optimum ground cover fraction was found. Next we found the optimum facet spacing for the optimal ground cover. When we compared sub-optimal designs, the tilt-tilt was superior. When both designs were optimized, the AZ-EL proved superior.

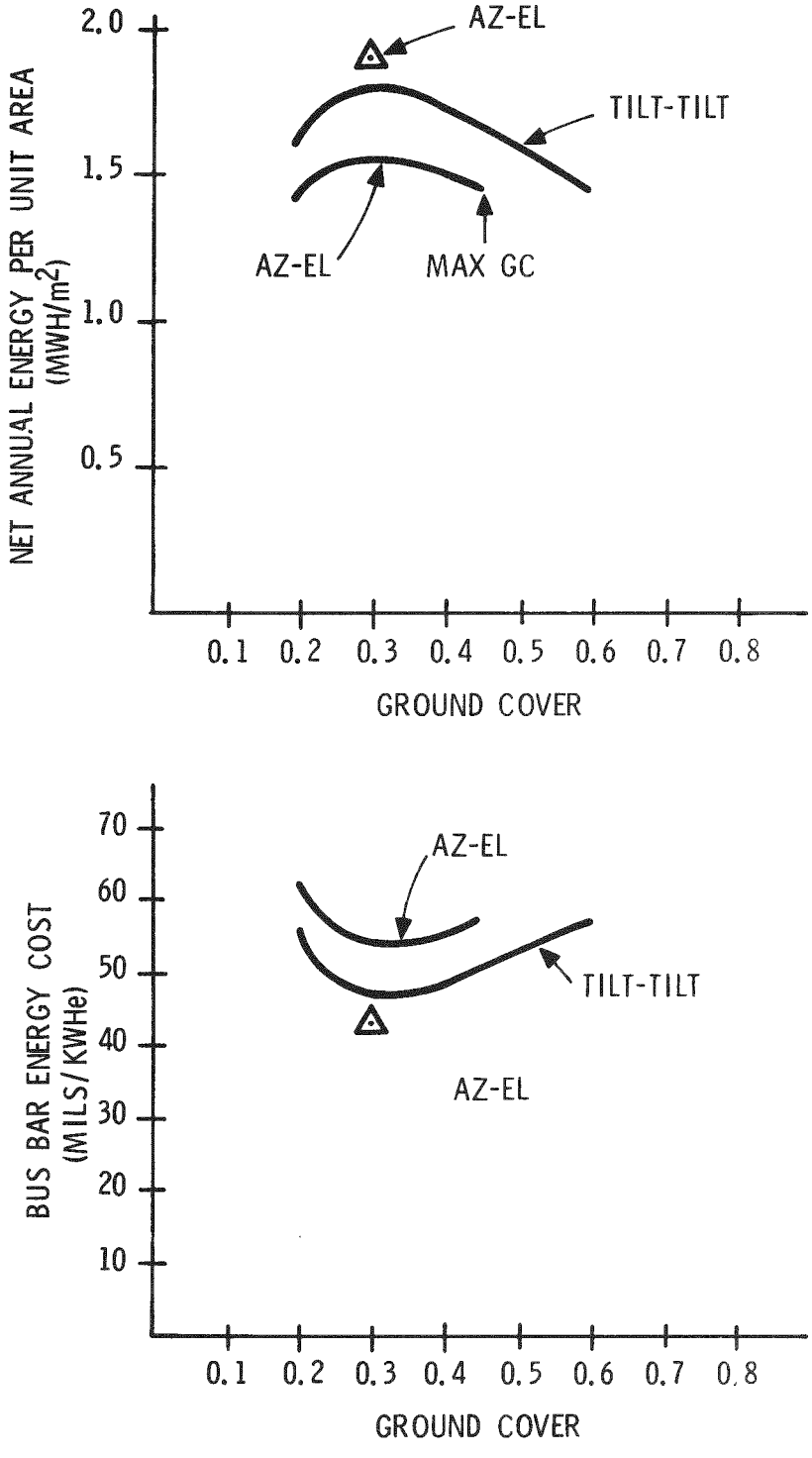


Figure 2-22. System Performance Versus Ground Cover

Systems Tradeoffs

Optics

To receive 90 percent of the normal incident radiation at China Lake, the heliostats must meet the pointing and tracking specification in an 18-mph wind.

The adjacent radiation duration curve is the result of correlating wind speed and normal incidence radiation at China Lake. The data was taken on hourly intervals for the year 1962. These results illustrate the importance of accurate pointing and tracking in relatively high wind conditions.

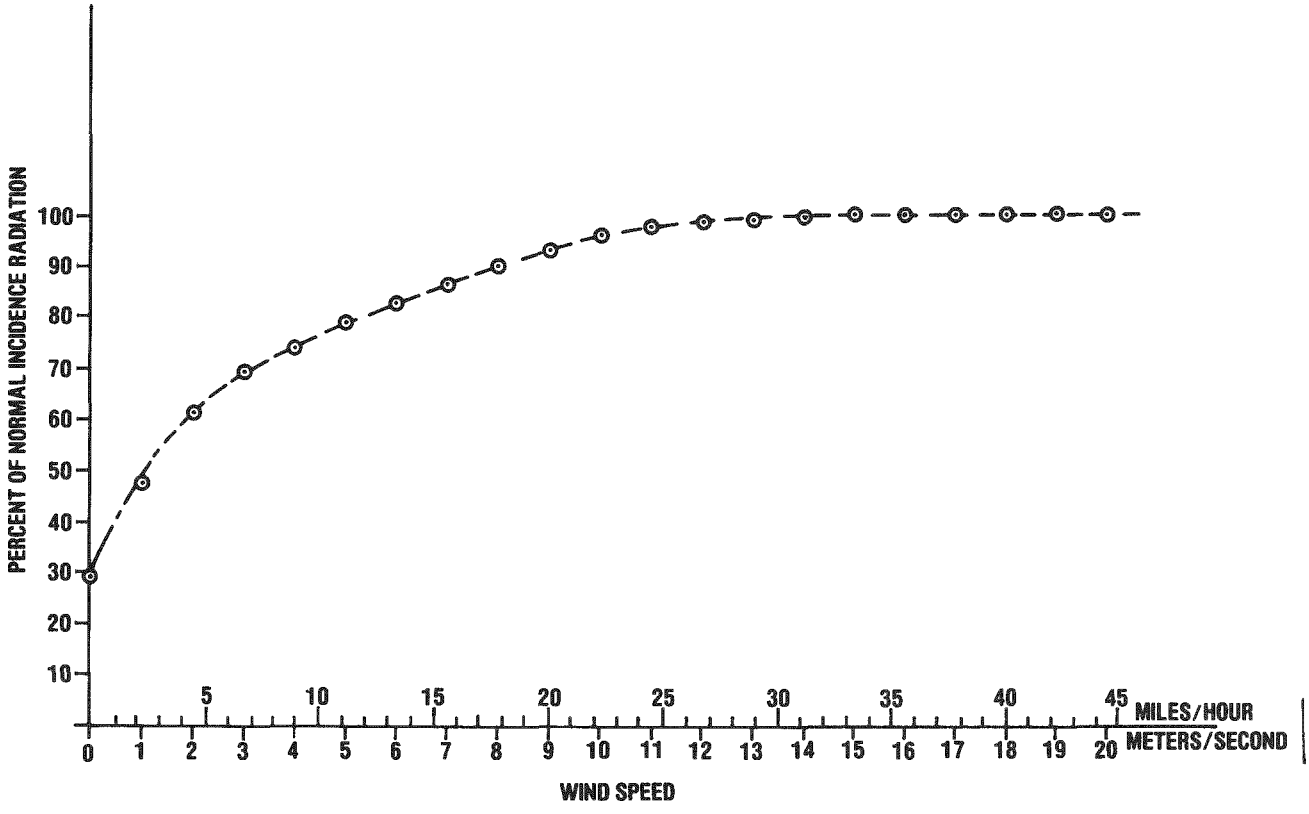


Figure 2-23. China Lake Wind Speed Versus Energy Correlation (China Lake Weather Tape Courtesy Aerospace Corp.)

Systems Tradeoffs

Optics

The number of complete startup and shutdown cycles that the steam generator must undergo per year is not significantly greater than the diurnal total (730 or 2 per day) in spite of cloud cover and wind perturbations. This issue is important to boiler lifetime predictions.

To determine the relative effect of clouds, we computer scanned weather tapes and counted the number of times the hourly average insolation went from on to completely off or completely off to on. The total extra on-off cycle count was two extra (beyond the diurnal count) at China Lake and 26 extra at Albuquerque due to cloud cover only.

Recall that there is a design operational wind speed for the heliostat. This means that the heliostat field (hence the receiver) must be shut down anytime the wind exceeds the design value. The number of cycles due to the wind-related shutdowns at a shutdown threshold speed of 10 meters per second (22 miles per hour) is 20 extra at China Lake. All other shutdown speed thresholds yield lower extra shutdown totals. If we had available measured weather data which shows instantaneous flux, we might find a much higher incidence of solar outages than is apparent in the chart.

	EXTRA CYCLES DUE TO CLOUDS	EXTRA CYCLES DUE TO CLOUDS AND WIND
CHINA LAKE	2	20
ALBUQUERQUE	26	(NO WIND DATA)

Figure 2-24. Extra Startup and Shutdown Cycles Per Year Due to Weather

System Engineering

SYSTEM EFFECTIVENESS

The Systems Effectiveness Program provides an on-going assessment of compliance with the 90 percent availability goal for the Solar Pilot Plant and provides timely system design recommendations to achieve this goal.

The primary objective of the Systems Effectiveness Program is to assess compliance with the 90 percent availability goal for the Solar Pilot Plant, as specified in Annex 1 of the RFP and to provide system design recommendations to achieve this goal. This objective is to be accomplished without compromising the safety requirements specified in Annex 1 of the RFP and with a design goal of minimizing total cost (initial and operating) per watt-hour. Pursuant to this objective, availability estimates (numerical values) will be determined for each identifiable subsystem comprising the overall Solar Pilot Plant. The System Effectiveness Program will allow a quantitative, orderly, and on-going assessment of the system design as it progresses through its various stages. The Systems Effectiveness Program will be accomplished by a reliability/maintainability engineer specifically assigned to the Honeywell Solar Pilot Plant engineering team. The Systems Effectiveness Program Plan provides a detailed description of the System Effectiveness Program tasks to be accomplished during the Solar Pilot Plant Phase I program contract. It is provided as Appendix 2B. Following is a synopsis of the primary system effectiveness program tasks.

Availability Allocation

Provides an allocation of the total Solar Pilot Plant availability goal, 90 percent, to the major subsystems.

Availability Model

Provides a mathematical model of the Solar Pilot Plant availability, reflecting the solar pilot plant operating modes and operating strategy/scenario.

Availability Analysis

Assesses compliance with the availability goal and provides the basis for system design recommendations to achieve this goal.

Failure Mode and Effect Analysis

Identifies potential failure modes of the solar pilot plant and the consequences of them occurring. Highlights single-point failure conditions and provides the basis for recommendations for failsafe provisions, redundancy, and failure warning systems/devices.

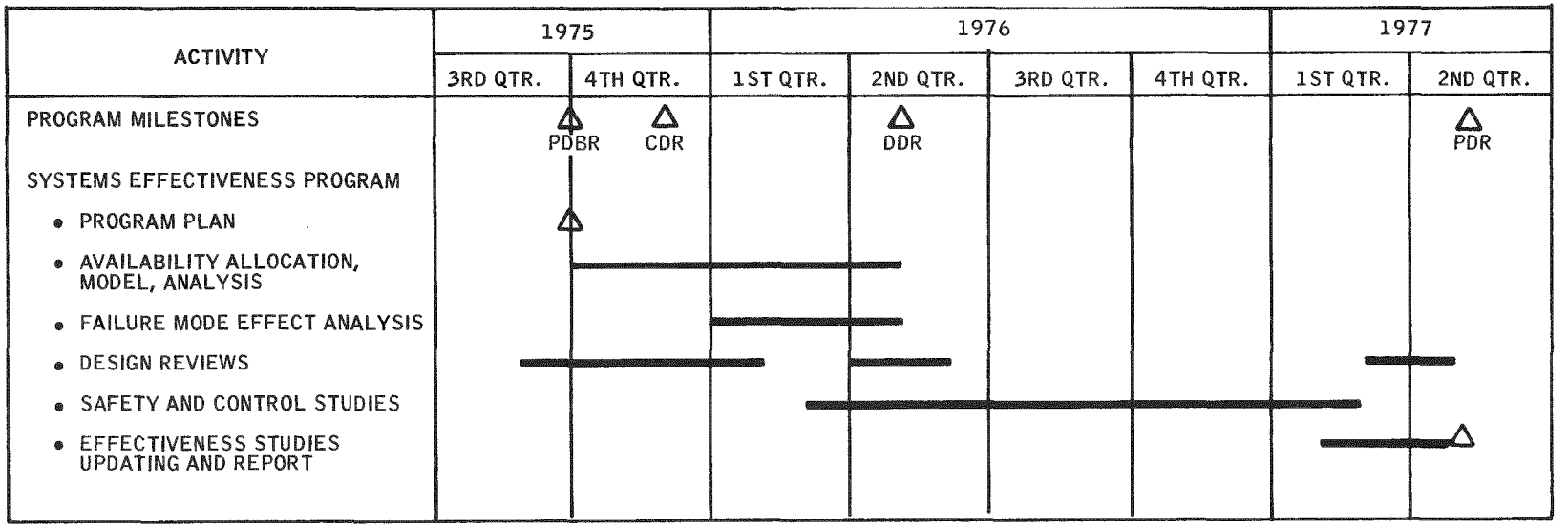


Figure 2-25. Systems Effectiveness Program
Solar Pilot Plant Phase I

Design Reviews

Provides assurance that systems effectiveness considerations (reliability, maintainability, and safety) are reflected in design decisions.

Safety and Control Studies

Assures that reliability and safety considerations which result from the above analysis and which are pertinent to the experiments are reflected in design tradeoffs and SRE test plans. Provides failure report documentation for problems which are surfaced during the SRE Test and Evaluation Program.

Effectiveness Studies

Provides the final updating of the Availability Allocation, Availability Analysis, and Failure Mode and Effect Analysis to be included in the Preliminary Design Review documentation (CDRL 2).

SECTION III
PILOT PLANT CONCEPT

	Page
Plant Layout	3-2
Subsystem Identification	3-9
Subsystem Interfaces	3-16

Pilot Plant Concept

Plant Layout

CONCEPT OVERVIEW

The pilot plant concept (Figure 3-1) has been designed to collect solar energy, convert it to thermal energy and use it to generate electrical power or store it for later use in generating electrical power.

1. Solar energy incident upon a circular field will be concentrated through the annulus aperture of an elevated central, cavity-type receiver.

2. The concentrated solar energy will be converted to thermal energy as it is absorbed by an array of boiler and superheater tubes located in the receiver cavity.

3. The superheated steam produced in the receiver can be used to generate electricity using a dual-pressure admission turbine generator.

4. The thermal energy generated in the receiver can also be stored by melting a eutectic salt. The thermal energy stored in the salt can be used to produce steam which is admitted to the low-pressure stage of the dual-admission turbine generator.

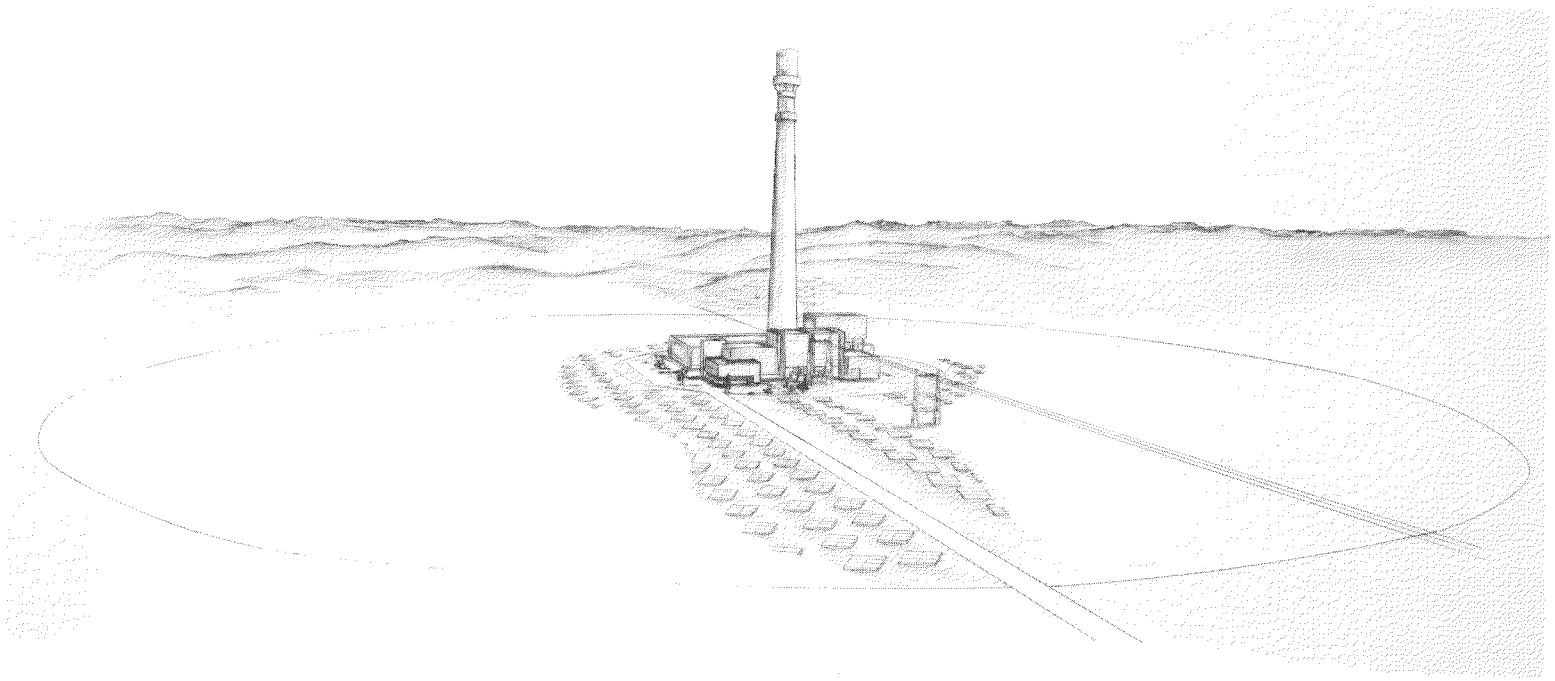


Figure 3-1. 10 MW Solar Pilot Plant

Pilot Plant Concept

Plant Layout

SITE ARRANGEMENT

The pilot plant site arrangement (Figure 3-2) was developed to facilitate a functional relationship between major plant systems.

1. Crossing of lines and interference between functional systems was minimized to reduce the complexity of plant operation and maintenance.

2. The site arrangement was developed by giving priority to those major plant facilities whose parameters could be manipulated least. These major plant facilities include the collector field, the central plant complex, an access road and a rail line and transmission lines integrating with the existing electrical network.

3. The collector field will be located by giving consideration to topographical features that accommodate the specified outer radius.

4. The central plant complex was located in the center of the collector field in a manner that would eliminate blockage of any heliostats on the collector field inner radius.

5. An access road and a rail line were located to facilitate plant operation and maintenance and to minimize collector loss.

6. The electrical transmission lines integrating the plant output with the existing network were located to minimize interference with other facilities or lines.

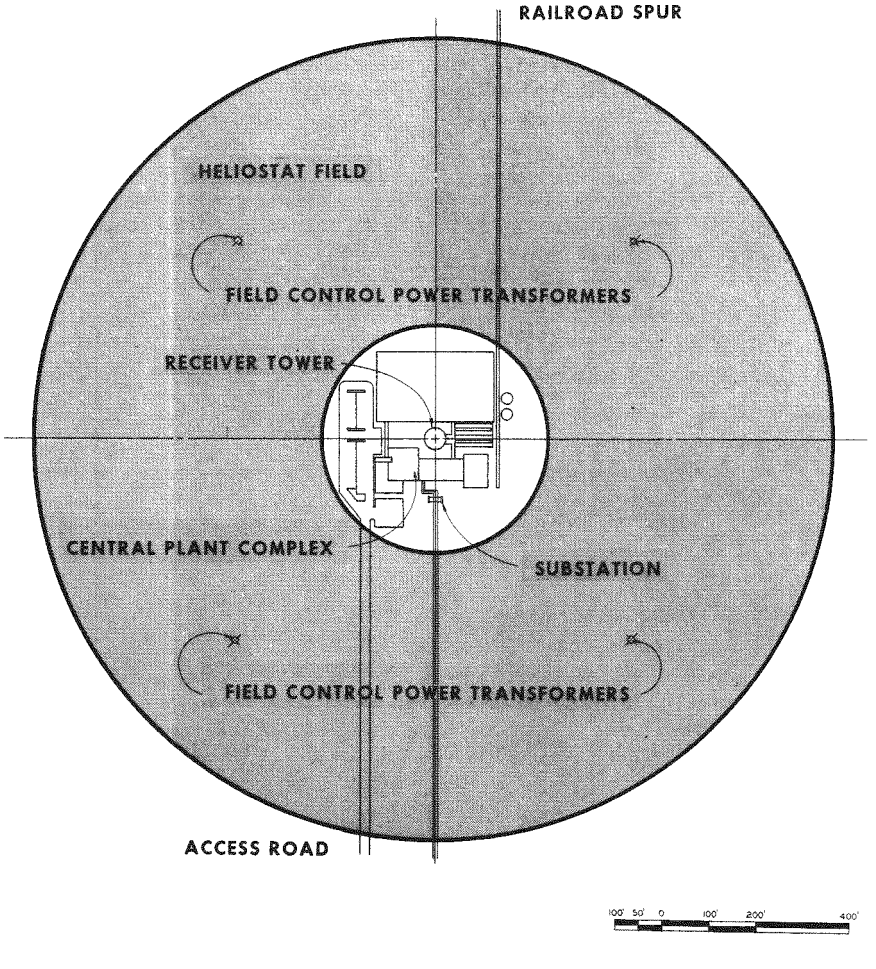


Figure 3-2. 10 MW Solar Pilot Plant - Site Plan

Pilot Plant Concept

Plant Layout

PLANT ARRANGEMENT

The central plant arrangement (Figure 3-3) was developed to minimize crossing and interference between functional systems with priority given to major plant facilities.

1. Crossing of lines and interference between functional systems was minimized to reduce the complexity of plant operation and maintenance.

2. The plant arrangement was developed by giving priority to those major plant facilities whose parameters could be manipulated least. These major plant facilities include the receiver tower, the electrical generation building, the thermal storage unit, and the air-cooled condensers.

3. The receiver tower was located at the center of the collector field to maximize annual solar energy collection.

4. The electrical generation building was designed and located to house the EGS equipment and serve as the operations center of the pilot plant.

5. The thermal storage unit was located to facilitiate interface with steam and feedwater lines and for convenient rail access.

6. The air cooled condensers were located to facilitate steam and condensate piping in a manner that blends with the overall plant arrangement.

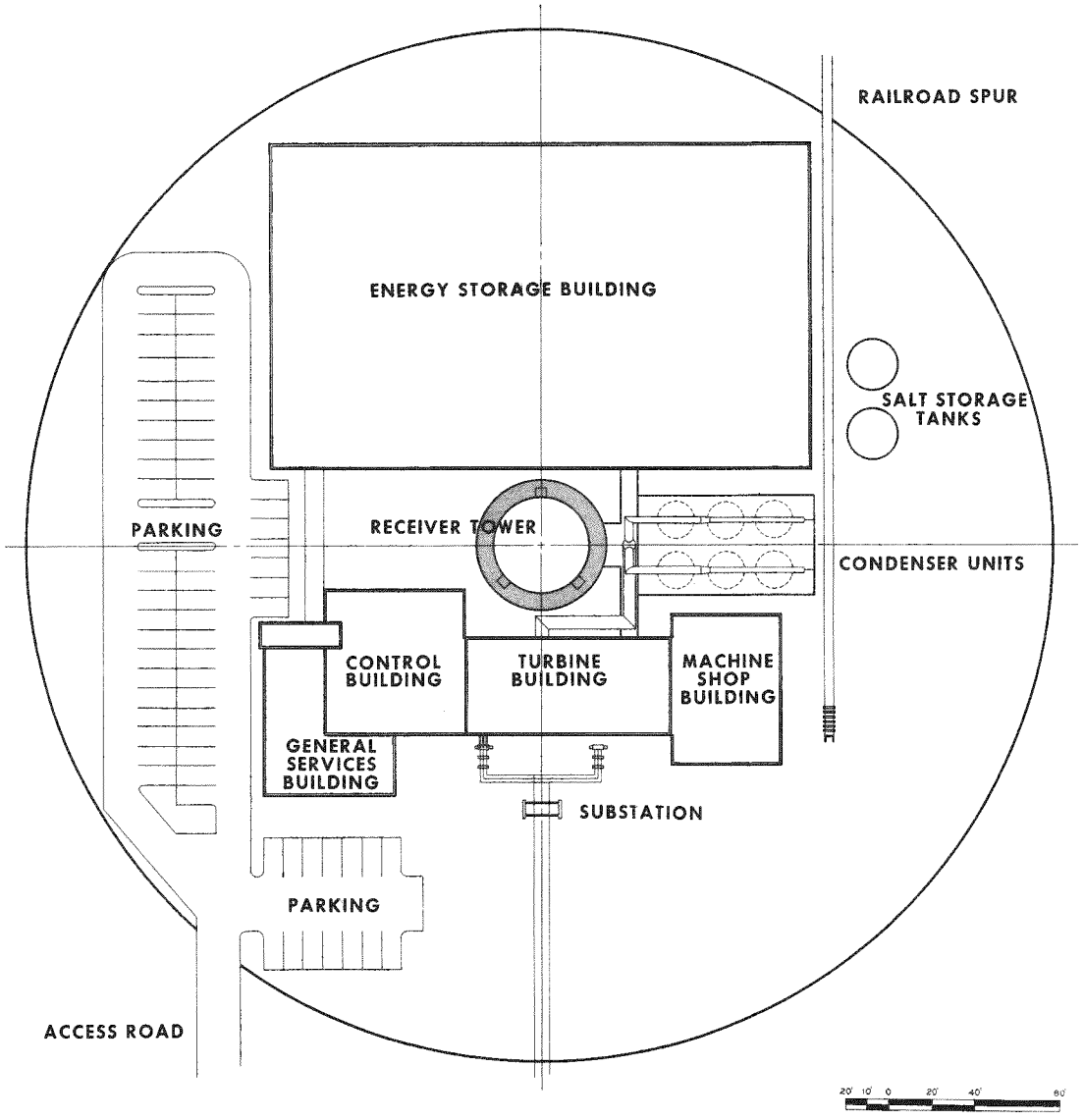


Figure 3-3. 10 MW Solar Pilot Plant - Central Plant Complex

Pilot Plant Concept

Plant Layout

MAJOR PLANT CHARACTERISTICS

Major characteristics (Table 3-1) have been identified for each of the plant subsystems.

1. The major characteristics of the collector subsystem include the field outer radius and the number of heliostats.

2. The major characteristics of the received subsystem include the tower height and the receiver cavity dimensions.

3. The major characteristics of the thermal storage subsystem are the thermal storage capacity and the total quantity of phase change materials.

4. The major characteristics of the electrical generation subsystem are the turbine name plate capacity, the high pressure steam turbine inlet conditions, and the low-pressure steam turbine inlet conditions.

Table 3-1. Major Plant Characteristics

	FPS	SI
Collector Subsystem		
Field Outer Radius	850 ft	259 M
Number of Heliostats	4968	4968
Receiver Subsystem		
Tower Height	400 ft	122 M
Cavity Diameter	32 ft	10 M
Cavity Height	46 ft	14 M
Thermal Storage Subsystem		
Thermal Storage Capacity	7×10^8 BTU	200 MWH(t)
Total Quantity of Phase Change Material ($NaCl-NaNO_3 - Na_2SO_4$, NaCl-NaOH)[3]	10×10^6 lb	4.5×10^6 KG
Electrical Generation Subsystem		
Turbine Name Plate Capacity		15,000 kW
High-Pressure Steam Turbine Inlet Conditions	1450 psi/950°F	100 BAR/510°C
Low-Pressure Steam Turbine Inlet Conditions	575 psi/534°F	40 BAR/280°C

Pilot Plant Concept

Subsystem Identification

COLLECTOR SUBSYSTEM

The collector subsystem (Table 3-2) was designed to gather and transmit as much solar energy as is economically feasible using focusing heliostats.

1. The tower-centered collector field was selected to optimize annual thermal energy.

2. A flat collector field has been selected because of the high earth moving costs and the ecological impact.

3. The collector field outer and inner radii were selected to optimize the annual thermal energy per unit mirror area and to accommodate the necessary generating plant structures.

4. Multi-faceted, low-profile focusing heliostats were designed to minimize wind loading effects and the cost per unit area.

Table 3-2. Collector Subsystem Characteristics

	FPS	SI
Field Outer Radius	850 ft	259 M
Field Inner Radius	237 ft	72 M
Number of Heliostats	4968	4968
Individual Heliostat Area	200 ft^2	19 M^2
Total Heliostat Area	941,760 ft^2	87,200 M^2
Peak Thermal Power into Aperture		55 MW
Annual Thermal Energy into Cavity Aperture	6.04×10^{11} BTU	1.77×10^5 MWH
Net Annual Thermal Energy Per Unit Mirror Area		$1.8 \frac{MWH}{M^2}$
Net Peak Power Per Unit Mirror Area (Thermal)		$0.6 \frac{kW}{M^2}$

Pilot Plant Concept

Subsystem Identification

RECEIVER SUBSYSTEM

The receiver subsystem (Table 3-3) was designed to efficiently convert solar energy to thermal energy using a cavity receiver with a full 360-degree annular aperture.

1. The receiver is a right-circular, cylindrical cavity located at the top of a reinforced concrete tower.

2. The cavity aperture subtends 360 degrees to accept solar energy from the entire circular collector field. The aperture was designed to maximize the total annual thermal energy collected.

3. The receiver cavity encloses boiler tubes, drum and superheater tubes. The cavity enclosure minimizes reflection, reradiation and convection losses and protects the steam generator from environmental extremes.

4. Feedwater and high-pressure steam lines provide the links between the steam generator at the top of the tower and other subsystems at grade elevation.

Table 3-3. Receiver Subsystem Characteristics

	FPS	SI
Tower Height	400 ft	122 M
Cavity Diameter	32 ft	10 M
Cavity Height	46 ft	14 M
Steam Generator Housing Height	65 ft	20 M
Steam Generator Housing Diameter	40 ft	12 M
Annulus Aperture Area	857 ft^2	80 M^2
Peak Absorbed Thermal Power		49 MW
Peak Wall Incident Thermal Power Flux	127,000 $\frac{BTU}{hr\text{-}ft^2}$	400 $\frac{kW}{M^2}$
Annual Thermal Energy Absorbed by the Cavity Working Fluid	5.43 x 10^{11} BTU	1.59 x 10^5 MWH

Pilot Plant Concept

Subsystem Identification

THERMAL STORAGE SUBSYSTEM

The thermal storage subsystem (Table 3-4) was designed to provide six hours of storage using eutectic salts in an underground storage unit.

1. The salts for the thermal storage subsystems have been selected because their liquid-solid phase change temperatures will generate steam suitable for the turbine low-pressure admission.

2. The thermal storage unit has been divided into individual cells for improved phase change performance.

3. Each cell will contain one charge cycle heat exchanger and one discharge cycle heat exchanger.

4. One set of cells will generate saturated steam while another set of cells will generate superheated steam.

5. Each cell will be insulated to minimize heat losses.

Table 3-4. Thermal Storage Subsystem Characteristics

	FPS	SI
Thermal Storage Capacity	7×10^8 BTU	200 MWH(t)
Total Quantity of Phase Change Materials ($NaCl$-$NaNO_3$-Na_2SO_4, Na Cl-NaOH)	10×10^6	4.5×10^6 KG
Maximum Thermal Power Input to Storage		49 MW
Maximum Thermal Power Output from Storage		29.8 MW
Net Annual Electrical Energy Produced if Storage is Charged and Discharged Daily		4.15×10^4 MWH
Net Annual Electrical Energy Produced if Storage is Not Used		4.4×10^4 MWH
Outlet Steam Conditions	600 psi/539 F	42 BAR/282°C

Pilot Plant Concept

Subsystem Identification

ELECTRICAL GENERATION SUBSYSTEM

The electrical generation subsystem (Table 3-5) was designed to efficiently transform thermal energy into electrical power using a steam cycle turbine.

1. A dual-pressure admission turbine was selected to generate electricity using either high-pressure receiver steam or lower pressure steam from thermal storage.

2. The turbine generator electrical output rating is 15 MW, 3-phase, 60 Hz, compatible with existing electrical networks.

3. An air-cooled condenser will be selected to convert turbine exhaust steam to condensate because of the expected lack of adequate water resources.

4. Auxiliary equipment required to provide complete power plant capabilities will be selected based on proven conventional design procedures.

Table 3-5. Electrical Generation Subsystem Characteristics

	FPS	SI
Turbine Name Plate Capacity		15,000 kW
Turbine Type	Dual Pressure Admission	
High-Pressure Steam Turbine Inlet Conditions	1450 psi/950°F	100 BAR/510°C
Low-Pressure Steam Turbine Inlet Conditions	575 psi/534°F	40 BAR/280°C
Peak Steam Flow Rate to Turbine Inlet	176,700 lb/hr	80,100 kg/hr

This page intentionally left blank.

Pilot Plant Concept

Subsystem Identification

CONTROLS

The plant controls (Figure 3-4) will be designed to provide centralized subsystem coordination and plant protection based on a philosophy of maximizing utilization of solar energy collected.

1. Plant controls, located in a centralized operating center, will provide coordination of subsystems and their interfaces and provide protection against dangerous operating conditions.

2. Receiver, thermal storage and electrical generation subsystems variables, input to the analog control system, will generate signals which activate subsystem control devices.

3. Limit signals from the analog control system will be input to the heliostat control digital computer. These limit signals, along with the collector subsystem inputs to the heliostat control computer, will send signals to the heliostat positioning devices.

4. Anticipatory signals from the heliostat control computer will be sent to the analog control system which will activate receiver, thermal storage and electrical generation subsystems control devices.

5. The underlying philosophy of the controls system is to utilize solar energy collected most effectively consistent with load demand and subsystem capability.

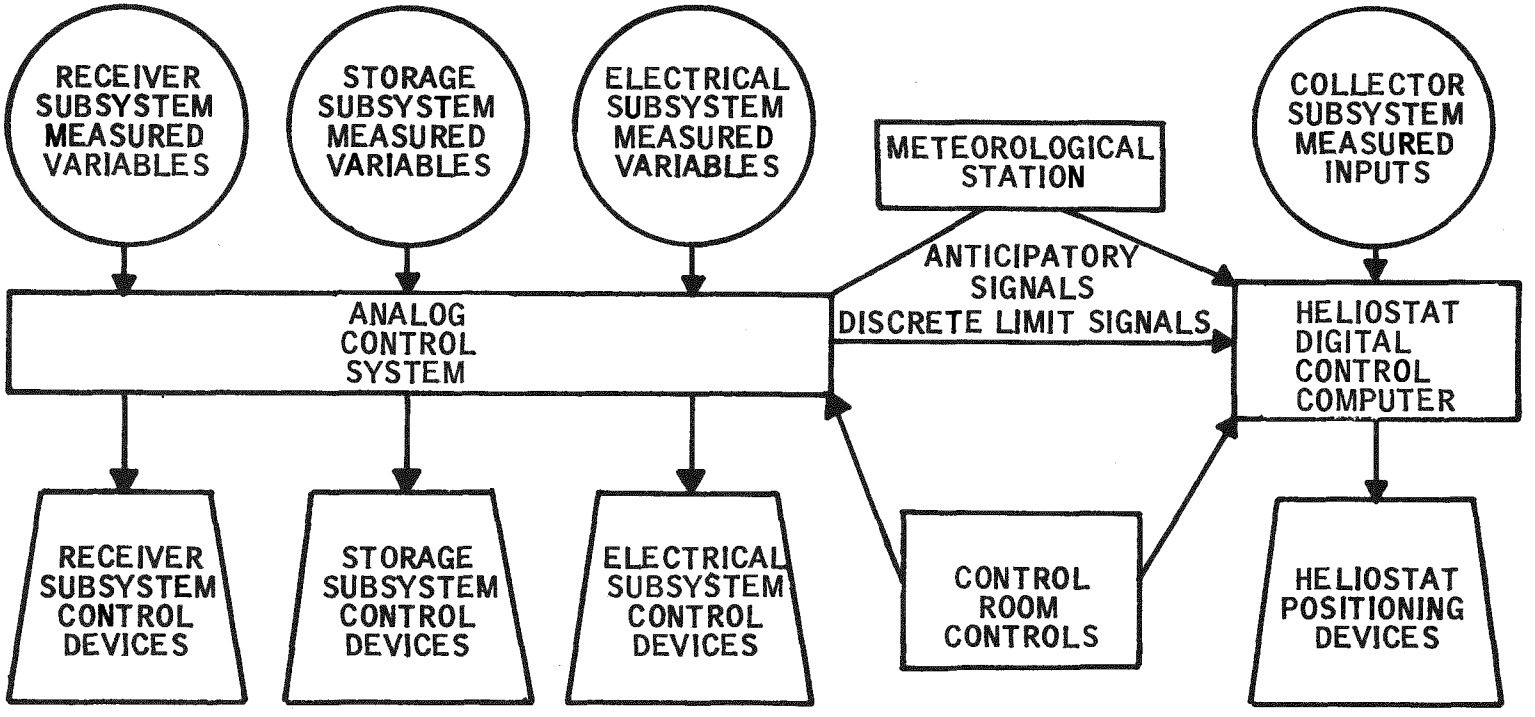


Figure 3-4. Control Coordination of Plant Subsystems

Pilot Plant Concept

Subsystem Interfaces

COLLECTOR SUBSYSTEM INTERFACES

The collector subsystem interfaces with the receiver subsystem, the electrical generation subsystem and the communication/control center.

1. Solar radiation is concentrated and redirected to the receiver subsystem.
2. Electrical power is provided by the electrical generation subsystem for heliostat motors and electronics.
3. Communications and controls signals are received from and sent to the communications/controls center.

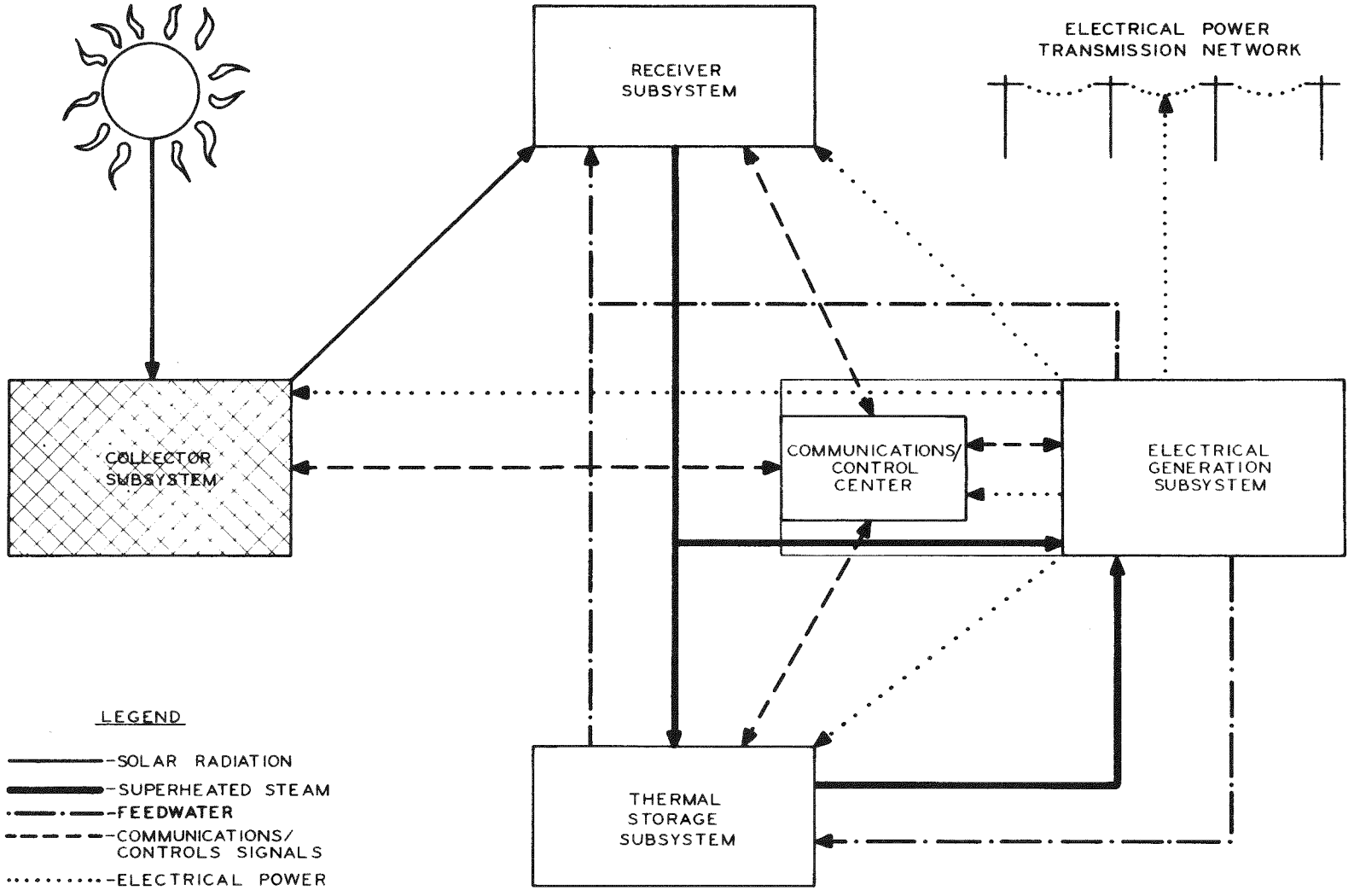


Figure 3-5. Collector Receiver Interface

Pilot Plant Concept

Subsystem Interfaces

RECEIVER SUBSYSTEM INTERFACES

The receiver subsystem interfaces with the collector subsystem, the thermal storage subsystem, the electrical generation subsystem and the communications/controls center.

1. Concentrated solar energy is received from the collector subsystem.
2. Feedwater from the thermal storage subsystem and/or the electrical generation subsystem is pumped to the receiver boiler tubes.
3. Superheated steam from the receiver flows to the electrical generation subsystem and/or to the thermal storage subsystem.
4. Electrical power is provided by the electrical generation subsystem for receiver pumps and electronics.
5. Communications and controls signals are received from and sent to the communications/controls center.

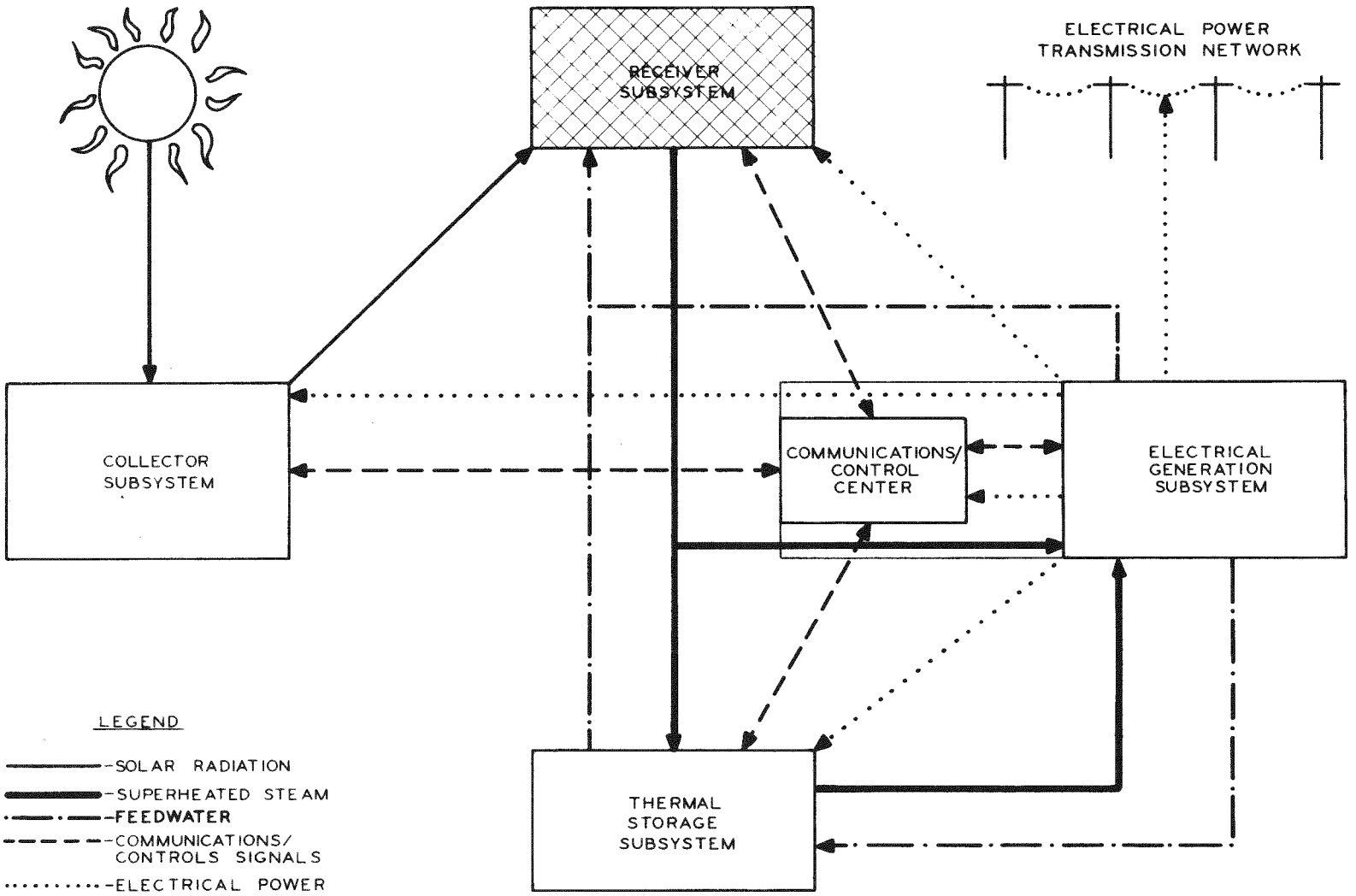


Figure 3-6. Receiver Subsystem Interfaces

Pilot Plant Concept

Subsystem Interfaces

THERMAL STORAGE SUBSYSTEM INTERFACES

The thermal storage subsystem interfaces with the receiver subsystem, the electrical generation subsystem and the communications/controls center.

1. Feedwater from the thermal storage subsystem is pumped to the receiver boiler tubes during the thermal storage charge cycle.

2. Superheated steam from the receiver flows to the thermal storage subsystem during the charge cycle.

3. Superheated steam from the thermal storage subsystem flows to the electrical generation subsystem during the thermal storage discharge cycle.

4. Feedwater from the electrical generation subsystem is pumped to the thermal storage subsystem during the discharge cycle.

5. Electrical power is provided by the electrical generation subsystem for thermal storage pumps, electric heaters and electronics.

6. Communications and controls signals are received from and sent to the communications/controls center.

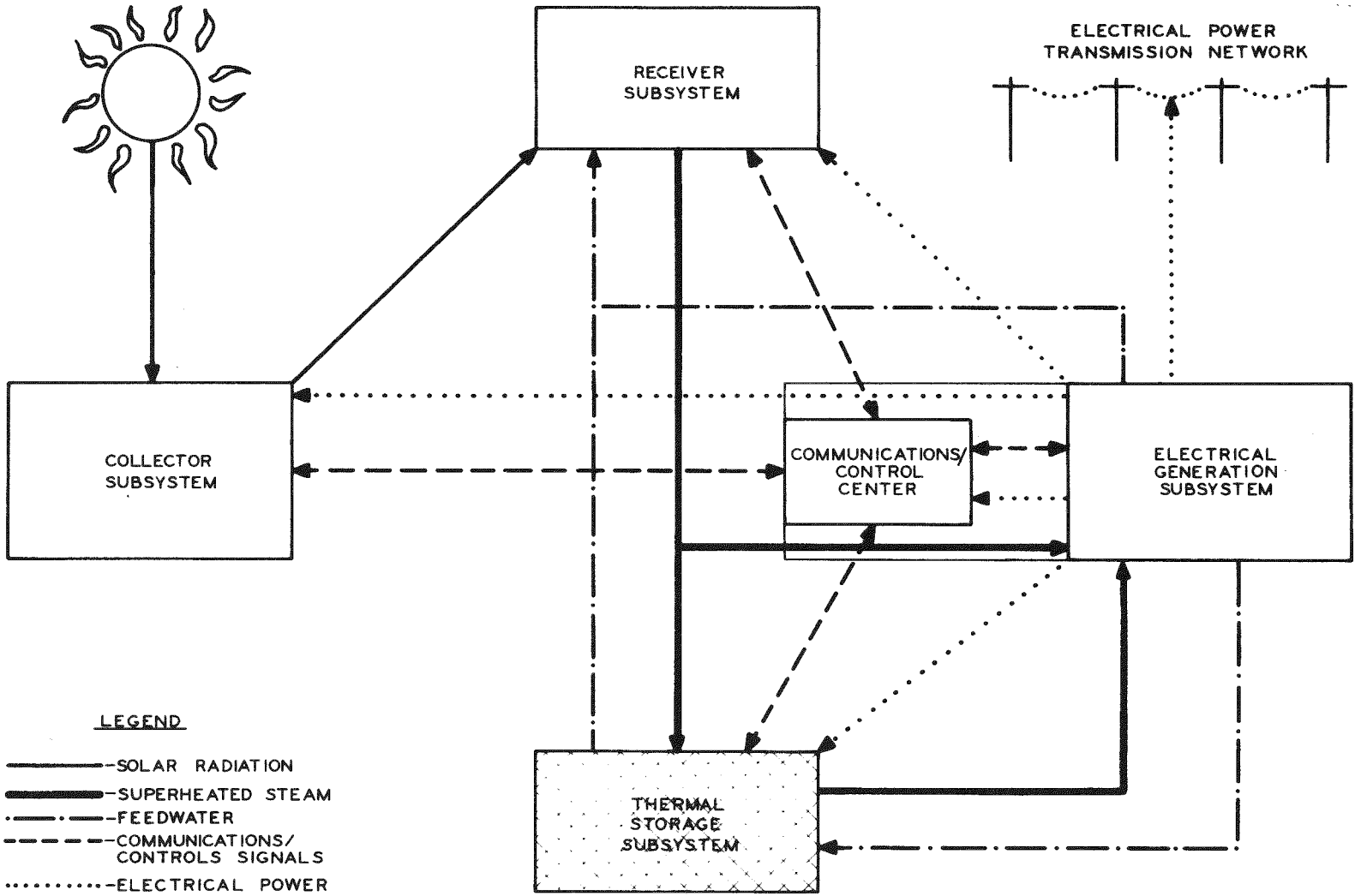


Figure 3-7. Thermal Storage Subsystem Interfaces

Pilot Plant Concept

Subsystem Interface

ELECTRICAL GENERATION SUBSYSTEM INTERFACES

The electrical generation subsystem interfaces with the collector subsystem, the receiver subsystem, the thermal storage subsystem and the communications/controls center.

1. Feedwater from the electrical generation subsystem is pumped to the receiver boiler tubes and/or the thermal storage subsystems.

2. Superheated steam from the receiver and/or thermal storage subsystem flows to the electrical generation subsystem.

3. Electrical power is provided by the electrical generation subsystem to the collector subsystem, the receiver subsystem, the thermal storage subsystem and the communications/controls center in addition to its own internal usage.

4. Communications and controls signals are received from and sent to the communications/controls center.

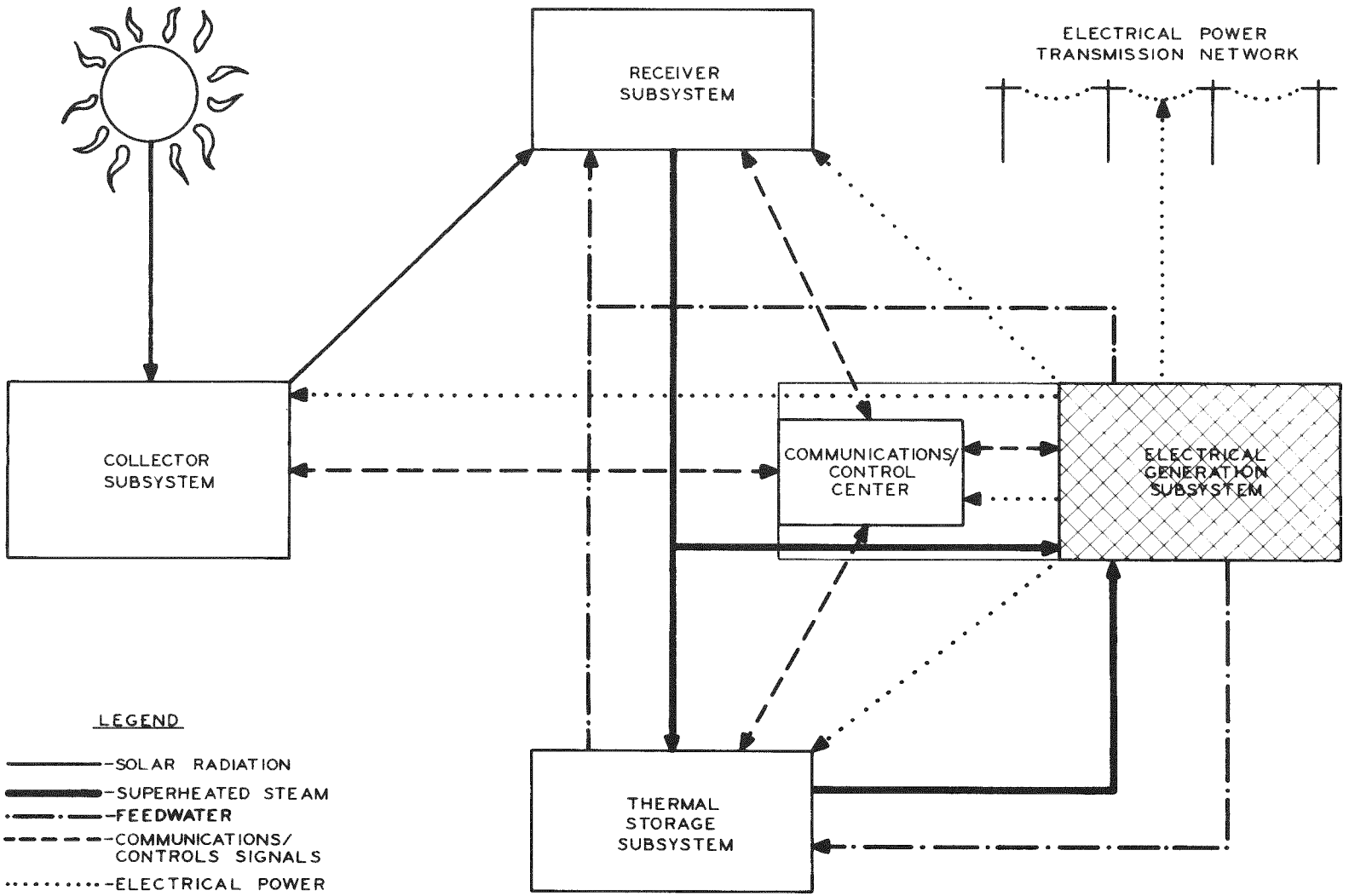


Figure 3-8. Electrical Generation Subsystem Interfaces

Blank

SECTION IV
COLLECTOR SUBSYSTEM

	Page
Program Overview and Derivation of a Baseline Subsystem	4-2
Baseline Subsystem Analysis and Tradeoffs	4-14
Analysis, Tradeoff, and Description of Heliostat Components	4-24
Analysis, Tradeoff, and Description of Power and Control System Components	4-36
Summary Characterization of Concept Design	4-56

Collector Subsystem

Program Overview and Derivation of a Baseline Subsystem

ESTABLISHING APPROPRIATE APPLICATION REQUIREMENTS

The most significant specification is the pointing accuracy with its temperature and wind environments.

The Collector Subsystem has only three interfaces with the power plant:

1. The reflected beam interface at the receiver
2. The central controller command interface with the power plant controller, and
3. The electrical power interface for the central controller and the heliostat field.

The first of these is the primary driver of the Collector Subsystem design. The other two are interface details to be defined during the design.

For pointing accuracies, the proper distribution between pointing requirements and optical requirements is important. Basic difference in off-axis performance between single mirrors and multiple segmented mirrors on individual axes of rotation means the specification is influenced by the concept.

The proposed change in time for return to stowage was based on maximum stepper motor speed at the gear ratios which yield the desired resolution in the tracking mode (0.66 arc-minute mirror normal per motor step). Motor command resolution also relates to Emergency Defocus, so the preferred approach at this time requires a finite time of approximately 12 seconds to move the beam approximately 3 degrees which gets it off the tower.

In the area of modes, the approach to sun location makes acquisition and synthetic tracking modes not applicable. An initialization mode was added to provide a known (0, 0) position for each gimbal from which beam erection starts. Thus, any time a heliostat is out of operation, a means of re-establishing a start position is available.

Table 4-1. Solar Collector Subsystem Requirements

	ITEM	SPECIFICATION	REMARKS
1.	FAR FIELD POINTING, MIRROR NORMALS	1 MR/AXIS, 1	GOAL
2.	OPTICS	1 MR TOTAL, 1	GOAL
3.	REDIRECTED PATTERN (95% WITHIN)	3.1 M X 3.1 M	DERIVED
4.	SURFACE REFLECTANCE (INITIAL)	>80%	
5.	RETURN TO STOWAGE	<12 MINUTES	DERIVED
6.	EMERGENCY DEFOCUS MAX TIME	<12 SEC/3° TRAVEL	DERIVED
7.	MODES ACQUISITION	–	N/A
	OFFSET POINTING	X	
	TRACKING OR FOLLOWING	X	
	SYNTHETIC TRACKING	–	N/A
	EMERGENCY SHUTDOWN	X	
	MANUAL CONTROL SINGLE UNITS	X	
	FAIL SAFE	X	
	RETURN TO STORAGE	X	
	LIMIT CONTROL	X	
	CALIBRATION AND CHECKOUT	X	
	INITIALIZATION	X	DERIVED
8.	TEMPERATURE – OPERATE AND SURVIVE	-20°C TO 60°C	
9.	WIND – OPERATE		
	SUSTAINED	4.5 M/SEC	
	GUSTS	13.5 M/SEC	
	SURVIVE		
	SUSTAINED	25 M/SEC	
	GUSTS	54 M/SEC	

Collector Subsystem

Program Overview and Derivation of a Baseline Subsystem

PERFORMANCE AND ENVIRONMENT DRIVE BASIC FUNCTIONAL DEFINITION AND MODES

The definition of a cost effective, cost competitive, Solar Collector Subsystem is constrained by primary performance requirements which stem from geometry of the problem, physical laws to be obeyed, and the certainty of environmental disturbance.

Expectations of a reasonable plant power output are biased by output levels associated with fossil fuel and nuclear plants, typically hundreds to a thousand megawatts. Due to the vast difference between these power levels and solar energy per unit area, extremely large area Solar Collector Subsystems are required to achieve power outputs in the range of interest. Large areas about a central receiver result in long distances to the farthest reflectors which establish the need for accurate pointing and optical surface contours. Thus, geometry factors create the need for thousands of accurately pointed heliostats positioned about the central receiver over areas as large as a square mile.

The physical laws of optics and reflection, coupled with the apparent daily and yearly motions of the Sun, further require that each reflective segment be accurately and continuously repositioned throughout each day for effective energy transmission.

Large precision pointed optical reflectors are adversely affected by typical outdoor environments such as wind, rain, hail, sand, and temperature variations. True performance requirements must be adjusted substantially to accommodate these unavoidable environmental factors which in turn drive the functional system definition and operating modes.

Coupling the foregoing with the desire for automatic operation of the field leads to the following basic functional definition of a Solar Collector Subsystem:

1. Central Controller - Computer plus Time Standard
   - Computes Sun vectors and commands to collector field.
   - Controls addressing and communication to field.
   - Perform monitoring, housekeeping and calibration.
2. Solar Collector - 5000 heliostat field, each unit containing:
   - 200 ft^2 reflective mirror assembly.
   - 2 gimbal structures, drive motors and mechanisms.
   - 2 initialization switches, 4 limit switches.
   - 1 motor controller, electronics, and power supply.

- 1 battery.
- 1 foundation.

3. Power Distribution System - AC power lines to each heliostat.

4. Communication System - Line drivers, receivers, address and command decoders and signal lines to each heliostat.

5. Calibration Arrays - 12 photocell arrays, 12 zones in field.

Five functional elements which comprise the Solar Collector Subsystem function in the following basic operational modes:

- Initialization - Automatic homing to (0, 0) position.
- Offset Pointing - Startup, shutdown, cloud balancing.
- Tracking - Normal operation.
- Calibration and Checkout - Periodic closed loop check on system.
- Manual Control - As required for maintenance.

The best solution to satisfy these functions is presented in this report.

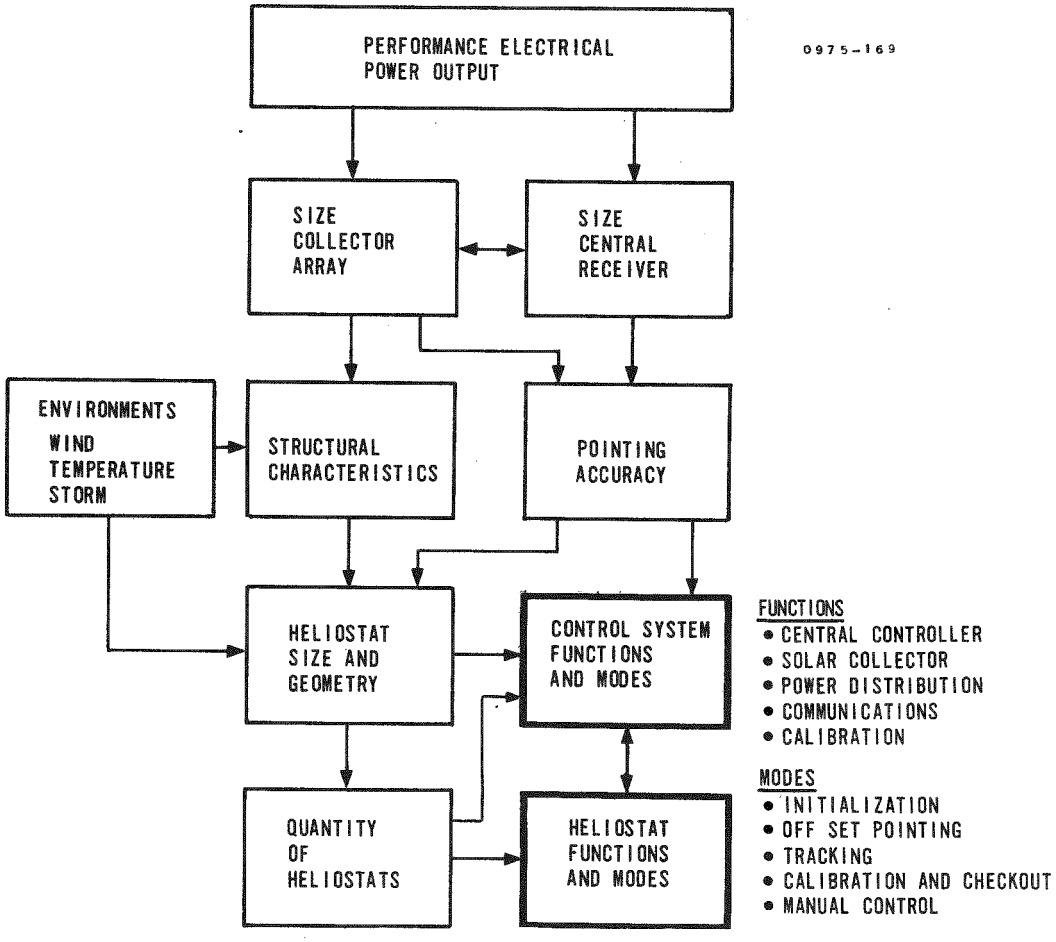


Figure 4-1. Performance and Environments Drive Primary Functional Definition of System and Operating Modes

SAFETY AND MAINTENANCE COSTS DETERMINE SECONDARY PERFORMANCE CHARACTERISTICS

Solar Collector Subsystem definition is further determined by secondary performance requirements which stem from design safety considerations and maintenance operating costs constraints.

Just as the definition of primary performance requirements is driven by power output (size), geometry, and environmental considerations, so the safety and maintenance cost criteria similarly establish additional performance requirements which modify the design definition.

Operational safety design considerations fall into two broad categories. The first is the need to react to major system failures and periodic external environment of stresses in a manner which protects the hardware from damage. This protection is accomplished by four operating modes: Emergency Defocus (protects the receiver), Return to Stowage (storm protection), Limit Control (self-destruction) and Fail-Safe (power loss). The threat of storm damage from wind, rain, hail and sand is met by reducing the heliostat mirror profile to a horizontal position, reflective surface downward.

The second safety category is personnel protection both for operating and maintenance staff as well as outsiders who might become exposed to inadvertently redirected energy. This category of protection is deemed to affect the detail design features of the collector subsystem and will be addressed in the detail design phase.

Life cycle maintenance cost versus plant output considerations, together with the necessity for sure operation of equipment safety critical portions of the Solar Collector Subsystem, establish a systems effectiveness design requirement. Availability is the measure of effectiveness of the reliability and maintainability features of the design. To achieve sufficient confidence that reasonable operational availability goals can be met, Honeywell has established a functional partitioning and redundance scheme for the stat power elements together with multiple partitioning of the signal and power distribution system. The product reliability and serviceability characteristics of the design directly impact plant operating costs and will be addressed in the detail design.

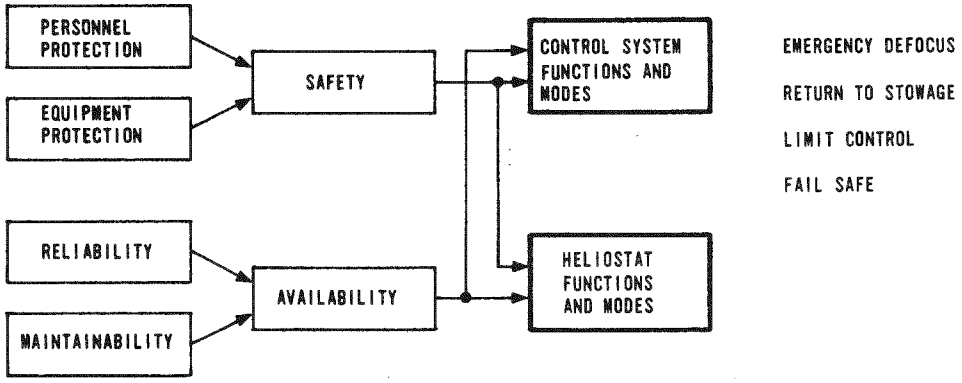


Figure 4-2. Secondary Performance Characteristics of the Solar Collector Subsystem are Established by Safety and Availability Factors

Collector Subsystem

Program Overview and Derivation of a Baseline System

HIGHLIGHTS OF SOLAR COLLECTOR SUBSYSTEM CONCEPT DESIGN

A low profile heliostat, under continuous control by the central processor, with calibration and recovery capability, is the best Solar Collector Subsystem design to satisfy the requirements.

The subsystem requirements for the heliostats have been defined and a conceptual design has been identified which will meet those requirements. This design concept is the end product of many detailed tradeoffs which show a cost effective design, a simple installation, a flexible operational control, and a reliable subsystem.

Some of the more significant concepts which are a basis for this study are:

1. Computed Sun tracking and calculation of heliostat commands based on line-of-sight vectors to the Sun and to the tower.

2. Low profile, 2-axis gimbaled heliostats.

3. Commands to two motors at each heliostat, issued from the central controller.

4. Periodic heliostat calibration, using the Sun, heliostat, and a target array on the tower near the receiver.

5. Continuous central control of heliostats for flexibility of power plant operation.

Some of the more significant tradeoff results are:

1. Selection of a tilt-tilt gimbal configuration for simple installation, minimum command rates and minimum power consumption.

2. Use of two pulse rates for the heliostat stepper motor controller which has communication and power loss detectors for failsafe operation.

3. Use of common hi-voltage a-c power distribution system, with step-down transformers to bring power to sectors of heliostats.

4. Local battery at each heliostat, trickle charged, to guarantee failsafe operation in the event of power failure.

5. Hard line serial data simplex communication link to carry computer commands to the individual heliostats.

6. Real-time command and control computations to improve pointing accuracy and maintain positive system control.

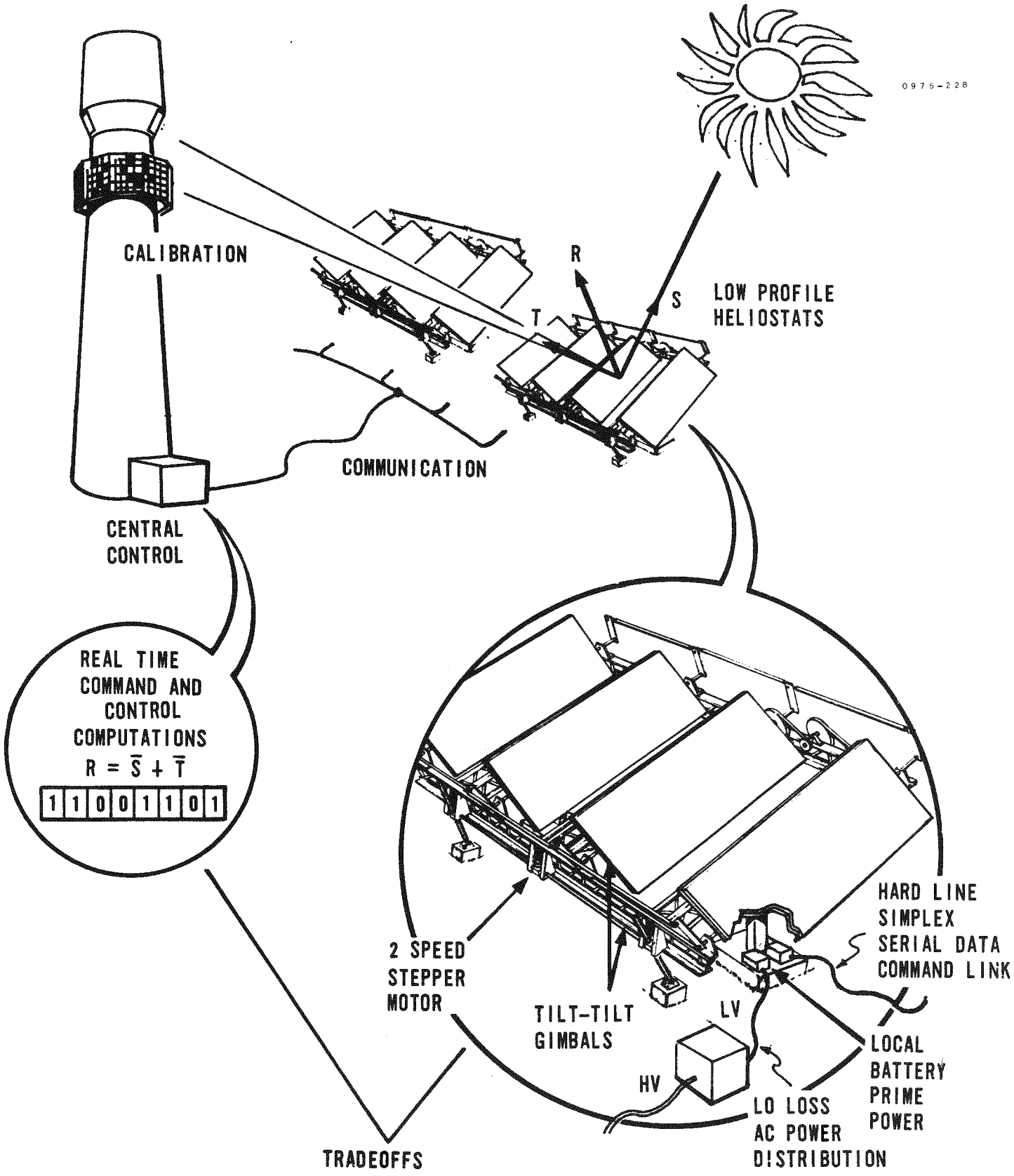


Figure 4-3. Solar Collector Subsystem Fundamental Characteristics and Concept Tradeoffs

APPORTIONMENT OF TRACKING ERRORS

An Error Budget must relate to the specifications, but it can be developed only after the concept is established so that the budget of error allocations is meaningful.

The tentative budgeting of errors during the concept phase is based on the premise that error sources that can be controlled must be. This leaves maximum margin for those error sources driven by environment which is less amenable to accurate prediction. It is also based on the premise that maximum cost effectiveness will be achieved by minimizing the structural stiffness requirements of each heliostat due to the massive cost leverage exerted by the large quantities involved. Hence, computational budgets have been held rather tightly and those associated with individual heliostat structures and drive systems have been allotted the greater share.

Probable error sources associated with the budget items are listed below. This list will be adjusted as necessary during the detailed design.

- Computation Sun Vector
  - Time Standard
  - Temperature Input
  - Pressure Input
  - Algorithm Accuracy
  - LSB Limitations
- Computation Mirror Normal
  - Heliostat LOS Inputs
- Computation Axis Commands
  - Residual Calibration Error
  - Residual Drive Train Scale Factor Error
- Delivery Commands to Motor Controller
  - Δ Time delivered versus time for which computed
- Foundation
  - Initial Installation
  - Residual Stability
- Heliostat
  - (0, 0) Gimbal Initialization
    - Initial Switch Alignment Errors
    - Repeatability
- Heliostat (Continued)
  - Motor and Drive System
    - Gear Train Backlash
    - Min Resolution/Step
    - Deviation from Nominal Drive Scale Factors
    - Initial Alignment Residual
    - Δ Wind Deflections
  - Mirror Support Structure
    - Initial Alignment
    - Δ "g" Vector Changes
    - Thermal Effects
    - Δ Wind Deflections
- Boresight Normal
  - Basic Pointing Accuracy at RSS
- Non-Boresight Normals
  - Cross Axis Coupling - conservatively taken as additive
- Optics
  - Residual Focus Misalignment
  - Initial Alignment to Structure
  - Thermal Changes
  - Δ "g" Changes
  - Δ Wind Deflections
  - Aberrations - mirror quality - Δ focus

Table 4-2. Collector Subsystem - Error Budget

SPECIFICATION

MIRROR NORMAL POINTING	±1 MR 1σ EACH AXIS
OPTICS ONLY	±1 MR 1σ TOTAL
HENCE, ASSUMING NORMAL DISTRIBUTION, 3σ	= ±3 MR

0975-259

BUDGET

SOURCE	EACH AXIS		
COMPUTATION AND COMMUNICATION			
COMPUTATION SUN VECTOR	±0.15		
COMPUTATION MIRROR NORMAL	±0.3		
COMPUTATION COMMANDS	±0.15		
DELIVERY COMMANDS TO MOTOR CONT	±0.15		
	SUBTOTAL ±0.4 RSS		
FOUNDATION			
RESIDUAL MISALIGNMENT	±0.14		
UNCOMPENSATED DRIFT RATE	±0.14		
	SUBTOTAL ±0.2 RSS		
HELIOSTAT			
(0.0) GIMBAL INITIALIZATION	±0.3		
MOTOR AND DRIVE SYSTEM	±1.2		
MIRROR SUPPORT STRUCTURE	±1.2		
	SUBTOTAL ±1.7 RSS		
BORESIGHT MIRROR NORMAL		TOTAL	±1.76 RSS
NONBORESIGHT MIRROR NORMAL		TOTAL	±1.24 ADDITIVE
MIRROR NORMAL POINTING BUDGET	GRAND	TOTAL	±3 MR 3σ
OPTICS (ONLY)		TOTAL	±3 MR 3σ

Collector Subsystem

Program Overview and Derivation of a Baseline Subsystem

COST SENSITIVITIES

A preliminary cost estimate for the pilot plant scale is necessary to serve as an aide to setting work priorities, expediting the tradeoff process, and identifying outstanding cost problem areas.

The basic ground rules for this costing exercise were to identify component cost for the configurations under consideration. Estimates were developed for cost-of-ownership over a 30-year operational life in addition to the acquisition cost. Estimates were developed at various levels of concept definition dependent upon tradeoff progress to that point in time. Specific part identification was sought whenever component cost was deemed significant.

The resulting heliostat cost apportionment depicts the major component cost for the tilt-tilt configuration. The major cost elements for this configuration varied little from other configurations when expressed as a percent of the heliostat cost. The mirror module developing 20.7 percent of the heliostat cost has as major cost elements 200 square feet of aluminum honeycomb in addition to the steel enclosure and axle assembly. These items constitute over 85 percent of the mirror module cost. The mirror module drive, adding 19.1 percent, attributes most of its cost to a speed reducer, sprockets and steel costs. The outer gimbal cost is represented in steel costs, while its drive assembly costs are primarily due to ball screw and bellows assemblies. Specific costs and cost comparisons are presented with the storyboard titled Selection of Heliostat Configuration.

Cost-of-ownership figures were developed for the power distribution system and for the processors and peripheral equipment. These figures provide for battery replacement at nominal periods considering the half-life effect of operation in an ambient +20°F above room temperature; or 3.5 battery changes over 30 years of operation. Cost associated with the processors and peripheral equipment is standard for the equipment.

Cost apportionment for major components was a basis for determining the application of tradeoff studies. Elements with cost exceeding 3.0 percent of the total heliostat cost required further investigation.

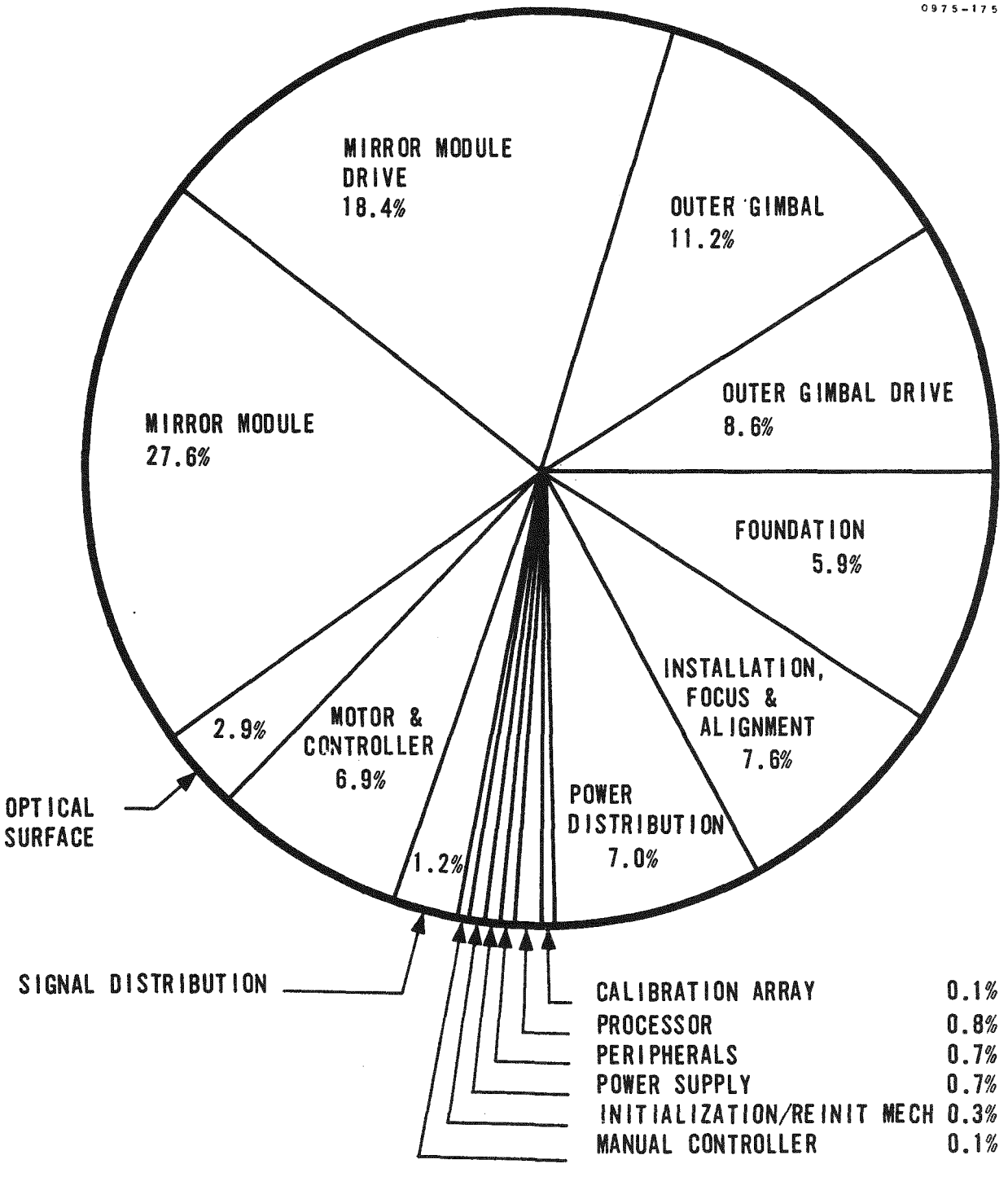


Figure 4-4. Cost Apportionment Percent of 200 Ft^2 Tilt-Tilt Heliostat Cost

Collector Subsystem

Baseline Subsystem Analysis and Tradeoffs

CHARACTERIZATION OF HELIOSTAT CONFIGURATION

A tilt-tilt configuration and an azimuth-elevation configuration are the best candidates for detail consideration, analysis, and tradeoff.

There are subsystem considerations that affect the configuration selection:

- Influence on Heliostat Design
- Optical Efficiency
- Tracking Rates
- Influence on Control System Design
- Pointing Accuracy
- Operation Ease

These are discussed in this section. Other considerations of various components are discussed in the next section.

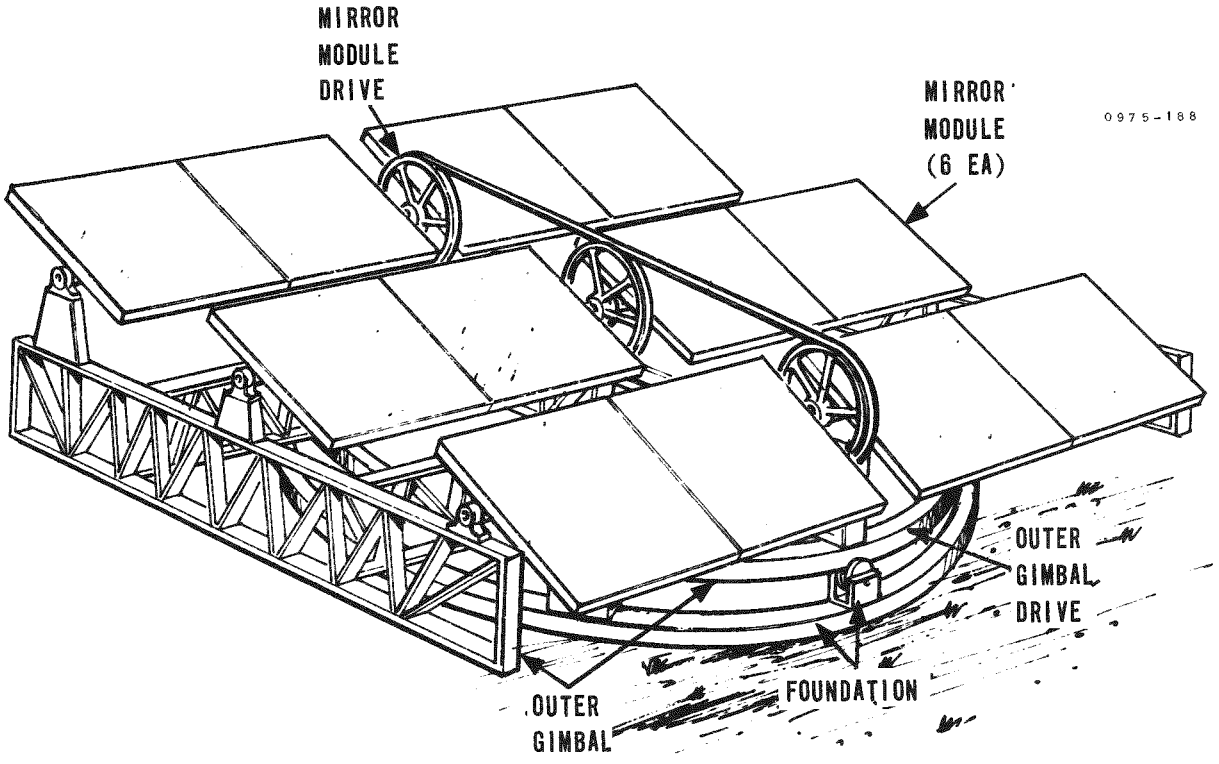


Figure 4-5. Az-El Configuration

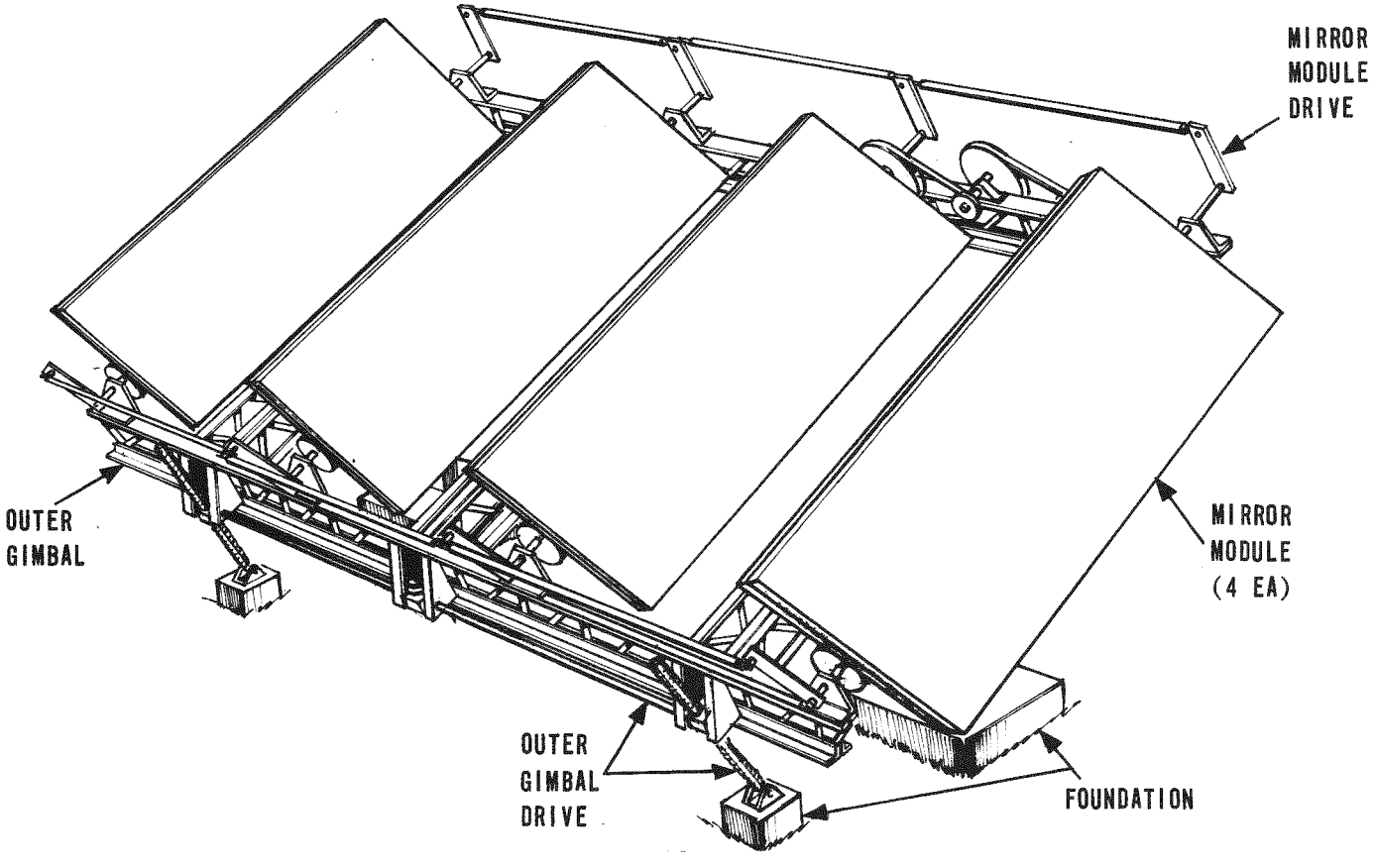


Figure 4-6. Tilt-Tilt Configuration

Collector Subsystem

Baseline Subsystem Analysis and Tradeoffs

AXIS SELECTION INFLUENCE ON HELIOSTAT AND CONTROL SYSTEM DESIGN

The tilt-tilt gimbal configuration provides the highest probability of success in designing to meet performance requirements because fewer parts in the foundation, frame and drive systems mean less assembly and alignment effort and fewer sources of pointing error.

Gimbal axis selection affects many elements of the heliostat design. Since initial cost estimates of the two basic gimbal concepts show little difference, the criteria then center on the probability of success of meeting design requirements with each approach. Tradeoffs for each of the five major heliostat elements show a strong total advantage for tilt-tilt.

Foundation -- The support of the heliostat has been reduced from six small support wheels and a center support to two steel posts. With the exception of one-time adjustments at the top of each post, there are no moving parts. Field survey and layout effort has also been reduced. The use of dual column support makes foundation costs less sensitive to local variations in ground level since the height of posts is easily varied.

Outer Gimbal Drive -- This part of the heliostat benefits the most from the tilt-tilt selection. Two angular contact bearings now perform the function of six support wheels, a center support, an 18-foot diameter precision ring and a takeup mechanism. Because of its large moment arm, the support ring/wheel interface in the azimuth/pitch configuration is susceptible to dirt on wheels or ring, dimensional variations and wildlife. Selection of the ball screw drive was made possible by the tilt-tilt heliostat and eliminates the need for spring loaded take-up mechanisms. Location of this drive at the outer edge of the frame simplifies both installation and maintenance. The lower inertial load and stiffer drive system reduce motor power and reduce pointing errors under wind load.

Outer Gimbal -- Shipping, handling and alignment are heavily influenced by frame size. The tilt-tilt frame is welded as a complete unit approximately 11 by 22 feet and is easily shipped by truck or rail. Precision alignment of two frame halves at the plant site is eliminated and the number of pieces is reduced from nine to five. The dual ball screw drive also eliminates the need for designing torsional stiffeners into this frame assembly.

Mirror Module Drive -- Relocation of the mirror drive system (inner gimbal) from the center of the heliostat to the outside allows easier access for assembly, alignment and maintenance. Workmen do not have to climb into or under the heliostat to the extent required for the azimuth/pitch configuration. Flex couplings and the associated alignment are eliminated. Toe-in adjustment of mirror modules is a less likely requirement for the tilt-tilt heliostat.

Mirror Module (MM) -- Potential cost savings exist here if mirror module toe-in can be eliminated in production heliostats. Toe-in is defined as rotation of the mirror surface about an axis through its center and parallel to the outer gimbal axis. Since the MM axes must remain coplanar and parallel, the toe-in adjustment requires movement of the mirror with respect to the MM axle and all the associated labor and hardware. The same hardware is also used to adjust focal length of the mirror module, however, so a constant focal length MM is implied.

Because of geometry constraints in the layout of the field, azimuth/tilt heliostats need to be as nearly square as possible. For heliostat sizes currently within optics and wind load constraints, the mirror module sizes are smaller on Az/El and increase the amount of alignment time required per square foot of mirror. The tilt-tilt allows the use of 5 by 10-foot mirror modules while Az/El modules are 4 by 8 feet.

0775-177

TILT-TILT IS BEST FOR HELIOSTAT DESIGN BECAUSE

- Foundation assembly has no moving parts and fewer adjustments
- Outer gimbal drive has no preload mechanism and predictable error sources
- Gimbal frame has five pieces instead of nine
- Mirror module drives are located on outside for easy access
- Four mirror modules are used instead of six

Axis Selection Influence on Heliostat Design

Collector Subsystem

Baseline Subsystem Analysis and Tradeoffs

TILT-TILT CONFIGURATION ELIMINATES ENERGY LOSS

Gimbal lock, inherent with azimuth-elevation gimbaling, is avoided with tilt-tilt gimbals, thereby eliminating energy loss in a rate limited system.

Significant loss of energy and potential damage to the receiver can occur with a rate-limited gimbal system. An average of 4 percent of the heliostats in the field cannot maintain track with a 40 deg/hr rate capability with the azimuth-elevation (Az-El) configuration. In contrast, the tilt-tilt gimbaling is able to maintain track at all times so that no loss of energy or receiver damage can occur with the same 40 deg/hr track rate capability. The yearly average percent of heliostats unable to maintain the Sun's energy on the target is plotted as a function of gimbal tracking rate limitation in Figure 4-7a.

Gimbal lock occurs for Az-El gimbals when the mirror normal becomes aligned with the outer gimbal axis. When this happens, complete loss of freedom occurs about the normal to mirror axis that is also normal to the elevation axis. This occurs when the horizontal components of the unit tower and sun vectors are equal in magnitude and opposite in sign. Locked heliostat location is shown in Figure 4-7b.

The azimuth gimbal rate requirement is proportional to the tangent of the elevation gimbal angle (α). For ω_1, ω_2, ω_3 equal to the east north and vertical components of mirror normal angular rate, the azimuth gimbal rate ($\dot{\psi}$) is: $\dot{\psi} = \tan\alpha(\omega_1 \cos\psi - \omega_2 \sin\psi) - \omega_3$. For a particular time, lines of constant required gimbal rates can be drawn across the heliostat field. A typical plot of required gimbal angle rates is shown in Figure 4-7c.

Tilt-tilt avoids gimbal lock by replacing the outer vertical axis with a horizontal one. With the outer axis (ϕ) oriented east-west, the outer axis command rate becomes $\dot{\phi} = \tan\theta\,(\omega_2 S\phi - \omega_3 C\phi) - \omega_1$ where θ is the inner axis angle. The large reduction in rate requirements comes about because θ does not reach 90 degrees as did α in the Az-El configuration. A typical plot of $\dot{\phi}$ is shown in Figure 4-7d. Comparing this with Figure 4-7c illustrates the significant reduction in rate requirements achieved with the tilt-tilt configuration. The highest $\dot{\phi}$ of 23 deg/hr occurred at sunrise of the summer solstice.

The proportion of the field unable to maintain track at one time point was computed for Az-El by determining the areas bounded by the rate capability and/or the heliostat field, and dividing by the area of the field. The yearly average was calculated by averaging the above over time of day and time of year for a particular rate limit. The average unavailable heliostats are plotted against rate limits in Figure 4-7a. Since the tilt-tilt command rate never exceeds the 40 deg/hr capability, the availability for tilt-tilt is 100 percent.

Details of the drive rate analysis are included in Appendix A.

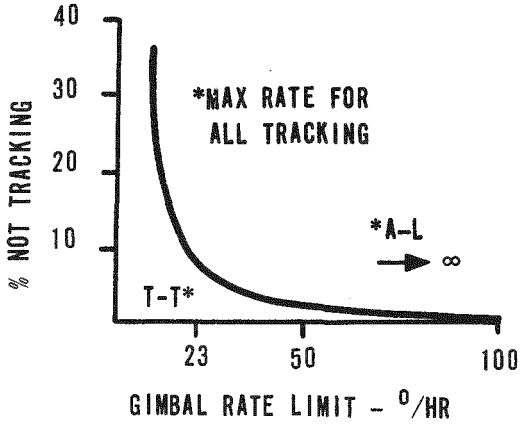


Figure A. Rate Limit Lowers Az-El Efficiency

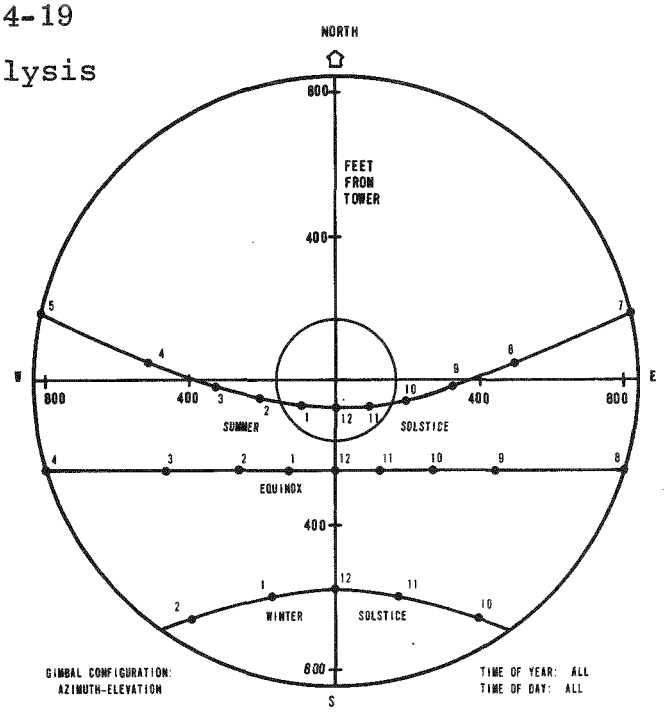


Figure B. Gimbal Lock Position

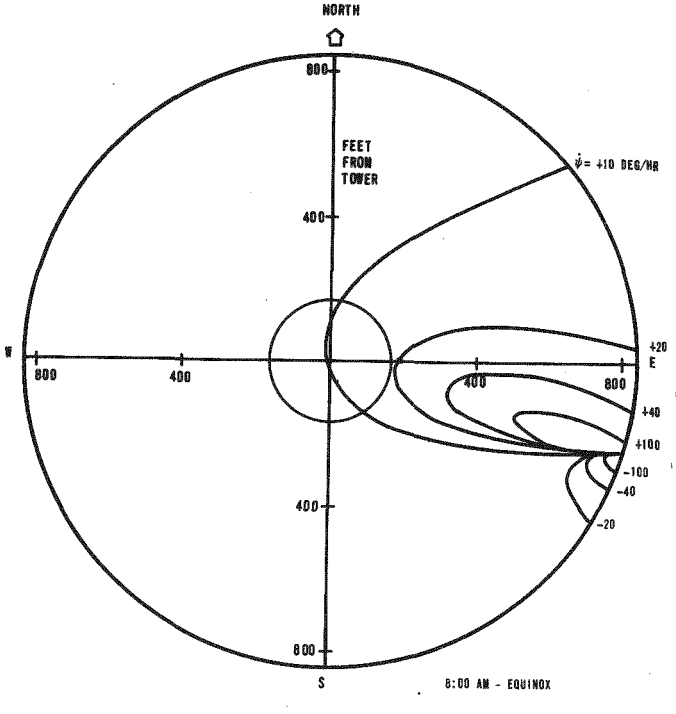


Figure C. Az-El Gimbal Command Rates

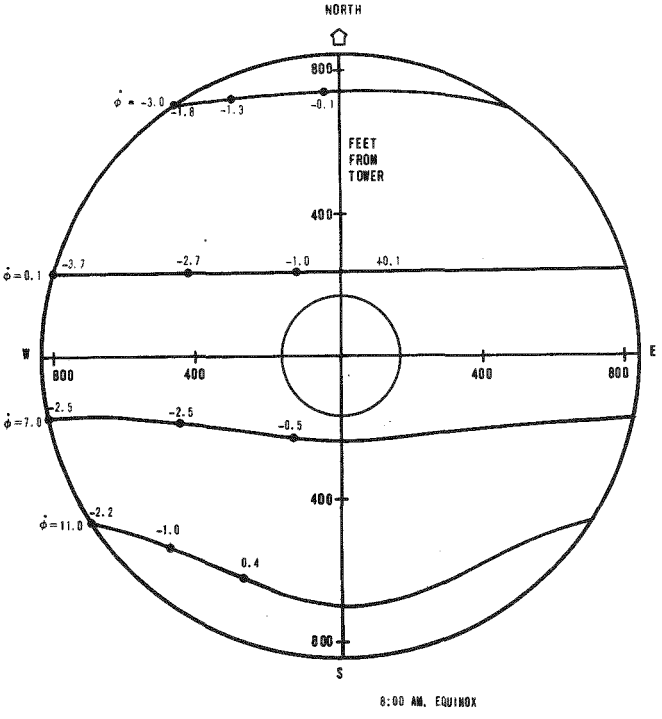


Figure D. Tilt-Tilt Gimbal Command Rates

Figure 4-7. Gimbal Tracking Rate Limitation

Collector Subsystem

Baseline Subsystem Analysis and Tradeoffs

AXIS SELECTION INFLUENCE ON CONTROL SYSTEM DESIGN

The choice of heliostat axis has a major impact on computation and communication rates, and on heliostat electronics design.

An azimuth-elevation gimbal configuration requires command rates five times larger than the tilt-tilt configuration. This is because of the gimbal lock condition experienced by about 45 percent of the heliostat field. To meet these higher rate demands, computation and communication rates would have to be increased proportionally to maintain the same degree of command resolution. Failure to do so would result in those heliostats in the lock condition drifting off the receiver for short periods of time which may be significant. The only other alternative is significantly increasing the command quantization value of 40 arc-seconds. This is unacceptable from a pointing accuracy standpoint.

Computation rate increases forced by the azimuth-elevation configuration place high-speed requirements on the processor for any given number of heliostats. This means that more computers would be needed to handle the same number of heliostats in a given field. A non-real-time solution would have to be invoked to reduce the number of computers at the expense of increased mass storage devices. Non-real-time means that all tracking commands are computed the night before, stored away, and then simply metered out the next day. That solution does not make use of the current temperature and pressure data, nor of the up-to-the-minute calibration data on the individual heliostat.

The tilt-tilt configuration yields significantly lower inertias for both gimbals particularly in the outer axis. Comparing both concepts, the inertia of the outer axis for the tilt-tilt version is lower by a factor of 8.4 resulting in a reduction of the reflected inertia to the drive motor of 8.4. This advantage can be used to reduce the drive gear ratio which in the case of the Az-El configuration was determined primarily from inertial load drive requirements rather than resolution requirements. By reducing the outer axis gear ratio by a factor of four, the following results:

1. The gear ratios for both axes can be made the same.
2. The power to drive the gimbal a given amount is reduced by a factor of 4.
3. The gimbal can be made to slew 4 times as fast.
4. The Motor Controller Electronics assemblies can be made identical.

While the inner axis inertia for the tilt-tilt configuration is one-half that of the other, no further reduction in gear ratio can be made because of resolution requirements. However, the reduction in reflected inertia will allow that gimbal to be slewed at a higher rate which is desirable in that axis in an emergency situation.

Also, by eliminating the gimbal lock condition mentioned above which is associated with Az-El configuration, the power required to do a gimbal flip maneuver in the outer axis to maintain tracking is saved.

	AZ/EL	Tilt/Tilt
Command Rates		+
Gimbal Lock	-	
Computation Rates		+
Inner Axis Inertia		+
Outer Axis Inertia		++
Driver Power		+
Slew Capability		+

Axis Selection Influence on Control System Design

Collector Subsystem

Baseline Subsystem Analysis and Tradeoffs

SELECTION OF HELIOSTAT CONFIGURATION

Based on the subsystem considerations discussed previously, plus the advantages presented here, the best choice, low profile heliostat, is a tilt-tilt configuration.

There are many advantages of a tilt-tilt configuration related to design features. All of these can be quantified but it is also reasonable to consider the inherent advantages in this summary.

TILT-TILT ADVANTAGES

Foundation
- Less adjustment required.
- No moving parts.

Outer Drive
- 8:1 reduction in inertial.
- Less torque required to overcome pressure center movements.
- No 400 lb preload required.
- No takeup mechanism required.
- Lower friction to overcome.
- Less susceptible to hang-up from contamination or irregularities on track or wheel.
- Higher resonant frequency.
- Rigid center control.
- Rigid radius arm control (no ring runout).
- No ring sag to overcome (that is; climb up)
- No high rates required during gimbal flip.
- Can initialize to local vertical.
- Very small overnight return angle.
- Lower annual motor drive energy required.

Outer Gimbal
- Single welded frame instead of two-piece assembly.

Mirror Module Drive
- Lower total wind load and, therefore, lower K_T.
- No center flex couplings.
- No adjust between end-to-end axles.
- Easy access to drive and adjustments.
- Less wind-up in Mirror Modules with crank arm drive.

Mirror Modules
- No toe-in adjustment.
- No stair stepping.

Operational Considerations
- Allows more flexibility in field layout.
- More commonality in heliostats.
- Smaller, lighter unit to ship and maintain.
- Smaller average excursion required for initialization.
- Safety improved because workmen do not have to climb into center of heliostat or work with 400-lb preload on takeup.
- Easier to maintain with improved access to both inner and outer drive systems.

Table 4-3. Gimbal Order Comparison

0975-218

	TILT-TILT	AZ/EL
ENERGY LOSS VERSUS DRIVE RATE	0% LOSS AT 23°/HR	4% LOSS AT 40°/HR
HELIOSTAT DESIGN		
FOUNDATION	NO MOVING PARTS	ADJUSTMENT OF SIX SUPPORT WHEELS
OUTER GIMBAL DRIVE	NO PRELOAD AND PREDICTABLE ERROR SOURCES	PRECISION 18 FOOT RING
OUTER GIMBAL	FIVE PIECES	NINE PIECES
MIRROR MODULE DRIVE	LOCATED OUTSIDE OF STRUCTURE	FLEX COUPLINGS
MIRROR MODULES	FOUR EACH 5 X 10 FEET	SIX EACH 4 X 8 FEET WITH TOE-IN ADJUSTMENT
CONTROL SYSTEM DESIGN		
GIMBAL LOCK	NO	YES
OUTER GIMBAL INERTIA	ONE UNIT	EIGHT UNITS
COMPUTATIONAL RATES	LESS	–
DRIVE POWER	–	MORE
OPTICAL EFFICIENCY	≈5 TO 10% GREATER NET ANNUAL ENERGY (GC = 0.45)	–
OPERATIONAL EASE		
FIELD LAYOUT	MORE FLEXIBLE	HEX CLOSE PACK
SAFETY	–	400 LB PRELOAD ON TAKE-up
MAINTAINABLE	BETTER ACCESS	–
POINTING ACCURACY	–	ROUGHLY EQUAL
COST	SLIGHTLY LESS	SLIGHTLY MORE

Collector Subsystem

Analysis, Tradeoff, and Description of Heliostat Components

SITE INFLUENCE ON FOUNDATION DESIGN

Local soil conditions influence foundation design with stiffness against wind load a primary concern.

Stiffness against wind loads and stability over temperature range are the controlling criteria in foundation design. Deflections of the gimbal supports must be held to 0.050 inch to keep pointing errors within 0.5 milliradian under 30 mph wind loads. Frost heave must be avoided to prevent errors due to support height variations. Life, initial alignment and dynamic response are secondary requirements.

Steel trunnions, cedar posts and reinforced concrete posts were among those considered. Deep driven piles were also traded against concrete foundations for obtaining the required stiffness at the soil interface.

Trunnions were dismissed because of the gimbal interface. The support must reach up into the box frame structure to the center of gravity of the gimbal without limiting angular travel. Wooden posts have a low modulus (1/15 of steel) and require special consideration to handle high local stresses at the gimbal interface. Concrete posts require extensive steel reinforcement to obtain the required stiffness within the size limitations but remain a "first" alternate concept. Driven piles have two disadvantages: one is dimensional control to assure fit to the gimbal frame. The second is the small soil bearing area per unit length; concrete is required to spread the stresses over a larger bearing area.

The foundation concept shown in the illustration provides a low-cost installation with adaptability to local soil and terrain conditions. The steel post is sized to provide the cantilever stiffness required against operational wind loads. The 6-inch by 10-inch steel tube is sized for the worst case where the outer gimbal is at its highest angle. This condition results in a longer cantilever and at the same time greater dependence on the tube to control pointing accuracy. As the elevation angle decreases, the tube can be shortened and made smaller. Variations in post height are easily used to vary heliostat height in different areas of the field as well as compensate for local variations in ground level.

The size of the concrete support depends on local soil conditions. Sample calculations for the four-foot-square slab show it will limit tilt under 30 mph winds to 0.1 milliradian for the concept heliostat. This is based on a shear modulus of 3000 psi, a typical test value for the sandy soil at Honeywell's Florida facility. Tests of each plant location will be required to assure the modulus is adequate. Other soil characteristics which affect foundation design are frost penetration and bearing load capacity. The foundation base must be below the frost line to prevent frost heave. Inyokern frost depth is only three to six inches and always allows the 12-inch slab to sit flush or slightly above ground level.

Pointing errors due to vertical bearing loads and spring rates are insignificant since the slab was sized for stiffness against tilting using a large bearing area.

The steel post is set and aligned prior to processing concrete to lock it in. The reinforcing rods can be welded to the tube if additional support is necessary.

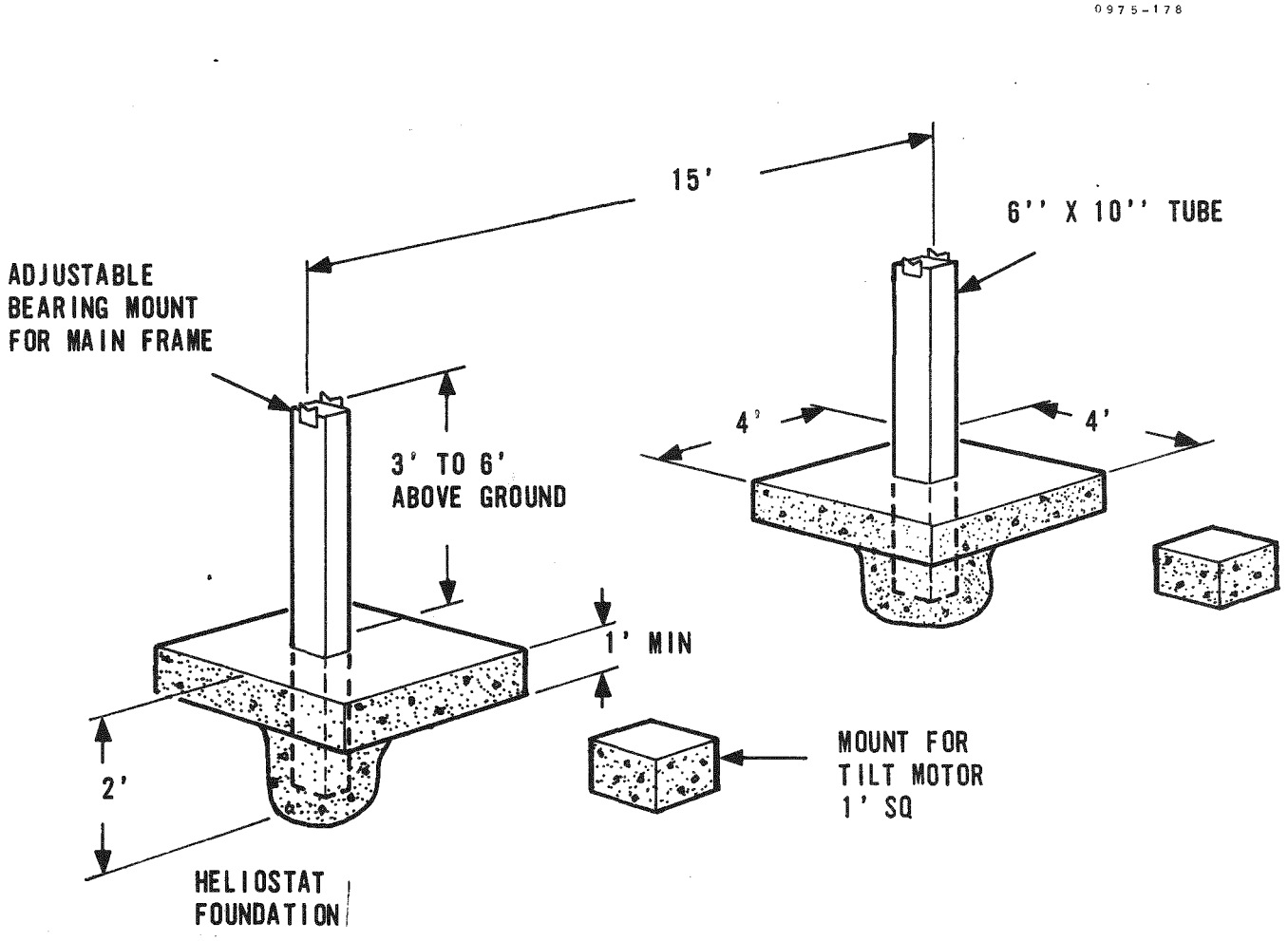


Figure 4-8. Foundation

Collector Subsystem

Analysis, Tradeoff, and Description of Heliostat Components

POINTING ACCURACY GOVERNS OUTER SIGNAL DRIVE SELECTION

A rugged outer gimbal drive is required to maintain pointing accuracy under environmental conditions.

The requirements for this drive system clearly show pointing accuracy to be the design driver. This is because so many different aspects contribute to pointing errors. These include:

- Resolution (determined by total reduction ratio).
- Backlash of drive components and connections.
- Windup (distortion under moments created by wind loads and gimbal imbalance.)
- Initial alignment.
- Differential thermal expansion.

These requirements indicate the need for a tight rigid drive system with good wear characteristics.

Candidate drive systems considered included axis-mounted gear drives, timing chains with spring loaded takeup, large diameter gear and sprocket segments, and ball screws.

Gear-mounted drives, that is, worm reducers, capable of handling the torque (775 ft-lbs at 30 mph wind) are large and expensive ($600) and can control backlash only through axial preloading of the output shaft which increases wear. Chains and belts were discarded because of the high spring rates required on idlers to resist wind moments. Large diameter gear and sprocket segments added inertia which increases motor power and reduces motor life. Another important consideration is the twisting of the outer gimbal frame about the roll axis. Providing torsional stiffness with adequate mirror module clearance and minimum inertia is a difficult design task. The advantages of a synchronous pair of drivers become obvious.

A pair of ball screws driven by a common motor/reducer set now appears the best tradeoff for meeting the design requirements.

The illustration shows the drive concept with the ball screws in line with the gimbal bearings. Structural deflections of importance are now limited to bending modes which are easily controlled with bar joist construction.

The ball screw drive is aligned differently for each heliostat (or group of heliostats) so that the screw axis is perpendicular to the plane of the outer gimbal at its nominal position. This optimizes drive torque for the operating range resolution is obtained by a total reduction ratio of approximately 8000:1. Each motor step of 90 degrees gives 0.2 milliradian of angular motion at the gimbal.

Backlash effects are minimized by mounting the drive system at the edge of the frame providing a long moment arm. Backlash in a standard rolled thread ball screw of 0.010 inch still gives only a 0.14 milliradian error at a 72-inch lever arm. Lower backlash is easily obtained.

Because of the high effective reduction ratio and compressive stiffness of the ball screw, windup is minimized. The drive shaft connecting the two nut drivers is controlling in this area but is far enough down the reduction chain so its angular deflection produces small errors at the gimbal.

Differential thermal expansion is not a problem since the support post, frame and drive system are all steel. Concrete's expansion coefficient is within 10 percent of steel.

Environmental resistance is obtained by flange mounting the stepper motor to the single worm reducer which has environmental seals at each output shaft; the right angle nut drives have similar seals. The ball screw itself has metal bellows above and below the drive nut to seal out dust and dirt.

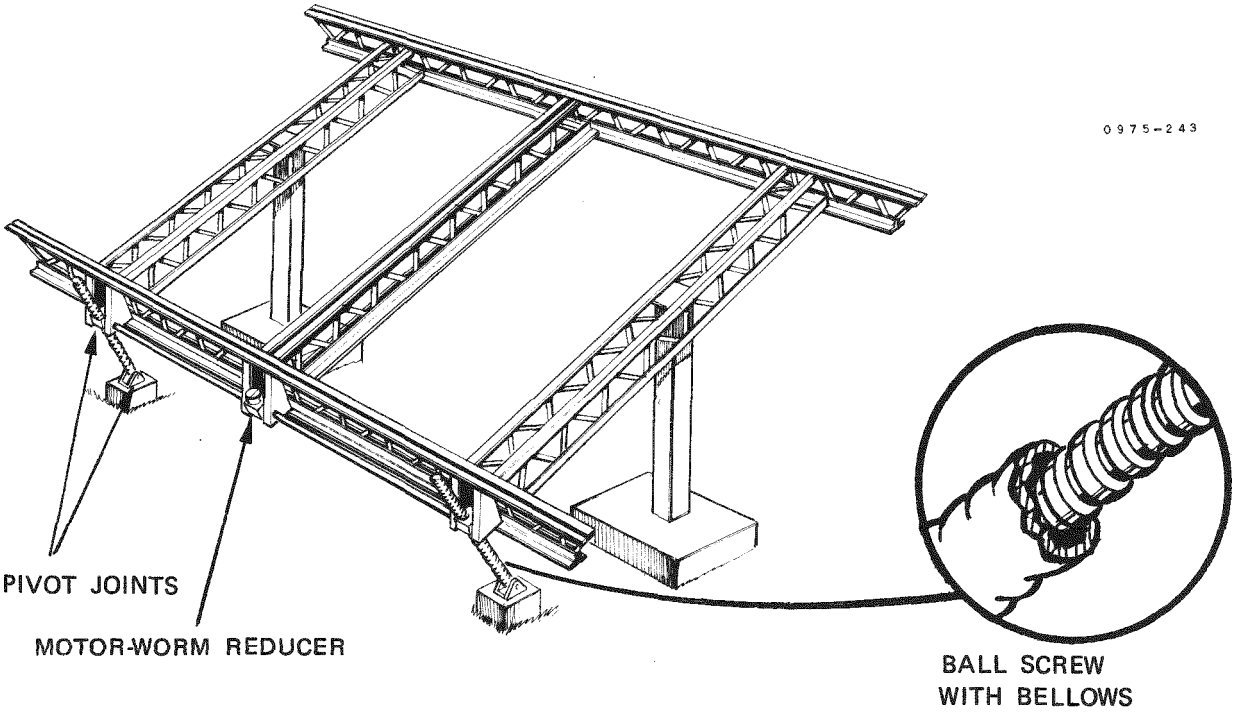
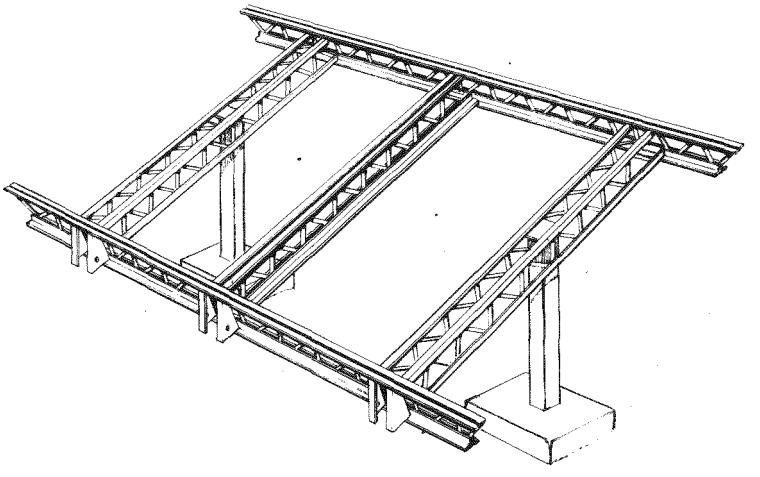
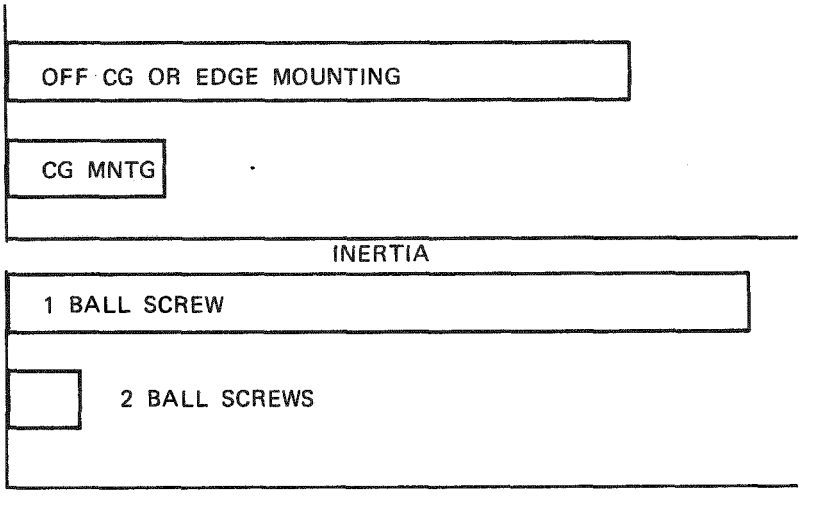


Figure 4-9. Outer Gimbal Drive Mechanism



0975-172

Figure 4-10. Outer Gimbal Assembly



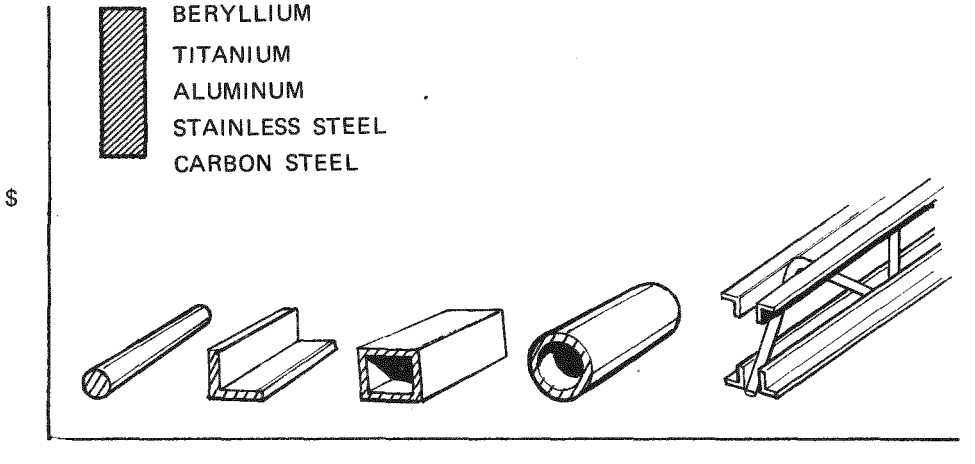


Figure 4-11. Stiffness

Collector Subsystem

Analysis, Tradeoff, and Description of Heliostat Components

WEIGHT MINIMIZATION OF OUTER SIGNAL

Bar joist construction and proper gimbal axis selection provide minimum weight and inertial load on drive motors.

Control of structural deflections under varying wind loads and gimbal angles is critical to maintaining 1 mr pointing accuracies. High stiffness and resulting weight and inertia was not compatible with low drive motor power. Two key design concepts will provide the required pointing accuracy with minimum weight and inertia. The first is a balanced frame assembly. By locating the axis at the center of gravity of the gimbal assembly the rotational inertia is minimized. With proper weight balancing of drive system components about the center line we get small relative displacements regardless of gimbal orientation. The second key design concept is actually the drive system. By using two synchronous ball screws, the requirement for torsional stiffness about the outer axis is minimized. Clearance required for mirror module rotation restricts the use of stiffening members normally used to gain torsional rigidity. Frame stiffness is important then, only in bending modes which are easily controlled with bar joist type construction.

Alternate frame configurations considered included those with pivot points other than the center of gravity to preload the drive for backlash control. This however resulted in higher torque and inertia loading of the drive motor. Drive system backlash was later found to be acceptable without preload. Other materials were considered for the frame including aluminum titanium, beryllium and stainless steel but none has the low cost per unit stiffness of structural steel. Matching of expansion coefficients with glass and concrete is also an asset of steel.

A welded tube frame was considered also but the cost of tubing was found to be higher per unit of stiffness than the rod and angle used in bar joists. The existence of a commercial industry (roof trusses) speaks for cost effectiveness of bar joist construction.

Support of the gimbal assembly is provided by two angular contact bearings set into pillow blocks.

Overall size of the frame is approximately 12 feet by 22 feet by 18 inches deep. This will allow stacking horizontally for shipping by truck or rail.

Collector Subsystem

Analysis, Tradeoff, and Description of Heliostat Components

PRECISION OF THE MIRROR MODULE DRIVE

Pointing accuracy is the primary design criteria for the mirror module drive. Backlash, windup and initial alignment were the considerations which most often caused the rejection of candidate concepts.

Worm gear reducers at each mirror module driven by a common shaft were eliminated due to backlash (1-4 milliradians at output shaft) and cost ($400 each). The need for long lever arms at the mirror module axle became apparent and led to the consideration of large diameter pulleys and sprockets (36-inch diameter or larger). Mirror shading, weight, rotational inertia and cost all detracted from these approaches. A standard 33-inch sprocket costs $200 and weighs 200 pounds. A standard 36-inch wire rope sleeve weighs 100 pounds and costs $200. Some additional problems were seen in the initial alignment area. Vernier adjustments are required at the outer diameter for relative mirror alignment and appeared difficult to mechanize using either chain or wire rope.

A crank arm drive overcomes the problems of the other candidates. It provides a long lever arm (24 inches) with minimum cost, inertia and shading while allowing the use of an inexpensive jackscrew adjustment for mirror alignment. Ball bearing rod ends are used to connect tie rods to the crank arms and provide tight positive control of mirror angle. A disadvantage of this approach is the limited angular range of the crank arm. This is overcome primarily by adjusting the crank arm/mirror relationship to the optimum angle at the center of the operational range on each heliostat. Turnover capability is obtained with a set of crank arms on the opposite end of the mirror module axle set at 90 degrees to the main crank arms.

All drive shaft interfaces have taper lock hubs for positive engagement and easy maintenance and repair. Crank arms will be counter balanced to reduce windup errors.

Drive power is supplied by a sealed stepper motor/reducer assembly which in turn drives a timing chain and sprocket system to one of the center mirror modules. Timing chain was selected over roller chain to control backlash.

Because of the larger dimensions and greater number of drive train components, the mirror module drive is susceptible to windup (angular deflection) due to moments induced by wind load. Based on preliminary analysis of worst case wind direction and attack angle, (see Appendix B) the concept drive system is capable of holding deflections to 0.1 milliradian at 10 mph wind speed. Wind speed versus insolation data from China Lake, California indicate that operation up to 25 mph is desirable to obtain maximum energy. Using the same torsion constants, deflections would reach 0.62 milliradian. This may be acceptable as a worst case condition and can be improved somewhat by furthering stiffening of the structure and drive system. The analysis to date shows, however, that the total stiffness is the sum of many terms of equal magnitude. Significant stiffening then is expensive since many parts must be changed instead of a few "weak links."

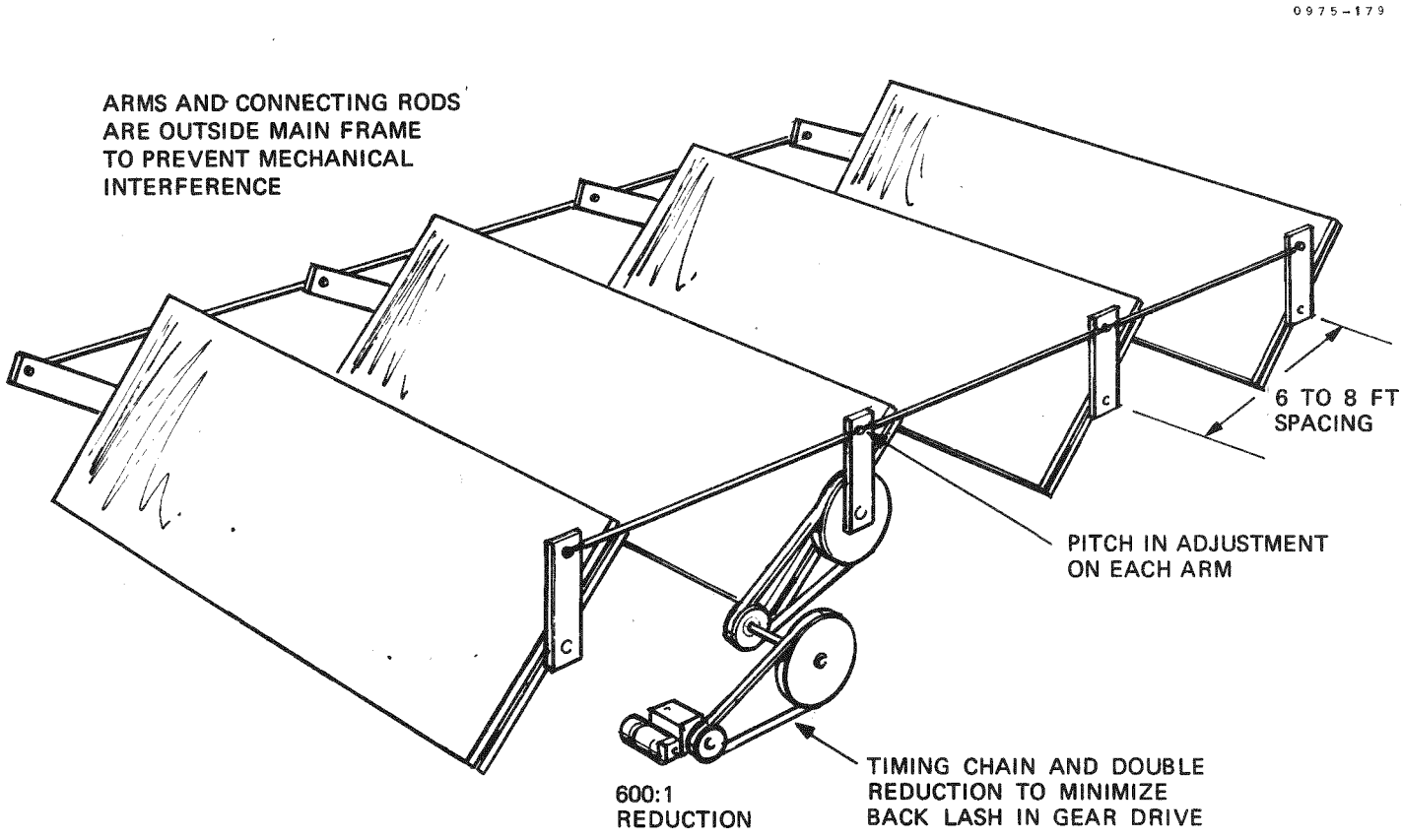


Figure 4-12. Mirror Module Drive System

Collector Subsystem

Analysis, Tradeoff and Description of Heliostat Components

REFLECTIVE SURFACE PROPERTIES AND CONTOUR CONTROL

A back surface silvered, commercial float glass mirror bonded to a honeycomb support gives protection for the reflective surface plus high stiffness to weight ratio to control the mirror contour under wind and variable "g" conditions.

A 3-mm, second surface, float glass mirror has been chosen for its cost effectiveness, environmental resistance, and inherent freedom from distortion. Also, these mirrors are currently in volume production by many sources. Reflectance is 83 percent according to one supplier but is subject to improvement by using low iron glass and possibly reducing thickness to 2 mm. Thicker mirrors would provide more rigidity but at the expense of lower reflectance (73 percent for 6-mm thick) and greater weight.

Although glass mirrors are flat over small areas they will sag (without breaking) by many times their thickness over large areas. Regardless of what surface contour is selected, that is, flat, spherical radius, etc., consistency of that shape under varying conditions of elevation angle and wind loading is required to control the size of the image at the receiver. Assembly and alignment of the mirrors to the axle assembly is, of course, the first place where the contour must be maintained. These requirements led to the selection of a one-inch thick honeycomb panel to support the mirrors.

The heliostat reflective surfaces must perform three functions: reflect as much energy as possible, focus the energy down to a beam size that will fit into the receiver and finally point the beam to the center of the receiver aperture. These functions are all included in a heliostat building block called a mirror module.

Selection of the reflective surface was driven heavily by spectral reflectance, environmental resistance and distortion characteristics. Flexural rigidity, initial alignment and thermal expansion were the main factors in the selection of a focus control concept. Torsional stiffness and balance control the mirror modules contribution to pointing error.

Candidate reflective surfaces included float glass mirrors, polished aluminum, aluminized plastics, laminated glass mirrors and aluminized plastics with thin glass laminated on the front surface. Polished aluminum surfaces such as Alcoa's ALZAK were deleted because of lower initial reflectance and poor environmental protection. Aluminized plastics have good reflectance and negligible weight but require lamination to a continuous flat surface. Laminated glass mirrors such as those made by Gardner Mirror Company have a poor stiffness to weight ratio. Thin glass laminated to aluminized plastics provides minimum weight but is too sensitive to temperature.

Each mirror module consists of a 5 foot by 10 foot panel with four bonded mirror segments. This assembly is mounted and aligned to a tubular axle at five points; center and four corners. This scheme allows alignment of 50 feet^2 of mirror with one adjustment without distortion of the contour. Focal length can also be adjusted by pulling the center after the corners are secured.

Thermal expansion effects are controlled by adhesive selection to provide shear compliance between the glass mirror and honeycomb skin. A cost reduction may be possible using the glass mirror as one of the honeycomb skins but the adhesive interface requires further development.

Mirror module pointing errors are controlled by using a single thin wall tube 12 inches OD by 0.05 wall for stiffness in both bending and torsion. The complete mirror module is balanced by placing the stub shafts in line with the center of gravity.

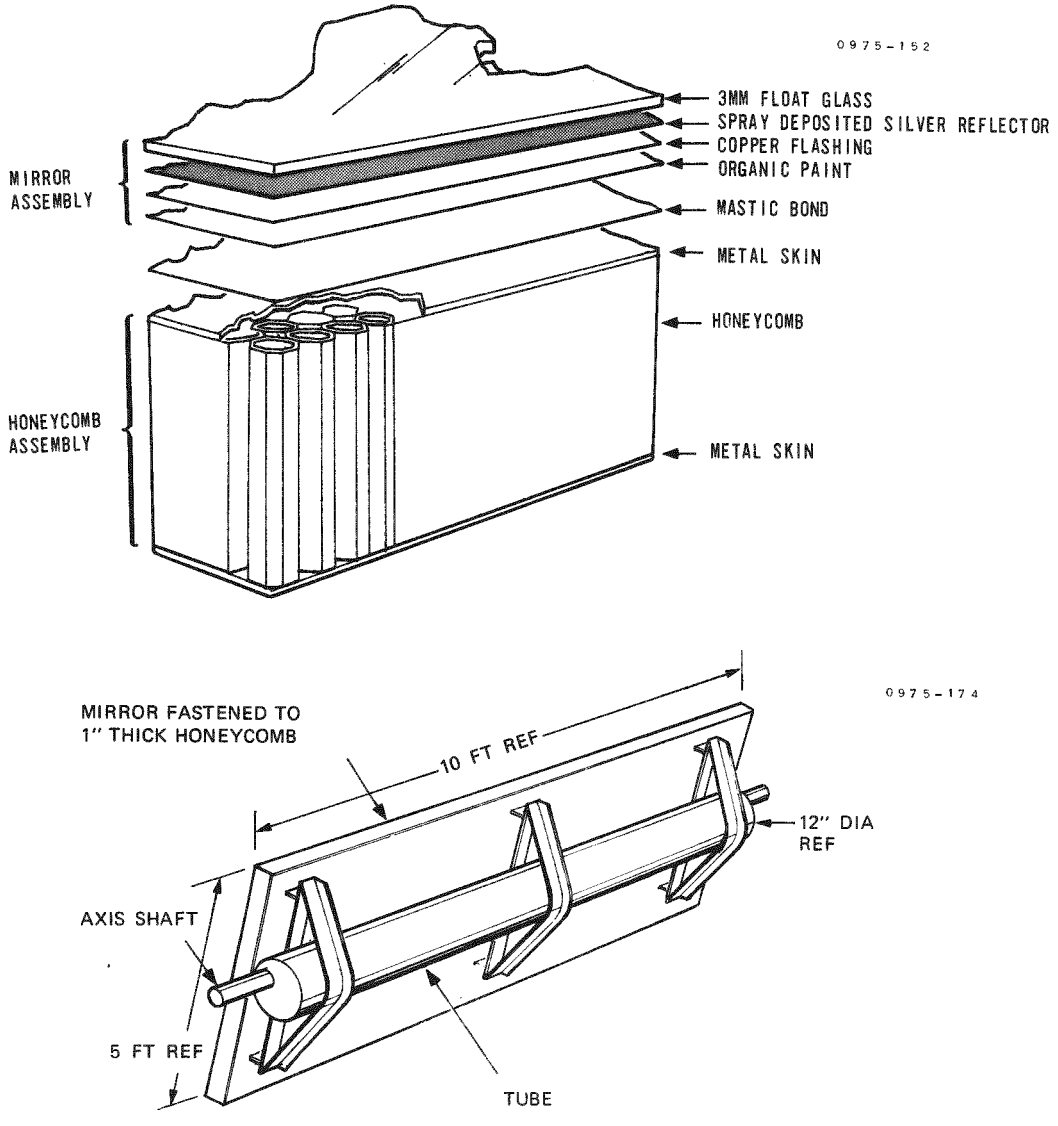


Figure 4-13. Mirror Module Configuration

Collector Subsystem

Analysis, Tradeoff, and Description of Heliostat Components

HELIOSTAT INSTALLATION AND ALIGNMENT

Built-in adjustments and optical calibration provide cost effective alternatives to piece part tolerance control.

Pointing and focusing accuracy requirements dictate that heliostat parts and subassemblies be aligned within as little as 0.010 inch. Even if these tolerances could be held on parts like the outer gimbal frame, the stresses seen during shipping would cause some change. A second consideration is the focusing requirement where relative alignment of parts is a function of field location. Interchangeable parts built to commercial tolerances with adjustment mechanisms built in are the key to low cost heliostats.

The individual adjustment mechanisms and their functions are described below.

- Foundation. Vertical adjustments are installed at the top of each support post to accept the stub shafts of the outer gimbal support. Adjustment is by a stiff lightweight tooling bar and level which spans the distance between posts and rests in the gimbal supports.

- Outer Gimbal Assembly. Pillow block supports for each stub shaft have jack screw adjustments to control the parallelism and coplanairty of the mirror module axes and the perpendicularity of the inner and outer gimbal axes. Fixtures set up on a stable concrete slab at the plant site are envisioned for this assembly operation.

- Outer Gimbal Drive. Alignment here is performed at the site. The outer gimbal is set at its nominal tilt angle and a level installed on the end of the mirror module axles and parallel to the outer gimbal axis. The right angle ball screw drives are operated independently until level is obtained, then the drives are locked to the motor/reducer output.

- Mirror Module Drive. The connecting rods have two independent adjustments at each crank arm excluding the drive arm. The first adjusts the length of the rod itself to prevent binding at top dead center and is completed during assembly of the heliostat at the plant site. After the heliostat is installed on its foundation, the second adjusts the relative alignment between mirror modules by an optical procedure. Taper lock hubs are used at each crank arm/stub shaft interface for course mirror alignment as well as easy repair and maintenance.

- Mirror Module. Tie points between honeycomb and axle assembly control pointing of mirror normal with respect to the axle pivot axis; center tie point allows variation in focal length although use of a common contour for all mirror modules is now a design goal.

- Optical Alignment. Heliostat alignment is completed at the assembly line and at the foundation to the largest extent possible using fixtures, level indicators or other instruments. Final focusing of the complete unit, however, is best done using feedback from the calibration array. Optical errors are magnified to provide high resolution at the line of sight distances between heliostats and calibration array.

  A set of modulated Xenon lamps are located on top of the tower and spaced to simulate collimated light, that is, parallel lines of sight to the four mirror modules. With one light at a time, each mirror module is aligned (and focused if necessary) per calibration array feedback. As each mirror module is aligned, the other three are temporarily shaded. Night time now appears the best for this operation for minimum interference from adjacent heliostats, the best resolution and longest lamp life.

- Electrical Adjustments. The only electrical adjustment required at the heliostat will be that needed to set the address for that particular location in the field. This can be a programmable switch array or a hard wired setting. All other major subassemblies such as the power supply, battery, motor controller electronics, and motors will be identical and interchangeable.

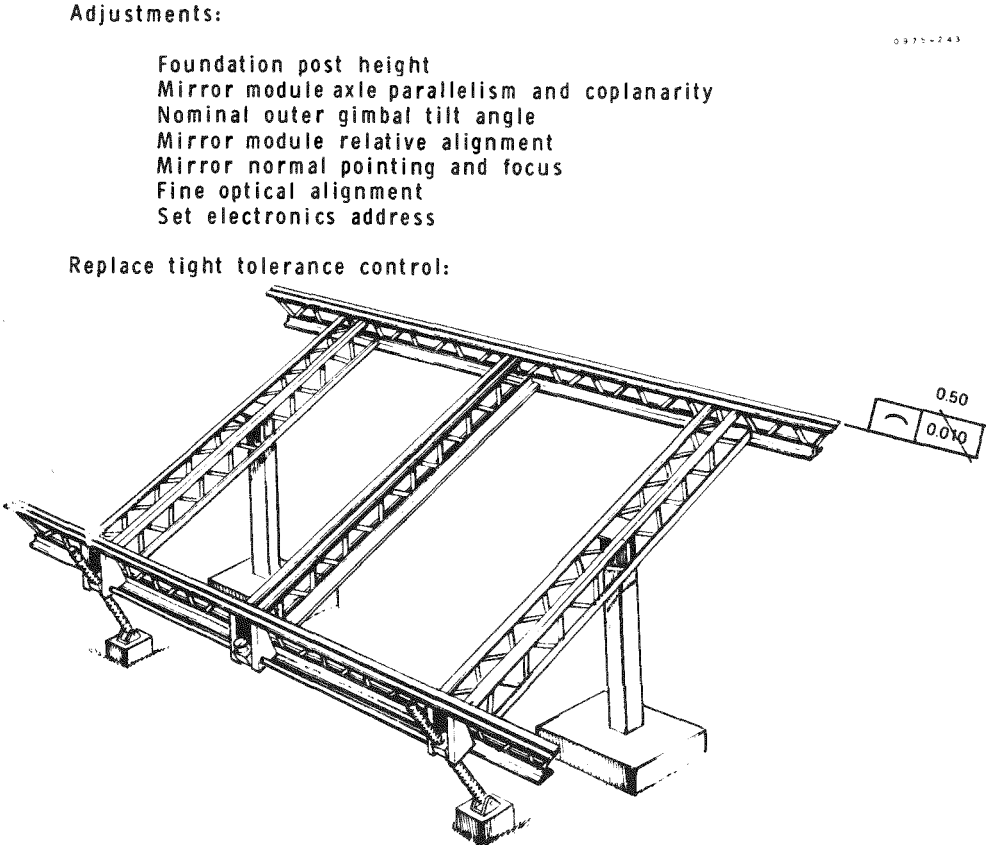


Figure 4-14. Heliostat Installation and Alignment

Collector Subsystem

Analysis, Tradeoff, and Description of Power and Control System Components

INTRODUCTION TO SYSTEM CONTROL

Central computer control of the heliostat arrays is the safest and most cost effective way to operate and maintain the solar collection station.

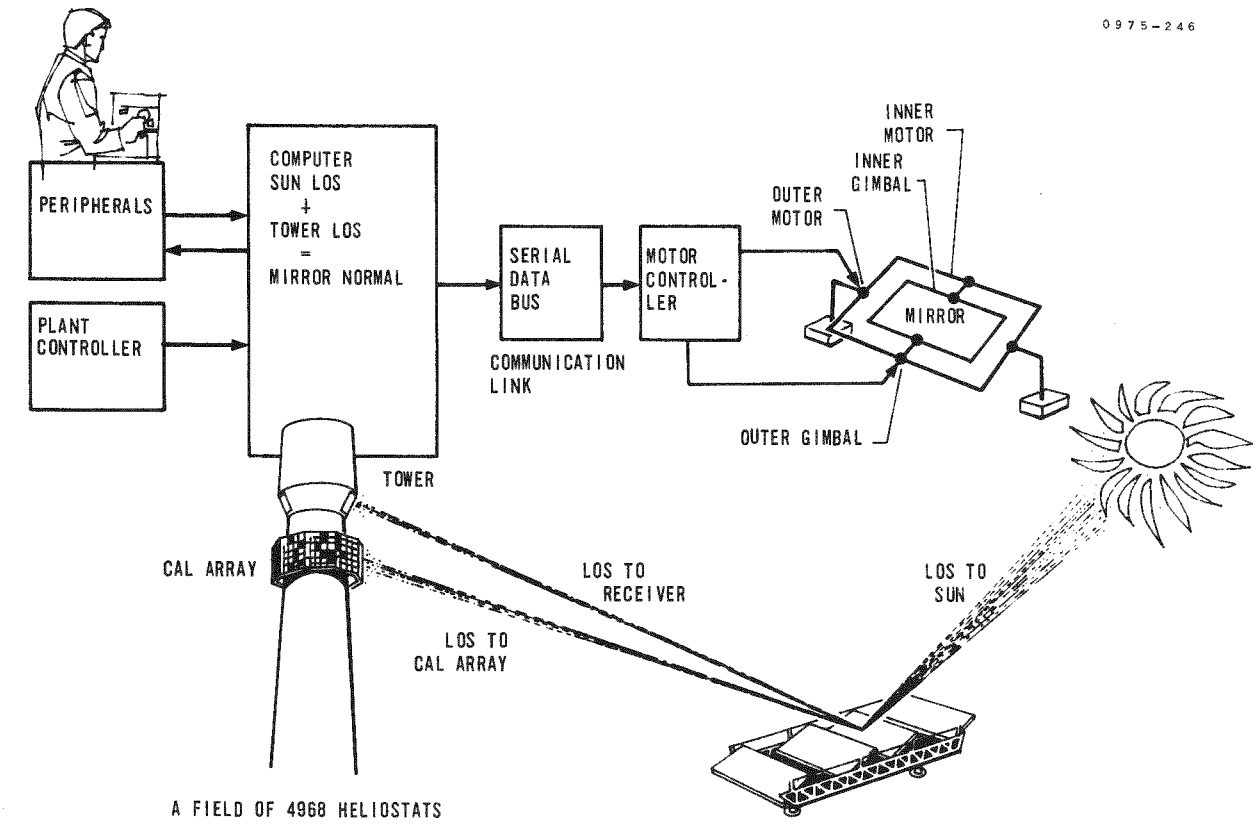
The central computer concept permits low cost, high speed minicomputers to service large numbers of heliostats. This means even lower costs when expressed on a per heliostat basis. Being centrally located, a wide variety of programmed options will be made available to the operator and/or to the central plant controller. These options will permit special start-up and turn-down sequencing, fine vernier control of the number of heliostats focused on the tower throughout the day, and the normal tracking, calibration and emergency control modes.

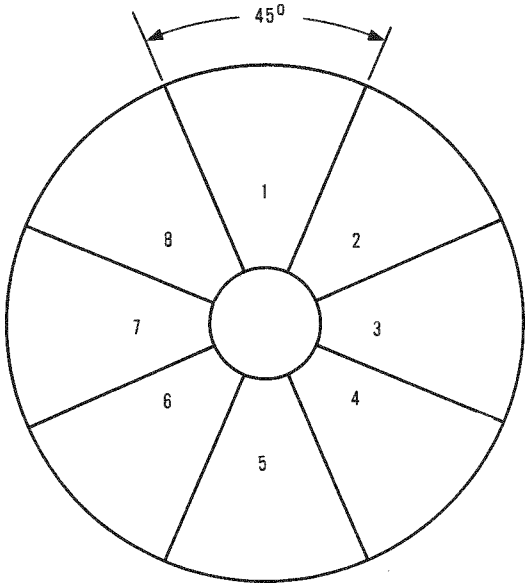
The heliostat field will be subdivided into 45 degrees octants of 621 heliostats each. Each octant will be further subdivided into six sectors, 7-1/2 degrees wide, each containing 103 or 104 heliostats. Each of four processors will have control over two such octants on opposite sides of the field to permit symmetrical balancing of the heliostat energy.

Each computer will operate in real-time to track the Sun and control the heliostats. This approach permits the use of real-time meteorology data for refraction corrections and the immediate application of calibration compensations as they become available. Operator and plant controller inputs will, of course, be processed in real-time so that system control can be effective and immediate.

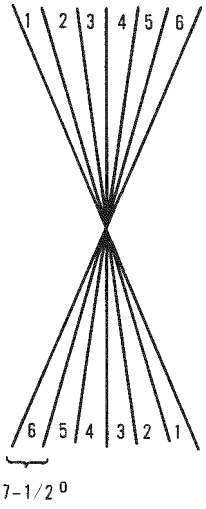
In the normal tracking mode, the line of site to the Sun will be added vectorily to the prestored line of site to the receiver. The resultant vector, which describes the mirror normal, will be resolved into outer and inner gimbal commands and sent to the heliostat. In other tracking modes such as offset pointing and calibration, the same technique will be used except that the receiver LOS vector will be replaced with the LOS of the calibration array of the LOS of the offset point. This allows the same software algorithms to be used for all tracking modes.

Calibration of one or two heliostats in each octant will be going on continuously throughout the operating day. This will be done by taking the heliostat off the receiver and slewing it down to the target array in the computation described above. Once on the target array, error coordinates will be returned to the computer and evaluated for reasonableness. If the errors are extreme, the operator will be advised and the heliostat will not be returned to service. If the errors are reasonable, the compensation parameters for that heliostat will be updated and then the heliostat will be returned to service.





EACH OCTANT CONTAINS 621 HELIOSTATS



COMPUTER NO 1 CONTROLS OCTANTS 1 AND 5 (1242 HELIOSTATS)
NO 2 CONTROLS OCTANTS 2 AND 6
NO 3 CONTROLS OCTANTS 3 AND 7
NO. 4 CONTROLS OCTANTS 4 AND 8

EACH PAIR OF OPPOSING OCTANTS IS SUBDIVIDED INTO 12 OPPOSING SECTORS OF 103 5 HELIOSTATS EACH

Figure 4-15. A Field of 4968 Heliostats

Collector Subsystem

Analysis, Tradeoff, and Description of Power and Control System Components

CONTROL SYSTEM OPERATION VIA SOFTWARE

Central Processor Control is the best solution to integrate Sun tracking, heliostat command and control and operator interface, particularly considering the variety of power plant situations.

Real time executive control logic will be used to tie Sun tracking and heliostat command and control to a fixed time base, synchronized with Greenwich Mean Time. A 20 Hz interrupt will be subdivided into 50 millisecond blocks of time. These blocks of time will be used to compute the Sun vector once each second and to service each sector of 103 or 104 heliostats. This requires the vector addition of the Sun LOS and the heliostat LOS, the extraction of two arc-tangents and the construction of the control word in about 485 microseconds. When the control word array is output via DMA, the processor is free to compute the next sector's array. The main system advantage of this approach is the staggered distribution of the heliostat power load, rather than having all heliostats trying to turn at the same time. In the software, other advantages are gained such as the sharing of subroutines and temporary storage between sectors. Meteorology data will also be input at this frequency so that digital filtering techniques may be used to smooth the raw data. Operator and plant controller inputs will also be input at these rates to guarantee the servicing of emergency commands within one second.

Visual display data to the CRT and printer will be handled on a no-priority basis. That is, when the computer is not responding to the 20 Hz interrupt routine, it will be free to format and transmit status data to the displays. This data is routine in nature and does not require a precise time base.

A high speed processor with a reasonable instruction repertoire and 32K of memory is required for this task. Add times should be on the order of two microseconds and multiply times no greater than eight microseconds. A sixteen bit machine with a double precision capability will provide sufficient computational accuracy for the problem. Hardwired arc-tangent and square root functions would be nice, but if they can be accomplished via software in 100 and 150 microseconds, respectively, this would be satisfactory.

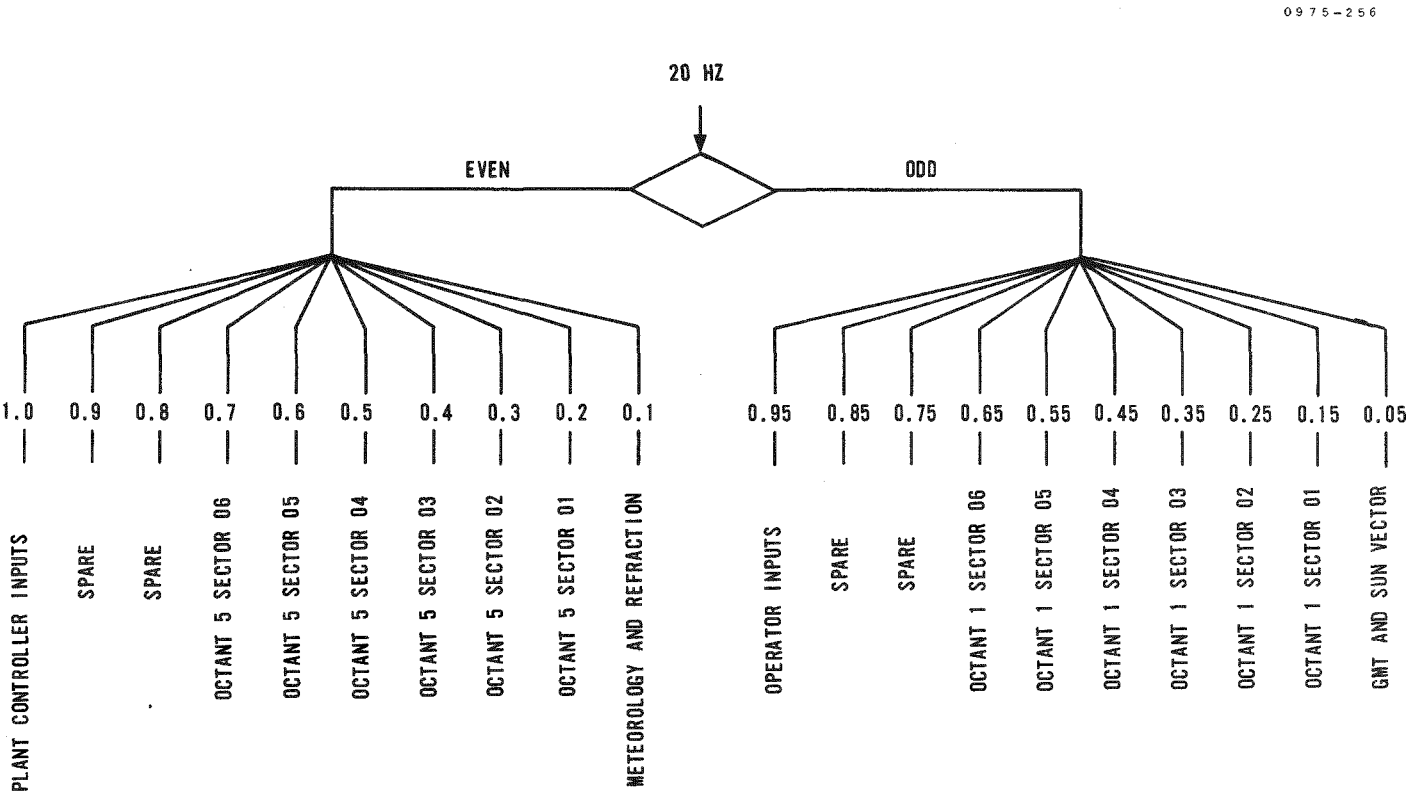


Figure 4-16. Real-Time Executive Control Logic

Collector Subsystem

Analysis, Tradeoff, and Description of Power and Control System Components

ACCURACY FACTORS IN SUN TRACKING

Accurate Sun tracking is best solved by a software approach with precise orbit parameters, knowledge of Greenwich Mean Time, and corrections for atmospheric refraction.

Two techniques were considered for Sun tracking. The first concept was a hardware concept using a central Sun tracker with precision gimbal readouts. Although this system would accurately track the apparent Sun, it was rejected because of high initial cost, a continuing maintenance and calibration cost, possible failure to track during periods of intermittent cloud cover and an additional computer interface link to design. In addition, it adds error sources of its own, such as gimbal readout error, etc.

The second concept, a software approach was chosen on the basis of lower cost, higher reliability, a reduced interface requirement and potentially greater accuracy. The only disadvantage of the software concept is the difficulty in predicting refraction corrections at low elevation angles. With appropriate data inputs, however, this error source can be eliminated for all practical elevation angles.

Computation of the Sun's position in the sky can be accurately done with the computer under any kind of weather conditions. No synthetic tracking requirements are imposed on the heliostats. The mean orbital elements of the Sun are given in the American Ephemeris and Nautical Almanac, published yearly, or they may be computed from equations documented in the same publication. See Appendix C-1 for details.

The strategy for obtaining the Sun's position is to treat the Sun as a satellite of the Earth. Using Greenwhich Mean Time to determine the days and fractions of the day and using the orbital parameters determined from the Almanac, the true anomaly, which describes the position of the Sun on the ecliptic, is computed. This value, in vector form, is rotated through the argument of perigee (ω) and the mean obliquity of the ecliptic (i) to transform the vector to an inertial coordinate frame; Equatorial, East and Polar. Then, with knowledge of GMT and latitude and longitude of the station, the Sun vector can be transformed to an Earth fixed local vertical frame; Up, East and North. See Appendix C-2 for details.

The true elevation of the Sun in the sky is not the apparent elevation due to atmospheric refraction. This error in elevation is zero when the Sun is directly overhead but it is in excess of one-half degree at sunrise and sunset. This error source can be sufficiently compensated for co-altitude angles up to 80 degrees by using the equation

$$R_{\widehat{Sec}} = \frac{206P}{273+T} \tan (\text{co-altitude})$$

where T is the local temperature in degrees centigrade, P the local barometric pressure in centimeters of mercury, and R is the refraction correction in arc-seconds. See Appendix C-3.

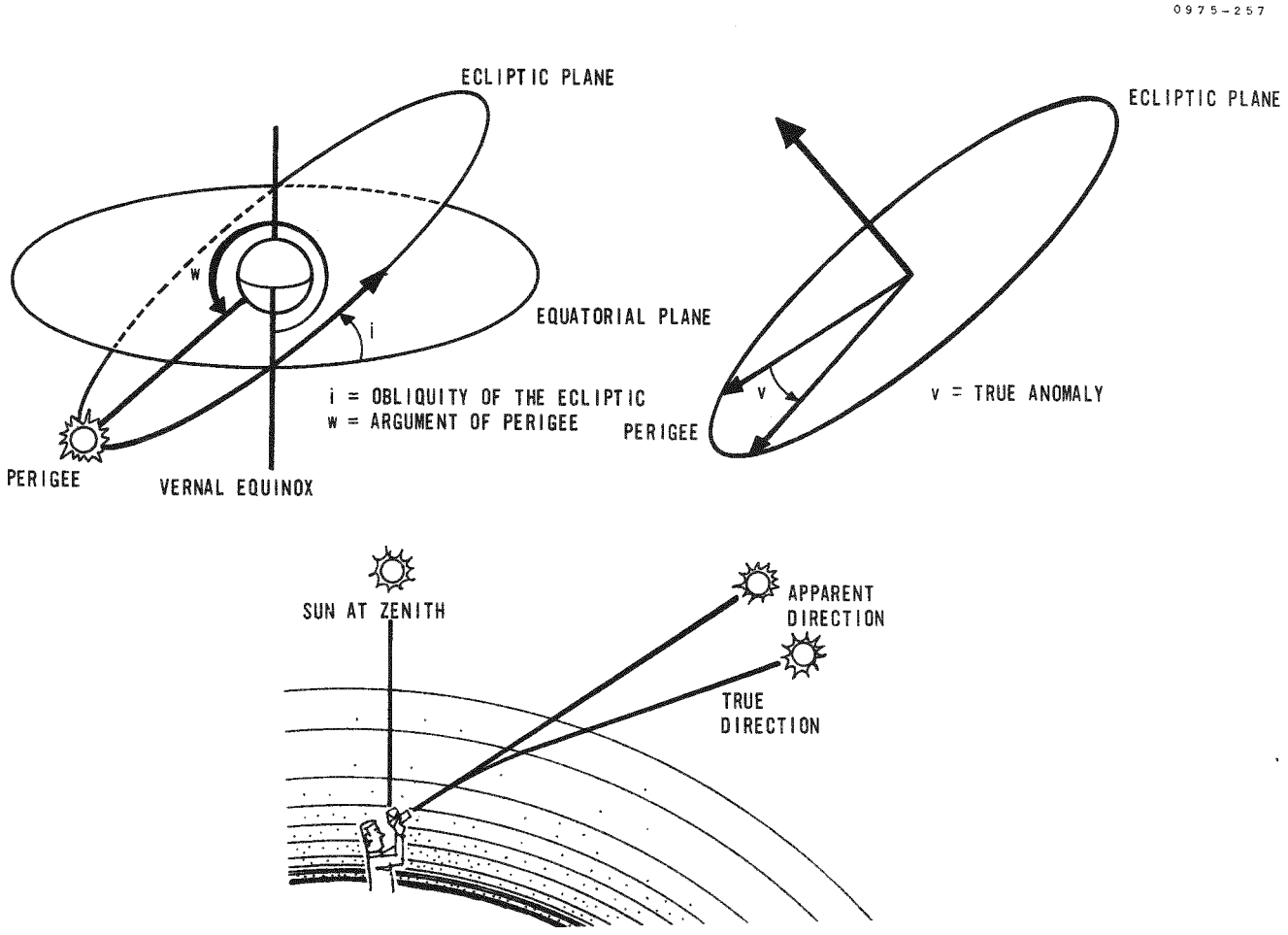


Figure 4-17. Atmospheric Refraction Increases the Sun's Altitude

Collector Subsystem

Analysis, Tradeoff, and Description of Power and Control System Components

FUNDAMENTALS OF HELIOSTAT CONTROL

Heliostat command and control requires computer summations of all commands given and an accurate reference starting point.

The heliostats are to be driven by stepper motors, in an open loop discrete fashion. Normal tracking rates for the tilt/tilt configuration will not exceed 23°/hour. This criteria is satisfied with the planned one command per second rate of 40°/hour. An additional slew rate of 640°/hour will also be available for calibration and emergency conditions.

The mirror normal vector will be found by adding the sun LOS unit vector(s) to the receiver LOS unit vector (T). The outer and inner gimbal commands will then be extracted from the resultant vector (R) using the arctangent subroutine.

Since the system is open loop, the computer must keep track of the gimbal angle positions of each heliostat by integrating all the commands sent out. The control law is then simply the commanded angle minus the actual angle. The resultant delta angle is then evaluated to determine which control bits are to be set in the control word for that particular heliostat. This control word and the heliostat address are then stored in an output DMA table. The same delta angle is then used to update the actual angle stored in the computer. This process is then repeated for both gimbal angles on all heliostats within the sector. When this is completed, the DMA output is initiated and the computer begins the same computations for the next sector.

If control is ever lost on any heliostat, the initialize bit is set and the heliostat control electronics drive the heliostat to a known reference position. Once there, recovery operations can begin.

Control can be lost in several different ways. One way is the loss of power to the heliostat control electronics. The battery system will hold up heliostat operation for some period of time but it will then, of its own, proceed to the stowage position. The computer will be aware of this by loss of receiver signals or failure to receive calibrate signals. A second way to lose control is to lose the communication link. The heliostat responds in the same manner to this type failure, and again the computer is aware of the condition by failure to calibrate. A third type of control loss is the failure to receive calibration signal after slewing to the calibration array. In this case we assume an intermittent loss of either power or communications which caused a loss of pulses to the motors. The strategy in all three cases is to command initialization and then try calibration again. If calibration fails a second time, the heliostat would be flagged as a failure and commanded to the stow position in the usual vector control fashion. Of course, it may not get there exactly depending on the nature of the error but it should be in a sufficiently safe position. If calibration is successful, the heliostat would be returned to service on the receiver.

1. $R = \bar{S} + \bar{T}$
2. OUTER COMMAND = ARCTAN $-R_3/R_1$
3. INNER COMMAND = ARCTAN $R_2/\sqrt{R_1^2 + R_3^2}$
4. FORM Θ COMMANDED – ΘACTUAL
5. CONSTRUCT HELIOSTAT CONTROL WORD AND STORE IN DMA OUTPUT ARRAY
6. UPDATE Θ ACTUAL IN COMPUTER
7. REPEAT 4–6 FOR SECOND AXIS
8. REPEAT 1–7 FOR ALL HELIOSTATS IN SECTOR
9. OUTPUT DMA TABLE
10. CONTROL WORD FORMAT

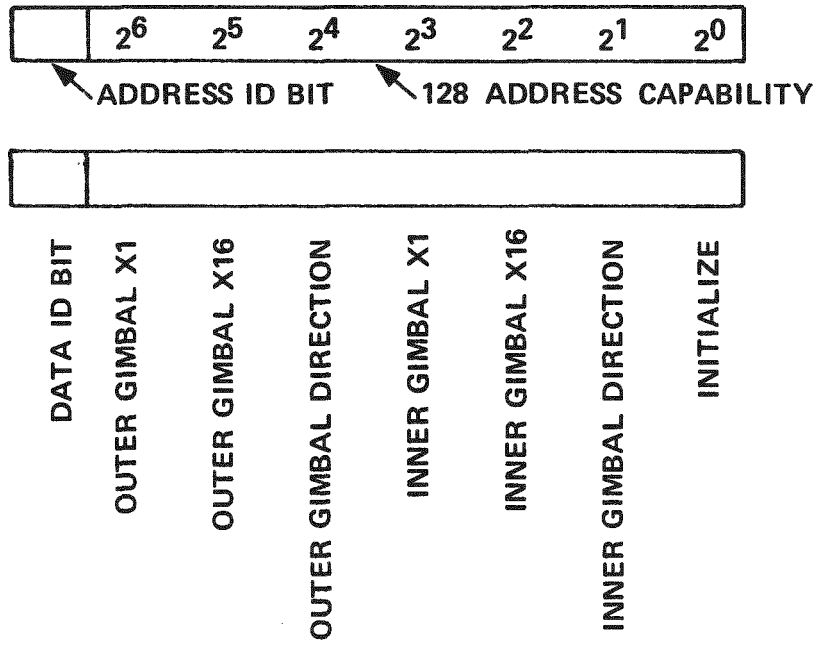


Figure 4-18. Command and Control

Collector Subsystem

Analysis, Tradeoff, and Description of Power and Control System Components

SERIAL DATA BUS PROVIDES HELIOSTAT COMMUNICATION

A serial data bus via a dedicated line provides the most reliable and cost effective communication link between the computer and the heliostat.

A communications link must be provided between the computer and the field heliostat. Three types of systems were considered for this link: (1) an RF transmitter/receiver combination, (2) transmission via the power lines, and (3) transmission by means of a separate dedicated wire. In an open-loop system such as ours, reliable communications is of prime importance. As such, the RF system, which would be subject to interference and the added unreliability of the additional parts required for the receiver ruled against this choice. Control via the power lines also required no additional wires but severe technical problems were foreseen in attempting to filter power and signal frequencies and line transients. While the dedicated line required field wiring it was felt that a significant part of the costs of installing a separate grid could be averted by bundling the communications lines in the jacket of the ac power grid lines which must be there in any case. It was further felt that a dedicated shielded hard line provided the most reliable interconnecting link and this system was chosen.

The overall serial data bus system consists of a transmitter section which interfaces the computer and the bus line, the bus line itself, and a receiver section which interfaces the line with the motor controller electronics. The transmitter under program control accepts data in parallel form from the computer memory via a DMA channel, formats the data, and meters it out serially on the bus. The receiver contains an address decoder which recognizes and accepts data addressed to it, reformats the data in parallel form and stores it for use by the controller electronics. Line driving and receiving will be high level differential. A complete message will consist of two 8-bit bytes, the first byte being an address word with the second being the data word. Communication rate is expected to be 4800 baud. Each serial data bus will service 100 heliostats, hence, 50 serial data bus lines will be required.

Only simplex communication is envisioned. As a future cost reduction, the control and sequencing logic of the serial data bus could be made into a custom LSI to further lower purchase and assembly costs.

0975-258

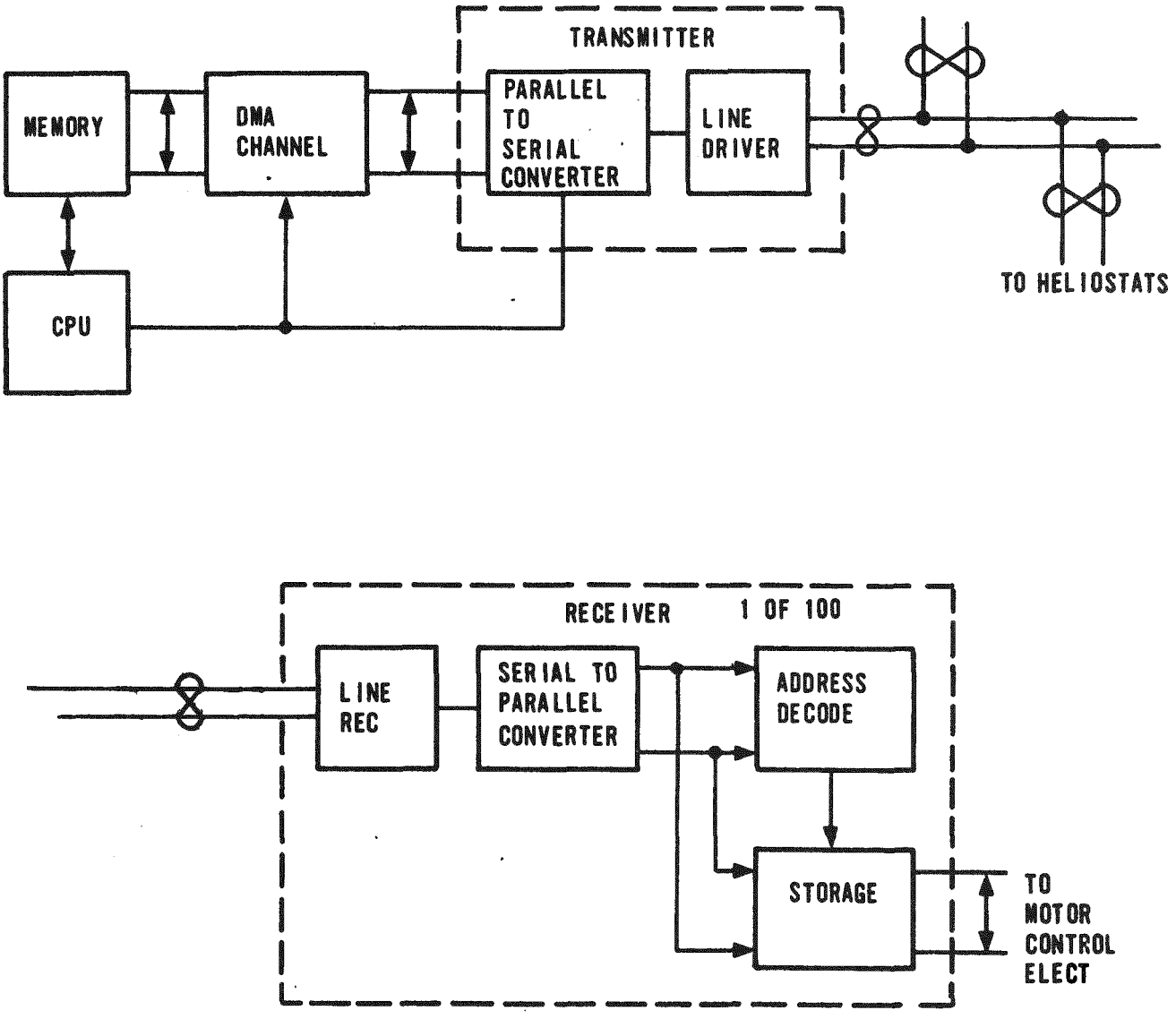


Figure 4-19. Serial Data Bus

Collector Subsystem

Analysis, Tradeoff, and Description of Power and Control System Components

MOTOR CONTROLLER FOR GIMBAL DRIVES

The motor controller electronics uses low power standard logic elements for efficiency and low cost.

The motor controller electronics will accept an 8-bit data word from the serial data bus line receiver and process the information as required to perform the commanded operations. Either 1 or 16 motor steps can be commanded by a single word bit representing 0.66 arc minute or 10.56 arc-minutes of mirror travel. Initialization is also commanded by a single word bit. In addition to the computer commanded inputs, the motor controller will also accept inputs from the Power and Communications Loss Detectors, and the Initialization and Limits Switches to provide directional sense and fail safe commands as required in the event of an emergency. Axis drive will be by means of a stepper motor. The inner and outer axes commands will be acted on sequentially. The controller assemblies for both axes will be identical. A block diagram of the Motor Controller Electronics is shown in the accompanying illustration.

Virtually all functions of the Motor Controller Electronics assemblies are digital functions and will be mechanized with Low Power Schottky or MOS type integrated circuits for power efficiency and low cost. So as not to waste power between updates, the motor power drivers will be disabled except when metering out commands. In the future when large quantities of these circuits would be required, custom large scale integration of these functions would reduce acquisition and fabrication costs even further.

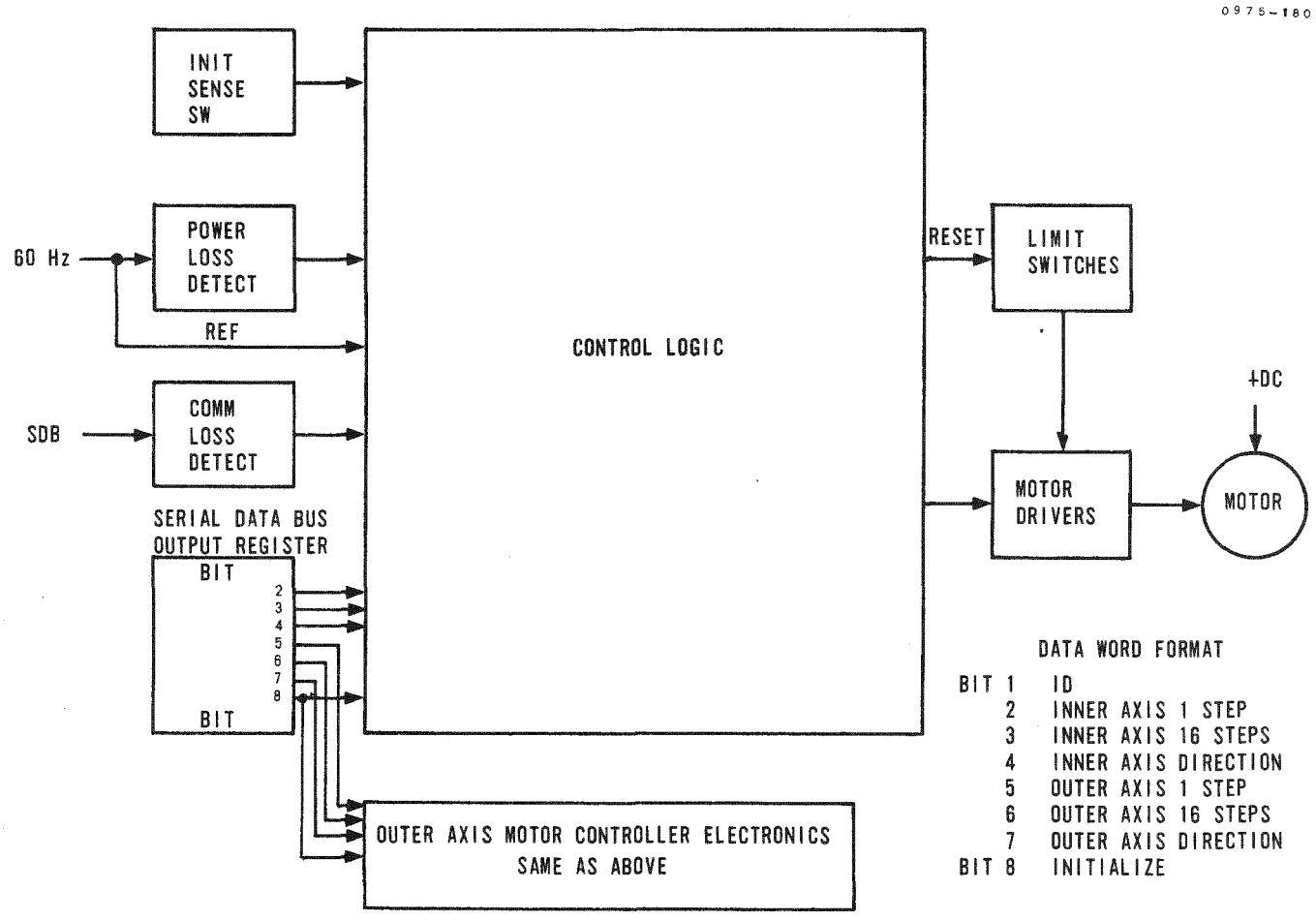


Figure 4-20. Motor Controller Electronics

Collector Subsystem

Analysis, Tradeoff, and Description of Power and Control System Components

EFFECTIVE HELIOSTAT CALIBRATION

Pointing errors can be detected and compensations applied by means of a photodetector sensor array in conjunction with the computer.

Photodetectors and thermistors were considered for the calibration sensor. Thermistors were considered slow acting, needing elaborate temperature and scaling compensation and protection from the wind. Among photodetectors, the photovoltaic type used in the short circuit mode of operation was considered superior to the photo resistive type. In the resistive type, the change in resistance is a nonlinear function of incident light having larger resistance changes for the same light deltas at lower levels than higher ones, thereby, amplifying the background light with a higher scale factor than the signal light.

Each photodetector will have its own operational amplifier. Photodiodes or phototransistors will be used as shown in Figure 4-21. The individual op-amp will provide a good low output impedance for line driving. It eliminates the detector leakage temperature problem by reducing the voltage across it to that of the input offset voltage of the amplifier. It also provides an easy means to calibrate by adjusting the feedback resistor with a calibrated light incident on the detector. Balanced input impedances will be used if common mode rejection is required.

Separate photodetectors will be mounted in the extreme parts of the array with their outputs averaged so as to provide a measure of background level. This level will be subtracted from the level detected by the calibration sensors so as to enhance the signal to background ratio and provide compensation for varying light and background levels. A signal to background ratio of TBD is expected at the array.

Three calibration schemes were considered. Two methods used dedicated hardware while one depended heavily upon the computer. In the latter method, the beam of the heliostat to be calibrated is swept across an X photodetector configuration. The time for the beam to reach the center of the array is computed and the time to intercept the two diagonals is measured. From the computed and measured times, two axis error information can be obtained. The objections to this system are that with sequential axis operation, the beam cannot be smoothly swept across the array. Irregular beam shapes could introduce errors and that real-time interrupts to the computer at the intercept times significantly impact the software. It also requires the longest time of the three methods to calibrate.

The other two methods use dedicated hardware to compute the energy centroid and only the two error coefficients are fed to the computer. In the second method, the beam is slewed to a point anywhere on the array where an energy centroid computation is made and the heliostat immediately returned to service. The third method is similar to the second except that the beam would be

servoed to the center of the array by feedback to the computer. Here photocells might be packed more closely for a finer error measurement. The second method, which required the minimum calibration time was chosen. The energy centroid will be computed by using the photocells as threshold detectors feeding a microprocessor or by an analog means similar to a moment of inertia calculation. The array is expected to be 12 feet by 12 feet with cells 1 foot apart. The array will be mounted ≈34 feet below the tower. Twelve arrays will be required for the entire field.

The inputs to the computer from the calibration array will be treated as delta azimuth and delta elevation increments. These errors will be projected back to the receiver and used to update the heliostat line of site to the receiver.

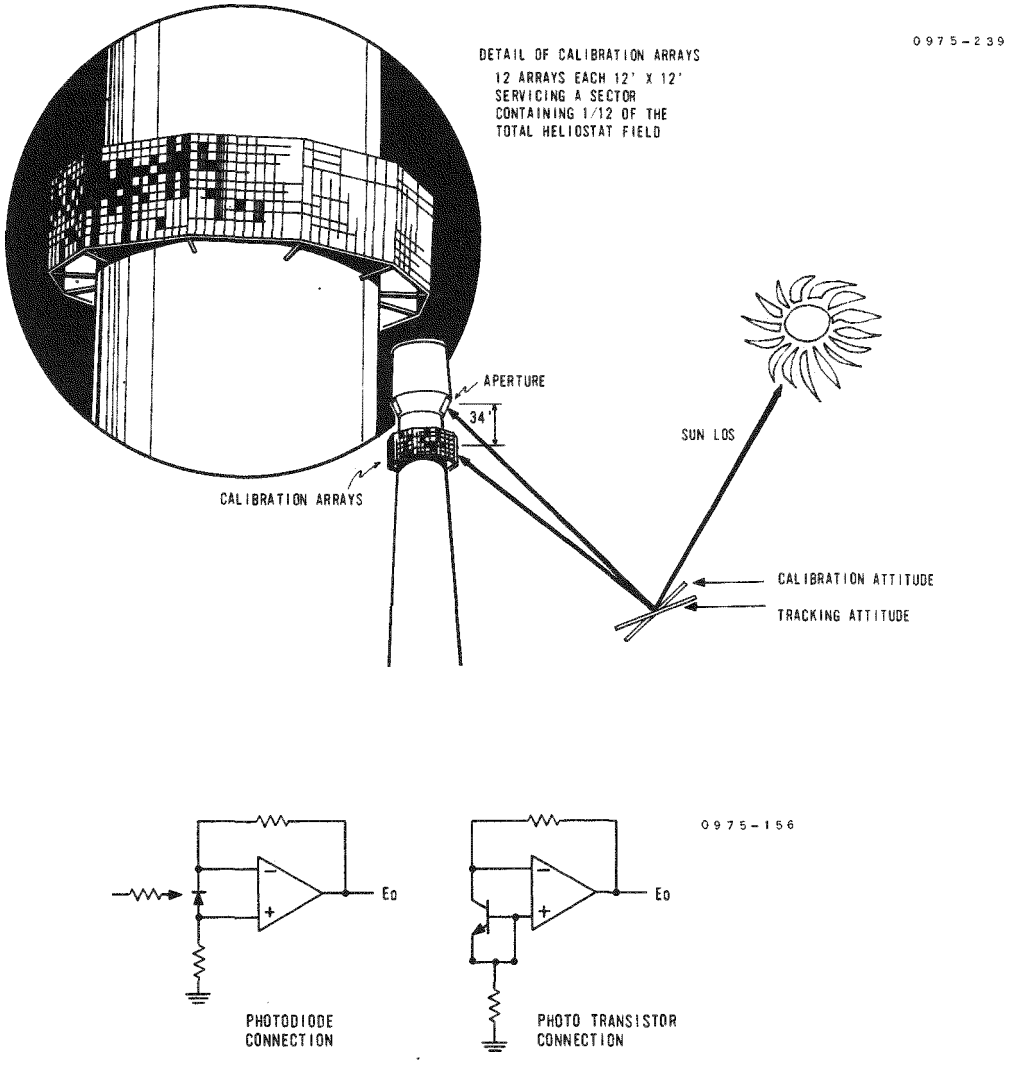


Figure 4-21. Calibration Geometry

Collector Subsystem

Analysis, Tradeoff, and Description of Power and Control System Components

EMERGENCY DEFOCUS FOR BOILER PROTECTION

The ramifications of inadequate boiler protection are so vast that emergency defocus and the subject of single failure versus multiple failure protection receives high priority.

The subject of emergency defocus for boiler protection becomes more clear once the problem is defined in terms of four submodes. These submodes are:

1. Initial rapid removal of reflected beam from boiler (greater than 3 degree motion in less than 12 seconds).

2. Follow-up maneuver to prevent the energy dome from drifting back onto the receiver.

3. Possible need to return to stowage in the event of an impending emergency condition such as wind, hail, sand storm.

4. Automatic reset and recovery mode that does not require operator service at each heliostat.

Of the many candidates that were considered, four were the most promising:

1. Stored energy mechanism operating the drive train.

2. Operational shutter to close over the mirrors.

3. Normal gimbal drive.

4. Normal gimbal drive with battery backup.

The mechanization of candidates 1, 2, and 4 include local detection of ac power or communication loss and self-command of the emergency defocus mode. All candidates respond to a computer issued emergency defocus command.

In reality, getting the energy off the tower within seconds is important and most of the candidates considered were able to accomplish this. However, for all cases but the operational shutter, a second maneuver will be required within minutes to maintain control over the moving energy dome left by a small mechanical deflection of mirrors.

At the same time it seems prudent to consider the possibility of at least a single failure. Two of the most obvious single failures would be loss of ac power or possibly loss of communications. However, the possibility of correlation between these type failures and impending high winds, hail, or sand storm leads to a second case wherein it may be required to place heliostats in a safe position by an emergency Return-to-Storage Command. The only means of insuring this maneuver is to provide a local backup battery source at each heliostat.

After accepting this conclusion, one could then return to candidates 1 through 3 and fill in all the "X's" if batteries were included with those candidates. However, the mechanical defocus mechanism may have questionable reliability if only exercised upon emergency conditions, and may tend to cause optical misalignment if subjected to repeated use. The operational shutter concept has other desirable properties but a good effective all weather design cannot compete with battery costs.

Hence the preferred approach becomes No. 4 using battery backup and normal gimbal drive to effect emergency defocus. Beam deflections of at least 3 degrees can be effected in less than 12 seconds by driving a single axis. Logic mechanization will automatically return each heliostat to storage after short term loss of communication or after a 30 minute interval of ac power loss.

Table 4-4. Emergency Defocus

0975-261

CANDIDATES	SUBMODE CAPABILITY EVALUATION							
	INITIAL RAPID REMOVAL		ENERGY DOME FOLLOW-UP MANEUVER		RETURN TO STOWAGE (POSSIBLE)		AUTOMATIC RESET AND RECOVERY	
	N	F	N	F	N	F	N	F
1. PROPOSED MECHANICAL STORED ENERGY DEVICE	X	X	X	O	X	O	X	O
2. SPRING LOADED MIRROR SHUTTER	X	X	X	X	X	O	X	O
3. NORMAL GIMBAL DRIVE	X	O	X	O	X	O	X	O
4. NORMAL GIMBAL DRIVE WITH LOCAL BATTERY BACKUP	X	X	X	X	X	X	X	X

N – NORMAL CONDITIONS
F – FAULT CONDITIONS: AC POWER OR CONTROL FUNCTION FAILURE
X – SUBMODE CAPABILITY PROVIDED
O – SUBMODE CAPABILITY NOT PROVIDED

Collector Subsystem

Analysis, Tradeoff, and Description of Power and Control System Components

DISTRIBUTION AND CONVERSION OF POWER

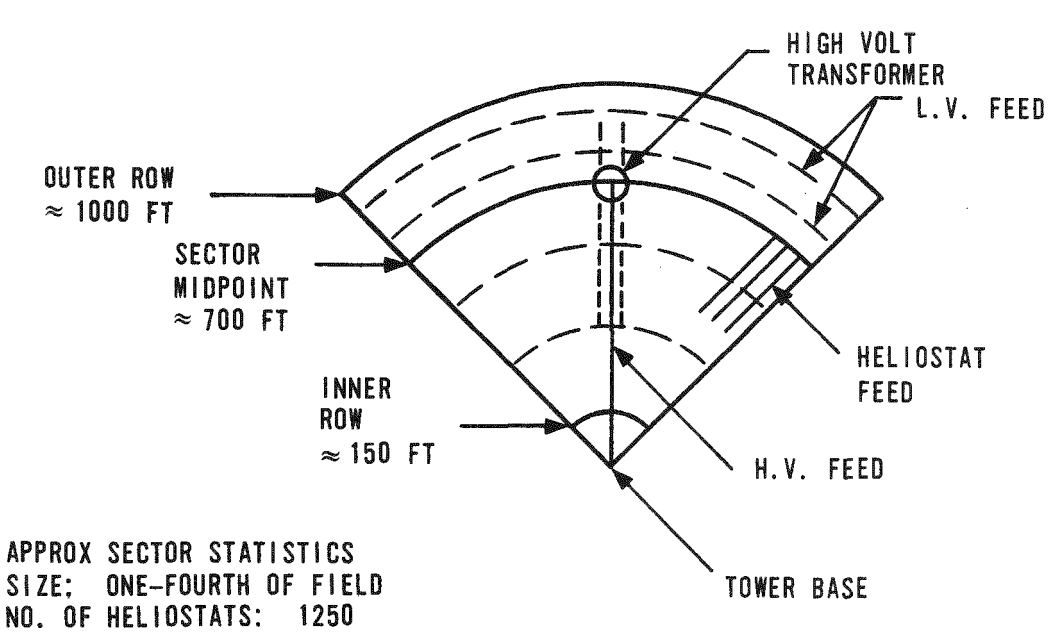
A high to low voltage ac grid with a battery at each heliostat provides the most efficient and failsafe method of providing power to the field of heliostats.

Three candidate systems were considered. They were (1) an ac grid capable of providing the heliostat peak power requirements, (2) a battery system with no grid, and (3) a battery system with a grid supplying only average recharge current. The pure battery system was eliminated because of high maintenance costs conservatively estimated to be $2700 per heliostat over a 30 year period. While the ac grid system was considered to be the least expensive of all, the ac grid and battery system was chosen because in the event of a failure in the grid, the battery would provide the power to (1) perform emergency defocus, (2) perform mirror stow and (3) continue operation for power interrupts of up to one hour or more.

The distribution system is mechanized as follows. To reduce line losses, as high a voltage as is both practical and in common use will be used to feed power to sectors of the field. Here it will be transformed to a more safe and usable level for distribution to the individual heliostats. At the heliostat a charger will continuously resupply the battery which will be of the sealed type for low maintenance. The charger will be of the constant current limited voltage type for prolonged battery life. The battery voltage will be used to supply the high motor current pulses directly, while an inverter with individual rectifiers and integrated circuit regulators will supply the low voltage requirements of the motor controller electronics. The ac grid distribution system is shown in Figure 4-22, with the heliostat power supply shown in Figure 4-23.

Areas around the high voltage transformers in the field will be contained in locked enclosures to prevent accidental contact by field personnel performing routine maintenance. High voltage feeder lines will also be made inaccessible and will probably be routed via underground means.

One of the expressed purposes of the field battery is to provide the power to continue tracking during an ac power interrupt condition. Further, it should have sufficient reserve to allow stowage of the mirror should the ac not be resumed in 0.5 to 1 hour. The 6 amp/hour battery proposed will provide the estimated requirements to 0°C over the life of the battery which is expected to be 8-9 years. To provide that same reserve to -20°C, it is estimated that a battery with twice this capacity will be required costing an estimated 43 percent more. Plant site characteristics and availability should be carefully weighed in trading off this environmental consideration versus cost.



APPROX SECTOR STATISTICS
SIZE: ONE-FOURTH OF FIELD
NO. OF HELIOSTATS: 1250
H.V. TRANSFORMER: 1 @ 30 KW SECONDARY RATING
AVERAGE POWER: 6.5 KW
PEAK BATTERY POWER: 116K
H.V. FEED: 700 FEET (ROUTE)

Figure 4-22. AC Grid Distribution System

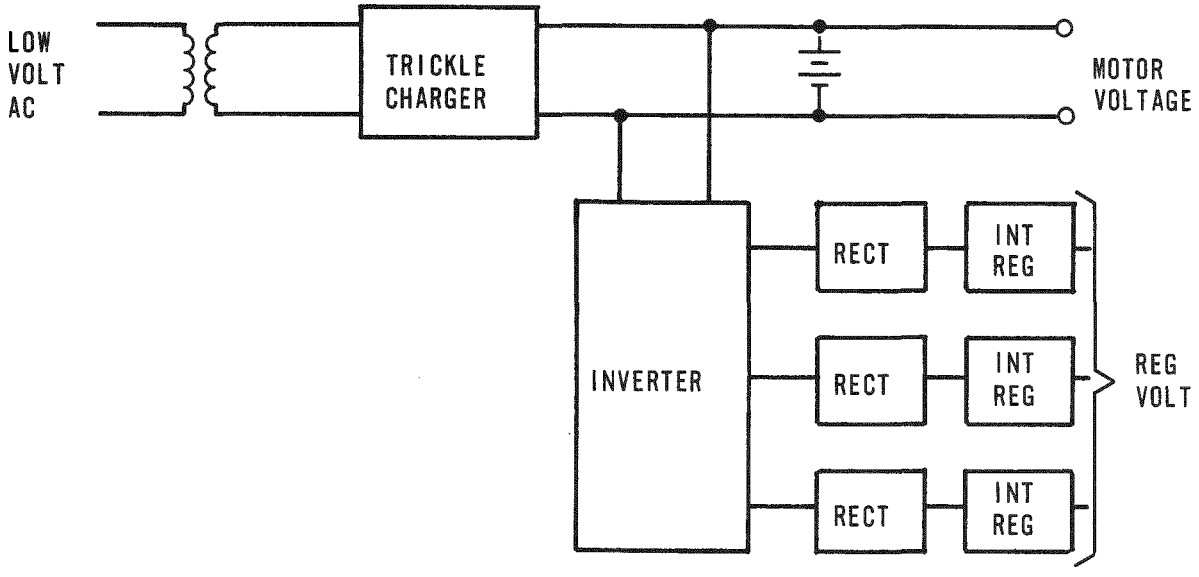


Figure 4-23. Heliostat Power Supply

Collector Subsystem

Analysis, Tradeoff, and Description of Power and Control System Components

MULTIPORT INPUT/OUTPUT SERVICES HELIOSTATS, PLANT CONTROLLER AND OPERATOR

The control of thousands of heliostats, their calibration and the input of GMT, meteorology data, plant and operator inputs requires a large I/O throughput which can be satisfied by direct memory access.

The method proposed for servicing heliostats consists of sending two 8-bit bytes for each heliostat each second. One byte will contain the address of the heliostat and the other byte contains the control information. To do this efficiently the computer selected must have multiple direct memory access (DMA) capability. This feature allows the computer to set up a table of values for a sector of heliostats, then initiate the DMA output once. The processor is then free to go compute the next sector values while the DMA meters out all the bytes to the previous sector. This technique will allow the selected computer to handle the largest possible number of heliostats.

A Greenwich Mean Time input of days, hours, minutes and seconds is an essential part of the Sun tracking algorithm. An always accurate digital clock monitoring the NBS radio station WWVB will provide this input. This station operates at 60 kHz from Boulder, Colorado, and is a very reliable signal in all areas of the country. Another advantage of using this time code, instead of a local oscillator, is the automatic reset at power turn on or after a power outage.

Meteorological data is readily available in analog form from a variety of sensors. An analog to digital converter will be necessary to input temperature and pressure inputs for refraction corrections, and wind speed and direction for safety purposes. For example, heliostats could be commanded to turn their mirror surfaces away from a blowing sand storm, or, automatic shut down on detection of high surface winds. Pyranometers are also available and would be useful for correlating insolation data with calibration performance data.

Inputs from the plant controller via a command serial data link will provide instructions to the processors for control of the heliostats. Special startup and shutdown sequencing or vernier temperature balancing are examples of such commands. A baud rate of 4800 would provide communications at 300 16-bit words per second.

An operator interface is required for status, maintenance and safety considerations. Each processor would drive a visual display constantly giving the status of its quadrant. This display would report such things as GMT, wind data, mode of operation, number of heliostats on receiver, number of heliostats on offset point, which heliostat is in calibration and a report of all anomalous conditions. These, of course, would be output on a printer so that maintenance functions could be scheduled.

An operator input will also be required to inform the processor of heliostats to be returned to service following maintenance, to request mode changes or to insert emergency commands. Another operator function would be to command the spare computer to take over the functions of any quadrant if its computer was suspected of malfunction.

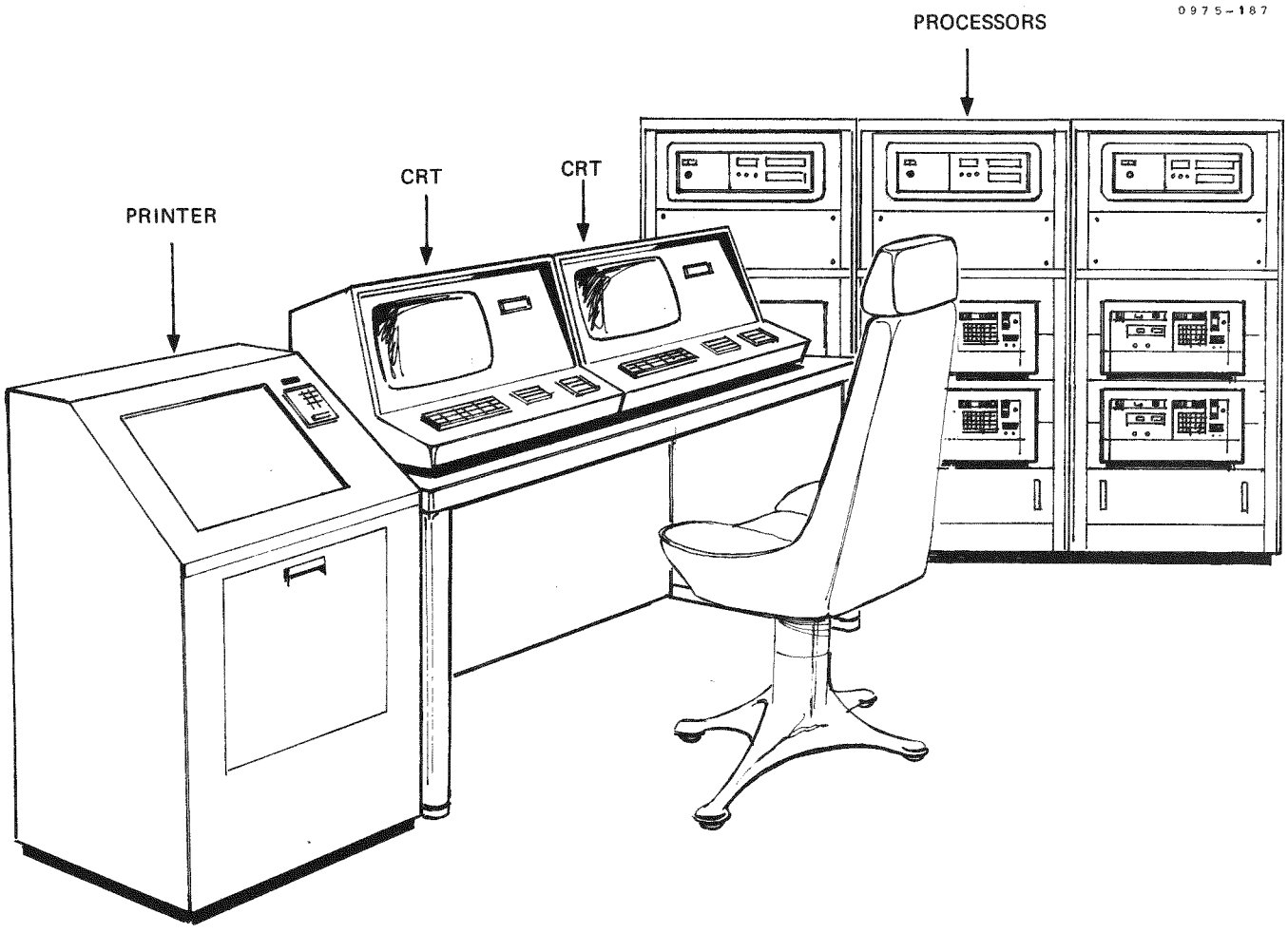


Figure 4-24. Control Panel

Collector Subsystem

Summary Characterization of Concept Design

ACHIEVING SYSTEM AVAILABILITY

The degree to which high availability of the Solar Collector Subsystem can be obtained is determined primarily by design and application feature which establish reliability and maintainability characteristics of the system.

The relationships of design reliability and maintainability to achieving high availability are reflected in the illustration.

The dawn to dusk mission reliability of the solar collector subsystem is enhanced in the design architecture by both functional partitioning and circuit redundancy techniques. Functional partitioning is employed for both operating power distribution and signal distribution. The heliostat power matrix is divided into 12 13K volt power busses with reductions to 110 volts for local distribution. Drive command pulses to heliostats are provided from four processors, one for each quandrant. The processor commands are further distributed by Global networks serving 400 heliostats, one hundred each on four output transmission lines. This partitioning scheme reduces the impact of individual signal or power failures consistent with minimum system complexity.

Redundancy is under continuing study to establish the most cost-effective points at which circuits or signals should be duplicated. Three areas have been identified as major candidates. These are the real-time clocks, processors (one or more backups to the four processor system) and batteries for each heliostat (which provide for emergency shutdown).

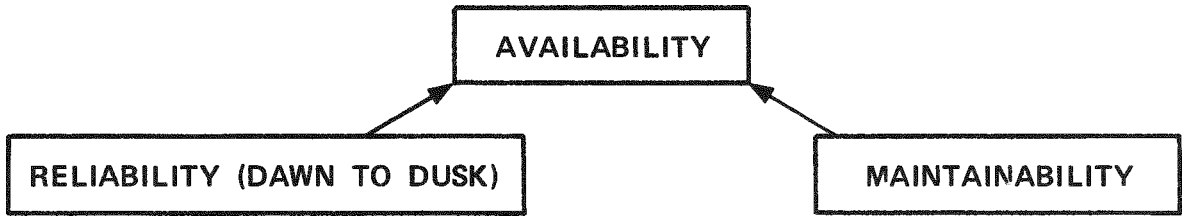
Operational reliability and installation cost are also direct functions of the quality of electronic and electromechanical products used in the manufacture of the heliostats. With well over a million electrical parts in just the drive signal distribution, it is clear that maintenance features and system tolerance to component failure will play a major role in determining the need for enhanced part level reliability.

The solar collector maintenance philosophy must be based upon the dual objectives of obtaining operational readiness at the beginning of the day and maintaining the operation of system critical functions during the day. Hence it is expected that overhauls, battery or stepper motor replacements and most individual heliostat repairs would be accomplished at night. Loss of critical functions such as global failure (affecting 400 heliostats), a processor which requires the backup to be switched in or failure in the calibration array would be repaired immediately upon detection.

The ease with which repairs can be made, or serviceability, is also a significant design parameter. Serviceability is a function of both the effectiveness of the fault detection scheme and the accessibility and modularity of the design. The primary fault detection feature of the collector subsystem is the periodic heliostat calibration. Failures to yield satisfactory calibration patterns (at

6-hour intervals) are output to the operators' teletype. Sensors at the heliostats also detect catastrophic loss of power which causes emergency shutdown of the affected unit to the storage position using battery power.

The simplicity and modularity of the concept design heliostats and their distribution system reduces repair and logistics problems of a large system to manageable proportions. It is anticipated that problem diagnosis will be straightforward and replacements swiftly executed by semi-skilled maintenance personnel. Easily replaceable items on the heliostats should include stepper motors, small gear boxes, batteries, limit switches, the interface circuit board and cable segments. Heliostat realignment is not expected to become necessary as a result of normal repairs.



- REDUNDANCY FEATURES
  - REAL-TIME CLOCKS
  - BATTERY BACKUP POWER
  - STANDBY SPARE PROCESSOR
- FUNCTIONAL PARTITIONING
  - SIGNAL DISTRIBUTION VIA GLOBALS
  - DEDICATED SECTOR PROCESSORS
  - POWER DISTRIBUTION MATRIX
- QUALITY GRADE OF COMPONENTS
- REPAIR PHILOSOPHY
  - DAYTIME REPAIR OF CRITICAL FUNCTIONS
  - ROUTINE MAINTENANCE AT NIGHT (OPERATIONAL READINESS)
- DESIGN FOR MAINTENANCE
  - FAULT DETECTION
  - SERVICEABILITY
  - MODULARITY

Figure 4-25. Solar Collector Subsystem Availability is Established by Reliability and Maintainability Features of the Design

Collector Subsystem

Summary Characterization of Concept Design

ESTIMATED COST FOR PILOT PLANT SCALE

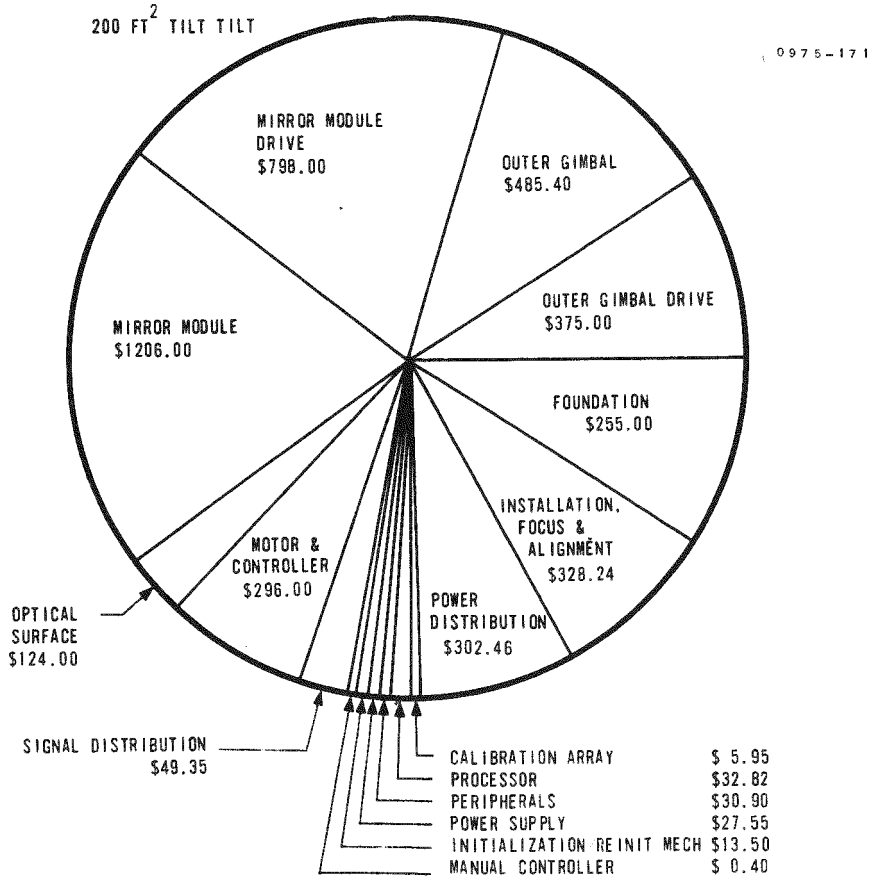
The credibility of the preliminary pilot plant ROM estimate summarized is the storyboard titled "Rough Estimate Identifies Cost Sensitivities" is established by a review cost makeup.

Table 4-5. Estimated Cost for Pilot Plant Scale

	Usage	Unit Cost	Cost Per Heliostat		Cost For 4968 Heliostat Field
Foundation			$ 255.00		$ 1,266,840
Support Tubes 6"x10"x8'	2	$ 62.50	$125.00		
Slab 4'x4'x1'	2	56.00	112.00		
Slab 1'x1'x1'	2	4.00	8.00		
Interface Brackets	2	5.00	10.00		
Outer Frame Drive			$ 375.00		$ 1,863,000
Ball Screw and Bellows	2	$ 150.00	$300.00		
Pivot Assembly	2	7.50	15.00		
Motor Mount and Reducer	1	60.00	60.00		
Outer Frame			$ 485.40		$ 2,411,467
Steel Frame	1	$ 300.00	$300.00		
Diagonal Braces	3	5.00	15.00		
Stub Shafts	2	2.50	5.00		
Collars	4	2.00	8.00		
Bearings and Axles	2	24.00	48.00		
Ball Drive Brackets	2	7.50	15.00		
PB Support - 12"	8	6.00	48.00		
Pillow Block Mounts	8	5.00	40.00		
Bolts - PB Assembly	32	.20	6.40		
Mirror Module Drive			$ 798.00		$ 3,964,464
Pillow Blocks	8	$ 14.00	$112.00		
Crank Arms 1/2"x4"x30"	8	12.00	96.00		
Tie Rods	6	17.50	105.00		
Drive Sprockets w/Chain	2	80.00	160.00		
Pillow Blocks	2	11.00	22.00		
Jack Shaft	1	1.00	1.00		
Lever Take-Up	1	10.00	10.00		
Speed Reducer	1	212.00	212.00		
Assembly		80.00	80.00		
Optical Surface			$ 124.00		$ 616,032
3/32 Mirrored Glass	200 ft^2	$.56/$ft^2$	$112.00		
Mirror Holes		12.00	12.00		
Mirror Module (4)			$1,206.00		$ 5,991,408
Mirror Mounting Hardware	75	$ .20	$ 15.00		
Honeycomb	200 sq ft	3.62/sq ft	724.00		
Butyl Sealant	64 ft		4.00		
Honeycomb Mounting Hardware			3.00		
Frame and Axle	4	112.50	450.00		
Ball Joint	1	10.00	10.00		
Power Supply			$ 27.55		$ 136,868
Transformer	1	$ 10.00	$ 10.00		
Diode	8	.35	2.80		
Capacitor	1	4.00	4.00		
Regulator	2	3.00	6.00		
LM309K	1	2.75	2.75		
Spark Gap	2	1.00	2.00		
Motors and Controller			$ 296.00		$ 1,470,528
Logic Elements	20	$ 1.00	$ 20.00		
Transistor - Power Output	6	1.50	9.00		
Vector Board	1	2.00	2.00		
Edge Connector	2	.50	1.00		
Connector-Manual Controller	1	3.00	3.00		
Jones Strip Connector	1	3.00	3.00		
Assembly Labor		58.00	58.00		
Stepper Motors	2	100.00	200.00		
Initialization Mechanism			$ 13.50		$ 67,068
Optical Pair	4	$ 2.00	$ 8.00		
Magnets	6	.25	1.50		
Housing and Armature	2	2.00	4.00		
Installation, Focus and Alignment			$ 328.24		$ 1,630,696
Assembly Labor			$328.24		
Power Distribution			$ 302.46		$ 1,502,621
Interconnect Cable	26.4 LF	$ .50/LF	$ 13.20		
Cable Installation	26.4	1.50/LF	39.59		
Batteries (Initial)	3	13.79	41.37		
Charger	1	13.50	13.50		
Inverter	1	20.00	20.00		
Cost of Ownership					
Battery Changes	3.5	$ 41.00	$144.80		
Installation		30.00	30.00		
Signal Distribution			$ 49.35		$ 505,480
Global	17	$8,500.00		$144,500.00	
Interconnect Cable	100,000 LF	.50		50,000.00	
Cable Installation	100,000 LF	.50		50,000.00	
Line Drivers	132	5.00		660.00	
Converter			$ 52.50		
Uart	1	8.00	$ 8.00		
Schottky, Low Power	12	1.00	12.00		
Assembly Labor		30.00	30.00		
Receiver	1	2.50	2.50		

Table 4-5. Estimated Cost for Pilot Plant Scale (Concluded)

		Usage	Unit Cost	Cost Per Heliostat		Cost For 4968 Heliostat Field
Calibration Array (12)				$ 5.95		$ 29,580
Photodiodes	1,728	$ 2.00			$ 3,456.00	
Operational Amps	1,728	1.50			2,592.00	
Column Area and Moment Mult						
Resistors	1,872	.05			93.60	
OP Amps	288	1.50			432.00	
Total Area and Moment Sum						
OP Amps	48	1.25			60.00	
Dividers	24	20.00			480.00	
PC Boards w/Conn	24	2.00			48.00	
+15V Power Supply	12	100.00			1,200.00	
-15V Power Supply	12	100.00			1,200.00	
Chassis, Hardware, etc.	12	25.00			300.00	
Assembly Labor	12	1,644.00			19,728.00	
Processor				$ 32.82		$ 165,800
DDP716 Processor	5	$18,760.00			$ 93,800.00	
Cost of Ownership	360 mo	40.00/unit			72,000.00	
Peripheral Equipment				$ 30.90		$ 153,525
CRT w/Keyboard	5	$2,350.00			$ 11,750.00	
NCR Printer	5	2,195.00			10,975.00	
Disc Storage	1	30,000.00			30,000.00	
Cost of Ownership						
CRT	360 mo	35/unit			63,000.00	
NCR Printer	360 mo	15/unit			27,000.00	
Disc Storage	360 mo	30			10,800.00	
Manual Controller	10	$ 200.00		$ .40		$ 2,000
TOTAL				$4,383.07		$21,790,095



Collector Subsystem

Summary Characterization of Concept Design

COST EFFECTIVENESS FEATURES OF THE OPERATIONAL PLANT SCALE

The cost effectiveness features at an operational point scale involve not only larger volume discounts but get into a region where custom components, dedicated production lines, and even new industries become feasible.

The projected average heliostat cost is $1,895 each, or $6.32 per square feet of mirror.

This assumes:

85 percent learning curve on labor

85 percent learning curve on material, except steel

No improvement in steel cost with higher volume

300 square feet of mirror per heliostat in operational plant configuration

Dedicated facility or division with low burden, G.O., and profit center.

Projected Average Heliostat Cost

0975-223

Single heliostat LBM cost with all distributed costs prorated to heliostat	$1,895
Assumed factory G.O. at 12 percent	227
Assumed factory profit at 8 percent	170
Total	$2,292

Total price per square foot $7.64

85 percent learning curve, except steel

300 square feet of mirror in operational plant configuration

Dedicated facility, low burden, G.O., profit

Blank

SECTION V
RECEIVER SUBSYSTEM

	Page
Concept	5-2
Tower Structure	5-4
Tower Piping	5-10
Steam Generator Housing	5-14
Costs	5-22
Steam Generator	5-24

Receiver Subsystem

CONCEPT

The receiver has been designed as a tower-mounted cavity with an annulus type aperture, as shown in Figure 5-1, because a cavity receiver has a higher throughput efficiency than any non-cavity-type receiver and because a circular, 360 degree, heliostat field has been shown to be the most efficient heliostat configuration in terms of annual redirected energy per unit area of mirror surface.

1. A right circular cylinder was chosen because of simplicity of construction and because the boiler and superheater tube configuration and construction can be similar to a conventional, fossil-fuel-fired steam generator.

2. The choice of a right circular cylinder for the steam generator housing also simplifies the design and construction of the cavity supports (corbels).

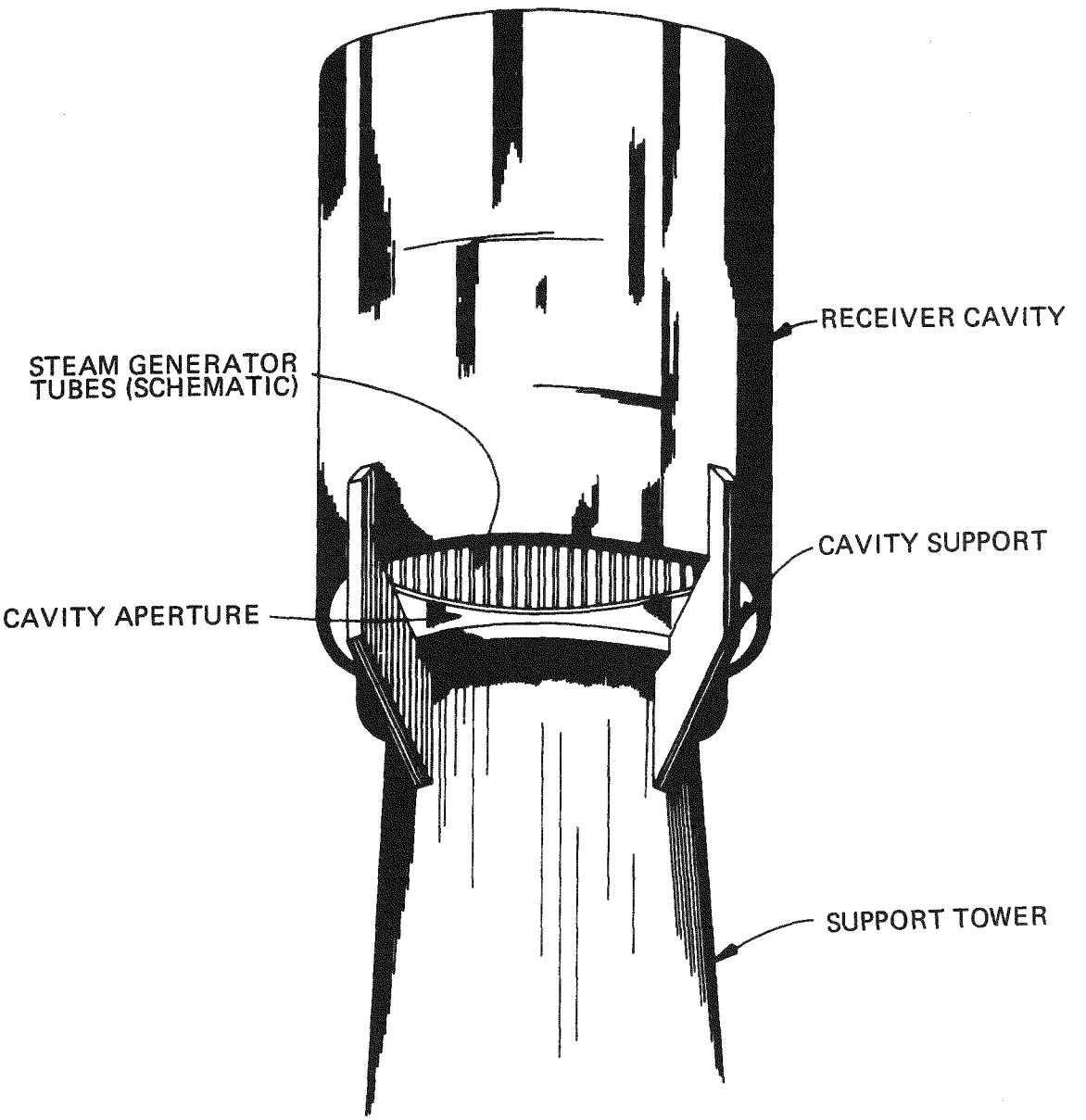


Figure 5-1. Receiver Concept

Receiver Subsystem

Tower Structure

TYPE OF CONSTRUCTION

The tower structure has been designed as a circular, tapered, column fabricated of reinforced concrete using a slipform technique because a tradeoff analysis with regard to reliability, load-carrying capacity, capital cost, speed of erection, available space for ancilliary equipment, and environmental protection for this ancilliary equipment indicated that this type of column is superior to alternatives such as welded steel and guyed steel columns.

1. Reinforced concrete chimneys have performed reliably in power plants for many decades.

2. A commercial size unit will require a tower height in excess of 1000 feet and a receiver weight in excess of 1000 tons. No other type of column can support this load at this height as inexpensively as a column of this type.

3. Rust Chimney Company recently won the largest chimney contract ever awarded, nearly $15,000,000, for two 1000-foot tall chimneys to serve a power plant in Arkansas. This demonstrates that the capital cost of very tall chimneys is not excessive.

4. The world's largest chimney is 1250 feet tall at the INCO Copper Cliff Smelter in Sudbury, Ontario. The chimney walls were erected in 12 weeks, by the M. W. Kellogg Company, using a continuous slipforming technique. In this technique, there are two movable collars which become the inside and outside forms for the chimney. Each of the two collars is made up of overlapping steel plates which squeeze together, as the chimney rises, to create the necessary taper. A slipforming setup is shown in Figure 5-2.

5. Because the central shaft is very large, there is adequate space for piping, wiring, and an elevator. The concrete shell provides environmental protection for all this equipment.

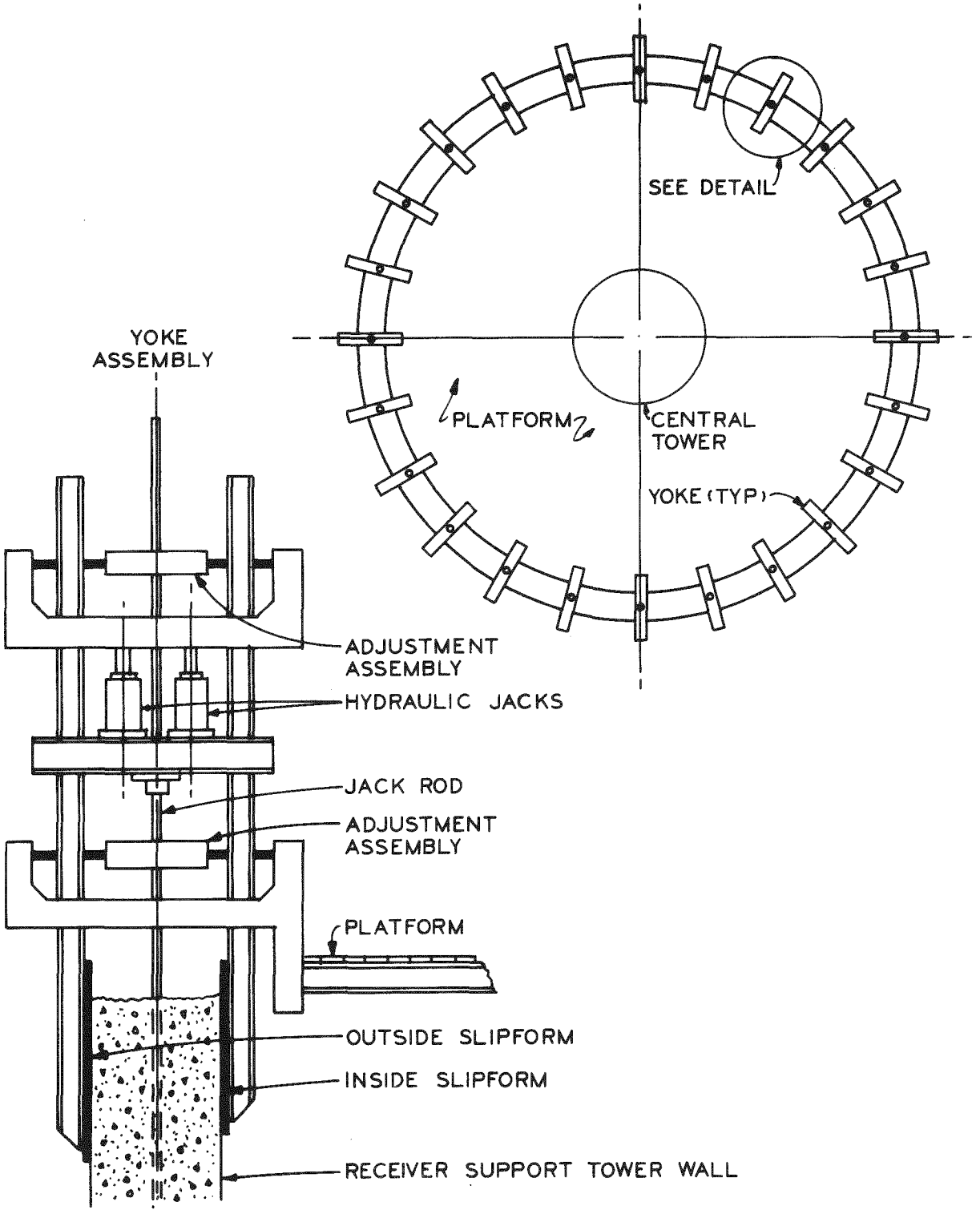


Figure 5-2. Slipforming Arrangement

Receiver Subsystem

Tower Structure

DIMENSIONS

The top diameter and height of the tower have been determined by optical tradeoff analyses, and the thickness and taper of the tower have been determined by structural considerations.

1. The top diameter and height of the tower have been chosen by raytrace analysis, to optimize the total energy absorbed by the cavity, over the year, per unit area of mirror surface.

2. The dimensions of the tower structure are shown in Figure 5-3.

3. The base on which the tower sits is also made of reinforced concrete. This base is an octagon 90 feet (27.4m) in diameter and 8 feet (2.4m) thick.

4. The tower base was designed for a soil-bearing pressure of 2 tons/ft^2 (0.191 x 10^6n/m^2). This is an average value for the Southern California area. The final design would depend on the soil conditions at the selected site.

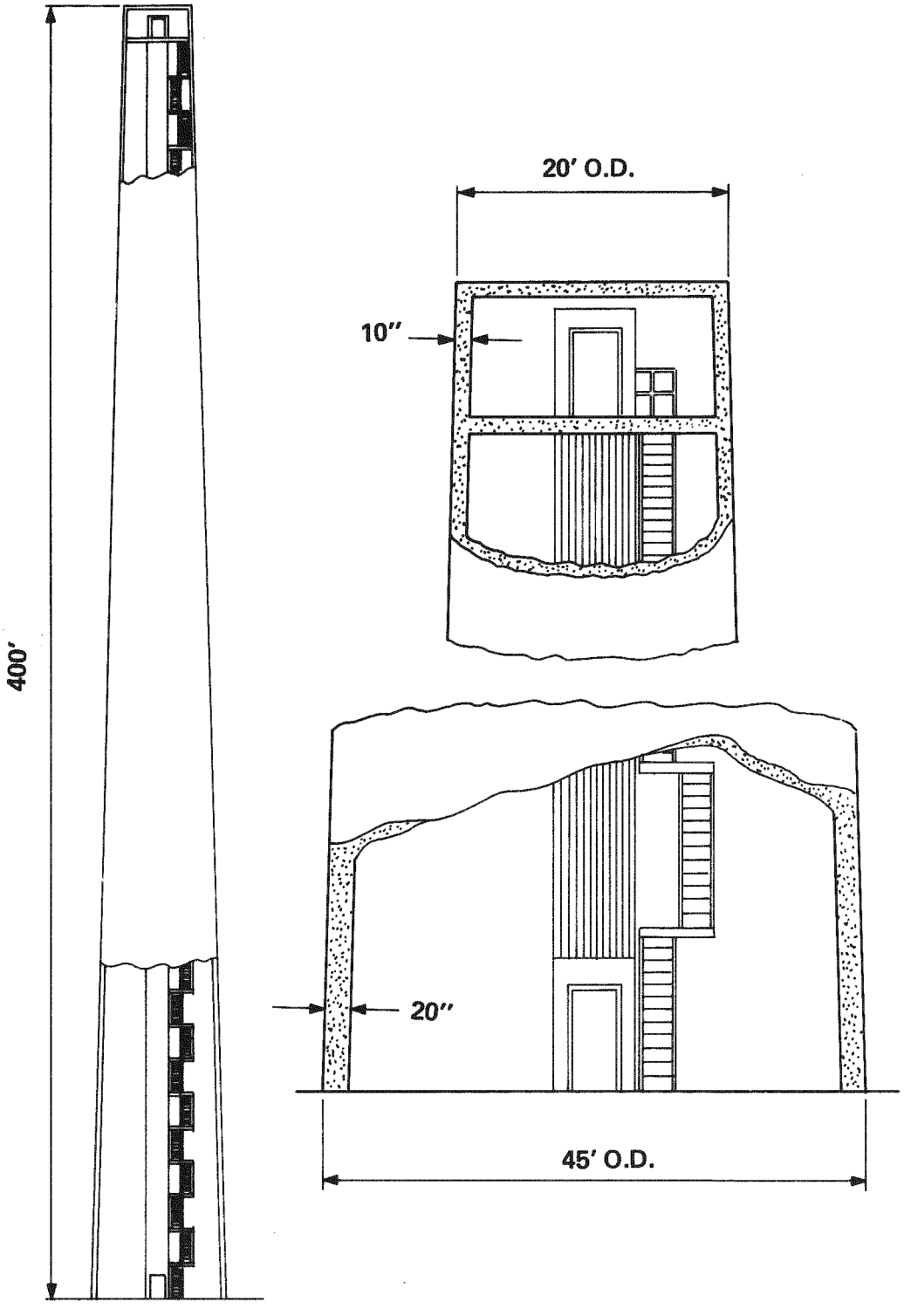


Figure 5-3. Support Tower

Receiver Subsystem

Tower Structure

RADIATION PROTECTION

The top of the tower structure, the base of the steam generator housing, and the three corbels will be protected from errant radiation by stainless steel radiation shields, as shown in Figures 5-4 and 5-5, because shields of this type are reliable, inexpensive, maintenance free, and will continue to function despite environmental degradation.

1. Analysis has shown that shields of this type can withstand a steady flux in excess of 200 kW/m^2. This analysis did not include the cooling effect due to wind. If any wind were present, the allowable flux would be significantly increased.

2. Shields of this type do not rely on polished or otherwise treated surfaces and will, therefore, function over the plant lifetime without periodic maintenance.

3. As shields of this type become hotter, the air inside the shielding is also heated. This heated air rises and provides forced convection cooling of the shielding surfaces.

4. Because the surfaces which make up the shielding are thin and flexible, they are free to expand in a bending mode when heated. Thermal stresses are, therefore, minimized.

5. Analysis has shown that the tower structure and corbels will have surface temperatures below 200°F (93°C). The corbels will, therefore, be suitable for containing electrical control and power distribution wiring.

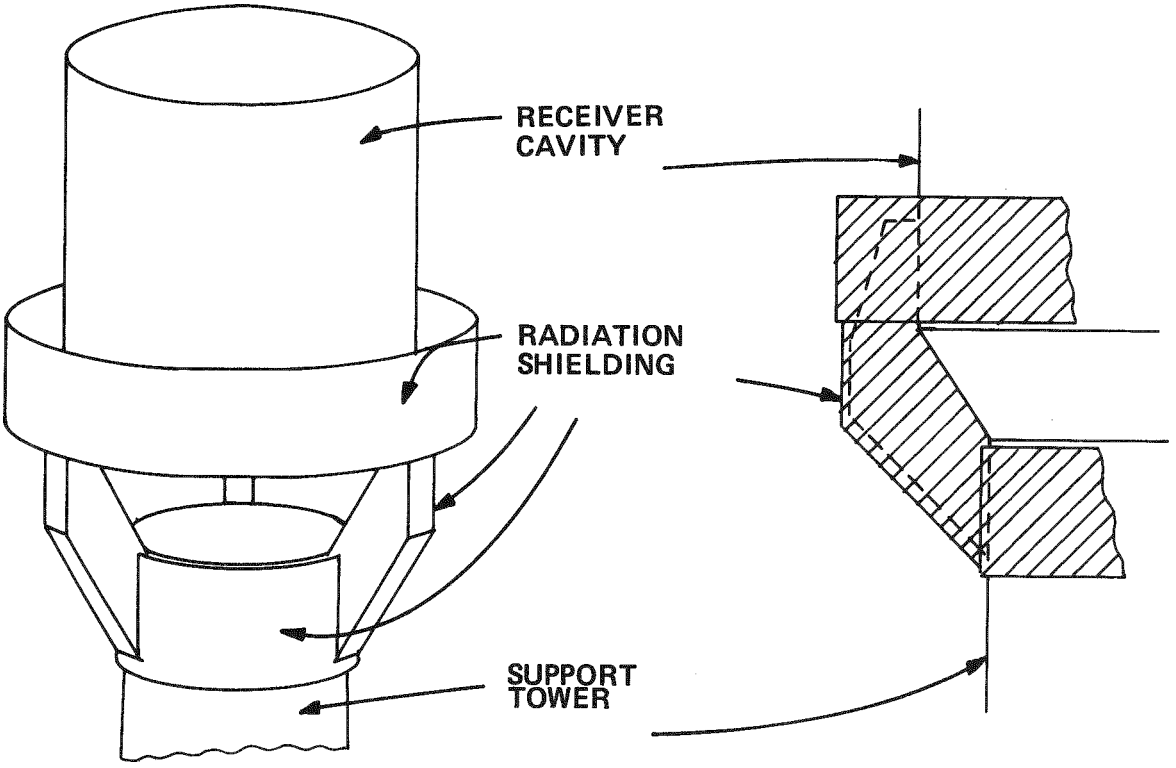


Figure 5-4. Radiation Shielding

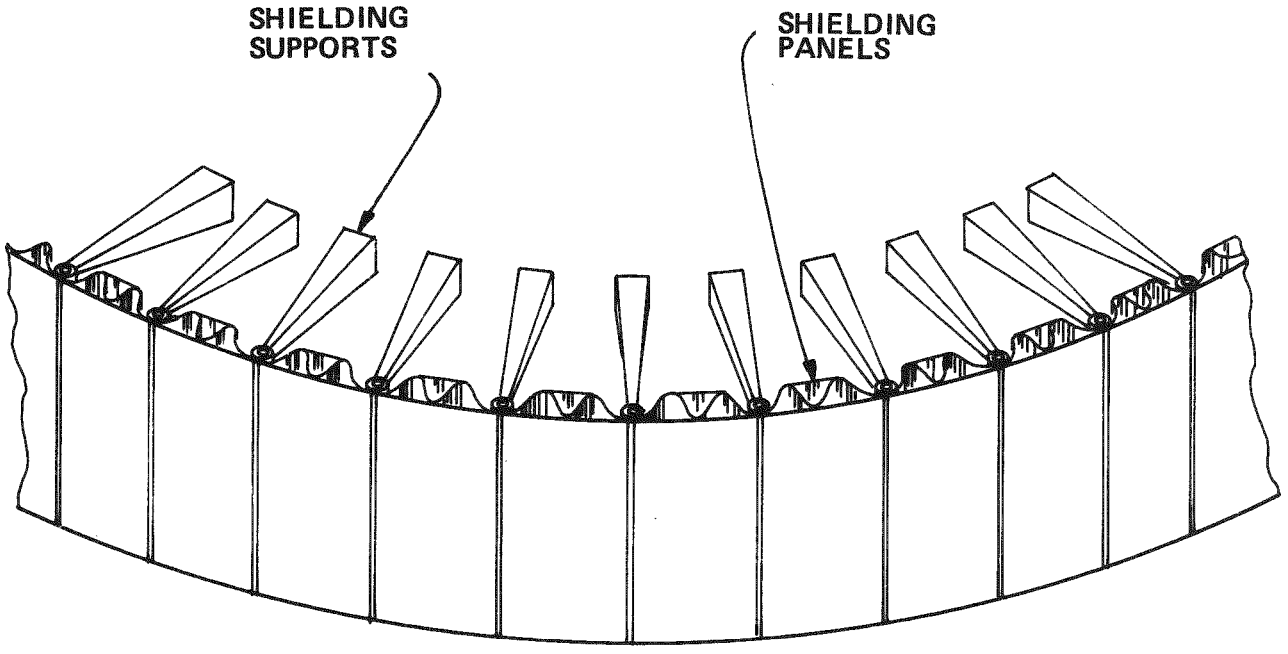


Figure 5-5. Radiation Shielding

Receiver Subsystem

TOWER PIPING

The tower piping has been sized, routed, and supported to provide reasonable fluid velocities, to yield reasonable pressure drops, and to withstand the stresses due to internal pressure, thermal expansion, dead loads, and seismic activity.

1. The feedwater line and main steam line were sized to contain the maximum rated mass flow at a steam velocity below 12,000 feet/minute (61.0 m/sec) and a water velocity below 750 feet/minute (3.81 m/sec).

2. At the maximum rated mass flow, the pressure drops due to friction are approximately 22 psi (0.151×10^6 n/m^2) in the feedwater line and 45 psi (0.310×10^6 n/m^2) in the main steam line.

3. The piping specifications, as given in Table 5-1, will withstand the stresses due to internal pressure at the operating temperatures. These specifications are in accordance with the ASME Boiler and Pressure Vessel Code.

4. The expansion loops, as shown in Figure 5-6, will provide sufficient flexibility to absorb the thermal expansion without causing unacceptable stresses. These expansion loops also provide sufficient flexibility to absorb the downward thermal expansion of the steam generator.

5. The hangers used, as shown in Figure 5-7, are designed to withstand the loads imposed by dead weight, thermal expansion, and seismic activity.

Table 5-1. Tower Piping Specifications

	Feedwater Line	Steam Line
Nominal Size	4 in.	8 in.
Schedule	120	140
Material	A106 B carbon steel	P12 alloy steel
Outside Diameter	4.500 in.	8.625 in.
Inside Diameter	3.624 in.	7.001 in.

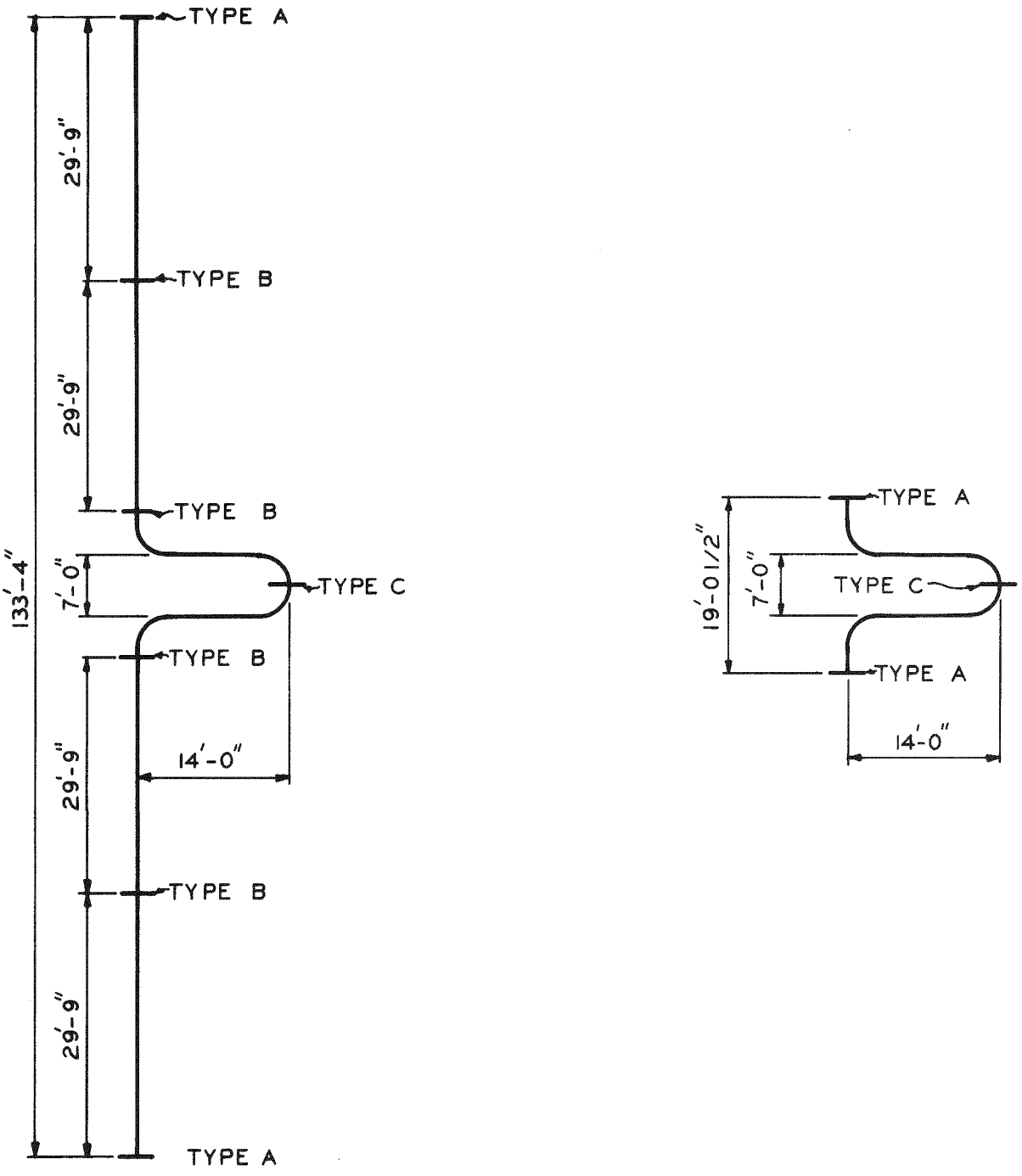


Figure 5-6. Tower Piping Expansion Loops

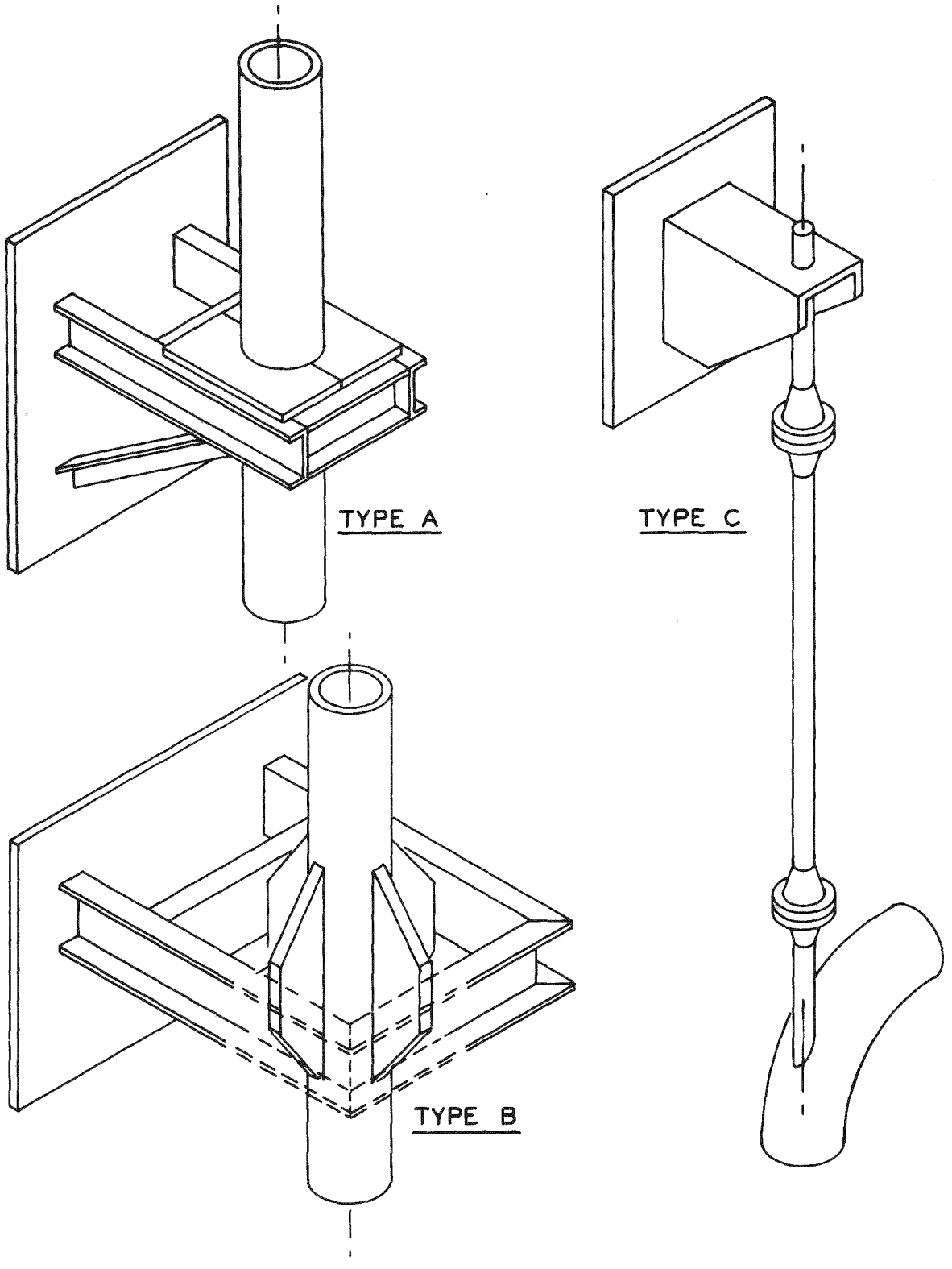


Figure 5-7. Tower Piping Hangars

This page intentionally left blank.

Receiver Subsystem

Steam Generator Housing

GEOMETRY AND MATERIALS

The steam generator housing and supports have been designed, as shown in Figures 5-8 and 5-9, based on wind loading, load-carrying capacity, seismic loading, weight, capital cost, and ease of erection.

1. Structural steel, rather than concrete, was selected for the steam generator housing and corbels because this choice reduces the weight of the steam generator housing and reduces the size of the corbels.

2. The corbels were designed, as shown in Figure 5-8, to withstand the stresses imposed by dead loads, wind loads, and seismic loads. The wind loads were calculated in accordance with the Black & Veatch Standard Practices Manual which is in accordance with the standards promulgated by the American National Standards Institute (ANSI). The seismic loads were calculated based on a Seismic Zone III Safe Shutdown Earthquake (SSE), in accordance with Nuclear Regulatory Commission (NRC) Reg. Guide 1.60.

3. The corbels were designed as box beams with internal stiffeners. The design was carried to sufficient detail to ensure that corbels of this type could withstand the applied loads. The design of the stiffeners was not finalized.

4. The radiation shields are not shown in these drawings.

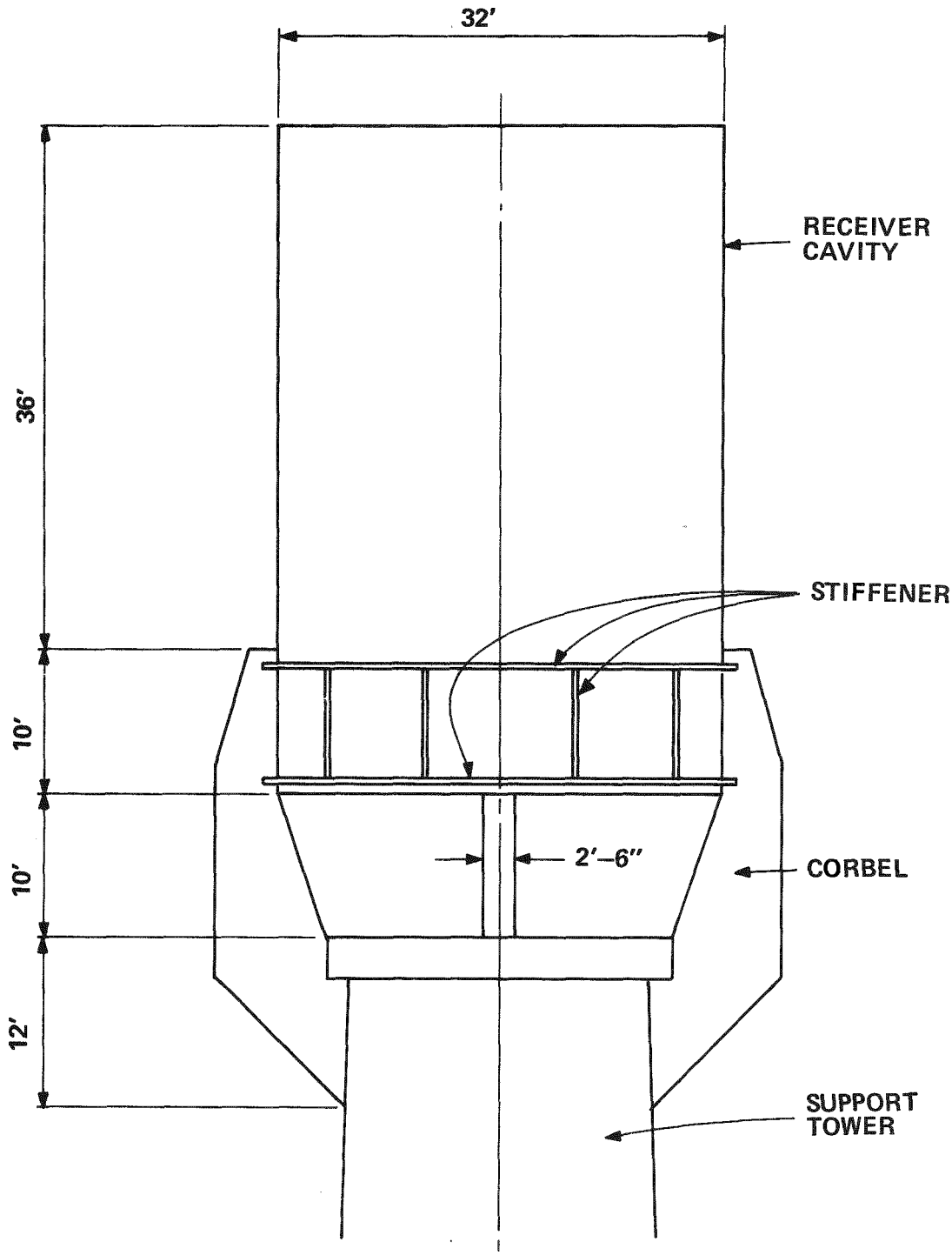


Figure 5-8. Steam Generator Housing and Supports

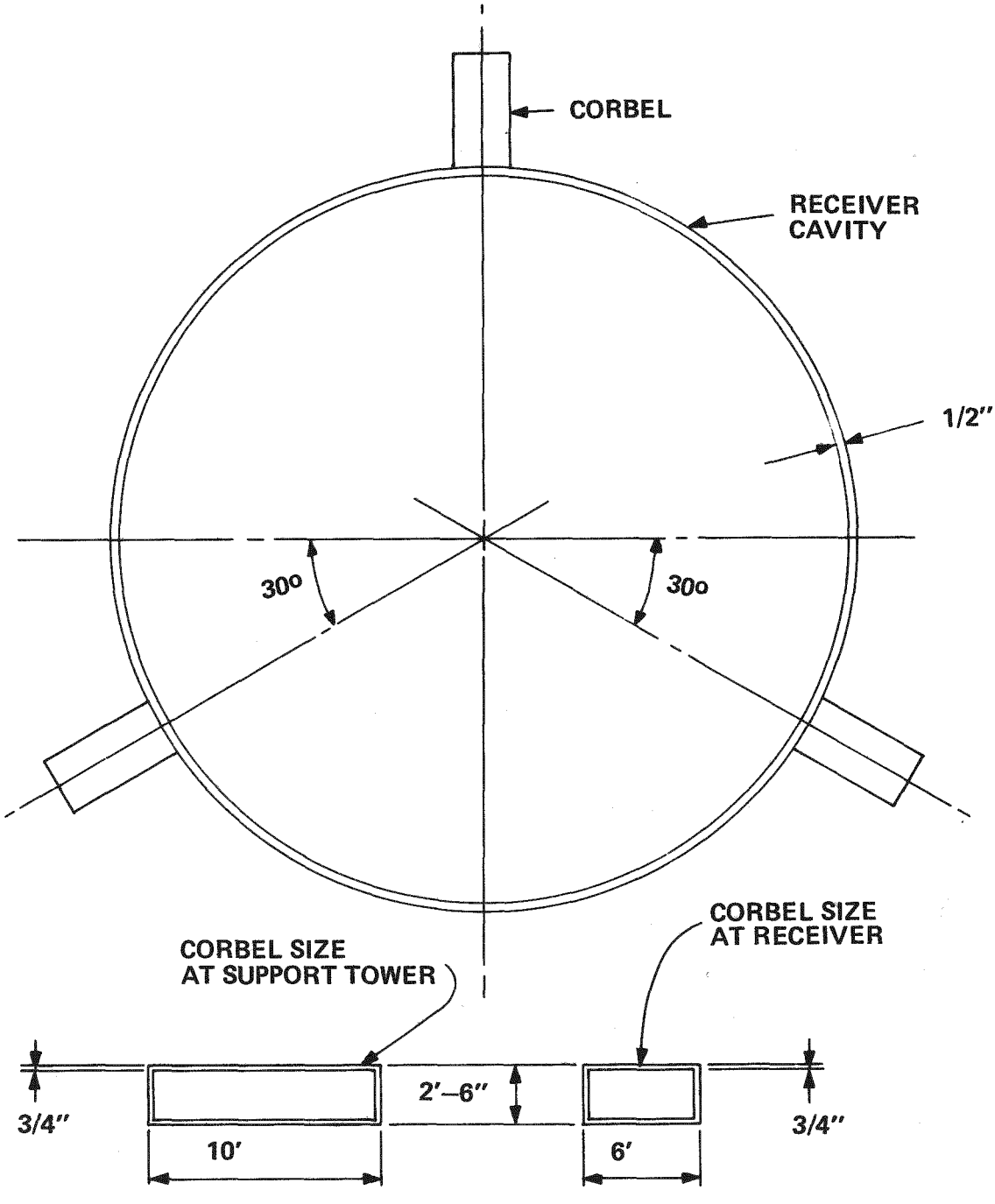


Figure 5-9. Steam Generator Housing and Supports

This page intentionally left blank.

Receiver Subsystem

Steam Generator Housing

APERTURE DOORS

The cavity will be provided with aperture doors, as shown in Figures 5-10 and 5-11, in order to minimize the loss of thermal energy during nighttime hours and in order to assist in maintaining an elevated cavity temperature and thereby reduce start-up time.

1. Doors of this type can be retracted into a position behind the radiation shields.

2. The operating mechanisms of these doors are also located behind the radiation shelds.

3. The hydraulic actuating mechanisms shown in Figure 5-11 are one possible design. No decision has been made on the actual method of operation of these doors.

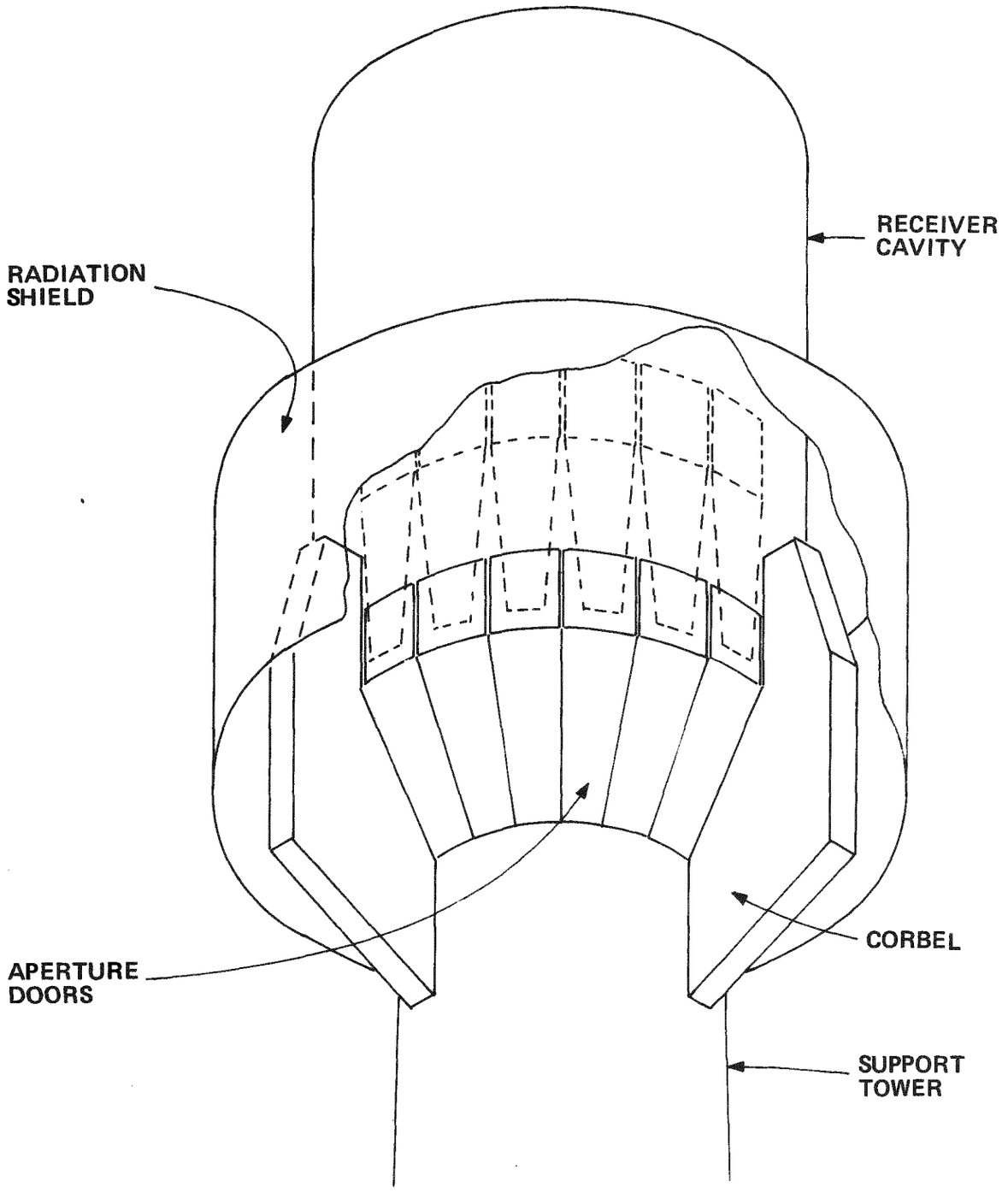


Figure 5-10. Aperture Doors - Closed Position

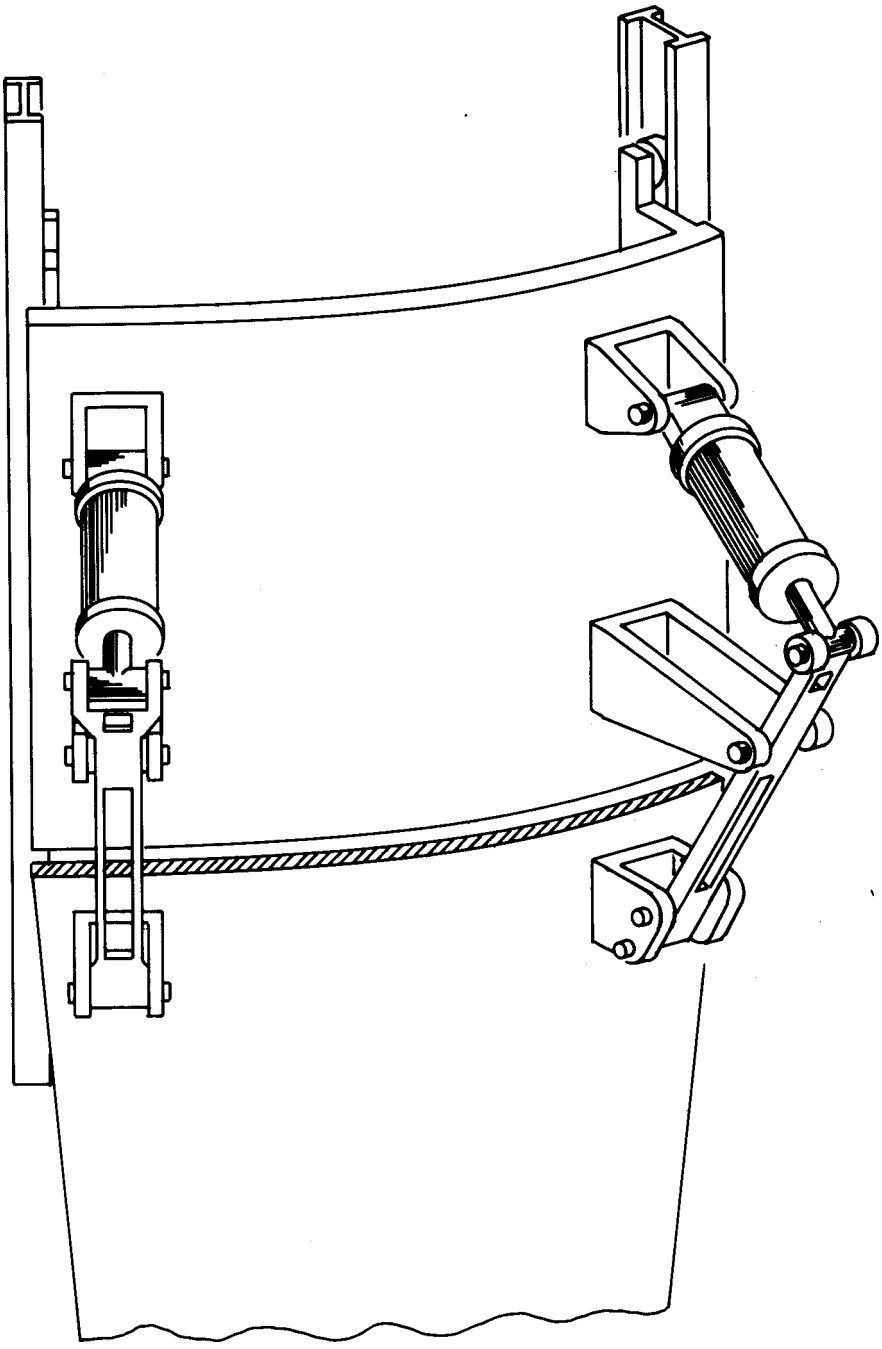


Figure 5-11. Aperture Door Operating Mechanism

This page intentionally left blank.

Receiver Subsystem

COSTS

The capital costs of the elements of the receiver subsystem, excluding the steam generator, are given in Table 5-2.

1. These costs were developed for orders placed presently, with construction to follow immediately.

2. The costs of auxiliary equipment such as the elevator, aircraft warning system, ladders and catwalks, and required safety equipment are not included in these costs. These additional costs are not expected to represent more than 10 percent of the receiver subsystem cost.

Table 5-2. Receiver Subsystem Capital Costs

Tower Structure (Including Base)		$ 930,000
Feedwater Line		
Pipe	5,000	
Pipe Installation	16,000	
Pipe Insulation	5,000	
Hangers	7,000	
Hanger Installation	12,000	
Subtotal		45,000
Steam Line		
Pipe	70,000	
Pipe Installation	90,000	
Pipe Insulation	13,000	
Hangers	19,000	
Hanger Installation	10,000	
Subtotal		202,000
Steam Generator Housing		100,000
Corbels		70,000
TOTAL		$1,347,000

Steam Generator

Steam Generator Requirement

GENERAL REQUIREMENT

The general requirement of the solar steam generator is to provide a means of transferring solar energy from the heliostats to the water-steam working fluid for generation of electrical energy.

The specific subsystem requirements are:

- Generate superheated steam
- Use the available solar energy
- Have a high reliability and availability
- Minimize heat loss

1. The solar steam generator must generate superheated steam to be supplied both to the storage system and the turbine-generator. The design conditions are presented in Table 5-3 for the steam cycle condition of 1450 psig throttle pressure and 950°F steam temperature.

2. The solar steam generator must use the available solar energy incident from a 360-deg heliostat field into a tower-mounted right circular cylinder cavity.

3. The solar steam generator must be conservatively designed for high reliability and availability to minimize outages.

4. The solar steam generator must be designed to minimize heat loss by:

   - reradiation and convection through the aperture,
   - conduction through the cavity walls and ceiling,
   - maintaining a gas-tight enclosure to prevent convection.

Table 5-3. Solar Steam Generator Steam Conditions

Throttle Conditions at the Turbine

Steam Pressure - 1450 psig

Steam Temperature - 950°F

	Summer Solstice @ 12:00 Noon	Winter Solstice @2:00 PM
	Maximum Capability	12,000 KW Rating 10 MW Net Electrical
Steam Pressure @ Outlet of Second-Stage Superheater, psig	1500	1470
Steam Temperature @ Outlet of Second-Stage Superheater, °F	955	955
Drum Operating Pressure, psig	1700	
Boiler and Superheater Design Pressure, psig	1800	
Feedwater Temperature @ Inlet of Drum, °F	520	471
Steam Flow, lb per hour	176,700	114,000

Steam Generator

Design Approach

USE EXISTING TECHNOLOGY

The recommended design approach to meet the general requirement is to use existing technology because of the time schedule constraints.

1. The time scheduled for the solar steam generator research experiment and the preliminary design of the pilot plant is shown in Figure 5-12.

2. The conclusion drawn from the schedule is that existing technology must be used to meet the general requirements within the time available. For example, the development of significantly new steam generator designs such as the supercritical fossil boiler and the once-through nuclear steam generator required 5 to 10 years from the initiation of development to the initial operation.

   In order to have a successfully operating pilot plant within 5 years, it will require maximum use of existing technology. New technology will be developed only if necessary to meet the requirements.

3. In the following sections we will:

   - Describe the steam generator concept
   - Explain why the concept was selected
   - Identify where existing technology can be used
   - Identify where new technology must be developed.

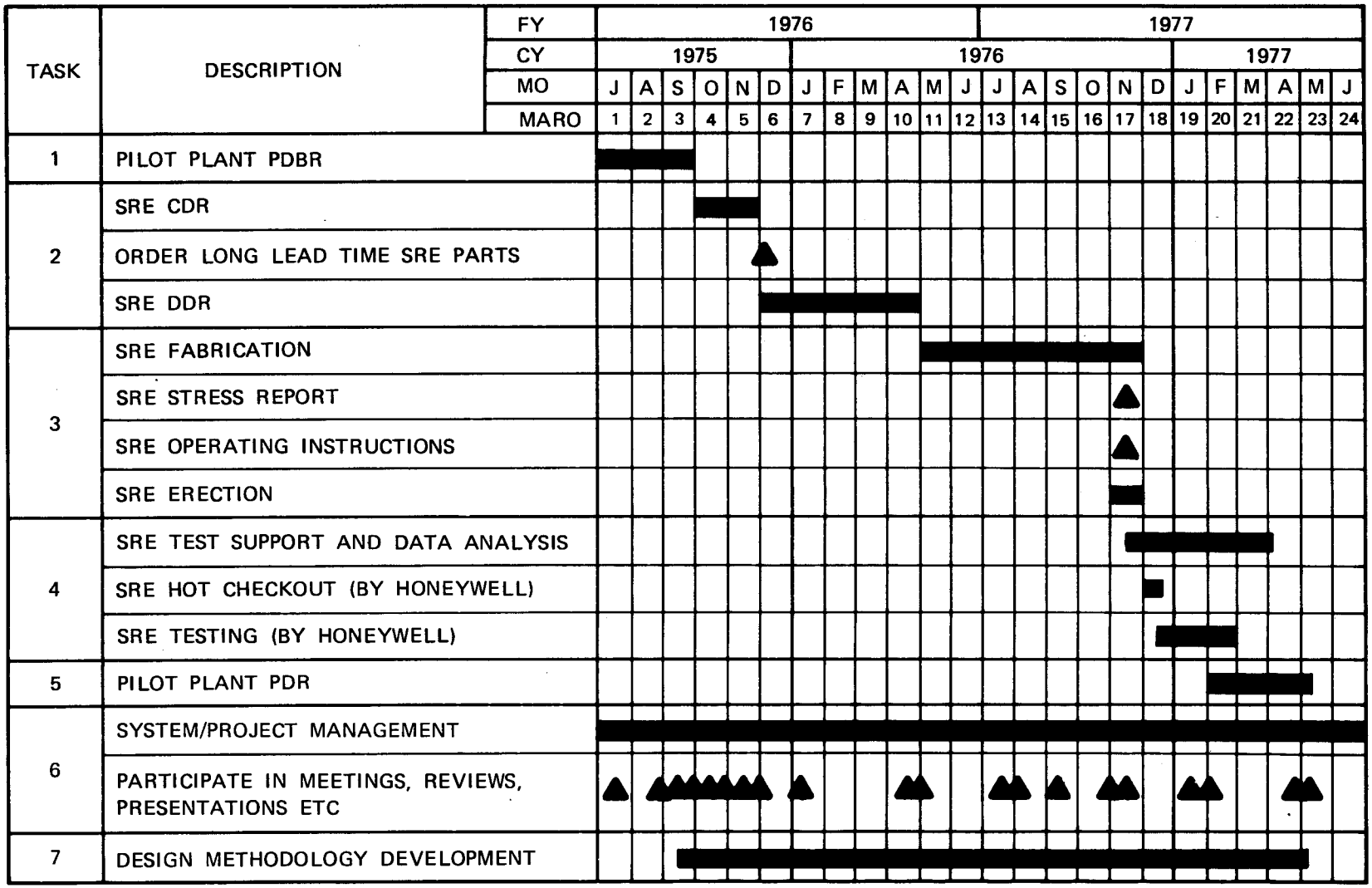


Figure 5-12. Program Schedule

Steam Generator

Preliminary Design Concept

PUMP ASSISTED RECIRCULATING DRUM BOILER

The recommended solar steam generator design concept is a pump-assisted recirculating drum boiler with a two-stage helical superheater because this concept best uses existing technology to meet the design requirements.

1. Recirculating Drum Versus Once Through. The recirculating drum boiler was chosen to meet the difficult control requirements associated with rapid startup.

2. Pump-Assisted Versus Natural Circulation. The pump-assisted drum boiler allows the use of smaller-diameter tubes,resulting in a lighter structure and reduced thermal stress.

3. A spray attemperator was selected to control steam temperature because this method allows the use of all the solar energy. Spray attemperators are commonly used in fossil boilers. Other methods of steam temperature control in fossil boilers are not applicable because they function by reducing the energy input rate, which would be wasteful in a solar steam generator.

4. Referring to Figure 5-13, the drum receives feedwater from the outlet of the feedwater heater and receives a steam-water mixture from the boiler section. Mechanical separators in the drum separate the steam from the steam-water mixture flowing into the drum from the riser(s). The saturated steam leaves the top of the drum and flows through the saturated steam line(s) to the first-stage superheater. The steam exiting the first-stage superheater passes through a spray attemperator where feedwater from the inlet to the feedwater heater is injected for superheat control. From the attemperator, the steam flows into the second-stage superheater where the desired superheat is reached.

   The saturated water separated with the mechanical separators mixes with the feedwater from the outlet of the feedwater heater, exits the bottom of the drum through a downcomer pipe connected to the recirculating pump. This pump discharges to the boiler.

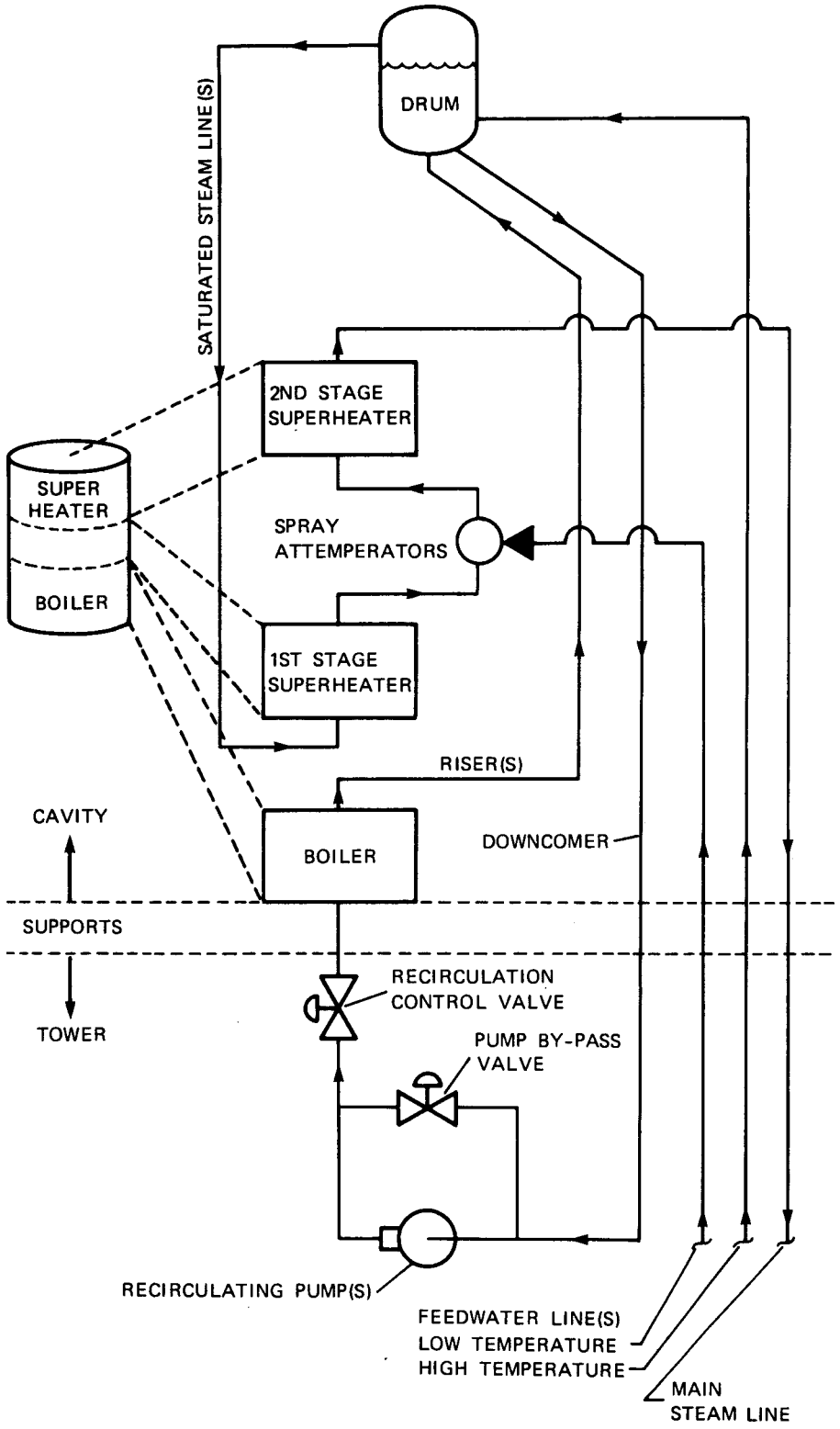


Figure 5-13. Solar Steam Generator - Flow Schematic

Steam Generator

Preliminary Design Arrangement

PHYSICAL ARRANGEMENT OF THE DESIGN CONCEPT

The design arrangement of the steam generator concept must utilize the cylindrical cavity configuration to meet the specific subsystem requirements.

1. The steam generator arrangement utilizing the pump-assisted recirculating drum boiler is shown in Figure 5-14. The boiler, first-stage superheater and second-stage superheater heat transfer surfaces are arranged to cover the surface area of the right circular cylinder of the cavity. The boiler section, which has the relatively cool heat transfer surface, is on the bottom portion of the cavity; there the reradiation losses through the cavity aperture are reduced. The first and second stages of the superheater are arranged on the remaining portion of the cavity such that the second-stage superheater has to be in the lowest heat input zone for metal temperature protection.

2. All piping and headers, spray attemperators, and drums will be placed beyond the thermal insulation and lagging covering the heat transfer surface. All of the above components will be internal to the steam generator housing.

3. The boiler and drum will be top supported to allow for thermal expansion. The piping and headers will be supported from the same structural frame from which the boiler is supported.

4. The recirculating pump will be located in the top portion of the support tower. The piping to and from this pump and the feedwater and main steam lines will be routed through the cavity supports (corbels).

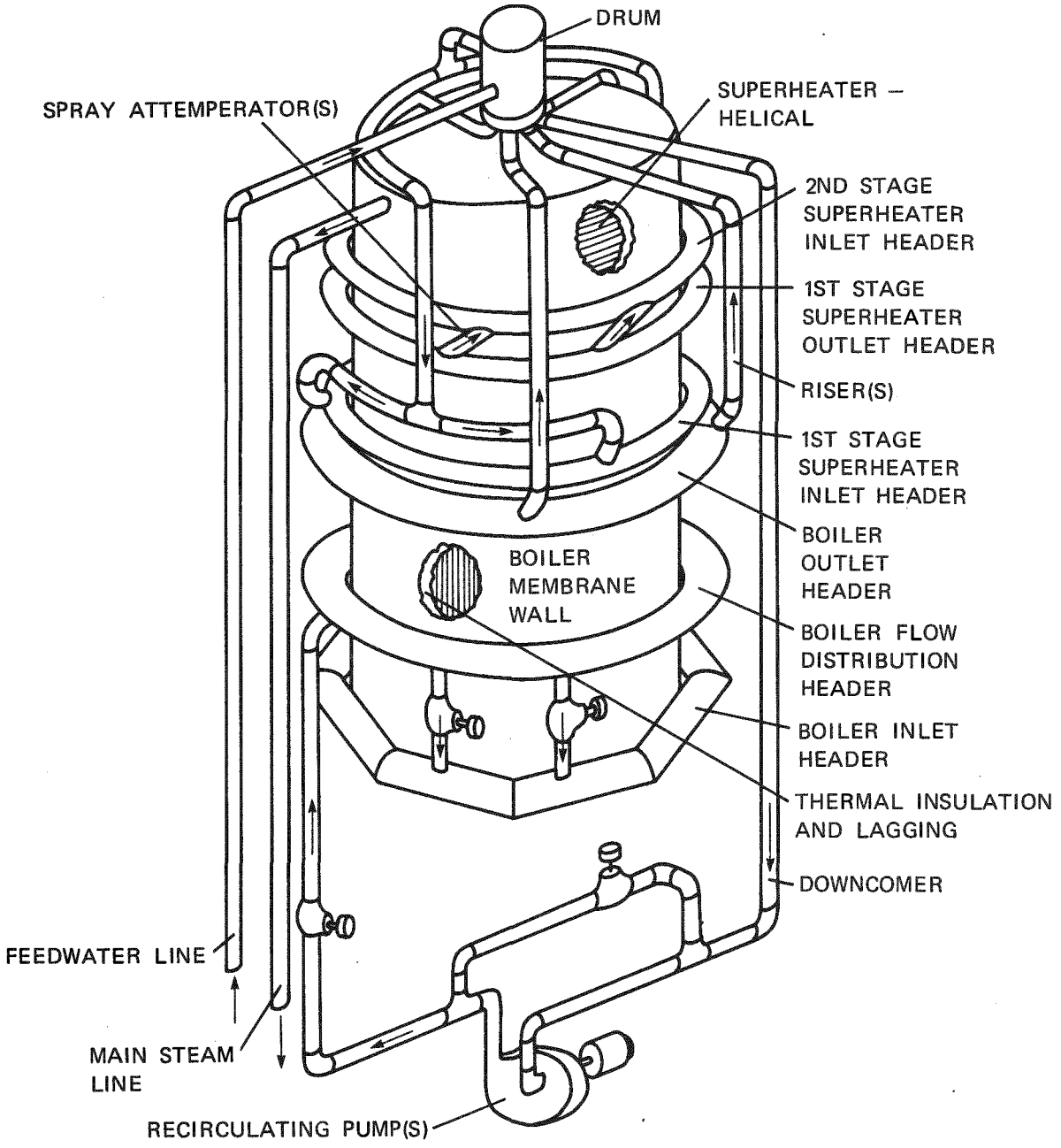


Figure 5-14. Preliminary Design Arrangement

Steam Generator

Steam Generator Components

HEAT TRANSFER SURFACE FOR THE BOILER SECTION

A membrane wall with vertical flow circuitry is recommended for the boiler section because this construction has been proven to be most economical for similar fossil boiler applications.

Modern fossil boiler furnaces all have walls which are water cooled. The furnace wall tubes are spaced on close centers to obtain maximum heat absorption. Membrane wall construction consisting of a steel bar or membrane welded between adjacent tubes (Figure 5-15) is used in the furnace. These panels are all shop fabricated. The furnace walls are composed of a number of membrane wall panels welded together. The result is a continuous wall surface of rugged, pressure-tight construction capable of transferring a maximum amount of heat to the tube.

The boiler section of the solar steam generator operates at conditions similar to those in the furnace of a fossil boiler. Thus, the membrane wall construction can be designed for the solar steam generator to withstand thermal and pressure stresses resulting from the high heat fluxes in the boiler section.

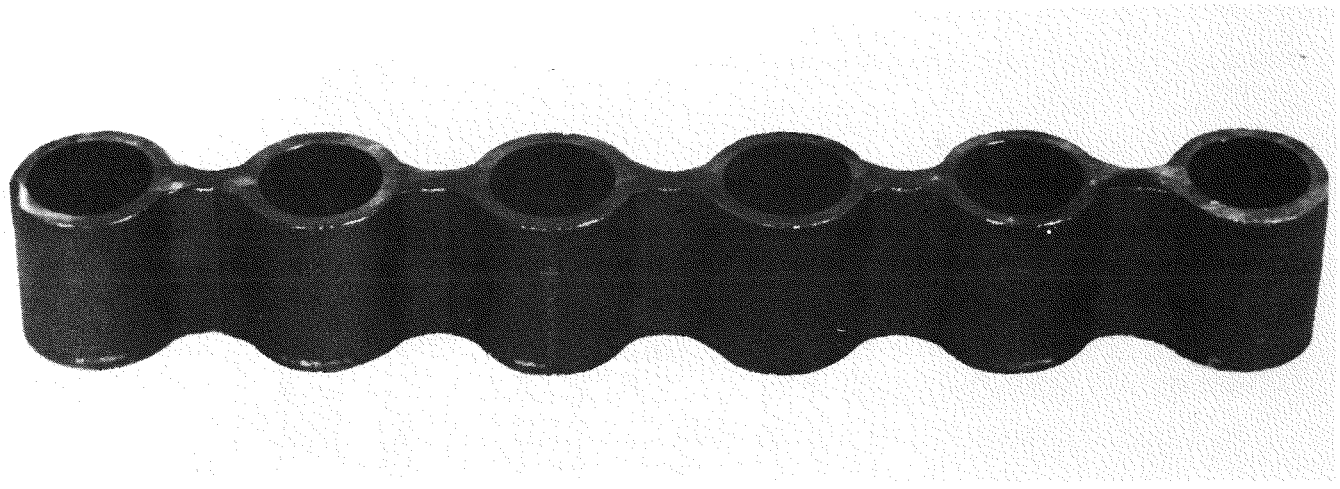


Figure 5-15. Membrane Wall

Steam Generator

Steam Generator Components

CONSTRUCTION OF THE MEMBRANE WALL FOR A CAVITY

Membrane wall panels have been constructed for round cavities.

The membrane wall for the boiler section of the solar steam generator will be 7/8-in. OD tubes on 1-3/8-in. centers. The web or membrane bar is carbon steel and the tube material is B&W alloy Croloy 1/2 (ASME Spec SA-213 T2). The pilot plant solar steam generator with a cavity diameter of 39 feet will have about 1070 tubes in the boiler section.

In Figure 5-16 a membrane wall section is shown assembled out of flat plate panels to approximate a cylindrical cavity. This structure forms a water-cooled hood for the basic oxygen furnace (BOF) used in the steel-making industry.

To reduce the heat losses to an economical minimum,flexible block insulation is installed on the outside of the membrane wall. In addition, a protective metal lagging is installed to protect the insulation from the environment. Figure 5-17 shows the membrane wall with its insulation and protective lagging. The lagging shown in Figure 5-17 is the ribbed type, but flat sheet lagging could also be used for covering the insulation. If the ribbed lagging is used, thermal barriers are provided to prevent the rise of warm air caused by the natural stack effect.

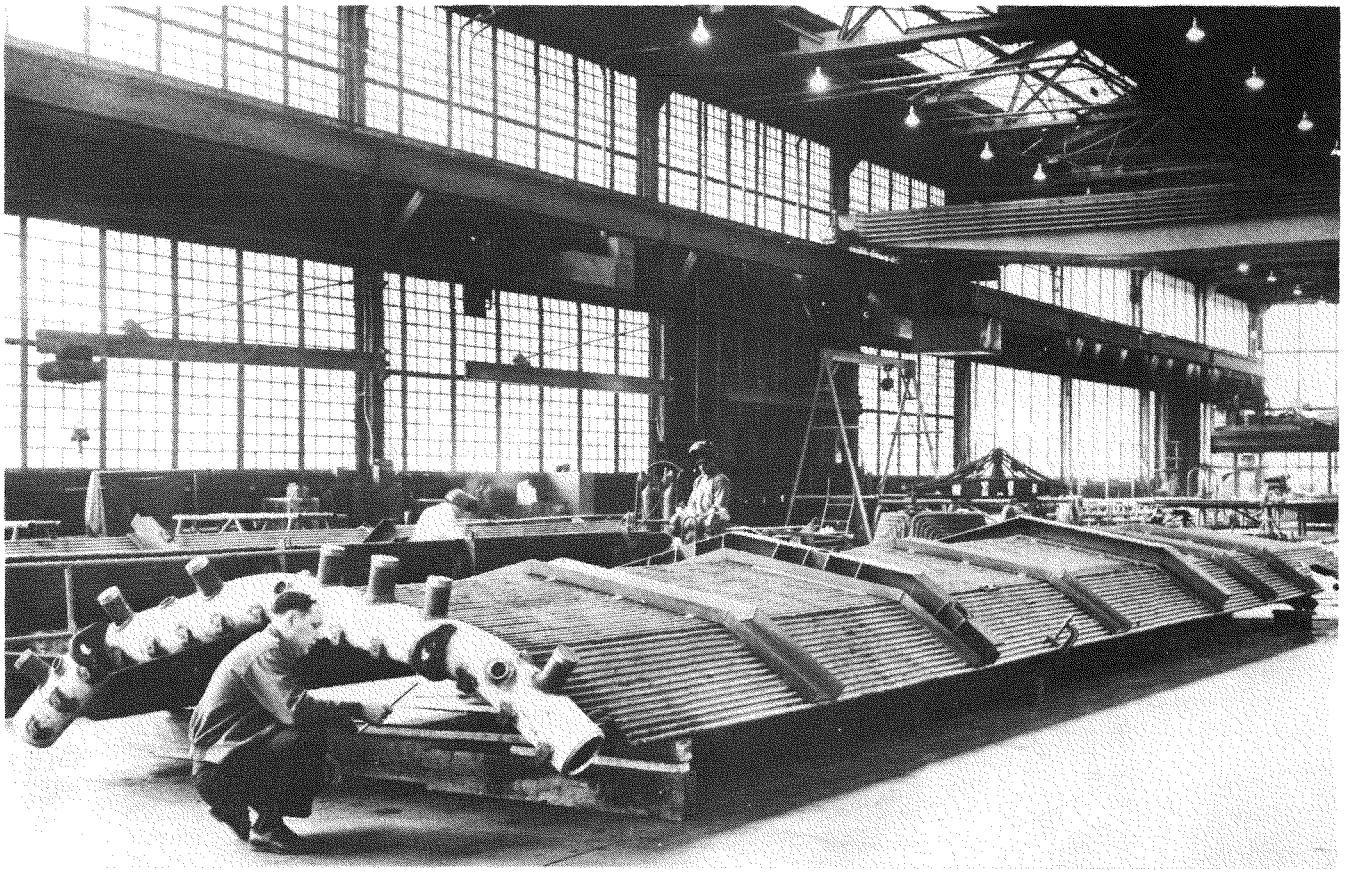


Figure 5-16. Membrane Wall Sections Assembled for Round Shape

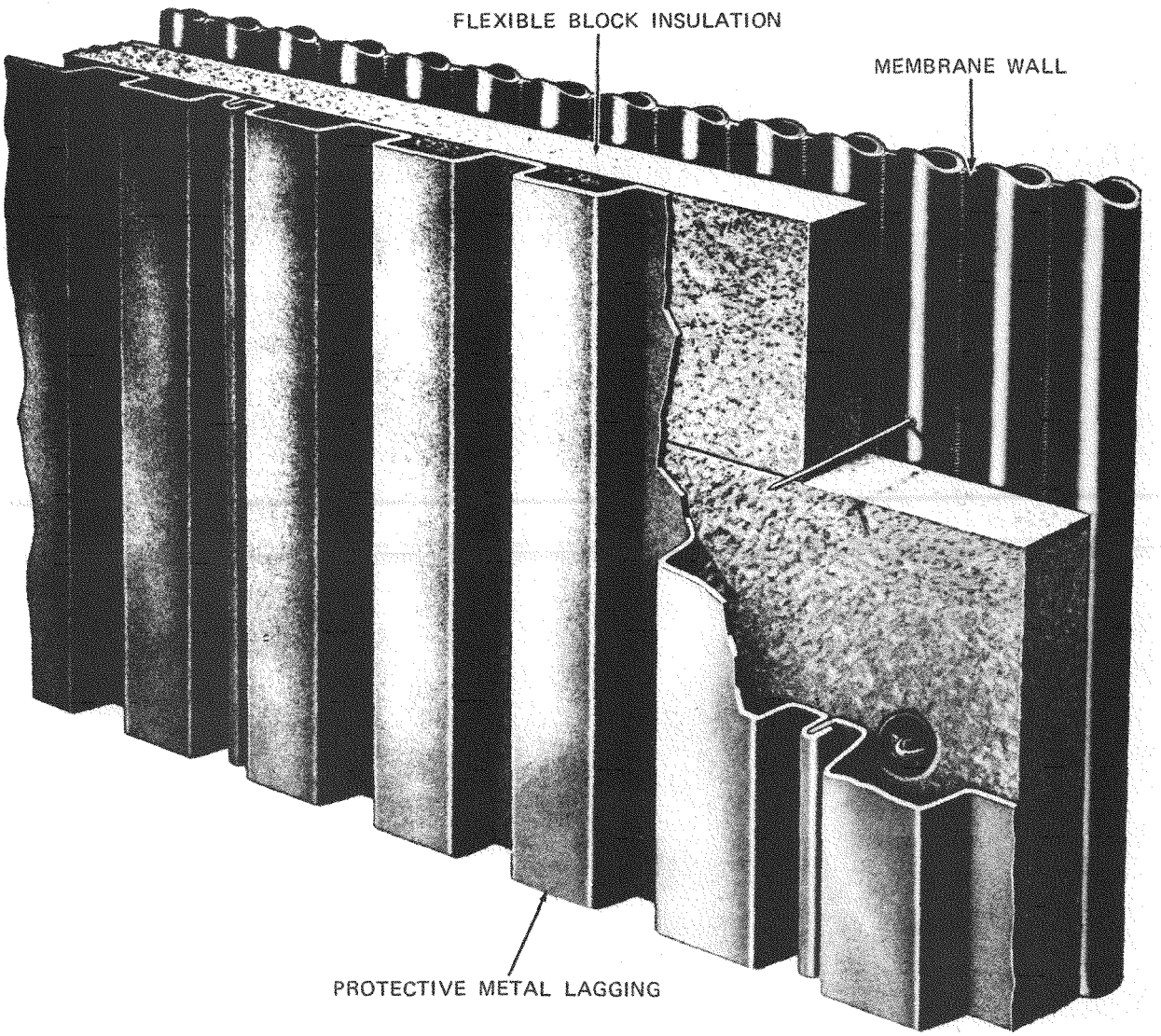


Figure 5-17. Membrane Wall with Block Insulation and Lagging

This page intentionally left blank.

Steam Generator

Steam Generator Components

HEAT TRANSFER SURFACE FOR THE SUPERHEATER

A helical flow circuitry is recommended for the superheater because this construction will improve flexibility and thermal averaging capability.

1. Helical flow circuits are used in European fossil steam generators to reduce the effect of heat flux variations. Since every tube passes completely around the circumference and through each azimuthal heat flux zone the unbalance effects of tower supports and cloud coverage will be averaged out. The solar superheater has to be designed to

   - Reduce thermal stress by relatively free radial expansion
   - Cover the receiver cavity surface and minimize reradiation losses
   - Provide a low ratio of steam flow area to heat transfer surface area for achievement of a high superheater heat transfer coefficient.

2. The design problems are expected to be related to the frequent stress cycles because of daily startup and shutdown as well as intermittent cloud coverage. The helical superheater completely covers the upper part of the cavity and thus receives heat on one side only as opposed to a fossil boiler superheater which is normally heated from all sides.

3. Depending on the cavity dimensions and the resulting heat flux distribution, there may be a heat input to the ceiling of the cavity. The flow circuitry for the ceiling superheater is presently undefined and will be determined when the heat flux distribution is defined.

SUPERHEATER

- CAVITY WALLS – HELICAL
  - ADVANTAGES
    - FLEXIBLE
    - THERMAL AVERAGING
  - DISADVANTAGES
    - ONE SIDED HEATING
- CEILING – UNDEFINED

Steam Generator

Steam Generator Components

DRUM AND INTERNALS

A vertical drum configuration was chosen for the solar steam generator to assure adequate flow distribution to the cyclone separators and to give a wider range of water level indication for control of feedwater flow.

1. The recommended drum and internals are shown in Figure 5-18. A vertical drum with internal dimensions of 48-in. ID and a height of 120-in. was chosen over the horizontal drum concept. Although the vertical drum will increase the required height of the boiler support structure by approximately 4 feet, its advantages of establishing an adequate flow distribution from the risers to the cyclones and wider range of water level indication overcome the disadvantage of increased height.

2. The cyclone steam separators are centrifugal steam-water separating devices. The cyclones make it possible for the steam drum to effect positive separation of steam and water even when handling variations in water level during wide load swings. They thus provide essentially steam free water in the downcomer circuit and assure proper circulation. The action of the cyclone steam separators also results in a positive indication of drum water level.

   Eight cyclone separators were chosen for the pilot plant design condition; these cyclones are not scaled up nor down to other design conditions but their number is either increased or decreased. For example, if the steam flow is double (a larger plant size) there will be 16 cyclone separators. The drum is then arranged to accommodate these 16 cyclones.

3. Secondary scrubbers are located above each cyclone separator to reduce the moisture and solids carryover. Moisture, with its entrained solids, is agglomerated in the corrugated passages of the scrubber plates and returned to the drum.

4. The water level indication will be used as a control element to increase feedwater flow (low water level) or reduce feedwater flow (high water level). The water level in the drum will vary as the heat input in the boiler section and system pressure are varied due to cloud passage and as load conditions are varied during daily startup and shutdown. Here the change in water level, "shrink and swell", is related to the steam voids in the boiler section and riser(s); once the circulation ratio is established the variation in the drum water level can be finalized.

Table 5-4 lists the actions initiated by high and low water level signals.

Table 5-4. Action Initiated by High and Low Water Level Signals

Condition	Drum Problem	System Problem	Action
High Water Level "Swell"	Water carryover	Water droplets to turbine	1) Blowdown drum
			2) Decrease FW flow
		Shock superheater tubes	3) Defocus heliostats
			4) Pump trips
	Loss of control range		1) Switch to manual control
			2) Blowdown drum
			3) Decrease FW flow
Low Water Level "Shrink"	Steam carryunder into downcomer	Insufficient NPSH for recirc pump	1) Increase FW flow
			2) Reduce steam flow
		Steam into recirc pump	3) Defocus heliostats
			4) Pump trips
	Loss of control range		1) Switch to manual control
			2) Increase FW flow
			3) Reduce steam flow
			4) Defocus heliostats
			5) Pump trips

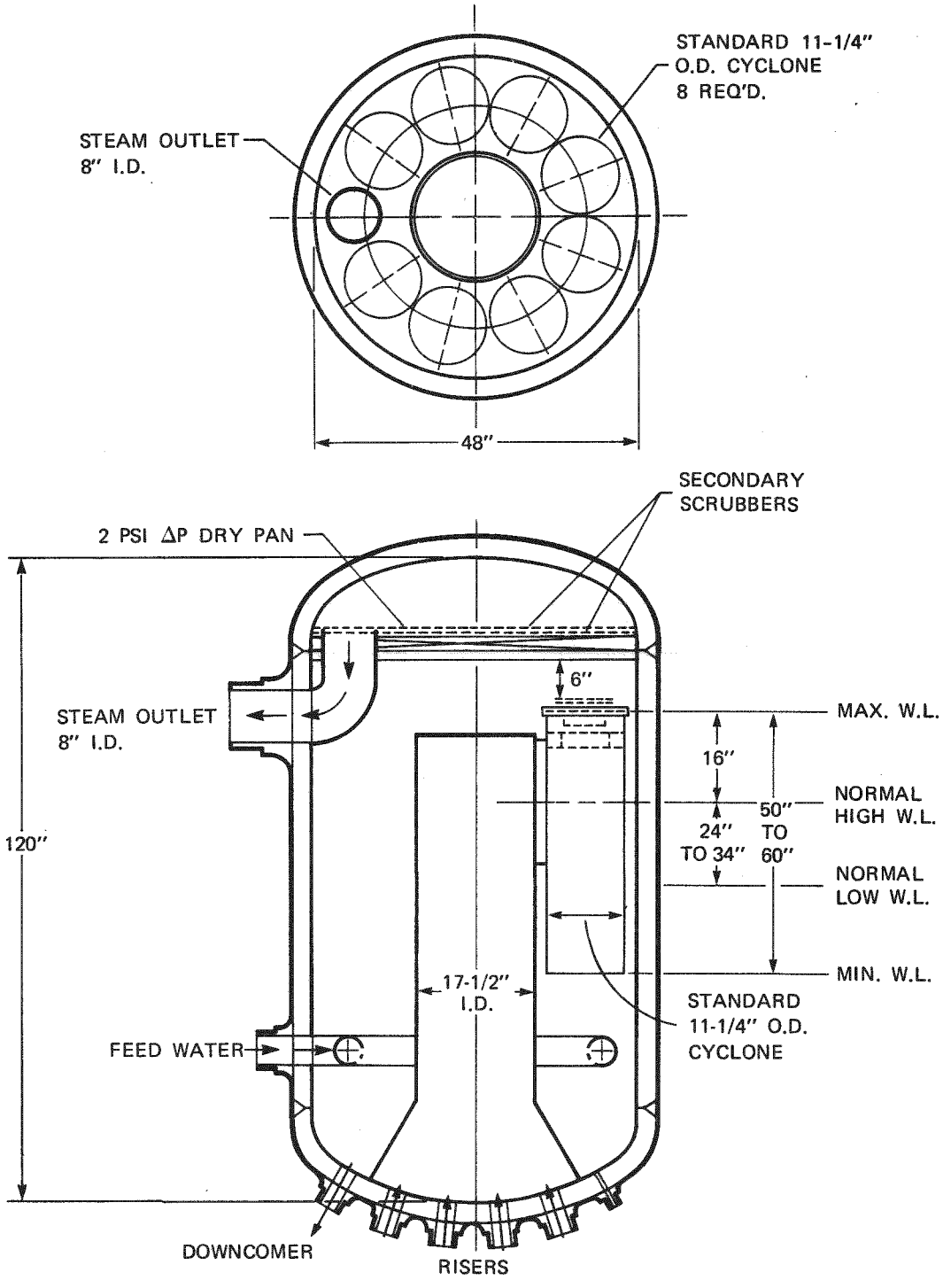


Figure 5-18. Drum and Internals - Solar Steam Generator

This page intentionally left blank.

Steam Generator

Steam Generator Components

CONTROL FOR NORMAL OPERATION

A spray attemperator between the two stages of the superheater provides for a superheat regulation to maintain optimum temperature at the turbine and to protect superheater and turbine from high temperatures.

1. Regulating steam temperature within required limits of control is necessary to correct variations in energy input. This control is required to hold the optimum heat rate at the turbine and provide superheater and turbine metal temperature protection. The superheater spray attemperator illustrated in Figure 5-19 has proven very satisfactory for regulating steam temperature in fossil boilers.

2. Superheat must be maintained after attemperation at all operating conditions in order to avoid the possibility of deposition of solids in the superheater. This is achieved by locating the attemperator after the first-stage superheater.

3. Water of high purity is introduced into the superheater steam line through a spray nozzle at the throat of a venturi section within the line. Because of the spray action at the nozzle and the high velocity of the steam through the venturi throat, the water vaporizes, mixes with, and cools the superheated steam. The venturi section is continued into a thermal sleeve, downstream from the spray nozzle, to protect the high-temperature piping from thermal shock that could result from any incompletely evaporated water droplets striking the hot surface.

   It is important that the spray water be of highest purity, since solids entrained in the spray water enter the steam and may, if excessive, cause troublesome deposits on superheater tubes.

4. This installation will offer the following advantages:

   - Control of outlet steam temperature
   - The average steam temperature in the second stage superheater is reduced;hence, the metal temperatures are lowered
   - Additional mixing of the steam exiting the first stage superheater will occur; hence, a more uniform steam temperature entering the second stage superheater.

5. The energy input (flow x enthalpy) to the spray attemperator will be defined once the two stages of the superheater are defined. The steam generator performance is calculated for a load range to define the load conditions and attemperator energy input to provide the desired outlet steam temperature and maintain superheater metal protection.

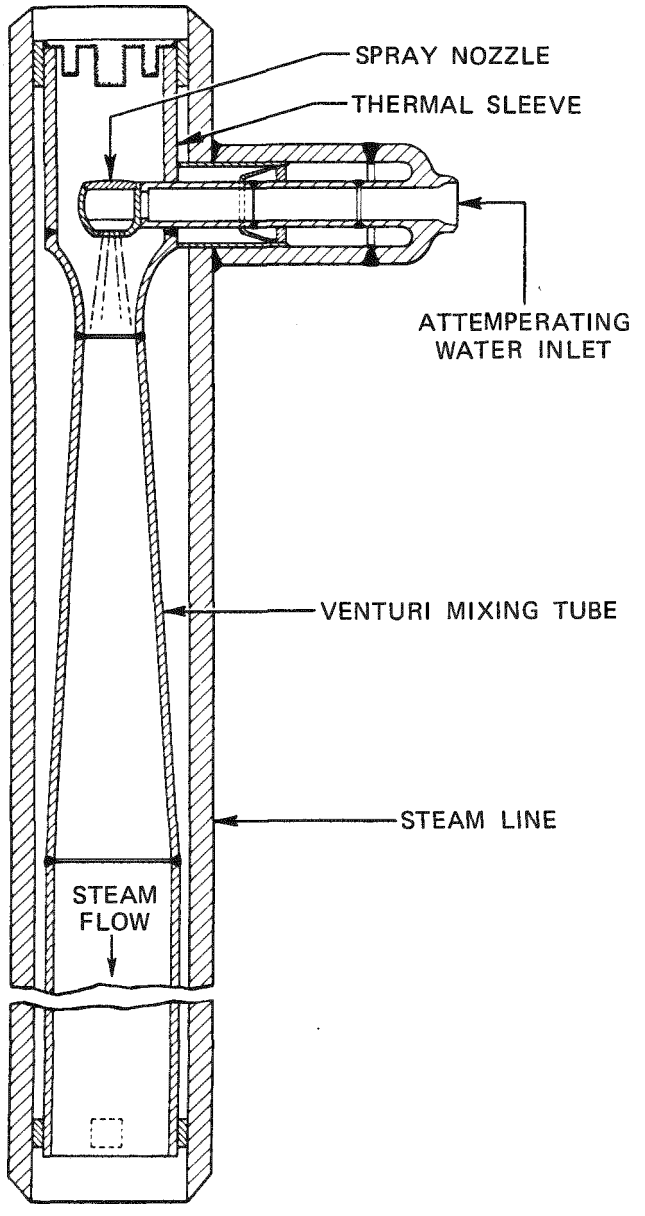


Figure 5-19. Superheater Spray Attemperator

Steam Generator

Steam Generator Components

CONTROL DURING STARTUP AND SHUTDOWN

A fossil boiler peaking unit startup control system is the best choice for the solar steam generator because of the inherent similarity between the solar and fossil applications.

1. A fossil boiler peaking unit must start up and shut down each day. The startup and shutdown rates are similar to those required of the solar steam generator.

2. For boiler applications that require a desired rate of startup, especially following weekend and overnight shutdowns, positive control of boiler steam conditions during startup and at low loads is important since the startup time depends on the degree of match between main steam temperature and critical turbine metal temperature.

3. The drum boiler bypass system, shown schematically in Figure 5-20, provides a means for positive control of steam conditions during startup and also shutdown. This system controls drum pressure by means of a superheater bypass to the condenser. From fossil experience it offers faster startups, controlled shutdowns in preparation for anticipated startup conditions, conservation of equipment life, and reliability and increased maneuverability during startup and over the load range.

4. The superheater bypass to the condenser provides a means to limit throttle pressure to the turbine presenting a number of advantages for hot restarts after cloud passage and starts following overnight shutdowns.

   - Reduces throttling temperature drop in the turbine
   - Allows maximum heat input without exceeding metal temperature limits
   - Reduces startup time by matching steam and turbine temperatures while maintaining maximum heat input.
   - Depressurization through this line during shutdown maintains heat storage in superheater outlet components and main steam leads, contributing to a close match of steam and turbine metal temperatures,thus reducing the time required for the next startup.
   - The drop of first-stage turbine temperatures can be minimized during shutdown by unloading the turbine with control valves in a fixed position and reducing boiler pressure.

The heliostat aim strategy and the operation of the superheater bypass system during startup and shutdown will be analyzed further when a transient model of the system is available. During the analysis work the possibility of passing the excess steam from the superheater by-pass to the storage system or to an auxiliary steam system will be considered.

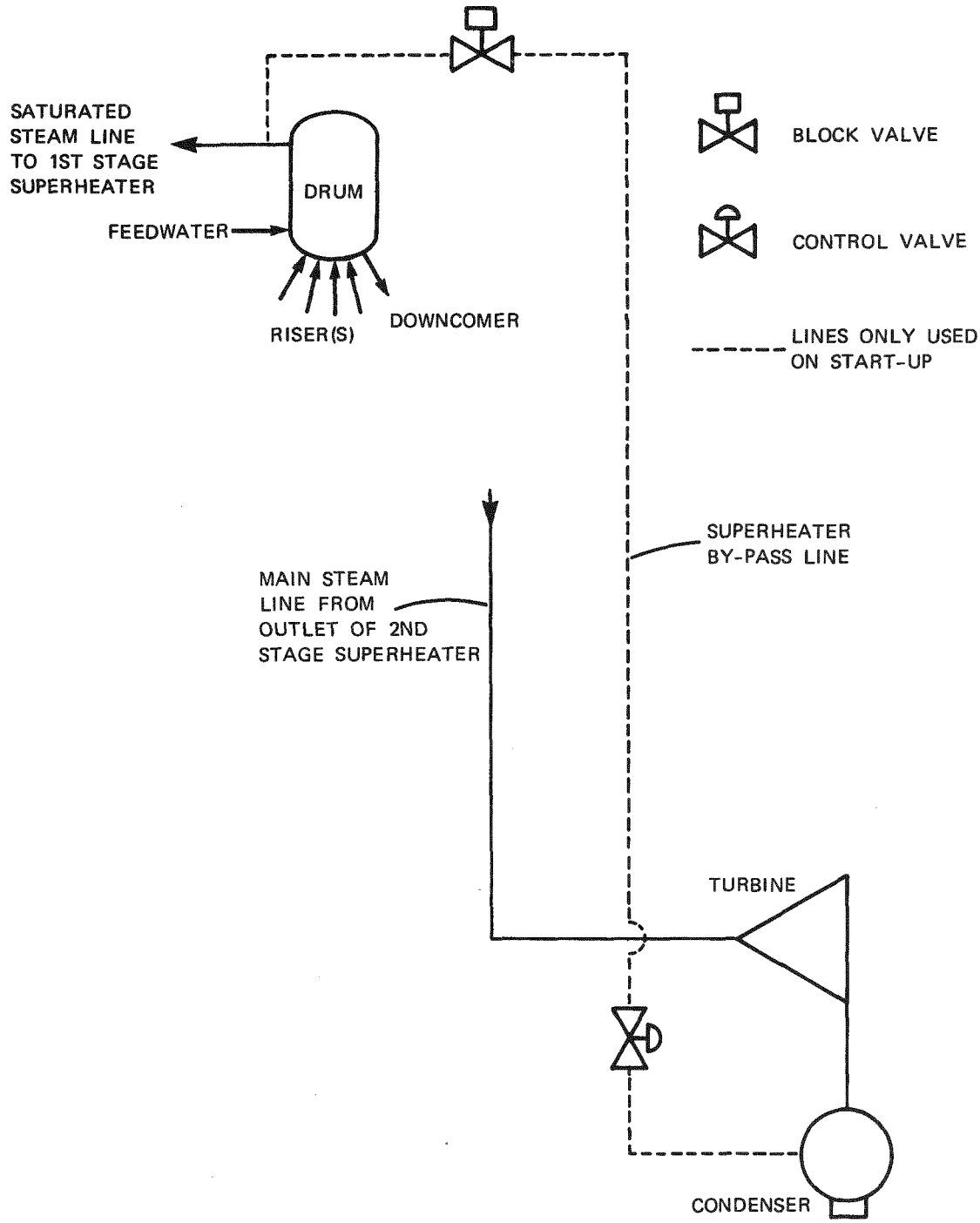


Figure 5-20. Superheater Bypass System for Solar Steam Generator

Steam Generator

Steam Generator Specifications

MATERIAL SPECIFICATIONS FOR THE HEAT TRANSFER SURFACE

The materials used for the heat transfer surface must be given due consideration in design to establish an adequate margin of safety, high reliability, and high availability.

1. The ferrous tube material specifications and maximum allowable metal temperatures (based only on resistance-to-oxidation characteristics) for typical boiler material are presented in Table 5-5. Tube materials from this table will be chosen for the construction of the membrane boiler wall and the helical superheaters.

2. Final material selection will depend on the maximum use temperatures, stress values in accordance with the ASME Code, and creep and fatigue resistance.

Table 5-5. Ferrous Tube Material Specifications and Maximum Allowable Metal Temperatures Based on Oxidation Characteristics

Material	ASME Specification	Max Allowable Metal Temp, °F
Carbon Steel	SA-192	950
B-Carbon Steel	SA-210 Grade A1	950
Carbon Steel	SA-210 Grade C	850
Carbon Moly	SA-209 Grade T1a	975
B, SH-Croloy 1/2	SA-213 Grade 2	1025[1]
SH-Croloy 1-1/4	SA-213 Grade T11	1050
Croloy 2	SA-213 Grade T3b	1080
SH-Croloy 2-1/4	SA-213 Grade T22	1125
Croloy 5	SA-213 Grade T5	1150
SH-Croloy 9	SA-213 Grade T9	1200
SH-Croloy 304H	SA-213 Grade TP-304H	1400
SH-Croloy 321H	SA-213 Grade TP-321H	1400

B - Materials in common use for membrane walls

SH - Materials in common use for superheaters

[1]The mean wall temperature for selecting tube thickness shall not exceed 1000 °F.

Steam Generator

Steam Generator Specifications

FEEDWATER AND ATTEMPERATOR WATER SPECIFICATIONS

Drum boilers designed for daily startup and shutdown require strict water quality and water quality control to minimize losses of capacity and efficiency because the greater off-line periods give rise to higher levels of contamination and greater rates of deposition.

1. Boilers for peaking service require strict control of water quality during the transient periods to which these units are subjected. The degree of corrosion protection that can be provided is related to the ability to prevent oxygen from entering the boiler-turbine system.

2. For overnight or weekend shutdowns, the best method to exclude oxygen from the system is to maintain condenser vacuum, thus enabling the steam side of the feedwater heaters, turbine, and reheater to become dry and to stay dry. Maintaining condenser vacuum should also decrease the incidence of condenser leaks by eliminating the transients that occur while making and breaking vacuum. Auxiliary steam is necessary to maintain turbine seals.

3. During shutdown the deaerator vents to the atmosphere should be closed when the cycle water temperature falls below the boiling point. Another method of preventing oxygen infiltration is to vent the deaerator to the condenser. In the latter method, a valve in the line from the deaerator to the condenser should automatically open when the deaerator pressure decays to atmospheric pressure. In either case, the deaerator should be designed to withstand full condenser vacuum.

4. Drum-type boilers normally do not require condensate polishing systems for satisfactory operation. However, the start-stop operation of a peaking boiler, with its consequent transients, and the greater off-line periods, give rise to higher levels of contamination in the feedwater and greater rates of deposition in the boiler. Therefore, condensate polishing for peaking boilers offers a unique and important advantage.

5. The feedwater and attemperator water specifications are presented below.

6. Figure 5-21 shows a typical water-steam cycle indicating control monitoring locations and instrumentation required to meet the water specs.

pH	8.5-9.2* 9.3-9.5**	Cu, ppm	0.005 max
		Total Hardness, ppm	0
Oxygen, ppm	0.007 (Pref. 0)		
		SiO_2, ppm	0.02 max
Fe, ppm	0.01		
		Organic, ppm	0

* With copper alloys in feedwater heaters.

** With carbon steel feedwater heaters.

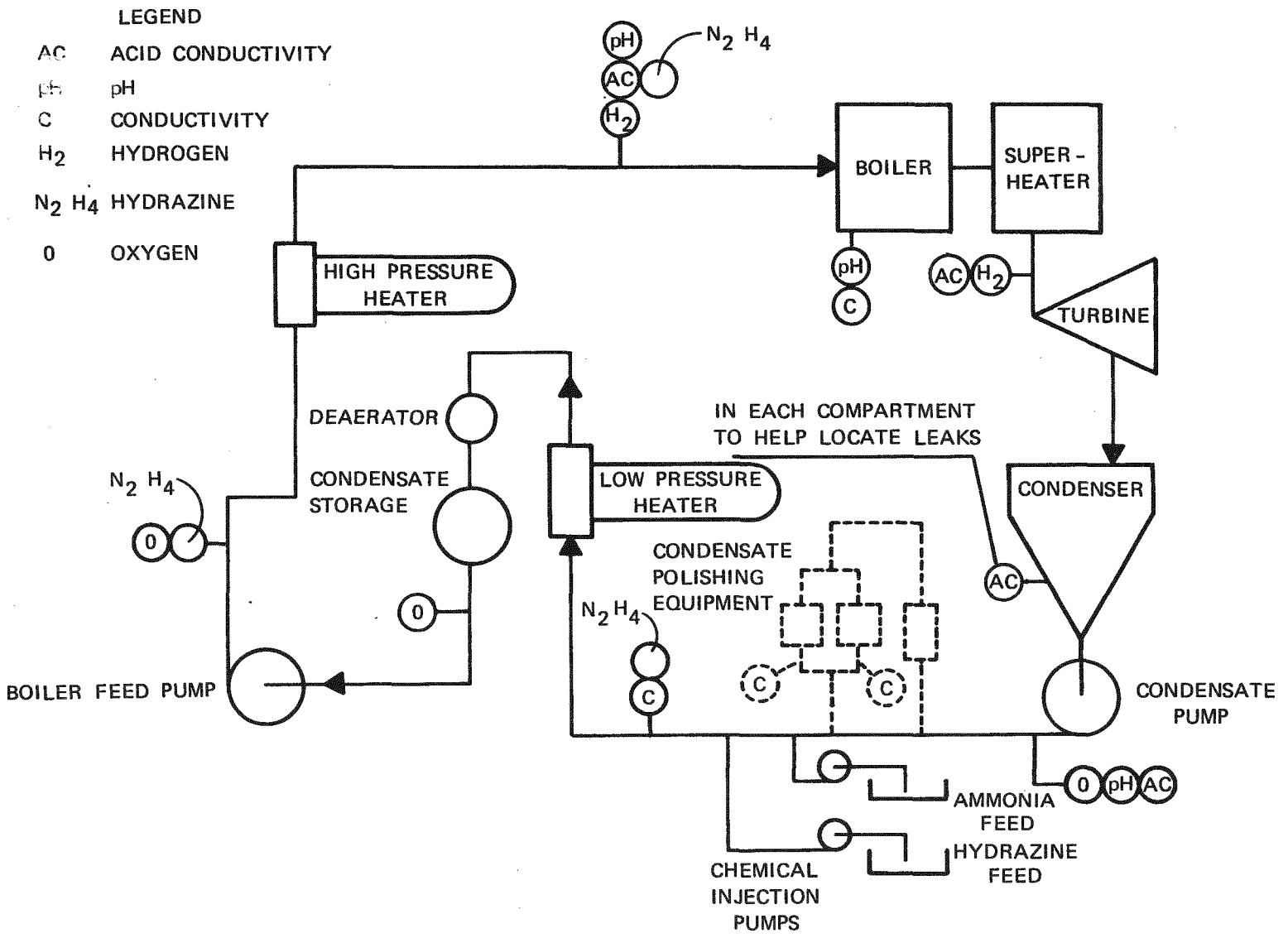


Figure 5-21. Typical Water-Steam Cycle Indicating Control Monitoring Locations and Instrumentation Required for Volatile Water Treatment

Steam Generator

Heat Transfer Surface Layout

HEAT FLUX DISTRIBUTION ON THE CAVITY WALL

The heat transfer surface layout will depend on the absorbed heat flux and its distribution on the cavity wall and ceiling.

1. Presented in Figure 5-22 is a three-dimensional computer drawing of the cavity wall heat flux distribution resulting from the ray trace analysis.

2. This figure shows that the heat transfer surface must be strategically positioned to operate with an azimuthal as well as longitudinal heat flux distribution.

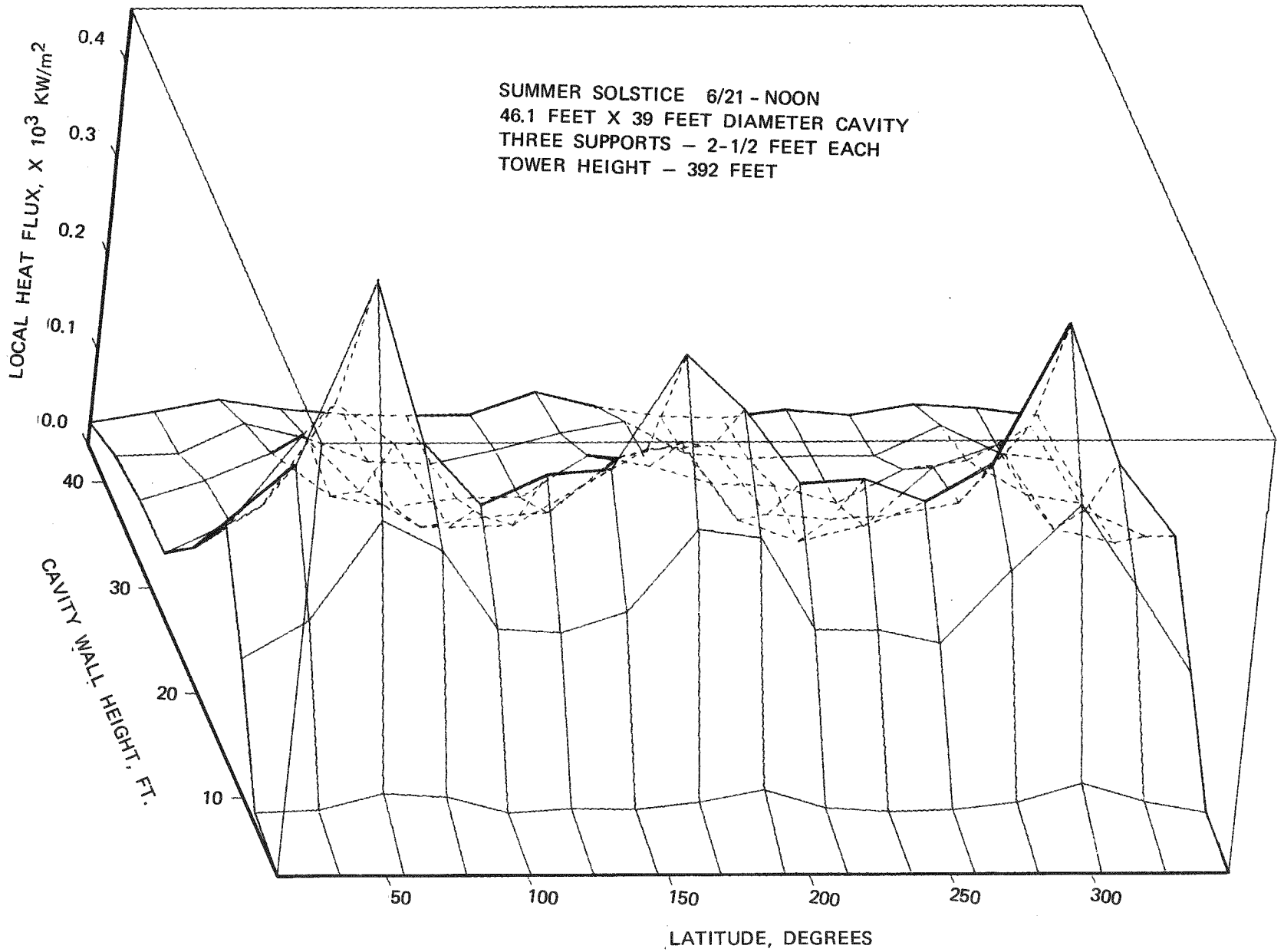


Figure 5-22. Flux Map of Pilot Plant Cavity Walls

Steam Generator

Heat Transfer Surface Layout

BOILER AND SUPERHEATER SURFACE LAYOUT ON THE CAVITY WALLS

The boiler and superheater heat transfer surface has to be designed and laid out such that the maximum and average absorbed heat fluxes will be within the range experienced with successful fossil steam generators to assure that the design will operate reliably.

1. In Figure 5-23 an example of the ratio of the local heat flux to the average heat flux on the cavity wall is shown for summer solstice (June 21, noon). These heat fluxes do not include reradiation.

2. For the 1450 psig/950°F steam cycle, the boiler section will require 70 percent of the heat input and the remaining 30 percent will be in the superheater. Integration of the azimuthal average heat flux results in a boiler height of 23 feet for the 46.1 x 39-foot diameter cavity and the heat flux distribution presented.

3. The heat flux distribution on the cavity wall is similar to that encountered in a modern fossil steam generator. The azimuthal distribution is similar to those expected in the burner zones of the lower portion of a fossil unit.

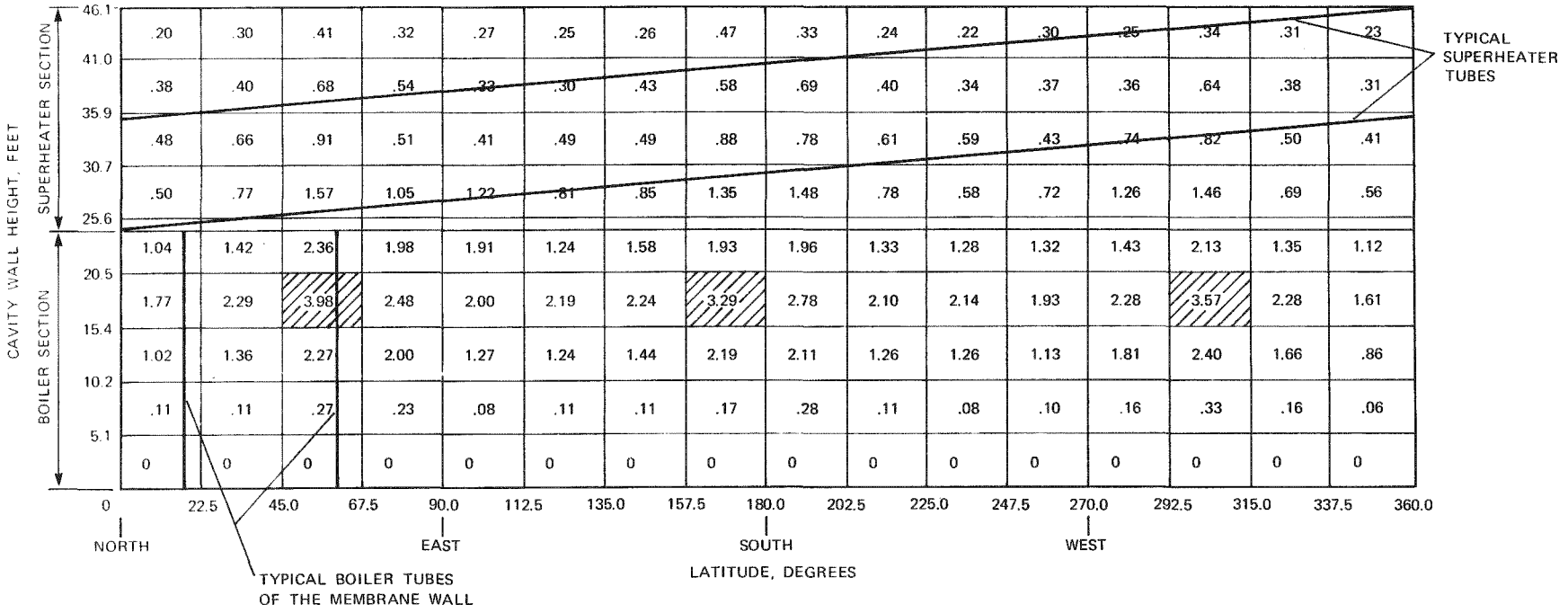
4. The membrane wall boiler section is placed in the lower portion of the cavity to take advantage of the more efficient heat transfer achieved by nucleate boiling with high heat fluxes. Also, the ratio of the peak heat flux to the average heat flux in the boiler section is about 2 (maximum heat flux is about 400 kW/m^2, average heat flux is about 200 kW/m^2) and is within that experienced in fossil steam generators in the burner zones of the furnace.

5. The flow distribution in the tubes of the membrane wall will vary because of the different heat inputs to each tube. A circulation ratio must be selected which will reduce flow maldistribution so that the heat transfer effectiveness of the boiler section will not be impaired.

6. The boiler section will be composed of individual membrane panels with separate inlet headers. The azimuthal heat flux distribution will determine the flow requirements for each panel.

7. Flow oscillations may occur in parallel channels containing two-phase flow. Flow oscillations can lead to loss of heat transfer capability and subsequent tube damage. The boiler section of the solar steam generator is composed of two levels of parallel flow circuitry:

    - Membrane panel wall circuits
    - Tubes within each membrane wall circuit



NUMBER IN BOX = LOCAL HEAT FLUX / AVE WALL HEAT FLUX

SUMMER SOLSTICE 6/21 – NOON

46.1' X 39' DIAMETER CAVITY
TOWER HEIGHT 392'
THREE SUPPORTS 2.5' THICK EACH

Figure 5-23. Layout of Heat Transfer Surface

Orifices at the inlet to each membrane wall panel may be necessary to achieve flow stability among panel wall circuits. Orifices at the inlet to each tube may also be required to achieve tube-to-tube flow stability. These orifices, if required, will be selected during the detailed design of the Research Experiment.

8. A typical superheater surface is laid out in the upper portion of the cavity wall. Here the local heat fluxes are generally less than the average wall flux. The advantage of a helical superheater is apparent from Figure 5-23 which shows that a given tube passes through various heat flux zones and indicates that the variation in total heat input should be reduced by the helical circuitry.

This page intentionally left blank.

Steam Generator

Steam Generator Summary

SUMMARY OF THE PRELIMINARY BASELINE DESIGN

The steam generator arrangement and the components make maximum use of existing technology in applying the design concept to satisfy the specific subsystem requirements.

1. The steam generator arrangement and the components will satisfy the specific subsystem requirements which are:

   - Generate superheated steam
   - Use the available solar energy
   - Have a high reliability and availability
   - Minimize heat loss

2. A review of the steam generator design concept results in the following conclusions:

   - The majority of the steam generator components can be selected from those standard in fossil boilers.
   - The areas we have identified where standard fossil components cannot be used are one sided heating of the helical superheater and the supports of the steam generator for seismic loading.
   - Further design and layout will be required to define the design concept for the above areas.

SUMMARY

- ARRANGEMENT/COMPONENTS
  - MET REQUIREMENTS
- SOLAR STEAM GENERATOR COMPONENTS
  - STANDARD IN FOSSIL BOILERS
  - NON-STANDARD IN FOSSIL BOILERS

Blank

SECTION VI

STORAGE SUBSYSTEM

	Page
Storage Concept	6-2
Baseline Design	6-4

Storage Subsystem

Storage Concept

DEFINING THE REQUIREMENTS

Using the latent heat of fusion of a phase change material is an ideal way to store thermal energy.

The thermal storage concept uses the latent heat of fusion of a eutectic salt to store thermal energy. The energy to charge the salt is obtained as heat of condensation from the steam supplied by the Receiver Subsystem. The condenser tube banks required to do this are located at the bottom of the tank. The heat transfer to the salt is by natural convection.

To discharge the heat energy in the tank, feedwater is circulated through boiler tubes. Using a forced recirculation scheme, the heated water is supplied to a drum and withdrawn as saturated steam. This steam is passed through a superheater before admission to the turbine. The boiler tubes are located at the top of the tank. The salt buildup on the tubes is removed by mechanical means.

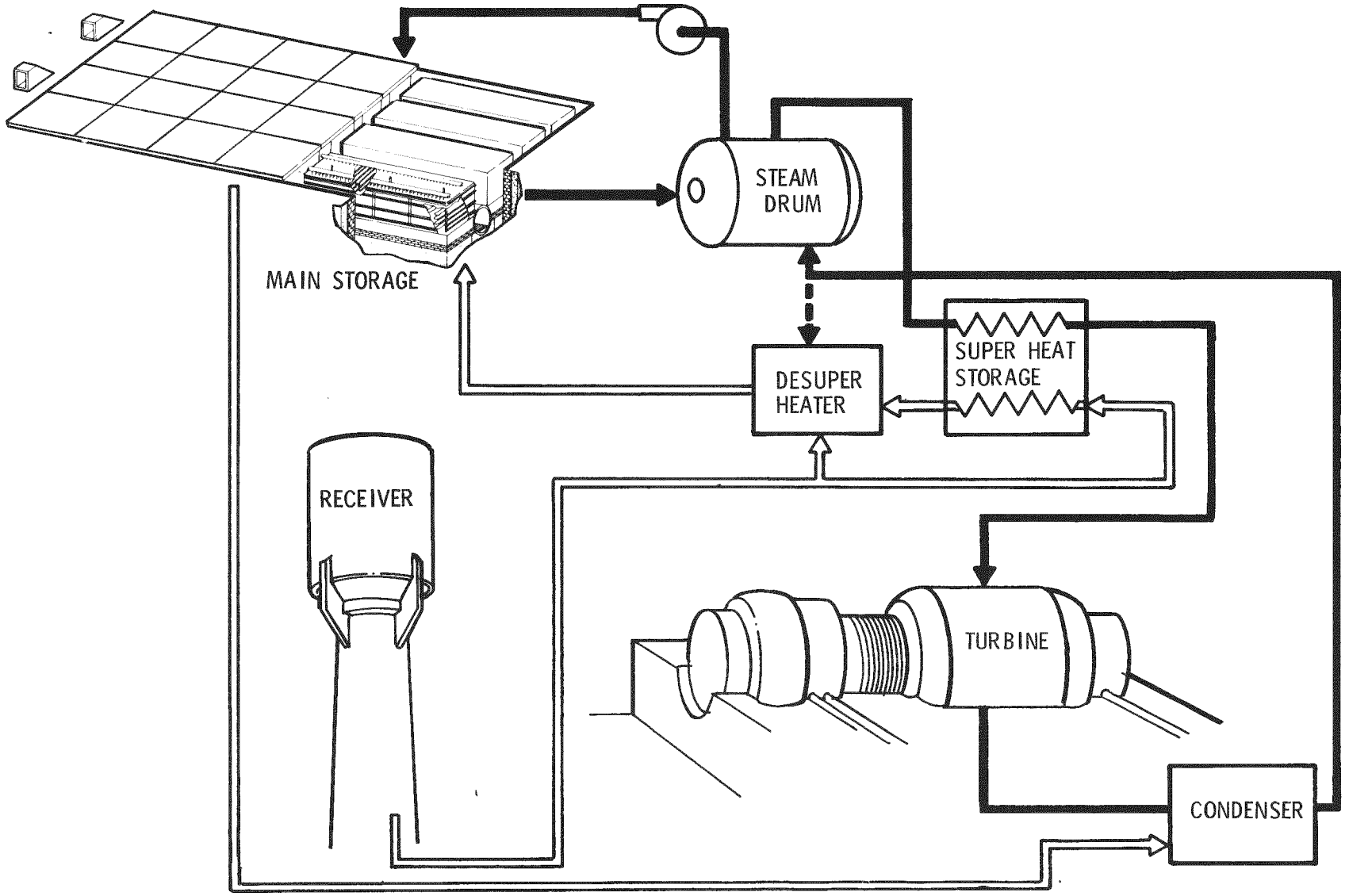


Figure 6-1. Thermal Storage Concept

Storage Subsystem

Baseline Design

STORAGE FIELD CAPACITY

The thermal capacity of the storage field must be sized to handle all auxiliary loads, inefficiencies and heat losses of the system.

The thermal energy storage capacity of the field is 196 MWH(t). The superheater storage requires 9.3 MWH(t) or 4.7%, and the main storage requires 186.8 MWH(t) or 95.3%. This capacity is predicated on the the thermal storage subsystem being capable of delivering a net of 7 MW(e) to the grid for a period up to six hours. To achieve this net means that the storage capacity must provide for the operation of the auxiliary electrical loads within the plant, allow for the reduced thermal efficiency of the turbine/generator when operating from storage, account for the storage cycle efficiency and supply the energy to account for the thermal losses in the system which are less than 1% of the capacity. The thermal efficiency is based on the 1450 psig/950°F cycle with turbine extraction steam for feedwater heating to 335°F. The storage cycle efficiency is the ratio of the thermal energy extracted to that stored. It is highly dependent upon the design. It will be one of the parameters quantified during the SRE program.

$$\text{DESIGN CAPACITY} = \frac{\left[\text{NET ELECTRICAL OUTPUT} + \text{AUXILIARY POWER SUPPLY}\right]}{\left[\text{ACTUAL THERMAL EFFICIENCY}\right] \times \left[\text{STORAGE CYCLE EFFICIENCY}\right]} \times \text{DISCHARGE TIME} + \text{HEAT LOSSES}$$

- NET ELECTRICAL OUTPUT = 7MW(e)
- AUXILIARY ELECTRIC LOAD = 1.05MW(e)
- THERMAL EFFICIENCY = 0.264
- THERMAL STORAGE CYCLE EFFICIENCY = 0.95
- DISCHARGE TIME = 6 HRS.
- HEAT LOSSES TO AMBIENT = 3.17MWH(t)/24 HRS

$$= \left[\frac{\text{WEIGHT FLOW FROM STORAGE LB/HR} \times \text{ENTHALPY RISE ACROSS STORAGE, } \frac{B}{LB}}{3413.10^{3} \ \frac{BTU}{MWH(t)} \times \text{STORAGE CYCLE EFFICIENCY}}\right] \times \text{DISCHARGE TIME} + \text{HEAT LOSSES}$$

- WEIGHT FLOW FROM STORAGE - 111,000 LB/HR
- ENTHALPY RISE ACROSS STORAGE -940 B/LB ($H_{SUP\ OUT} - H_{BOILER\ IN\ AT\ 335^{o}F}$)

Figure 6-2. Thermal Storage Field Capacity Design

Storage Subsystem

Baseline Design

THERMAL STORAGE CHARGING RATE

The thermal storage must be capable of charging at a rate equal to the maximum generated power from the steam generator.

The maximum charging rate to the Thermal Storage Subsystem is 49 MW(t). This is the peak power output from the Receiver Subsystem on 6/21 annual summer solstice at 12:00 noon. This assumes a boiler efficiency of approximately 90%. This corresponds to a flow rate of 177,000 lb/hr at 1450/950 from the Receiver Subsystem.

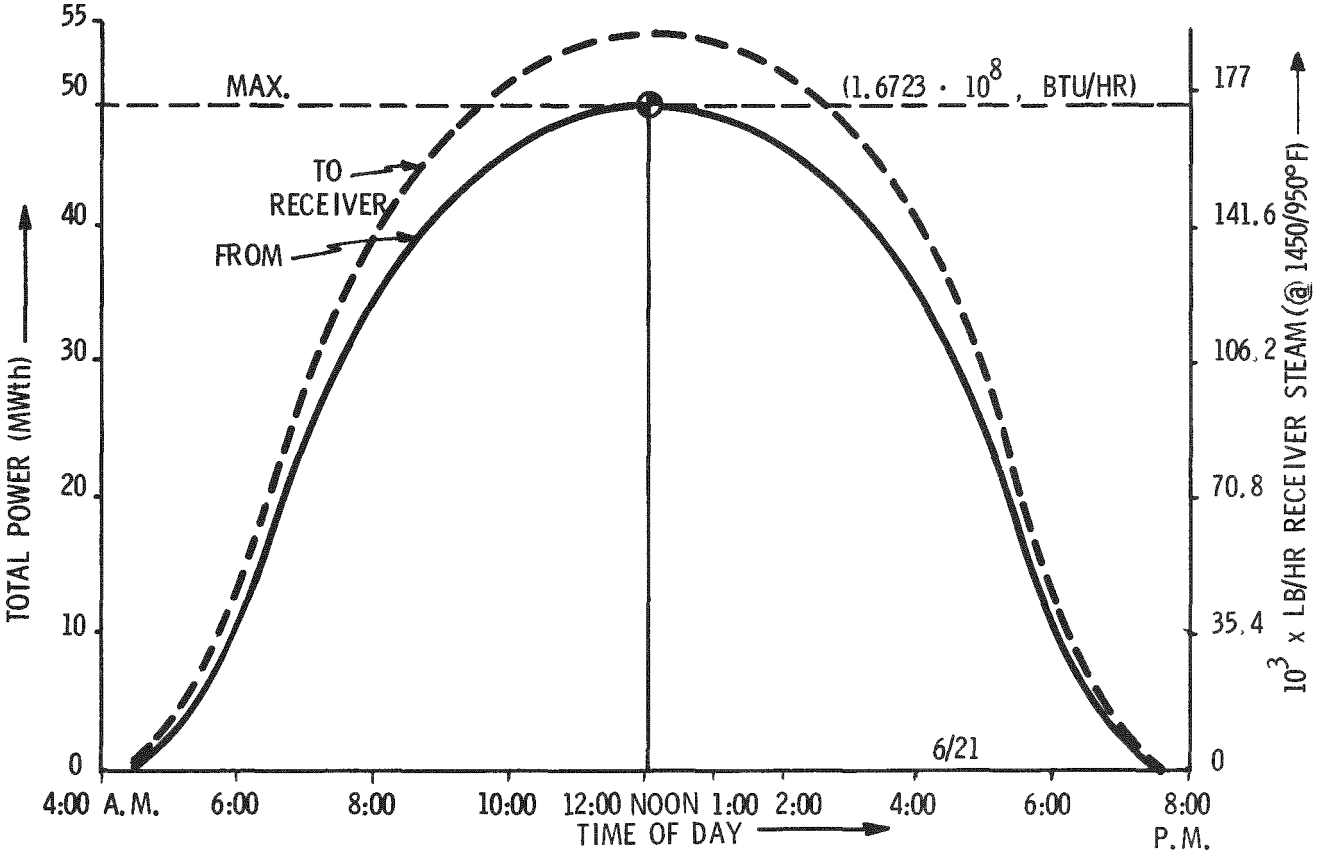


Figure 6-3. Thermal Storage Charging Rate

Storage Subsystem

Baseline Design

THERMAL STORAGE DISCHARGE RATE

The discharge rate for the thermal storage subsystem must provide 7WM(e) net electrical power for six hours when fully charged.

The steam discharge rate required from storage to the turbine inlet at 575 psig/538°F is a function of the extraction steam used for feedwater heating. Without extraction steam and a 3.5 psia turbine exhaust pressure, a flow of 97,500 lb/hr of steam is required with storage feedwater at 146°F. When sufficient extraction steam is used to provide storage feedwater at 337°F, the flow increases to 111,000 lb/hr to maintain the same net heat rate of 1.04×10^8 Btu/hr [30.54 MW(t) or 8.05 MW(e)]. As a result of extraction, the thermal efficiency increases to 0.264. Consequently, with 335°F feedwater and 111,000 lb/hr at 600 psig/538°F, a net of 7 MW(e) for 6 hours is provided.

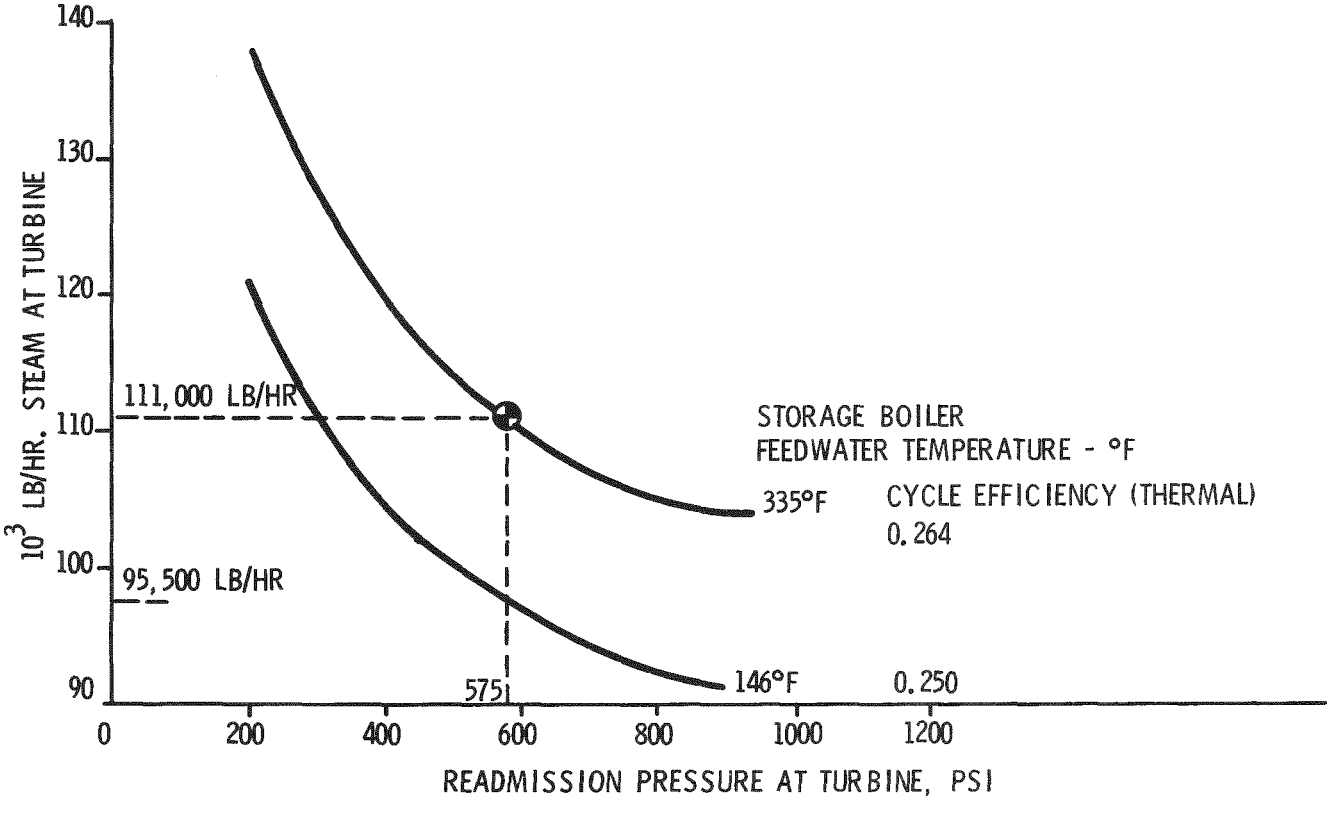


Figure 6-4. Thermal Storage Discharge Rate

Storage Subsystem

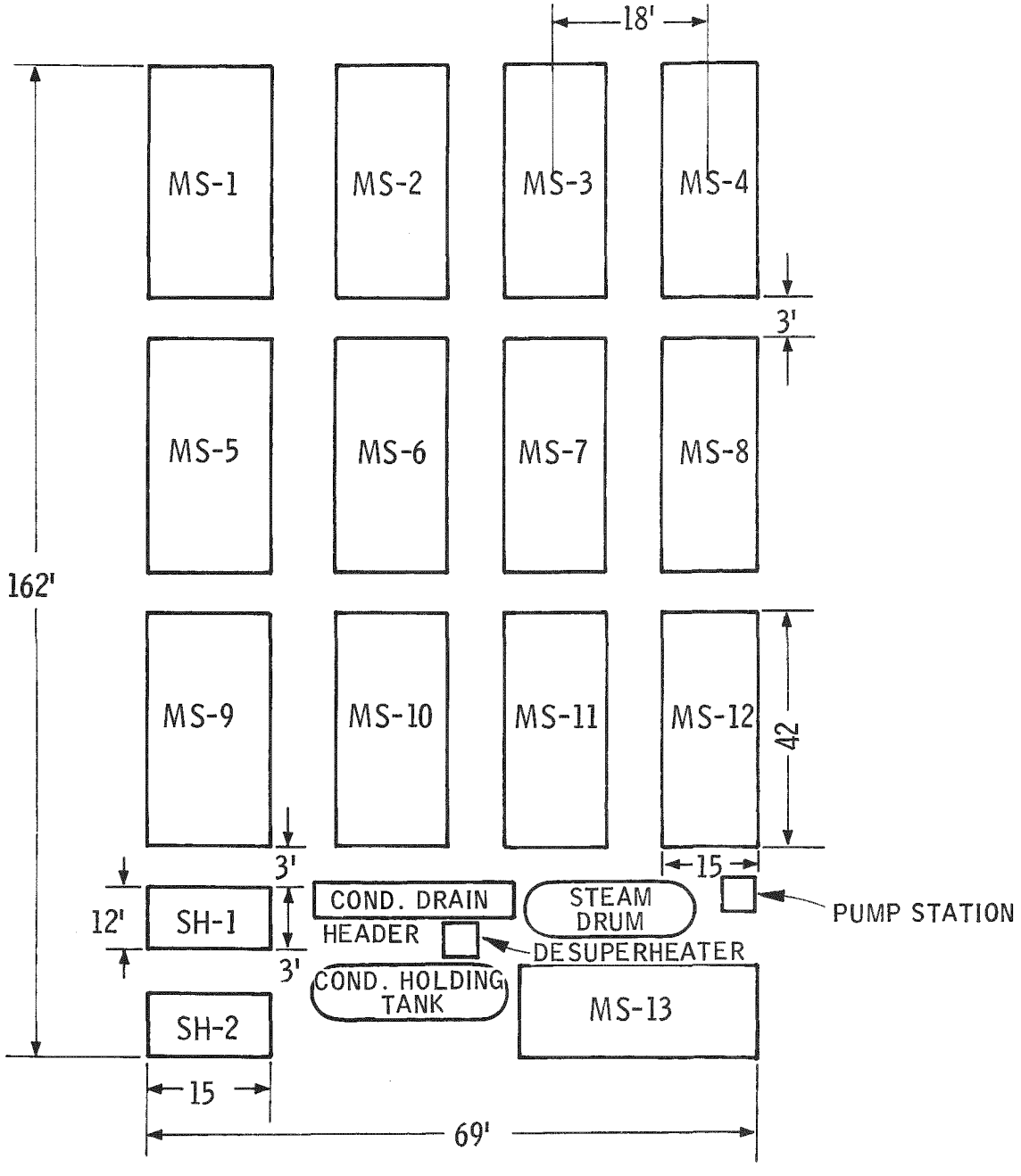
Baseline Design

DETERMINING THE EQUIPMENT LAYOUT

The Thermal Storage Subsystem can be designed to be compatible with standard steam power plant equipments.

The Thermal Storage Subsystem will store approximately 196 MWH(t) within the storage field of 70' by 162'. Twelve main storage tanks (12' x 15' x 42') contain a total of approximately 9.5 million pounds of a eutectic combination of sodium chloride, sodium nitrate and sodium sulfate. The superheater tank contains approximately 200,000 pounds of a eutectic combination of sodium chloride and sodium hydroxide. One extra main storage and superheater tank is provided for the required system availability. The tanks will be installed below ground to grade level on a foundation of three to four courses heavy duty fireclay-firebrick and spaced approximately three feet apart. The foundation bed will be suitably stabilized with pilings to support the brick foundation. A combination of castable/block insulation will be used over the entire field to maintain an acceptable field heat loss. A steam drum equipped with level controls will be located above ground and will supply the requisite saturated steam.

The Desuperheater Station provides saturated steam at the required operating pressure to the main storage tanks. Feedwater is provided to the station to condition the superheated vapor. The condensate will drain from the base of the tank heat exchangers into the condensate drain header. The condensate drain system will be installed below grade. Condensate in the headers will be transferred to the Deaerator. A condensate holding tank is provided in the event that a salt concentration is detected within the Thermal Storage Subsystem. With such an event the condensate would then be transferred to the holding tank to prevent possible contamination of the plant water supply system.



SH - SUPERHEATER
MS - MAIN STORAGE

Figure 6-5. Thermal Storage Field Layout

Storage Subsystem

Baseline Design

STORAGE FIELD HEAT LOSS

The heat loss from the Thermal Storage Field can be maintained less than: 0.2 MWH(t)/hr (6.8×10^5 Btu/hr).

The results from computer simulation of the field heat loss problem indicate that 0.12 MWH(t)/hr or 4×10^5 Btu/hr can be achieved with the following design.

A field 70 ft x 130 ft x 16 ft deep is excavated and prepared. The field base is covered with 18 in. of heavy duty structural firebrick such as H-W-Woodland x Brank firebrick. The perimeter of the field is lined with 9 in. of insulating firebrick and backed by a retaining wall. Uninsulated storage tanks 15 ft x 12 ft x 42 ft are installed with 3-ft spacings on the structural firebrick base. The entire field is covered with an equivalent of 1 foot thick H-W Block insulation.

Under these conditions the heat loss is estimated to be as follows:

Top of Field	(25%)	97,980 Btu/hr
Perimeter	(57%)	225,600 Btu/hr
Bottom	(18%)	73,800 Btu/hr
Total		397,380 Btu/hr

The fact that the individual unit cell sidewalls require no insulation results in considerable cost savings.

The temperature within the field enclosure will approach 550°F during steady-state operations.

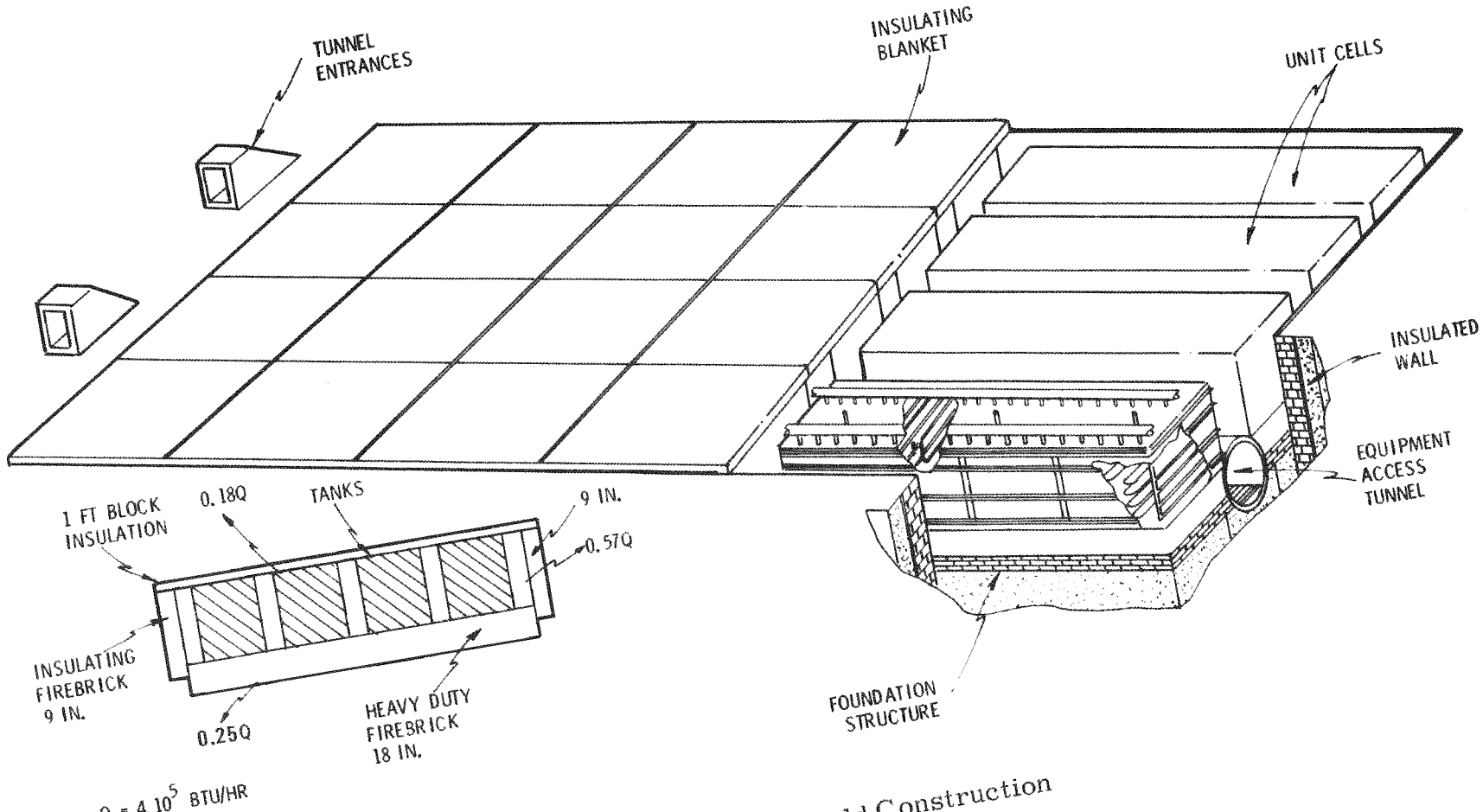


Figure 6-6. Storage Field Construction

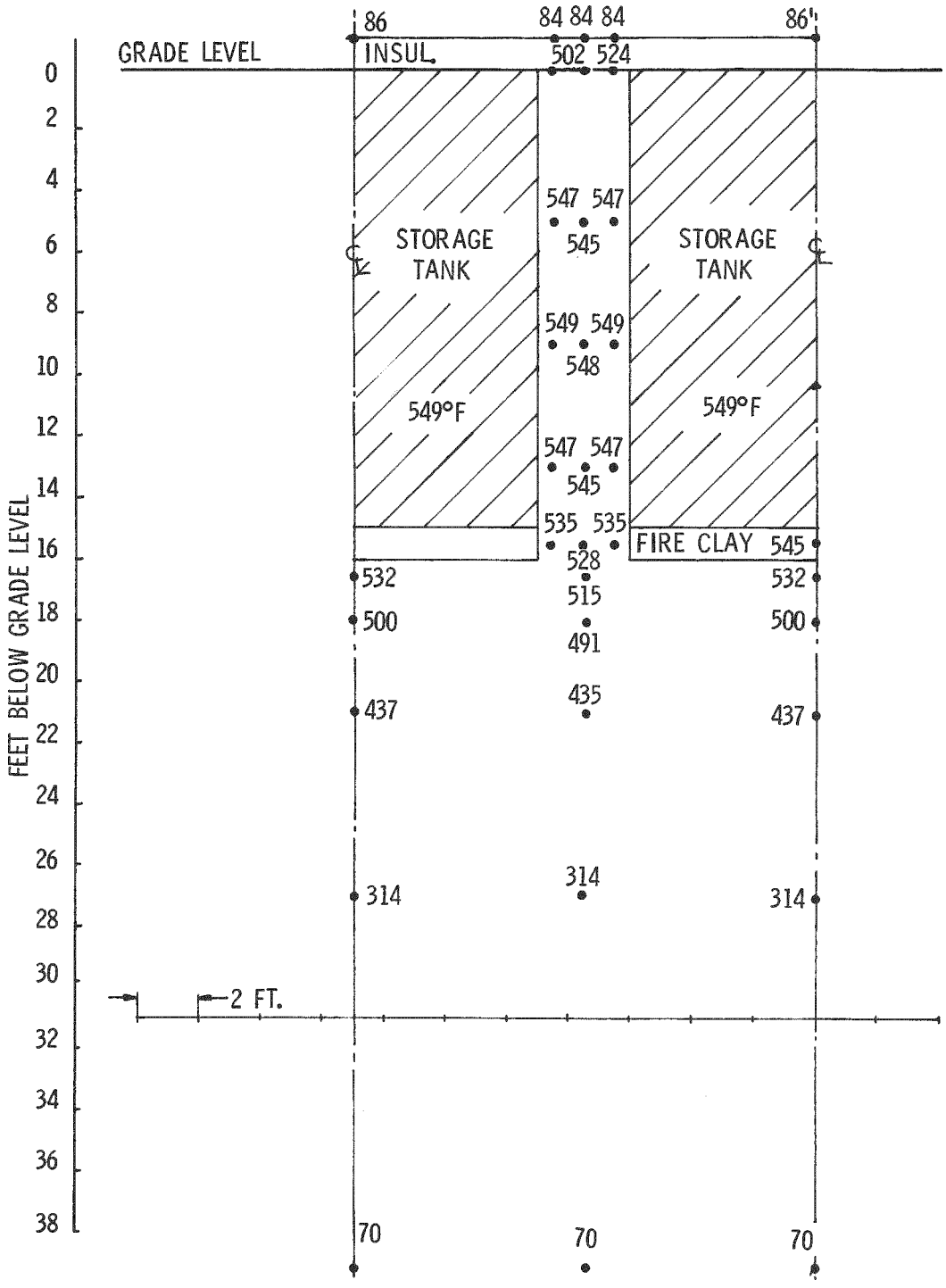


Figure 6-7. Temperature Drop

This page intentionally left blank.

Storage Subsystem

Baseline Design

MAIN STORAGE UNIT CELL

A battery of unit cells is the most practicable solution for storing large quantities of eutectic salts.

Twelve unit cells were selected for the main storage field as a compromise between cost, maintainability, control, and developmental scaling capabilities. Each cell, when fully charged, can hold approximately 16 MWH(t). The charge of 737,000 pounds of $NaCl$-$NaNO_3$-Na_2SO_4 salt mixture is contained within a mild steel tank 15 feet wide, 12 feet high and 42 feet long. The tank, designed to a 40-year life, consists of 3/8" mild steel thick base and side plates welded together. An external frame of U and L channels and gusset plates are provided to structurally unitize the entire unit. Corrosion, unfired high temperatures, handling loads (empty weight only), and long life are primary design considerations. The cover is designed to support the entire boiler unit and will have a lip seal for tank closure. The tank will be an atmospheric, vented, unpressurized vessel.

The weight of a charged tank, estimated to be approximately 840,000 pounds, will be distributed onto the foundation of super-strength heavy duty firebrick. The maximum cell base unit area loading will be less than 10 psi. This is well below the ultimate strength in compression for the firebrick.

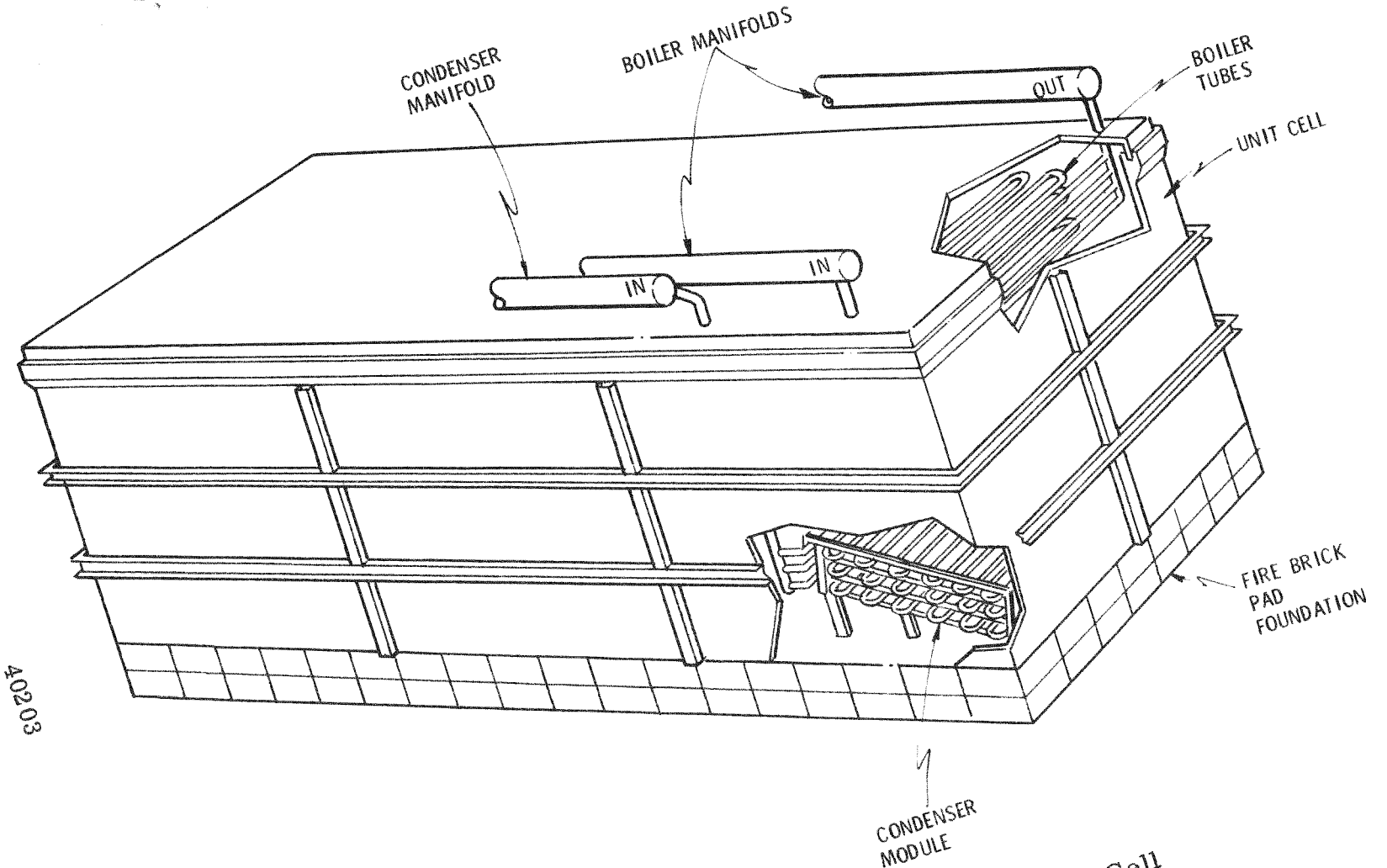


Figure 6-8. Main Storage Unit Cell

Storage Subsystem

Baseline Design

BOILER DESIGN SUMMARY

A forced recirculation boiler scheme with mechanical salt removal and heat extraction from the top of the tank is a viable method for heat energy discharge.

A maximum steam rate of 9250 lb/hr at 700 psig/503°F is required from each tank using the forced recirculation scheme. With a design condition of 43F°ΔT and an overall U_{aver} = 448 B/hr-ft^2-F°, a heat flux of 4480 B/hr-ft is possible. For a 10 ft/sec velocity in the 1" IPS schedule 80 pipes, a recirculation ratio of 5:1 and scraping time of 4 sec, 1500 lineal feet of pipe is required. Using 12-ft length of pipe per leg in a serpentine bundle configuration containing 20 legs results in 8 bundles per cell. Likewise, stacking two bundles per module allows four modules to be integrated into the top of the tank.

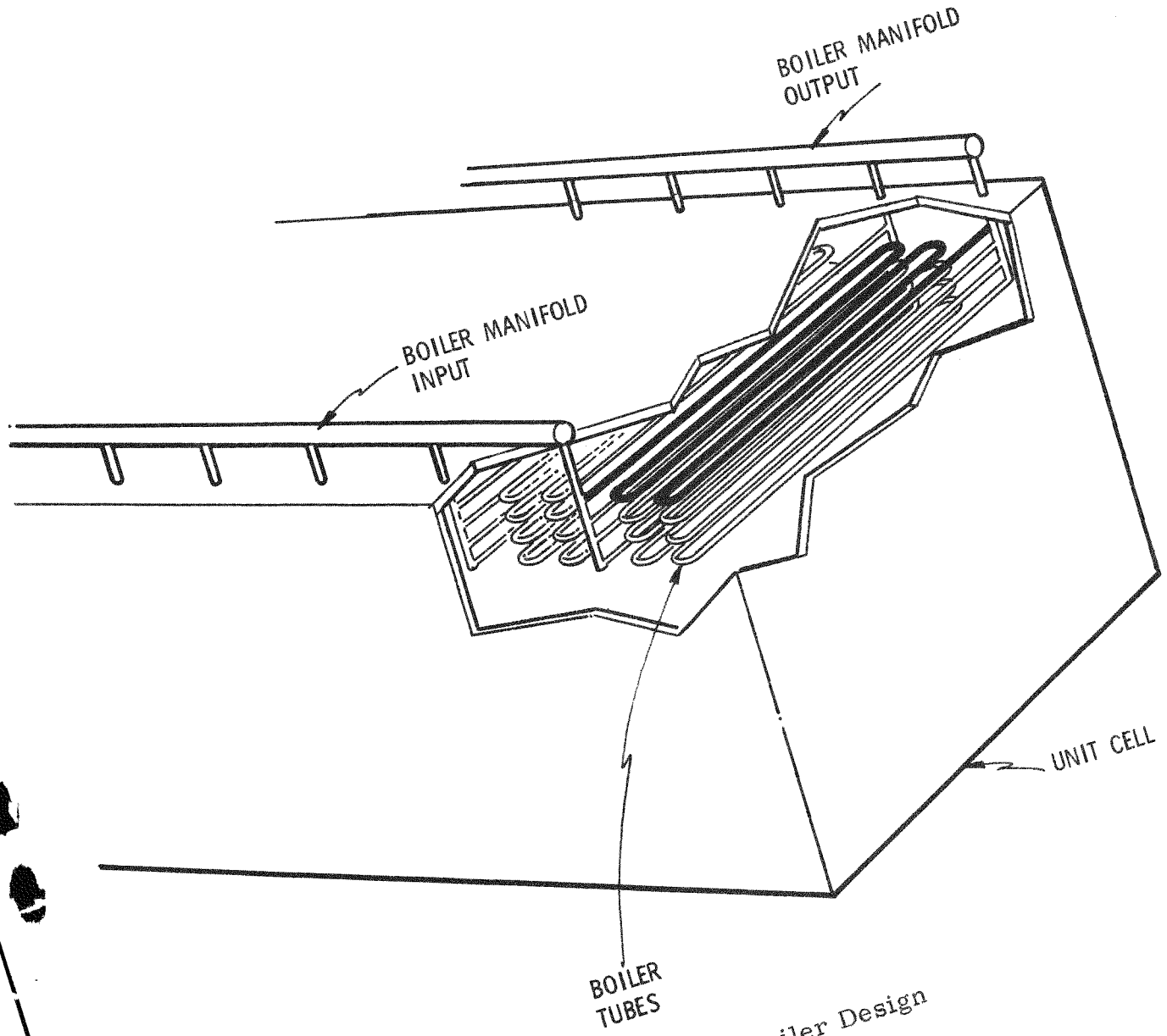


Figure 6-9. Boiler Design

Storage Subsystem

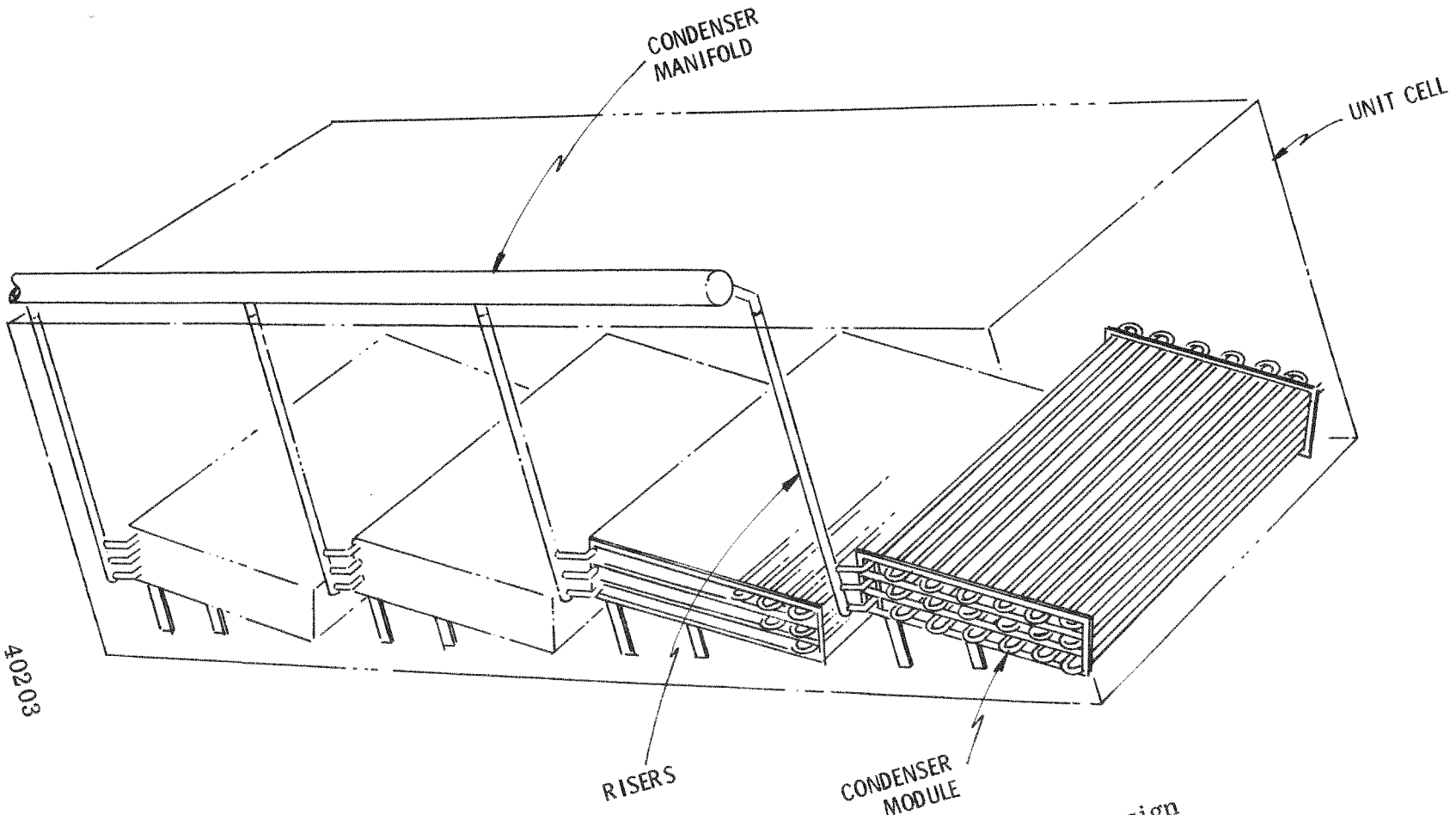
Baseline Design

CONDENSER DESIGN SUMMARY

A viable method for heat energy charging is an externally finned tube heat exchanger unit located at the bottom of the tank with natural convection heat transfer from steam condensing on the inside.

The maximum design steam rate to the Storage Subsystem from the steam generator is 177,000 lb/hr at 1450/950. When this steam is conditioned with feedwater 244,000 lb/hr of saturated steam is available to the main storage. The design ΔT at the condenser is 44°F. Using 1" IPS schedule 160 pipes with eight extended surfaces to achieve a 10/1 area ratio and an outside heat transfer coefficient of 80 B/hr-ft^2-F° fixes the condensate loading factor at 2.6 lb/hr-ft, a heat rate of 1464 B/hr-ft is possible. The total length of pipe required per cell to condense the steam at design conditions is 5760 feet. If a serpentine configuration is used with 30-12-foot legs packaged four to a module, then four 10 x 12 modules can be conveniently located at the base of the unit cell. The modules are tilted so the condensate will drain into the condensate header.

The external helical fins are spaced at three per inch, with a fin height of 3/4" and a thickness of 0.024".



40203

Figure 6-10. Condenser Design

Storage Subsystem

Baseline Design

SUPERHEATER DESIGN SUMMARY

A superheater unit consisting of a tube and plate heat exchanger in a eutectic salt bath can be effectively designed for both the charge and the discharge cycle over the operating conditions.

The superheater unit consists of a 12 ft x 12 ft x 17 ft long steel tank containing 200,000 lb of NaCl-NaOH eutectic mixture. This unit will have a gross weight of approximately 300,000 lb.

A tube and plate type heat exchanger has been designed to provide this minimum of 50°F superheat to the discharge steam at about 700 psig and saturated at inlet to the unit and discharge conditions of 600 psig/538°F. The maximum pressure drop across the superheater is estimated as 100 psi. A eutectic mixture of NaCl-NaOH having melting temperature of 698°F, provides a LMTD of 175°F for the discharge and 164°F for the charge at the design conditions. An overall U of 150 Btu/hr-ft^2°F was utilized for design. To achieve this, the shell side required sixty 10 ft x 7 ft plates, 1/4 inch thick spaced at four per foot. A plate efficiency of 60% was estimated. On the tube side, 52 1-inch IPS Sch 160 pipes, 15 ft long spaced on 17 in. centers is required to distribute a maximum of 111,000 lb/hr of discharge steam, with a distributed flow of 2135 lb/hr at 77 ft/sec. During charge, a maximum of 177,000 lb/hr of superheated steam at 1450 psig supplied from the Receiver Subsystem will flow through the same pipe bundle. Pressure balanced headers on the inlet/outlet allow a uniform steam velocity of 123 ft/sec in the pipes.

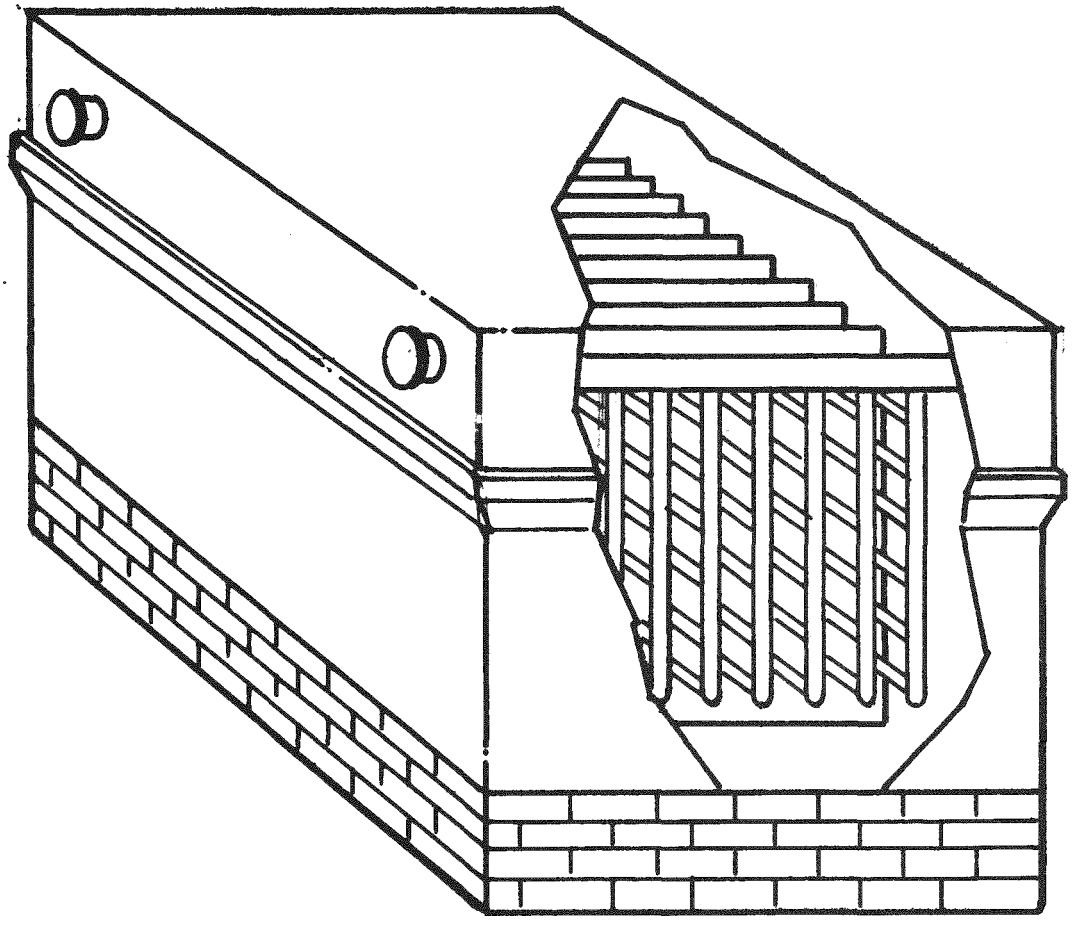


Figure 6-11. Superheater Design

Storage Subsystem

Baseline Design

SALT SELECTION

A low cost per KWH(e) eutectic salt can be found that is ideally suited to the operating cycle and is compatible with steam generating plant equipment and common materials.

The salt selected for the main storage is a ternary eutectic mixture of NaCl (5.72 wt %) - $NaNO_3$ (85.5 wt %) - Na_2SO_4 (8.78 wt %) with an experimentally determined eutectic temperature and heat of fusion of 549°F and 9250 B/ft^3 respectively. This temperature is ideally suited for the cycle selected. The current unit weight cost based on carload quantities is less than $.10 a pound [$3.49/KWH(t)] FOB at chemical plants in east and south. It is a nonhydroscopic, low-corrosivity, stable mixture of common salts. The design ΔT across the condenser unit is 43°F and that of the boiler is 44°F. The superheater storage cell salt is a binary eutectic misture of NaCl (26.8 wt %) and NaOH (73.2 wt %). The salt eutectic temperature is 698°F and has a heat of fusion in excess of 17,000 B/ft^3. For design, the log mean temperature difference (LMTD) for the charge and discharge cycles is given as 164°F and 178°F, respectively. One heat exchanger will be designed to accomplish both charge and discharge cycles.

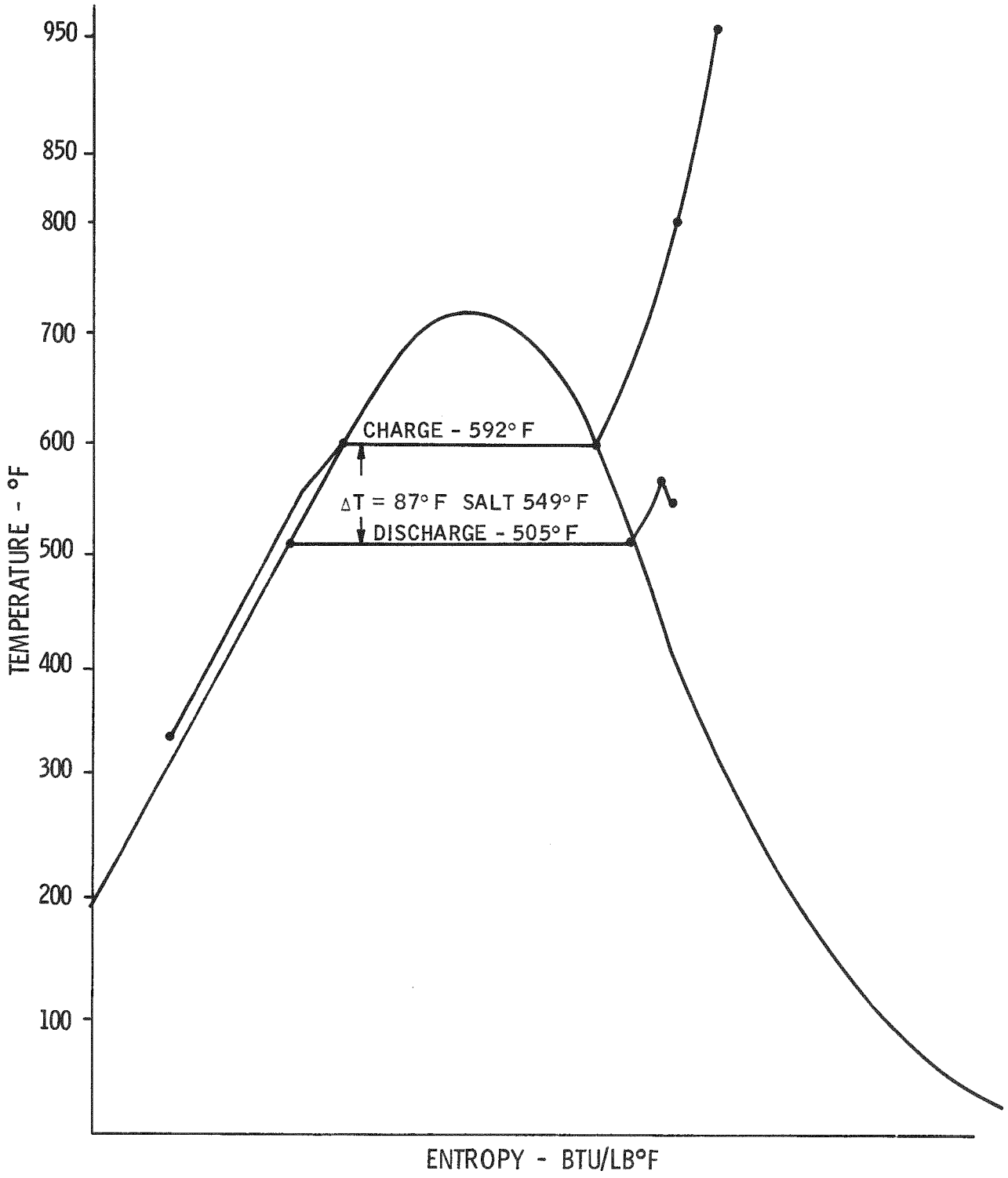


Figure 6-12. Thermal Storage Cycle

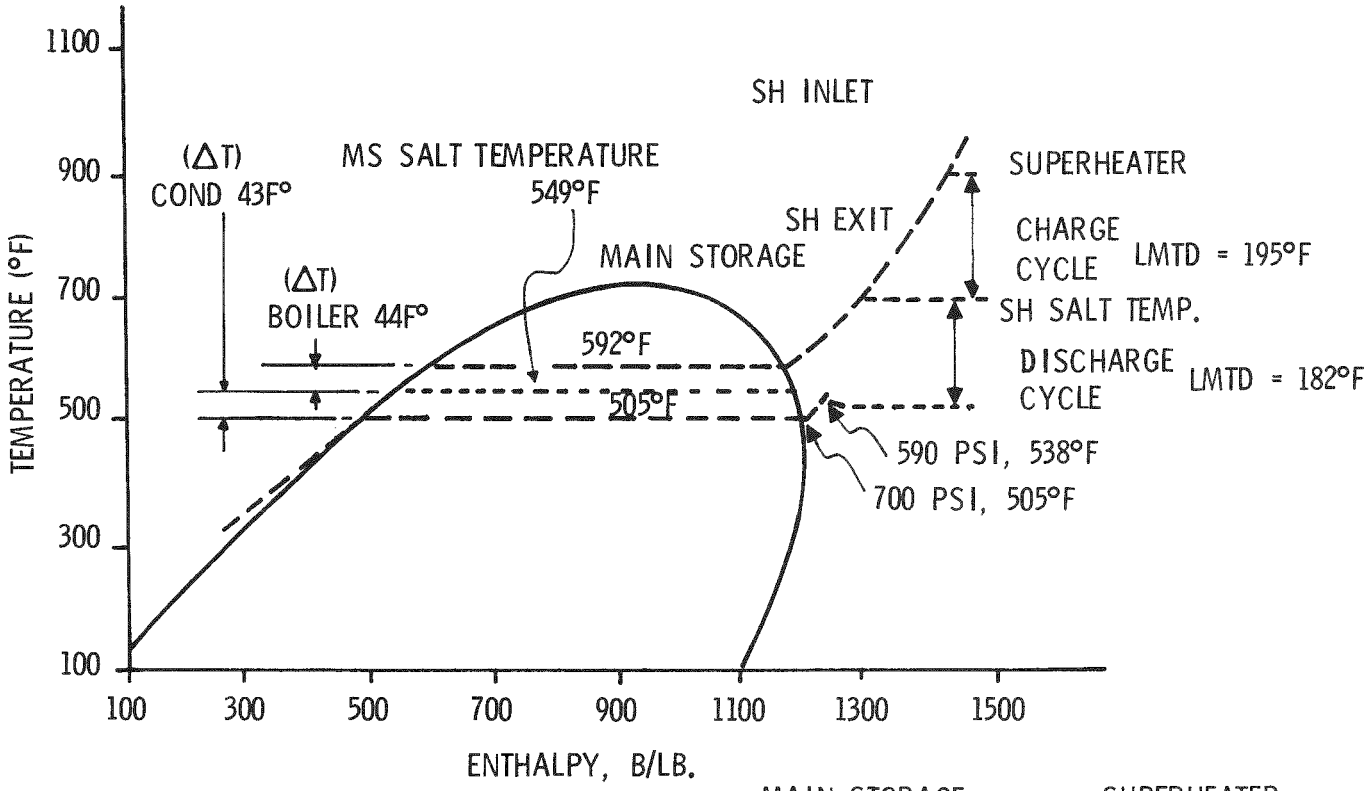
Storage Subsystem

Baseline Design

THERMAL STORAGE CYCLE AND STORAGE DESIGN

A Thermal Storage Subsystem can be designed to efficiently perform at a 1450 psig/950°F plant cycle.

The design of the Thermal Storage Subsystem is predicated on the 1450/950 pilot plant cycle with secondary injection at 575 psig/534°F. Charging steam from the Receiver Subsystem is supplied at 1450 - 1000 psig at either the main storage or superheater cell. The charging steam when flowing through the superheater exits at approximately 800°F and is reduced to near saturation temperature conditions at the desuperheater. The desuperheater station is capable of conditioning the steam with feedwater to within 14°F of the saturation valve of 592°F. The steam is then distributed to the main storage field unit cells. The steam is condensed and discharged from the field as saturated water at approximately 1450 - 1000 psig. When the superheater is fully charged, the steam will be valved to enter the desuperheater directly. When discharging, feedwater at 335°F enters the steam drum is mixed with resident water and pumped through the boiler section of the unit cell in the field. The flow will depend upon the turbine demand as determined by the throttle valve setting. The discharge from the main storage will be at 700 psig/538°F. A minimum of 50°F superheat must be available at the turbine throttle at all times. An alternate superheater tank will be charged and available in the event that the main superheater malfunctions.



MAIN STORAGE

$$Q_{bo} = Q_{co} = W_s H_f$$

$$\frac{A_b}{A_c} = 1 \frac{U_{bo}}{U_{co}} = 1.0$$

$$T_e = \frac{T_b + T_c}{2}$$

SUPERHEATER

$$LMTD = \frac{U_o \, 2 \, r_o \, L}{W_h \, C_{ph}}$$

$LMTD_c = 195F°$

$LMTD_d = 182F°$

Figure 6-13. Thermal Storage Operating Cycle

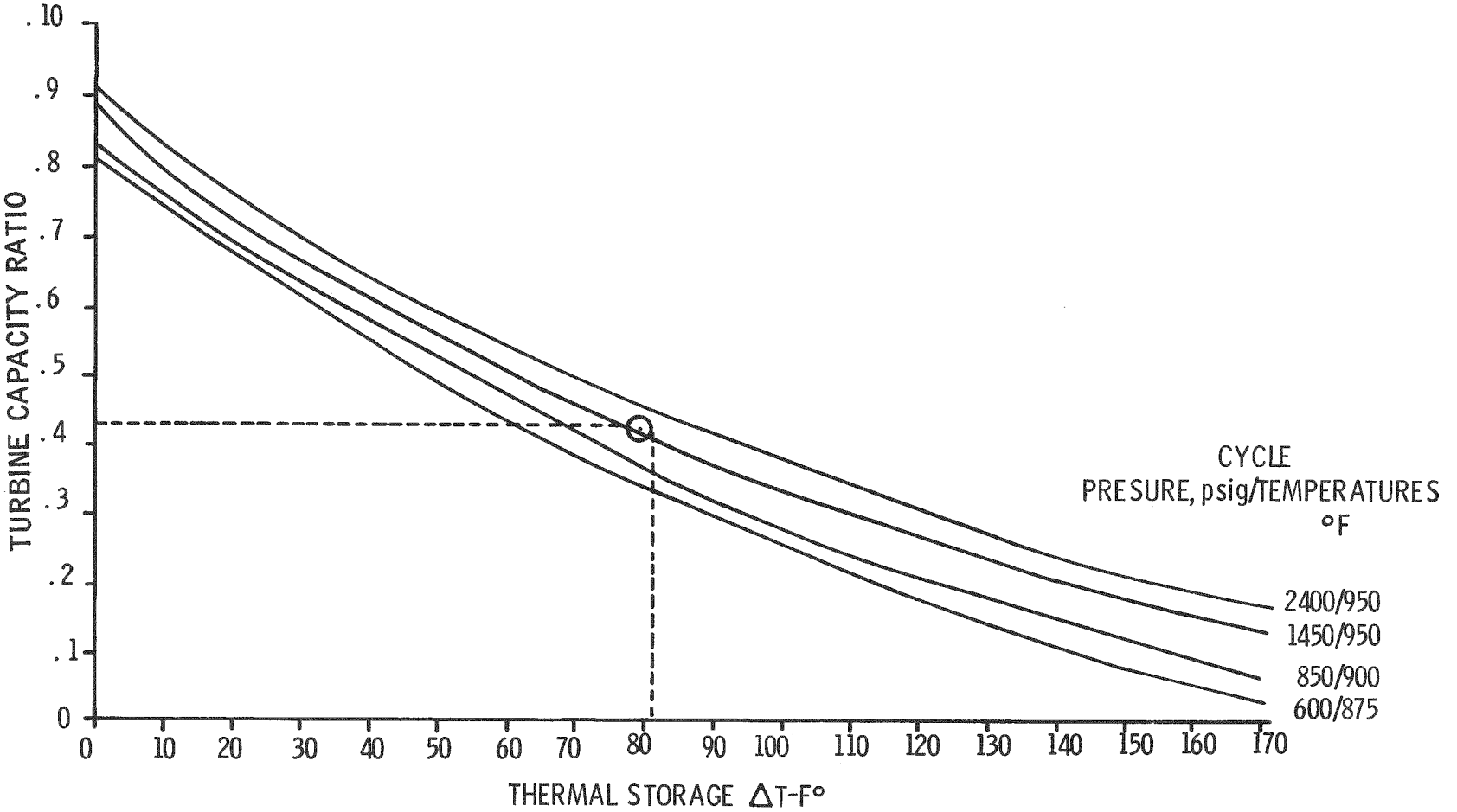


Figure 6-14. Thermal Storage ΔT Versus Single-Admission Turbine Loading for Power Plant Cycles Assuming 50% Superheat

This page intentionally left blank.

Storage Subsystem

Baseline Design

THERMAL STORAGE CONTROL

The thermal storage control system will follow input and output demands with a minimum of restrictions on the operation of the plant.

The thermal storage system will operate all 12 cells in parallel, charging and discharging evenly. This will allow the system to follow any input or output demand from 0 to maximum design flow as long as there is heat available. Flow distribution will be through the velocity difference between feeder lines and headers. Maximum velocity in the heat exchangers will be 600 feet per minute at the design condition. Charge input following will be controlled by a single condensate trap-level control. Steam output pressure will be controlled by automatically regulating the feedwater recirculation flow.

Charging

The charging steam input will be distributed evenly to all storage cells. A single condensate drain header system trap with level control will allow the output to follow the input demand. At input flow rates below the design condition, the heat exchangers will have excess capacity, causing the saturation temperature and pressure to decrease.

The maximum charging rate is 49 mw(t). This is the peak power output from the Receiver Subsystem on 6/21. This corresponds to a flow rate of 177,000 lb/hr at 1450/950°F. There is no minimum charge flow rate. However, the minimum pressure that steam will condense is 1000 psi, and maximum flow rate will be restricted at pressures below 1450 psi.

Discharging

Steam pressure will be held constant at all output levels, from 0 to maximum flow, by regulating feedwater recirculation flow. At output rates below the design condition, recirculation flow will decrease. Excess capacity will increase boiler output quality up to 70 percent. Above 70 percent the heat transfer coefficient will fall off enough to produce the required amount of steam.

The steam discharge rate required from storage to the turbine inlet at 575 psig/538°F is a function of the extraction steam used for feedwater heating. Without extraction steam and a 3.5 psia turbine exhaust pressure, a flow of 97,500 lb/hr of steam is required with storage feedwater at 146°F. When sufficient extraction steam is used to provide storage feedwater at 337°F, the flow increases to 111,000 lb/hr to maintain the same net heat rate of 1.04×10^8 Btu/hr (30.57 MW(t) - 8.05 MW(e). However, as a result of extraction, the thermal efficiency increases to 0.264. A discharge rate based on the unit cell is 11,700 lb/hr.

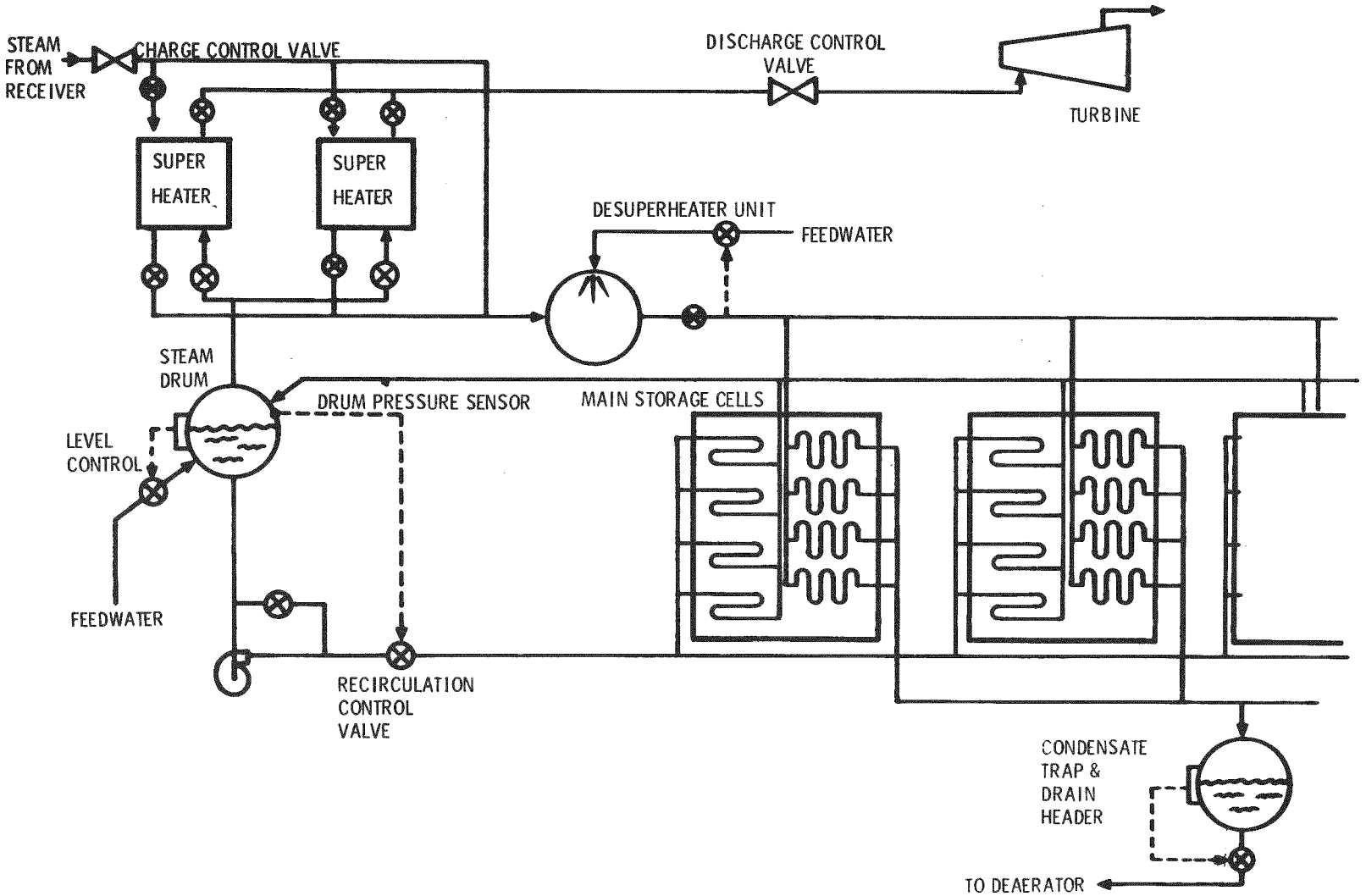


Figure 6-15. Thermal Storage Control

Superheater

Discharge steam will circulate through one superheater cell while the second cell is used for backup or charging. At steam flow rates below maximum, the superheat temperature will increase slightly. The heat transfer coefficient drops off almost as fast as the flow rate. At 0.1 of design flow, the superheat temperature will increase 50 percent. If the superheat temperature drops below the desired value, the flow will automatically switch to the backup cell.

This page intentionally left blank.

OPERATIONS

The Thermal Storage Subsystem is capable of providing an efficient, flexible energy management program for plant operation.

For the baseline design three basic operating strategies are employed. The first two require charge and discharge both separately and concurrently from the Storage Subsystem and the third requires a hold or store capability. Based on the baseline mechanization it has been determined that storage will be in a 30% full status at the end of a given day. The thermal power profile required of storage with either operating strategy is one of steadily increasing demand. For example, for Strategy "A" at summer solestice (6/21) the storage will come on the line at 4:30 P.M., be at full load at 7:30 P.M., and shut down at 7:45 P.M. with the required 30% residual for the next day's operation.

In the winter (12/21) using the same strategy gives a similar result. The rate of change of the demand power is typically 335 KW/min over the operating period.

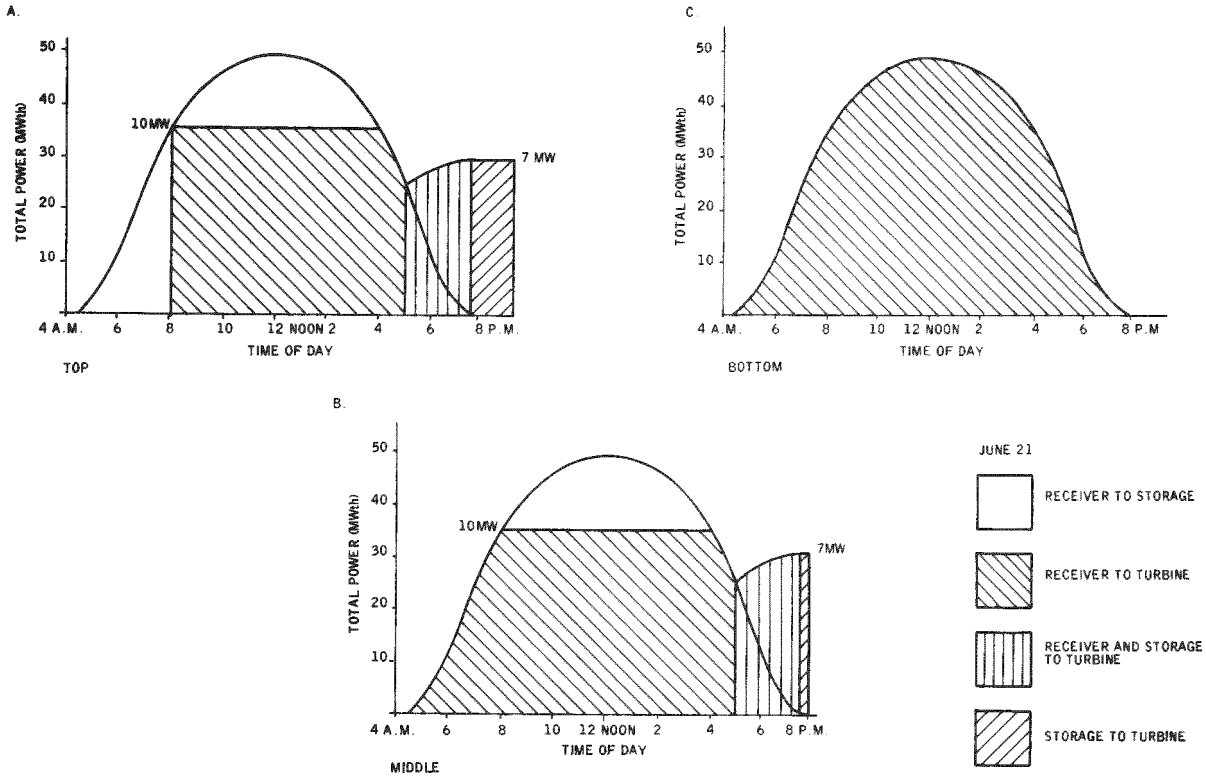


Figure 6-16. Three Operating Strategies

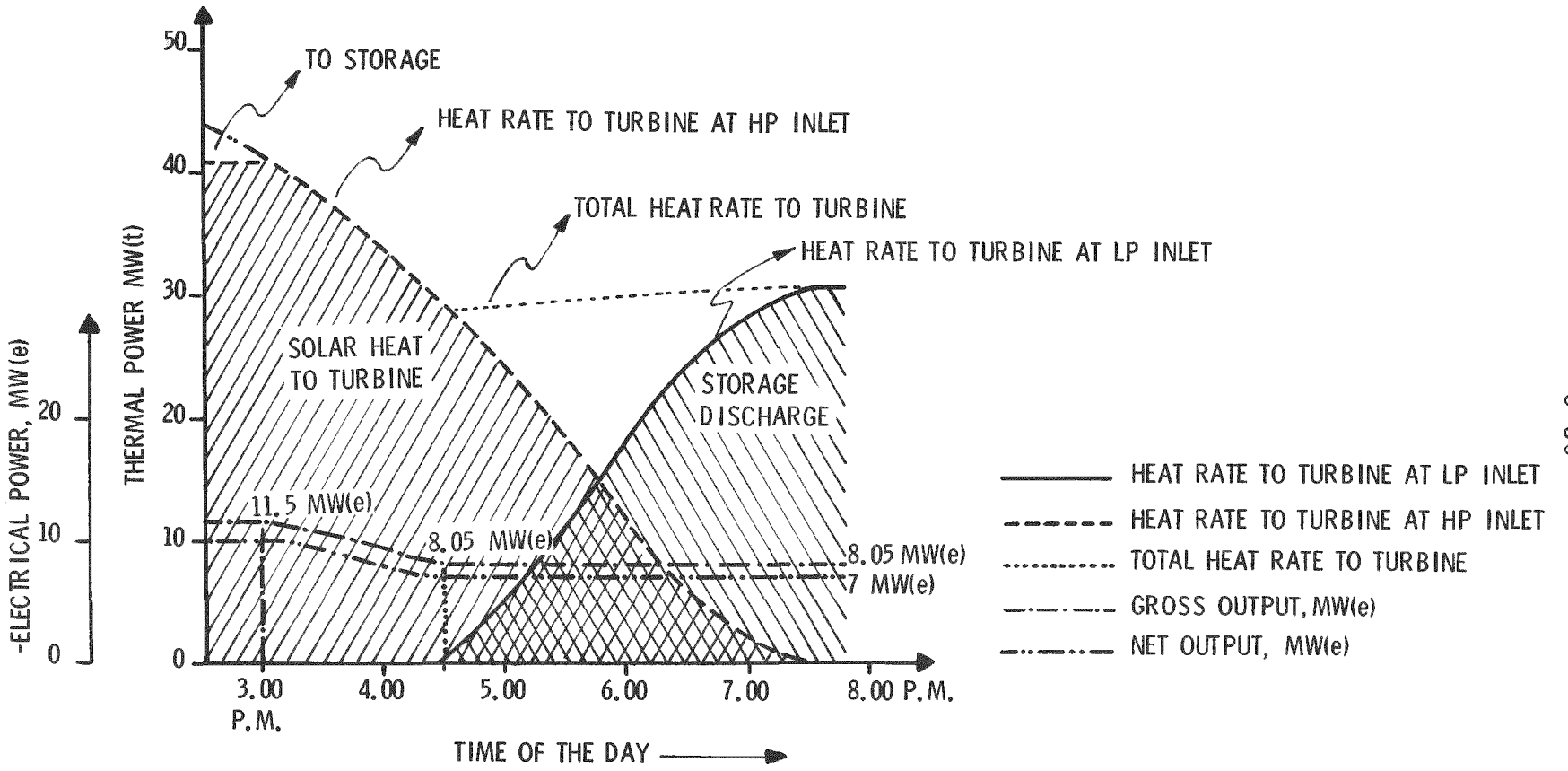


Figure 6-17. Thermal Power Profile A

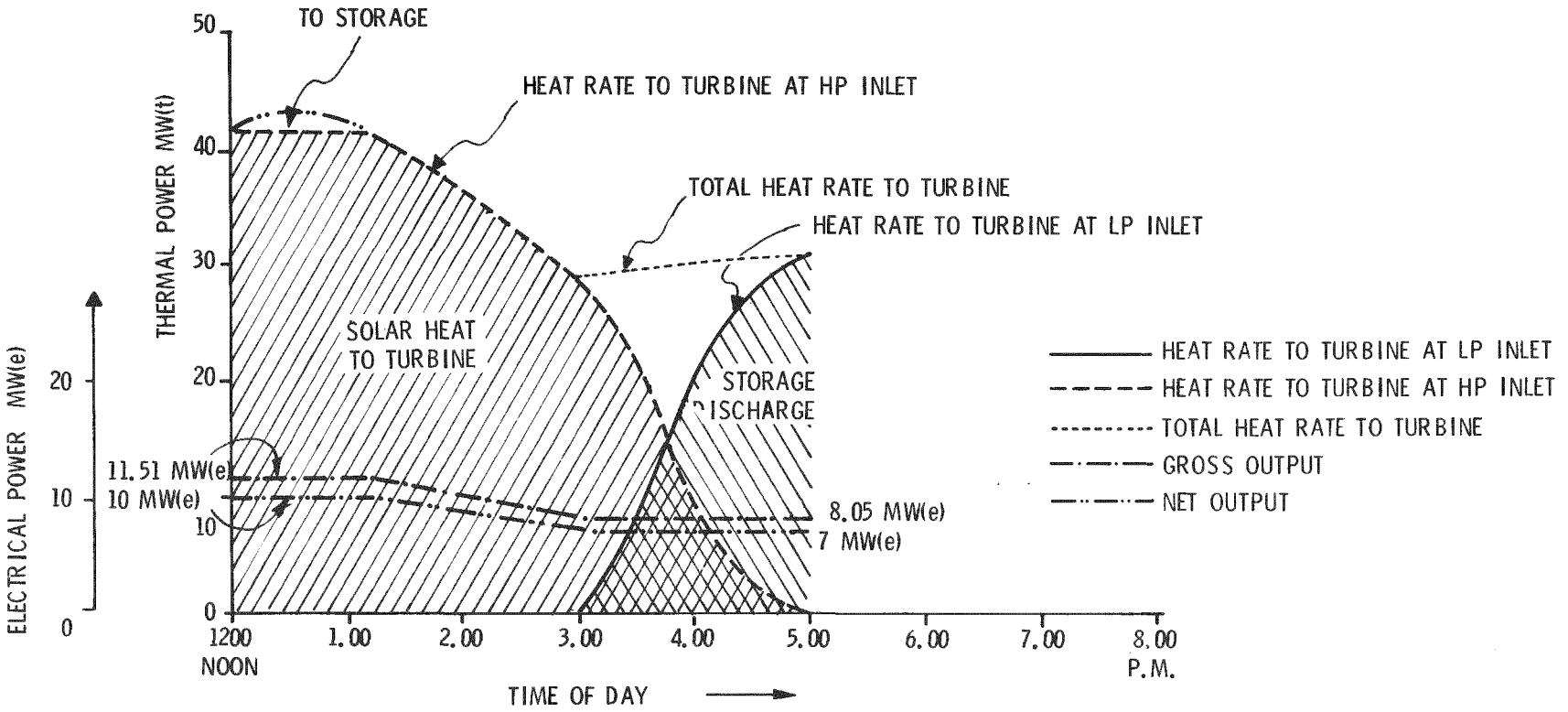


Figure 6-18. Thermal Power Profile B

Table 6-1. Thermal Storage Subsystem Specific Costs and Goals

ITEM	DOLLARS/KWH(e) NET OUTPUT	
	CURRENT ESTIMATE NON-RECURRING INSTALLED	GOAL
MAIN STORAGE ($NaCl$-$NaNO_3$-Na_2SO_4)	16.3	10.3
SUPERHEATER SALT ($NaCl$-$NaOH$)	0.6	0.5
TANKAGE (MS, SH AND AUX)	7.4	6.0
CONDENSER SYSTEM	12.9	9.2
BOILER SYSTEM	9.5	8.0
STORAGE FIELD PIPING	1.2	1.0
INSTALLATION	6.3	5.0
	54.2	40.0

SECTION VII
ELECTRICAL GENERATION SUBSYSTEM

	Page
Concept and Requirements	7-2
Tradeoffs and Analysis Review	7-12
Major Component Specifications and Layout	7-22
Major Piping and Instrument System Description	7-34
Control Concept and Requirements	7-50
Plant Operating Modes	7-60

Electrical Generation Subsystem

Concept and Requirements

GENERATE ELECTRICAL POWER USING RECEIVER STEAM OR THERMAL STORAGE UNIT STEAM

The EGS is being designed to efficiently generate electrical power using a water/steam cycle with the thermal energy being supplied by solar radiation either directly through the receiver or indirectly through the thermal storage unit.

1. The EGS will provide the means for transforming and using, in an efficient manner, the thermal output of the Receiver and/or Thermal Storage Subsystems into 60-cycle electrical power at 13,800 volts. The EGS electrical output will be regulated for integration into an existing electrical power system.

2. The EGS is being designed to transport, control and condition the cycle working fluid during all anticipated operating modes. The design will attempt to maintain maximum plant efficiency during all modes of operation with primary consideration given to meeting the performance requirements which have been established for the 10-MW Solar Pilot Plant. These performance requirements are:

   - Generate a 10-MW net busbar electricity at 2 pm on a clear day on winter solstice using superheated steam supplied directly from the Receiver Subsystem.
   - Generate a 7-MW net busbar electricity for a period of six hours using superheated steam supplied directly from the Thermal Storage Subsystem.
   - Generate a 7-MW net busbar electricity when using steam from the Receiver and Thermal Storage Subsystems simultaneously.
   - Operate safely and reliably with the maximum steam flow that will be generated by the Receiver Subsystem during maximum insolation and ambient air temperature periods.

3. Figure 7-1 depicts the basic cycle arrangement of the plant and illustrates the major working fluid flow paths between the primary EGS components and the Receiver and Thermal Storage Subsystems.

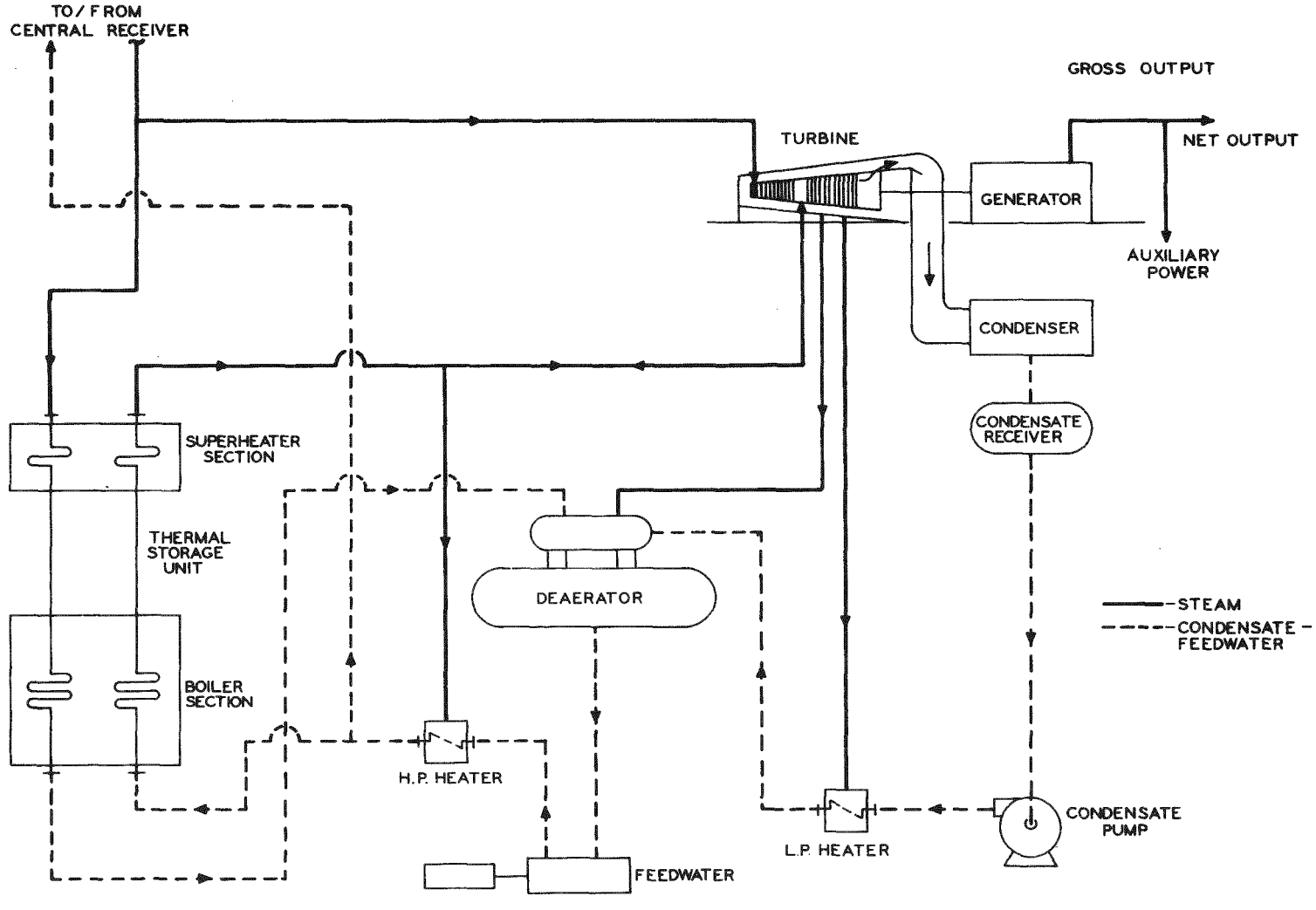


Figure 7-1. Electrical Generation Subsystem

Electrical Generation Subsystem

Concept and Requirements

PERFORMANCE AND OPERATIONAL REQUIREMENTS USING RECEIVER SUBSYSTEM STEAM

The EGS is being designed to generate 10-MW net busbar electricity at 2 pm on a clear day at winter solstice using superheated steam supplied directly from the Receiver Subsystem.

1. The EGS will generate a 12,000-kW gross capacity and a 10,000-kW net capacity when operating with Receiver Subsystem steam leaving the receiver superheater outlet at 1470 psi and 955°F. The turbine design throttle steam conditions will be 1450 psi and 950°F. The 20-psi and 5°F temperature differences between the receiver superheater outlet and the turbine inlet will account for frictional and thermal losses between the two points. The turbine throttle flow required at these conditions and load has been estimated to be 114,000 pounds per hour. Based on this flow and the 20-psi pressure drop, a steam header size of eight inches has been chosen.

2. During steady-state periods of operation at these conditions and load, both the high-pressure (HP) and low-pressure (LP) feedwater heaters will be in service. The deaerator will also be in service as will be one condensate pump and one feedwater pump.

3. The steady-state operation of the EGS during this performance mode is shown schematically in Figure 7-2.

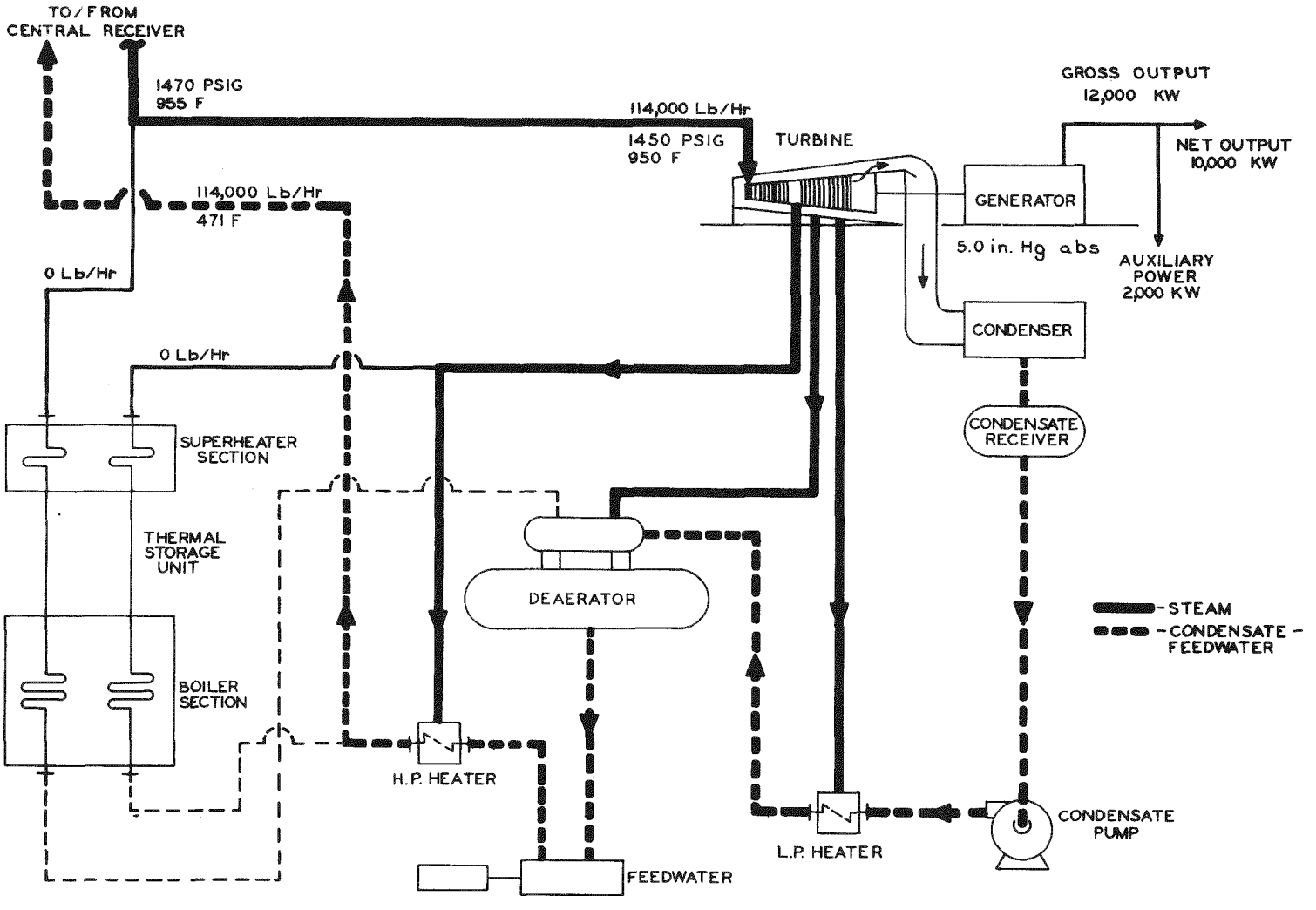


Figure 7-2. Performance Using Receiver Subsystem Steam

Electrical Generation Subsystem

Concept and Requirements

PERFORMANCE AND OPERATIONAL REQUIREMENTS
USING STORAGE SUBSYSTEM STEAM

The EGS is being designed to generate 7-MW net busbar electricity for a period of six hours using superheated steam supplied directly from the Storage Subsystem.

---

1. The EGS will generate an 8050-kW gross capacity and a 7000-kW net capacity when operating with Thermal Storage Subsystem steam leaving the storage unit superheater outlet at 600 psi and 539°F. The turbine LP admission design steam conditions will be 575 psi and 534°F. The 25-psi and 5.0°F temperature differences between the storage unit superheater outlet and the turbine LP admission inlet will account for frictional and thermal losses between the two points.

2. During steady-state periods of operation at these conditions and load, the HP feedwater heater will be taken out of service. The LP feedwater heater and deaerator will be in service as will be one condensate pump and one feedwater pump.

3. The steady-state operation of the EGS during this performance mode is shown schematically in Figure 7-3.

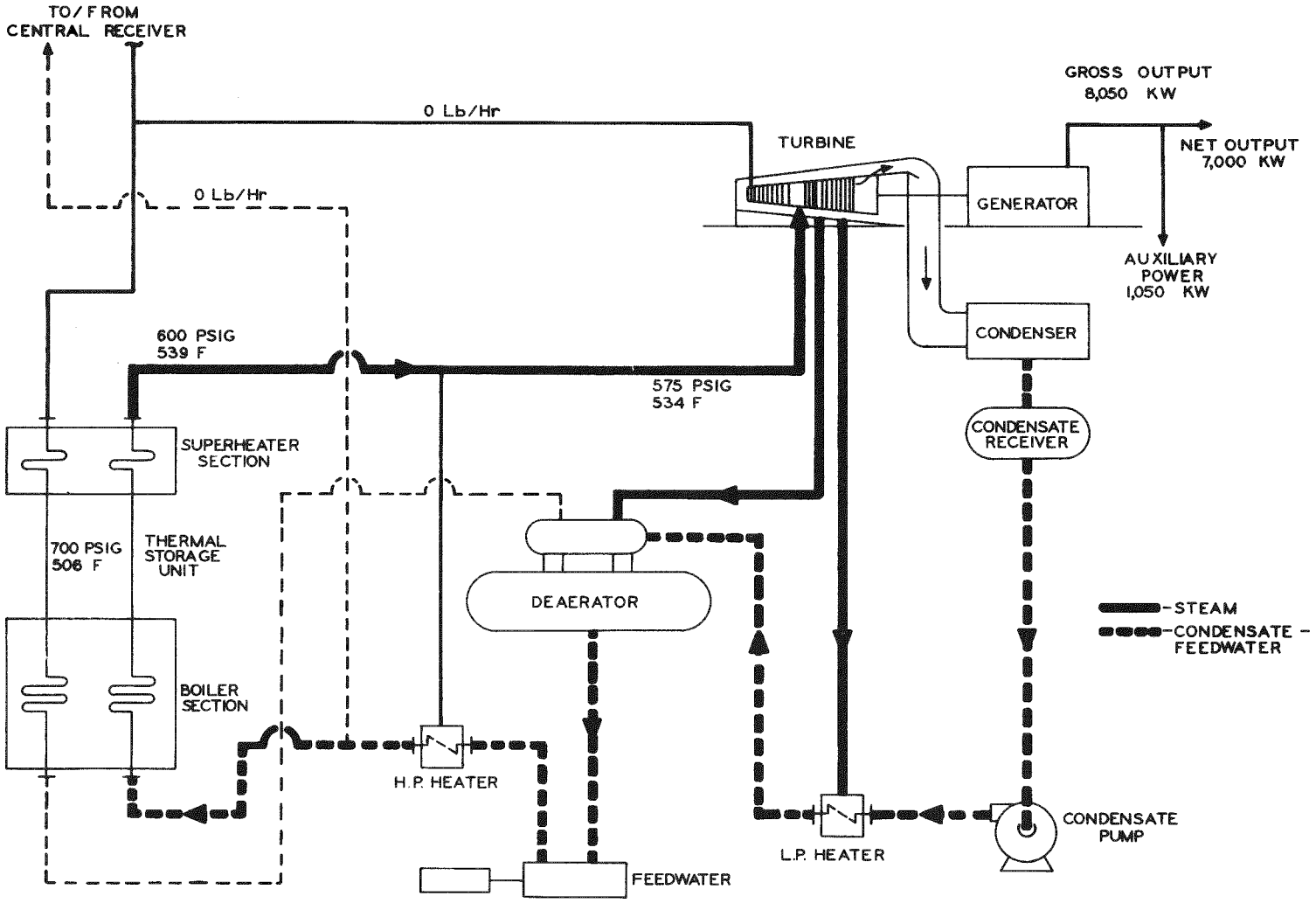


Figure 7-3. Performance Using Storage Subsystem Steam

Electrical Generation Subsystem

Concept and Requirements

PERFORMANCE AND OPERATIONAL REQUIREMENTS USING RECEIVER SUBSYSTEM AND STORAGE SUBSYSTEM STEAM SIMULTANEOUSLY

The EGS is being designed to generate 7-MW net busbar electricity when using steam from the Receiver and Storage Subsystems simultaneously.

1. The EGS will generate an 8050-kW gross capacity and a 7000-kW net capacity when operating with Receiver and Thermal Storage Subsystem steam simultaneously. The turbine HP inlet throttle conditions will be 1450 psi and 950°F. The turbine LP admission steam conditions will be 575 psi and 534°F.

2. During steady-state periods of operation at these conditions and load, the HP feedwater heater will be taken out of service. The LP feedwater heater and the deaerator will be in service as will be one condensate pump and one feedwater pump. The feedwater pump discharge flow will be divided and controlled to maintain the proper amount of flow to the receiver and thermal storage unit.

3. The steady-state operation of the EGS during this performance mode is shown schematically in Figure 7-4.

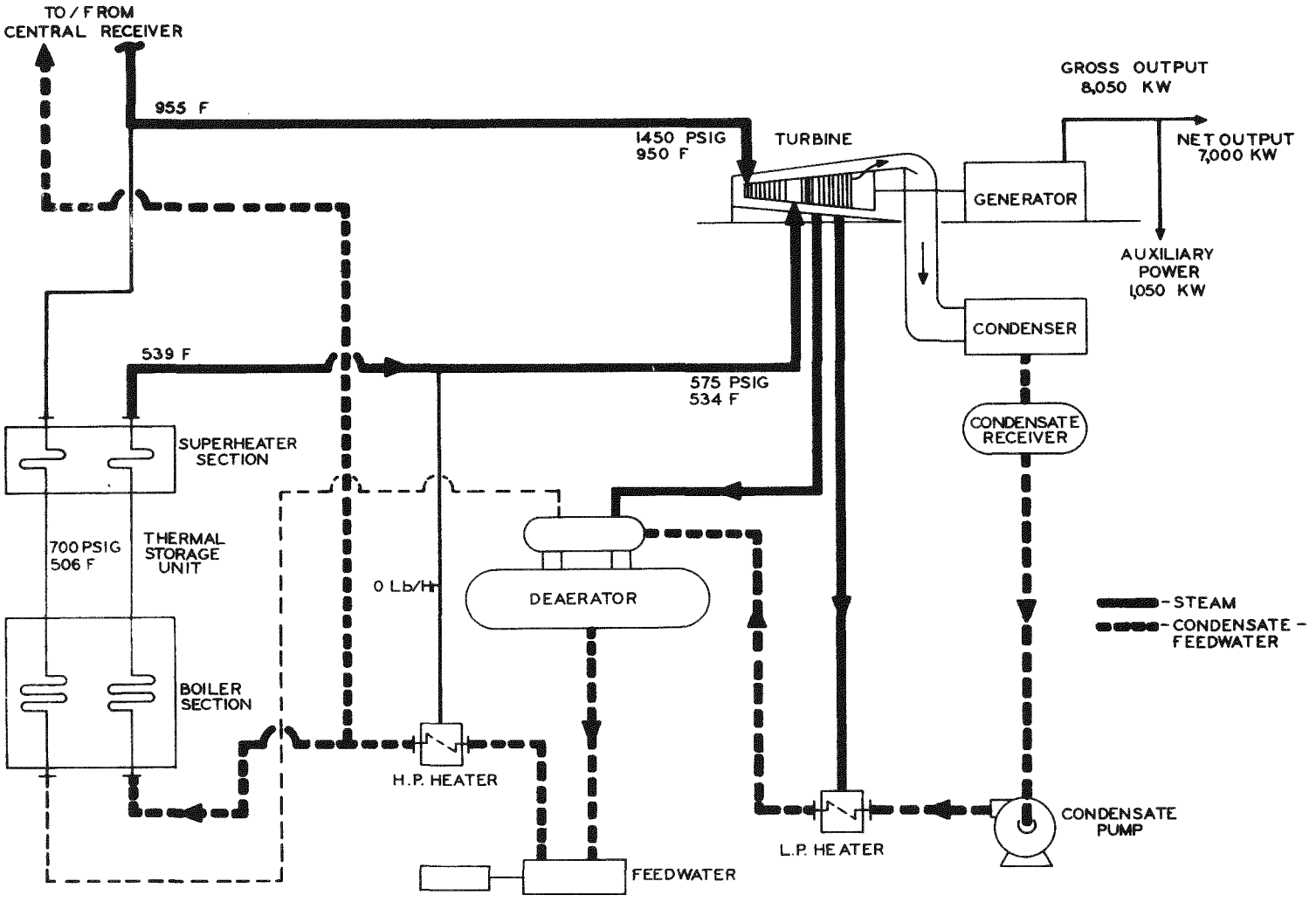


Figure 7-4. Performance Using Receiver Subsystem and Storage Subsystem Steam Simultaneously

Electrical Generation Subsystem

Concept and Requirements

GENERATION CAPABILITIES DURING HIGH SUMMER FLUX PERIODS

The EGS is being designed to operate safely and reliably with the maximum steam flow that can be generated by the Receiver Subsystem during maximum insolation periods with an ambient temperature of 115°F.

1. The EGS, with its major components such as the turbine generator and heat rejection system, will be capable of safe and reliable operation when handling the maximum receiver steam output. This flow rate has been defined to be 55 percent more than the design flow that will be required to generate 10-MW net busbar electricity at 2 pm on the winter solstice.

2. The turbine design HP throttle conditions will be 1450 psi and 950°F. The receiver superheater outlet steam conditions will be 1500 psi and 955°F. The 50-psi pressure and 5°F temperature differences between the receiver superheater outlet and the turbine inlet will account for frictional and thermal losses between the two points. The turbine throttle flow at these conditions and load, based on 55 percent more than the estimated 114,000 pounds per hour requirement at 10-MW net, will be 176-700 pounds per hour. The amount of gross generation during this performance mode will be dependent upon the turbine generator design.

3. During steady-state periods of operation at these conditions, both the HP and LP feedwater heaters will be in service. The deaerator will be in service and two condensate and two feedwater pumps will be used. Two pumps will be required in order to handle the increased flow rates.

4. The steady-state operation of the EGS during this performance mode is shown schematically in Figure 7-5.

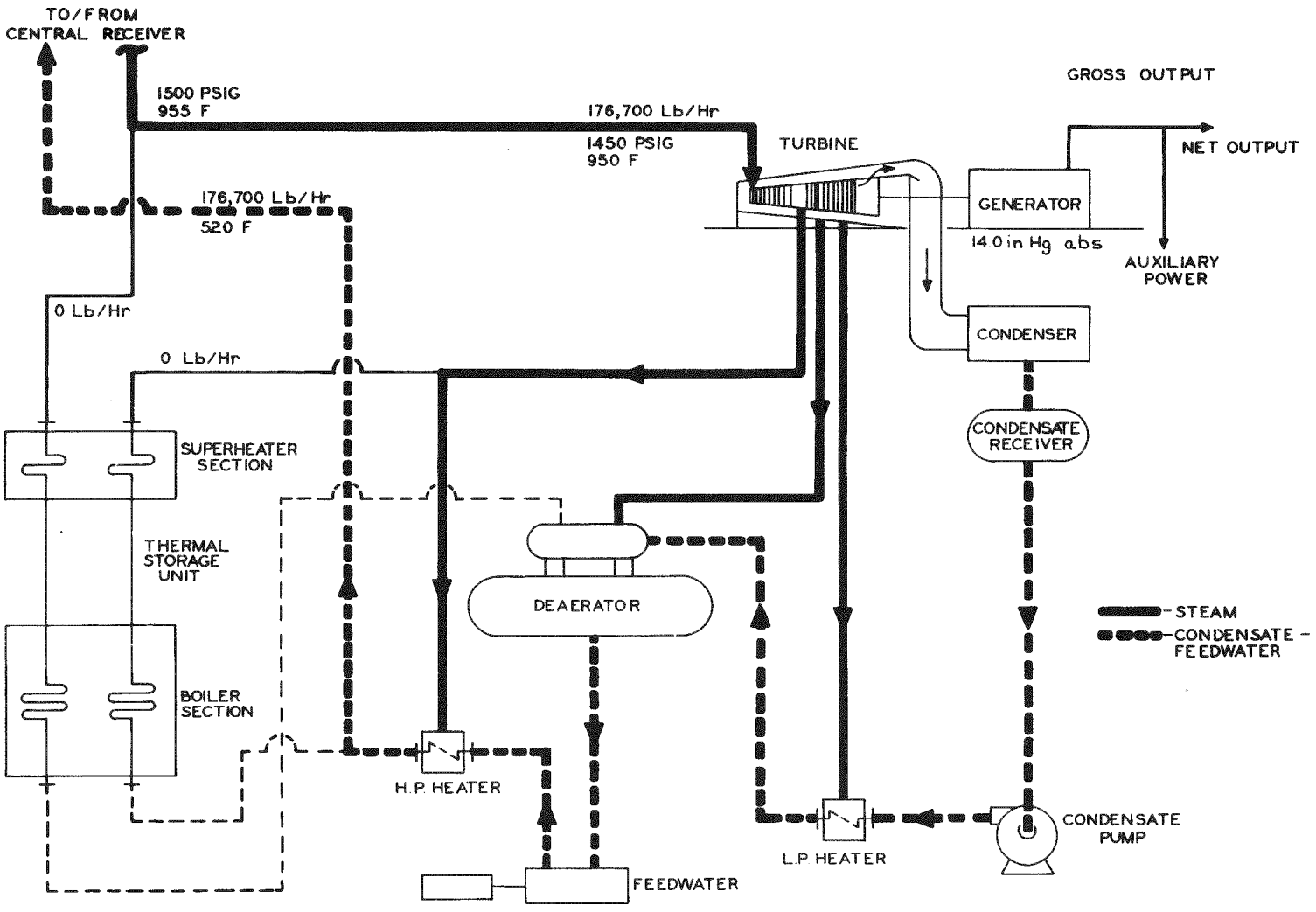


Figure 7-5. Performance With Receiver Maximum Capability Steam Flow

Electrical Generation Subsystem

Tradeoffs and Analysis Review

SELECTION OF TURBINE THROTTLE CONDITIONS WHEN USING RECEIVER SUBSYSTEM STEAM TO MEET PERFORMANCE, OPERATING AND EXTRAPOLATION REQUIREMENTS

The 1450 psi/950°F turbine throttle conditions have been selected because they result in efficient turbine operation, are the upper limits recommended for cycling overnight-startup design and they provide a high thermal driving force for Storage Subsystem charging.

1. Steam turbine generators can essentially be built to operate at any steam conditions. The turbine throttle steam conditions that have been considered for the 10-MW Solar Pilot Plant are:

   625 psi/825°F
   850 psi/950°F
   1250 psi/950°F
   1450 psi/950°F
   1800 psi/950°F

   These throttle conditions are the most commonly used and industry accepted break points. The exception would be that the 850-psi pressure condition is generally used with 900°F.

2. The 625-psi/825°F conditions were eliminated because turbine generator equipment is not available in sizes above 100 MW.

3. The 950°F temperature was selected because it provides the maximum increase in cycle efficiency to be obtained while still allowing materials that have good cyclic thermal cracking properties to be used for the turbine casing and motor. At 950°F and below, carbon moly steels can be used which have good cyclic thermal cracking properties. Above 950°F, chrome moly steels will be required for creep rupture strength, but these materials are not as ductile and would be less resistant to cyclic thermal cracking.

4. The cycle heat rate or efficiency is improved as the higher throttle pressures are used. The net heat rate gain; however, for each progressive increase in throttle pressure, decreases due to the higher pumping power requirements associated with the higher throttle pressures. This trend is shown in Figure 7-6.

5. The higher throttle pressures will also provide a higher saturation temperature driving force for thermal storage unit charging. This is shown in Figure 7-7.

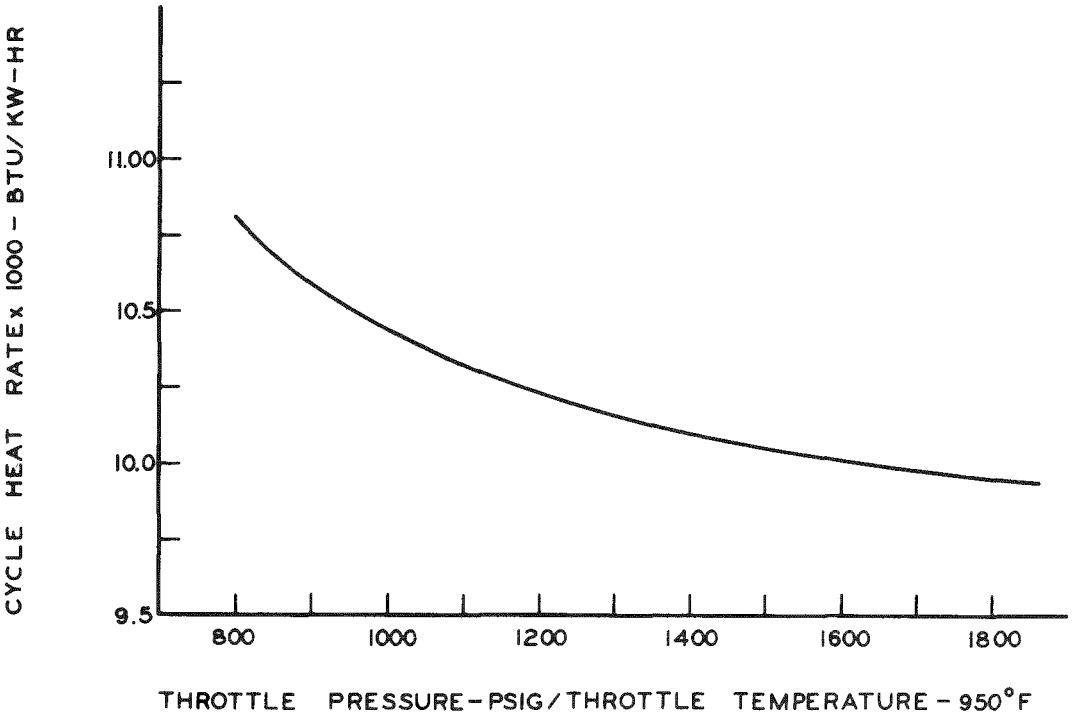


Figure 7-6. Comparative Cycle Heat Rates

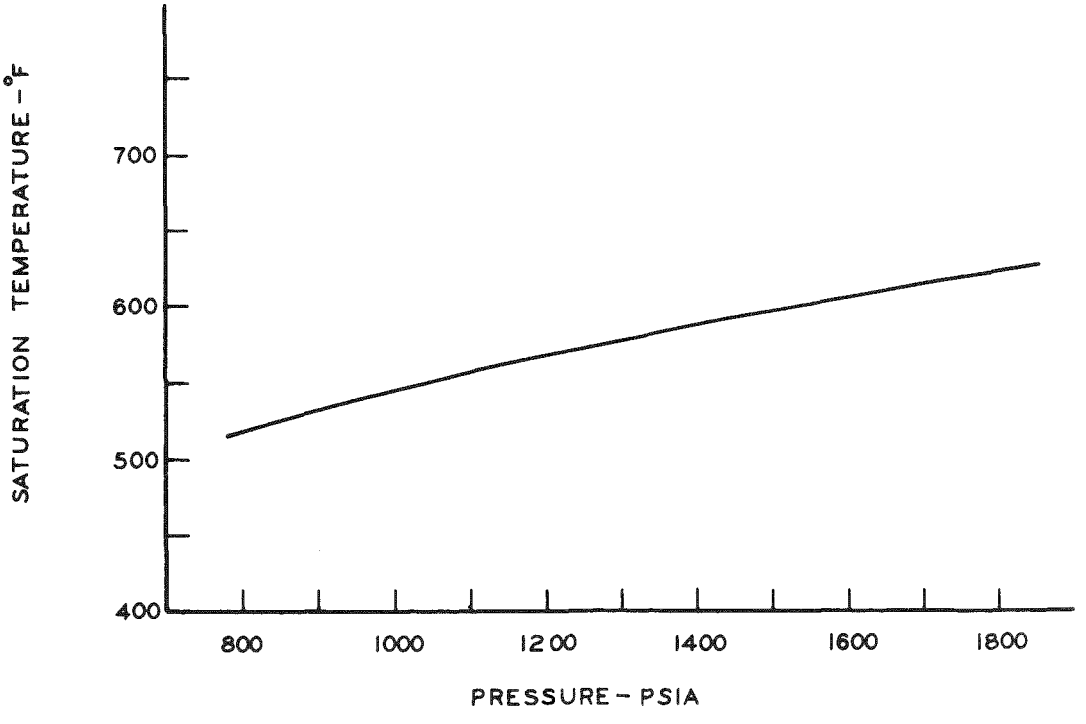


Figure 7-7. Saturation Temperatures

6. Consideration of items 4 and 5 implies that possibly the 1800-psi throttle pressure should be selected. However, the following considerations have resulted in our selection of the 1450-psi throttle pressure for the 10-MW Solar Pilot Plant:

   - The 1450-psi and 950°F is the upper limit at which General Electric will build a single casing or shell turbine.
   - The 1800-psi throttle pressure would require a double-shell design. General Electric has never built a double-shell design in the size required for the 10-MW Pilot Plant.
   - The cost for an 1800-psi design would be much higher due to the double-shell requirement and the fact that General Electric has never built such a small double-shell unit.
   - The heavier metal HP shell and nozzle block parts, plus possibly the longer shaft required due to a double shell design, would require longer startup times.
   - The 1450 psi/950°F would be more conventional from General Electric's standpoint for the pilot plant size and would still be extrapolatable to the 100-MW or 300-MW size.

This page is intentionally left blank.

Electrical Generation Subsystem

Tradeoffs and Analysis Review

SELECTION OF A TURBINE DESIGN TO FACILITATE DUAL STEAM SOURCE OPERATING MODES

A mixed pressure (high and low pressure admission) turbine design was selected because it allows the Receiver and Storage Subsystem's steam supplies to be used separately or simultaneously with a minimum of thermal shock to the turbine during a steam source transfer.

1. A dual-pressure admission type turbine has been selected, rather than a more conventional single HP inlet turbine, in order to more fully accommodate the varied performance and operating requirements of the 10-MW Solar Pilot Plant.

2. A dual-pressure admission type turbine has the following advantages in regards to these requirements:

   - It will allow both Receiver and Thermal Storage Subsystem steam to be used simultaneously.
   - The transfer of steam sources will be able to occur more efficiently with greater speed and smoothness of transition.
   - The thermal shock to the turbine, piping and valves will be greatly reduced during a steam source transfer.
   - The turbine will not have to be overrated in order to meet the 7.0-MW net generation requirement when using thermal storage steam.

3. The reduction in the amount of thermal shock that will be experienced by the turbine is shown in Figure 7-8. As shown on this Mollier Diagram, if a transfer of steam sources was made with a single HP inlet turbine, the turbine would experience a temperature shock of 416°F depending upon the rate of transfer. Too fast a transfer would result in a decrease of the life expectancy of the turbine and would not be recommended for normal operation. The rate at which the transfer could take place would be controlled to meet allowable turbine metal temperature rates of change. The allowable rates of temperature change would be dependent upon the turbine design, frequency of the temperature change and required life expectancy of the unit.

4. With the dual-pressure admission type turbine, the thermal shock during a steam source transfer will be as a maximum in the order of 150°F to 200°F. This amount of temperature mismatch could be reduced by adding more superheat in the thermal storage unit superheating section. The exact amount of temperature mismatch that will be used is dependent upon the turbine design limitations.

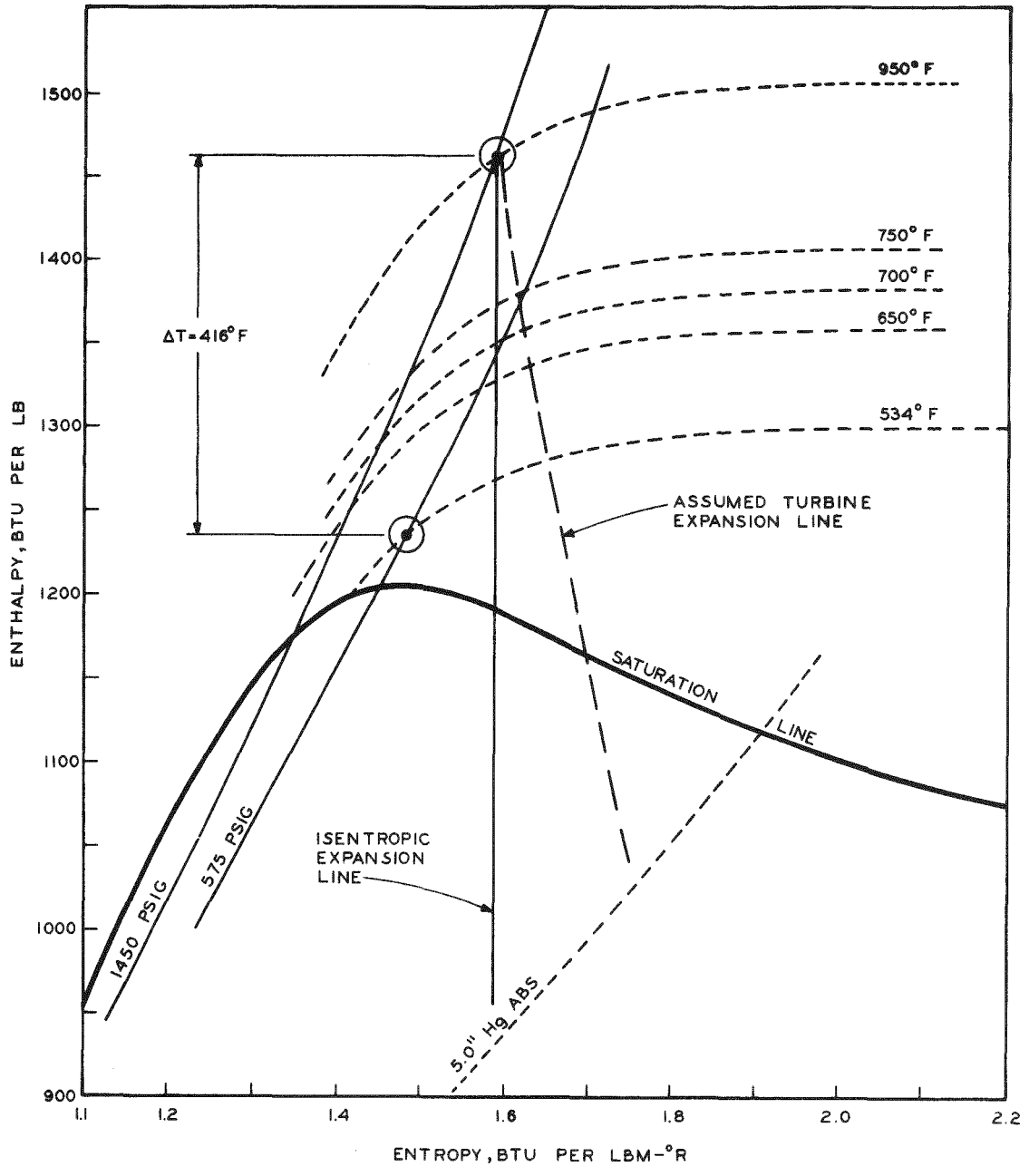


Figure 7-8. Mollier Diagram

5. The dual-pressure admission design will allow the turbine, as listed above, to be designed and selected without excess capacity. Due to the volume flow limitations of a given turbine inlet, a single HP pressure inlet turbine would have to be overrated in order to meet the 7.0-MW net generation requirement when using the LP and temperature thermal storage steam. Listed below, for four throttle design conditions, is an estimation of what size turbine would be required in order to generate 8050-kW when using 500 psi and 520°F steam at the turbine HP Inlet.

Turbine Throttle Design Conditions	Estimated Turbine Size Required to Generate 8050 kW with 500 psi/ 520°F Throttle Conditions
850 psi/950°F	15 MW
1250 psi/950°F	24 MW
1450 psi/950°F	29 MW
1800 psi/950°F	38 MW

This page is intentionally left blank.

Electrical Generation Subsystem

Tradeoffs and Analysis Review

DETERMINATION OF AIR-COOLED CONDENSER CAPACITY FOR OPTIMUM PLANT PERFORMANCE

The air-cooled condenser will be sized to result in the minimum plant generating cost determined by an economic analysis of the major plant component costs as a function of turbine back-pressure.

1. The most important factor affecting the physical size of the air-cooled condenser and its associated cost is the initial temperature difference (ITD). ITD is the amount, at the design point, by which the saturated temperature of the steam at the turbine exhaust flange exceeds the ambient air temperature. The physical size of the condenser, and its cost, is larger or smaller roughly in inverse proportion to the ITD. This principle is shown in Table 7-1, which is a summary of performance, cost and size data for three different ITD air-cooled condenser designs for the same turbine exhaust flows and ambient air temperatures.

2. By increasing the turbine back-pressure design point, the cost of the air-cooled condenser decreases. However, this will also reduce the turbine generation efficiency and cause a loss of generating capacity. In order to make up the lost capacity, the number of heliostats, receiver capability, turbine design and other miscellaneous equipment could be modified. A yearly load or generation model can be analyzed in conjunction with a plant site design temperature duration curve to make an economic determination of the condenser design that will result in the minimum plant generating costs.

3. For PDBR purposes, two minimum or base design constraints were considered. The first requirement is that the condenser is capable of condensing the estimated turbine exhaust steam flow when 10-MW net load is being generated on the hottest day in December. The second requirement is that the condenser is capable of condensing the estimated maximum turbine exhaust steam flow when the unit is operating with the receiver maximum steam output on the hottest day during the summer months. This second condition must be met without exceeding a turbine back pressure of 14 in-Hg abs which is 1 in-Hg abs below the maximum safe operating pressure that the turbine will be able to operate. The temperatures selected for PDBR purposes are the maximum temperatures ever recorded at China Lake, California. These temperatures are 86°F for December and 115°F for July.

4. From Table 7-1, it can be seen that a condenser designed for the 14 in-Hg abs condition will also be able to achieve the 5 in-Hg abs condition which is required to meet the PDBR turbine design. This design ITD also results in the minimum cost and physical size, and has been selected for PDBR purposes.

5. When the receiver, heliostat and thermal storage performance and cost characteristics are more clearly established along with the establishment of a yearly generation model, the question of whether or not it will be economically justifiable to decrease the condenser design ITD will de addressed.

Table 7-1. Air-Cooled Condenser Performance and Cost Comparison

SUMMER OPERATION			
TURBINE EXHAUST FLOW, LB/HR	118,000	118,000	118,000
AMBIENT AIR TEMP, F	115	115	115
DESIGN BACKPRESSURE, IN HGA	8	10	14
DESIGN ITD, F	37	47	61
PLOT AREA REQ'D	60' x 90'	60' x 75'	50' x 70'
NUMBER FANS & MOTORS REQ'D	6	6	6
FAN SHAFT POWER, HP	785	635	480
FAN MOTOR, HP	200	125	100
UNIT WEIGHT, TONS	490	400	300
WINTER OPERATION			
TURBINE EXHAUST FLOW, LB/HR	83,000	83,000	83,000
AMBIENT AIR TEMP, F	86	86	86
BACKPRESSURE (FANS AT FULL SPEED), IN HGA	3.0	3.5	4.7
UNIT CAPITAL COST, $	1,160,000	940,000	710,000

Electrical Generation Subsystem

Major Component Specifications and Layout

TURBINE GENERATOR

The turbine and generator will be specified to use conventional and proven materials, and accessories to the maximum extent possible.

1. The turbine will be a 3600-rpm, nonreheat condensing, bottom exhaust, single-shell, dual-pressure admission type turbine designed for high-back pressure operation. The LP admission stage will also be the HP extraction point. Two additional extraction points will be provided for a deaerating heater and an LP feedwater heater. The turbine will be directly connected to a rotating field, synchronous, totally enclosed, air-cooled generator.

2. The turbine will be designed to meet both the 10-MW net requirement, when operating solely off receiver steam, and the 7-MW net requirement, when operating solely off thermal storage steam. In addition, the turbine generator unit will be designed to operate safely and reliably with the maximum receiver output steam flow of 1.55 times the flow required to generate the 10-MW net load.

3. The turbine will be designed to meet the following requirements:

	10-MW Net Load	7-MW Net Load	Maximum Flow Capability
Turbine			
Steam inlet	HP Inlet	LP Admission Point	HP Inlet
Steam pressure, psi	1,450	575	1450
Steam temperature, F	950	534	950
Exhause pressure, in-Hg abs	5.0	5.0	14.0
Number of extraction stages used for feedwater heating	3	2	3
Generator output, kW	12,000	8,050	Vendor Supplied

4. Figure 7-9 shows a cross-sectional view of a General Electric Single Automatic Extraction Steam Turbine. This diagram illustrates the same design principles that will be used for a dual-pressure admission type turbine.

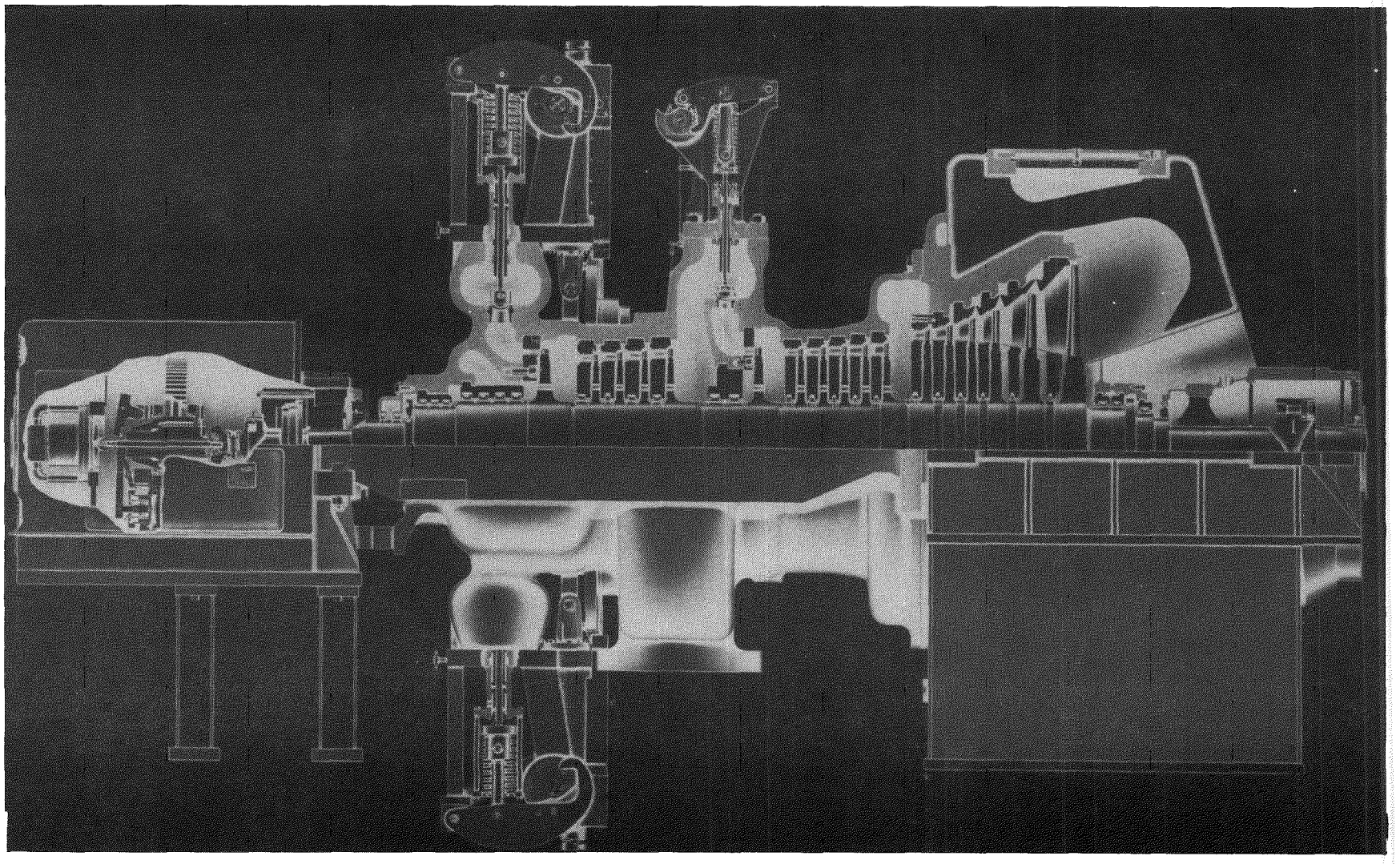


Figure 7-9. Typical General Electric Single Automatic Extraction Steam Turbine

Electrical Generation Subsystem

Major Component Specifications and Layout

CONDENSER - HEAT REJECTION SYSTEM

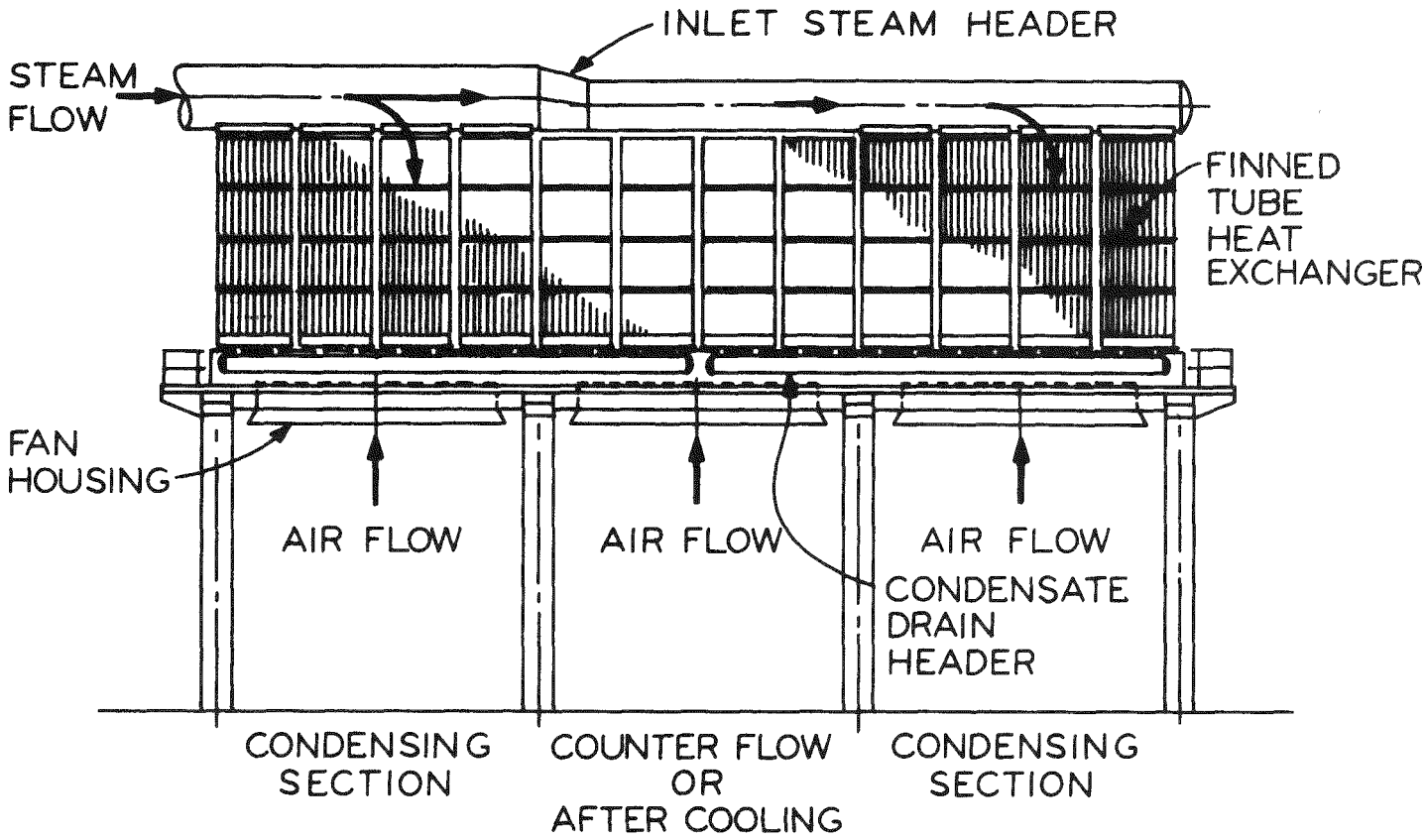
The condenser will be designed and selected to condense the turbine exhaust flows, during all operating modes, while maintaining the turbine back-pressure at or below acceptable limits.

1. The EGS condensing or heat rejection system will be a direct, dry-type system. The turbine exhaust steam will be condensed directly in finned-tube heat exchangers by forced air circulation without the use of a direct-contact condenser or any circulating water. The air-cooled condenser unit will consist of six sections and fans. Figure 7-10 illustrates the condenser layout arrangement. Only three of the six sections are shown in this view.

2. The turbine exhaust steam will be routed to the top of the air-cooled condensing units, which will consist of inclined heat exchanger finned-tube sections arranged in an inverted V-form. Air will be supplied to the center of this inverted V-arrangement by large fans similar to those used in conventional evaporative-type cooling towers. The fans will be variable speed with individual control to minimize power consumption. The steam will enter the top headers of the condensing sections, pass down through the finned tubes and into the lower headers. Approximately 70 percent of the steam will be condensed in the condensing sections. A steam and liquid condensate mixture will exist in the lower headers. The remaining steam and non-condensables will be drawn off from the headers upward through additional after-cooling sections. The remaining steam will be condensed and the non-condensables will be drawn off from the top of the after-cooling sections by the condenser air removal equipment.

3. The after-cooling sections will be located between two condensing sections, as shown in Figure 7-10, with each section (condensing and after-cooling) having its own fan. The primary purpose of the after-cooling sections will be to control and prevent subcooling of the condensate with results in a thermal loss to the turbine cycle.

4. The tubes and fins of the heat exchanger sections will be made of steel. Protection against external corrosion, and the binding of the fin to the tube will be accomplished by hot-dipped galvanizing. The galvanizing of the fin to the tube will also provide better heat transfer characteristics.



AIR-COOLED CONDENSER DESIGN CONDITIONS

	WINTER DESIGN CONDITIONS	SUMMER DESIGN CONDITIONS
TURBINE EXHAUST FLOW, LB/HR	DEPENDENT UPON TURBINE DESIGN	DEPENDENT UPON TURBINE DESIGN
AMBIENT AIR TEMPERATURE F.	86	115
TURBINE EXHAUST PRESS., IN HG ABS	5.0	14.0
CONDENSER ITD, F	48	61

Electrical Generation Subsystem

Major Component Specification and Layout

TURBINE AREA GROUND FLOOR LAYOUT

The turbine area ground floor layout was adopted to provide adequate space for inspection, maintenance and safe operation of turbine auxiliary equipment, pumps and piping.

1. The layout of the major EGS components, which will be located on the ground floor, and the location of various auxiliary rooms and maintenance areas is shown in Figure 7-11. Space will be provided on the ground floor, in addition to the turbine room proper, for the following:

   - Visitors center with reception desk, lounge and vending area, toilet facilities and a media room
   - Water treatment and demineralization equipment and a water treatment laboratory
   - Machine shop with manual hoist
   - Electrical equipment and instrument repair shop
   - Tool crib and small parts storage
   - Welding shop, warehouse and storage areas
   - Locker and lunch rooms for operating personnel

2. All large rotative EGS equipment will be located at the ground floor level, with the exception of the turbine generator unit, to facilitate maintenance and minimize vibration. Service hoists and monorails will be provided as required for maintenance of major pieces of equipment.

3. An enclosed corridor, reaching in height from the ground level to the plant mezzanine floor level, will be provided for piping runs and personnel movement between the turbine area, receiver tower base and thermal storage building.

4. The turbine area proper ground floor slab will have a separate finish over the structural slab. The separate finish will encase equipment drains and conduits.

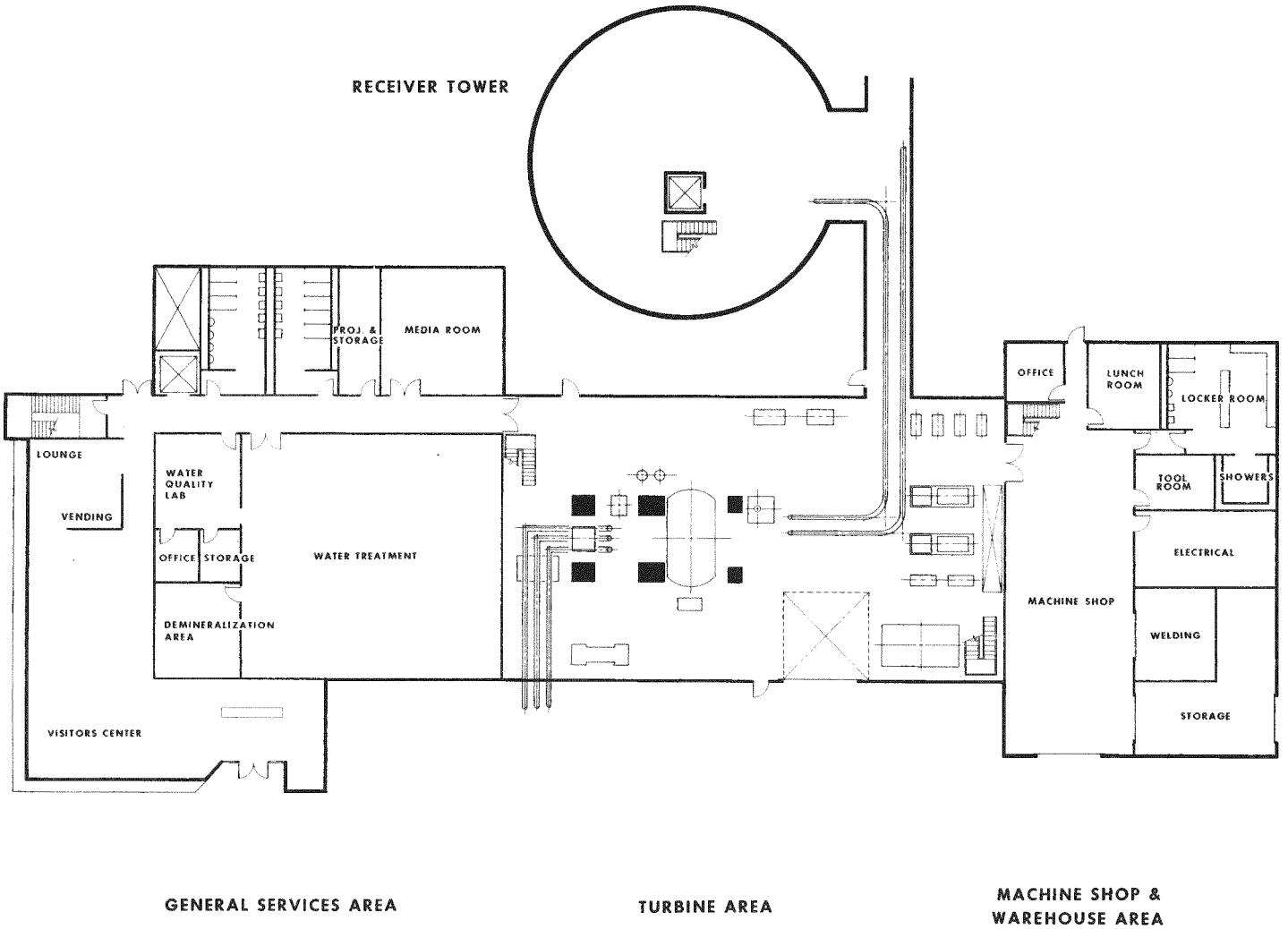


Figure 7-11. Turbine Area Plant Arrangement-Ground Floor Plan

Electrical Generation Subsystem

Major Component Specifications and Layout

TURBINE AREA MEZZANINE FLOOR LAYOUT

The turbine area mezzanine floor layout was adopted to provide adequate clearance for turbine main steam and extraction piping.

---

1. The layout of the major EGS components which will be located on the mezzanine floor, and the location of various auxiliary rooms, is shown in Figure 7-12. Space will be provided on the mezzanine floor, in addition to the turbine room proper, for the following:

   - General offices for administrative personnel with toilet facilities
   - Lunch room with kitchen facilities
   - Mechanical equipment room
   - Battery and inverter room
   - Computer wiring room
   - Motor control center and relay room

2. The turbine exhaust duct, which will transport the turbine exhaust steam to the air-cooled condenser units, will be routed out of the building at this level. The duct will be supported on top of the ground floor piping and personnel corridor, which is connecting the turbine room with the receiver tower and thermal storage building.

3. Condensate storage tanks will be located at this level inside the receiver tower. The elevational difference between the tanks and the condensate receiver, which is on the ground floor and will not be under vacuum during startup, will ensure that adequate pressure is available for condensate makeup at all times without the use of a pump. This location for the tanks will use the space available at the receiver tower base, and will remove the tanks from view.

4. Service hoists and monorails will be provided on the mezzanine floor for maintenance of major pieces of equipment.

5. Galvanized welded steel grating will be provided for miscellaneous turbine room proper walkways and platforms. Concrete slabs will be used where heavy loads are anticipated.

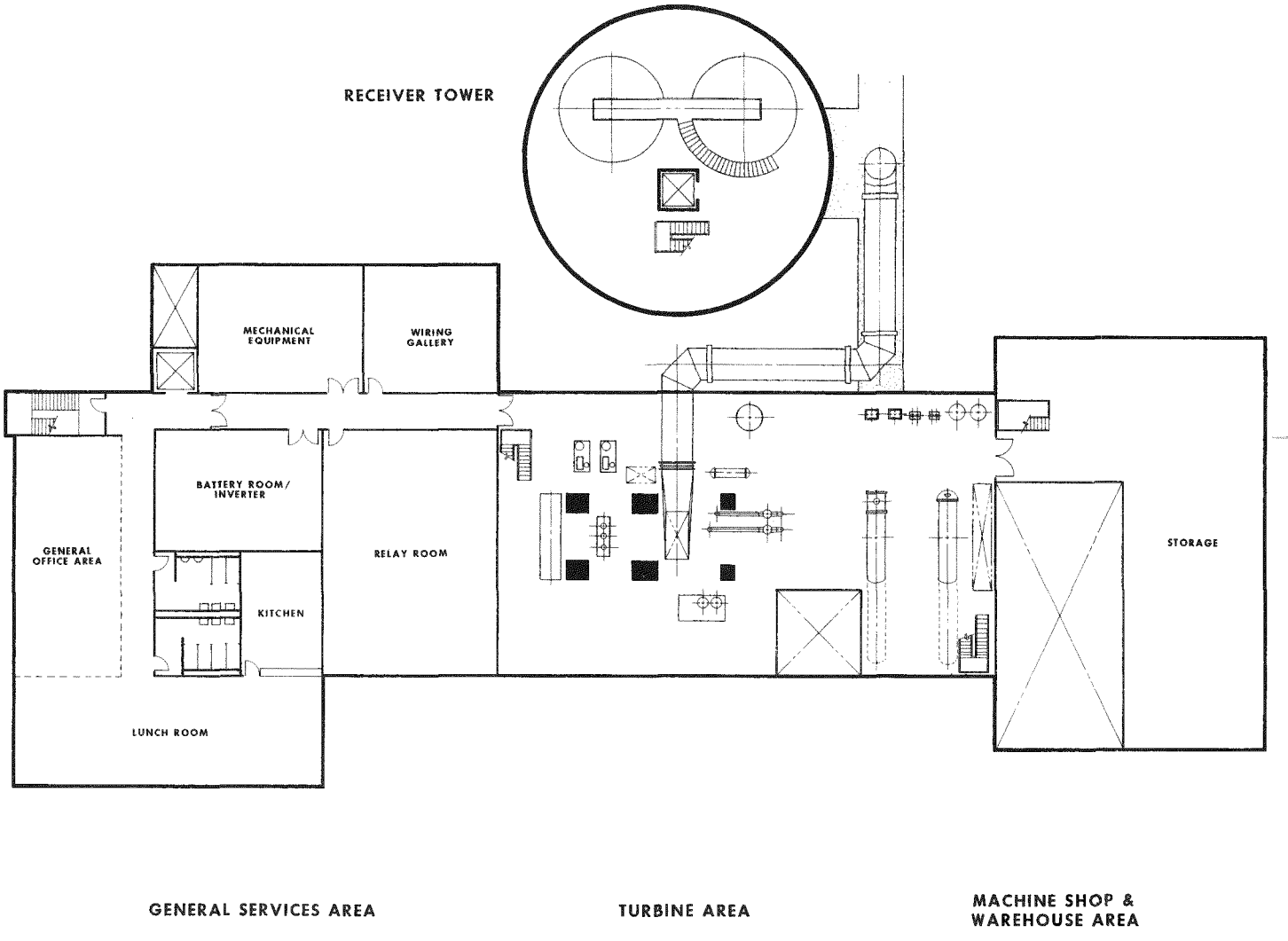


Figure 7-12. Turbine Area Plant Arrangement-Mezzanine Floor Plan

Electrical Generation Subsystem

Major Component Specifications and Layout

TURBINE AREA OPERATING FLOOR LAYOUT

The turbine area operating floor layout was adopted to provide adequate space for inspection and maintenance of the turbine and space for the central plant control room.

1. The layout of the major EGS components which will be located on the operating floor, and the location of the control room and various auxiliary rooms, is shown in Figures 7-13 and 7-14. Space will be provided on the operating floor, in addition to the turbine room proper, for the following:

   - Centralized control room
   - Computer and computer storage rooms
   - Electronic equipment checkout room

2. The entire plant will be operated from the centralized control room. Computer facilities will be located adjacent to the control room with a computer programming console in the control room itself .

3. The turbine generator will be located on the operating floor. The longitudinal axis of the turbine generator will be perpendicular to the receiver tower centerline. A turbine room crane will be furnished which will be capable of lifting turbine generator maintenance pieces. An access hatch will be provided for lifting and lowering equipment from the ground to operating floor.

4. Galvanized welded steel grating will be provided for miscellaneous turbine room proper platforms. The operating floor will consist of slabs and beams cast-in-place.

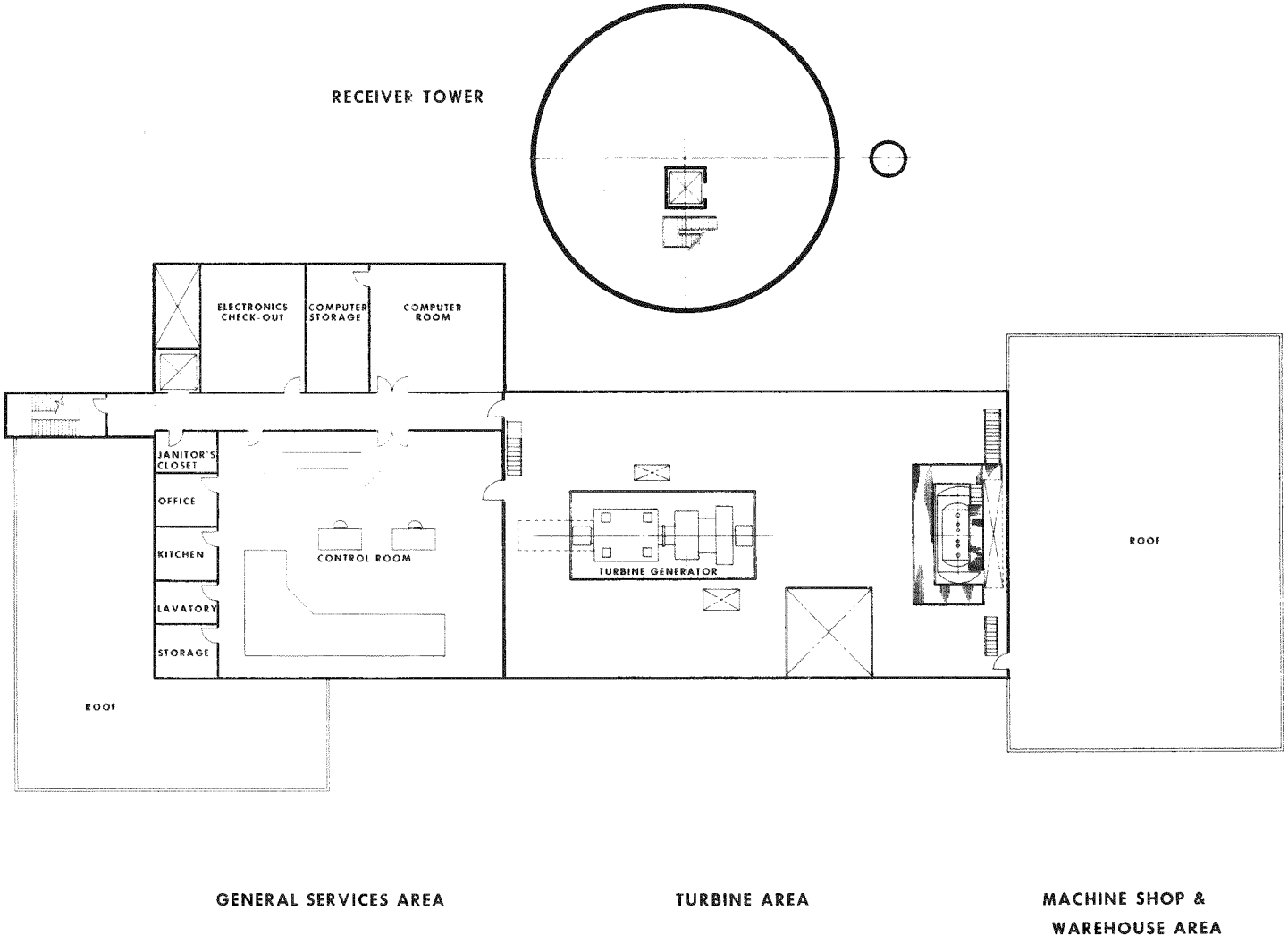


Figure 7-13. Turbine Area Plant Arrangement-Operating Floor Plan

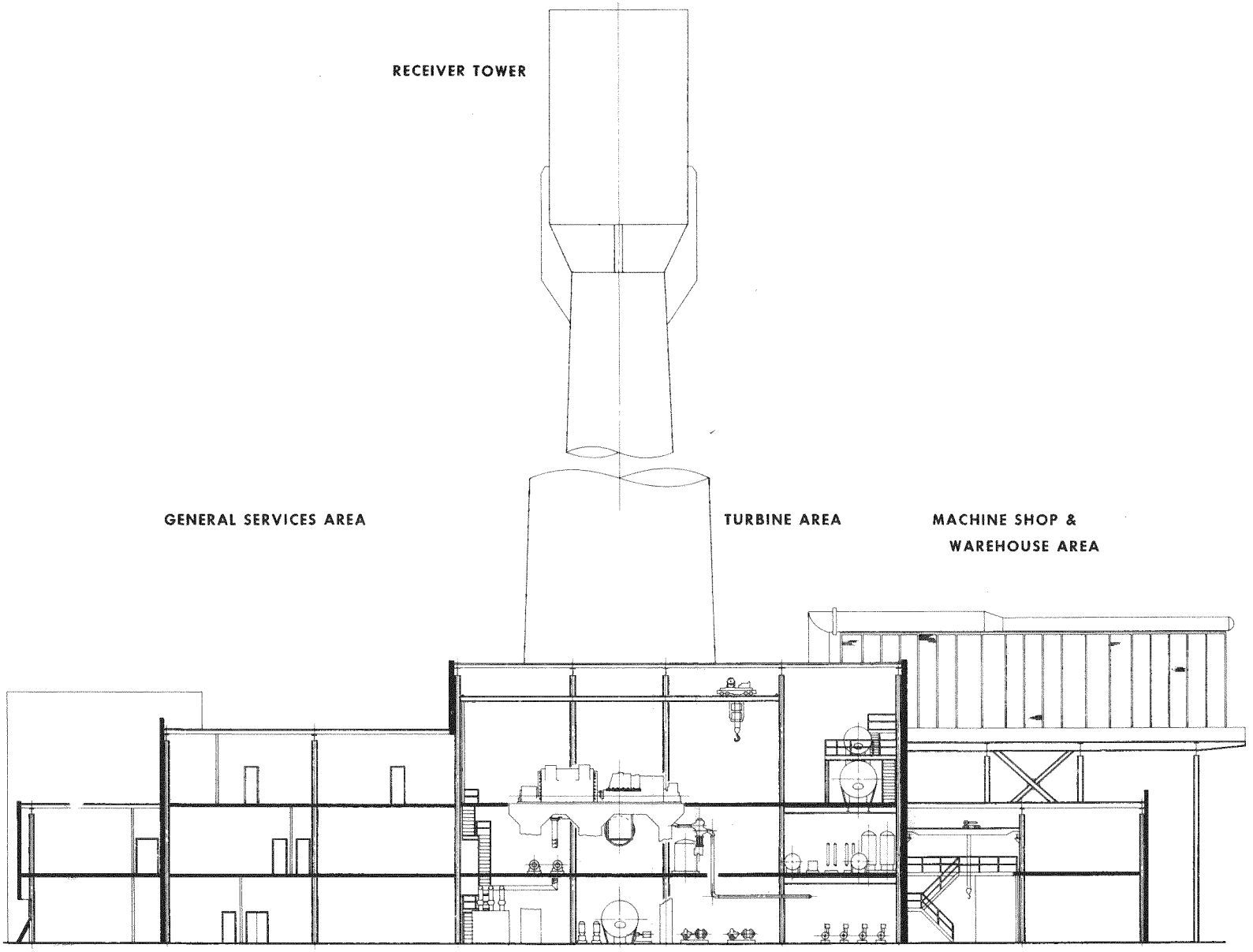


Figure 7-14. Turbine Area Plant Arrangement-Cross Section

This page is intentionally left blank.

Electrical Generation Subsystem

Major Piping and Instrument System Description

HIGH PRESSURE STEAM SUPPLY

The HP steam supply piping system is being designed to transport and control the design steam flows between the plant subsystems in a manner consistent with functional performance requirements.

1. The high-pressure steam supply piping system will transport superheated steam from the receiver to the steam-turbine, HP inlet and from the receiver to the thermal storage unit. The HP steam supply piping system will also transport thermal storage unit superheated steam to the turbine LP, admission-extraction connection and to the receiver drum for pressurization and warming during shutdown. Extraction steam for the HP heater will be supplied from the turbine LP admission-extraction line. This is the same line that thermal storage unit steam will be supplied through. The system is shown schematically on Figure 7-15.

2. Warming steam drain lines to the condensate receiver for both receiver and thermal storage steam will be provided. These lines will be used in warming up the HP steam headers prior to steam being admitted to the turbine and also to facilitate obtaining required superheat temperatures during startup.

3. A steam line from each of the turbine steam supply heaters will be routed to the turbine seal steam regulator. This will provide a source of seal steam from both supply headers for use in startup, before there is adequate seal steam from the turbine for self-sufficiency. The seal steam line from the thermal storage supply header will also be used to seal the turbine during shutdown periods so that vacuum can be maintained in the condensing system.

4. Drip legs, power operated drain valves, level controls and drain lines will be located at the low points of all steam supply lines to prevent the accumulation of condensed steam and possible water induction damage to the turbine. The power operated drain valves will open automatically in the event of a water level being detected in the associated drip leg and/or turbine tip. The drain valves will also be controllable from the control room.

5. The HP steam supply piping system is being designed in accordance with the applicable standards of the ASME Boiler and Pressure Vessel Code and ANSI Power Piping Code. The piping specifications for the HP steam supply piping system will be as listed on Table 7-2.

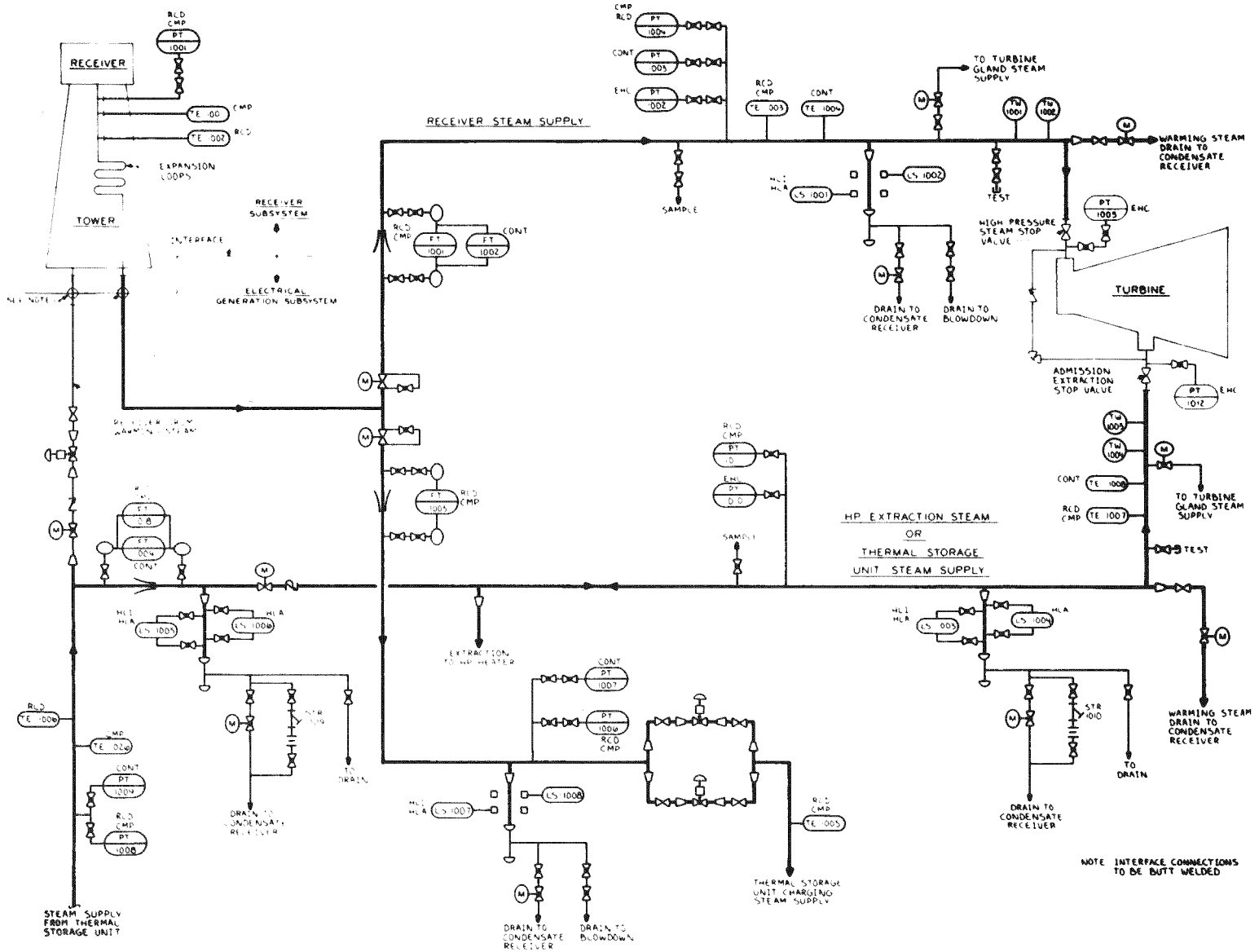


Figure 7-15. High Pressure Steam Piping and Instrumentation

Table 7-2. High-Pressure (HP) Steam Piping Specifications

Pipeline Listing	Pressures and Temperatures Operating	Design	Test Pressure psi	Pipe	Valves 2" and Smaller	Valves 2 1/2" and Larger	Insulation Class	Special Features
1. Receiver steam supply from receiver superheater outlet to turbine high pressure inlet; to thermal storage unit superheater section inlet; drain lines thru last valve; instrument and test piping	1500 psi 955°F	1600 psi 965°F	2400	ASTM A335 GR P12 8": SCH 140 6": SCH 160 5" & 4": SCH 120 3" and smaller: SCH 160	1500 lb 1-1/4 CR SW	1500 lb 1-1/4 CR BW	A	Inert-arc first pass welding on all butt welds. Shot blast cleaning on all piping 2-1/2" and larger. Radiographic examination on all butt welds.
2. Thermal storage steam supply from storage unit superheater outlet to turbine low pressure inlet; to HP heater; drain lines to condensate receiver; instrument and test piping	600 psi 539°F	750 psi 575°F	1125	ASTM A106 GR B 2-1/2" thru 12": std wt 2" and smaller: SCH 80	1500 lb 1-1/4 CR	400 lb CS, BW	B	Inert-act first pass welding on all butt welds. Shot blast cleaning on all piping 2-1/2" and larger

This page is intentionally left blank.

Electrical Generation Subsystems

Major Piping and Instrument System Description

TURBINE EXTRACTION STEAM AND HEATER DRAINS SYSTEM

The turbine extraction steam piping and heater drains system is being designed to transport and efficiently use the design extraction steam flows for regenerative feedwater heating and deaeration

1. The extraction steam and heater drains piping system will utilize turbine extraction steam to increase the thermal efficiency of the cycle. The system is shown schematically on Figure 7-16, Extraction Steam and Heater Drains Piping and Instrumentation.

2. The extraction steam from the turbine will be used for regenerative feedwater heating. The lowest pressure extraction will supply steam to one LP, shell and tube type, regenerative feedwater heater. The intermediate pressure extraction will supply steam to one direct contact type, deaerating heater with a storage tank. The single HP, shell and tube type, regenerative feedwater heater will be supplied steam from the turbine extraction-admission point. When the turbine is operating solely on receiver steam the HP heater will be supplied turbine extraction steam through the same pipe used to admit steam to the turbine from the thermal storage unit. Whenever the turbine is operating on thermal storage steam or a combination of receiver and thermal storage steam the HP heater will be taken out of service.

3. The heater drains system will dispose of condensed extraction steam in the feedwater heaters by passing it to a lower pressure region in the cycle. This will provide for maximum heat recovery from the condensed extraction steam. The HP heater drips will be cascaded to the deaerator during normal operation, and to the condensate receiver during startup or abnormal (maintenance or high heater level) operations. The LP heater drips will be cascaded to the condenser.

4. Each extraction steam line will be provided with drip legs, power-operated valves, level controls and drain lines to the condensate receiver to prevent the accumulation of condensed steam which could damage the turbine. The power-operated drain valves will open automatically in the event of a water level being detected in the associated drip leg and/or turbine trip. The drain valves will also be controllable from the control room.

5. The extraction steam and heater drains piping system is being designed in accordance with the applicable standards of the ANSI Power Piping Code. The piping specifications for the HP heater extraction piping will be as previously stated. The piping specifications for the deaerator and LP heater extraction piping will be dependent upon the turbine design and associated design extraction pressures and temperatures.

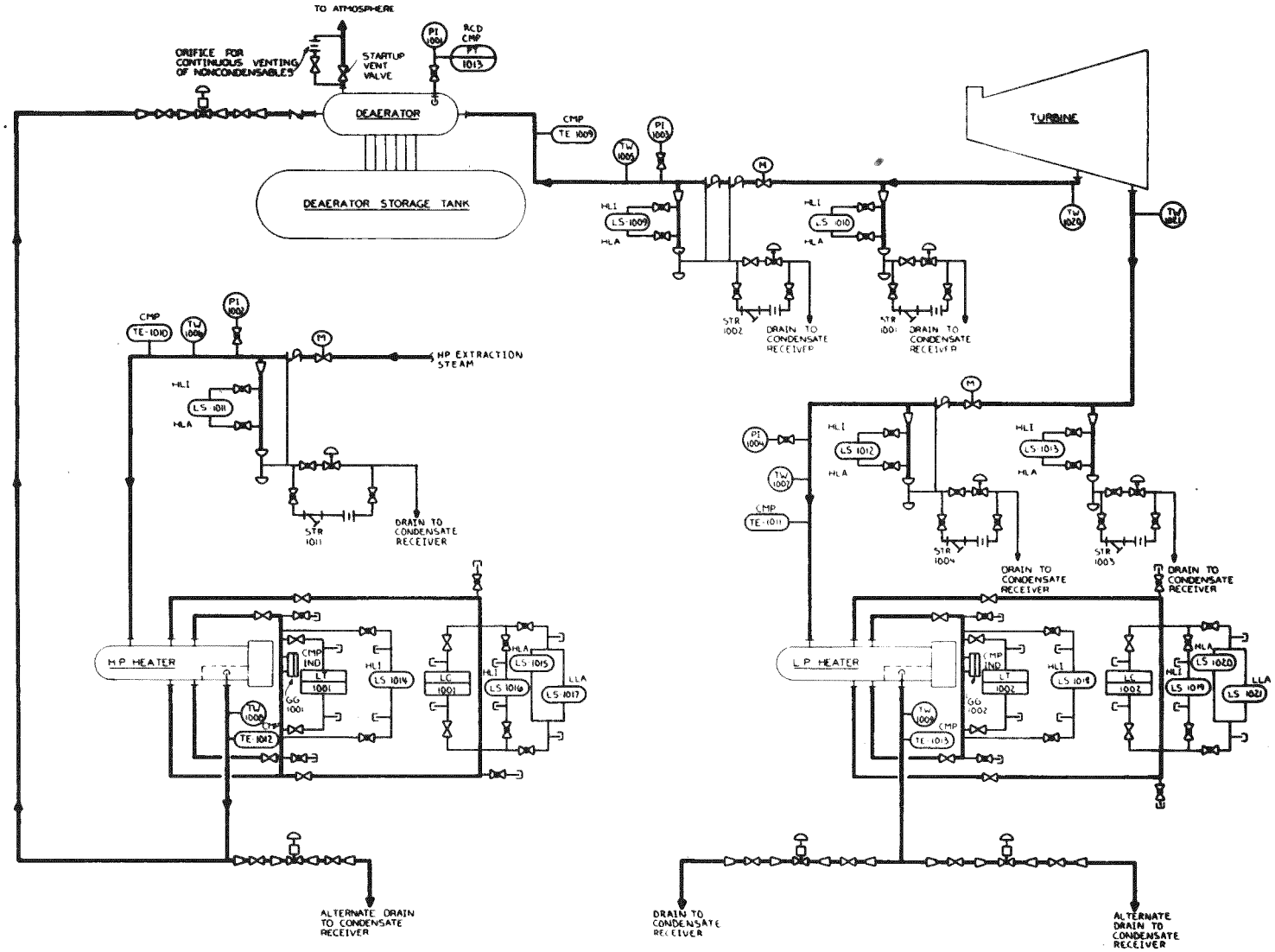


Figure 7-16. Extraction Steam and Heater Drains Piping and Instrumentation

Electrical Generation Subsystem

Major Piping and Instrument System Descriptions

FEEDWATER SYSTEM

The feedwater piping system is being designed to transport and control the maximum deaerated condensate flow from the deaerator to the Receiver and/or Storage Subsystems in a manner consistent with functional performance requirements.

1. The feedwater piping system will supply deaerated condensate (feedwater) from the deaerator storage tank to the receiver and/or thermal storage unit. Feedwater will also be supplied to the receiver and thermal storage unit desuperheaters. The system is shown schematically on Figure 7-17.

2. The feedwater will be regeneratively heated by passing through the HP heater, which will be supplied extraction steam from the turbine during operation of the turbine using receiver steam only. Whenever thermal storage unit steam is being supplied to the turbine, the extraction steam line to the HP heater will be closed and the feedwater will not receive additional heat as it passes through the HP heater. The desuperheating spray flows will be piped from the main feedwater line before the HP heater. This flow will use the cooler feedwater and decrease the amount of spray water required. Feedwater will be used for desuperheating spray water rather than the much cooler condensate because the injection spray pressure must be higher than the steam line pressure being desuperheated.

3. Two feedwater pumps will take suction from the deaerator storage tank and discharge to the Receiver and/or Thermal Storage Subsystems. Each pump will be rated full capacity at the net unit load of 10 MW. Both feed pumps will operate simultaneously to attain the increased flow capacities required during high flux and maximum receiver output periods. Feedwater pump minimum flow requirements (to prevent flashing within the pumps at low loads) will be maintained by automatic recirculation of feedwater to the deaerator storage tank.

4. The feedwater piping system is being designed in accordance with the applicable standards of the ANSI Power Piping Code. The main feedwater line will be sized to not exceed a velocity of 20 feet per second with consideration given to the total pressure drop of the system. The feedwater pump suction piping will be designed to accomodate sufficient NPSH at the pump suction nozzles to prevent flashing of the feedwater at the eye of the flood stage impeller. The piping specifications for the feedwater pump suction and discharge piping systems will be listed on Table 7-3.

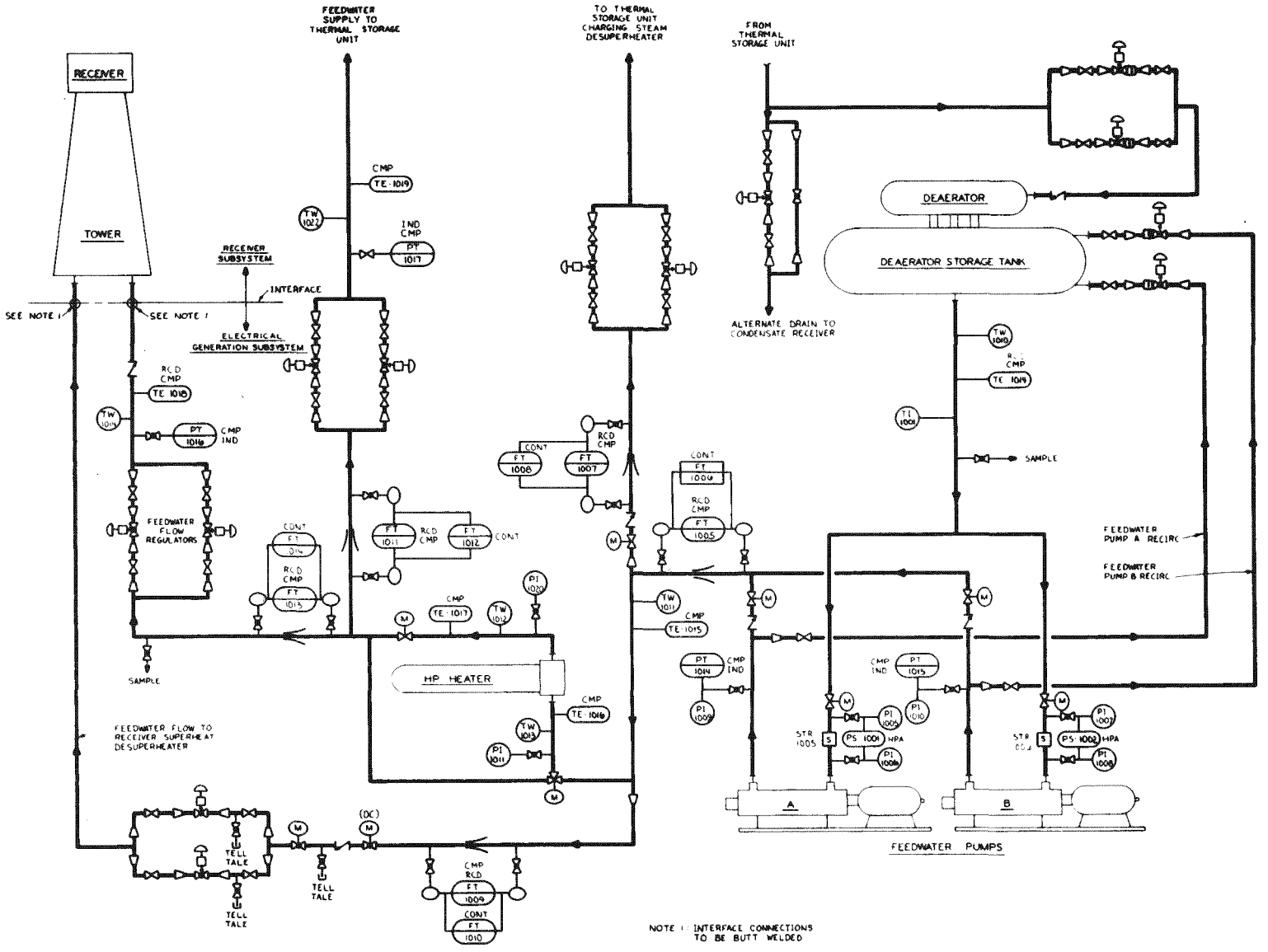


Figure 7-17. Feedwater Piping and Instrumentation

Table 7-3. Feedwater Piping Specifications

Pipeline Listing	Pressures and Temperatures Operating Design		Test Pressure psi	Pipe	Valves		Insulation Class	Special Features
					2" & Smaller	2 1/2" & Larger		
1. Feedwater pump suction piping; instrument, vent drain and test piping	125 psi 336°F	200 psi 400°F	300	ASTM A196 GR B 2-1/2" & larger; Std wt 2" & smaller: SCH 80	600 lb CS, SW	150 lb CS, BW	C	Inert-arc first pass welding on all butt welds. Shot blast cleaning on all piping 2-1/2" and larger
2. Feedwater pump discharge to receiver to thermal storage unit; spray water to receiver desuperheater; spray water to thermal storage desuperheater; recirculation to deaerator; instrument, vent, drain and test piping	1800 psi	2500 psi	3700	ASTM A106 GR B 6": SCH 160 4" & 5": SCH 120 3" & smaller: SCH 160	1500 lb 1-1/4 CR	1500 lb CS, BW	C	

This page is intentionally left blank.

Electrical Generation Subsystem

Major Piping and Instrument System Descriptions

CONDENSATE SYSTEM

The condensate piping system is being designed to transport and control the maximum condensed turbine exhaust flow from the condensate receiver to the deaerator.

1. The condensate piping system will supply condensed steam (condensate) from the condensate receiver to the deaerating section of the deaerator. The condensate will be regeneratively heated by passing through the LP feedwater heater. The water quality required by the Receiver Subsystem will be maintained by passing the condensate through a condensate polisher for removal of suspended and dissolved solids. The system is shown schematically on Figure 7-18.

2. Two condensate pumps will take suction from the condensate receiver and discharge to the deaerator. Each pump will be rated full capacity at the net unit load of 10 MW. Both condensate pumps will operate simultaneously to attain the increased flow capacities required during high flux and maximum receiver output periods. Condensate pump minimum flow requirements will be maintained by automatic recirculation of condensate to the condensate receiver.

3. The condensate piping system will be designed in accordance with the applicable standards of the ANSI Power Piping Code. The main condensate line will be sized to not exceed a velocity of 10 feet per second with consideration given to the total pressure drop of the system. The condensate pump suction piping will be designed to accommodate the NPSH requirements of the pumps.

4. The piping specifications for the condensate pump suction and discharge piping systems will be as listed on Table 7-4.

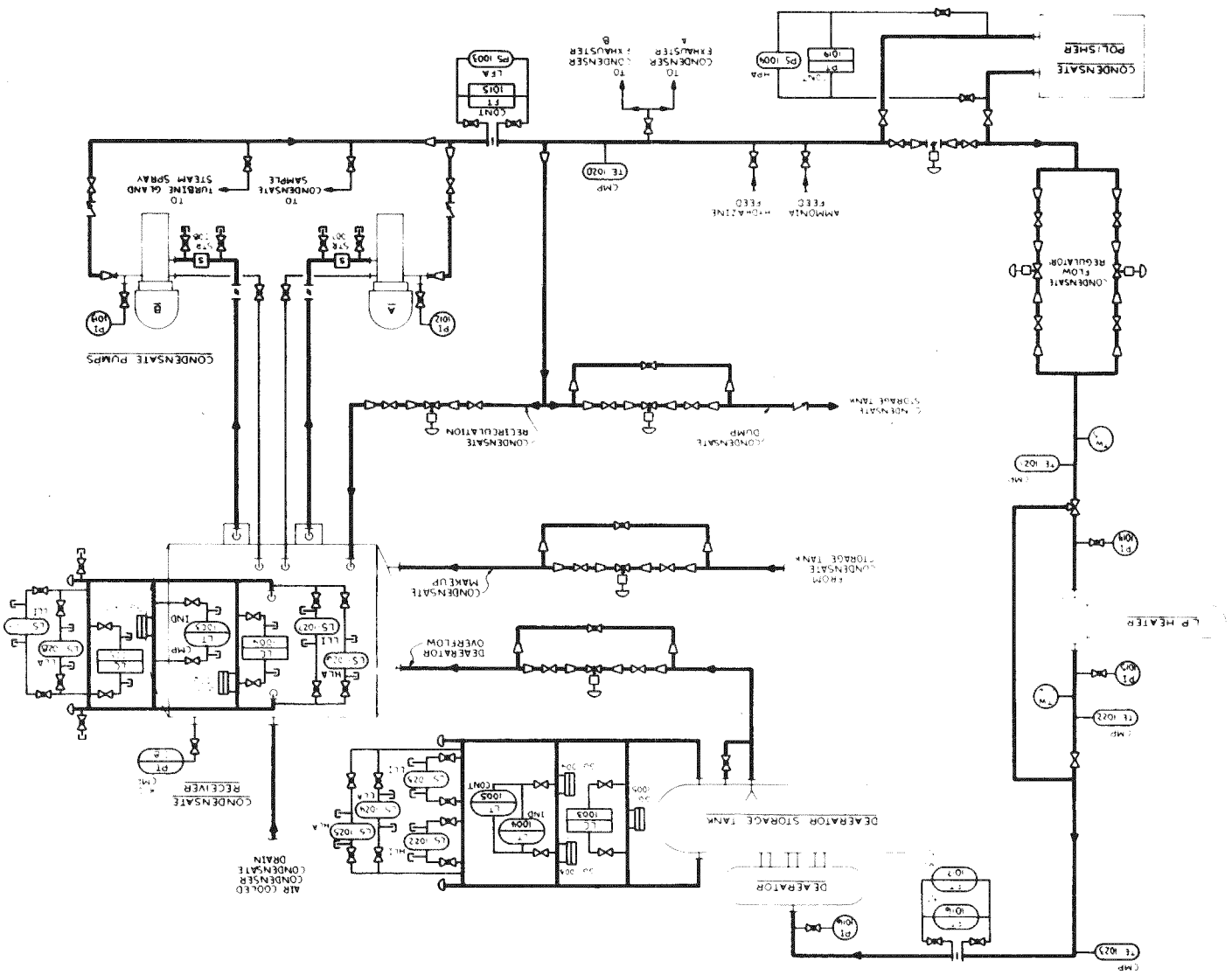


Figure 7-18. Condensate Piping and Instrumentation

Table 7-4. Condensate Piping Specifications

Pipeline Listing	Pressures and Temperatures Operating	Design	Test Pressure psi	Pipe	Valves 2" & Smaller	Valves 2 1/2" & Larger	Insulation Class	Special Features
1. Condensate pump suction piping; instrument, vent, drain and test piping	Vacuum 134°F	50 psi 200°F	75	ASTM A106 GR B 2 1/2" &larger: Std wt 2" &smaller: SCH 80	600 lb CS, SW	150 lb CS, BW 50 lb BFLY CI, wafer	D	Inert-arc first pass welding on all butt welds. Shot blast cleaning on all piping 2-1/2" and larger
2. Condensate pump discharge to deaerator; thru condensate polisher; condensate recirculation line thru isolation valves; condensate dump line thru isolation valves; instrument, vent, drain and test piping	215 psi 234°F	300 psi 300°F	450	ASTM A106 GR B 2 1/2" &larger: Std wt 2" & smaller: SCH 80	600 lb CS, SW	300 lb CS, BW	D	Inert-arc first pass welding on all butt welds. Shot blast cleaning on all piping 2-1/2" and larger.

This page is intentionally left blank.

Electrical Generation Subsystem

Major Piping and Instrument System Descriptions

LOW PRESSURE STEAM AND HEAT REJECTION SYSTEM

The low pressure steam and heat rejection system is being designed to transport, control and condense turbine exhaust steam flow with minimum cycle efficiency losses.

1. The LP exhaust duct will transport the turbine exhaust steam to the air-cooled condenser steam distribution headers. Branch lines to individual condenser sections will be provided with power operated valves for isolation purposes. The system is shown schematically on Figure 7-19.

2. The duct will be designed to accommodate the maximum turbine exhaust flow, which will occur during high flux and maximum receiver output periods, with a pressure drop of approximately 1.0 in. Hg abs between the turbine exhaust flange and the condenser units. The specifications for this exhaust duct will be dependent upon the turbine design exhaust flow.

3. The duct will be provided with a drip leg, with a power operated drain valve, level controls and drain lines to the condensate receiver to prevent the accumulation of condensed steam which could damage the turbine. The power operated drain valve will open automatically in the event of a water level being detected in the drip leg and/or a turbine trip. The drain valve will also be controllable from the control room.

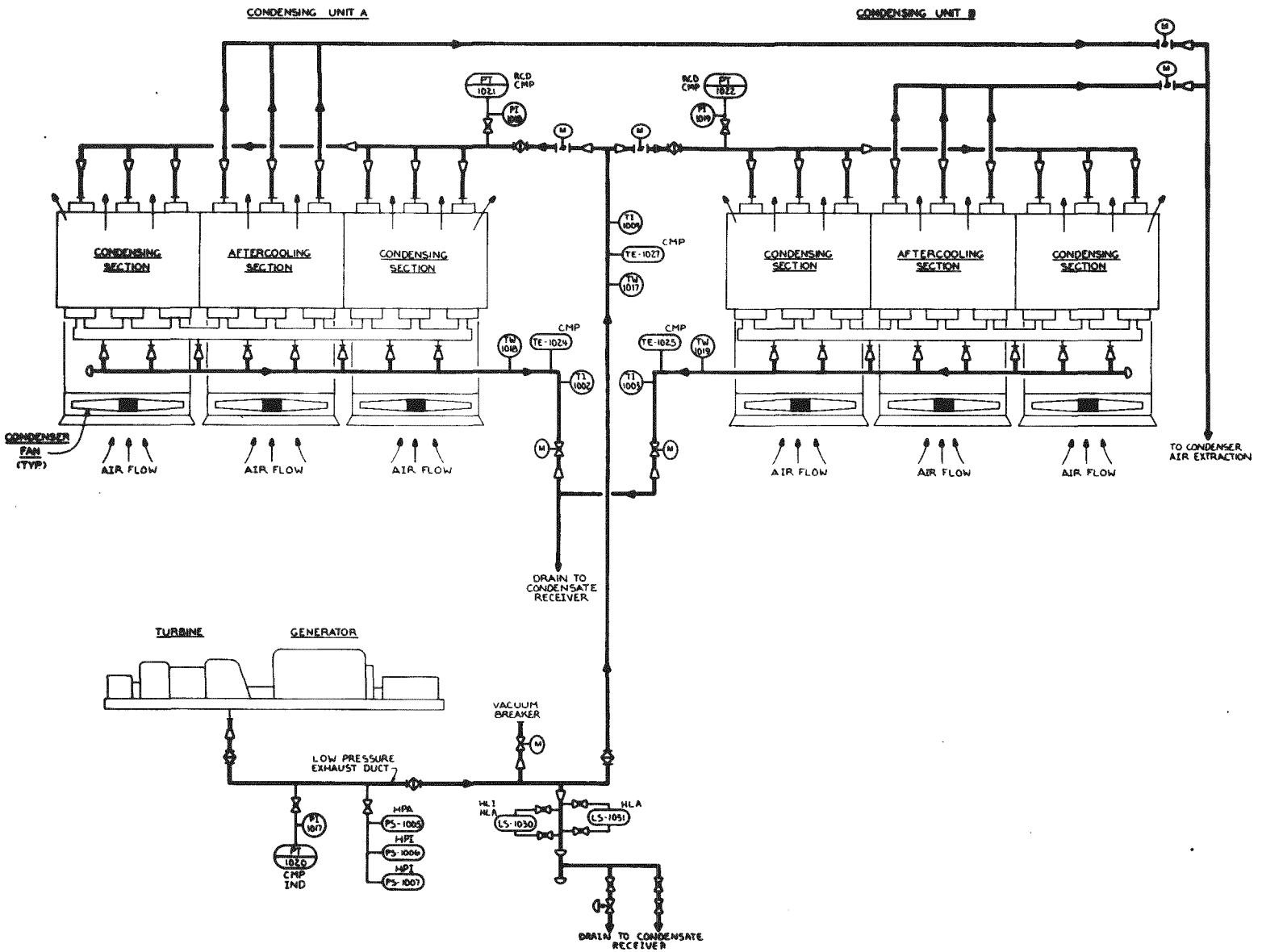


Figure 7-19. Low-Pressure Steam and Heat Rejection Piping and Instrumentation

Electrical Generation Subsystem

Control Concept and Requirements

OBJECTIVE OF PLANT CONTROL

A control objective of allowing the plant to be operated at all times in a manner which uses solar energy most efficiently consistent with load demand and plant subsystem capability has been adopted.

1. With the plant energy source available during a limited number of hours each day, an operating strategy which maximizes use of the solar energy collected becomes the most practical method of plant operation. Because equipment availability and electrical grid requirements may change daily, the operating strategy may also vary from day to day. The plant control systems must have the flexibility required to accommodate these variations in operation.

2. The concept of maximizing the collection of solar energy requires collector subsystem controls be designed to maximize receiver flux while the electrical generation subsystem and the thermal storage subsystem adjust to the varying receiver output.

3. One operating strategy which may be used at times consists of bringing the turbine generator to rated speed with receiver steam as the sun rises. After the generator is connected to the electrical grid, the electrical output is increased as receiver output increases until a predetermined electrical output is reached. The generator is then held at a constant output and excess receiver steam is used to charge the storage unit. In the evening, storage charging steam is stopped as the receiver output drops to the level required to produce the generator output. The generator output is then reduced as the receiver output decreases, until the evening generating level is reached. Storage steam is used to drive the turbine at the evening generation level until the storage unit is approximately 65 percent discharged. The generator is then shut down for the night.

4. A second operating strategy uses all receiver steam for charging the storage unit until the receiver output is sufficient to drive the generator at 10 MW net output. The generator is then placed into operation using receiver steam for a limited number of hours, after which the electrical output is reduced to the evening level and driven from storage steam. When the storage unit is approximately 65 percent discharged, the generator is shut down for the night.

5. A third operating strategy uses all receiver output for operating the turbine generator, with electrical output following the level of insolation.

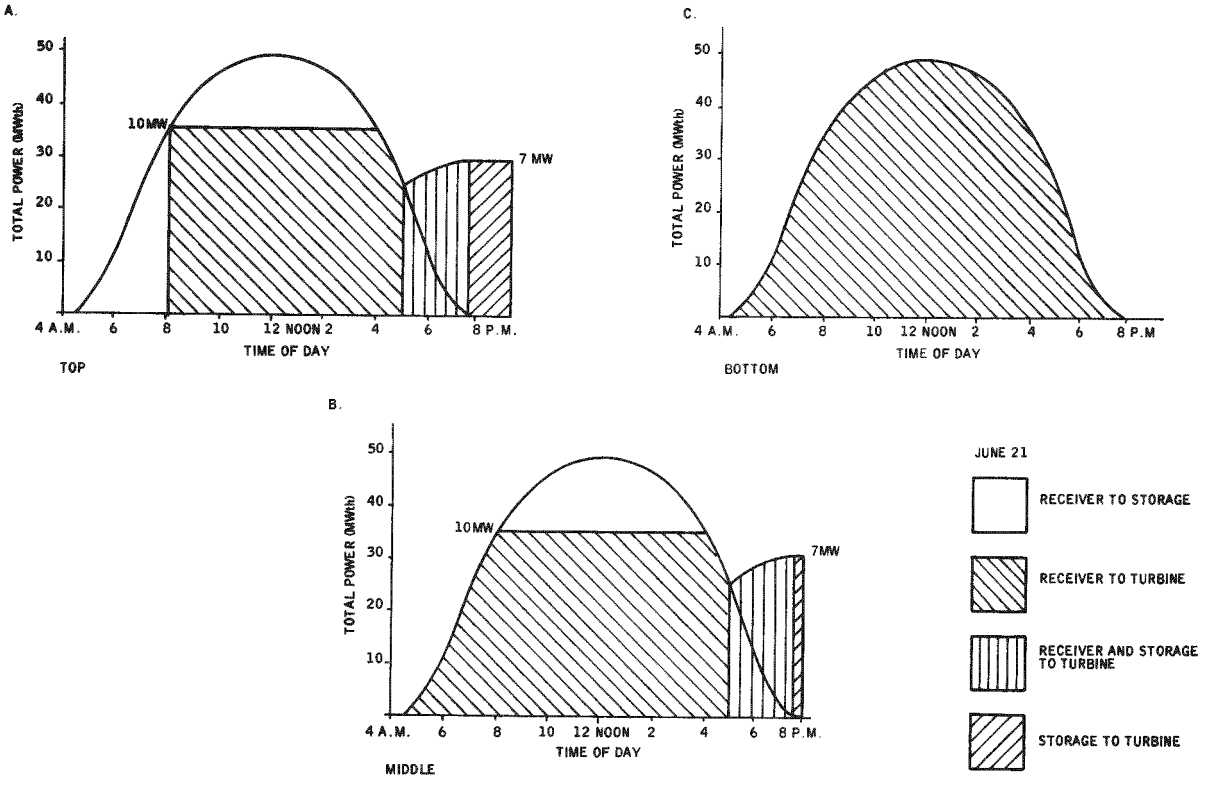


Figure 7-20. Typical Daily Operation

Electrical Generation Subsystem

Control Concept and Requirements

PLANT SUBSYSTEM CONTROL COORDINATION

A plant control system which uses one central analog control unit for control of all major subsystem process variables has been selected to provide subsystem control coordination.

1. The concept of operating the plant in a manner which most efficiently uses the solar energy collected requires the electrical generation and the thermal storage subsystems to follow the power output of the receiver. This requirement, along with the fact that a variation in one subsystem's level of operation has an interacting effect on the other subsystems, establishes the need for subsystem control coordination.

2. To provide subsystem coordination, all analog control loops for subsystem process variables, with the exception of the collector subsystem, will be implemented in a central analog control system. As illustrated in Figure 7-21, major process variables (e.g., pressure, temperature, flow, level, and density) will be measured in each subsystem and the values electronically transmitted to the central analog system. In the analog system, the measured variables will be used in analog logic circuits. Outputs from the analog system will position subsystem control devices (e.g., valves) to provide process control. Interconnected logic between the various analog loops will be used to provide control coordination and improve system stability.

3. Analog control stations in the control room will be used for operator interface with the analog controls. Adjustment of rates, set points and limits, as well as manual positioning of control valves, will be possible through these analog control stations.

4. The collector subsystem control logic (heliostat aiming) will be implemented in dedicated digital computers. The plant operator will interface with the collector controls through computer interface equipment located in the control room.

5. Although implemented by means of digital computer, the collector control will be integrated into the overall plant control by limit signals generated in the central analog control system. These limit signals will cause the computer to defocus heliostats when required due to the lack of subsystem capability to absorb full receiver output.

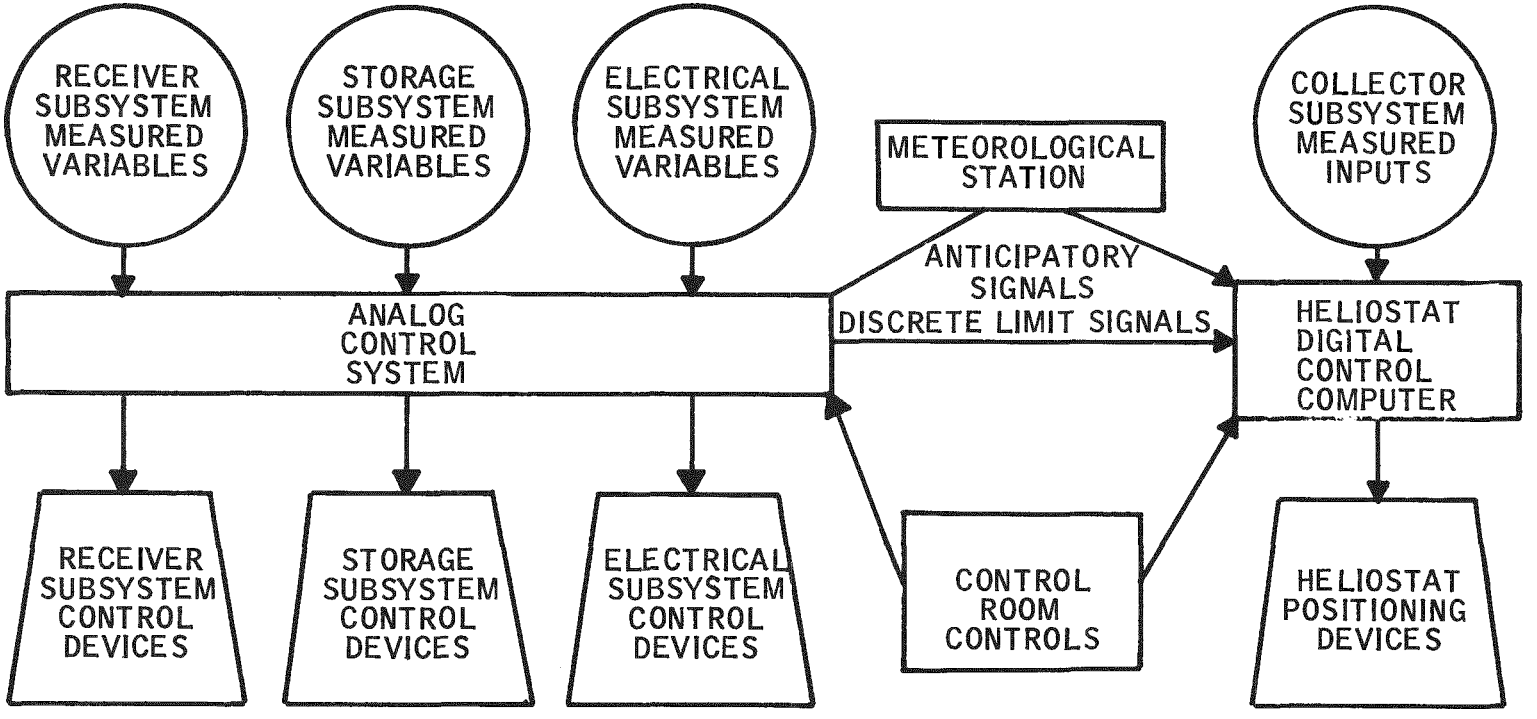


Figure 7-21. Control Coordination of Plant Subsystems

Electrical Generation Subsystem

Control Concept and Requirements

REQUIREMENT FOR A PLANT PROTECTIVE SYSTEM

A plant protective system is incorporated into the plant control to detect dangerous operating conditions and to initiate required protective actions.

1. A separate plant system will be used to monitor the status of essential plant equipment and to initiate protective control actions when necessary. The protective actions will fall into one of two categories: system runback or system shutdown.

2. System runback actions will be initiated when operating plant equipment has insufficient capacity to support the unit load. An example of this situation occurs when the receiver is operated at a load which requires both boiler feed pumps to be in operation. If one of the feed pumps trips, the protective system initiates signals to reduce the solar flux to a level which can be supported with the capacity of the remaining boiler feed pump.

3. System shutdown actions will be initiated when plant conditions develop which could cause major equipment damage. An example of this situation occurs when both boiler feed pumps trip.

4. The protective system will be designed to provide individual subsystem runbacks or trips, allowing the remaining plant subsystems to remain in operation if possible. Sufficient interlocks will be incorporated to cause multiple subsystem runbacks or trips if required.

5. The protective system will consist of hard wired electromagnetic control relays, time delays and sensing devices. The relays will be mounted in a fully enclosed cabinet assembly located in the controlled environment of the relay room. Where required for system integrity, redundant input devices will be used.

6. Trip condition and runback conditions monitored by the protective system are listed in Table 7-5.

Table 7-5. System Protective Conditions

System Shutdown Conditions

- Receiver
  - Manual emergency trip pushbutton operated
  - Loss of sufficient boiler circulating pumps
  - Drum level out of limits
  - Turbine tripped and storage system out of service
  - Both boiler feed pumps tripped
  - High receiver enclosure temperature
- Turbine
  - Generator lockout relay tripped (electrical fault)
  - Thrust bearing wear high
  - Hydraulic fluid pressure low
  - Turbine vibration high
  - Condenser vacuum low
  - Loss of turbine speed signal
  - Exhaust hood temperature high
  - Water detected in steam line
- Storage Unit
  - High charging steam temperature in boiler section
  - Water leak detected
  - Loss of output steam superheat

System Runback Conditions

- Receiver
  - Loss of one condensate pump
  - Loss of one boiler feed pump
- Turbine
  - Partial loss of condenser cooling fans
  - Loss of generator cooling water

Electrical Generation Subsystem

Control Concepts and Requirements

CENTRALIZED PLANT CONTROL

A central plant control room will be used because locating the majority of control operator interfaces in one location is the most practical design for a power plant.

1. A control room located in the plant control wing at turbine floor level will be used to centralize the plant control interfaces with the main plant operator. A control panel of the bench and vertical section type will be used for control switches, analog control stations, cathode ray tube displays, recorders, annunciator windows and other control/operator interface equipment. The controls on the control panel will be located in groups according to plant subsystems. Figure 7-22 shows the control room layout.

2. A data acquisition system using a plant computer will monitor temperatures, flows, pressures and other analog variables in the plant and display this information upon operator request. Cathode ray tube displays in the control panel and printer terminals will be used for display purposes.

3. Control switches will be located on the control panel for control of major motors in the plant.

4. Due to the experimental nature of the solar power plant, additional space has been provided in the control room for locating data acquisition equipment, when required. In addition, the computer programming console has been located in the control room to facilitate communication between the programmer and the plant operator while program modifications are being made.

5. Electronic control cabinets, relay cabinets and computer equipment will be located in environmentally controlled rooms for proper equipment protection.

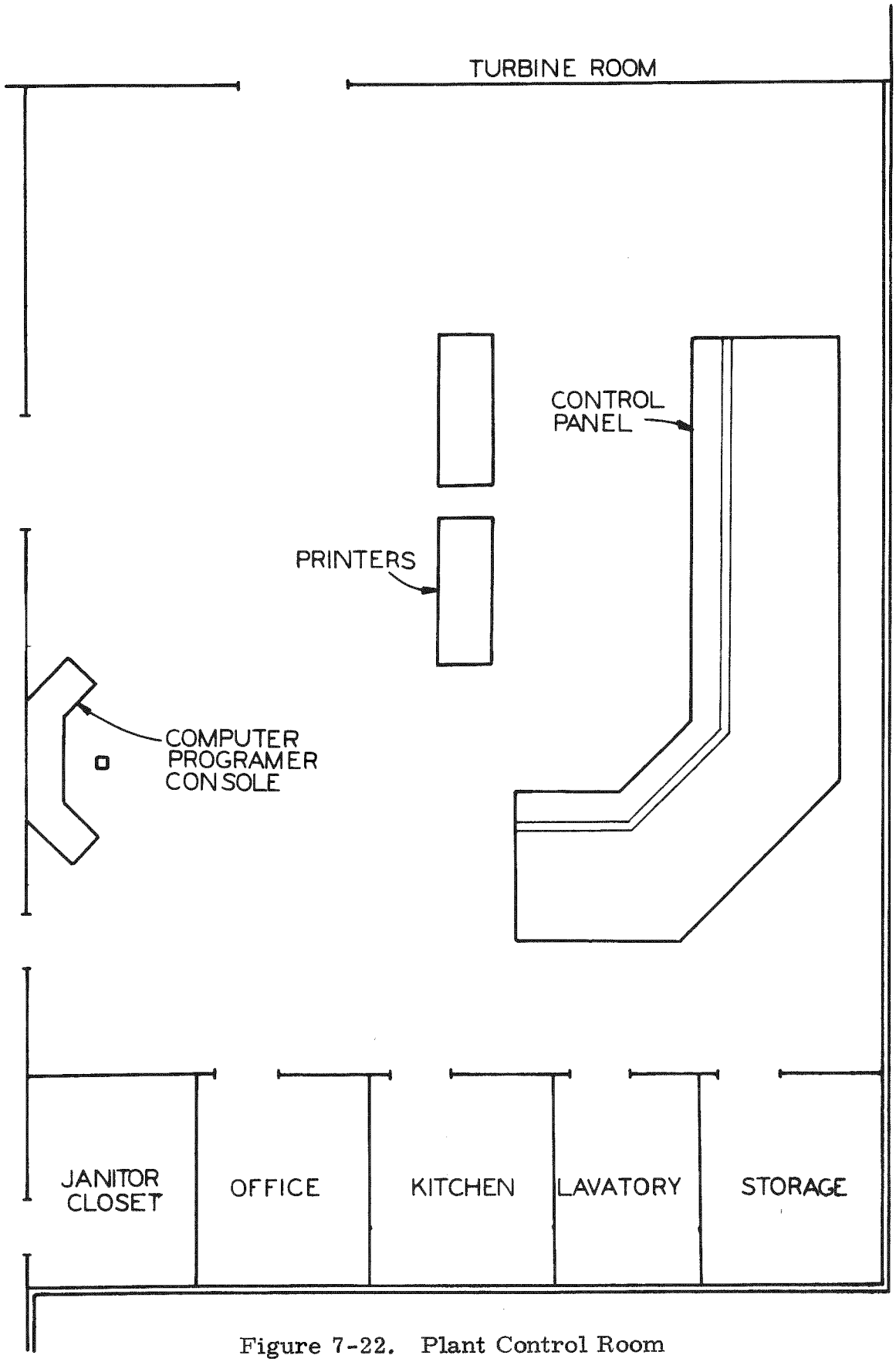


Figure 7-22. Plant Control Room

Electrical Generation Subsystem

Control Concepts and Requirements

INDIVIDUAL SUBSYSTEM CONTROL REQUIREMENTS

Special subsystem control loops are required for proper functioning of the various subsystems.

1. Special control requirements for the Collector Subsystem and the Storage Subsystem have been discussed in previous sections.

2. The controls for the receiver subsystem and the electrical generation subsystem are similar to those used in conventional fossil plants. Analog control logics for two of the more important control loops (feedwater and steam temperature) are shown in Figure 7-23. The logic presentation employed uses standard symbols developed by the Scientific Apparatus Markers Association (SAMA) and by the Instrument Society of America (ISA). These symbols have been adopted as industry standards. Appendix 7A.6 lists the analog diagramming symbols and defines their meanings.

3. One variation from conventional fossil plant controls in the electrical generation subsystem concerns the air-cooled condenser. Because of the efficiency of air-cooled condensers, high-fan power is required when high-ambient temperatures occur. Although turbine efficiency improves with lower condenser backpressure, the increased fan power required to obtain low-condenser pressure may more than offset increased turbine efficiency. In order to provide the highest overall plant efficiency, a special fan management program will be used in the plant computer. Monitoring generator output, steam and air temperatures, and condenser absolute pressure, the program will determine the most economical speed and number of condenser fans to be operated. Provisions will be made for allowing the computer to assume direct control of the fans, if desired by the operator. Manual fan control by the operator will always be possible.

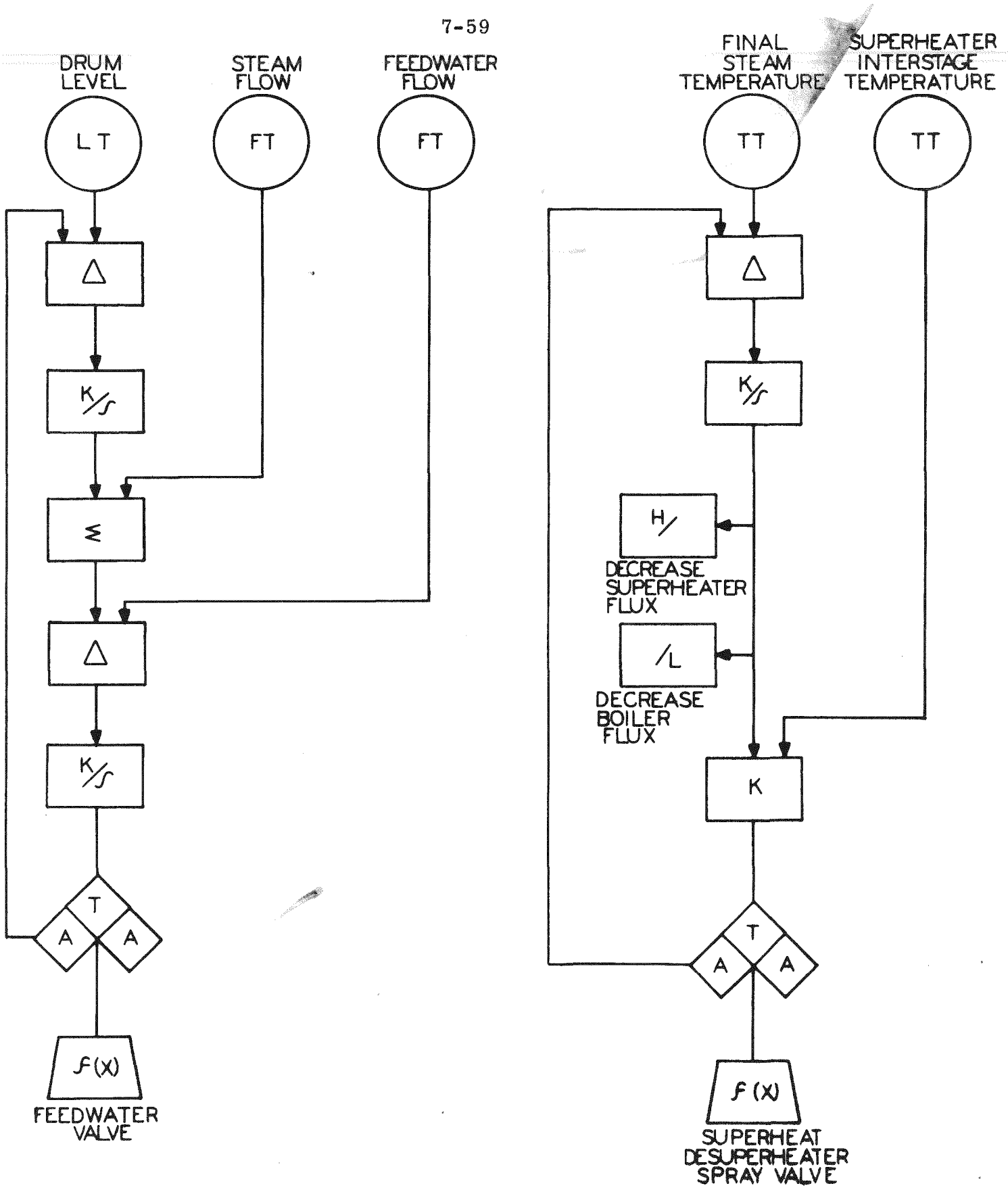


Figure 7-23. Feedwater and Steam Temperature Controls

Electrical Generation Subsystem

Plant Operating Modes

TRANSITIONS BETWEEN STEADY-STATE MODES

A detailed study will be performed to determine that the plant control systems are capable of making all possible transitions between steady-state operating modes.

1. Table 7-6 shows the six steady-state operating modes which occur during plant operation. The possibility exists that at some time the plant may be required to make a transition from any steady-state mode to one of the five remaining modes. With six allowed modes, 50 possible mode transitions exist.

2. After all system control design has been initially completed, a detailed examination of the capability of the controls to maintain system stability during each possible transition must be performed. If control problems occur during any transition, control design modifications must be made.

3. A complete transition analysis as described above will be performed prior to completing the final control design.

4. The control system will also be modified as required to allow for dynamic system characteristics discovered during the period of subsystem experimental testing.

Table 7-6. Solar Power Plant Steady-State Operating Modes

Subsystem	Steady-State Mode					
	A	B	C	D	E	F
Receiver	ON	ON	ON	OFF	ON	OFF
Turbine	ON (Receiver Steam)	ON (Receiver Steam)	ON (Receiver & Storage Steam)	ON (Storage Steam)	OFF	OFF
Storage	Holding	Charging	Discharging	Discharging	Charging	Holding

Electrical Generation Subsystem

Plant Operating Modes

MODE A - RECEIVER ON, STORAGE UNIT HOLDING, TURBINE ON

The first steady-state operating mode occurs when receiver steam is only used for driving the turbine generator.

1. Control parameters used while operating in Mode A are shown in Figure 7-24. The symbols used are standard SAMA analog logic symbols. Only basic analog control loops are shown for illustrative purposes. More complex logics using such items as feedforward and feedback signals will actually be employed.

2. This steady-state mode of operation would normally occur if the thermal storage unit were either fully charged or unavailable because of maintenance or malfunction.

3. During this steady-state mode, the unit is operated in a control mode conventionally known as a turbine following. All heliostats are on their assigned aim points, thus maximizing solar collection. The turbine control valves are positioned to maintain receiver pressure at a set value.

4. With this method of control, the generator output varies directly with solar energy collection.

5. If solar energy exceeds generator capacity some heliostats must be defocused to reduce solar input to the receiver. Under these conditions, some available power is rejected and the objective of using all available power is not achieved.

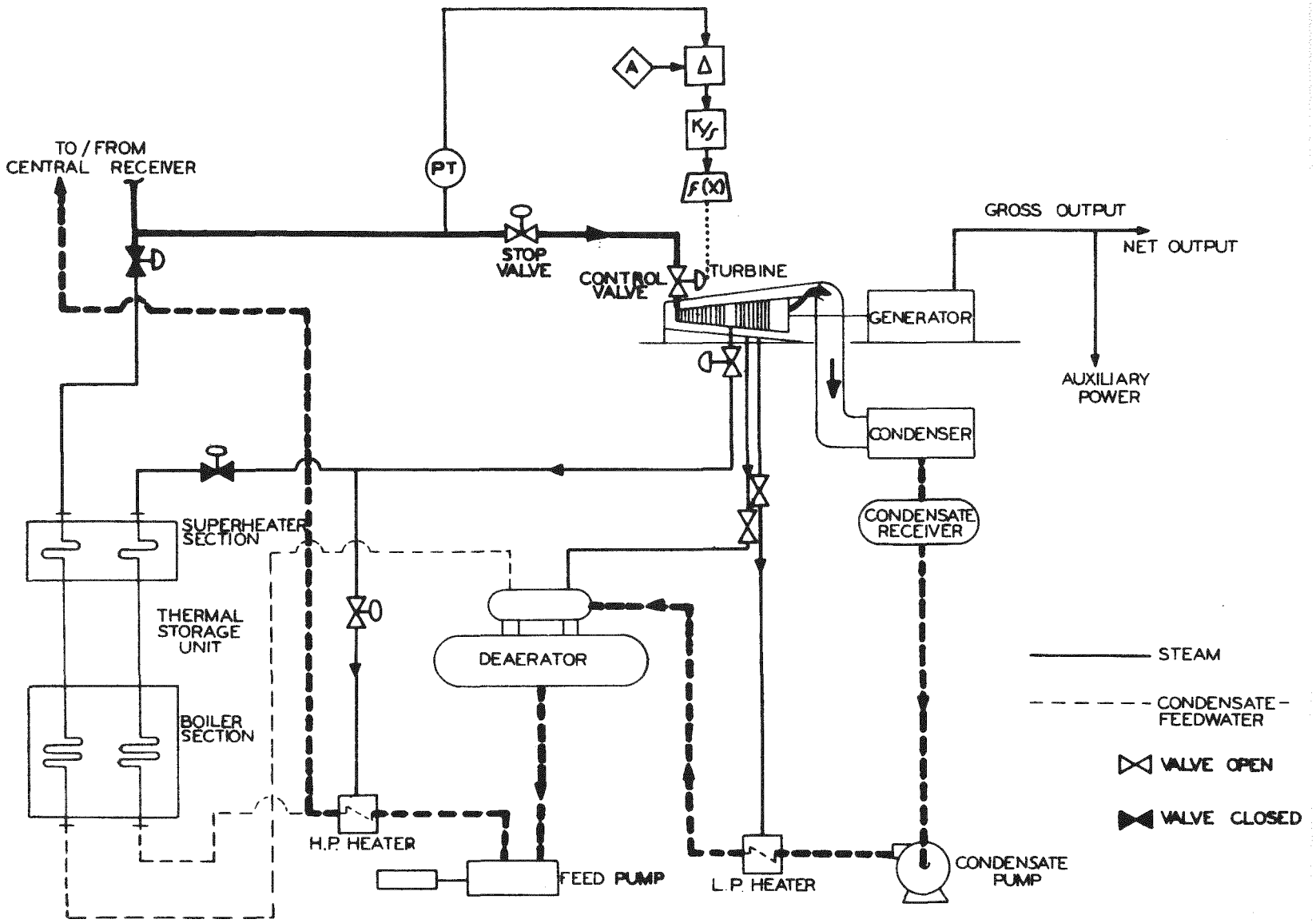


Figure 7-24. Mode A-Receiver on, Storage Holding, Turbine Generator On

Electrical Generation Subsystem

Plant Operating Modes

MODE B - RECEIVER ON, STORAGE UNIT CHARGING, TURBINE GENERATOR DRIVEN BY RECEIVER STEAM

The second steady-state operating mode occurs when receiver steam is used for simultaneously driving the turbine generator and charging the thermal storage unit.

1. Control parameters used while operating in Mode B are shown in Figure 7-25.

2. This steady-state mode of operation normally occurs during the middle of the day when excess receiver output is available.

3. During this steady-state mode, the turbine control valves are positioned to maintain a set generator output. The thermal storage charging steam valve is modulated to maintain receiver outlet pressure at a set value. All heliostats are on their assigned aim points; thus, maximizing solar collection.

4. When operating in this steady-state mode, the electrical output remains constant, with excess receiver output used for charging the thermal storage unit.

5. Normally, the combined steam requirements of the turbine and the storage unit are sufficiently great to avoid any solar collection restrictions.

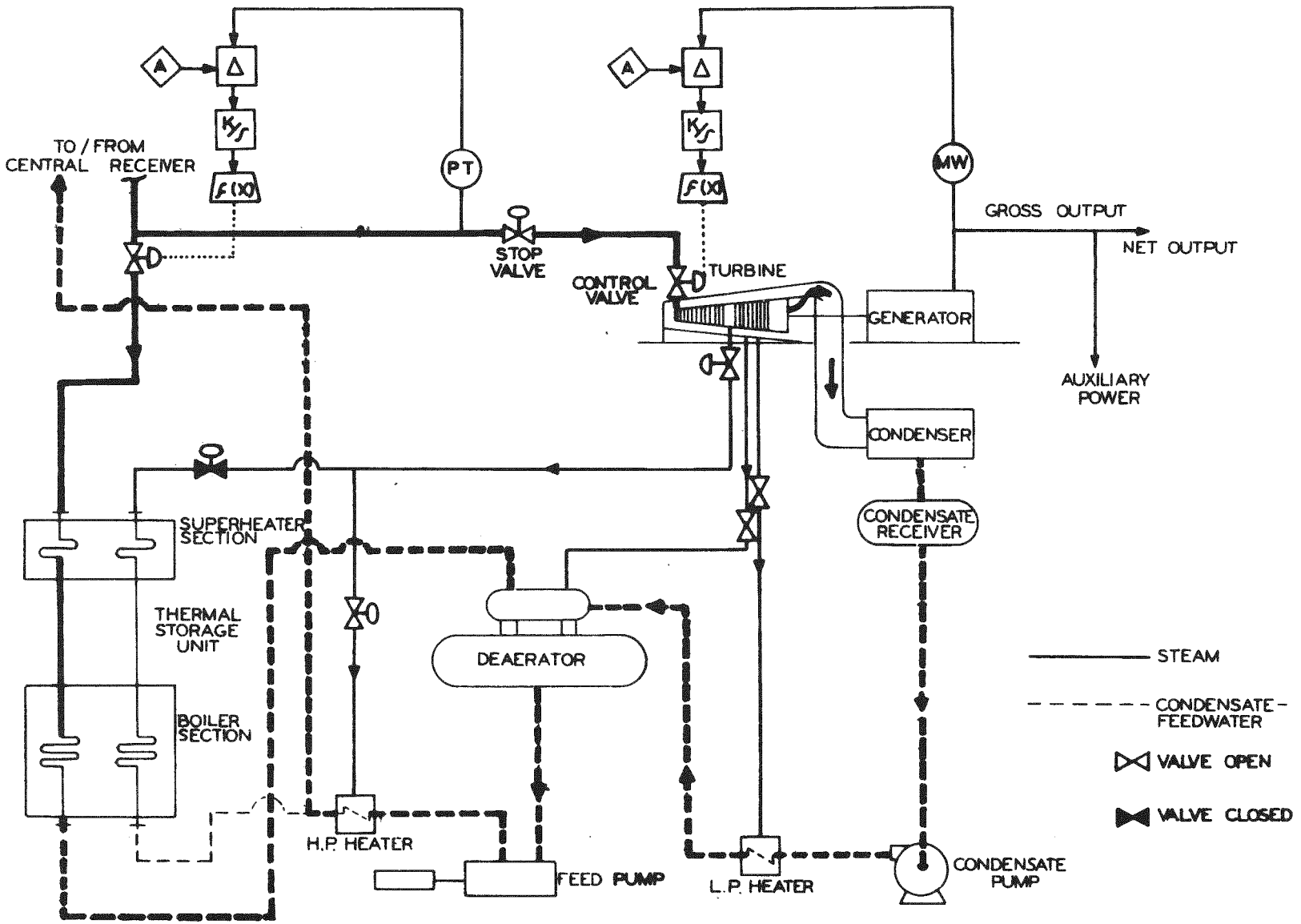


Figure 7-25. Mode B-Receiver on, Storage Charging, Turbine Generator Driven by Receiver Steam

Electrical Generation Subsystem

Plant Operating Modes

MODE C - RECEIVER ON, STORAGE UNIT DISCHARGING, TURBINE USING BOTH RECEIVER STEAM AND STORAGE STEAM

The third steady-state operating mode occurs when both receiver steam and storage steam are used to drive the turbine generator.

1. Control parameters used while operating in Mode C are shown in Figure 7-26.

2. This steady-state mode of operation occurs on most days as the turbine generator is transferred from receiver steam to storage steam. Under these conditions, the operating mode could be considered a transition mode rather than a steady-state mode. Conditions will exist on certain days of the year; however, prolonged cloud cover will limit receiver output to a level below that required to maintain desired generator output. If the storage unit is sufficiently charged, unit operation as described for Mode C would be employed for a prolonged period of time; thus, the operation becomes a steady-state mode.

3. During this mode, the turbine control valves are positioned to maintain receiver outlet pressure at a set value. The receiver output is not sufficient to drive the turbine at the desired output. Extraction steam to the HP heater is shut off and steam from the storage unit is admitted to the turbine in order to increase the generator output to the desired value. The valve for controlling storage steam flow to the turbine is positioned in response to generator output.

4. When operating in this steady-state mode, the generator output remains constant.

5. No solar collection restrictions are required in this steady-state mode.

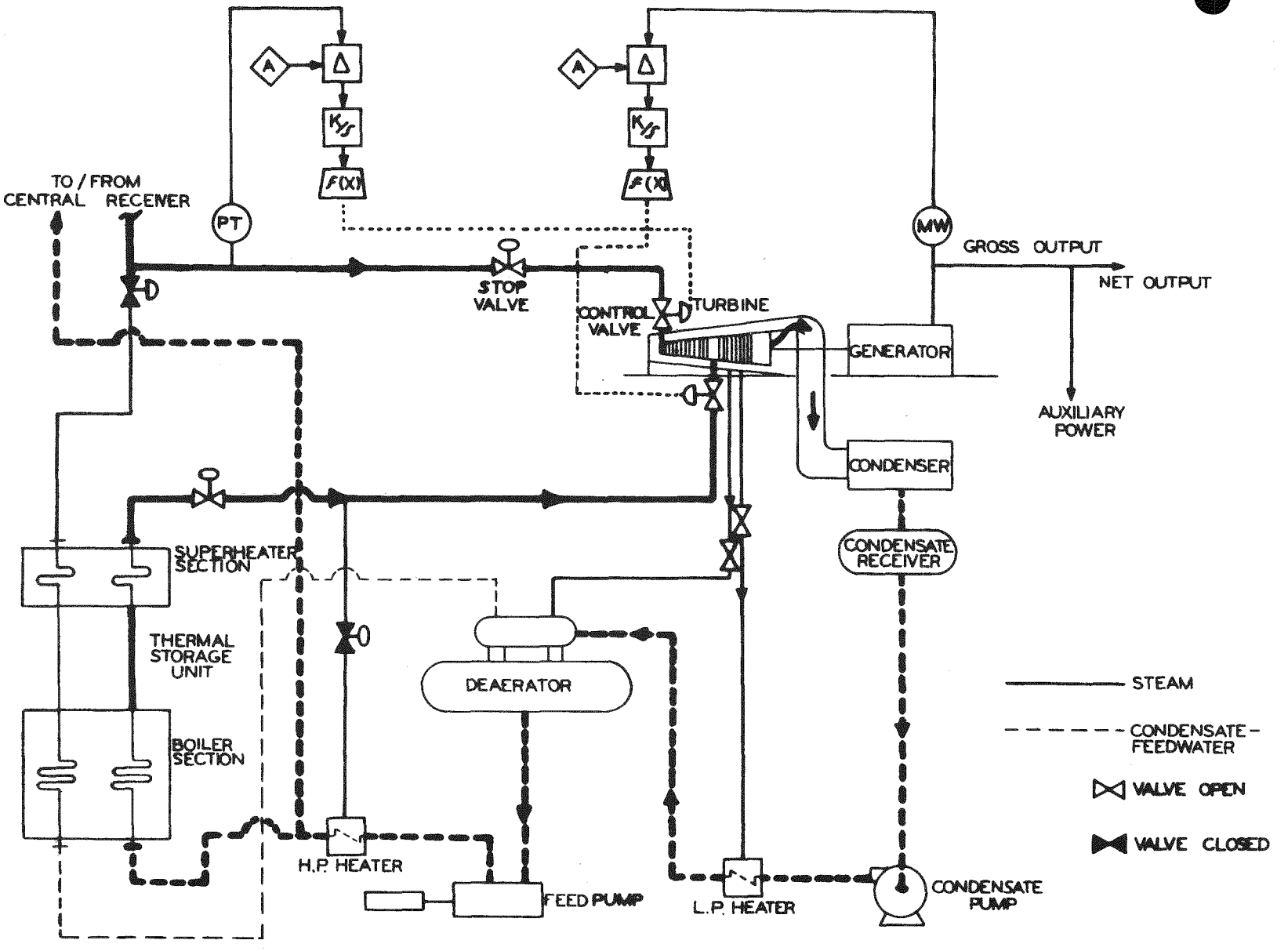


Figure 7-26. Mode C-Receiver on, Turbine Generator Driven by Receiver Steam and by Storage Steam

Electrical Generation Subsystem

Plant Operating Modes

MODE D - RECEIVER OFF, STORAGE UNIT DISCHARGING, TURBINE DRIVEN BY STORAGE STEAM ONLY

The fourth steady-state operating mode occurs when the receiver is off and steam from the thermal storage unit is used to drive the turbine generator.

1. Control parameters used while operating in Mode D are shown in Figure 7-27.

2. This steady-state mode of operation normally occurs during evening hours when the generating unit is maintained in operation.

3. During this steady-state mode, the valve for controlling storage steam flow to the turbine is modulated to maintain generator output at a set value. The heliostats are in their stored position and the receiver is secured. While operating the turbine with storage steam only, a small amount of steam is continuously admitted to the turbine through the HP steam control valves. This steam is required for cooling the first-stage blading in the turbine. Also, a small amount of storage steam is continuously fed to the receiver drum to aid in maintaining receiver temperatures.

4. When operating in this steady-state mode, generator output remains constant as long as the thermal storage unit can provide sufficient output.

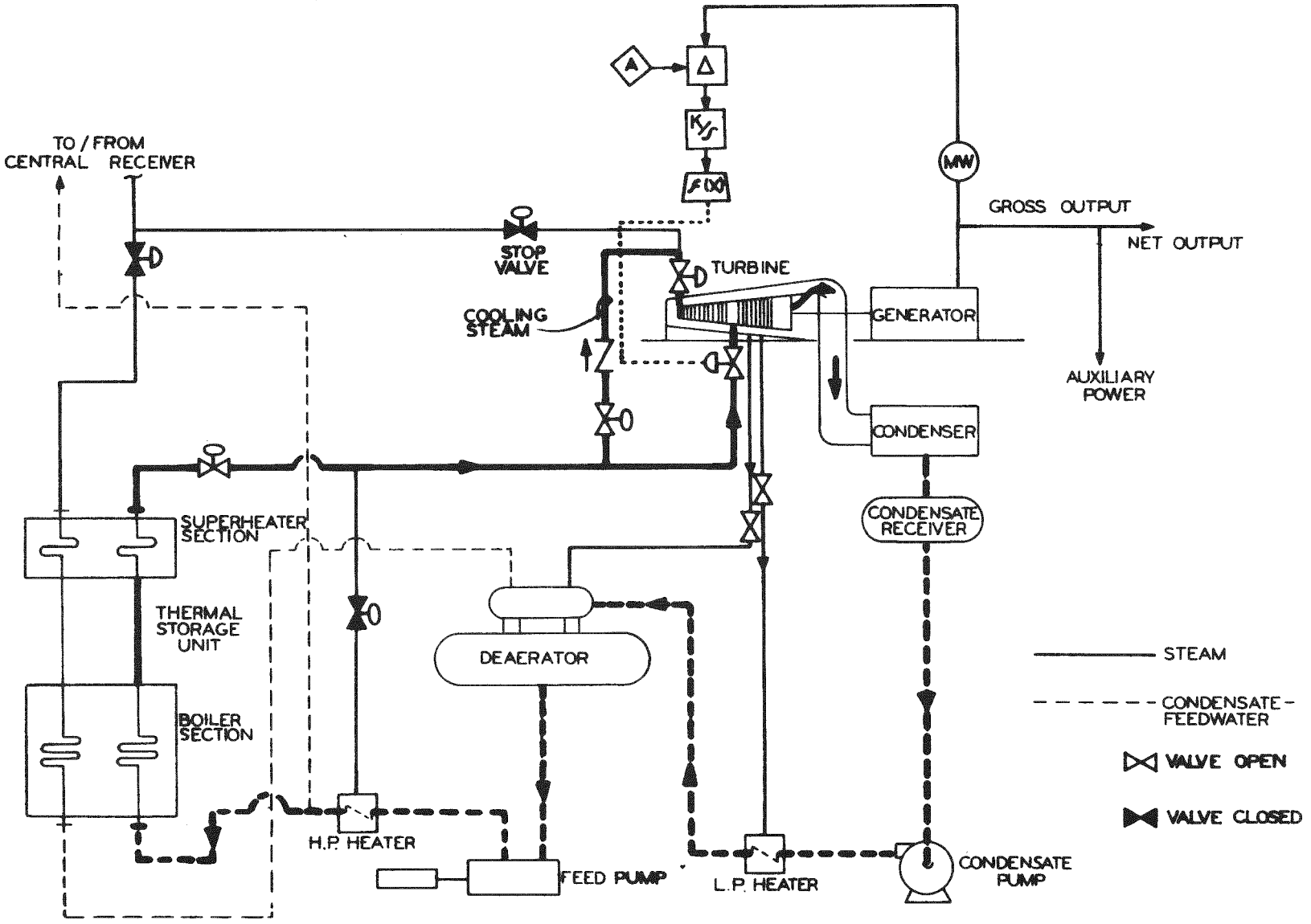


Figure 7-27. Mode D-Receiver Off, Turbine Generator Driven by Storage Steam

Electrical Generation Subsystem

Plant Operating Modes

MODE E - RECEIVER ON, STORAGE UNIT CHARGING, TURBINE OFF

The fifth steady-state operating mode occurs when the receiver output is used only to charge the thermal storage unit.

1. Control parameters used while operating in Mode E are shown in Figure 7-28.

2. This steady-state mode of operation would normally occur if the turbine generator is out of service due to malfunction or maintenance.

3. During this steady-state mode the thermal storage charging steam valve is modulated to maintain the receiver outlet pressure at a set value. All heliostats are on their assigned aim points, thus maximizing solar collection. Steam valves to the turbine are closed.

4. Full solar collection is possible in this steady-state mode. However, if the thermal storage unit becomes sufficiently charged such that it can no longer accept the full receiver output, heliostat defocusing is required.

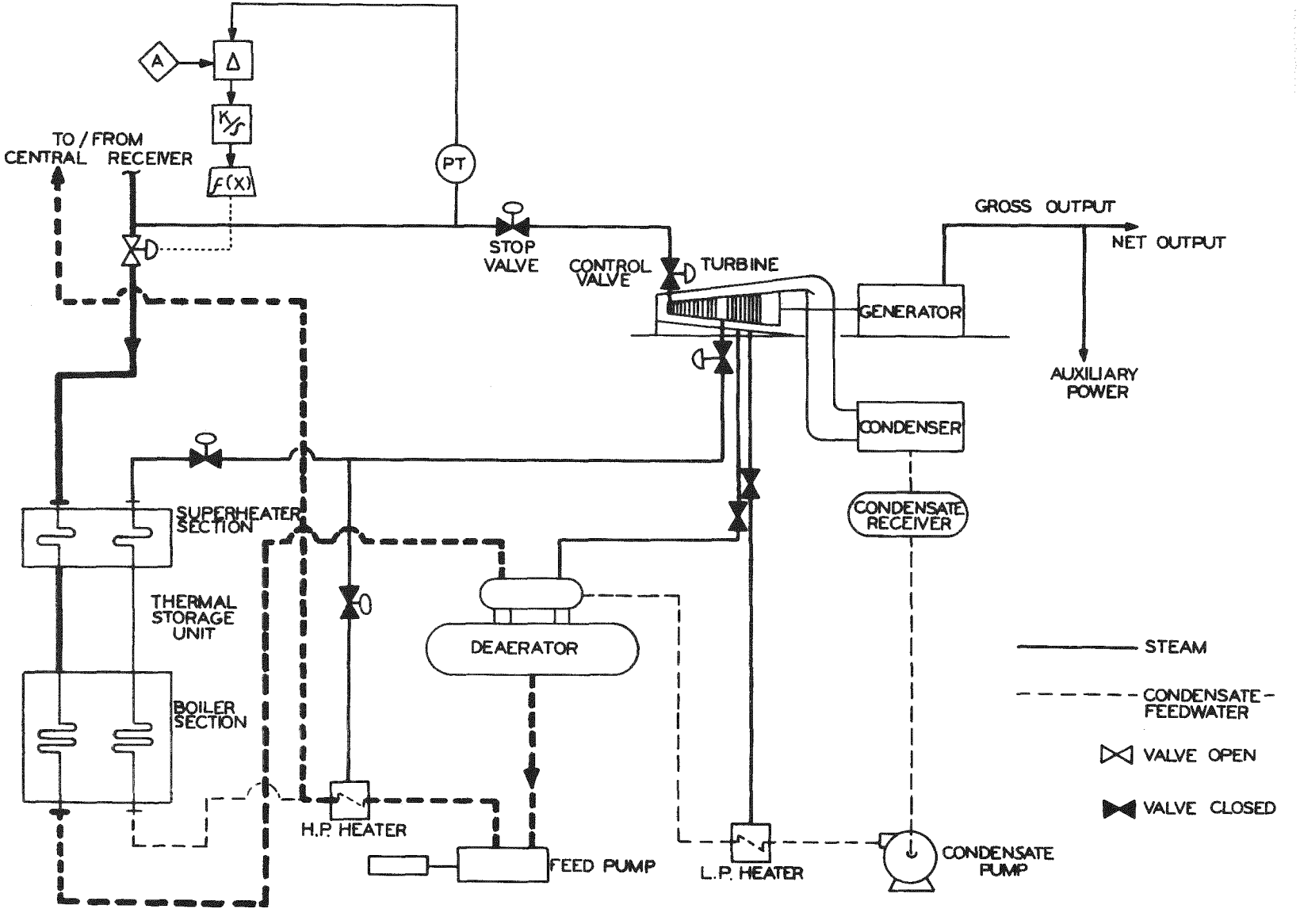


Figure 7-28. Mode E-Receiver On, Storage Charging, Turbine Generator Off

Electrical Generation Subsystem

Plant Operating Modes

MODE F - RECEIVER OFF, STORAGE UNIT HOLDING, TURBINE OFF

The sixth steady-state mode occurs when the receiver is off and the turbine generator is not in operation.

1. Control parameters used while operating in Mode F are shown in Figure 7-29.

2. This steady-state mode of operation is the normal plant shutdown condition. On a daily basis, this mode would regularly occur when the generator was shut down during night-time hours.

3. During this steady-state mode, each of the four plant subsystems is essentially in a non-operating status. All heliostats are in their stored position, the receiver is secured, and the turbine generator is on turning gear. The thermal storage unit is holding, with one exception. If the storage unit is charged, a small amount of steam from the storage unit is used for plant purposes, such as maintaining steam seals on the turbine and maintaining receiver drum temperatures.

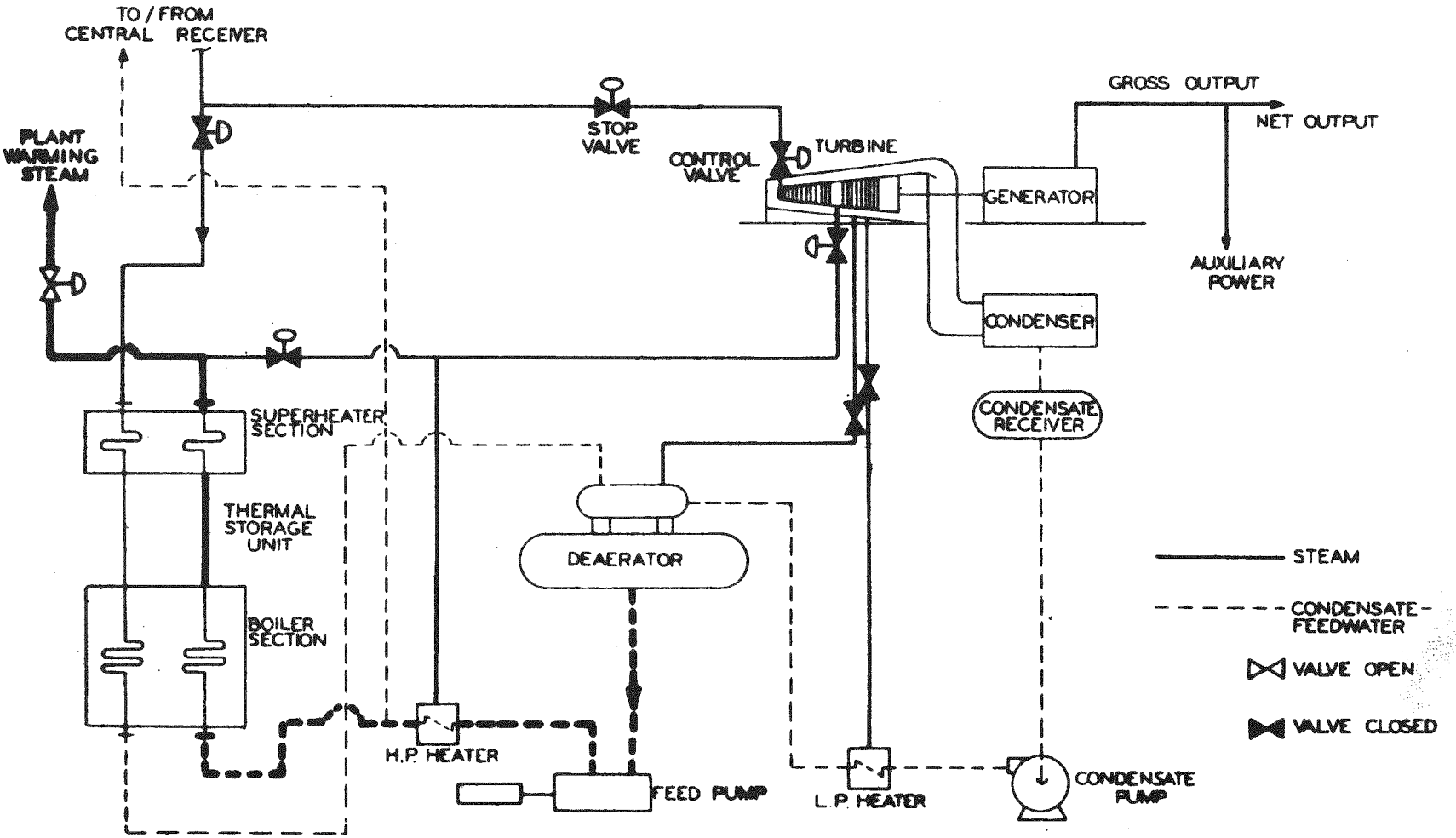


Figure 7-29. Mode F-Receiver Off, Storage Holding, Turbine Generator Off

APPENDIX 2A
ECONOMIC ANALYSIS ASSUMPTIONS

APPENDIX 2A

ECONOMIC ANALYSIS ASSUMPTIONS

I. COST PARAMETERS USED IN CYCLE OPTIMIZATION

Steel Cost = $.43/lb

Storage Insulation Cost = $20/ft^2

Coal Cost = $.50/10^6 BTU

Cost of Coal Plant = $400/kW

Cooling Tower Cost = $.0115/BTU heat load per hr

Turbine Cost = $58.5/kW turbine capacity

Salt Cost = $.08/lb

Oil Cost = $1.50/gallon

Tank Cost = 770* (Tank Volume)$^{-.613}$ $/ft^3

Tower Cost = an extrapolation between the following points:

100 ft	$ .5 x 10^6
500 ft	$ 1.1 x 10^6
700 ft	$ 2.0 x 10^6
1000 ft	$ 3.8 x 10^6
1250 ft	$ 5.0 x 10^6
2000 ft	$14.5 x 10^6

Balance of Plant Cost = $42/kW of turbine capacity

Indirect Costs = .21* (Total Cost)

Fixed Charge Rate = $.16

II. PERFORMANCE PARAMETERS USED IN CYCLE OPTIMIZATION

Storage Superheater Pressure Drop = 100 psia

Superheater Heat Transfer Coefficients = 8 BTU/hrF°ft^2

Fraction of Annual Thermal Energy Collected Which is Sent Through Storage = .45

Efficiency of Coal-Fired Plant Turbine = .33

Efficiency of Coal-Fired Boilers = .85

Redirected Power to Tower at 12/21 2 PM = .48 kW/m^2 mirror area

Output Electric Power Desired at 12/21 2 PM = 10 MW(e)

Cavity Efficiency = .9

Total Annual Energy Collected = 1.8 MW (thermal) per $meter^2$ mirror area

Ground Cover Ratio = .45

Overall Condensing Heat Transfer Coefficient for Salt Storage = 90

Overall Boiling Heat Transfer Coefficient for Salt Storage = 110

Overall Condensing Heat Transfer Coefficient for Oil Storage = 125

Overall Boiling Heat Transfer Coefficient for Oil Storage = 100

Flux in Receiver = 200 kW/m^2 (Average)

Safety Factor in Sizing Storage = 1.15

Turbine Outlet Pressure = 5 in. Hg

Feedwater Temperature Ratio = .8

Peak Energy Collected = 0.6 kW (thermal)/hr - m^2

Output Power from Storage = 8.05 MW(e)

Storage Capacity = 6 hr

Bus Bar Power from Storage = 7.00 MW(e)

III. IDEALIZATIONS, ASSUMPTIONS, AND ALGORITHMS

Real Efficiency = .9 (Ideal Efficiency) - .05

Turbine Capacity Needed for Normal Turbine to get Desired Output Rate =

$$\left[\frac{\text{Desired Output Rate}}{\left(\frac{P_{reduced}}{P_{design}}\right)\sqrt{\frac{P_{design}\,\bar{V}_{design}}{P_{reduced}\,\bar{V}_{reduced}}}\left(\frac{\Delta H_{design}}{\Delta H_{reduced}}\right)}\right]$$

Turbine capacity needed for secondary injection turbine is calculated by the following algorithm.

1) Set turbine capacity for the steam which comes through the front

2) Pick reduced pressure

3) Calculate the ideal efficiency of the turbine when running off the steam injected from the front end

4) Calculate the ideal efficiency of the turbine when running off of steam at the reduced pressure conditions

5) Calculate the steam flow rates necessary when running from front end steam and the reduced pressure (storage) steam

6) Isoentrophically expand the steam from the turbine front-end conditions to the reduced pressure - calculate the volume flow rate at this point

7) Calculate the volume flow rate for the desired output rate when running off of storage steam (reduced pressure) conditions

8) If the volume rate in (7) is less than that in (6), turbine capacity is the same as in (1)

9) If the volume rate in (7) is greater than that in (6), we increase the size of the back end of the turbine to handle the increased volume, assign the increased volume to the reduced pressure steam, and calculate the turbine capacity from the capacity in (1) plus the added capacity

Receiver, Condensor, Boiler Costs = 4 x cost of the steel (bulk metal) used 2 in. piping is assumed throughout.

Tower Height = .25 (Field Radius)

APPENDIX 2B
SYSTEMS EFFECTIVENESS PROGRAM PLAN

APPENDIX 2B
SYSTEMS EFFECTIVENESS PROGRAM PLAN
SOLAR PILOT PLANT PHASE I
SECTION I
INTRODUCTION

SCOPE

This document describes Honeywell's plan to accomplish the System's Effectiveness Program on the Solar Pilot Plant Phase I program contract. This plan is prepared in accordance with the reference plan Work Breakdown Structure (WBS), SC061A.04 (6.1.1.4) Systems Effectiveness and is compatible with the Solar Pilot Plant Program Master Schedule, Figure 3-1 of the reference plan.

Reference: Honeywell Report F3419-PP1 (2852-40140), "Solar Pilot Plant Phase I Program Plan" (CDRL NO. 9) 3 July 1975, Revised 10, September 1975.

PURPOSE

The primary objective of the Systems Effectiveness Program is to assess compliance with the 90 percent availability goal for the Solar Pilot Plant, as specified in Annex 1 of the RFP and to provide system design recommendations to achieve this goal. This objective is to be accomplished without compromising the safety requirements specified in Annex 1 of the RFP and with a design goal of minimizing total cost (initial and operating) per watt-hour. Pursuant to this objective, availability estimates (numerical values) will be determined for each indentifiable subsystem comprising the overall Solar Pilot Plant. The System Effectiveness Program will allow a quantitative, orderly, and ongoing assessment of the system design as it progresses through its various stages. The Systems Effectiveness Program will be accomplished by a reliability/maintainability engineer specifically assigned to the Honeywell Solar Pilot Plant engineering team.

Section II of this document presents the Systems Effectiveness Program schedule and Section III describes the Systems Effectiveness Program tasks to be conducted during the Solar Pilot Plant Phase I program contract.

SECTION II
SYSTEMS EFFECTIVENESS PROGRAM SCHEDULE

The schedule for accomplishing the Systems Effectiveness Program tasks during the Solar Pilot Plant Phase I program contract is shown in Figure 2-25.

SECTION III
SYSTEMS EFFECTIVENESS PROGRAM
TASK DESCRIPTION

This section provides a description of the specific Systems Effectiveness Program tasks which will be conducted in fulfillment of the following three Work Breakdown Structure (WBS) elements of the reference plan.

- SC061A.04 (6.1.1.4) Systems Effectiveness
- SC061B.03 (6.1.2.3) Safety and Control Studies
- SC061D.03 (6.1.4.3) Effectiveness Studies

SC061A.04(6.1.1.4) SYSTEMS EFFECTIVENESS

Systems Effectiveness Program Plan

This document describes the specific systems effectiveness program tasks and the schedule for conducting these tasks (Figure 2-25) during the Solar Pilot Plant Phase I program contract. It is being submitted to ERDA as part of the Preliminary Design Baseline Review (PDBR) documentation (CDRL 1) of the Pilot Plant.

Availability Allocation

A primary objective of the systems effectiveness program is to assess compliance with the 90 percent availability goal for the Solar Pilot Plant, as specified in Annex 1 of the RFP and to provide system design recommendations to achieve this goal. Availability goals will be assigned to each major subsystem i.e. Collector, Receiver, Thermal Storage, and Electric Power Generation such that the overall systems effectiveness goal (90 percent availability) will be achieved if each subsystem meets its apportioned goal. The initial subsystem availability allocation will be established per the schedule shown in Figure 2-25. As the Pilot Plant design progresses, the availability parameters of each subsystem will be estimated. When the availability parameters of the subsystems have been estimated, the estimates will be compared with the apportionment. In the event that the estimate exceeds the apportionment, the excess will be reapportioned to the remaining subsystems using standard reapportionment procedures. In the event that an estimate falls

short of an apportionment, the deficit will be used to either identify areas requiring system improvement or as the basis for an availability reapportionment to achieve the systems availability goal.

Availability Model

An availability model will be developed which is compatible with the Solar Pilot Plant operating modes and operating strategy/scenario. Pilot Plant operating modes to be considered in this model include:

- Power generation from Solar Energy only and simultaneously recharging thermal storage.
- Power generation from solar energy only with thermal storage, holding.
- Power generation using stored thermal energy only.
- Power generation using both solar energy and stored thermal energy.

The model will consider availability parameters such as hardware reliability, redundancy, scheduled maintenance, and unscheduled maintenance. The availability model as initially established will be utilized in the availability analysis and in establishing the availability allocation. It will be updated as required to reflect changes in system design, operating modes, and operating strategy/scenario.

Availability Analysis

Availability analysis of the Solar Pilot Plant will be conducted to assess compliance with the 90 percent availability goal and to highlight areas of the system which may require improvement to achieve the availability goal. An initial assessment will be completed according to the Figure 2-25 schedule. This assessment basically entails establishing numerical values for the availability parameters i.e. hardware mean time between failure, life, scheduled/unscheduled maintenance time, and modeling them in the aforementioned availability model. Historical data of related hardware will be utilized as the basis for the availability parameter numerical values where they are available. Engineering estimates and data sources such as Government Industry Data Exchange Program (GIDEP) will also be utilized where no directly related experience is available.

Failure Mode and Effect Analysis (FMEA)

A functional level FMEA will be conducted of the Solar Pilot Plant which will identify potential failure modes and the consequences of them occurring. The identification of the potential failure modes and their consequences will consider worst case design requirements for solar flux variations, thermal power variations, environment, and startup/shutdown extremes. The FMEA results will include the probable consequences of possible failure modes, the identification of single point failures, and recommendations for failsafe provisions, redundancy provisions, and failure warning systems/devices. The initial FMEA will be completed in a time frame to allow the results which potentially impact reliability/safety of the subsystem research experiments (SRE) to be transmitted to the SRE Design team for incorporation in the SRE test plans.

Design Reviews

The Honeywell reliability/maintainability engineer assigned to the Solar Pilot Plant program will participate in all Design Reviews to assure that reliability

and safety considerations are properly reflected in the SRE specifications and test plans and to assure that these parameters are not compromised as a result of design decisions resulting from these reviews. In addition to reliability and safety, the reliability/maintainability engineer will also assure that design decisions relating to the Pilot Plant do not compromise maintainability and availability.

SC061B.03(6.1.2.3) SAFETY AND CONTROL STUDIES

Subsystem Experiment Design Support

Reliability engineering support will be provided to the subsystem experiment design effort to assure that reliability and safety considerations are properly reflected in design tradeoffs and in the SRE test plans. The primary input to this effort will be the initial FMEA, wherein the FMEA results which have a potential impact on reliability/safety of the SRE's will be determined. In a coordinated effort with Design, the desirability of additions and/or changes to the development tests and experiments will be assessed.

Failure Reporting Analysis Corrective Action (FRACA)

FRACA will be performed during the SRE Test and Evaluation Program to assure that problems which are surfaced during this testing are properly documented. The failure reports will be segregated into two classifications--those which are relevant to the Solar Pilot Plant and those which relate exclusively to the SRE. Recommended corrective action will be established for those failures which are relevant to the Pilot Plant. Those which relate exclusively to the SRE will be documented as such and dismissed with no further action.

SC061D.03(6.1.4.3) EFFECTIVENESS STUDIES

A Systems Effectiveness Study Report will be provided as part of the Preliminary Design Review (PDR) documentation (CDRL 2) of the Pilot Plant. This report will include the final Phase 1 contract updating of the Availability

Allocation, Availability Analysis, and the FMEA, based on the latest Pilot Plant design definition and the SRE results.

Availability Allocation

An updated Availability allocation will be made to each of the four major subsystems (Collector, Receiver, Thermal Storage, and Electric Power Generation) such that the overall Solar Pilot Plant 90 percent Availability goal will be met if each subsystem meets its allocation.

Availability Analysis

An updated Availability Analysis will be made to assess compliance with the 90 percent availability goal and to document areas of the system which may require improvement to achieve the availability goal.

Failure Mode and Effect Analysis (FMEA)

A functional level FMEA will be conducted of the Solar Pilot Plant to identify potential failure modes and the consequences of them occurring. Single point failure conditions will be highlighted and recommendations for failsafe provisions, redundancy, and failure warning systems/devices will be made.

APPENDIX 4A
DRIVE RATE ANALYSIS

APPENDIX 4A

DRIVE RATE ANALYSIS

SUMMARY

The azimuth-elevation configuration with a gimbal drive rate limit of 40 degrees/hour results in an average of four percent of the heliostats being off target at any time. The tilt-tilt configuration has no rate limited heliostats at any time for the same 40 degree/hour limit.

THE APPROACH TO THE ANALYSIS

The analysis begins with the control law and develops the gimbal configuration-dependent command angles. The derivative of these angles are taken to determine angular rate. The resulting equations are solved for heliostat position in the field for constant required command rate. These isopleths of gimbal angle rates are then plotted.

DEVELOPING THE COMMAND LAW

Snell's law of reflection states that, relative to the mirror normal, the angle of the incoming ray equals the angle of the reflected ray. Referring to Figure 1, $\hat{S}$ is the Sun's unit direction vector, $\hat{T}$ is the tower unit direction vector from a point P in the field, and $\hat{N}$ the required mirror normal unit direction vector for the reflected Sun's ray to hit the target. One way to express the command law is: "The cross product of the Sun vector into the mirror normal must equal the cross product of the normal into the tower vector" or $\hat{S} \times \hat{N} = \hat{N} \times \hat{T}$

$$\hat{N} \times \hat{T} + \hat{N} \times \hat{S} = 0$$

$$\hat{N} \times (\hat{S} + \hat{T}) = 0$$

This expression can only be zero if:

1. The angle between $\hat{N}$ and $\hat{S} + \hat{T}$ is zero-- the condition we wish to establish.

2. $\hat{N}$ is zero which by definition cannot occur since $|\hat{N}| \equiv 1$.

3. $\hat{S} = -\hat{T}$ which can only occur when the Sun is below the horizon.

Therefore, an acceptable definition for the mirror normal direction is

$$\hat{N} = \hat{S} + \hat{T}$$

COMPUTATION OF SUN VECTOR, $\hat{S}$

The flow diagram for the computation of the Sun's unit vector direction cosines in the east, north, vertical coordinate frame is shown in Figure 2. For the purposes of calculating gimbal angles and rates, the Earth's orbital rotation was held fixed throughout each day, the precession of the Earth's axis was held fixed, and a latitude of 33 degrees was assumed. The rates of the unit vectors are obtained by taking the time derivatives of the cosines.

THE TOWER VECTOR, $\hat{T}$

Calculation of the unit tower direction vector simply unitizes the distance vector from the heliostat to the tower as measured in the east, north and vertical coordinate frame located at the heliostat.

CALCULATION OF MIRROR NORMAL, $\hat{n}$

The mirror normal $\hat{n}$ is computed by summing the Sun vector $\hat{S}$ and the tower vector $\hat{T}$ in east, north and vertical components.

$$\hat{n} = (S_1 + T_1)\ \hat{E} + (S_2 + T_2)\ \hat{N} + (S_3 + T_3)\ \hat{V}$$

DETERMINING AZ-EL GIMBAL ANGLES AND RATES

The azimuth-elevation gimbal is pictured in Figure 3 at the assumed zero angle orientation together with the transformation equation flow diagram. The gimbal angles ψ and α are positioned so that $\hat{n}$ always lies on the $\hat{y}$ mirror axis. By inspection then,

$$n_1 \cos \psi + n_2 \sin \psi = 0$$

or

$$\psi = \tan^{-1} - \frac{n_1}{n_2}$$

where

$$n_1 = S_1 + T_1,\ n_2 = S_2 + T_2,\ n_3 = S_3 + T_3$$

and

$$n_3 \cos \alpha - (n_1^{\ 2} + n_2^{\ 2})^{1/2} \sin \alpha = 0$$

or

$$\alpha = \tan^{-1} \frac{n_3}{(n_1^{\ 2} + n_2^{\ 2})^{1/2}}$$

Required gimbal angle rates can be computed using the ω_1, ω_2, ω_3 angular rate cosines of the normal vector and computing $\dot{\psi}$ and $\dot{\alpha}$ required to maintain zero rates on the $\hat{x}$ and $\hat{z}$ mirror axes. By inspection:

$$\omega_1 C\psi + \omega_2 S\psi + \dot{\alpha} = 0$$

or

$$\dot{\alpha} = -\omega_1 C\psi - \omega_2 \sin\psi$$

and

$$-S\alpha(\omega_2 C\psi - \omega_1 S\psi) + (\omega_3 + \dot{\psi})C\alpha = 0$$

or

$$\dot{\psi} = \tan\alpha\ (\omega_2 C\psi - \omega_1 S\psi) - \omega_3$$

Examination of the last equation shows that as α, the inner gimbal angle, reaches 90 degrees, the outer gimbal rate goes to infinity--commonly called the gimbal lock position. This occurs when the mirror normal becomes aligned with the outer gimbal axis so that there is no axis with which to null input rates about the mirror axis that is perpendicular to the mirror-normal and the outer gimbal axis. This occurs when the north and east components of the Sun vector are equal in magnitude and opposite in sign to the tower vector. Figure 4 shows a plot of heliostat position for which this occurs as a function of time of day and time of year.

DETERMINING TILT-TILT GIMBAL ANGLES AND RATES

The tilt-tilt configuration flow diagram is shown in Figure 5. The steps are the same as for the AZ-EL configuration. By inspection:

$$n_2 \cos\phi + n_3 \sin\phi = 0$$

or

$$\phi = \tan^{-1} - \frac{n_2}{n_3}$$

and

$$n_1 C\theta + (n_3 C\phi - n_2 S\phi)\ S\theta = 0$$

or

$$\theta = \tan^{-1} \frac{n_1}{n_2 C\phi - n_3 S\phi} = \tan^{-1} \frac{n_1}{(n_2^2 + n_3^2)^{1/2}}$$

and

$$\dot{\theta} + \omega_2 C\phi + \omega_3 S\phi = 0$$

or

$$\dot{\theta} = -\omega_2 C\phi - \omega_3 S\phi$$

and

$$(\omega_1 + \dot{\phi})\ C\theta + (\omega_3 C\phi - \omega_2 S\phi)\ S\theta = 0$$

or

$$\dot{\phi} = \tan\theta\ (\omega_2 S\phi - \omega_3 C\phi) - \omega_1$$

The last equation shows that $\dot{\phi}$ is a function of the $\tan\theta$ but as opposed to α in the AZ-ELEV configuration, θ never approaches 90 degrees in the tilt-tilt approach so that gimbal lock does not occur.

CALCULATION OF RATE ISOPLETHS FOR AZ-EL

The equation for the azimuth gimbal angle was found to be

$$\psi = \tan^{-1} - \frac{n_1}{n_2}$$

Taking the derivative with respect to time gives

$$\dot{\psi} = \frac{d\omega}{dt} = \frac{1}{1 + \left(\frac{n_1}{n_2}\right)^2} \left[\frac{n_2\dot{n}_1 - n_1\dot{n}_2}{n_2^2}\right] = \frac{n_2\dot{n}_1 - n_1\dot{n}_2}{n_1^2 + n_2^2}$$

but

$$\hat{n} = n_1\hat{E} + n_2\hat{N} + n_3\hat{V} = (S_1+T_1)\hat{E} + (S_2+T_2)\hat{N} + (S_3+T_3)\hat{V}$$

and

$$\dot{T} \equiv 0 \qquad \text{so that } \dot{n}_1 = \dot{S}_1 \text{ and } \dot{n}_2 = \dot{S}_2$$

giving

$$\dot{\psi} = \frac{n_2\dot{S}_1 - n_1\dot{S}_2}{n_1^2 + n_2^2} = \frac{(S_2 + T_2)\dot{S}_1 - (S_1 + T_1)\dot{S}_2}{S_1^2 + 2S_1T_1 + T_1^2 + S_2^2 + 2S_2T_2 + T_2^2}$$

which can be rearranged as a quadratic in T_1:

$$T_1^2 + \left[2S_1 + \frac{\dot{S}_2}{\dot{\psi}}\right] T_1 + \left[(S_2 + T_2)^2 + S_1^2 - \frac{(S_2+T_2)\dot{S}_1 + \dot{S}_2S_1}{\dot{\psi}}\right] = 0$$

At a fixed point in time S_1, S_2, $\dot{S}_1$ and $\dot{S}_2$ are determined as described in the section above on the computation of the Sun vector. A value of $\dot{\psi}$ is assumed.

T_1 is then computed for selected values of T_2 and $T_3 = \sqrt{1 - T_1^2 - T_2^2}$

Finally the north and east distance coordinates for the heliostat are computed by multiplying T_1 and T_2 by the tower height divided by T_3.

Coordinates for constant gimbal rates over the field were calculated for $\dot{\psi}$ = 10, 20, 40 and 100 degrees/hour for the summer and winter solstices and for the equinox for two times of day, noon and either early in the morning or late in the afternoon. Plots of these rate isopleths are shown in Figures 6 through 11.

RATE ISOPLETHS FOR TILT-TILT

The tilt-tilt rate calculations follow the same pattern and steps as for AZ-EL. Starting with

$$\phi = \tan^{-1} - \frac{n_2}{n_3}$$

and taking the time derivative gives

$$\dot{\phi} = \frac{n_2\dot{n}_3 - n_3\dot{n}_2}{n_2^2 + n_3^2} = \frac{(T_2+S_2)\dot{S}_3 - (T_3+S_3)\dot{S}_2}{T_3^2 + 2T_3S_3 + S_3^2 + T_2^2 + 2T_2S_2 + S_2^2}$$

Rearranging terms gives T_2 in quadratic form:

$$T_2^2 + \left[2S_2 - \frac{\dot{S}_3}{\dot{\phi}}\right] T_2 + \left[(T_3+S_3)^2 + S_2^2 + \frac{(T_3+S_3)\dot{S}_2 - S_2\dot{S}_3}{\dot{\phi}}\right] = 0$$

From the above discussion on determining tilt-tilt gimbal angles and rates,

$$\theta = \tan^{-1} \frac{n_1}{(n_2^2 + n_3^2)^{1/2}}$$

Taking the derivative and rearranging terms gives:

$$\dot{\theta} = \frac{1}{n_1^2+n_2^2+n_3^2} \left[(n_2^2+n_3^2)^{1/2} \dot{n}_1 - n_1(n_2^2+n_3^3)^{-1/2} (n_2\dot{n}_2+n_3\dot{n}_2) \right]$$

$\dot{\theta}$ and T_2 are then calculated for selected values of T_3 and $\dot{\phi}$ at values of S_1, S_2, S_3, $\dot{S}_1$, $\dot{S}_2$ and $\dot{S}_3$ for a fixed point in time.

The heliostat locations in the field for the selected values of $\dot{\phi}$ are then calculated by multiplying T_1 and T_2 by the scale factor term of tower height/T_3 and plotted. Values for $\dot{\theta}$ are included for each computed set of coordinates. Curves 12 through 18 are plots made for selected times of day and times of year.

CALCULATING THE RATE LIMIT EFFECT ON UNAVAILABILITY

The average proportion of heliostats unable to maintain the reflected Sun on the target is estimated by determining the field area encompassed by the rate isopleth and dividing by the total field area. The average for each day is then averaged over the year. The results are summarized in the following table.

Gimbal Rate Limit (deg/hr)	Yearly Average Percent of Non-Tracking Heliostats	
	AZ-EL	Tilt-Tilt
20	10	0
40	4	0
100	1	0

CONCLUDING REMARKS

Gimbal command rate limits can significantly affect the number of heliostats capable of delivering energy to the receiver. The tilt-tilt gimbal configuration compared to AZ-EL significantly reduces the command rate required for a given percent of non-tracking heliostats.

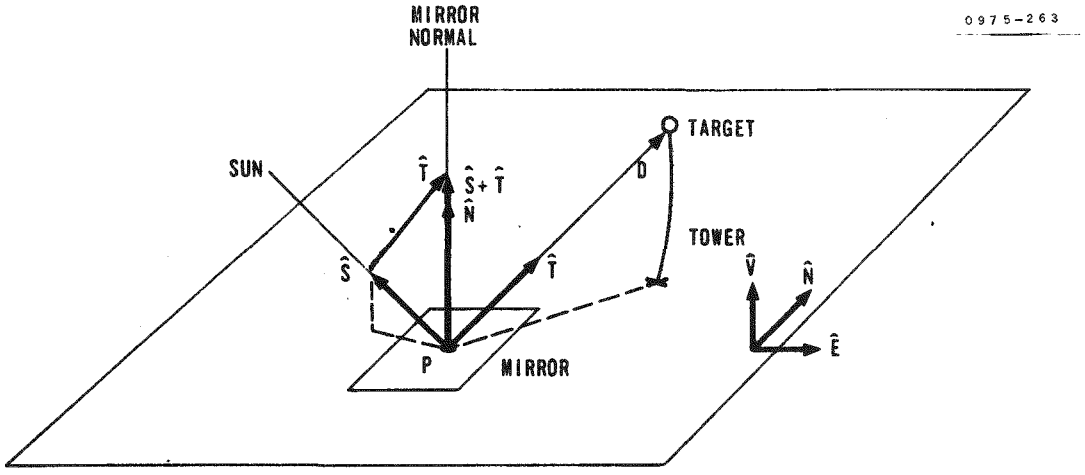


FIGURE 1. COMMAND LAW VECTOR DIAGRAM

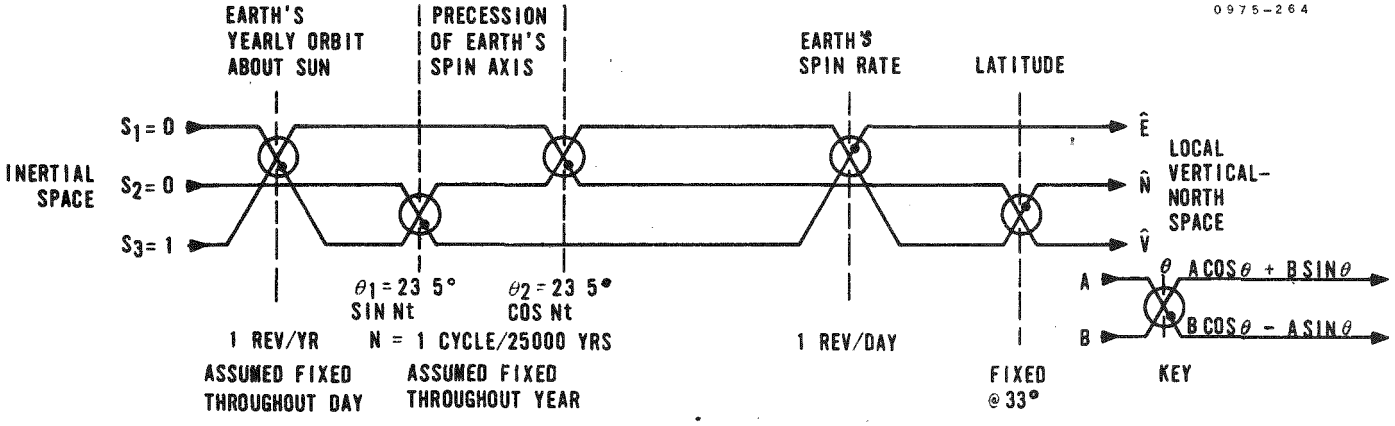


FIGURE 2. COMPUTATION OF SUN VECTOR COSINES

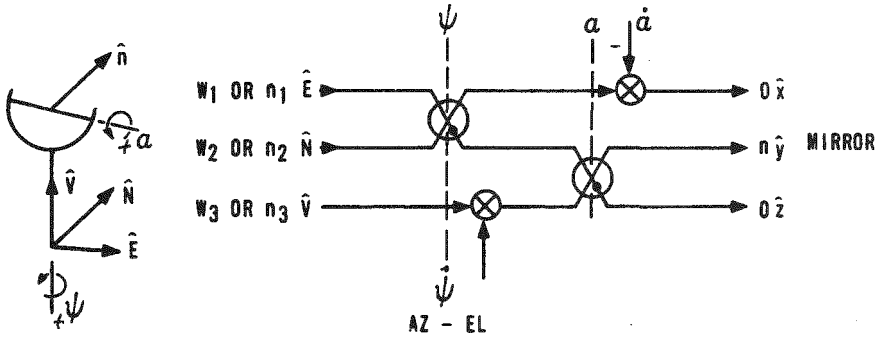


FIGURE 3. DETERMINING AZ-EL GIMBAL ANGLES AND RATES

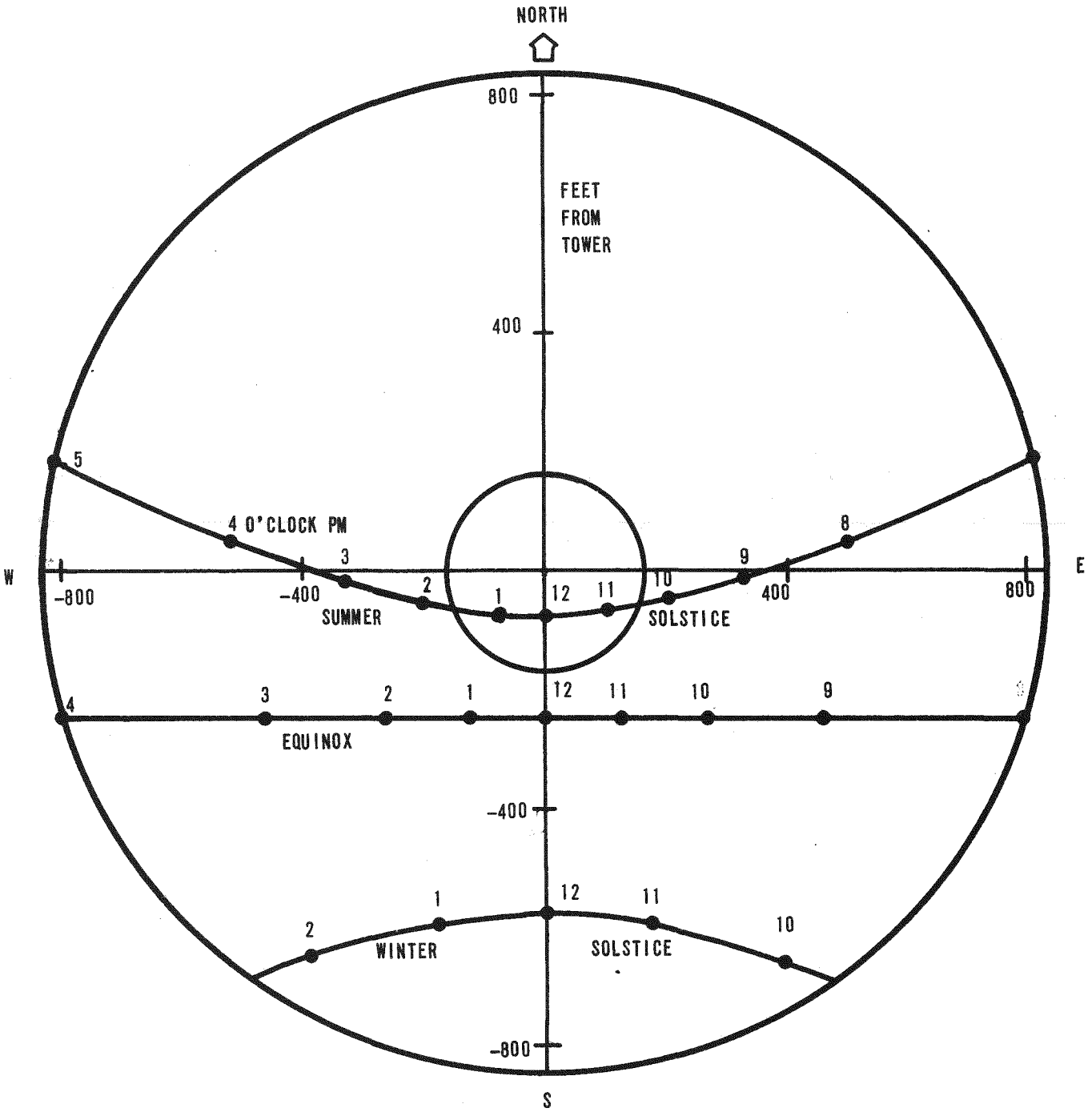


FIGURE 4. POSITION OF HELIOSTAT IN GIMBAL LOCK

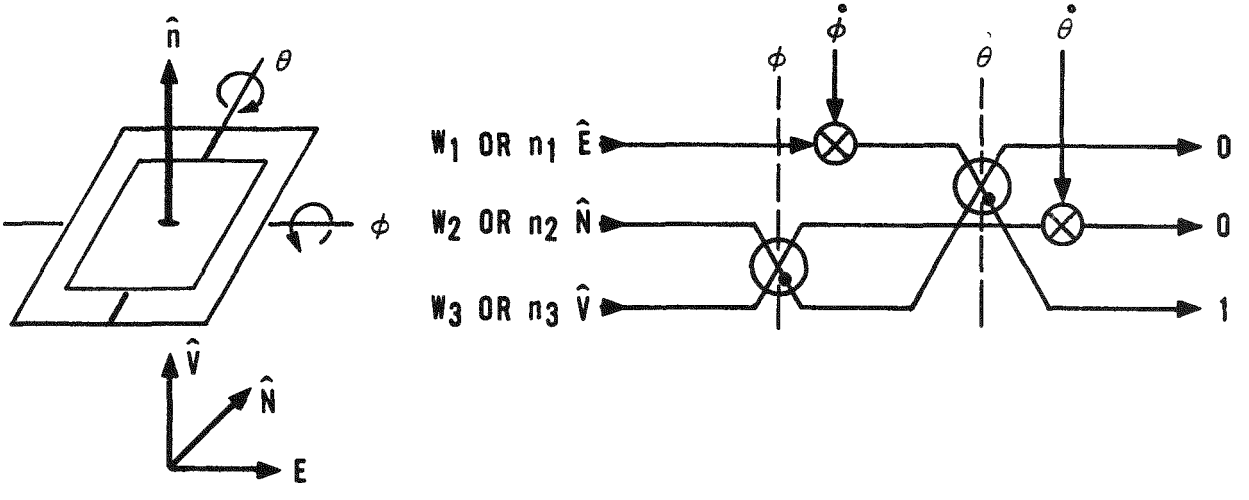


FIGURE 5. DETERMINING TILT-TILT GIMBAL ANGLES AND RATES

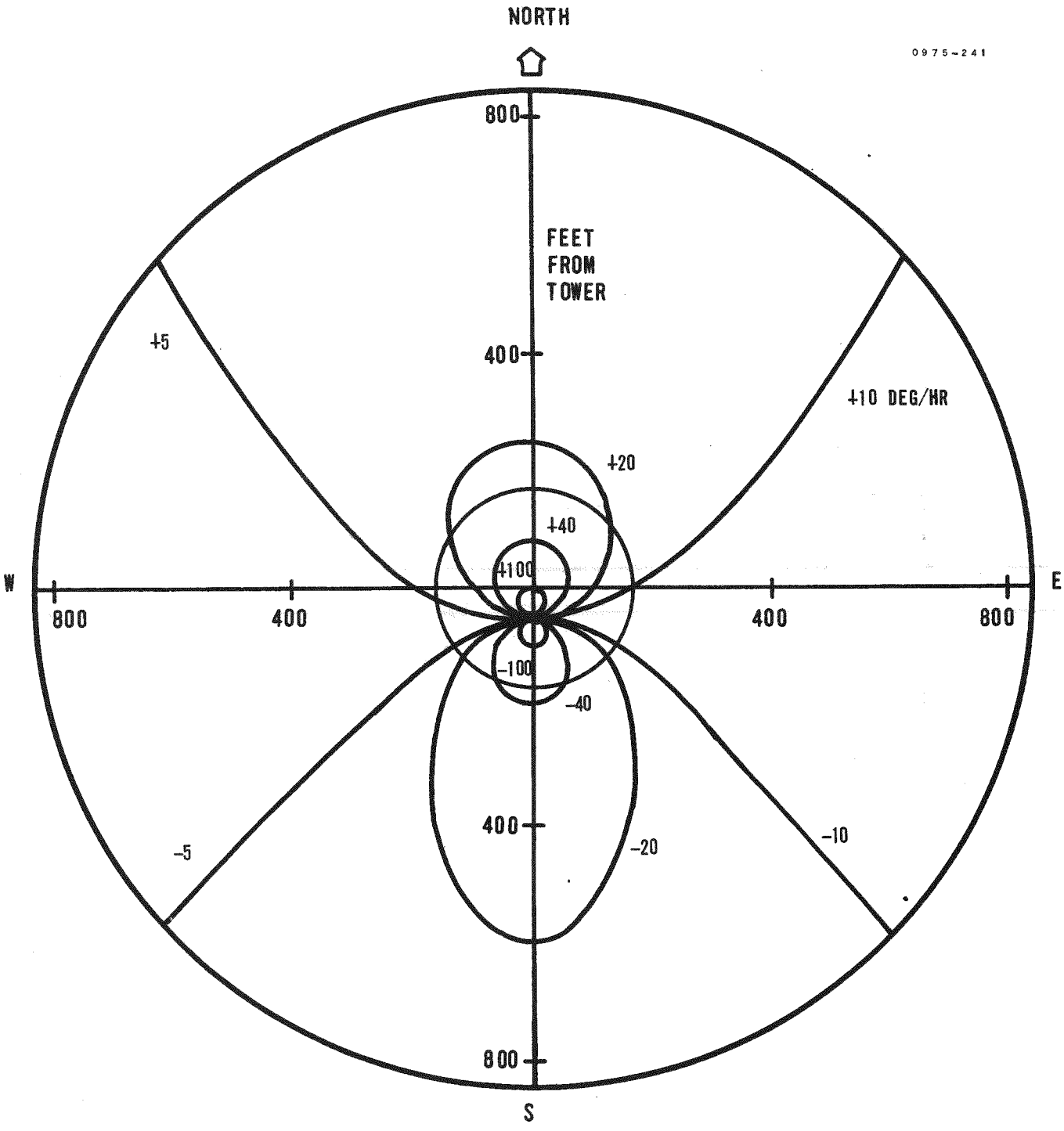


FIGURE 6. ISOPLETH OF AZ GIMBAL COMMAND RATES

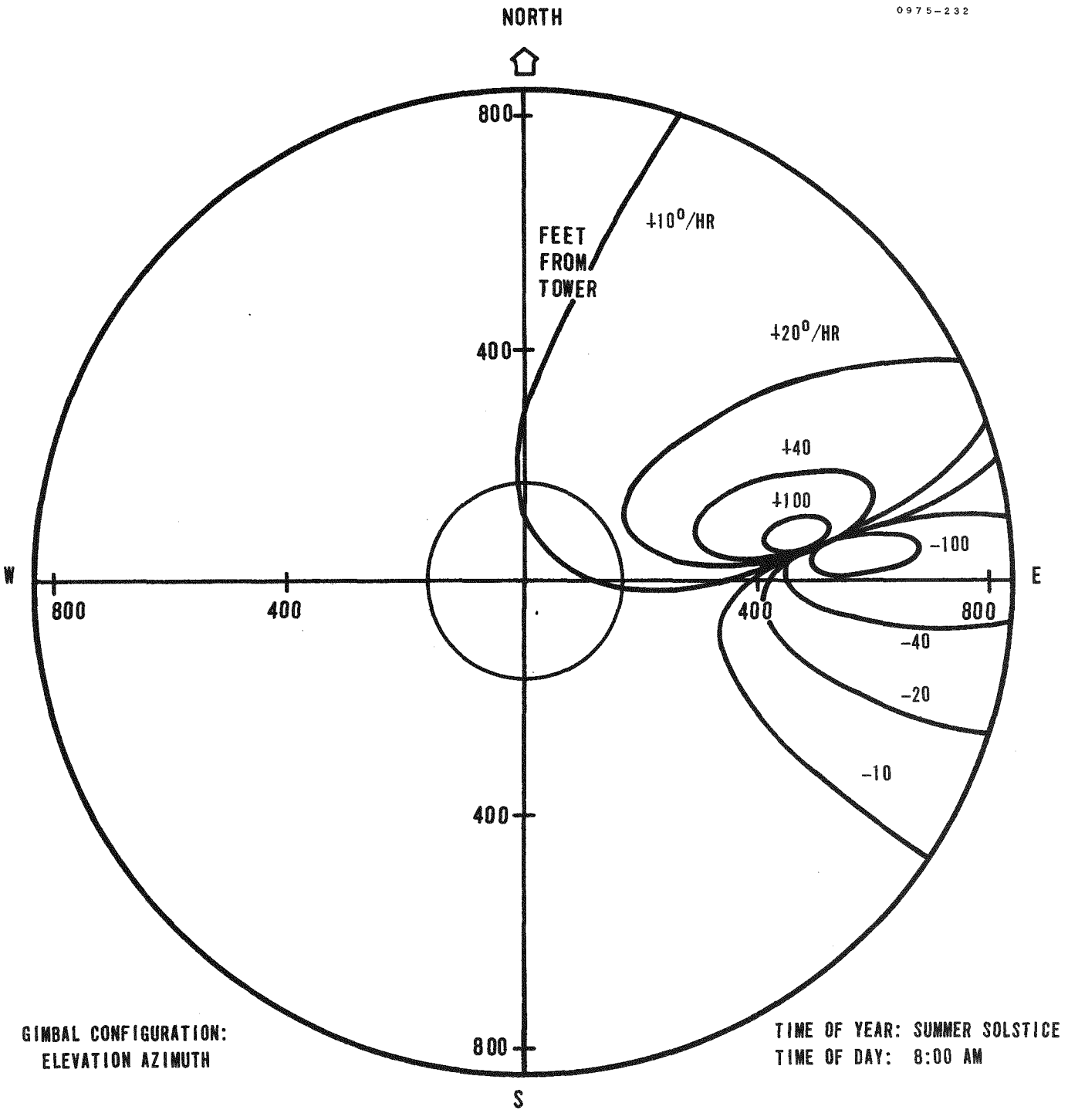


FIGURE 7. ISOPLETH OF AZ GIMBAL COMMAND RATES

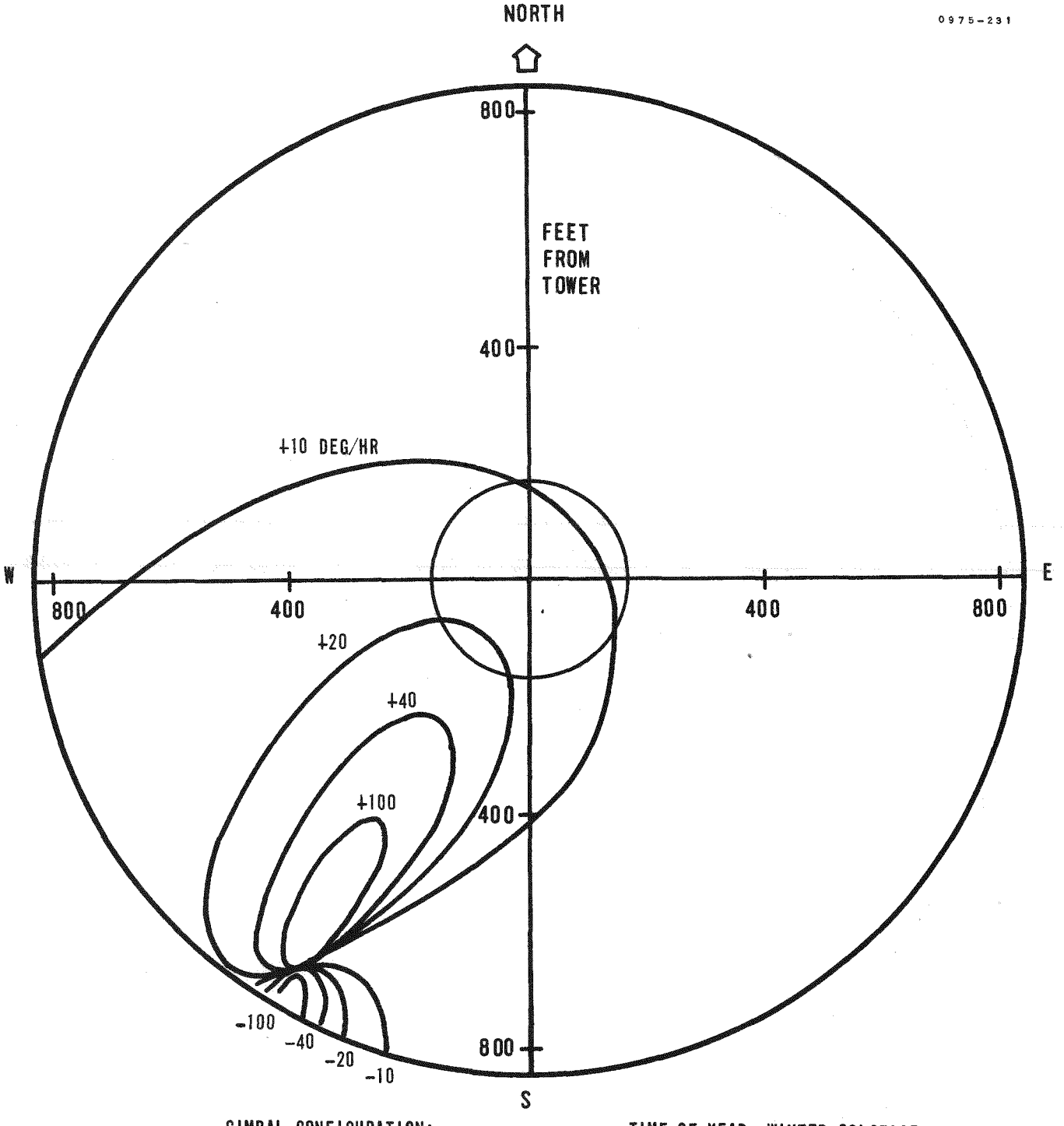


FIGURE 8. ISOPLETH OF AZ GIMBAL COMMAND RATES

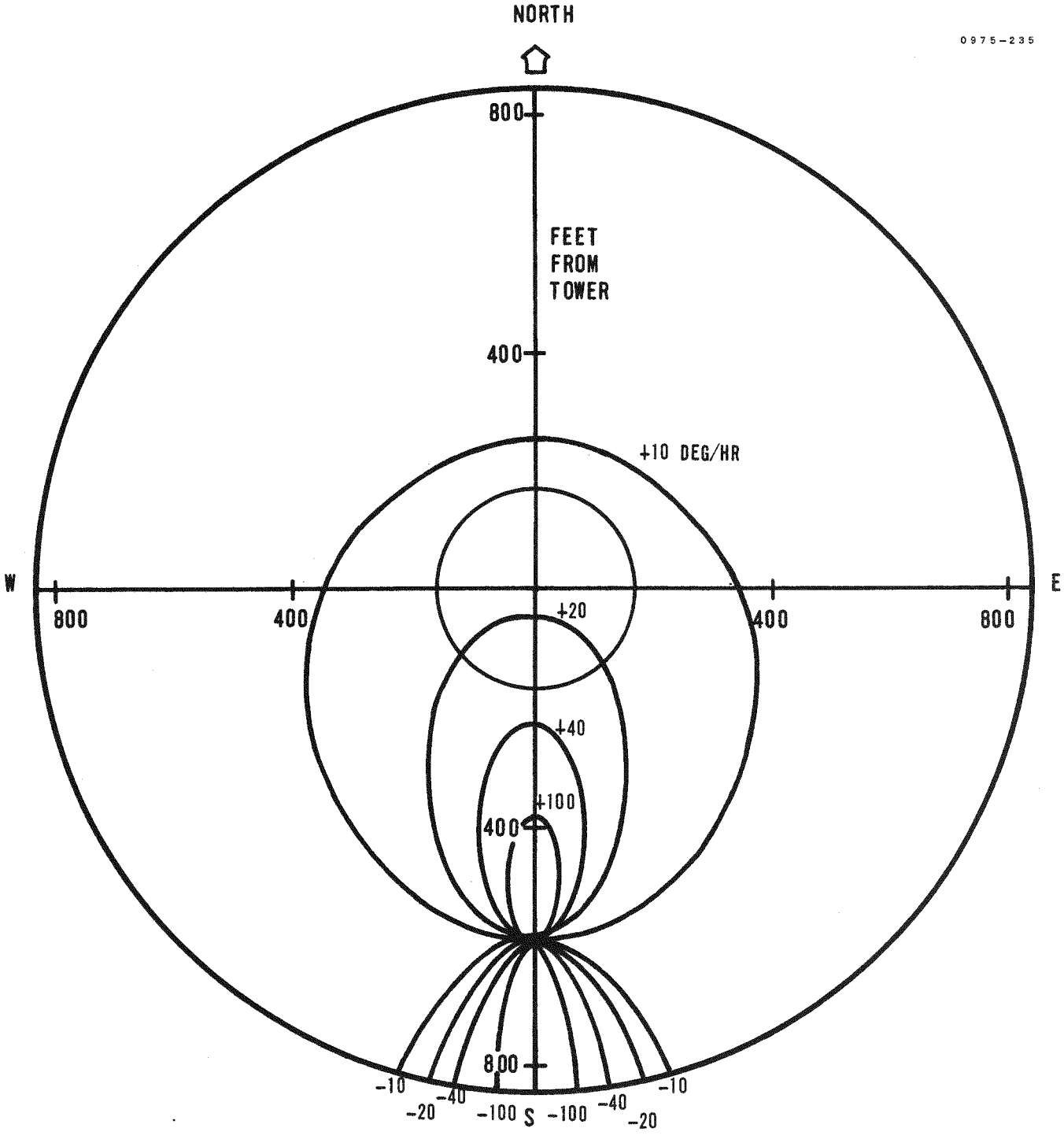


FIGURE 9. ISOPLETH OF AZ GIMBAL COMMAND RATES

0975-248

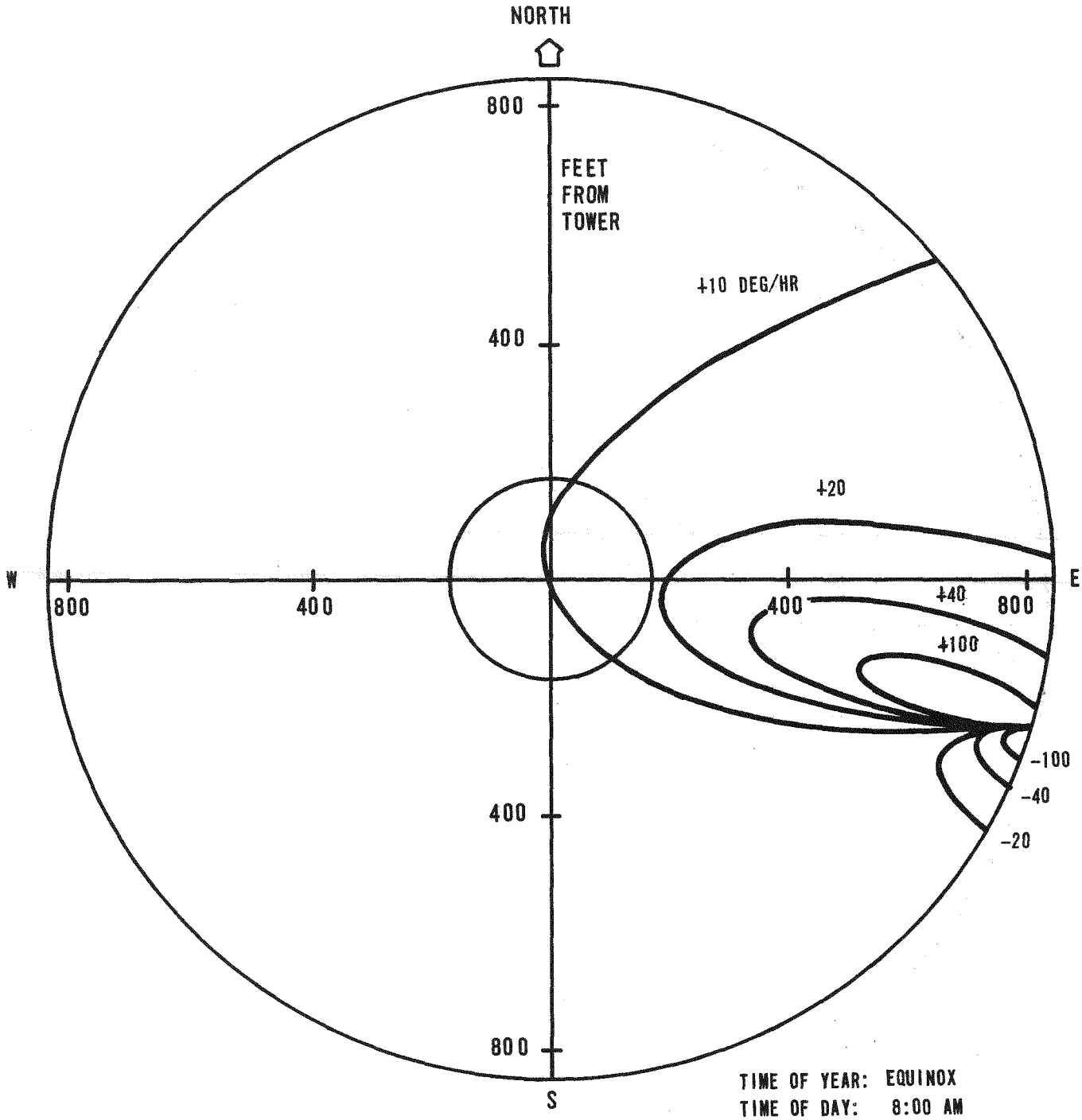


FIGURE 10. ISOPLETH OF AZ GIMBAL COMMAND RATES

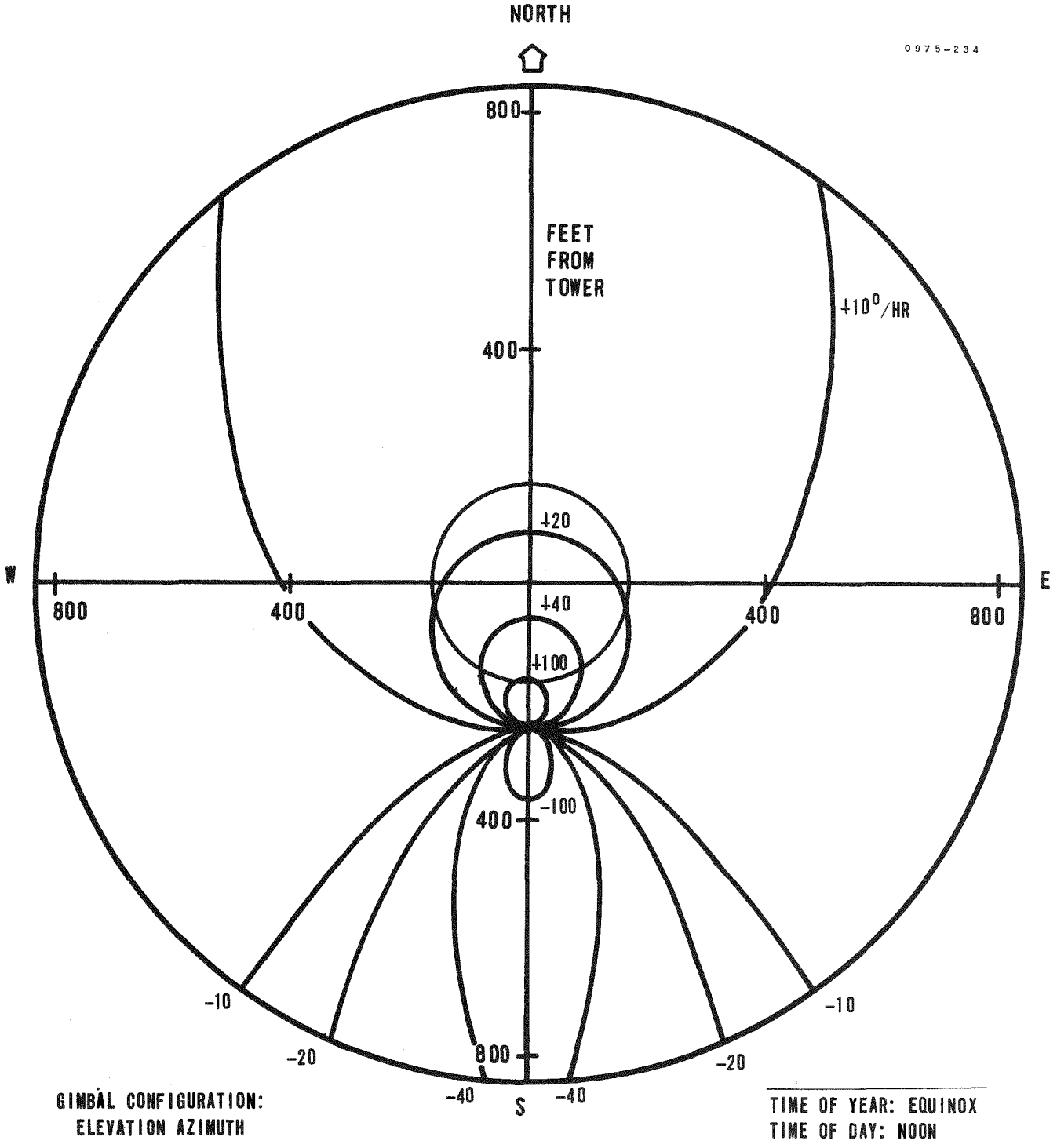


FIGURE 11. ISOPLETH OF AZ GIMBAL COMMAND RATES

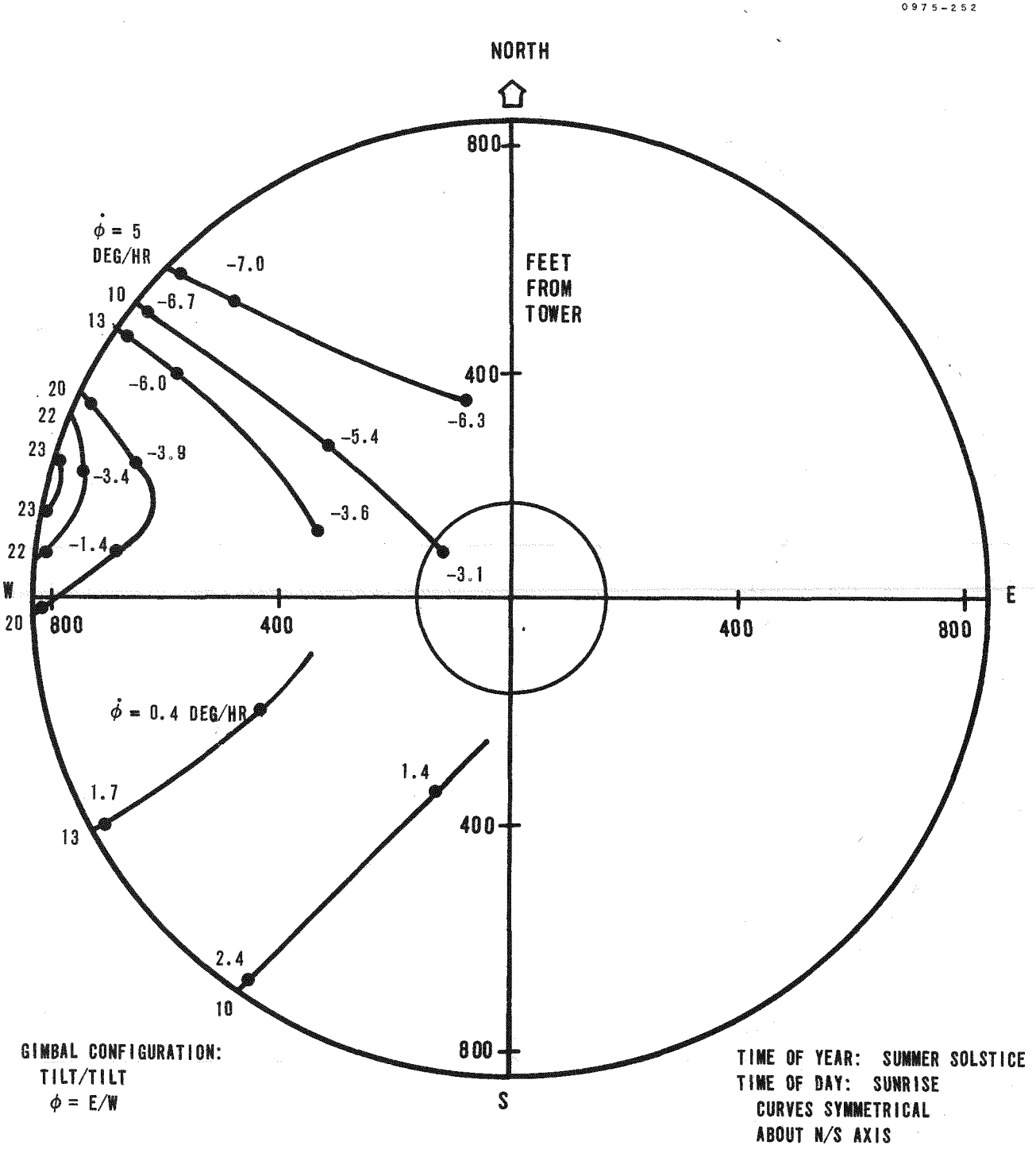
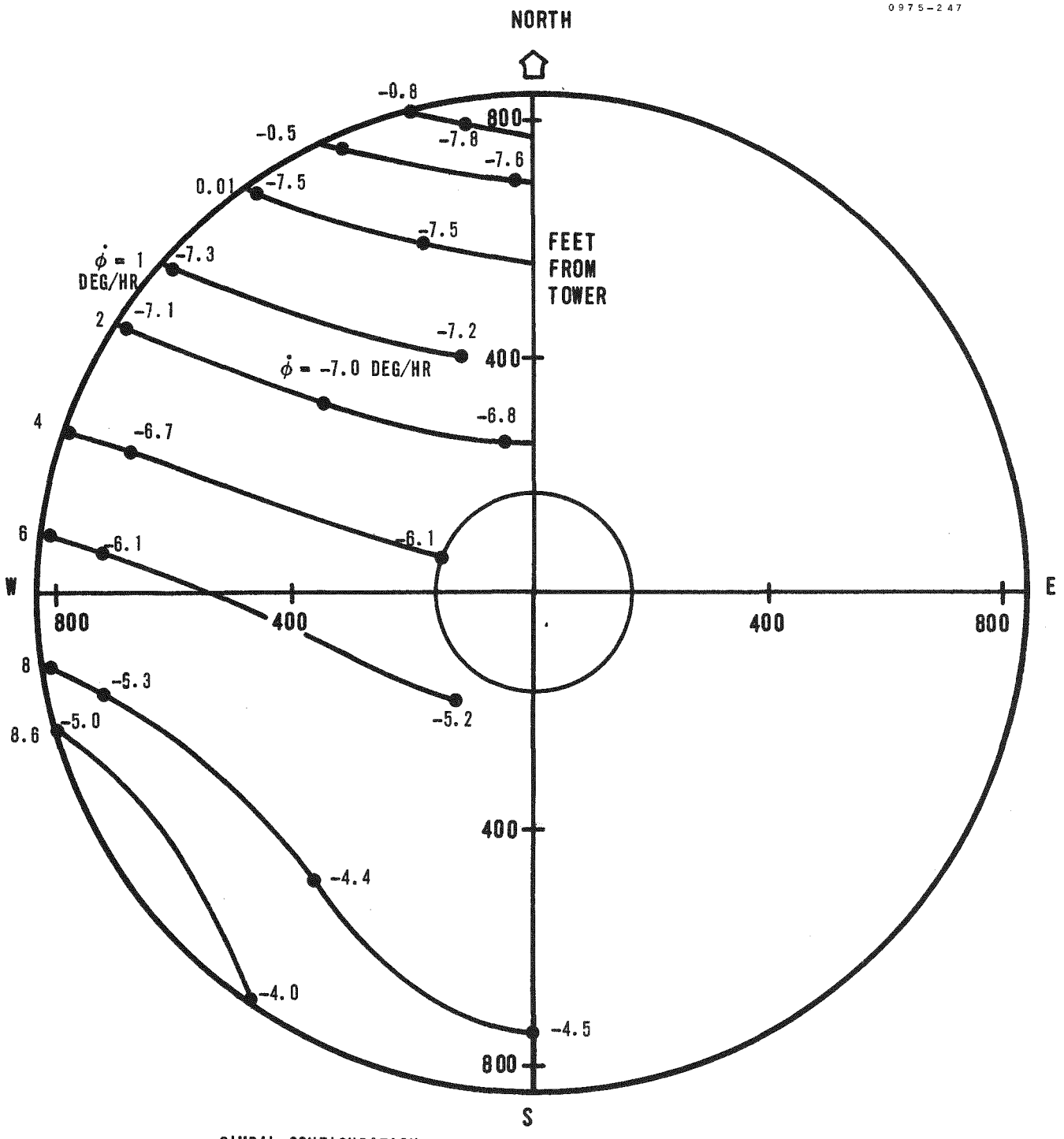


FIGURE 12. ISOPLETH OF $\dot{\phi}$ GIMBAL COMMAND RATES WITH $\dot{\theta}$



GIMBAL CONFIGURATION:
TILT-TILT
ϕ = E-W AXIS

TIME OF YEAR: SUMMER SOLSTICE
TIME OF DAY: 8:00 AM
CURVES SYMMETRICAL ABOUT THE NORTH-SOUTH AXIS

FIGURE 13. ISOPLETH OF $\dot{\phi}$ GIMBAL COMMAND RATES WITH $\dot{\theta}$

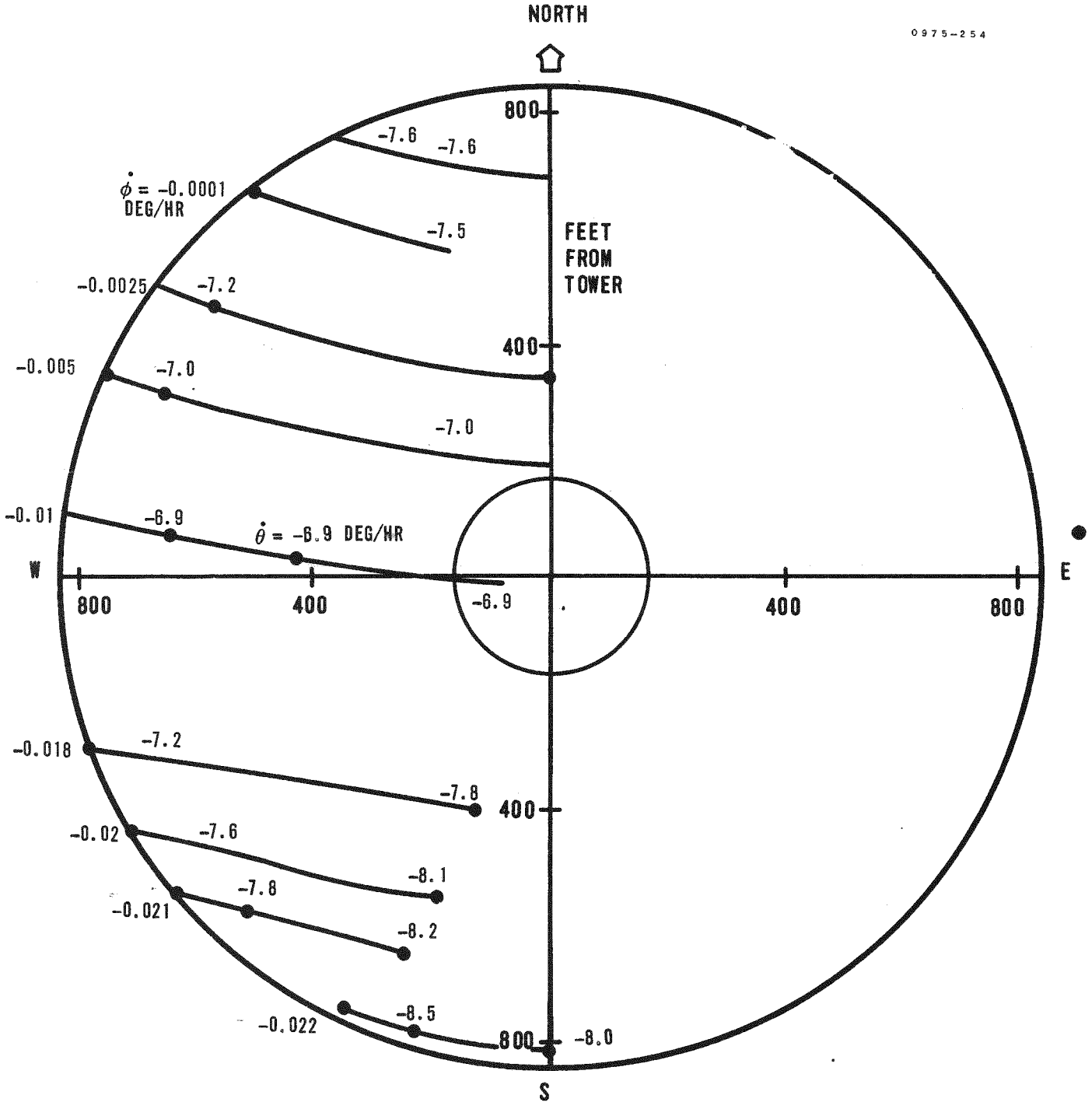


FIGURE 14. ISOPLETH OF $\dot{\phi}$ GIMBAL COMMAND RATES WITH $\dot{\theta}$

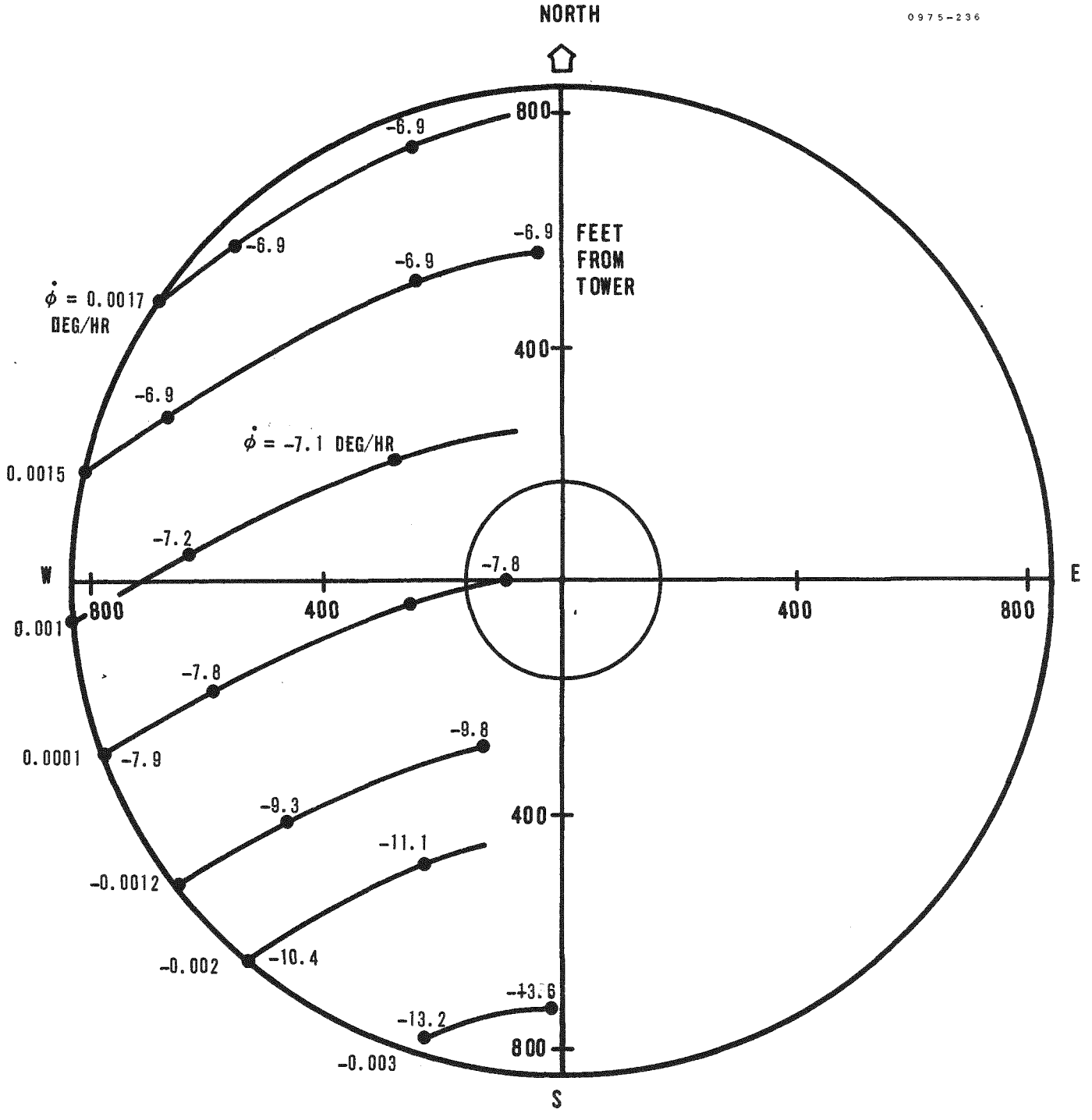


FIGURE 15. ISOPLETH OF $\dot{\phi}$ GIMBAL COMMAND RATES WITH $\dot{\theta}$

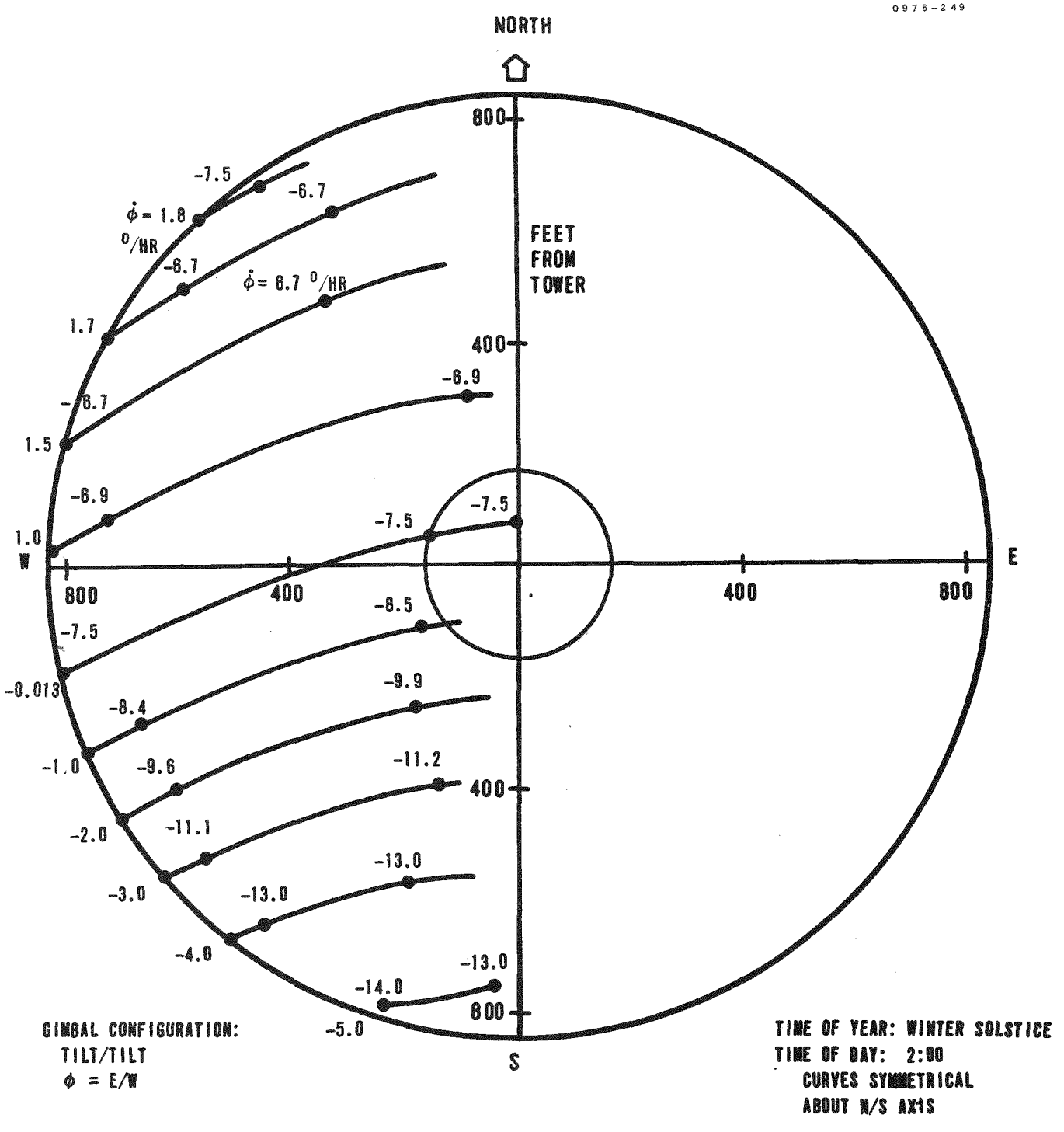
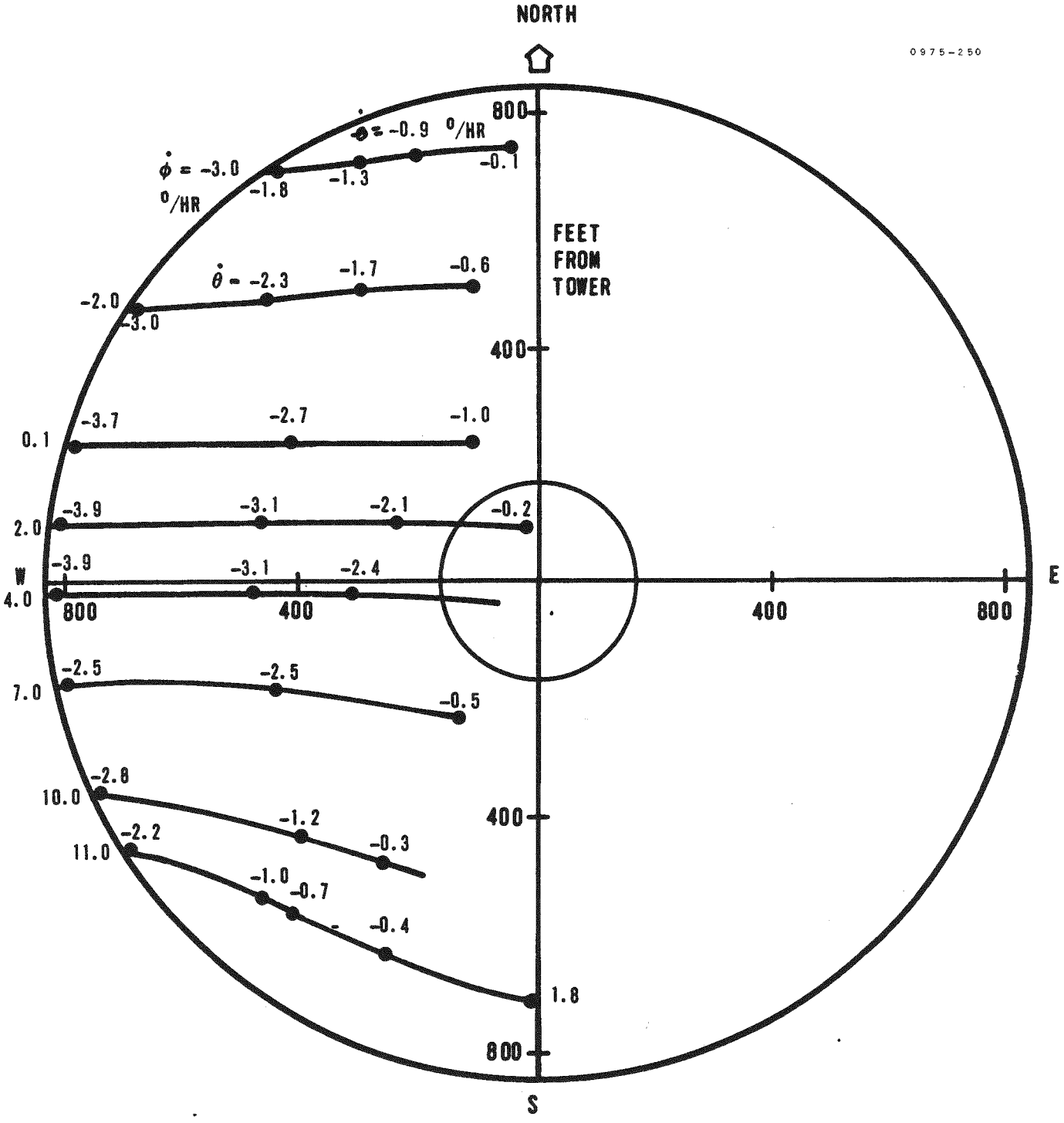


FIGURE 16. ISOPLETH OF $\dot{\phi}$ GIMBAL COMMAND RATES WITH $\dot{\theta}$



GIMBAL CONFIGURATION:
TILT-TILT
ϕ = E-W

TIME OF YEAR: EQUINOX
TIME OF DAY: 8:00 AM
CURVES SYMMETRICAL
ABOUT NORTH-SOUTH AXIS

FIGURE 17. ISOPLETH OF $\dot{\phi}$ GIMBAL COMMAND RATES WITH $\dot{\theta}$

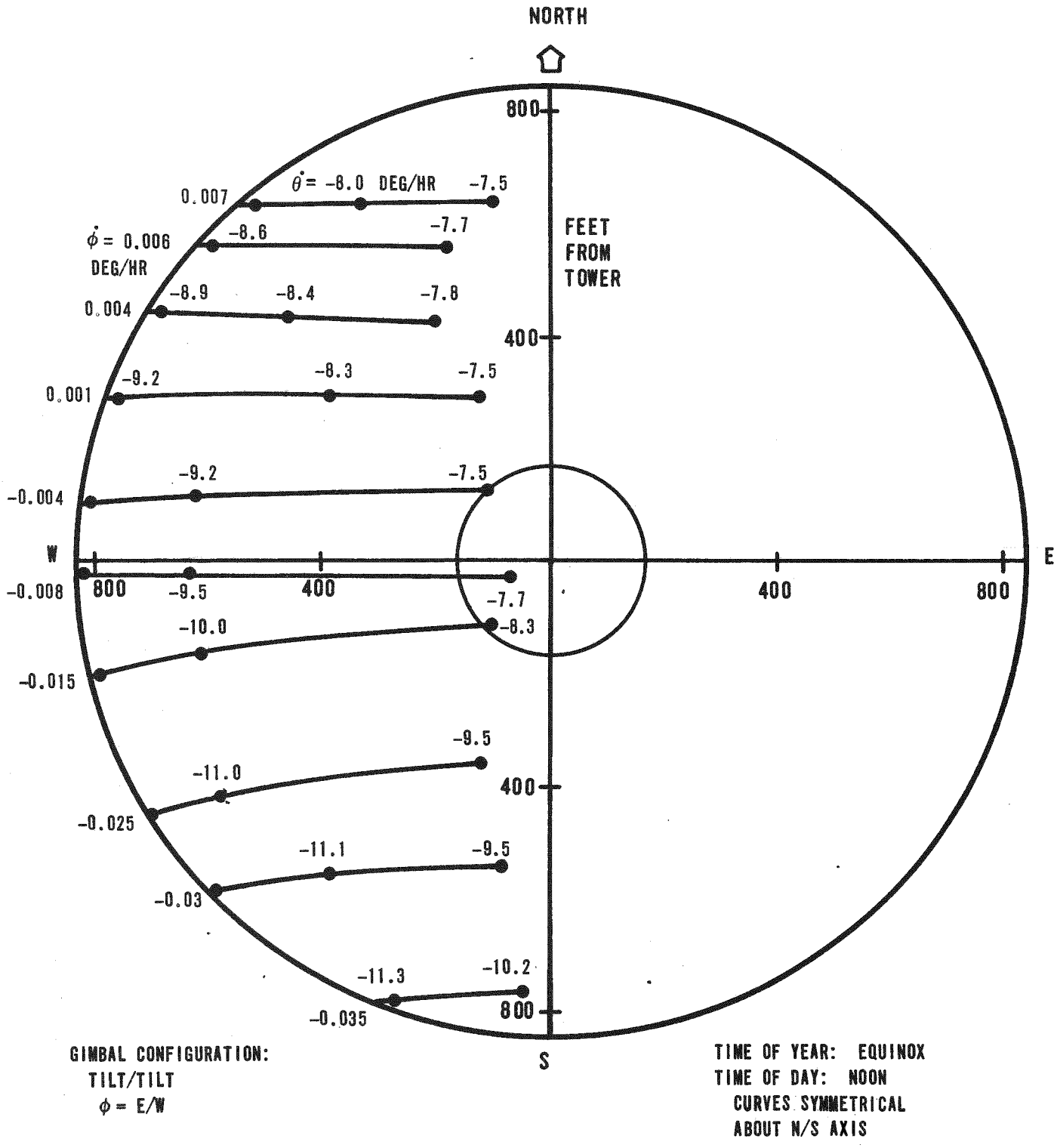


FIGURE 18. ISOPLETH OF $\dot{\phi}$ GIMBAL COMMAND RATES WITH $\dot{\theta}$

APPENDIX 4B

AERODYNAMIC STUDY OF HELIOSTAT DESIGN CONCEPTS

APPENDIX 4B

AERODYNAMIC STUDY

OF HELIOSTAT DESIGN CONCEPTS

An aerodynamic study was performed on two heliostat concepts defined by Aerospace Division Engineering, Florida. These are shown as AZ-EL configuration and Tilt-Tilt configuration. Aerodynamic forces and moments were estimated for each configuration in an attempt to define conditions of maximum airloads. A pure flat plate analysis was used throughout this study.

Azimuth-Elevation Configuration

For this design (Figure B-1), the airloads were determined for the mirror panels pitched to 90 degrees. Azimuth angles were variable for a wind vector parallel to the ground surface. Forces and moments were calculated for mirror panel dimensions of 6 feet by 12 feet and 5 feet by 10 feet. It will be noted that the 5 feet by 10 feet panels reduce the 6 feet by 12 feet panel moment by $1/\sqrt{3}$ and the force by $1/\sqrt{2}$ approximately.

Results for this configuration using 6 feet by 12 feet mirror panels were as follows:

1. Maximum moment about the azimuth axis occurs at a wind angle of attack of 25 degrees and has a value of M/q = 885 foot/pounds per PSF (where q is the dynamic pressure in pounds/square foot). With a 10 miles-per-hour wind speed, q = 0.255 PSF and the moment becomes 226 feet pound. A force normal to the panel surfaces at this angle of attack was also calculated and found to be F/q = 527 lb/PSF or 135 pounds total at a 10 miles-per-hour wind speed.

2. The same procedure for a set of 5 feet by 10 feet mirror panels results in a maximum M/q = 512 feet/pound at a 10 miles-per-hour wind speed and an F/q = 355 lb/PSF or 92 pounds at 10 miles-per-hour all calculated at the same angle of attack of 25 degrees.

3. The point of maximum force normal to the panel surface occurs at an angle of attack of 35 degrees. The resulting maximum F/q = 751 lb/PSF or 192 pounds at 10 miles-per-hour wind speed on the 6 feet by 12 feet panels. This force reduces to F/q = 522 lb/PSF or 134 pounds at 10 miles-per-hour wind speed for the 5 feet by 10 feet panels.

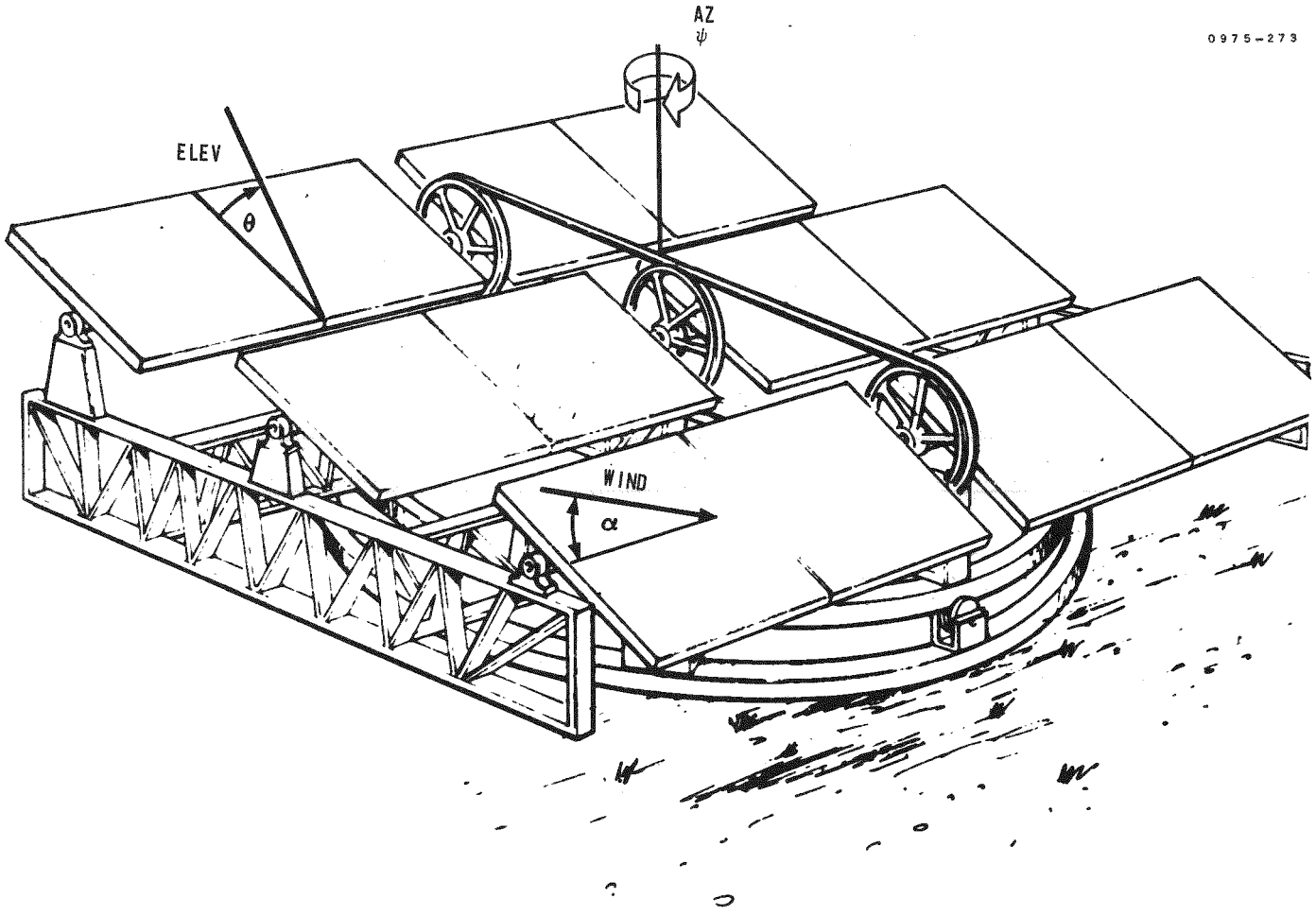


FIGURE B-1. AZIMUTH-ELEVATION CONFIGURATION

Tilt-Tilt Configuration

Before the aerodynamic estimates were made on this configuration (Figure B-2), an examination on the location of the primary hinge line was conducted. In this examination a minimum weight of 500 pounds was assumed for the heliostat structure. With this weight and a hinge line location at one end of the panels, a moment on the order of 3000 foot/pounds is produced. The aerodynamic moments, on the other hand, are small in comparison ranging between 3 and 15 percent of this weight moment value. The conclusion from this very simple analysis is that the primary heliostat hinge line location should be along the centerline of the panels. The large weight moments are eliminated and only the aerodynamic moments remain. Other criteria must also be weighed in the final decision.

Airloads were estimated for the configuration with the following results:

1. The maximum moment about the primary hinge line again occurs at 25 degrees angle of attack and has a value M/q = 435 feet lb/PSF or 111 feet/pound at 10 miles-per-hour for the 6 feet by 12 feet panels. For the 5 feet by 10 feet panels, M/q = 252 feet lb/PSF or 64 feet/pound with 10 miles-per-hour winds.

2. A maximum force normal to the heliostat panels also occurs at α = 35 degrees with a value of F/q = 375 lb/PSF or 96 pounds at 10 miles-per-hour.

COMPUTATION OF STATIC LOADS ON MIRROR ASSEMBLY

Figure B-3, presents the results of estimated static forces and moments on a 6 by 12 foot mirror mounted in a truss support concept. The truss members were assumed to be 4 inches wide.

The analysis was performed for two geometric cases; edge-on, in which the wind is blowing perpendicular to the long side of the assembly; and end-on, in which the wind is blowing perpendicular to the short side of the assembly. See Figure B-3, which also defines the forces and moments. The forces are expressed as normal force, N, perpendicular to the mirror surface; axial force, A, parallel to the mirror surface; and moment, M. The moment is shown about the secondary hinge axis for the edge-on case, and about the primary axis as proposed for the end-on case. The moment is easily transferred to other hinge lines.

The method used involved adding approximate components of axial force, normal force, and moment due to the truss to the values predicted from available data for thin flat plates. The axial force due to the finite thickness of the mirror frame was also approximated.

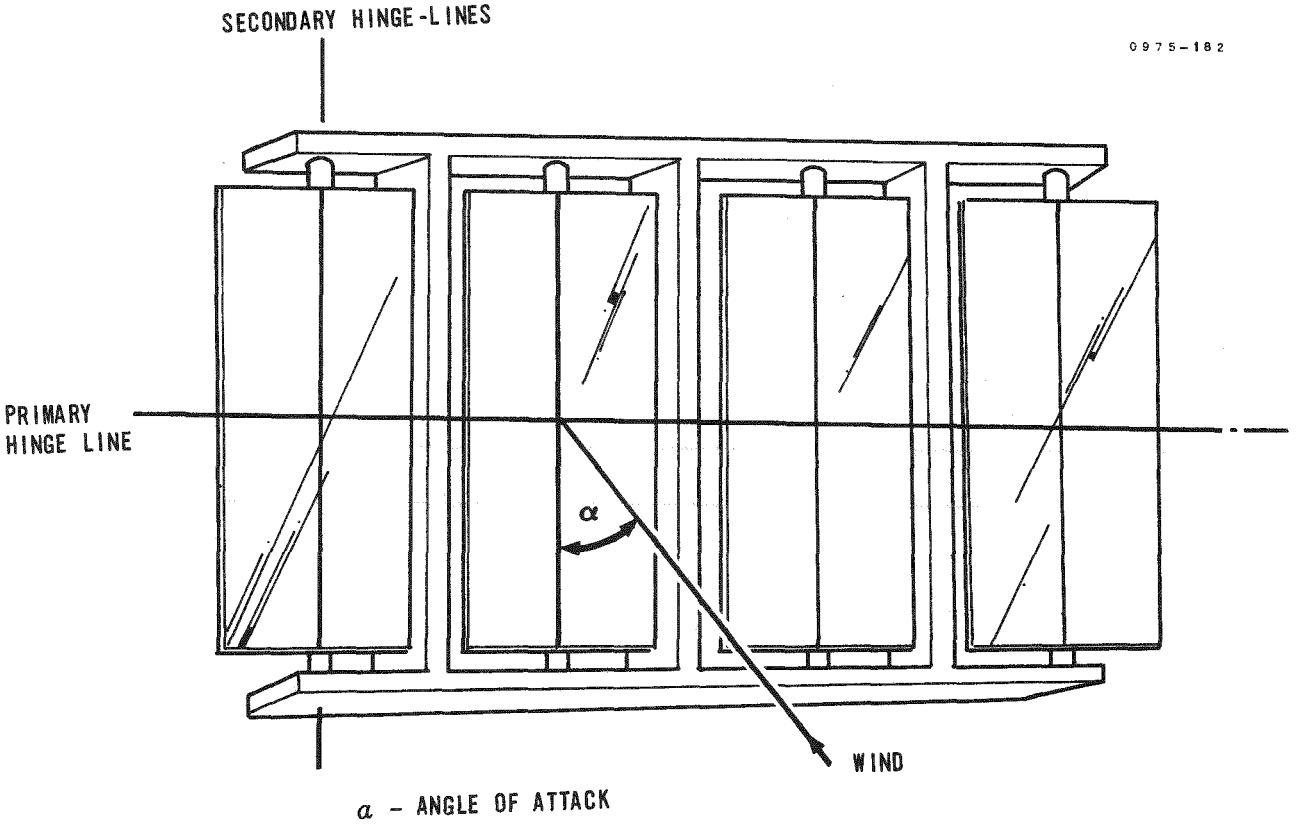


FIGURE B-2. TILT-TILT CONFIGURATION

The basic aerodynamic assumption for the truss was that the only significant force on a truss member was a cross-flow drag force perpendicular to the member produced by a component of velocity perpendicular to that member. The cross-flow drag coefficient was assumed to be 2 and the cross-flow area was the length, $3\sqrt{3}$. times the assumed 1/3 foot width.

Depending on the angle of attack, the cross-flow force vectors add to produce net axial and normal force. Except for the bottom horizontal member (edge-on) the equilateral geometry of the truss produced individual member forces which pass through the pivot point. The truss contributions turned out to be very similar for both edge-on and end-on. Except for the longer reference length, the mirror contributions differed because of the difference in aspect ratios between edge-on (2) and end-on (1/2).

The results shown in Figure B-3, were normalized to dynamic pressure $q = 1/2\ pv^2$ for a 6 feet by 12 feet configuration. It was assumed that if the mirror size were changed, the truss would be changed by the same scale so that forces would scale with scale factor squared and moments by scale factor cubed.

As indicated on Figures B-3a and B-3b, the maximum moments on the assembly occur at different angles of attack for the 2 wind direction cases because of aspect ratio effects.

It was also assumed that the mirror and truss were unaffected by each other, by other assemblies or by the rest of the heliostat structure.

It should be noted that the truss design adds only about 15 percent to the mirror normal force and moment and may, therefore, be neglected in these preliminary estimates.

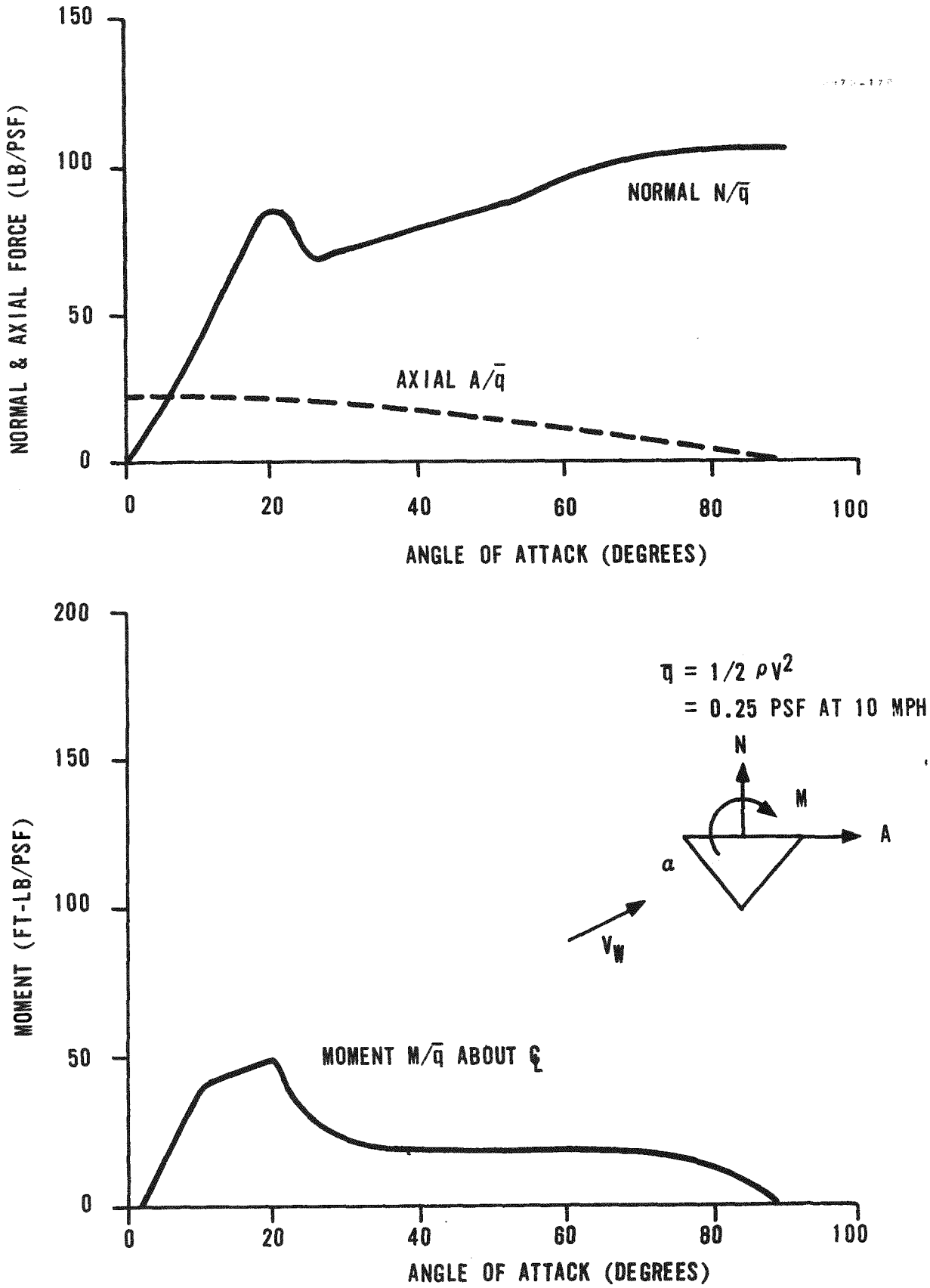


FIGURE B-3a. WIND FORCES AND MOMENT ON MIRROR-TRUSS ASSEMBLY EDGE ON, 6 FEET BY 12 FEET

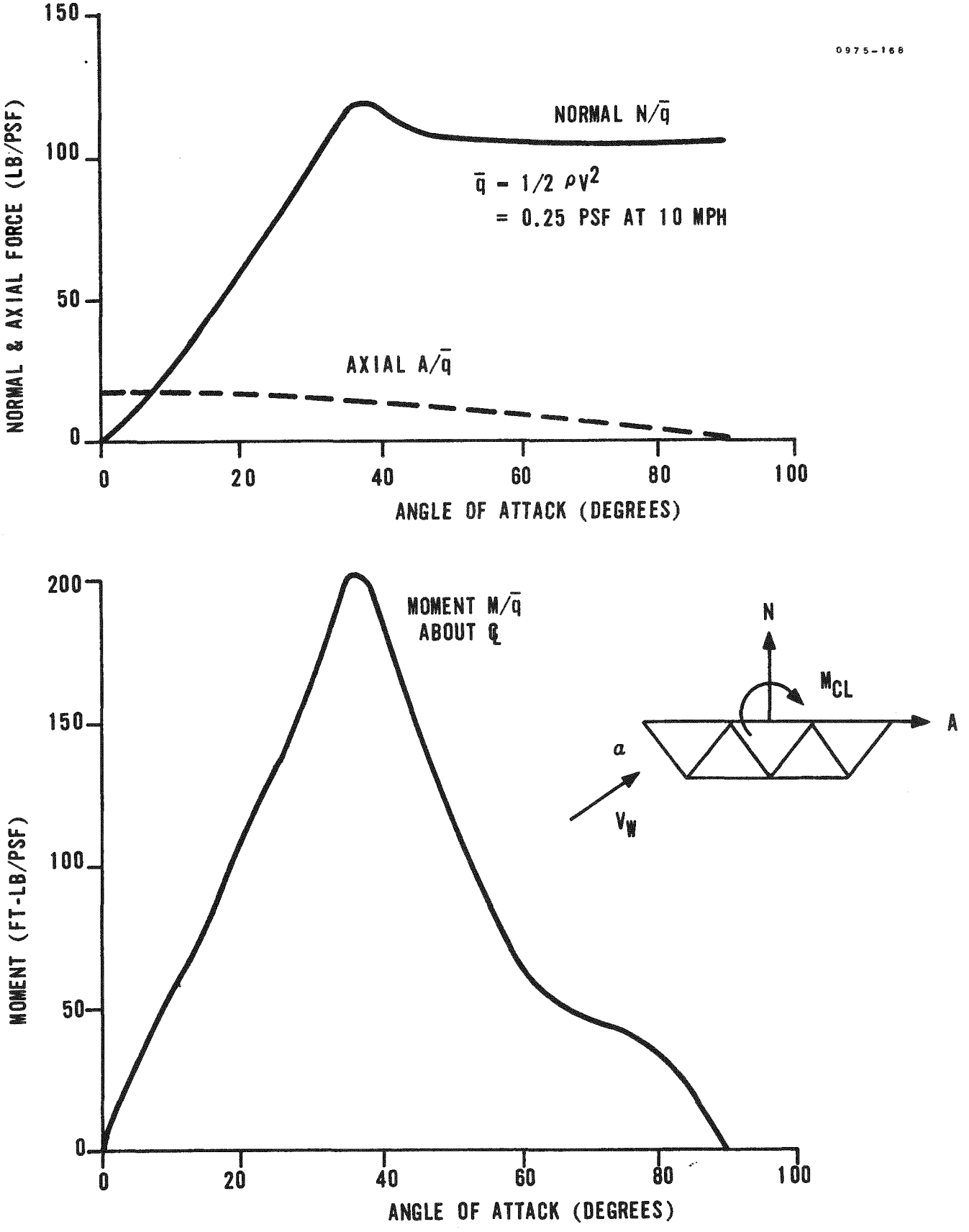


FIGURE B-3b. WIND FORCES AND MOMENT ON MIRROR-TRUSS ASSEMBLY END ON, 6 FEET BY 12 FEET

APPENDIX 4C
MATHEMATICS OF SUN TRACKING

APPENDIX 4C

MATHEMATICS OF SUN TRACKING

Appendix C-1

SUN'S MEAN ORBITAL ELEMENTS

1975 JAN 0^d 0^h E.T. J.D. 2442412.5

Julian Date at 0^h on 1975 Jan 0 = 2442412.5
Julian Date at epoch of tables = 2415020.0
Interval in days (d) = 27392.5
Fraction of Julian Century (T) = 0.749966

ω_o = Mean longitude of perigee, mean equinox of date
= $281.220833 + 0.0000470684d + 0.000453T^2 + 0.000003T^3$
= 282.51040 degrees

M_o = Mean anomaly
= $358.475845 + 0.9856002670d - 0.000150T^2 - 0.000003T^3$
= 356.531056 degrees

i = Mean obliquity of the ecliptic
= $23.452294 - 0.0130125T - 0.00000164T^2 + 0.000000503T^3$
= 23.442534 degrees

Y = Length of tropical year
= $365.24219878 - 0.00000614T$
= 365.2422033 $\qquad 360/Y = 0.9856473232$

m = Mean Light/time correction
= 20.47 arc seconds
= 0.005686 degrees

Ref: American Ephemeris and Nautical Almanac

Appendix C-2

COMPUTATION OF SUN'S POSITION IN ORBIT PLANE

Given:

$\omega = \omega_o + \dot{\omega}d = 282.51040 + 0.0000470684d$

$M = M_o - m + (360/Y)d = 356.531056 - 0.005686 + 0.985647d$

$i = 23.442534$

$e = 0.01672$

d = Number of days

Then:

E_{i+1} = Eccentric anomaly
$= M + e \sin E_i * 180/\pi$

Solve iteratively, three passes, $E_1 = 0$

Cos v = Cosine of true anomaly

$$= \frac{\text{Cos } E - e}{1 - e \text{ Cos } E}$$

Sin v = Sine of true anomaly

$$= \frac{\sqrt{1-e^2} \sin E}{1 - e \cos E}$$

$$\text{Sun vector} = \begin{bmatrix} \cos v \\ \sin v \\ 0 \end{bmatrix}$$

Rotate Sun vector to equinox

$X = \cos v \cos \omega - \sin v \sin \omega$

$Y = \cos v \sin \omega + \sin v \cos \omega$

$Z = 0$

Rotate ecliptic to equatorial plane

$Eq = X$

$E = y \cos i$

$P = y \sin i$

We now have the unit Sun vector in equatorial, east, polar coordinates

To transform unit Sun vector in inertial coordinates to an Earth fixed UEN reference frame compute first

GHA_γ 1975 0^d 0^h E.T.	=	6^h 36^m $9^s.628$
GMT_{DAYS} * 0.065709822 hrs/day	+	
GMT_{HRS}	+	
Longitude	-	
Longitude * 9.85654 arc sec/deg	+	

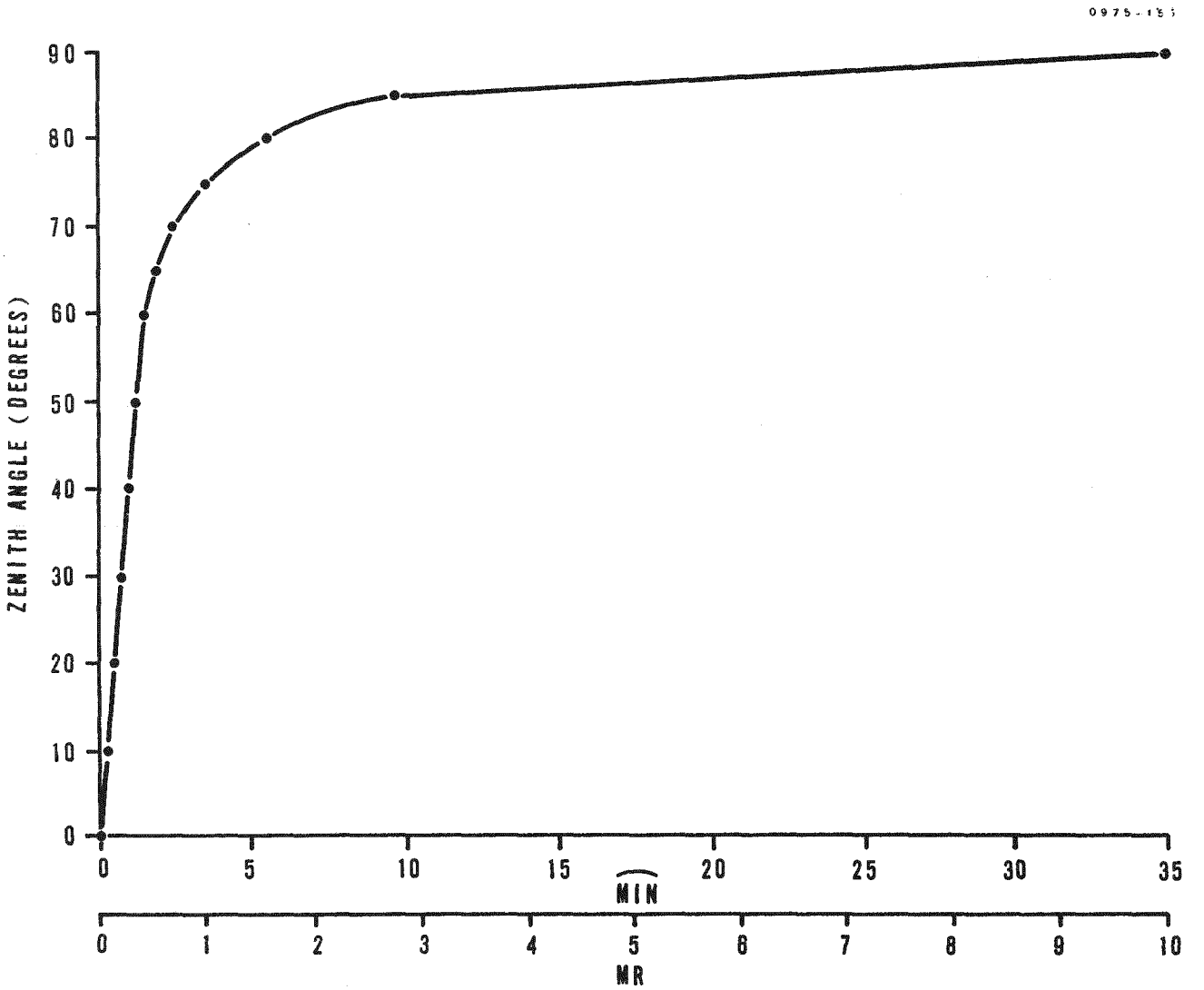
Convert time to angle Ω =

Now make the following transformations:

$$\begin{bmatrix} U \\ E \\ N \end{bmatrix} = \begin{bmatrix} \cos\lambda & 0 & \sin\lambda \\ 0 & 1 & 0 \\ -\sin\lambda & 0 & \cos\lambda \end{bmatrix} \begin{bmatrix} \cos\Omega & \sin\Omega & 0 \\ -\sin\Omega & \cos\Omega & 0 \\ 0 & 0 & 1 \end{bmatrix} \begin{bmatrix} Eq \\ E \\ P \end{bmatrix}$$

λ = local geodetic latitude

We now have a unit Sun vector in local UEN coordinates



Appendix C

REFRACTION CORRECTION FOR ZENITH ANGLES AT SEA LEVEL
0°C 76 CM HG

$$R_{\overset{\frown}{sec}} = 206 \frac{Pcm}{T_K} \tan z$$

		-4°		32°		68°		104°			F
z^o	-30	-20	-10	0	10	20	30	40	50	60	70°C
0	0	0	0	0	0	0	0	0	0	0	0
10	11	11	11	10	10	9	9	9	9	8	8
20	23	23	22	21	20	19	19	18	18	17	17
30	37	36	34	33	32	31	30	29	28	27	26
40	54	52	50	48	46	45	43	42	41	40	38
50	77	74	71	68	66	64	62	60	58	56	54
60	112	107	103	99	96	93	90	87	84	82	79
70	177	170	164	158	152	147	142	138	133	129	126
75	240	231	222	214	206	199	193	187	181	176	170
80	366	351	338	326	314	303	293	284	275	267	259
85	736	708	680	655	632	611	591	572	555	538	522

at 76 cm Hg

z^o	73	76	79
0	0	0	0
10	9	9	9
20	18	19	20
30	29	30	31
40	42	43	45
50	59	62	64
60	86	90	93
70	137	142	148
75	185	193	200
80	282	293	305
85	568	591	615

at 30°C

73 cm = 28.74 in Hg
76 cm = 29.92 in Hg
79 cm = 31.10 in Hg

APPENDIX 4D

DETAIL SPECIFICATION

PART I

SOLAR COLLECTOR SUBSYSTEM

(SEE RESEARCH EXPERIMENT
REPORT, APPENDIX B)

APPENDIX 4E

DETAIL SPECIFICATION

PART I

HELIOSTAT

(SEE RESEARCH EXPERIMENT
REPORT, APPENDIX C)

APPENDIX 4F

DETAIL SPECIFICATION

PART I

HELIOSTAT CONTROL SOFTWARE

(SEE RESEARCH EXPERIMENT
REPORT, APPENDIX D)

APPENDIX 4G

DETAIL SPECIFICATION

PART I

CALIBRATION ARRAY

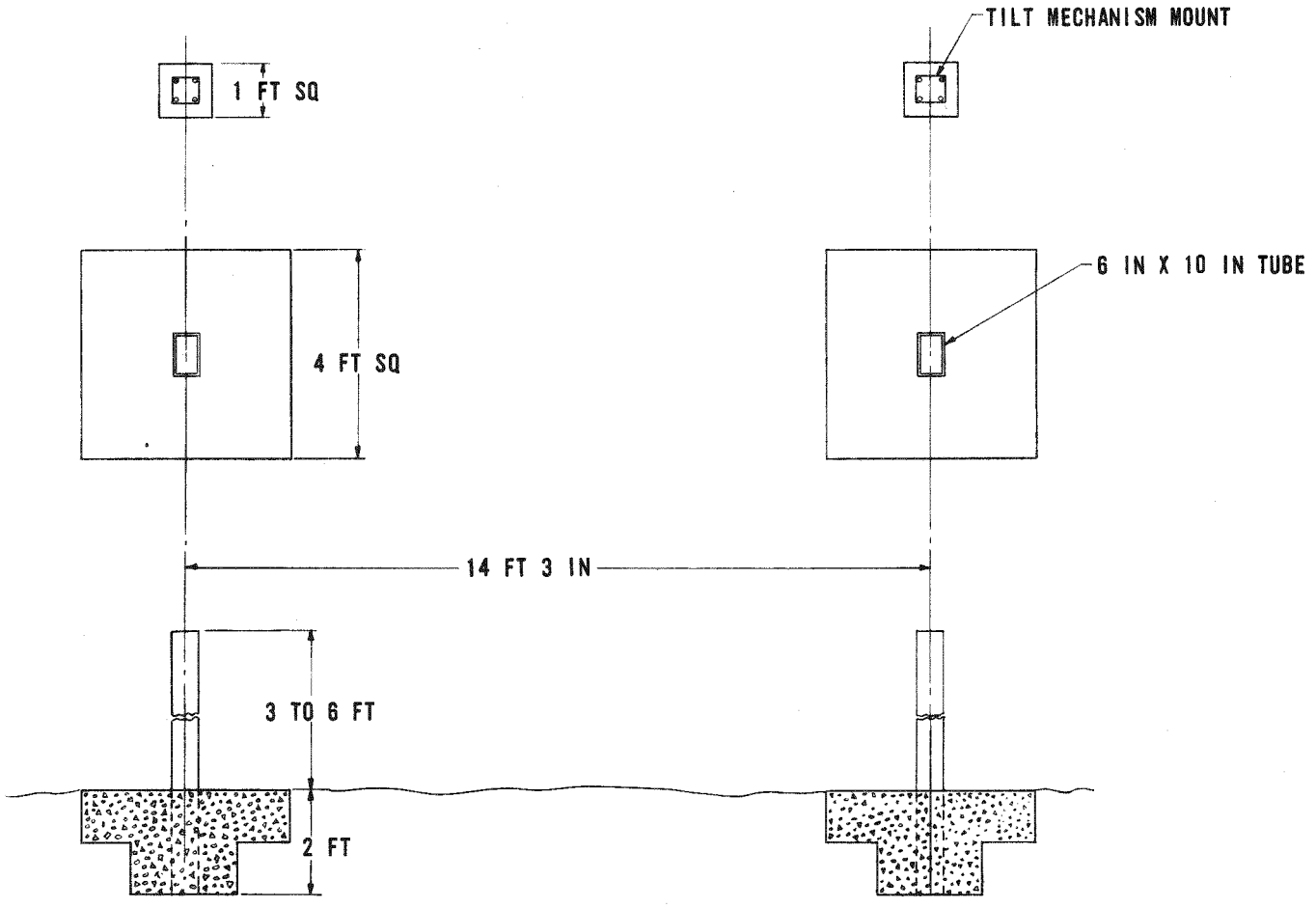
(SEE RESEARCH EXPERIMENT
REPORT, APPENDIX E)

APPENDIX 4H
HELIOSTAT FOUNDATION

APPENDIX 4H

HELIOSTAT FOUNDATION

0975-266

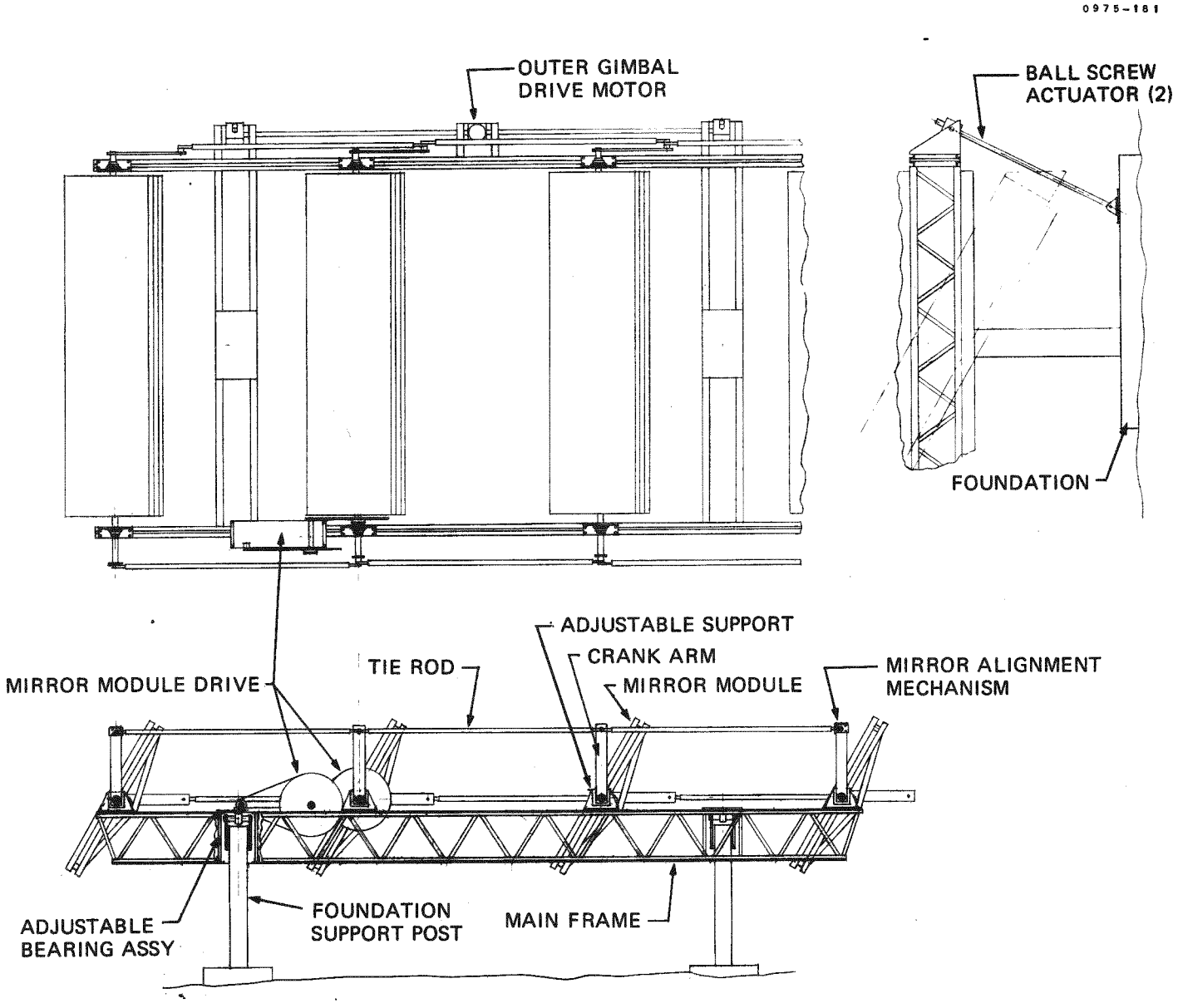


PRELIMINARY CONFIGURATION HELIOSTAT FOUNDATION

APPENDIX 4I
OUTER GIMBAL AND DRIVE ASSEMBLY

APPENDIX 4I

OUTER GIMBAL AND DRIVE ASSEMBLY



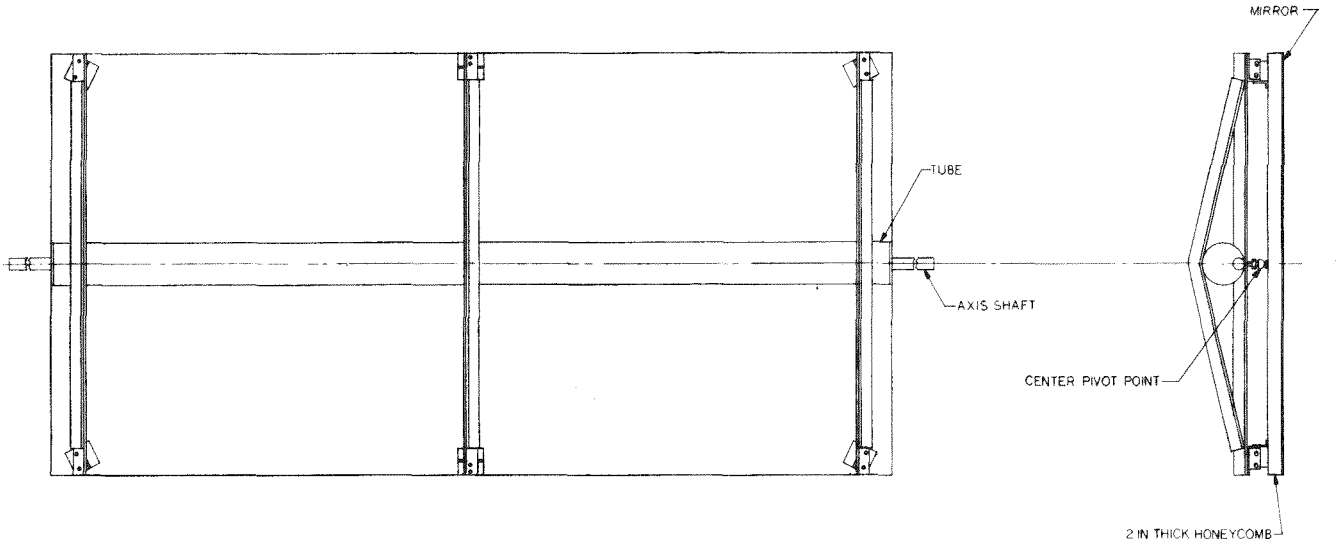
PRELIMINARY CONFIGURATION HELIOSTAT CONCEPT

APPENDIX 4J
MIRROR MODULE ASSEMBLY

APPENDIX 4J

MIRROR MODULE ASSEMBLY

0975-260



PRELIMINARY CONFIGURATION MIRROR MODULE

APPENDIX 6A

THERMAL STORAGE SALT TRADEOFF SELECTION ANALYSIS

APPENDIX 6A

THERMAL STORAGE SALT TRADEOFF SELECTION ANALYSIS

The concept to be mechanized for the Pilot Plant and SRE Demonstration for storing heat energy was based on utilizing inorganic salt mixtures at or near the best eutectic point. Therefore, this analysis considered only inorganic salts and salt mixtures in the temperature range compatible with a fixed turbine cycle operation. The pilot plant requirement is thermal storage to provide 7 MW(e) for 6 hours.

PILOT PLANT TURBINE CYCLES

This analysis considers a total of four turbine cycles for baseline, i.e.:

Case I	600/825
Case II	850/900
Used	890/950
Case III	1450/950
Case IV	2400/950

The temperature ranges for boiler were set between the saturation temperatures at the charge cycle and discharge cycle pressures.

SALT CHARACTERIZATION

One of the primary difficulties in conducting this analysis is obtaining valid and relevant data on promising inorganic salts and salt mixtures for the boiler and superheater storage. This data includes thermal, chemical, physical and transport properties, handling characteristics and costs. Laboratory investigations and analytical studies have proved extremely beneficial. Measurement of heats of fusion and heat capacities of candidate salts have proved some literature values to be in error. Investigations of thermal stability, corrosion and containment and nucleation are extremely important on selecting the "best" thermal storage salt. However, this information is sparse to say the least, and costly to determine for large numbers of samples. Additionally, valid and relevant salt price/quantity data are difficult to obtain. The data in this analysis was based principally on data contained in the Chemical Marketing Reporter for December 1973. These data were supplemented with informal pricing information based on inquiries. Consideration has been given to the fact that with the large quantities of salt required for pilot and commercial plants operations the supply/demand curve may be drastically affected depending upon the salt selected.

METHODOLOGY

A procedure was developed to permit a systematic screening of salts to ensure that the final candidates contain the "best" and true salt, with a high degree of confidence.

1. To be a true candidate the eutectic temperature must fall within temperature ranges for the cycle considered. Operating on an isopleth other than that at or near the eutectic composition is questionable. This is due primarily to unpredictability of nucleation, the question as to the availability of heat of fusion and sensible heat, solid growth characteristics of bulk quantities of the excess component, etc.

2. Those salts within the temperature limits are rated according to their location to the arithmetic mean temperature. The mean arithmetic temperature was selected on the basis that the (UA) condenser was essentially equal to the (UA) boiler. This assumption may require modification dependent upon the results of continuing thermal analysis. It is suspected that the (UA) condenser may be somewhat larger which would tend to lower the "desired" eutectic temperature.

3. Compare the salts on the basis of specific cost density ($ per cu. ft. of salt) and energy density (BTU per cu. ft. of salt). This study considered only salt costs.

4. Select several promising candidates from the chosen turbine cycle case.

5. Conduct more detailed characterization studies only on the selected candidates. This means for example that the heats of fusion and capacities would be experimentally determined, pass/fail corrosion and containment evaluations and preliminary tests to quantify nucleation "capability." Additionally, analysis was conducted to evaluate more fully the thermal, chemical, physical, transport properties and handling characteristics and costs.

6. If one or more of the leading candidates is eliminated as a result of (5) above a search for a suitable replacement(s) will be made.

SELECTION OF PCM (PHASE CHANGE MATERIALS)
FOR THERMAL STORAGE

Eutectic salts having melting temperatures within the boiler and superheater cycle conditions were selected. Salts containing heavy metal components (like Cd, Ag, Pb, Cs, Sr, etc.) were eliminated because of their nonavailability and most likely high cost. The next screening was based on the energy density, cost, physical and chemical properties. A salt with a low cost per unit capacity ($/KWH) melting in a range close to the median temperature for the cycle and with compatible properties was considered as a most desirable candidate. Tables 6A-1 and 6A-2 list the boiler and superheater salts after initial screening. The following was the procedure for selection:

1. Salts with low cost per KWH(t) were considered first.

2. Salts with melting temperatures close to (generally less than 10°F difference) the minimum and maximum temperatures of the particular cycle were eliminated. However, salts melting at temperatures below the median were considered good since they do give a better driving force (ΔT) to the condenser and besides it would be possible to run off the eutectic with such salts.

3. Some of the salts were eliminated because of their incompatible properties.

Case 1 Boiler - 435°F to 492°F (464°F)

The following salts were selected for further analysis.

(9) $NaNO_3$ - NaOH (475°F)
(6) $NaNO_2$ - NaOH (460°F)
(2) KOH - LiOH (441°F)

Salt 1, even though cheap, is eliminated because it has a low melting point and higher cost than 9. Salts 3, 4, 5 and 8 have a low energy density. Salts 7, 10, 11 and 12 are priced high. Salt 13 has a high temperature.

Salt 2, even though it has a low melting point, was selected because it has a high energy density and melting temperature could be raised by running off the eutectic point. If the containment costs are high then this could be a promising candidate.

Table 6A-1. Superheater

Salt	T_f (°F)	Mole (%)	Weight (%)	Density at M. Pt. (lb/ft^3)	B/lb	B/ft^3	$/lb	$/ft^3	Viscosity (Cp)	$/kWh	$/lb**	$/kWh**
1. LiBr-KBr	590	68	60.8	162.3	64.82	10,520	1.21	196.40		52.67	2.197	95.65
2. KOH-LiOH	597	60	77.8	110.8	146.6	16,241	0.24	26.00		5.52	0.415	9.66
3. KCl-KNO_3	608	6	4.5	118.1	64.46	7,613	0.106	12.52		5.61	0.17	9.01
4. KNO_3-K_2CO_3	608	98	97.3	118.1	63.0	7,439	0.11	12.86		5.905	0.177	9.56
5. KNO_3-K_2SO_4	626	98	96.6	117.5	64.2	7,540	0.113	13.28		6.00	0.178	9.43
6. $BaCl_2$-KCl-LiCl	639	6.38 - 39.4	20.2 - 44.8	130.0	103.5	13,463	0.42	54.73		13.85	0.555	18.30
7. KCl-LiCl-$CaCl_2$	644	45 - 45	52.8 - 29.9	110.2	112.63	12,412	0.30	33.30		9.09	0.445	13.50
8. KBr-KCl-KNO_3	648	10 - 10	4.7 - 7.3	120.0	60.19	7,223	0.16	19.20		9.07	0.192	10.88
9. KCl-LiCl-NaCl	655	24 - 43	32.4 - 32.8	107.5	120.7	12,972	0.31	34.80		8.76	0.52	14.68
10. LiCl-KCl	671	58	44	106.5	121.12	12,900	0.424	45.16		11.95	0.64	17.95
11. KBr-KCl-LiCl-LiBr	675	21.3 - 37.7 - 3.5	34.4 - 38.6 - 2.0	117.5	91.95	10,804	0.48	56.60		17.82	0.79	29.28
12. NaF-NaOH	680	10	10.5	113.7	170.06	19,336	0.085	9.66		1.71	0.163	3.28
13. NaCl-NaOH	698	20	26.75	109.0	158.9	17,321	0.054	5.89		1.16	0.126	2.71
14. K_2CO_3-Li_2CO_3-LiOH	701.6	16.4 - 26.4	40 - 35	122.9	151.4	18,607	0.3884	47.74		8.755	0.637	14.35
15. $FeCl_2$-NaCl	705	44	63		96.3							
16. $FeCl_2$-KCl	716	52.2	65		87.2							
17. KCl-LiCl-NaCl	723	30 - 15	41.2 - 42.7	105.6	130.3	13,761	0.40	41.80		10.477	0.672	17.60
18. K_2CO_3-Li_2CO_3-Na_2CO_3	741	25 - 43.5	34.5 - 32.5	130.3	108.54 (118.8)*	14,149 (15,580)*	0.223	29.00		7.01	0.332	10.43

*Experimental values.
**Supplier's quotation.

Table 6A-1. Superheater (Concluded)

Salt	T_f (°F)	Mole (%)	Weight (%)	Density at M. Pt. (lb/ft^3)	B/lb	B/ft^3	$/lb	$/ft^3	Viscosity (Cp)	$/kWh	$/lb**	$/kWh**
19. $KCl-MgCl_2-NaCl$	744.8	22 - 51	20.4 - 60	110.25	112.2	12,370	0.085	9.33		2.57		
20. $BaCl_2-Ca(NO_3)_2$	755.6	41.7	47.6	170.9	60.0	10,254	0.2365	40.42		13.45	0.081	4.6
21. $Ba(NO_3)_2-NaCl$	766.4	62	88	178.0	52.4	9,326	0.1338	23.82		8.175		
22. $CaCl_2-Ca(NO_3)_2$	768	42.5	33	130.0	78.0	10,149	0.055	7.18		2.41	0.27	11.83
23. KCl-KOH	770	35	41.9	107.2	117.9	12,638	0.08	8.33		2.316	0.138	3.98
24. $BaCl_2-MgCl_2-NaCl$	784	13.8 - 39.9	30.6 - 40.5	144.15	100.56	14,496	0.186	26.17		6.30		
25. $BaCl_2-CaCl_2-KCl-NaCl$	790	14 - 45 - 8	27.9 - 47.8 - 5.7	156.6	92.98	14,380	0.133	20.56		4.88	0.036	1.31
26. $KCl-LiCl-CaCl_2$	797	10 - 60	11.3 - 38.3	119.8	131.0	15,715	0.38	45.70		9.90	0.62	16.07
27. $KCl-NaCl-Li_2SO_4$	799	34 - 24.2	29.8 - 16.5	123.4	114.8	14,170	0.652	80.50		19.4		
28. LiBr-LiF	838	89	77.25	160.26	97.11	15,562	1.70	272.00		59.75	2.80	98.56
29. $K_2CO_3-Li_2CO_3$	916	52	66.9	124.2	124.5 (157.5)*	15,462 (19,564)*	0.36	43.00		7.8	0.382	8.27
30. $LiCl-CaCl_2$	925	40	20.3	129.0	129.2	16,671	0.21	26.84		5.55	0.326	8.61
31. $NaCl-CaCl_2$	932	47.2	32	127.7	122.42	15,628	0.023	27.75		0.641	0.042	1.18
32. $K_2CO_3-Li_2CO_3$	932	73	78.65	130.0	97.78	12,712	0.77	100.52		26.88	0.31	10.78

*Experimental values.
**Supplier's quotation.

Table 6A-2. Boiler

Salt	T_f °F	Mole %	Wt %	Density at M. Pt. lb/ft^3	B/lb	B/ft^3	$/lb	$/ft^3	Viscosity (Cp)	$/kWh**	$/lb	$/kWh**
1. $NaNO_2$-$NaNO_3$	439	65	60	118.1	72.24	8,532	0.08	9.45		3.78	0.148	6.99
2. KOH-LiOH	441	30	50	110.8	160.7	17,810	0.39	43.21		8.28	0.78	16.56
3. KNO_2-$NaNO_2$	447	70	74	117.25	68	7,940	0.34	39.90		17.065	0.1817	9.12
4. $Ca(NO_3)_2$-KNO_3	450	40	52	122.9	51.84	6,373	0.11	13.52		7.24	0.159	10.46
5. $LiNO_3$-$Ca(NO_3)_2$	453	26	13	123.1	53.7	6,611	0.25	13.54		15.39		
6. $NaNO_2$-NaOH	460	27	39	114.1	115 (105)	13,188 (11,983)*	0.084	10.00	8.34	2.73	0.158	5.14
7. $CaCl_2$-$LiNO_3$	460	8.1	12.4	114.25	79 (126.3)*	9,062 (14,400)*	1.10	126.00	6.22	29.7		
8. KCl-NaCl-KNO_3-$NaNO_3$	471	20-10-40	17.3-6.7-46.6	119.5	64.3	7,683	0.07	8.00		3.715	0.1026	5.46
9. $NaNO_3$-NaOH	475 (482)	70	83	120.4	78.4 (72.0)	9,440 (8,500)*	0.035	4.20 (4.12)	(7.05 at 475°F)	1.66	0.087	3.12
10. $LiNO_3$-$LiSO_4$	482	98	97	112.3	81.7	9,175	1.25	140.00		52.2		
11. $LiNO_3$-Li_2CO_3	482	98	95	111.5	82.55	9,167	1.24	138.00		51.26		
12. $Ba(NO_3)_2$-$LiNO_3$	485	2.8	10	118.8	78	10,390	1.14	152.00	6.5	49.90		
13. $LiNO_3$	490	---	---	111	160 (148)*	17,798 (16,465)*	1.25	139.00	6.25	34.59		
14. NaBr-NaOH	500	22.3	42.5	126.1	106	13,430	0.21	26.50	17.2	6.76	0.357	21.60
15. LiOH-LiCl	504	63	49	107.8	182	19,600	0.80	86.30	4.24	15.00	1.34	25.20
16. Na_2CO_3-Na_2O-NaOH	505	6.5-7.4	15-10	117.4	135	15,850						
17. $Ca(NO_3)_2$-LiCl	509	40.85	73	116.6	76	8,860	0.28	32.76	15.0	12.57	0.48	21.50
18. $Ba(NO_2)_2$-KNO_2	509	95	98	199.1	38	7,586						
19. LiBr-LiOH	527	55	81.6	158.6	101.1	16,031	1.51	240.00		50.97	2.78	94.00

* Experimental Values

**Supplier's Quotation

Table 6A-2. Boiler (Concluded)

Salt	T_f °F	Mole %	Wt %	Density at M. Pt. lb/ft^3	B/lb	B/ft^3	$/lb	$/ft^3	Viscosity (Cp)	$/kWh**	$/lb	$/kWh**
20. KCl-LiCl-LiOH	536	11.5-45	22.6-50	106.87	156.6	16,735	0.652	69.70		14.21	1.654	36.04
21. $Ca(NO_3)_2$-NaCl-$NaNO_3$	536	5.8-7.9	16.27-5	130.6	66.2	8,664	0.047	6.14		2.42	0.074	3.81
22. NaCl-$NaNO_2$	538	1.1	1	113.3	86.84	9,839	0.106	12.00		4.17	0.195	7.65
23. NaCl-Na_2CO_3-NaOH	540	7.8-6.4	10-14.9	117.26	135.9	15,941	0.0607	7.12		1.524	0.116	2.92
24. KCl-LiCl-LiOH	541.4	1.5-36.5	3.6-49.1	106.32	190.75	20,290	0.77	81.90		13.77	1.296	23.18
25. Na_2CO_3-NaOH	541	7.2	1,205	117	146	17,068	0.066	7.72		1.54	0.132	3.08
26. $Ba(NO_3)_2$-$NaNO_2$	543	15.2	40.4	119	66	13,117	0.124	24.70		6.41		
27. KNO_3-$NaNO_2$	545	45.5	49.8	115.7	65.3 71.2	7,554 8,705	0.108	12.50		5.65	0.1865	9.76
28. NaCl-$NaNO_3$-Na_2SO_4	549*	8.4-86.3	5.72-85.5	122.26	(75.66)	(9,250)*	0.0354	4.34		1.597	0.0773	3.49
29. LiOH-LiCl	554	63	49	104	185.6	19,301	0.84	86.90		15.45	1.344	24.72
30. KNO_3-$Ba(NO_3)_2$	554	87	72	142.3	53.16	7,564	0.12	17.08		7.704		
31. NaCl-$NaNO_3$	563	6.4	5	119.1	73.63	8,770	0.03	3.53		1.39	0.073	3.35
32. LiOH-LiCl	567	50	36.15	114.2	197.6	22,567	0.80	91.12		13.82	1.393	24.06
33. LiBr-KBr	590	68	60.8	162.3	64.8	10,520	1.21	196.40		52.67	2.197	95.65
34. KOH-LiOH	597	60	77.8	110.8	146.6	16,241	0.237	26.00		5.52	0.415	9.66
35. KCl-KNO_3	608	6	4.5	118.1	64.46	10,520	0.106	12.52 (20.19)		5.61	0.17	9.01
36. KNO_3-K_2CO_3	608	98	97.3	118.1	63	7,439	0.109	12.86		5.905	0.177	9.56
37. KNO_3-K_2SO_4	626	98	96.6	117.5	64.2	7,540	0.113	13.28		6.00	0.178	9.43
38. $BaCl_2$-KCl-LiCl	639	6.38-29.4	20.2-44.8	130	103.5	13,463	0.42	54.73		13.85	0.555	18.30

* Experimental Values

** Supplier's Quotation

Case 2 Boiler 466° - 528°F (497°F)

The following salts were selected for further analysis.

(9) $NaNO_3$ - NaOH (475°F)
(14) NaBr - NaOH (500°F)
(15) LiOH - LiCl (504°F)
(13) $LiNO_3$ (490°F)

Salts 10, 11, 12 and 13 fall within the same cost bracket. Salt 13 was selected because it has a high energy density and a melting temperature close to the median. Salt 16 contains Na_2O which is believed to form a slag with the container and is an expensive salt. Salt 17 has a high melting temperature. However, lithium salts and $NaNO_3$ deliquesce in moist atmosphere while NaBr absorbs moisture. Even though lithium salts are relatively expensive they are being considered at this time because of supply/demand evaluation and recycle potential.

Case 3 Boiler - 505° - 592°F (535°F)

The following salts were selected:

(28) NaCl - $NaNO_3$ - Na_2SO_4 (549°F)
(31) NaCl - $NaNO_3$

Salts (29), (32) and (33) are lithium salts and are expensive.

Case 4 Boiler 579° - 655°F (617°F)

The following were selected for further analysis.

(35) KCl - KNO_3 (608°F)
(34) KOH-LiOH (597°F)
(37) KNO_3 - K_2SO_4 (626°F)

Salt 33 is expensive and has a low energy density; salts 36 and 37 fall in the same category. Salt 37 was selected primarily for further investigation. Salt 38 is expensive in comparison to those selected.

Case 1 Superheater - 495° - 825°F (660°F)

The following salts were selected for further analysis.

(13) NaCl - NaOH (698°F)

(12) NaF - NaOH (680°F)

(2) KOH - LiOH (597°F)

Salts 1, 6, 7, 9, 10 and 11 have high costs. However, 7 and 9 could be possible candidates if LiCl could be obtained at a relatively lower price. Salts 3, 4, 5 and 8 have low energy density, which could lead to high-containment cost. However, they melt at lower temperatures which could lower the insulation costs. For this reason salt 2 was selected. Salts 12 and 13 are the best as of now; however, experiments on NaBr - NaOH system have shown that it has a lower ΔH_f (heat fusion) than calculated value.

Case 2 Superheater - 528°F - 950°F (739°F)

The following were selected for further analysis.

(13) NaCl - NaOH (698°F)

(12) NaF - NaOH (680°F)

(18) K_2CO_3 - Li_2CO_3 - Na_2CO_3 (741°F)

(19) KCl - M Cl_2 - NaCl (745°F)

(20) $BaCl_2$ - $Ca(NO_3)_2$ (756°F)

(23) KCl - KOH (770°F)

Salts 10, 11, 14 and 26 are relatively expensive. However, for salts 14 and 17 LiCl is the prime cost factor. Salt 15 could be a promising candidate.

Case 3 Superheater - 590° - 950°F (759°F)

Same as Case 2 Superheater.

Case 4 Superheater - 655° - 950°F (803°F)

The following are selected for further analysis.

(13) NaCl - NaOH (698°F)

(12) NaF - NaOH (680°F)

(29) K_2CO_3 - Li_2CO_3 (916°F)

(23) KCl - KOH (770°F)

(18) K_2CO_3 - Li_2CO_3 - Na_2CO_3 (741°F)

Salt 8 has a low energy density and melts at a temperature close to lower limit; salts 9, 10, 11, 17 and 26 are relatively expensive. From the salts 18, 30, and 32 belonging to the same category one of them (15) is selected for further investigation. If salts 12 and 13 do not satisfy the heat exchanger requirements then salt 18, 30 or 32 would emerge as a promising candidate.

It should be noted that the values indicated inthe table are calculated values. However, this approach narrows the study down to a few salts for which experimental investigation can be managed. Actual selection of the salt should be based on the total installed cost. Therefore, some of the salts with higher energy density and some promising salts with low energy density were selected. If the containment cost per unit capacity is high then it would be profitable to select a salt with a high energy density. But if the salt cost is of significance in total cost then a salt with lowest cost should be selected even though it has a lower energy density.

APPENDIX 6B
MATERIALS EVALUATION FOR THERMAL ENERGY STORAGE

APPENDIX 6B
MATERIALS EVALUATION FOR THERMAL ENERGY STORAGE

Several promising inorganic eutectic mixtures and compounds with the melting points in the range of 220 to 290°C have been examined from the literature and nine most promising ones identified. For these, the eutectic compositions have been prepared, their melting points measured, densities at the melting point determined and given in Table 6B-1.

The thermodynamic properties like the molar heat capacity for these eutectics and/or compounds covering the temperature range of 25°C below the fusion temperature and 25°C above the fusion temperature have been measured using differential scanning calorimeter and the average value obtained. The heats of fusion for these materials have been calculated using Richards' Rule based on entropy of fusion and the heats of fusion have been experimentally measured using differential scanning calorimeter and these values are given in Table 6B-2.

As a result of this investigation and taking into consideration the temperature range of interest for the main storage and cost of the material, two eutectic mixtures were chosen for further studies. These are $NaNO_3$-NaOH and NaCl-$NaNO_3$-Na_2SO_4. These two eutectics have been studied for their thermal stability. The eutectic $NaNO_3$-NaOH was evaluated for thermal stability in differential scanning calorimeter holding a known weight of the sample in the calorimeter at a known temperature for a known length of time and after that period, running the heat of fusion curve. The area under the curve and the fusion temperature will give information on the thermal stability of the material. In the case of $NaNO_3$-NaOH eutectic mixture, there is a slight shift of one degree when the eutectic is kept at 375°C for 20 minutes and one hour. When the same material is maintained for 20 minutes at 400°C, there is no change in its fusion temperature; whereas, when it is maintained at 425°C for 20 minutes and then the heat of fusion curve run, there is a slight shift in fusion temperature. When the eutectic is maintained at 475°C for 15 minutes and the heat of fusion curve run, the heat of fusion temperature shifts by 5°C and the area under the curve becomes smaller as shown in Figure 6B-1. In the case of NaCl-$NaNO_3$-Na_2SO_4, when the eutectic mixture is held at 400°C for 10 minutes and the heat of fusion curve run, there is no change in the fusion temperature; whereas, the same eutectic mixture when held at 450°C for 10 minutes and the heat of fusion curve run, there is a shift of one degree in fusion temperature. When the same eutectic mixture is held at 500°C for 20 minutes and the heat of fusion curve run, there is a shift of 5°C in the fusion temperature and at the same time the area under the curve becomes much smaller compared to the earlier curves as shown in Figure 6B-2.

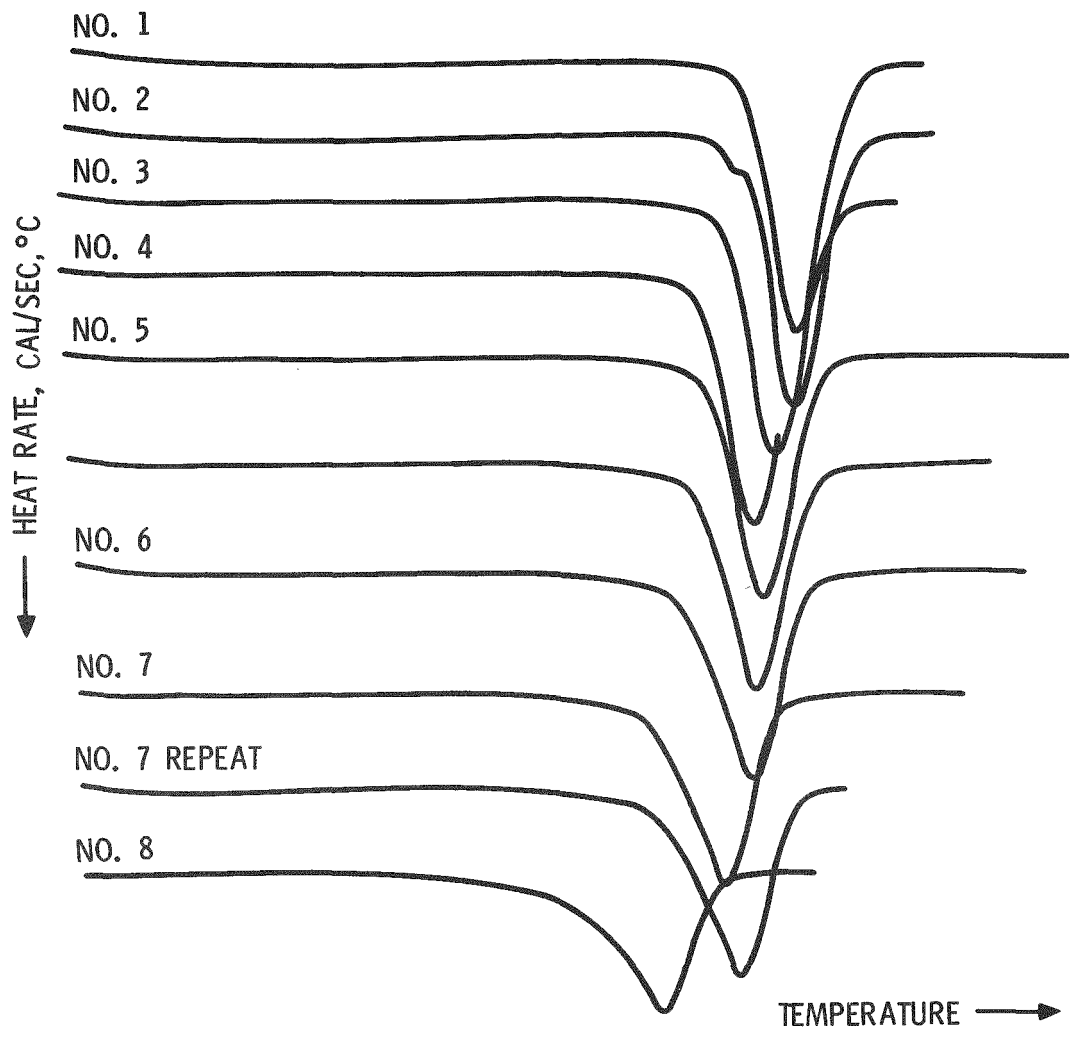
Table 6B-1. Physico-Chemical and Thermodynamic Properties of Eutectic Materials

Eutectic Mixture	Composition Mole %	Melting Point Literature		Melting Point Measured	Density at mp
		°C	°F	°C	gm/cc
Na_2CO_3-Na_2O-NaOH	6.5 - 7.4 - 86.1	263	505	288.3	1.8814
$NaNO_2$-NaOH	27 - 73	238	460	240	1.8290
$NaNO_3$-KNO_3	54 - 46	222	432	222.2	1.9600
$NaNO_3$-NaOH	70 - 30	246		247.5	1.9103
NaCl-$NaNO_3$-Na_2SO_4	8.4 - 86.3 - 5.3	278		286.5	1.9363
NaBr-NaOH	22.3 - 77.7	260	500	261	2.0195
$LiNO_3$		254	490	254	1.782
$Ba(NO_3)_2$-$LiNO_3$	2.6 - 97.4	252	485	253	2.133
$Ca(NO_3)_2$-LiCl	40.85 - 59.15	265	509	269.7	1.868

Table 6B-2. Physico-Chemical and Thermodynamic Properties of Eutectic Mixtures

Eutectic Mixture	Specific Heat Measured	Heat of Fusion (caltd)			Heat of Fusion (measured)		
	Cals/mole-degree	KCals/mole	Btu/lb	Btu/ft^3	KCals/mole	Btu/lb	Btu/ft^3
Na_2CO_3-Na_2O-NaOH	13.07	3.44	135	15,850	2.59	101.5	11,920
$NaNO_2$-NaOH	20.24	3.07	115	13,188	2.79	105.0	11,991
$NaNO_3$-KNO_3	19.16	2.97	58	7,070	2.18	50.5	6,178
$NaNO_3$-NaOH	23.33	3.12	78.5	9,360	2.7	68.0	8,108
NaCl-$NaNO_3$-Na_2SO_4	24.46	3.45	72.4	8,750	3.64	76.4	9,235
NaBr-NaOH	13.54	3.2	106	13,430	2,088	69.6	8,774
$LiNO_3$	29.69	3.162	82.5	9,176	6.27	163.7	18,210
$Ba(NO_3)_2$-$LiNO_3$	26.67	3.19	78	10,390	6.47	157.5	20,970
$Ca(NO_3)_2$-LiCl	22.24	3.89	76	8,860	3.68	72.0	8,395

$NaNO_3$-NaOH



NO. 1	SAMPLE PREVIOUSLY HEATED TO 260°C FOR 5 MIN.
NO. 2	REPEAT 1 FOR REPRODUCIBILITY
NO. 3	375°C FOR 20 MIN.
NO. 4	375°C FOR 30 MIN.
NO. 5	375°C FOR 1 HOUR
NO. 6	400°C FOR 20 MIN.
NO. 7	425°C FOR 20 MIN.
NO. 8	475°C FOR 15 MIN.

Figure 6B-1. $NaNO_3$-NaOH

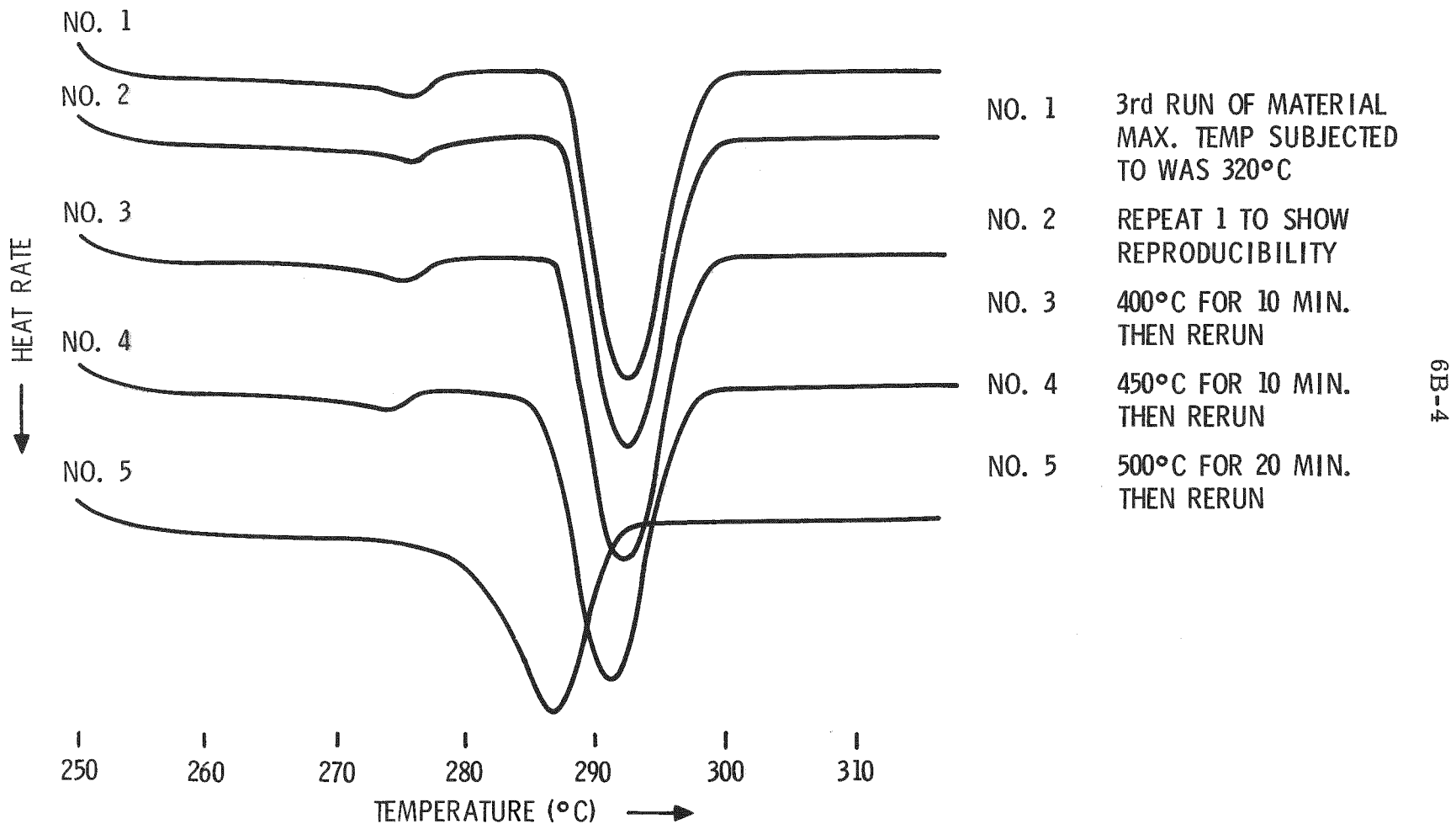


Figure 6B-3. $NaCl-NaNO_3-Na_2SO_4$

APPENDIX 6C

STORAGE SUBSYSTEM SALT CHARACTERISTICS

MAIN STORAGE SALT CHARACTERISTICS

- Nacl - $NaNO_3$ - Na_2SO_4 - - - - - - - - - - - ternary eutectic
- Phase Diagram - - - - - - - - - - - - - - - - - $549^{0}F$/mole : 8.4 - 86.3 - 5.3
- Thermal Properties:
  - heat of fusion - - - - - - - - - - - - - 75.6 B/lb, 9250 B/ft^3
  - specific heat - - - - - - - - - - - - - - 0.2851 cal/mole - degree
  - thermal conductivity - - - - - - - - - -
- Fluid Properties:
  - Viscosity - - - - - - - - - - - - - - - -
- Physical Properties:
  - Density - - - - - - - - - - - - - - - - - 120.3 lb/ft^3
- Mechanical Properties of Solid:
  - Shear Strength - - - - - - - - - - - - -
  - Porosity - - - - - - - - - - - - - - - -
- Chemical Properties:
- Cost - $0.077/lb; $3.49/KWH(t)

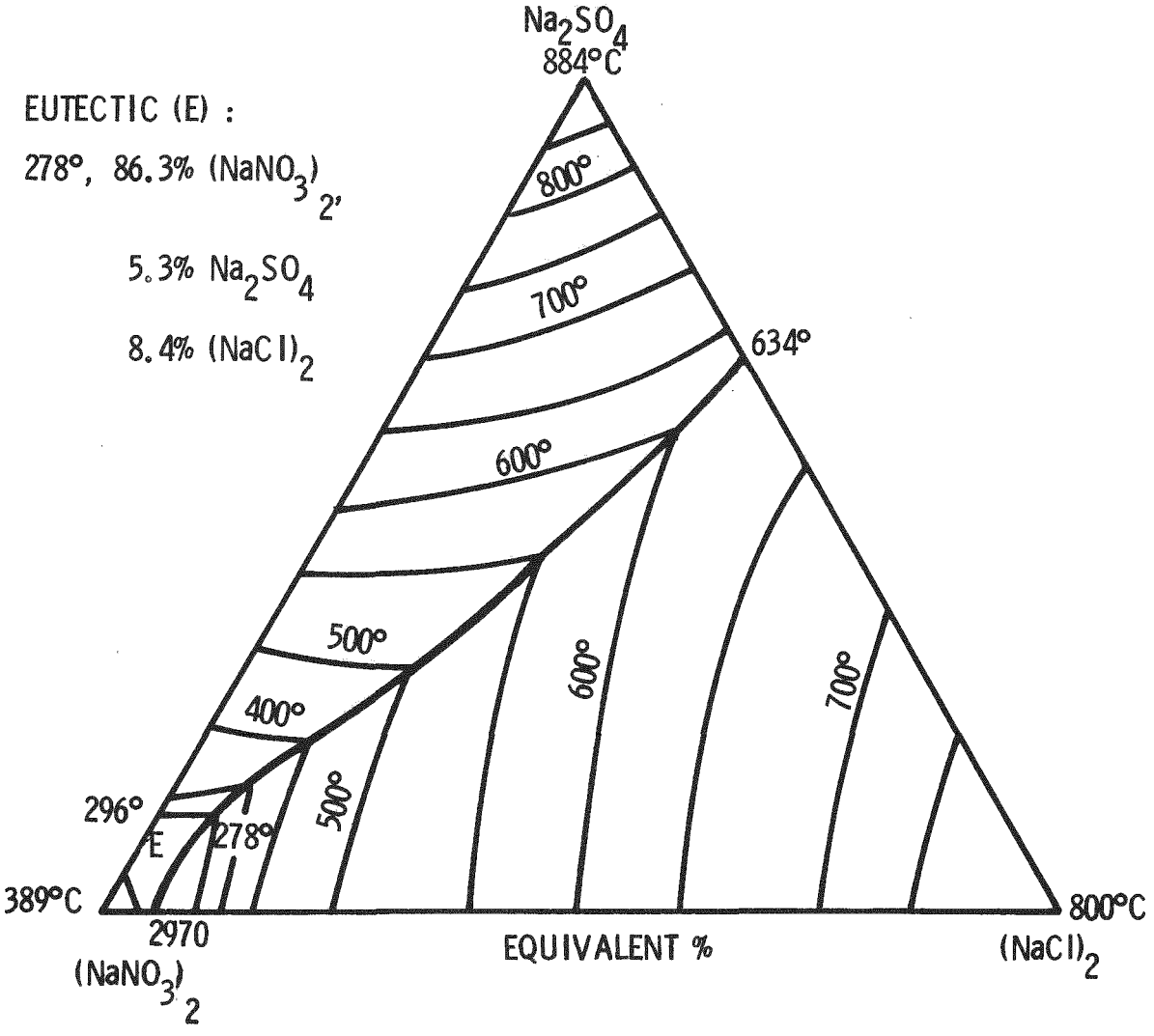


Figure 6C-1. Trinary Eutectic Phase Diagram

SUPERHEATER SALT CHARACTERISTICS

- Nacl - NaOH
- Phase Diagram - - - - - - - - - - - - - - - - - $698^{o}F$/Mole% - 20-80
- Thermal Properties:
  - heat of fusion: - - - - - - - - - - - - - - 158.9 B/lb; 17,321 B/ft^3
  - specific heat:
  - thermal conductivity:
- Fluid Properties:
  - Viscosity
- Physical Properties:
  - Density - - - - - - - - - - - - - - - - - - $109\ lb/ft^3$
- Mechanical Properties of Solid:
  - Shear Strength
  - Porosity
- Chemical Properties
- Cost - $0.126/lb; $2.71/KWH(t)

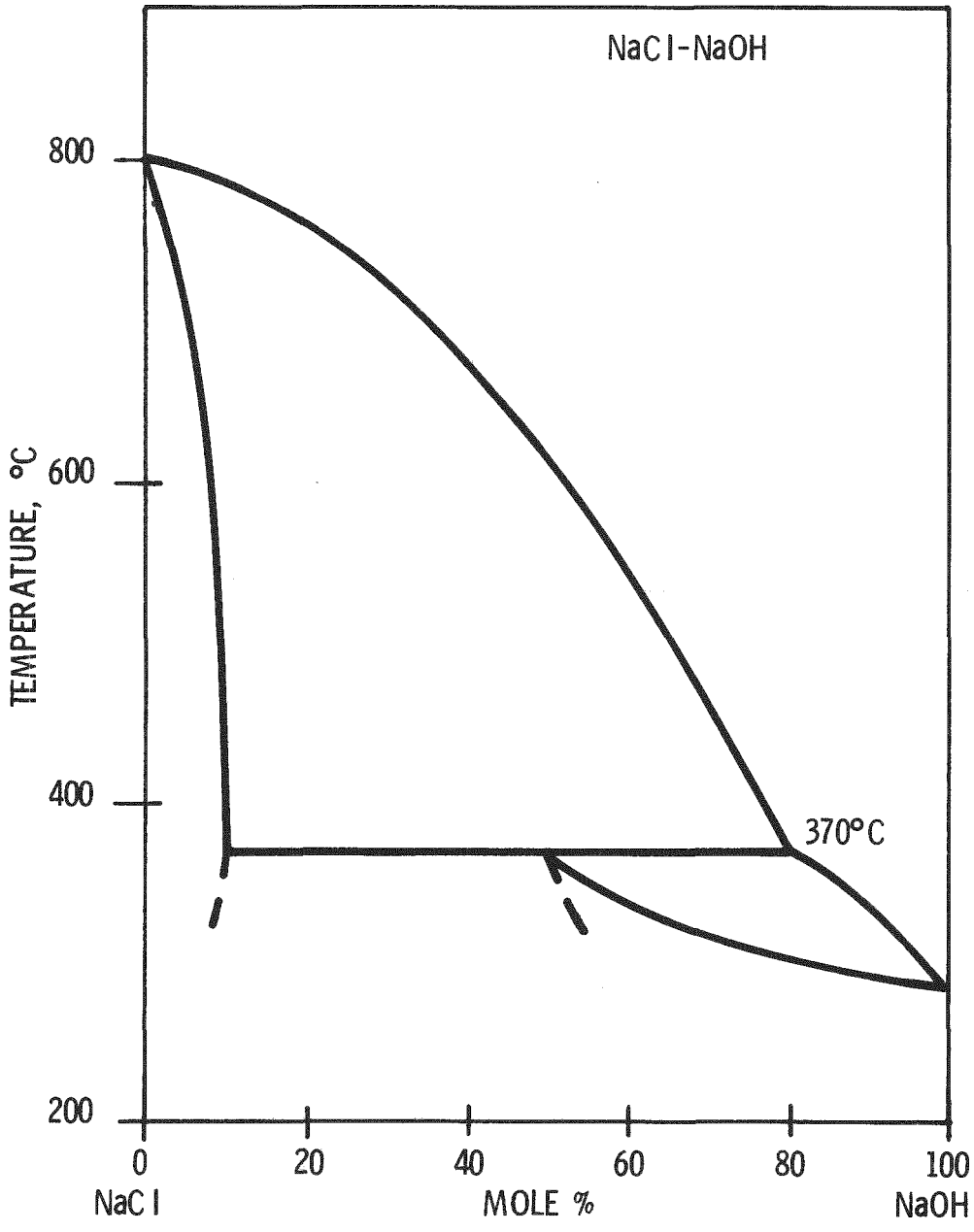


Figure 6C-2. Phase Diagram for Binary Eutectic

HEAT TRANSFER COEFFICIENTS

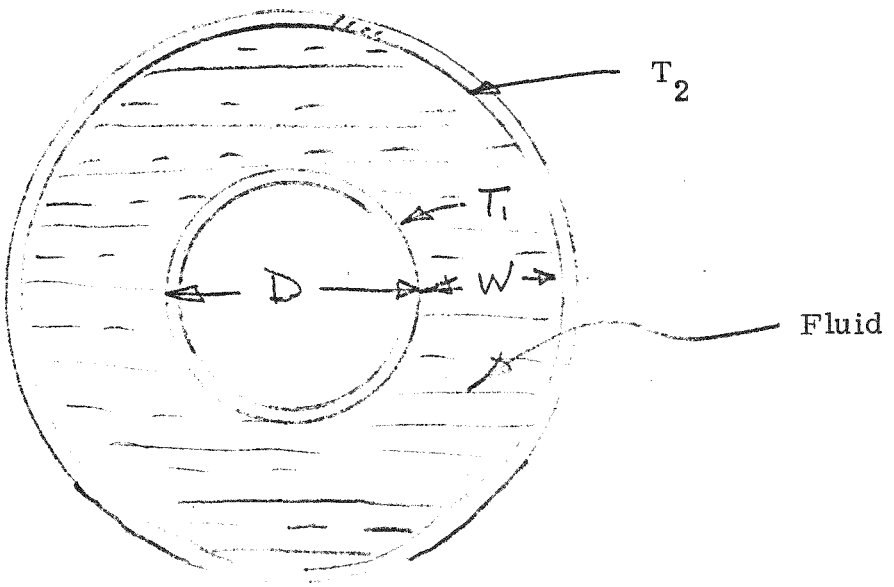
UNIT	CONDITIONS	VALUE	SOURCE
Superheater	Near end of discharge cycle	$U_o = 8 \frac{B}{hr\ ft^2\ F^o}$	Thermal conductivity of salt (assumed) Inside h.t.c. from J.H. Perry Handbook pp. 10-30
M.S. Condenser			
Inside h.t.c.	Condensate loading, $\Gamma = 2.6 \frac{lb}{hr\text{-}ft}$	$h_i = 585 \frac{B}{hr\ ft^2\ F^o}$	J.H. Perry pp. 10-15, 10-20 (Nusselt Eqn.)
Outside h.t.c.	Convection	$h_o = 80 \frac{B}{hr\ ft^2\ F^o}$	
Overall h.t.c.		$U_o \approx 33 \frac{B}{hr\ ft^2\ F^o}$	
		$U_i \approx 334 \frac{B}{hr\ ft^2\ F^o}$	
M.S. Boiler	Scraping time of 4 secs, using mechanical scrapers, and velocity of 0.673 ft/sec.		

Table 6C-1. Off Design Heat Transfer

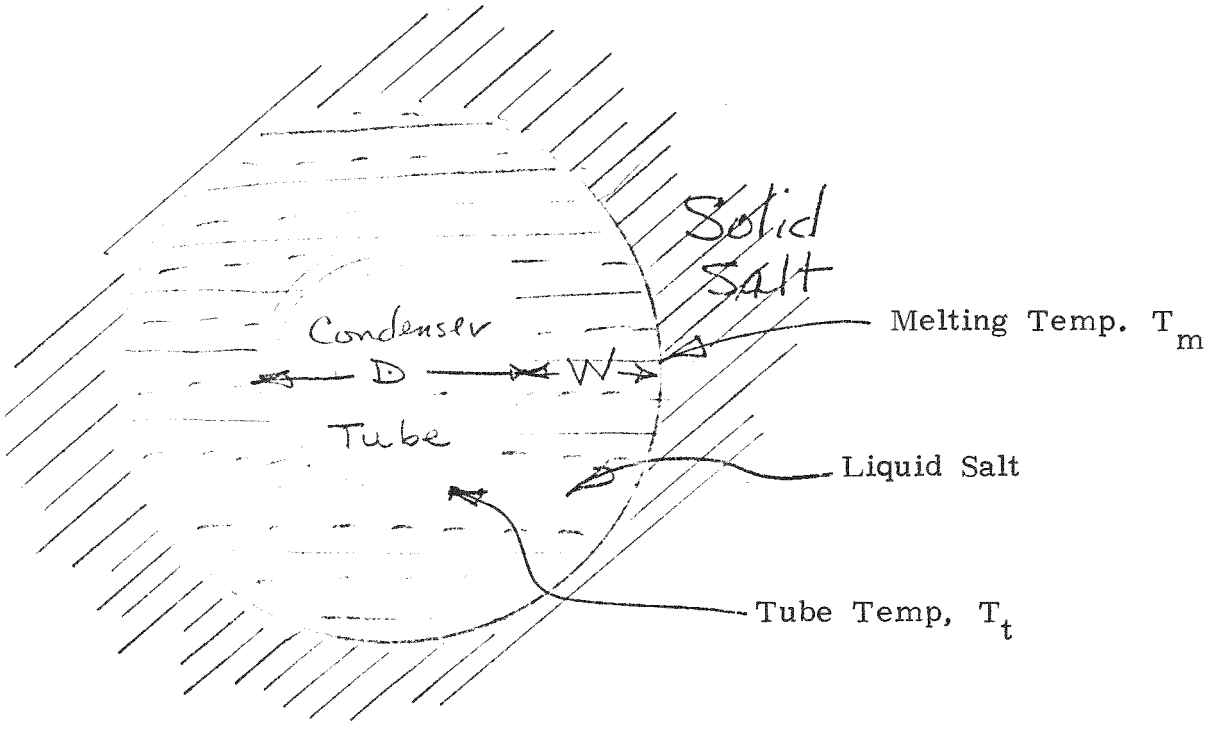
CONTINUITY OF ENERGY FLUX	HEAT FLOW OUT OF PIPE =	HEAT FLOW INTO PIPE
	$C_p \dot{m} \left(T_{OUT}-T_{IN}\right)$	$U A \left(T_{SALT}-T_{STEAM}\right)$
SUPERHEATER	$\dot{m} \alpha V$ SUPERHEAT $\alpha \frac{1}{V^{0.2}}$	$U \alpha V^{0.8}$
CONDENSER	$\dot{m} h_{fg}$	$U A \left(T_{SAT}-T_{SALT}\right)$
	LOWER $\dot{m}$	$U \alpha \dot{m}^{0.5}$ AREA USED & T_{SAT} WILL DECREASE
BOILER	$x \dot{m} h_{fg}$	$U A \left(T_{SALT}-T_{SAT}\right)$
	LOWER $\dot{m}$ QUALITY WILL INCREASE	U FIXED BY SALT UNTIL QUALITY EXCEEDS 70%

HEAT TRANSFER ON CONDENSER TUBES

- General Review of Phase Change Heat Transfer Conducted
- Best approximation given by recent work by R. Goldstein and T. Kuehn
  - -- Combined conduction and natural convection in an annular region bounded by isothermal surfaces
  - -- Analytic and experimental studies
  - -- Predicts heat transfer for wide range of annulus thicknesses, W



- Analagous Heat Storage Problem



Assumptions

-- Quasi Steady State

-- Effects of eccentricity are small (Goldstein, Kuehn studies tend to confirm)

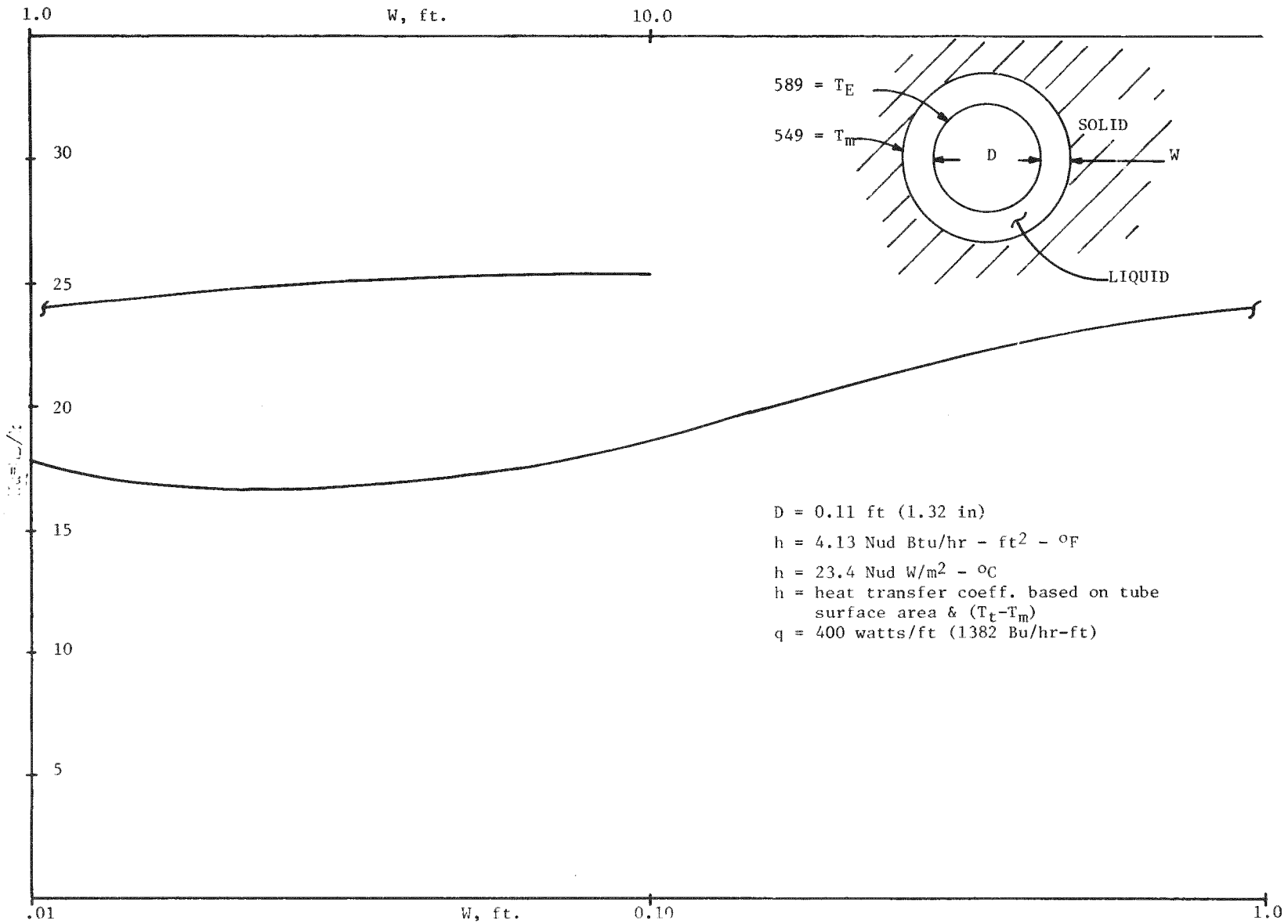


Figure 6C-3. Heat Transfer from Condenser Tube to Storage Medium

APPENDIX 7A

SECTION VII EGS SYSTEMS AND SUBSYSTEMS SPECIFICATIONS

SECTION VII EGS APPENDIX MATERIAL

APPENDIX 7A - SYSTEMS AND SUBSYSTEMS SPECIFICATIONS

7A.1 EGS MAJOR MECHANICAL DESIGN COMPONENT SPECIFICATIONS

7A.1.1 Feedwater Heaters
7A.1.2 Deaerator
7A.1.3 Feedwater Pumps
7A.1.4 Condensate Pumps
7A.1.5 Condenser Exhausters
7A.1.6 Piping
7A.1.7 Valves
7A.1.8 Insulation

7A.2 EGS MAJOR ELECTRICAL DESIGN COMPONENT SPECIFICATIONS

7A.2.1 Generator
7A.2.2 Excitation System
7A.2.3 Generator Neutral Grounding
7A.2.4 Generator Connection Equipment
7A.2.5 Surge Protection Equipment and Potential Transformers
7A.2.6 Generator Breaker
7A.2.7 Generator Transformer
7A.2.8 Protective Relaying
7A.2.9 Secondary Unit Substation
7A.2.10 Motor Control Center
7A.2.11 Conductors
7A.2.12 Motors
7A.2.13 Raceway System
7A.2.14 Essential Service Power System
7A.2.15 Communications System
7A.2.16 Lighting System
7A.2.17 Station Grounding System
7A.2.18 Cathodic Protection
7A.2.19 Construction Power

7A.3 EGS GENERAL STRUCTURAL DESIGN CRITERIA

7A.3.1 Design Standards
7A.3.2 Design Loads
7A.3.3 Foundations

SECTION VII EGS APPENDIX MATERIAL (CONTINUED)

7A.4 EGS GENERAL CHEMICAL DESIGN CRITERIA

7A.4.1 Cycle Makeup Water Facilities
7A.4.2 Condensate Polishing Equipment
7A.4.3 Service Water Facilities
7A.4.4 Cycle Makeup Water and Service Water Storage Facilities
7A.4.5 Water Quality Control System

7A.5 MAJOR PLANT SERVICES DESIGN SPECIFICATIONS

7A.5.1 Air Compressors
7A.5.2 Closed Cooling Water Equipment
7A.5.3 Turbine Lube Oil Conditioner
7A.5.4 Building Space Conditioning
7A.5.5 Fire Protection Equipment

7A.6 SAMA ANALOG SYMBOL STANDARD

7A.1 EGS MAJOR MECHANICAL DESIGN COMPONENT SPECIFICATIONS

7A.1.1 FEEDWATER HEATERS

7A.1.1.1 General. This section covers the design and performance criteria for the feedwater heaters.

7A.1.1.2 Type. The low pressure and high pressure feedwater heaters will be horizontal shell and U-tube type with carbon steel shells and copper-nickel tubes. Both the LP and HP heaters will be provided with an internal drain cooling section for obtaining maximum heat from the extraction steam. De-superheating zones will be provided in the heaters as required.

7A.1.1.3 Codes and Standards. The feedwater heaters will be designed and constructed in accordance with the latest applicable requirements of the Heat Exchange Institute Standards for Closed Feed Water Heaters, the ASME Boiler and Pressure Vessel Code, ANSI B31.1 Code for Pressure Piping and in accordance with the applicable requirements of the Federal Occupational Safety and Health Standards".

7A.1.1.4 Design Criteria. The feedwater heaters will be designed to operate under the following conditions with condensate flow and steam pressures in accordance with the turbine design parameters.

	Outlet Feedwater Approach to the Heater Shell Saturation Temperature, F	Outlet Drains Approach to the Inlet Feedwater Temperature, F
LP Heater	10	15
HP Heater	10	15

7A.1.1.5 Materials. The following materials satisfy the minimum requirements of the conditions encountered in feedwater heater service. If the manufacturer's standard construction materials are of equal or superior quality, the manufacturer's standard construction will be used.

Channel and channel cover	Carbon steel - ASME SA285 Gr C
	Forged steel - ASME SA181 Gr II
Shell	Carbon steel - ASME SA285 Gr C
Tubes	Carbon steel - ASME SA210
	Stainless steel - ASME SA213
	ASME SA249
	Copper alloy - ASME SB395 alloy as specified
Tube sheet	Carbon steel - ASME SA285 Gr C
	Forged steel - ASME SA181 Gr II
Support Plates	Carbon steel - ASME SA283
Air and segmental baffles	Carbon steel - ASME SA283
Inpingement baffles	Stainless steel - ASTM A167 Type 304
Desuperheating and drain - cooling zone shrouds	Carbon steel - ASME SA283 or alloy steel if required
Tie rods and spacers	Carbon steel - ASME SA306
Bolting	
Stud and stud bolts	Alloy steel - ASME SA193 Gr B7
Nuts	Alloy steel - ASME SA194 C1 2H

The maximum metal temperature for pressure parts will be limited to the following:

Material	Temperature, F
Carbon stell	800
Low alloy steels	
Carbon - 1/2 moly	875
1/2 chrome - 1/2 moly	975
Tube materials	
Carbon steel	800
Stainless steel	800
Copper - Nickel	700

Full information will be submitted which substantiates the manufacturer's cognizance of the erosion-corrosion phenomena occurring in carbon steel and copper alloy tubed feedwater heaters.

Information will be submitted which demonstrates that the proposed design and construction will satisfactorily minimize or eliminate the phenomena. The manufacturer will submit recommendations for construction features and supplemental devices such as grillage, baffle plates, diffuser baskets, or stainless steel inserts which, in his opinion, should be incorporated as part of the feedwater heaters to control the erosion-corrosion phenomena.

7A.1.1.6 Construction. Heater construction will conform to the ASME Boiler and Pressure Vessel Code, the Standards of the Heat Exchange Institute, and the following requirements.

All channels will be provided with covers or access manholes which will be removable without disturbing the piping connections. The channels for the low pressure heater will be of fabricated or forged steel construction and will have covers attached with flanged and bolted joints. The channels for the high pressure heater will be of forged steel construction of hemispherical design of sufficient depth for maintenance requirements. Access manholes will be provided.

Pass partition plates of both heaters will be constructed so that the differential pressure created by the tube side friction will tend to seal the pass partition plate sealing joints.

Heater shell and shell skirt wall thickness will be determined in accordance with the Code utilizing the allowable stress value for the shell material at the design pressure and temperature and will be limited to a 3/8 inch minimum wall thickness. The shells will be of all welded construction with a minimum of two designated cutting planes for the tube bundle access. Permanent stainless steel backup plates will be provided inside the shell at all cutting planes to prevent torch and weld spatter damage when removing or replacing a section of the shell. The location of cutting planes will be clearly indicated on outline drawings and marked on the shell. Heater shell guides for expansion control will be furnished as required.

Tubes will be of the material and not less then the minimum size and gage specified and will be suitable for the operating pressures, temperature, and type of construction specified. U-tubes will not be lighter than .050 inch wall thickness for carbon steel, 18 gage for copper alloy or 20 gage for stainless steel. Straight tubes of stainless steel will be not less than 22 gage. Type 304 stainless steel tubes will contain not more than 0.05 percent carbon.

Tubes for the low pressure heater will be rolled into the tube sheets and the tubes of high pressure heater will be welded to the tube sheets and rolled or explosively expanded after welding. All tubes will be supported to prevent tube sagging and excess vibration. Tubes will be expanded into the tube sheets by methods which will not change the size of the tube sheet openings. All carbon steel tube bends will be stress relieved.

Tube sheets will be of adequate thickness for the design pressures and physical dimensions of the heaters with a minimum thickness of one inch. Tube holes will be laid out on a triangular pitch. Tube hole edges will be chamfered on the shell side. The bridge between tube holes will not be less than nominally 3/16 inch or 25 percent of the tube diameter, whichever is greater.

All steam and drip return openings in the heater shells will be properly baffled to prevent impingement damage to the heater tubes and heater shell. All drip return baffles and surrounding shell interior areas will be adequately protected with stainless steel construction.

All heaters will be provided with an integral type drain subcooler. The subcoolers will be designed to prevent reheating of the drips by heat transfer from the condensing or desuperheating zones.

The drain cooling section will have sufficient free surface area to provide stable liquid level control. The free surface area of the water in the drain cooling section will be not less than 1.5 square feet for each 100 gpm of flow through the drain cooler at the design conditions.

All necessary air baffling and air vent openings will be provided for properly removing noncondensable vapors from the heater shell. Heaters will be provided with a properly sized vent orifice constructed integrally with the vent connection.

Drain connections will be provided to drain all low points and pockets on the shell and tube side not otherwise drained by nozzles. The final construction drawings of the internal construction of the heaters will show the provisions made to satisfy this requirement.

The heaters will be provided with connections as required. Both heaters will be provided with permanent connections that are suitable for nitrogen blanketing of shell and tube sides of the heaters. All butt welding connections will have weld-end preparation machined in accordance with details to be furnished by the Engineer. Rough flame cuts will not be accepted. The location, number, and size of all connections will be acceptable to the Engineer.

7A.1.2 DEAERATOR

7A.1.2.1 General. This section covers the design, performance and construction criteria for the deaerator.

7A.1.2.2 Type. The deaerator will be a direct-contact, tray-type heater with integral vent condensing equipment and stainless steel trays. The deaerator and the deaerator storage tank will be horizontal, cylindrical steel sheels with the deaerator supported above the deaerator storage tank.

7A.1.2.3 Codes and Standards. The deaerator will be designed and constructed in accordance with the latest applicable requirements of the ASME Boiler and Pressure Vessel Code, the Standards and Typical Specifications for Deaerators and Deaerating Heaters of the Heat Exchange Institute, ANSI B31.1 Code for Pressure Piping, and all governing state and local regulations; and in accordance with the applicable requirements of the Federal "Occupational Safety and Health Standards." The deaerator will bear an ASME code stamp.

7A.1.2.4 Design Criteria. The deaerator will be designed for safe and reliable operation with condensate flows, drain flows and steam pressures in accordance with the turbine and thermal storage unit design parameters.

The deaerator will be designed to remove all dissolved oxygen in excess of 0.005 cc per liter at all loads from 5 per cent to and including rated capacity. During short duration peaking loads the deaerator will be designed to remove all dissolved oxygen in excess of 0.05 cc per liter.

7A.1.2.5 Materials. The following materials satisfy the minimum requirements of the conditions encountered in deaerating feedwater. If the manufacturer's standard construction utilizes materials of equal or superior quality, the manufacturer's standard construction will be used.

Shell	
Deaerating section	Carbon steel - ASTM A515-70
Storage section	Carbon steel - ASTM A515-70
Shell supports	Carbon steel - ASTM A36
Trays	Stainless steel - ASTM A176 Type 430 or ASTM A167 Type 304
Tray supports	Stainless steel - ASTM A167 Type 304 or ASTM A176 Type 430
Vent condenser	
Shell internals	Stainless steel - ASTM A167 Type 304
Baffles and liners	Stainless steel - ASTM A167 Type 304
Spray tubes and vent piping	Stainless steel - ASTM A269 Type 304
Nozzles	Stainless steel - ASTM A276 Type 304
Internal bolting	Stainless steel - ASTM A193 Type 321
Piping, except as otherwise specified	Carbon steel - ASTM A53 Gr B
Fittings	
Butt weld	Carbon steel - ASTM A234
Socket weld	Carbon steel - ASTM A234
Valves	Carbon steel

7A.1.2.6 Construction. Deaerator construction will conform to the ASME Boiler and Pressure Vessel Code, Section VIII, Typical Specifications for Deaerators and Deaerating Heaters of the Heat Exchange Institute, the Code for Pressure Piping ANSI B31.1, and all governing state and local regulations, and the following requirements.

Deaerator shell wall thickness will be determined in accordance with the code utilizing the allowable stress value for the shell material at the design pressure and temperature. Corrosion allowance will be 1/8 inch.

Shells will be all welded steel construction with semiellipsoidal type shell heads.

The shells will be provided with lugs for attachment of platforms as required for accessibility to all parts of the unit. The platforms will be furnished under separate specifications.

The deaerating section and storage section shells will be provided with lifting lugs designed for lifting total assembled weights.

The internal surfaces of the deaerating section shell and shell head will be provided with seal welded stainless steel liners and shields as required to prevent contact with noncondensable gases. Liners and shields will be not less than 1/8 inch thickness and securely attached to avoid possible liner collapse during transient load conditions.

Equalizing piping will be provided between the deaerating and storage sections. The equalizing pipes will be shop fitted so that only a single field weld per pipe will be required. The equalizing piping will protrude into the deaerating section as far as possible without restricting the flow area due to the proximity of the impingement baffles. The equalizing pipes

will be baffled to prevent impingement on the bottom of the trays. The equalizing piping will be of sufficient size and quantity to prevent pressure buildup in the storage section during transient conditions or a unit trip or load reduction when steam supply is lost or reduced. The piping will be liberally sized to limit the pressure differential between sections to 0.5 psi or less.

The deaerating section shell will be provided with a hinged flanged and bolted manhole at each end of adequate size for tray removal but not less than 16 inches by 24 inches.

The storage section shell will be provided with a hinged flanged and bolted manhole at each end not less than 16 inches by 24 inches.

Manholes will be of an acceptable type complete with Flexitallic gaskets. All gaskets will be suitable for use during acid cleaning.

Full information will be submitted on the materials, method of construction of the trays, and the provisions made to prevent chloride stress corrosion.

Deaerating trays and tray supports will be fabricated from 18 USS gage minimum thickness stainless steel. Any welded parts will be bright annealed at not less than 1400 F for Type 430 stainless steel or 1900 F for Type 304 stainless steel.

All trays will be of a convenient size and weight for easy handling and will be interchangeable. Tray racks will be designed to hold the trays securely so that they will not become dislodged while in service.

The bottom of the tray section will not be less than 27 inches from the bottom of the deaerating section shell.

All surfaces which will contact noncondensable vapors will be constructed from stainless steel. All bolting within the unit will be stainless steel.

The deaerator will be furnished with a vent condenser of the internal direct contact spray type. The vent condenser will have adequate condensing capability to limit the oxygen content of the deaerated condensate to the specified maximum and to perform satisfactorily throughout the load range with the maximum condensate inlet temperature specified. All spray valves will be readily accessible for inspection, maintenance and removal without disturbing any internal piping. Spray valve gaskets will be suitable for acid cleaning.

All internal surfaces of the vent condenser including shell, baffles and spray tubes will be constructed from 18-8 stainless steel.

The deaerator will be provided with vent connections as required for discharge of noncondensable gases.

The deaerator will be furnished with spring loaded spray valves. The valves, springs and related components will be stainless steel.

The valves will be hydraulically balanced and not require close fitting guides. Valve springs will be heat trated to retain their elastic properties at the temperature to be encountered.

The storage section will be provided with an internal standpipe overflow having a formed entrance to reduce entrance loss and vortex action. The overflow level will be not less than 1'-0" below the inside top of the storage section.

All inlet distribution pipes will be constructed of Schedule 40, ASTM A269 Type 304 stainless steel and will have provisions to prevent steam from backing into the piping during conditions of low load or no flow.

A distribution system will be provided to minimize stratification in the storage section.

All steam, drip return, condensate return and vent connections and all spray pipes will be provided with ASTM A167 Type 304 stainless steel baffles or shell liners to prevent impingement of steam, water or noncondensable gases on any part of the carbon steel shells. Baffles and liners will be ruggedly constructed of plate not less than 1/4 inch in thickness.

All returns having a temperature 35 F lower than the saturation temperature and flashing mixtures will be introduced evenly into the deaerating section by distribution system.

Pump suction connections will be provided with special antivortex construction.

The feedwater pump recirculation flows will be introduced into the storage section above the water level through a spray pipe or other suitable distribution system. The distribution system will be arranged to introduce the flow with a minimum of disturbance to the stored water.

All interconnecting piping furnished with the deaerator for overflow, vent traps and other devices will be in accordance with the following:

Pipe	- Seamless carbon steel ASTM A53 Schedule 80
Valves	- 2 inch and smaller: 600 lb carbon steel socket welding
Fittings	- 2 inch and smaller: 2000 lb carbon steel socket welding
Fittings	- 2-1/2 inch and larger: Schedule 80 butt welding ASTM A234

The drips from the high pressure heater will be introduced into the inlet steam dome by means of a distribution pipe to evenly distribute the drips.

7A.1.3 FEEDWATER PUMPS

7A.1.3.1 General. This section covers the design and performance criteria for the feedwater pumps.

7A.1.3.2 Type. The pumps will be of the double case barrel, multistage centrifugal type designed for continuous operation in receiver feed service. Each pump will be direct driven by an electric motor. Two feedwater pumps will take suction from the deaerator storage tank and discharge to the receiver and thermal storage subsystems. Each pump will be rated full capacity at the net unit load of 10 MW. Both pumps will operate simultaneously to attain the high flux test mode capacity.

7A.1.3.3 Codes and Standards. All equipment and materials furnished under these specifications will be designed and constructed in accordance with the latest applicable requirements of the standard specifications and codes of ANSI, ASME, ASTM, NEMA, IEEE, EEI, the Hydraulic Institute, and other such regular published and accepted standards.

7A.1.3.4 Design and Performance Criteria. The pumps will be designed to operate reliably in continuous service under the following conditions. The performance indicated will be guaranteed for each of the two pumps.

Number of pumps	2
Capacity, each pump, gpm at 336 F	280
Total head, ft	4730
Maximum rotative speed, rpm	3600
Suction conditions	
Design temperature, F	336
Maximum temperature, F	400

The pumping capacity will be regulated by throttling the pump discharge across feedwater regulators. The pumps will be designed for continuous operation in boiler feedwater service. They will be suitable for operation in parallel at all loads.

The pumps will be specifically designed for pumping water ranging from 55 F to the temperature specified without setting up destructive temperature strains causing warping, buckling, misalignment, rubbing, or other objectionable effects. Adequate clearances will be provided in the pump to accommodate shaft deflections and loss of suction head. Reliability during all operational conditions is a major consideration and the apparent long term reliability of the pump would be emphasized in the evaluation of proposals.

Each pump will be designed to have a head-capacity characteristic which rises steadily from the rated capacity to shutoff. At shutoff the pump head will be not less than 110 per cent nor greater than 125 per cent of the head at the rated capacity.

7A.1.3.5 Materials. Pump materials will be equivalent to or will exceed the strength and corrosion-erosion resistance of the following listed materials:

Casing barrel	Forged carbon steel - ASTM A266 Cl I
Casing head	Forged carbon steel - ASTM A266 Cl I
Inner casing	Stainless steel - ASTM A217, Gr C5
Shaft	Stainless steel - ASTM A276 Type 410 HT
Impellers	Stainless steel - ASTM A296 Gr CA-15
Wearing rings	Stainless steel - AISI Type 416 hardened
Diffusers, diaphragms, and stage pieces	Stainless steel - ASTM A296 Gr CA-15
Balancing drum	Stainless steel - AISI Type 416 hardened

Throttle bushing	Stainless steel - ASTM A362 Gr CA-40 HT
Shaft sleeves	17-4 PH stainless steel or ASTM A362 Gr CA-15 HT
Warmup orifices	Stainless steel - AISI Type 416

All high pressure sealing joint surfaces in the barrel and head and areas subject to high water velocity will be lined with an overlay of 18-8 stainless steel deposited by welding.

7A.1.3.6 Construction. The pumps will be constructed in accordance with the requirements stated in the following paragraphs.

The pump outer casing will be horizontal center line supported and will be of the barrel type arranged so that the pump may be disassembled without disconnecting the suction or discharge piping. Pump inner casing joints will be of the pressure seal type constructed so that the pump discharge pressure acts to seal the joints.

The suction and discharge nozzles will be on top of the pump and project upward and will be prepared for butt welding connections.

All strength welds in the casing will be in strict accordance with the ASME Boiler and Pressure Vessel Code and will be radiographed. All stress levels in the barrel and head will be within the limits of the code requirements.

All impellers will be of the enclosed type, of one-piece case construction, carefully machine finished.

Renewable casing wearing rings designed for ease of replacement will be furnished to prevent excessive leakage between stages.

The pump will be arranged with opposed impellers and/or balancing drum so that hydraulic thrusts are in balance throughout the operating range. The impellers will be individually statically and dynamically balanced and the entire rotating assembly will be assembled and statically and dynamically balanced.

The pump shaft will be conservatively designed for rigidity to limit shaft deflection to not more than one mil at any operating condition. Bearing spans will be kept to the minimum practicable.

The shaft ends will be tapered to permit easy installation of the shaft seal cartridges and to receive the coupling half.

The pump will be provided with shaft seals of the throttle bushing type using condensate injection. Complete information on the type of seal, quantity, temperature, pressure and quality of injection water required will be submitted.

Injection water will be controlled by differential pressure sensing of the seal water pressure and shaft seal pressure to maintain a small outleakage of feedwater through the shaft seals. All injection water control system components required will be furnished. This will include all pressure controllers, sensing elements, control valves, filters, air filter regulators, and pressure gages. Control valves will have adjustable mechanical stops. The controllers and indicating equipment will be mounted on a flush type insert panel suitable for incorporation into a remote gage panel furnished under separate specifications.

The pump seal design will be such as to permit the pumping unit and turbine to coast to a stop following emergency plant trip-out when no injection water will be available.

Radial bearings will be of the split sleeve or tilting pad babbitt lined type. Kingsbury type thrust bearings will be provided in the pump to carry unbalanced end thrust in either direction.

A complete forced feed lubrication system will be provided to supply oil to each pump. The lubrication system will consist of, but not necessarily be limited to, an oil reservoir, main shaft driven oil pump, electric motor driven auxiliary oil pump, filters, heat exchangers, piping, valves and instrumentation.

Heat exchangers will be suitable for 95F cooling water.

The auxiliary oil pump will provide lubrication during startup and shutdown of the feed pump and upon failure of the shaft driven oil pump. The main shaft driven pump will provide lubrication during normal operation.

The feedwater pump and drive motor will be designed for coast-down without damage to the bearings on loss of station service power to the electric motor driven oil pump.

The oil reservoir will be coated internally with "Rustban".

A minimum of three pressure switches will be provided to control the auxiliary oil pump and to annunciate low oil pressure.

All oil piping will be carbon steel, ASTM A53 or A106, Schedule 40 minimum. Socket weld fittings and steel body valves will be used. All oil piping will be provided with sufficient numbers of flanged joints to facilitate assembly.

All miscellaneous piping for the pumps will be installed in a neat workmanlike manner within the confines of the pump base plate.

The pump will be provided with all drain piping required to interconnect bracket drains and other points of drainage and convey them to a common outlet connection. Each bracket drain outlet will be provided with a sight flow fitting.

Pump running clearances will be selected consistent with the requirements for turning gear operation, long term durability, and pumping efficiency.

7A.1.4 CONDENSATE PUMPS

7A.1.4.1 General. This section covers the design and performance requirements for the condensate pumps.

7A.1.4.2 Type. The pumps will be of the vertical shaft, submerged suction "can" type designed for continuous heavy duty service. Two condensate pumps will take suction from the condensate receiver and discharge to the deaerator. Each pump will be rated full capacity at the net unit load of 10 MW. Both pumps will operate simultaneously to attain the high flux test mode capacity.

7A.1.4.3 Codes and Standards. All equipment and materials furnished under these specifications will be designed and constructed in accordance with the latest applicable requirements of the standard specifications and codes of the Hydraulic Institute, ANSI, ASME, ASTM, AGMA, and other such regular published and accepted standards.

7A.1.4.4 Design and Performance Criteria. The pumps will be designed to operate reliably in continuous service under the following conditions. The performance indicated will be guaranteed for each of the two pumps.

Number of pumps	2
Capacity, each pump, gpm	200
Total head, ft.	540
Nominal motor speed, rpm	1800
Suction conditions	
Design temperature, F	134
Maximum temperature, F	200
Allowable shutoff head, ft	
Maximum	675
Minimum	620

The pumps will be designed to operate singly or in parallel with capacity regulated by throttling the discharge. Each pump will be designed to operate satisfactorily both in two pump parallel operation and single pump operation and when bringing on or taking a pump out of service with another pump in service.

The design of the pump shaft will be such that no critical speed will occur within a safe margin of the operating speed range.

Special attention will be given to the selection of pump materials, differential hardening of materials, and running clearances to allow the use of reasonably coarse suction strainers for prevention of galling.

7A.1.4.5 Materials. Pump materials will be equivalent to or will exceed the strength and corrosion-erosion resistance of the following listed materials:

Outer barrel and discharge head	Carbon steel - ASTM A36
Bowls	Carbon steel - ASTM A216 Gr WCB
Impellers	11.5-14 per cent cr stainless steel ASTM A296 Gr CA-15
Shaft	12-14 percent cr stainless steel AISI Type 416 hardened
Shaft sleeves	Stainless steel AISI Type 440C heat treated
Wearing rings	12-14 percent cr stainless steel AISI Type 416 hardened
Bearings	Carbon or graphalloy sleeve
Shaft seal type	Mechanical
Bowl bolting	12 percent cr stainless steel ASTM A193 Type 416
Base plate	Carbon steel ASTM A36

7A.1.4.6 Construction. The pumps will be constructed in accordance with the following requirements.

Suction and discharge piping connections will be flanged with ANSI drilling. Renewable casing wearing rings will be provided. Suitable vent connections will be provided to vent the pump casings and discharge heads to the condenser shell. Each pump discharge will be provided with a one inch pressure gage connection.

The rotating parts of each pump will be statically and dynamically balanced. Impellers will be provided with renewable wearing rings. The pump shafts will be sized to transmit the power requirements of the pumps. Shaft sleeves will be provided. Bearing spans will be the minimum practicable.

Mechanical type shaft seals will be furnished. If the temperature of the pumped liquid exceeds the seal manufacturer's recommendations, a seal liquid heat exchanger suitable for use with a 95 F cooling water supply and all interconnecting piping will be furnished.

All bearings will be of the sleeve type. Pump axial thrusts will be resisted by a thrust bearing located in the motor driver.

The pump bowl sections will be joined by bolted flanges. Screwed joints will not be acceptable. A flanged joint with special seal groove and rubber O-ring will be provided between the discharge head and "can" to permit removal of the pumping element without removal of the "can". Each pump and "can" will be fully shop assembled and shipped as a single unit.

Each condensate pump will be provided with a cylindrical fabricated steel motor support base for mounting the motor directly on the pump discharge head. Access holes sufficiently large and of sufficient quantity will be provided for dismantling the coupling and maintenance and inspection of the pump seal.

The support will be machined and drilled as required to receive and provide for proper alignment and securing of the drive to the support base. All bolting, nuts, washers, and pins required for securing the drives to the support bases will be furnished. Drive motor mounting provisions will be subject to the approval of the motor manufacturer.

Shaft couplings between the pumps and motors will be furnished. The couplings will be of the rigid adjustable type. The pump half couplings will be mounted on the pump shafts. The motor half couplings will be shipped to the motor manufacturer for mounting on the shafts prior to shipment of the motors. Dimensions for the motor half couplings will be subject to approval by the motor manufacturer.

7A.1.5 CONDENSER EXHAUSTERS

7A.1.5.1 General. This section covers the design and performance criteria for the condenser exhauster units.

7A.1.5.2 Type. The condenser exhauster units will be two stage units consisting of an atmospheric air ejector and a water seal ring vacuum pump. The two full capacity condenser exhausters will remove non condensable gases such as air, ammonia and carbon dioxide from the air-cooled condenser. The units will provide vacuum hogging of the condenser and maintenance of condenser vacuum. Each unit will be furnished complete with an air ejector, exhauster pump, separator, seal water pumps, and heat exchanger.

7A.1.5.3 Codes and Standards. All equipment and materials furnished under these specifications will be designed and constructed in accordance with the latest applicable requirements of the standard specifications and codes of ANSI, ASME, ASTM, NEMA, IEEE, EEI, AMCA, AGMA, the Heat Exchange Institute and other such regular published and accepted standards.

7A.1.5.4 Design Criteria. The condenser exhausters will be designed in accordance with the following criteria:

Number of condenser exhausters	2
Holding capacity, each unit, free dry air in a saturated air vapor mixture at 71.5 F and 1.0 in Hg absolute pressure, scfm minimum	8
Hogging capacity, each unit, dry air at 15 in Hg absolute pressure acfm minimum	700
Cooling water supply	
Pressure, psi maximum	125
Temperature, F	95

7A.1.5.5 Construction. Each exhauster will be the manufacturer's standard unit complete with motor, vacuum pump, seal water pump, seal water separator, seal water heat exchanger, jet ejector, pump discharge silencer, control valves, shutoff valves, check valves, pressure and temperature switches, air meter, control air filter regulators, solenoid valves, and all other accessories required for complete remote and automatic operation.

A heavy rectangular steel tube baseplate with drain trough and drain connection suitable for grouting to a concrete foundation will be furnished for each unit.

An air leakage meter for measuring air leakage into the condenser will be provided on each unit.

A discharge silencer will be provided on each seal water separator for a low operating noise level.

The seal water heat exchangers will be suitable for the maximum cooling water pressure of 125 psi.

All parts of the heat exchangers in contact with the seal water will be Type 316 stainless steel.

Pneumatic diaphragm operated check valves will be provided for the condenser exhauster inlets. The quantity and arrangement of the inlet valves will be such as to meet the requirements of automatic operation. The valves will be designed to isolate each unit when idle from the condenser air header, without leakage.

7A.1.6 PIPING

7A.1.6.1 General. This section covers the material requirements for the piping to be furnished under these specifications.

7A.1.6.2 Code Requirements. Except as otherwise specified herein, piping materials and applications of piping materials will be in accordance with the latest requirements of the Code for Pressure Piping ANSI B31.1, the appropriate sections of the ASME Boiler and Pressure Vessel Code, and all state and local regulations where applicable.

7A.1.6.3 Pipeline Listing. Each piping system will be identified and divided into categories on a pipeline listing. Piping materials, wall thicknesses, and operating and design conditions will be designated on the pipeline listings.

7A.1.6.4 Pipe Materials. Materials to be incorporated in permanent piping systems will be new, unused, and undamaged.

Pipe materials will be in accordance with the requirements stated herein. Pipe will be in accordance with the ASTM and ANSI standards designated herein and in the Pipeline Listing.

Schedule numbers, sizes, and dimensions of carbon steel and alloy steel pipe will conform to ANSI B36.10. Schedule numbers, sizes, and dimensions of stainless steel pipe will conform to ANSI B36.19 except where specifically designated in the Pipeline Listing as std wt, Schedule 40, Schedule 60, Schedule 80, Schedule 160, extra strong, or double extra strong, in which case the wall thicknesses will conform to ANSI B36.10.

Carbon steel and alloy steel pipe will be ungalvanized, seamless type unless

otherwise specified in the Pipeline Listing. Stainless steel pipe will be seamless type unless otherwise specified in the Pipeline Listing.

Where standard weight (std wt) pipe is specified, 10 inch and smaller pipe will be Schedule 40; and 12 inch and larger pipe will have 0.375 inch wall thickness.

Either ASTM A106 Grade A or Grade B pipe can be used wherever ASTM A106 Grade A pipe is specified in the Pipeline Listing.

Fittings will be constructed of materials equivalent to the pipe with which they are used. Unless otherwise specified herein or indicated on the drawings, steel fittings 2-1/2 inches and larger will be of the butt welding type; steel fittings 2 inches and smaller will be of the socket welding type.

Wall thicknesses of butt welding fittings will be equal to the pipe wall thickness with which they are used. Fittings will be manufactured in accordance with ANSI B16.9, ANSI B16.28, and ASTM A234 or ASTM A403. Unless otherwise indicated on the drawings, elbows will be of the long radius type.

Forged steel fittings will be used for socket weld and steel threaded connections. Socket weld and threaded fittings will conform to ANSI B16.11. Metal thicknesses in the fittings will be adequate to provide actual bursting strengths equal to, or greater than, those of the pipe with which they are to be used.

Minimum pressure classes of socket weld and threaded fittings to be used with various pipe schedules will be as follows:

Pipe Schedule No.	Minimum Fitting Pressure Class	
	Threaded	Socket Welding
40 or less	2000	2000
80	3000	3000
120	3000	3000
160	6000	4000
Double extra strong	6000*	6000*

Cast carbon steel flanged fittings will conform to ANSI B16.5, and will be of materials conforming to ASTM A216 WCB.

* If the design pressure-temperature conditions listed in the Pipeline Listing exceed the pressure-temperature service ratings stated in ANSI B16.11 for this class of fittings, fittings will be certified by the fitting manufacturer as being suitable for the design pressure-temperature conditions.

7A.1.7 VALVES

7A.1.7.1 General. This section covers the design and construction requirements for valves.

7A.1.7.2 Code Requirements. Valves will be designed and constructed in accordance with the latest applicable requirements of the ANSI B31.1 Code for Pressure Piping and the ASME Boiler and Pressure Vessel Code, except where modified or supplemented by these specifications.

Except as otherwise specified, all steel body valves will be constructed in accordance with the latest applicable requirements of ANSI B16.34 and will be desinged using stress values which do not exceed the maximum allowable stresses specified in the ASME Boiler and Pressure Vessel Code.

Flanged and butt-welding valves will have face-to-face and end-to-end dimensions which conform to the latest requirements of ANSI B16.10.

7A.1.7.3 Valve Materials. Valve body materials will be indicated on the Pipeline Listings and on a Valve List. The following table defines the abbreviations used:

Abbreviations	Description
CS	Carbon steel, ASTM A216 Grade WCB
1-1/4 CR	1-1/4% chromium alloy steel, ASTM A217, Grade WC6
2-1/4 CR	2-1/4% chromium alloy steel, ASTM A217, Grade WC9
5 CR	5% chromium alloy steel, ASTM A217, Grade C5

Stainless steel for stems, discs and seat facings will be AISI Type 410, 420, or ASTM A182 Grade F6. Nickel alloy for seat facing will be Monel metal or other alloy having not less than 60 per cent nickel content.

Except as specified otherwise in the Valve List, valve trim materials for Class 600, 900, 1500, 2500, 4500, and interpolated pressure class valves will be as follows:

Stem	Stainless steel
Disc	Equivalent to body material
Seating surfaces	Stellite faced

Except as otherwise specified in the Valve List, valve trim materials for Class 150, 300, and 400 valves will be as follows:

Stem	Stainless steel
Disc	Equivalent to body material
Seating surfaces	Stainless steel and nickel alloy or hardened stainless steel and stainless steel

7A.1.7.4 Class 600, 900, 1500, 2500, 4500, and Interpolated Pressure Class Valves. The Class 600, 900, 1500, 2500, 4500 and interpolated pressure class valves will be in accordance with the following requirements.

All check valves will be designed for satisfactory operation in both horizontal and vertical piping. Check valves will be of the swing check type unless otherwise specified. Where specified, check valves will be of the nonslam tilting disc type or the stop check type.

All stop check valves will have Y-pattern globe type bodies. Feedwater stop check valves will be checked for size and flow volume by the manufacturer to assure proper operation. The minimum flow to open the valve will be stated in proposal data.

All gate, globe and angle valves will be of the outside screw and yoke design. Valve bodies and bonnets will be heavy pattern type designed to support the valve operators (handwheel, gear, or motor) with the valve in any position and without external support. The valves will be provided with backseating construction.

Bonnet joints will be of the pressure seal or breechlock type.

All Class 600 valves which are 6 inches and larger and all Class 900, 1500, 2500, 4500, and interpolated pressure class valves will have grease lubricated antifriction bearing yoke sleeves.

Gate valves 4 inches and larger will have flexible wedge discs. Split discs will not be acceptable.

All globe valves will be suitable for throttling service.

7A.1.7.5 Class 150, 300, and 400 Valves. Bonnet joints will be of the bolted flange type having flat faced flange facings for Class 150 valves and male and female facings for Class 300 and 400 valves. Bolting for flanged bonnets and yokes will be bolt studs conforming to ASTM A193, Grade B7, with nuts conforming to ASTM A194, Class 2H.

Valve bodies and bonnets will be designed to support the valve operators (handwheel, gear, or motor) with the valve in any position and without external support.

Gate valves 4 inches and larger will have flexible wedge discs. Split discs will not be acceptable.

All gate and globe valves will be of the outside screw and yoke design. Gate and globe valves will be provided with backseating construction.

All check valves will be designed for satisfactory operation in both horizontal and vertical piping. Check valves will be of the swing check type unless otherwise specified. Where specified, check valves will be of the nonslam tilting disc type or the stop check type.

7A.1.8 INSULATION

7A.1.8.1 General. Insulation and lagging materials for the piping and equipment will be furnished as specified below.

All miscellaneous materials required for complete field installation of insulation and lagging will be furnished. This will include such items as insulating cements, sealers, plastic insulation materials, moisture barrier materials, wire, straps, bands, insulation lugs and special supports, lagging attachment screws, and neoprene washers.

7A.1.8.2 Materials. Except as otherwise specified, insulation materials will be calcium silicate in accordance with ASTM C533. Insulation materials will contain no asbestos. Insulation materials will be Johns-Manville Type Thermo-12, or acceptable equal.

All insulating cements for use with calcium silicate insulation will be in accordance with ASTM C195.

Mineral fiber blanket insulation will conform to ASTM C592, Class II, and will have a density of not less than 8 pounds per cubic foot. Insulation conforming to ASTM C592 will have an expanded metal lath facing on one side.

Mineral fiber preformed pipe insulation will conform to ASTM C547.

Antinoise and antisweat insulation, Class H, will be flexible foamed plastic insulation, Armstrong "Armaflex" or acceptable equal. Adhesive for use with this antisweat and soundproofing insulation will be Armstrong No. 520 or acceptable equal.

Piping insulation will be in sectional or segmental forms and equipment insulation will be in rigid block form unless otherwise specified.

Aluminum foil will be single wrap 0.004 inch thickness, dead soft, plain finished.

Wire for securing insulation to piping will be Type 302, dead soft, stainless steel wire in the following gages:

	Size of Pipe		
Insulation	4" & Smaller	6" thru 18"	20" & Larger
Inner layer of double thickness insulation or single layer insulation	18 ga	18 ga	16 ga
Outer layer of double thickness insulation	18 ga	16 ga	14 ga

Straps or bands for securing insulation to equipment will be 3/4 inch by 0.020 inch stainless steel. Wire for use in connection with equipment insulation will be not less than 14 gage, Type 302, dead soft stainless steel.

Studs used for attachment of insulation will be Nelson carbon steel studs in lengths suitable for the insulation thickness.

7A.1.8.3 Jacketing and Lagging Materials. Jacketing and lagging materials will be as specified below.

Aluminum jacket material will be ASTM B209 Alclad 3004, or acceptable equal. All aluminum jacket material will have a stucco embossed finish.

The minimum thickness will be 0.020 inch for jackets used on piping having insulated outside diameters 12.75 inches and smaller. The minimum thickness will be 0.024 inch for jackets used on equipment and on piping having insulated outside diameters larger than 12.75 inches.

Aluminum sheets will be machine rolled and formed to accurately fit insulation curvatures.

Piping elbows with insulated diameters smaller than 13 inches will be jacketed with preformed smooth aluminum elbow jackets, "Aluminels" as manufactured by Preformed Metals Products Company, or acceptable equal.

Aluminum jackets for out-of-doors installation will be provided with an asphalt and kraft paper moisture barrier. The moisture barrier will be attached to the inside surfaces of the jacketing or will be cemented to the insulation before application of aluminum jackets.

Aluminum pigmented sealer will be Benjamin Foster No. 30-45 or 60-64, or acceptable equal.

Screws for attachment of aluminum jackets will be 1/2 inch or 3/4 inch as required and will be of the self-tapping type made from stainless steel or 6061-T6 aluminum alloy. Screws for fastening aluminum to steel will be stainless steel. Screws in out-of-doors lagging will be provided with neoprene washers.

7A.1.8.4 Insulation Supports. Vertical runs of 2-1/2 inch and larger prefabricated steel piping which will be insulated will have insulation support lugs and collars.

7A.1.8.5 Insulation Classes. The letter designations indicated in the Pipeline Listing refer to the following insulation classes and corresponding thicknesses:

Class	Temperature	Pipe Size	Insulation Thickness Inner Layer	Outer Layer	Total
A	801 F to 1005 F	1-1/2" & Smaller	2"	None	2"
		2" - 3"	2"	1-1/2"	3-1/2"
		4" - 8"	2"	2"	4"
		10" & Larger	3"	2"	5"
B	501 F to 800 F to	1-1/2" & Smaller	2"	None	2"
		2" - 4"	1-1/2"	1"	2-1/2"
		5" - 10"	1-1/2"	1-1/2"	3"
		12" & Larger	2"	2"	4"
C	301 F to 500 F	2" & Smaller		1-1/2"	1-1/2"
		2-1/2" - 10"		2"	2"
		12" & Larger		2-1/2"	2-1/2"
D	150 F to 300 F	2" & Smaller		1" or Std	1" or Std
		2-1/2" - 10"		1-1/2"	1-1/2"
		12" & Larger		2"	2"
E	501 F to 800 F	Equipment	1-1/2"	1-1/2"	3"
F	301 F to 500 F	Equipment		2"	2"
G	150 F to 300 F	Equipment		1-1/2"	1-1/2"
H	Antinoise and Antisweat	All Pipe Sizes and Equipment		1/2"	1/2"
I	Antifreeze for Piping Below 150 F	All Pipe Sizes		1"	1"

7A.2 EGS MAJOR ELECTRICAL DESIGN COMPONENT SPECIFICATIONS

7A.2.1 GENERATOR

7A.2.1.1 Design Basis. The generator kVA rating will be based on the kilowatt capability of the turbine at maximum receiver output steam flow.

7A.2.1.2 Description. The generator will be an alternating current unit especially designed for direct connection to a steam turbine. The generator will be totally enclosed, self-ventilated, non-salient pole type with water to air cooling.

7A.2.1.3 Design Conditions. The preliminary generation design criteria is as follows:

Rated kVA at maximum	18,750
Output voltage, kV	13.8
Output characteristics	3 phase, 60 hertz
Power factor, per cent	80.0
Short circuit ratio, minimum	0.58
Telephone influence factors, maximum	
Balanced	100
Residual	75
Stator insulation	Class B
Field insulation	Class B

7A.2.2 EXCITATION SYSTEM

7A.2.2.1 Design Basis. The exciter will be the manufacturer's standard arrangement and will be rated at the same conditions as the generator.

7A.2.2.2 Description. A complete voltage regulation and static excitation system will be furnished with the generator. The major components of the excitation section will be the excitation potential transformers (EPT), the excitation current transformers (ECT), a field breaker, independent three-phase, full wave bridge rectifier assemblies and collector assembly. The voltage regulator section will consist of an automatic, a-c voltage regulator with reactive current compensator, maximum excitation limit equipment, a d-c voltage regulator for generator field voltage control, and an excitation system start-up circuit.

7A.2.2.3 Design Condition. The exciter will be designed for a response ratio of 0.5.

7A.2.3 GENERATOR NEUTRAL GROUNDING

7A.2.3.1 Design Basis. The neutral grounding equipment will be capable of limiting the generator ground current to approximately 5 amperes and will be capable of withstanding a generator ground fault for a minimum time of one hour duty cycle.

7A.2.3.2 Description. The equipment will be contained in a metal-enclosed, floor mounted enclosure and will consist of the following:

A single phase, nonflammable liquid filled distribution type transformer.

A loading resistor connected shunt to the secondary of the distribution transformer.

A single-pole single-throw, hook operated, disconnecting switch for isolating grounding equipment from the generator neutral.

A voltage relay for remote ground fault annunciation.

7A.2.3.3 Design Conditions. The design conditions for the neutral grounding equipment will be as follows:

Distribution Transformer

Primary voltage, kV class	Approximately 14
Secondary voltage, volts	120/240

The kVA rating will be determined from calculations involving the capacitances of the generator, the surge capacitors, the generator leads, and the generator transformers. The rating will be selected for a minimum of one hour duty cycle.

Loading Resistor

The resistance and current rating will be determined from the above calculations. The resistor will be sized for a minimum of one hour duty cycle.

7A.2.4 GENERATOR CONNECTION EQUIPMENT

7A.2.4.1 Design Basis. The generator connection equipment consists of the generator main leads, the generator current transformers, the non-segregated phase bus duct, and the neutral closure.

The generator will have six high voltage main leads.

The generator will be supplied with 16 bushing current transformers for relaying and metering service.

The non-segregated phase bus duct will be designed to carry 1200 amperes from the generator bushings to the generator breaker and from the generator breaker to the generator transformer at its self-cooled continuous current rating. The bus tap to the secondary unit substation transformers will be sized to carry the full load current of one transformer. Both the main bus and the tap will be designed to carry the maximum short circuit current deliverable by the generator and the external system.

The neutral closure will be furnished with the generator.

7A.2.4.2 Description. All six main leads will be brought out of the machine through bushings such that either end of the windings can be used for grounding or as generator power terminals. The main power terminals are to be suitable for connection to the non-segregated phase bus duct.

Seven current transformers, three of which are to be factory calibrated for metering accuracy, will be installed on the three high voltage bushings. The other nine current transformers will be installed on the three neutral bushings.

A terminal box with shorting type terminal blocks will be provided for mounting near the current transformers and all current transformer secondary leads will be wired to these terminal blocks.

The bus duct will be non-segregated phase construction with a tap for the potential transformer and surge protection equipment from the main bus. The tap to the secondary unit substation will be made in the generator breaker equipment. The bus duct conductors will be insulated aluminum mounted on glass polyester insulator supports and are enclosed in a steel rectangular housing.

The neutral closure equipment will consist of a complete set of materials and accessories necessary to electrically close the generator neutral at the generator neutral terminals. A suitable clamp type connector will be furnished on the netural buswork for connecting an insulated cable in conduit which will extend from the closed neutral to the grounding unit. A metal enclosure will completely encase the generator neutral bushings and associated connecting buswork.

7A.2.4.4 Design Conditions. Each current transformer will have 10L800 relaying accuracy or be in the .3B2 metering accuracy class.

The non-segregated phase bus duct will be designed for the following conditions:

Rated voltage, kV	15
Insulation level - BIL, kV	110
Current rating, amps	1200
Momentary asymmetrical current rating, amps	up to 80,000
Temperature rise above 40°C Ambient, C	65
Type cooling	self

7A.2.5 SURGE PROTECTION EQUIPMENT AND POTENTIAL TRANSFORMERS

7A.2.5.1 Design Basis. The surge protection equipment will be designed to protect the generator windings from the effects of overvoltages due to transient and switching surges. The potential transformers will be used for metering, relaying and voltage regulating functions and will have the capacity and accuracy to allow proper operation.

7A.2.5.2 Description. The equipment will be contained in a floor mounted metal enclosure and will consist of the following:

Three station type lightning arresters designed for rotating machine protection with low flashover breakdown.

Two sets of three single bushing potential transformers with each set to be connected grounded wye-wye. The transformers will have current limiting fuses on the primary side. Secondary fuses will be provided for circuitry protection and isolation.

Three surge capacitors designed for rotation machine protection.

7A.2.5.3 Design Conditions. The surge protection equipment and potential transformers will be designed for the following conditions:

Lightning Arrester

Line to ground voltage of machine, root mean square, kV	7.98
Arrester rating, kV	15

Potential Transformers

Rated voltage - primary, kV	15
Operating voltage	
Primary, kV	7.98
Secondary, volts	63.5
Insulation level - BIL, kV	110
Accuracy	Not less than 0.3 for W, X, Y and Z burdens.

Surge Capacitors

Capacitance, microfarads per phase	0.125
Machine voltage - phase to neutral, kV	7.98
Voltage rating, kV	15

7A.2.6 GENERATOR BREAKER

7A.2.6.1 Design Basis. The generator breaker will be designed to carry the full load amperes of the generator and interrupt the maximum available short circuit current deliverable by the generator or the external system.

7A.2.6.2 Description. The generator breaker will be used to isolate the generator from the utility system and to synchronize the generator to the utility system. It will be a stored-energy type breaker located in metal-clad switchgear. The breaker will be capable of being operated remotely from the station control room.

Included with the breaker will be potential transformers for synchronizing and relaying and a tap for making the connection to the secondary unit sub-station.

7A.2.6.3 Design Conditions. Preliminary ratings of the generator breaker are as follows:

Nominal voltage, kV	13.8
Rated voltage, kV	15
Nominal fault rating, MVA	500
Continuous current rating, amperes	1200

7A.2.7 GENERATOR TRANSFORMER

7A.2.7.1 Design Basis. The generator transformer will be designed to deliver at its high voltage terminals the full load of the generator minus transformer losses and minus maximum auxiliary power. The generator transformer will be designed to deliver its maximum ouput at the maximum ambient air temperatures that prevail at the site.

7A.2.7.2 Description. The generator transformer will have two windings and will be of outdoor construction.

Cooling equipment will have two sources of power with an automatic throwover switch.

Provisions for mounting station type lightning arrestors near each high voltage bushing.

The transformer low voltage bushings will be arranged for connection to the non-segregated bus duct.

Two relaying accuracy current transformers will be provided on each high voltage bushing and one relaying accuracy current transformer will be provided on the neutral bushings.

7A.2.7.3 Design Conditions. Preliminary ratings for the transformer are as follows:

Number of phases	Three
Maximum capacity at 55°C rise, MVA	20
Maximum capacity at 65°C rise, MVA	22.4
Class	OA/FA/FA

Coolant	Transformer oil
Frequency, Hz	60
High voltage, kV grounded wye, nominal voltage	138
Basic impulse level (BIL), kV	450
Low voltage, kV delta, nominal voltage	13.8
Vector relationship	ANSI Standard
Impedance	Minimum Industry Standard
Taps	Standard no-load taps

7A.2.8 PROTECTIVE RELAYING

7A.2.8.1 Design Basis. The protective relaying system will be designed so that any 3-phase, phase-to-phase or phase-to-ground fault which might occur in the plant electrical system will be detected and cleared through a coordinated application of relays.

7A.2.8.2 Description. In detecting the existence of faults or other electrical abnormalities on the plant system, the protective relaying scheme will be designed to provide for the following:

Generator protection

Generator transformer protection

480 volt secondary unit substation protection

In addition, any relays selected will coordinate with the protective devices supplied with major equipment items and with the thermal limits of electrical equipment (transformers and motors).

7A.2.8.3 Design Conditions. Protection for each of the plant subsystems will be provided as follows.

Generator protection will be selected to protect against the following faults and malfunctions.

Generator phase faults

Generator ground faults

Stator open circuits and unbalanced currents

Backup protection for external system faults

Loss of excitation

Potential circuit monitoring

Excessive volts per hertz

Reverse power flow

Generator transformer protection will be selected to protect against the following faults and malfunctions.

Phase faults

Ground faults

High pressure

Combustible gas

High temperature

The 480 volt Secondary Unit Substation. Protection will be selected to protect against the following faults and malfunctions.

Overcurrent

Phase faults

Ground faults

High temperature

7A.2.9 SECONDARY UNIT SUBSTATION

7A.2.9.1 Design Basis. The secondary unit substation will be designed to serve as the distribution center for the larger motors and to smaller distribution centers. It will be capable of interrupting the maximum short circuit current deliverable by the generator and utility system.

7A.2.9.2 Description. A double ended substation will be used with an electrically operated tie breaker provided to supply backup power to either end of the SUS should a loss of normal power occur.

Transformers will be of the ventilated dry type suitable for indoor use and furnished with two 2-1/2 percent taps above and below rated primary voltage. Provisions will be made for further forced-air cooling.

Provisions for connection to non-segregated phase bus duct will be made for incoming feeders to the SUS transformers.

7A.2.9.3 Design Conditions. Preliminary ratings are as follows:

Transformers	
High voltage, KV nominal, delta	13.8
Low voltage, V nominal, wye grounded	480
Impedance, percent	5.75
Switchgear rating, KVA	1500
Main breakers, amperes	
Continuous	3000
Symmetrical interrupting	65,000
Feeder Breakers, amperes	
Continuous	600
Symmetrical interrupting	30,000

7A.2.10 MOTOR CONTROL CENTER

7A.2.10.1 Design Basis. Distribution of 480 volt auxiliary power to motors 100 horsepower and smaller and to other 480 volt loads will be provided by motor control centers.

7A.2.10.2 Description. Motor control centers will utilize plug-in type circuit breaker combination starters for motor control circuits and molded case circuit breakers for power feed applicaitons. Starters will be the full voltage type, complete with 3 phase manual reset thermal overload relays, 120 voltac operating coils, and 480-120 volt control transformers.

7A.2.10.3 Design Conditions. Circuit breakers will be rated not less than 22,000 amperes rms symmetrical interrupting capacity at 480 volts. Magnetic only trip devices will be used when circuit breakers are a part of a combination motor starter. Circuit breakers will be furnished with thermal magnetic trip devices when used as feeder breakers.

7A.2.11 CONDUCTORS

7A.2.11.1 Design Basis. Electrical conductors will be designed for the insulation level applicable to the system voltage on which they are used, and will have ampacity ratings suitable for the load being served.

7A.2.11.2 Description. The physical characteristics of the required types of cables are as follows:

Medium voltage cable	Single conductor
Low voltage cable	1/0 AWG and larger -single conductor. Less than 1/0 - three conductors
Multiconductor control cables	Several types such as 2/C, 3/C, 5/C, & 7/C as well as several sizes such as #14 AWG, #12 AWG, and #10 AWG will be used
Multiconductor instrumentation cable	Twisted pair of #16 AWG shielded
Thermocouple extension cables	
Communication cable	
Lighting	Single conductor

7A.2.11.3 Design Conditions. Insulated electrical conductors will be designed to distribute power and to provide control, instrumentation, and monitoring circuits.

The selection of the insulating and jacketing materials, and the conductor configuration for various types of cables will be based on economic, environment and installation considerations. Cables will conform to the latest applicable standards of the Insulated Power Cables Engineers Association (IPCEA).

Cable insulations will be specified for 90 degree C maximum conductor temperature. Cable jackets will be specified with chemical substances that are flame resistant. Individual conductors of multiconductor cables will have flame resistant insulation or jackets.

Control cable will be multiconductor with overall jacket. Color coding of individual conductors will be in accordance with IPCEA S-19-81, Part 5, Method 1.

Thermocouple extension cable conductors will be the same material as the thermocouples and will be of suitable accuracy class as defined by the Instrument Society of America (ISA).

7A.2.12 MOTORS

7A.2.12.1 Design Basis. Electrical motors will be designed for maximum load requirements and service conditions of the mechanical equipment to be driven.

7A.2.12.2 Description. The motors will be the manufacturer's proven standard design, will be self-cooled and will have enclosures suitable for the location in which they are to be installed.

All motors will have nonhygroscopic insulation rated for temperature rise and ambient temperature in accordance with NEMA MG1 standards for motors having a service factor of 1.0. The allowable temperature rise for motors having a service factor greater than 1.0, when operating at service factor load, will not exceed that rise allowed for motors with a service factor of 1.0. The allowable temperature rise will be reduced in accordance with NEMA MG1 standards when ambient temperatures greater than 40 C are specified.

7A.2.12.3 Design Conditions. All ac motors less than 3/4 horsepower will be rated 120 volts, single phase, 60 hertz. All motors 3/4 horsepower and larger will be rated 460 volts, 3 phase, 60 hertz. The loading of motors having a service factor of 1.0 will be specified not to exceed 87 percent of the motor nameplate rating, while those with a service factor of 1.15 will be specified not to exceed the motor nameplate rating.

Direct current motors for emergency use will be rated 125 volts dc.

Motors in high temperature areas will be designed for operation in 50 C or 65 C ambient temperature. Motors in other areas will be designed for operation in 40 C ambient temperature.

7A.2.13 RACEWAY SYSTEM

7A.2.13.1 Design Basis. The raceway systems will be designed to support and protect electrical cable at the lowest possible cost.

7A.2.13.2 Description. Direct buried cables and various types of raceway will be used including cable trays and conduit.

7A.2.13.3 Design Conditions. Specific design conditions will be as follows.

Individual tray systems will be established for the following services:

15 KV power cables

480 KV power calbes

Control cables & plant communication cables

Special noise sensitive circuits & instrumentation cables

Direct buried cables will have at least 2 feet of earth cover.

7A.2.14 ESSENTIAL SERVICE POWER SYSTEM

7A.2.14.1 Design Basis. The essential service power system is designed to maintain an electrical supply under normal or abnormal operating conditions to those loads which are necessary for personnel and major equipment protection.

7A.2.14.2 Description. The essential service power system will consist of a d-c power system and an a-c power system.

The d-c power system will include a 125 volt station type battery, two battery chargers and d-c distribution panels. Normally only one battery charger will serve the battery and its associated loads with the other battery charger being available as a backup source of power.

The a-c power system will consist of a reliable 3-phase 480 volt a-c bus and a continuous or uninterruptible 120 volt a-c bus. The 480 volt bus will be connected to either a second incoming feeder from the utility or a small site-installed diesel generator set. The uninterruptible power supply will be fed from the d-c power system through static inverters and a static switch that will automatically switch to a regulated 480-120 volt transformer should the inverter fail. The configuration of this uninterruptible power supply is shown in Figure 7C-1.

7A.2.14.3 Design Conditions. Equipment ratings for this system will be determined after loads are identified.

7A.2.15 COMMUNICATIONS SYSTEM

7A.2.15.1 Design Basis. The following three types of communications systems will be provided:

Station-to-off site voice communications

Intrastation voice communications

Checkout and maintenance communications

7A.2.15.2 Description. The station-to-off-site voice communications system will be supplied and installed by the local telephone utility. Commerically leased dial-type telephone handsets will be provided in the main control room and offices for person-to-person communication.

The intrastation voice communications system will consist of a network of telephone type receiver-transmitter handsets, circuit selector switches, speaker-amplifiers, and loudspeakers all connected as one unit. Each handset station will have one page circuit and five party line circuits.

The checkout and maintenance communications system will consist of a permanently interconnected series of jacks and portable headsets. Stations of this system will be located in the control room and in the vicinity of equipment or devices requiring periodic testing, calibration, or maintenance. Consideration will be given to the use of radio communication for work in the heliostat field.

7A.2.16 LIGHTING SYSTEM

7A.2.16.1 Design Basis. The lighting systems will be designed to provide at least the minimum illumination levels recommended by the Illuminating Engineering Society (IES).

7A.2.16.2 Description. The lighting systems required will consist of a temporary construction lighting system and the permanent lighting system which will include an emergency lighting system.

7A.2.16.3 Design Conditions. Temporary construction lighting will be required in many plant areas until such time as the permanent system is installed. Temporary lighting will conform with the Occupational Safety and Health Act (OSHA) title 29, Chapter 17, Part 1926, Subparts D&K.

The permanent lighting system will be supplied 120 volt ac power from panelboards fed from a motor control center. The emergency lighting system will be provided with 125 volt dc standby power as well as its normal 120 volt ac power and will be switched to the 125 volt dc power when the 120 volt ac power is lost.

Types of light sources, control, convenience outlets and fixture supports will be developed later.

7A.2.17 STATION GROUNDING SYSTEM

7A.2.17.1 Design Basis. The station grounding system will be designed for protection of personnel and equipment from the hazards of electric circuit faults and lightning.

7A.2.17.2 Description. The station grounding system will consist of bare copper standard cable and ground wells. The ground cable will be buried in the soil below the plant ground floor concrete slab in a grid pattern. Each junction of the grid pattern will be securely bonded together by a thermal welding process. The grid will be connected to driven ground rods or a ground well and, where required, cable will be extended upward from the grid for connection to building steel columns, major electrical equipment and the lightning protection system.

7A.2.17.3 Design Conditions. The size of the ground grid conductors will be based on the following information.

The calculation of touch potential will be with an assumed body resistance of 1000 ohms, a duration of fault for 8 cycles and a touch contact resistance of 1.5 ρ_s (where ρ_s is the resistivity in ohm - meters of the soil near the surface).

Maximum fault on the transmission line will be determined after site selection.

Ground resistivity will be determined at the site.

Calculations will be made according to IEEE-80, 1961, "Safety in Alternating - Current Substation Grounding."

7A.2.18 CATHODIC PROTECTION

7A.2.18.1 Design Basis. Buried steel pipe will be adequately protected to minimize corrosion.

7A.2.18.2 Description. Protective measures to prevent rapid corrosion of underground piping will include:

Electrical isolation

Dielectric coating

Cathodic protection or concrete encasement

7A.2.18.3 Design Conditions. Selection of the protective measures to be employed for each buried pipe section will be determined on an individual basis after the extent, location, type material, and other features of each pipe have been determined.

7A.2.19 CONSTRUCTION POWER

7A.2.19.1 Design Basis. A construction power system will be designed to assure electrical power is available for all construction activities when, where and in the quantities required.

7A.2.19.2 Description. Arrangements will be made with the local electric utility for line construction from existing facilities, to the station site at the time required to properly coordinate with site construction requirements.

17.2.19.3 Design Conditions. The temporary power system will be designed to maximize personnel safety and to minimize interference with construction activities and permanent equipment.

7A.3 EGS GENERAL STRUCTURAL DESIGN CRITERIA

7A.3.1 DESIGN STANDARDS

7A.3.1.1 General. The designs and specifications of all structural, architectural and general construction components will be in accordance with the applicable local codes and ordinances, with the laws and regulations of the state in which the plant is built, and with recognized industry standards.

7A.3.1.2 Design Standards. Specifications for materials will refer to one or more of the sta ndard specifications of the American Society for Testing Materials (ASTM) and the American National Standards Institute (ANSI) insofar as they are applicable.

Field and laboratory testing of materials will follow standard specification procedures of ASTM.

The design and placement of structural concrete will follow the codes and standard practices of American Concrete Institute (ACI).

The design, fabrication and erection of structural steel will follow the applicable specifications of American Institute of Steel Construction (AISC).

The fabrication and erection of grating will follow applicable standards of the National Association of Architectural Metal Manufacturers (NAAMM).

Welding procedures and qualification of welders will follow codes and recommended practices of the American Welding Society (AWS).

Railroad design and track work construction will follow standard specifications and recommended practices of the American Railway Engineering Association (AREA).

Plumbing design and construction will follow practices of the National Plumbing Code (NPC).

The design will conform to the requirements of the Occupational Safety and Health Administration (OSHA).

Occupancy requirements will be based upon recommendation of the Uniform Building Code (UBC). Materials and construction practices for wood and masonry will be specified in accordance with the Uniform Building Code.

Wind and snow loading will be calculated and applied in accordance with the provisions of the American National Standards Institute (ANSI) A58.1, 1972.

Seismic design and analysis will be in accordance with the 1973 edition of the Uniform Building Code (UBC).

7A.3.2 DESIGN LOADS

7A.3.2.1 General. Design loads for all structures will be determined using the following criteria.

7A.3.2.2 Dead Loads. Dead loads will be determined using the actual weights of the structure and all equipment of a permanent or semi-permanent nature, including tanks, piping, electrical trays, bus ducts, and the contents of tanks, pipe, etc..., measured at full capacity.

7A.3.2.3 Live Loads. Live loads will be determined using assumed unit loadings deemed sufficient to provide for movable or transitory loads such as people, portable equipment, and fixtures and parts laydown during maintenance.

Ground floor slabs of all major structures will be designed for a minimum of 250 psf in all areas where a 2-ton fork lift truck can operate. Appropriate areas of the ground floor slabs will also be designed to support the operating loads of construction cranes. Ground floor slabs of auxiliary buildings will be designed for a live load of 150 psf. The live load to the supporting pile caps will be not less than 150 psf for all structures.

Suspended concrete floor slabs will be designed for a uniform loading of 100 psf with the exceptions as listed herein. The turbine generator area building operating floor will be designed for the weights of specifically located major parts or skid loads of the turbine or generator components as imposed during construction and maintenance, but not less than 250 psf uniform loading over the entire area. Grating in this area, if any, will be designed for 250 psf uniform loading. Control and computer room floors will be designed for the weights of equipment, but not less than 150 psf uniform loading. Storage areas will be designed as appropriate for the weight and height of material stored, but not less than 100 psf.

Grating floors will be designed for a uniform loading of 75 psf to the support beams. The grating will be selected for a uniform loading of 175 psf to minimize deflection.

Floors and supporting members which are subject to heavy equipment live loads will be designed on the basis of the weight of the equipment plus a uniform live load of 50 psf, or the preceding live loads, whichever is greatest. Each member in the floor system subject to these moving loads will be designed for the heaviest piece or pieces of equipment in the most critical position.

7A.3.2.4 Impact Loads. The following minimum impact loads will be used in addition to other loads for components supporting reciprocating or rotating machines, elevators, hoists, cranes, or other equipment creating dynamic forces.

Elevators	100 percent of lifted load
Hoists and Cranes	
Vertical	25 percent of lifted load
Horizontal	20 percent of the sum of the lifted load plus the weight of the hoisting component
Logitudinal	10 percent of the total moving load
Rotating and Reciprocating	
Equipment	50 percent of the machine weight
Hangers Supporting	
Floors and Platforms	33 percent of the sum of the dead load and reduced live load

Consideration will be given to problems of vibration isolation and dampening. Rational analysis will be used to dissipate forces in structural systems or to isolate foundations from abutting structures by dampening materials or vibration isolators.

7A.3.2.5 Pipe Hanger Loads. Pipe hanger loads for the high pressure steam, boiler feed, condensate and extraction systems will be specifically determined and located. Piping expansion and dynamic loads will be considered on an individual basis. Loads imposed on perimeter beams around pipe chase areas will also be considered on an individual basis.

Pipe loads for other areas will be treated as uniform loads per square foot of floor area and will be carried to columns and foundations as dead loads. These loads will be determined on a bay basis. In addition to the uniform dead load, a concentrated load will be applied at the center of all primary beams for purposes of sizing the beam. This load will not be carried over to the sizing of other beams or columns.

7A.3.3 FOUNDATIONS

7A.3.3.1 Soil Data. A soils investigation program will be required to determine the soil classification and structural properties of the soils at the site. The data and report on these borings will be studied prior to detail design of substructures and foundations to establish foundation design criteria based on the site soil conditions.

7A.3.3.2 Foundation Types. The foundations for the main plant structure will be on piling of low bearing capacity. Load tests will be made on a minimum of three piles to establish a minimum length, blow count, and to confirm the design load carrying capacities. Designs requiring cluster piles will take into account the group effect by derating the load carrying capacity of individual piles by a fixed percentage.

The foundation system for miscellaneous structures could be spread footings on select compacted fill where the load concentration on the soil allows. If the load concentration would result in excessive settlements, or construction restrictions preclude use of spread footings, piling will be used.

7A.4 EGS GENERAL CHEMICAL DESIGN CRITERIA

7A.4.1 CYCLE MAKEUP WATER FACILITIES

7A.4.1.1 General. The cycle makeup water facilities will supply high purity water to the high pressure steam and feedwater cycle. Cycle makeup water will be required at a rate of about one per cent of maximum steam flow.

7A.4.1.2 Description. Initial fill and makeup to the steam cycle will be provided by a demineralization system capable of providing high purity water. The demineralization system effluent would be characterized as follows:

Total dissolved solids (TDS)	50 micrograms/liter
Silica (SiO_2)	10 micrograms/liter
Dissolved oxygen (DO)	20 micrograms/liter

The purity limits listed above for cycle makeup are desirable, as feedwater to receiver and/or thermal storage unit should at all times have characteristics equal to or better than as follows:

TDS	25 micrograms/liter
SiO_2 (soluble)	5 micrograms/liter
SiO_2 (total)	20 micrograms/liter
Suspended solids	10 micrograms/liter
Total iron	5 micrograms/liter
Total copper	2 micrograms/liter

The demineralization process selected will be based on the quality of the water supply to the demineralization system. A multiple bed system is probable as the most appropriate selection.

7A.4.2 CONDENSATE POLISHING EQUIPMENT

7A.4.2.1 General. Condensate polishing equipment will enable the quality of the condensate and feedwater of the cycle to be maintained at a high purity level during both normal operation and startup. The use of high purity feedwater will allow operation of the receiver and thermal storage unit at essentially zero blowdown, while at the same time allowing production of high purity steam. Without the use of high purity feedwater, the receiver, thermal storage unit and turbine capability will not be maintained. Experience with both small and large fossil fuel power plants, which are subjected to numerous startup and shutdowns, has also proven that condensate polishing will allow quicker startups with minimal problems due to solids in the boiler water.

7A.4.2.2 Description. Suspended and dissolved solids will enter the water/steam cycle continuously during normal operation. Suspended solids will result from oxygen inleakage and are generally corrosion products. Dissolved solids may be introduced through water-to-water or water-to-steam heat exchanger leaks, or they may be introduced in the makeup water. A properly designed and properly operated demineralizer, however, will assure little contribution of dissolved solids to the cycle through makeup water.

There is also potential leakage into the water/steam cycle of salt from the thermal storage unit. If salt leakage is designed for, then condensate polishing by mixed bed ion exchange will be required to remove the salts.

If salt leakage is determined to not be a possibility, and the dissolved solids load is established to be light then filters could be used for

condensate polishing instead of ion exchange. Solka-Floc may be an appropriate filter material. The high temperature of the condensate, due to the higher than normal turbine backpressures that are anticipated, could also eliminate the possibility of using mixed bed ion exchange equipment. For such a case, powdered resin and/or Solka-Floc filters (filter-demineralizers) could be used.

The type of polishing equipment to be used will be determined after more specific system parameters are established.

7A.4.3 SERVICE WATER FACILITIES

7A.4.3.1 General. Water will be provided to supply the demineralization system, general service and potable water uses. To avoid complexities and potential dangers of a dual water system, "service water" will be of potable water quality. The type of water pretreatment system required, if any, will depend on the characteristics of the available water supply.

7A.4.3.2 Description. Possible pretreatment steps might be aeration, lime softening or clarification, or iron removal, or a combination of these steps, followed by filtration. The capacity needed may be on the order of 25 to 50 gpm, assuming storage of service water is provided for in adequate manner. The type of treatment, type of equipment employed, as well as storage capacity will influence the system capacity selected.

7A.4.4 CYCLE MAKEUP WATER AND SERVICE WATER STORAGE FACILITIES

7A.4.4.1 General. Storage of condensate, demineralized water, and service water will be provided to supply high rate of flow demands as well as large volume demands. Separate storage tanks will contain the high purity demineralized water and condensate, and service water.

7A.4.5 WATER QUALITY CONTROL SYSTEM

7A.4.5.1 General. Chemical conditioning of the main steam and feedwater cycle, and of the closed cooling water system, will be required. Hydrazine, and possibly ammonia, will be fed into the water/steam cycle. The hydrazine would serve in the removal of dissolved oxygen not removed by mechanical deaeration. The hydrazine and ammonia would be used to adjust water condition to minimize corrosion of steel and copper alloy components. The closed cooling water system, containing high purity water, would be conditioned by chromate feed to minimize corrosion.

Sampling and analysis would be provided to allow monitoring of water/steam systems, thus providing operating personnel with necessary intelligence to allow proper station operation.

7A.5 MAJOR PLANT SERVICES DESIGN SPECIFICATIONS

7A.5.1 AIR COMPRESSORS

7A.5.1.1 General. This section covers the design and performance requirements for the air compressors.

7A.5.1.2 Type. The air compressors will be of the single stage, double acting, heavy-duty, water cooled, V-belt driven, horizontal or vertical cylinder type. The instrument air compressor will be of the oil-free non-lubricated type. The service air compressor will be of the standard oil lubricated type. The compressors will be furnished complete with receivers, filters and dryers.

7A.5.1.3 Codes and Standards. All equipment and materials furnished will be designed and constructed in accordance with the latest applicable requirements of the standard specifications and codes of ANSI, ASME, ASTM, NEMA, IEEE, AMCA, AGMA, HEI, and other such regular published and accepted standards.

7A.5.1.4 Design Criteria. The air compressors will be designed and constructed to operate reliably in continuous service under the following conditions. The performance indicated will be guaranteed for each of the two compressors.

	Instrument Air Compressor	Service Air Compressor
Number of compressors to be furnished	2	2
Discharge pressure, psi	100	100
Capacity, free air with inlet conditions at 14.7 psia and 60F, scfm	100	100

	Instrument Air Compressor	Service Air Compressor
Cooling water supply		
Pressure, psi	125	125
Temperature, F	95	95
Discharge air temperature from aftercooler, maximum, F	105	105
Maximum motor speed, rpm	1800	1800
Receiver design pressure, psi	125	125

7A.5.2 CLOSED COOLING WATER EQUIPMENT

7A.5.2.1 General. This section covers the design and performance requirements for the closed cooling water equipment.

7A.5.2.2 Type. The closed cooling water equipment will consist of horizontal split case centrifugal pumps, an air-cooled water cooler, and a humidifying air precooler or mechanical refrigeration unit. The closed cooling water will provide a heat sink in which the heat rejected by plant equipment (air compressors, turbine oil coolers, generator air coolers) can be controlled and the proper operating temperature of such equipment can be maintained.

7A.5.2.3 Codes and Standards. All equipment and materials furnished will be designed and constructed in accordance with the latest applicable requirements of the standard specifications and codes of the Hydraulic Institute, ANSI, ASME, ASTM, NEMA, IEEE, EEI, TEMA, the Heat Exchange Institute, and other such regular published and accepted standards.

7A.5.2.4 Design and Performance Criteria. The closed cooling water equipment will be designed to operate reliably in continuous service. The system pumping capacity, auxiliary equipment heat loads and cooling water design temperature will be determined from equipment requirements and ambient design temperatures.

Treated condensate quality water will be circulated in a closed loop system to all auxiliary equipment requiring cooling water. The temperature of this circulating water will be controlled and maintained to some temperature in

the range of 95 F to 110 F. The circulating water, after absorbing the heat load rejected by the plant auxiliaries being cooled, will be passed through an air-cooled heat exchanger and cooled to the design temperature for reuse. During periods when the ambient air temperature becomes too high for cooling purposes, a humidifying air precooler or some means of mechanical refrigeration will be used to lower the air temperature. During periods when the ambient air temperature drops below freezing level the circulating water passing through the air-cooled exchanger will be protected from freezing by diverting warm air from the exchanger air discharge to the exchanger air inlet. The warm air will mix with and heat the incoming colder air to maintain the air temperature entering the cooling section above freezing.

7A.5.3 TURBINE LUBE OIL CONDITIONER

7A.5.3.1 General. This section covers the design and construction requirements for the turbine lube oil conditioning unit.

7A.5.3.2 Type. The turbine lube oil conditioner will be specifically designed for filtration of turbine lube oil which contains rust and/or oxidation inhibitor additives. The unit will require no water or other substances, including supplementary heat for effective operation. The lube oil conditioner will be Keene Corporation (formerly Bowser Incorporated) type, or acceptable equal. The unit will serve the main turbine lubricating system.

7A.5.3.3 Codes and Standards. All equipment and materials furnished will be designed and constructed in accordance with the latest applicable requirements of the standard specifications and codes of ANSI, ASME, ASTM, NEMS, IEEE, EEI and other regular published and accepted standards.

7A.5.3.4 Design Criteria. The turbine lube oil conditioner will be designed and constructed for the following conditions:

Location	Indoors
Approximate quantity of oil in system, gal	To be determined from turbine design data
Oil inlet temperature range, F	60 - 120
Oil SAE No.	10 - 20
Viscosity @ 100 F, SSU	150
Filtering capacity, gph	Will be a minimum of 10% of the turbine oil system capacity
Filtering effectiveness	Down to 2 microns

7A.5.4 BUILDING SPACE CONDITIONING

7A.5.4.1 General. This section covers the design, construction and performance requirements for the heating, ventilation and air conditioning equipment.

7A.5.4.2 Type. Heating, ventilation and air conditioning equipment will control the environment of critical equipment such as the computers and provide for personnel comfort. Building heating will be accomplished by electric heaters located throughout the structures of the central plant complex. Ventilation will be accomplished by power roof ventilators and fans. Air conditioning will be accomplished by air handling and condensing units.

A ventilation system will be provided for the turbine bay, auxiliary bay, water treatment area, machine shop, thermal storage unit building, receiver tower and outlying plant buildings as required by the type of structure.

The general services and control room area including the visitors center, media room, water treatment laboratory, general offices, lunch room, electronics check-out room, electrical equipment and relay room, computer room and control room will be air conditioned to maintain temperatures of 75 F and 50 per cent relative humidity.

7A.5.4.3 Codes and Standards. The heating, ventilation and air conditioning equipment will be designed and constructed in accordance with the latest applicable requirements of the standard specifications and codes of NEC, ASME, ANSI, AEMA, IEEE, EEN, TEMA, ARI, AMCA, and other such regular published and

accepted standards except where supplemented or modified by these specifications; and in accordance with the applicable requirements of the Federal "Occupational Safety and Health Standards".

7A.5.5 FIRE PROTECTION EQUIPMENT

7A.5.5.1 General. This section covers the design, performance, and construction requirements for the fire protection equipment.

The fire protection systems will be designed, furnished, and installed by a supplier specializing in fire protection systems which is acceptable to the Engineer.

The fire protection equipment contractor will furnish complete fire protection systems including spray nozzles, sprinkler heads, heat sensing and actuation devices, valves, piping, fittings, strainers, pipe hangers, expansion joints, controls, and instrumentation as required for a complete system.

7A.5.5.2 Type. The fire protection system, based on preliminary plant information, will include the following individual systems:

Equipment or Area Protected	Type of Protection
Yard and Building Exteriors	Fire Hydrants and Hose Houses
Control Room, Relay Room, Computer Room, Electronics Checkout Room	Halon 1301 System
Turbine Generator	Carbon Dioxide Hose Stations
Electrical Transformers and Lubricating Oil Equipment	Water Fog Systems
Building Interiors	Fire Extinguishers and Hose Cabinets

7A.5.5.3 Codes and Standards. The fire protection systems and their component parts will comply with all governing regulations and with applicable standard specifications and codes of ANSI, ASTM, ASME, NEMA, EEI, IEEE, UL, AIA, NEPA, and other such regular published and accepted standards, and in accordance with the applicable requirements of the Federal "Occupational Safety and Health Standards". The regulation, specification or code applied in each case will be the latest publication of such regulations, specification or code.

The fire protection systems will be designed in accordance with NFPA Pamphlet 13 and NFPA Pamphlet 15 except where more stringent requirements are specified.

7A.5.5.4 Design Criteria. The fire water supply system will be dependent upon the site selection and available water sources.

Portable hand carry fire extinguishers that are either multipurpose dry chemical or carbon dioxide type will be provided in the main plant buildings for general fire protection. The multipurpose dry chemical extinguishers will be suitable for Classes A, B and C fires and the carbon dioxide extinguishers will be suitable for Classes B and C fires. Carbon dioxide extinguishers will be located in areas of electrical equipment since carbon dioxide does not leave a dry powder residue, as do the multipurpose dry chemical extinguishers.

Hose cabinets will be provided so that all parts of the working areas in the main plant can be reached by a water stream from a hose not over 100 feet long, in accordance with NFPA Standards.

The control, relay, computer and electronics rooms will have automatic actuating fire protection systems using Halon 1301. Underwriter's Laboratories have certified that concentrations of 5 per cent Halon 1301 will extinguish electrical fires and that concentrations below 7 per cent will produce no ill effects in humans for brief (4-5 minutes) exposures.

7A.6 ANALOG DIAGRAMING SYMBOLS

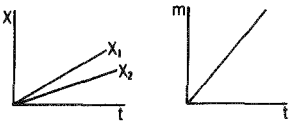
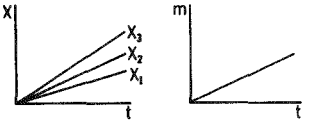
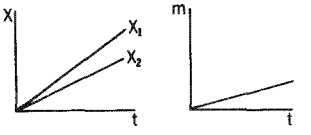
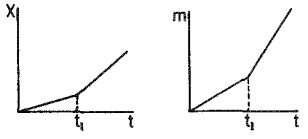
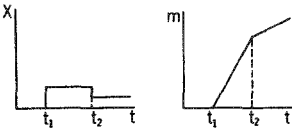
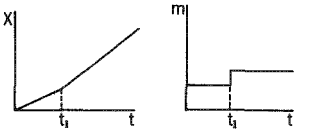
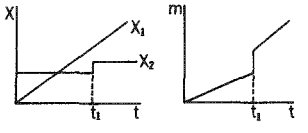
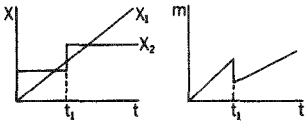
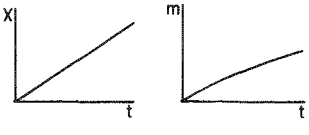
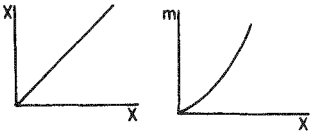
MEASURING/READOUT LETTERS

PROCESS VARIABLE		FUNCTION
A = Analysis**		**R** = Recording
C = Conductivity	**FR**	**I** = Indicating
D = Density		**T** = Transmitter
F = Flow		**RT** = Recording Transmitter
L = Level		
M = Moisture	**FRT**	**IT** = Indicating Transmitter
P = Pressure		
S = Speed		
T = Temperature		
V = Viscosity		
W = Weight		
Z = Position		

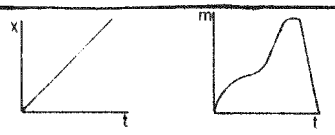
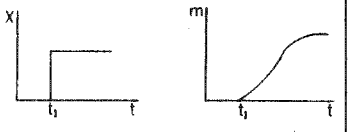
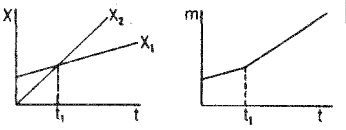
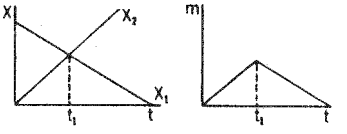
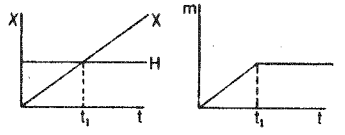
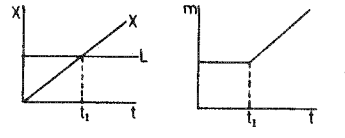
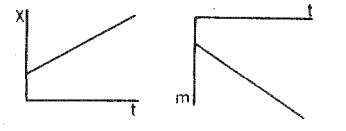
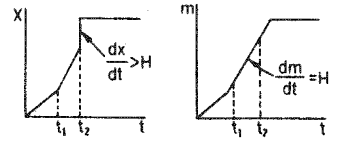
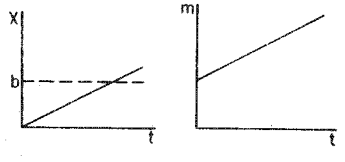
ENCLOSURE SYMBOLS

FUNCTION	SYMBOL
Measuring Or Readout	
Manual Signal Processing	
Automatic Signal Processing	
Final Controlling	

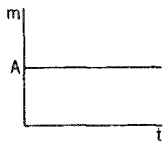
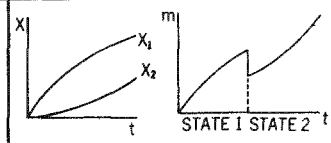
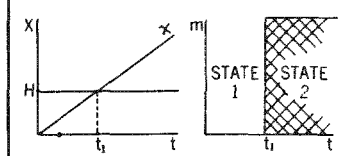
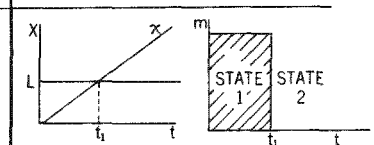
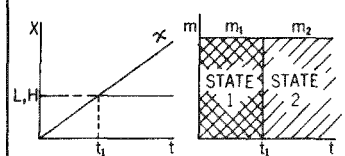
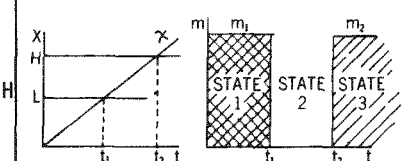
SIGNAL PROCESSING SYMBOLS

FUNCTION & SYMBOL	MATH EQUATION	GRAPHIC REPRESENTATION	DEFINITION
SUMMING Σ	$m = x_1 + x_2 + \ldots + x_n$		The output equals the algebraic sum of the inputs.
AVERAGING Σ/n	$m = \frac{x_1 + x_2 + \ldots + x_n}{n}$		The output equals the algebraic sum of the inputs divided by the number of inputs.
DIFFERENCE Δ	$m = x_1 - x_2$		The output equals the algebraic difference between the two inputs.
PROPORTIONAL K	$m = Kx$		The output is directly proportional to the input.
INTEGRAL ∫	$m = \frac{1}{T_I} \int x dt$		The output varies in accordance with both magnitude and duration of the input. The output is proportional to the time integral of the input.
DERIVATIVE d/dt	$m = T_D \frac{dx}{dt}$		The output is proportional to the rate of change (derivative) of the input.
MULTIPLYING X	$m = x_1 x_2$		The output equals the product of the two inputs.
DIVIDING ÷	$m = \frac{x_1}{x_2}$		The output equals the quotient of the two inputs.
ROOT EXTRACTION √	$m = \sqrt{x}$		The output equals the root (i.e., square root, fourth root, 3/2 root, etc.) of the input.
EXPONENTIAL x^n	$m = x^n$		The output equals the input raised to a power (i.e., second, third, fourth, etc.)

SIGNAL PROCESSING SYMBOLS (CONTINED)

FUNCTION & SYMBOL	MATH EQUATION	GRAPHIC REPRESENTATION	DEFINITION
NONLINEAR OR UNSPECIFIED FUNCTION **f (x)**	$m = f(x)$		The output equals some nonlinear function of the input.
TIME FUNCTION **f(t)**	$m = x\,f(t)$ $m = f(t)$		The output equals the input times some function of time or equals some function of time alone.
HIGH SELECTING **>**	$m = \begin{cases} x_1 \text{ FOR } x_1 > x_2 \\ x_2 \text{ FOR } x_1 < x_2 \end{cases}$		The output is equal to that input which is the greatest of the inputs.
LOW SELECTING **<**	$m = \begin{cases} x_2 \text{ FOR } x_1 \geq x_2 \\ x_1 \text{ FOR } x_1 \leq x_2 \end{cases}$		The output is equal to that input which is the least of the inputs.
HIGH LIMITING **⊁**	$m = \begin{cases} x \text{ FOR } x \leq H \\ H \text{ FOR } x \geq H \end{cases}$		The output equals the input or the high limit value whichever is lower.
LOW LIMITING **⊀**	$m = \begin{cases} x \text{ FOR } x > L \\ L \text{ FOR } x < L \end{cases}$		The output equals the input or the low limit value whichever is higher.
REVERSE PROPORTIONAL **−K**	$m = -Kx$		The output is reversely proportional to the input.
VELOCITY LIMITING **V⊁**	$\frac{dm}{dt} = \frac{dx}{dt}$ $\begin{cases} \frac{dx}{dt} \leq H \text{ and} \\ m = x \end{cases}$ $\frac{dm}{dt} = H$ $\begin{cases} \frac{dx}{dt} \geq H \text{ OR} \\ m \neq x \end{cases}$		The output equals the input as long as the rate of change of the input does not exceed a limit value. The output will change at the rate established by this limit until the output again equals the input.
BIAS **+, −, or ±**	$m = x \pm b$		The output equals the input plus (or minus) some arbitrary value (bias).

SIGNAL PROCESSING SYMBOLS (CONTINED)

FUNCTION & SYMBOL	MATH EQUATION	GRAPHIC REPRESENTATION	DEFINITION
ANALOG SIGNAL GENERATOR **A**	$m = A$	DOES NOT APPLY 	The output is an analog signal developed within the generator.
TRANSFER **T**	$m = \begin{cases} x_1 \text{ FOR STATE 1} \\ x_2 \text{ FOR STATE 2} \end{cases}$		The output equals the input which has been selected by transfer. The state of the transfer is established by external means.
SIGNAL MONITOR **H/**	STATE 1 $x \leq H$ STATE 2 (ENERGIZED OR ALARM STATE) $x > H$		
/L	STATE 1 (ENERGIZED OR ALARM STATE) $x < L$ STATE 2 $x \geq L$		
H/L	STATE 1 (FIRST OUTPUT m_1 ENERGIZED OR ALARM STATE) $x < H, L$ STATE 2 (SECOND OUTPUT m_2 ENERGIZED OR ALARM STATE) $x > H, L$		The output has discrete states which are dependent on the value of the input. When the input exceeds (or becomes less than) an arbitrary limit value the output changes state.
H//L	STATE 1 (FIRST OUTPUT m_1 ENERGIZED OR ALARM STATE) $x < L$ STATE 2 (BOTH OUTPUTS INACTIVE OR DE-ENERGIZED) $L \leq x \leq H$ STATE 3 (SECOND OUTPUT m_2 ENERGIZED OR ALARM STATE) $x > H$		

The variables used in the table are:

A — An arbitrary analog signal

b — Analog bias value

$\frac{d}{dt}$ — Derivative with respect to time

H — An arbitrary analog high limit value

$\frac{1}{T_I}$ — Integrating rate

L — An arbitrary analog low limit value

m — Analog output variable

n — Number of analog inputs or value of exponent

t — Time

T_D — Derivative time

x — Analog input variable

$x_1, x_2, x_3, \ldots, x_n$ — Analog input variable (1 to n in number)

APPENDIX 7B
LEGENDS, SYMBOLS AND WIRING SCHEMATIC

APPENDIX 7B
LEGENDS, SYMBOLS AND WIRING SCHEMATIC

The abbreviations used in the piping and instrumentation drawings are defined in Tables 7B-1 through 7B-4. In addition, a schematic for an uninterruptable power supply system and a one-line diagram of plant power distribution are indluded as Figures 7B-1 and 7B-2.

TABLE 7B-1. LEGEND ABBREVIATIONS

APT - ABSOLUTE PRESSURE TRANSMITTER
BS - BELLOWS SEAL
CC - CONDUCTIVITY CELL
CDR - CONTROL DRIVE
CP - CONTROL PANEL
DC - DRAIN COLLECTOR
DPT - DIFFERENTIAL PRESSURE TRANSMITTER
EH - EXHAUST HEAD
EJ - EXPANSION JOINT
"F" - FURNISHED WITH ASSOCIATED EQUIPMENT
FC - FLOW CONTROL
FD - FLOOR DRAIN
FE - FLOW ELEMENT
FI - FLOW INDICATOR
FS - FLOW SWITCH
FT - FLOW TRANSMITTER
FXH - FLEXIBLE HOSE
GG - GAUGE GLASS
GP - GAUGE PANEL
HLA - HIGH LEVEL ALARM
HLI - HIGH LEVEL INTERLOCK
HPA - HIGH PRESSURE ALARM
HPI - HIGH PRESSURE INTERLOCK
HTA - HIGH TEMPERATURE ALARM
HTI - HIGH TEMPERATURE INTERLOCK
L - LEVEL
LC - LEVEL CONTROLLER
LFA - LOW FLOW ALARM
LFI - LOW FLOW INTERLOCK
LI - LEVEL INDICATOR
LLA - LOW LEVEL ALARM
LLI - LOW LEVEL INTERLOCK
LPA - LOW PRESSURE ALARM
LPI - LOW PRESSURE INTERLOCK
LS - LEVEL SWITCH
LT - LEVEL TRANSMITTER
LTA - LOW TEMPERATURE ALARM
LX - LOCAL TRANSMITTER
PC - PRESSURE CONTROLLER
pH - pH CELL
PI - PRESSURE INDICATOR
PS - PRESSURE SWITCH
PT - PRESSURE TRANSMITTER
RD - ROOF DRAIN
RR - RELAY RACK
SC - SAMPLE COIL
SJ - SWIVEL JOINT
SS - STAINLESS STEEL
STR - STRAINER
TC - TEMPERATURE CONTROLLER
TE - TEMPERATURE ELEMENT
TI - TEMPERATURE INDICATOR
TR - TRAP
TS - TEMPERATURE SWITCH
TT - TEMPERATURE TRANSMITTER
TW - TEMPERATURE ELEMENT TEST WELL
VPT - VACUUM PRESSURE TRANSMITTER
VS - RELIEF VALVE VENT SEAL
XP - TRANSMITTER PANEL

TABLE 7B-1. LEGEND ABBREIVATIONS (CONCLUDED)

APT - ABSOLUTE PRESSURE TRANSMITTER
BS - BELLOWS SEAL
CC - CONDUCTIVITY CELL
CDR - CONTROL DRIVE
CP - CONTROL PANEL
DC - DRAIN COLLECTOR
DPT - DIFFERENTIAL PRESSURE TRANSMITTER
EH - EXHAUST HEAD
EJ - EXPANSION JOINT
"F" - FURNISHED WITH ASSOCIATED EQUIPMENT
FC - FLOW CONTROL
FD - FLOOR DRAIN
FE - FLOW ELEMENT
FI - FLOW INDICATOR
FS - FLOW SWITCH
FT - FLOW TRANSMITTER
FXH - FLEXIBLE HOSE
GG - GAUGE GLASS
GP - GAUGE PANEL
HLA - HIGH LEVEL ALARM
HLI - HIGH LEVEL INTERLOCK
HPA - HIGH PRESSURE ALARM
HPI - HIGH PRESSURE INTERLOCK
HTA - HIGH TEMPERATURE ALARM
HTI - HIGH TEMPERATURE INTERLOCK
L - LEVEL
LC - LEVEL CONTROLLER
LFA - LOW FLOW ALARM
LFI - LOW FLOW INTERLOCK
LI - LEVEL INDICATOR
LLA - LOW LEVEL ALARM
LLI - LOW LEVEL INTERLOCK
LPA - LOW PRESSURE ALARM
LPI - LOW PRESSURE INTERLOCK
LS - LEVEL SWITCH
LT - LEVEL TRANSMITTER
LTA - LOW TEMPERATURE ALARM
LX - LOCAL TRANSMITTER
PC - PRESSURE CONTROLLER
pH - pH CELL
PI - PRESSURE INDICATOR
PS - PRESSURE SWITCH
PT - PRESSURE TRANSMITTER
RD - ROOF DRAIN
RR - RELAY RACK
SC - SAMPLE COIL
SJ - SWIVEL JOINT
SS - STAINLESS STEEL
STR - STRAINER
TC - TEMPERATURE CONTROLLER
TE - TEMPERATURE ELEMENT
TI - TEMPERATURE INDICATOR
TR - TRAP
TS - TEMPERATURE SWITCH
TT - TEMPERATURE TRANSMITTER
TW - TEMPERATURE ELEMENT TEST WELL
VPT - VACUUM PRESSURE TRANSMITTER
VS - RELIEF VALVE VENT SEAL
XP - TRANSMITTER PANEL

TABLE 7B-2. LEGEND VALVE SYMBOLS

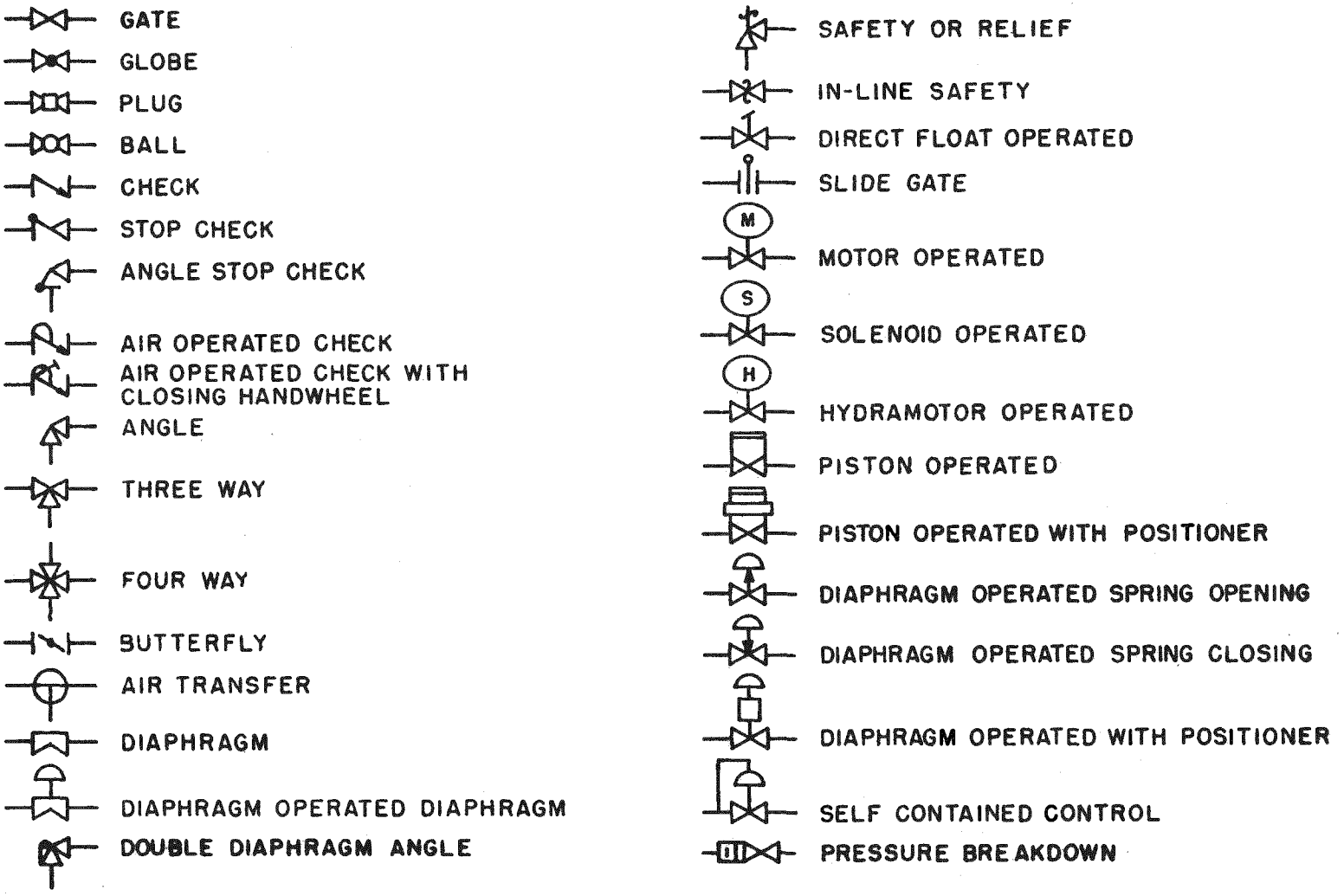


TABLE 7B-2. LEGEND VALVE SYMBOLS (CONCLUDED)

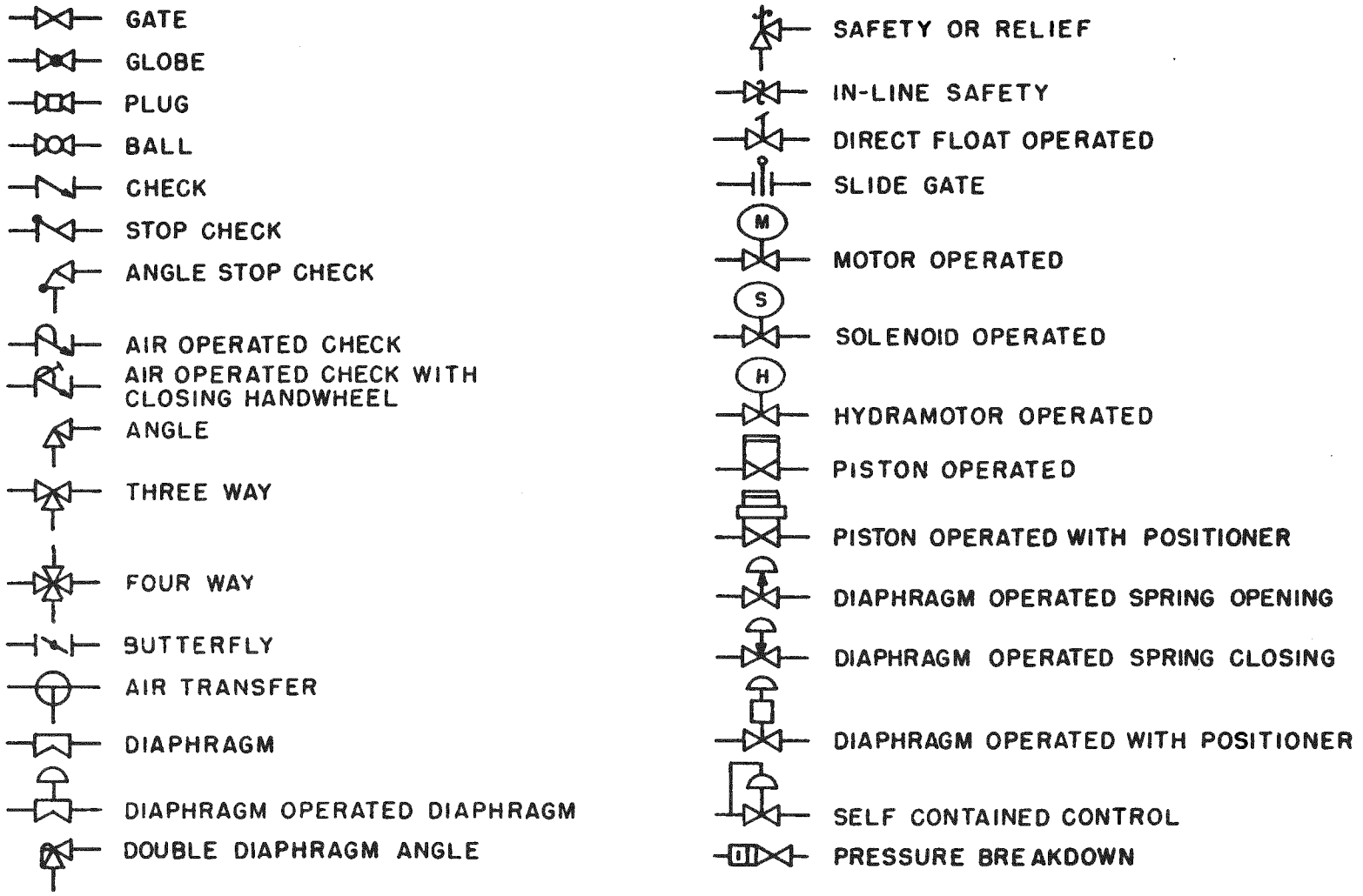
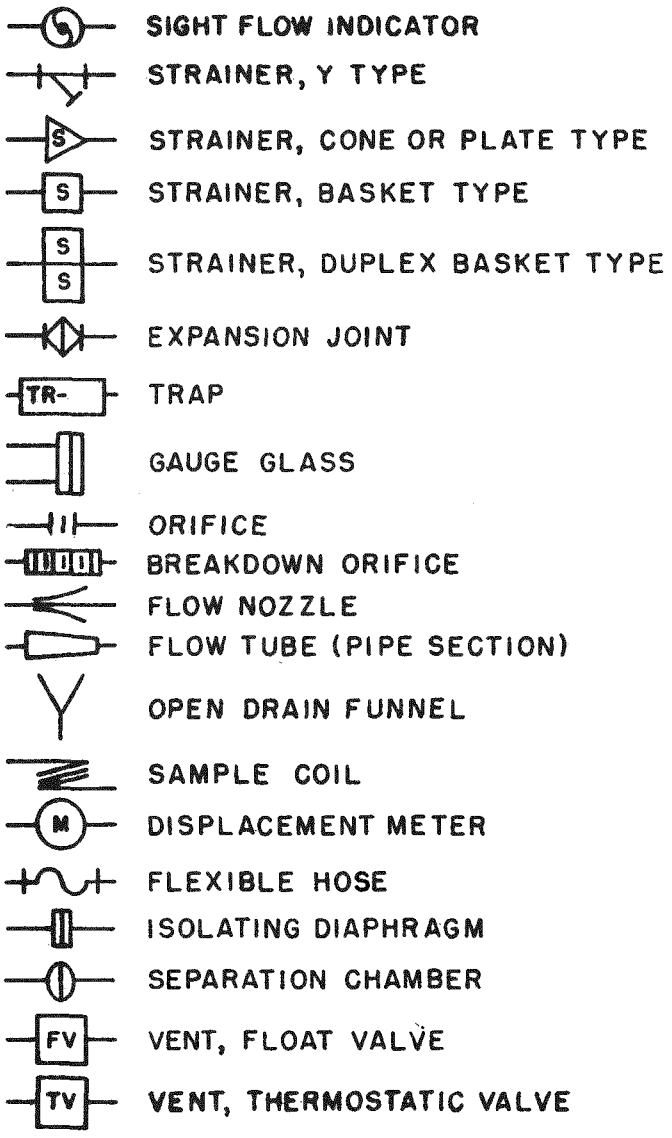


TABLE 7B-3. LEGEND ACCESSORY SYMBOLS



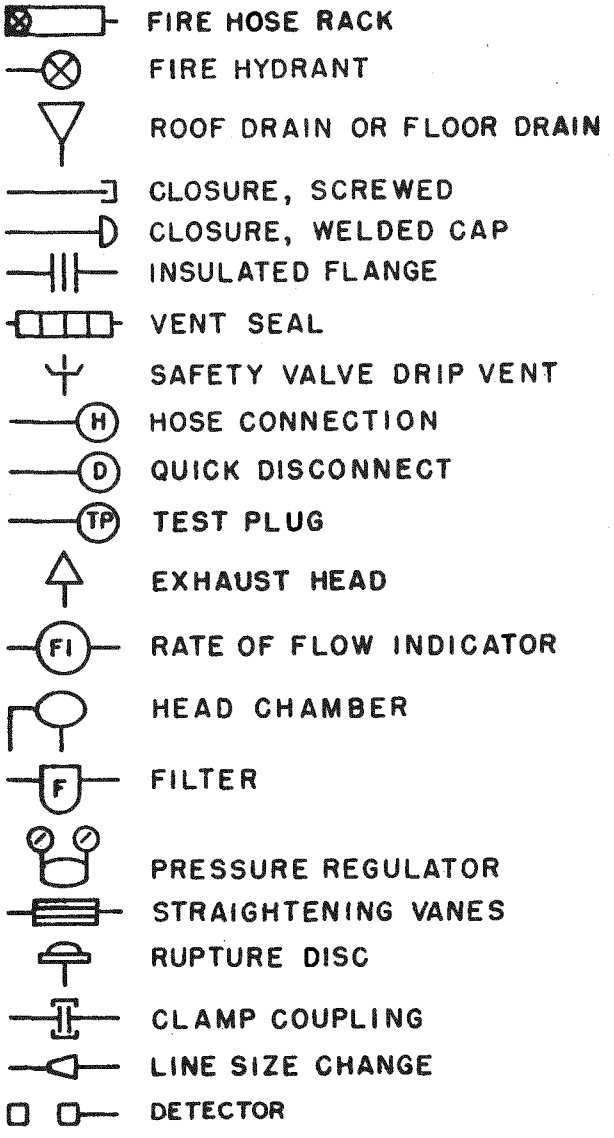


TABLE 7B-3. LEGEND ACCESSORY SYMBOLS (CONCLUDED)

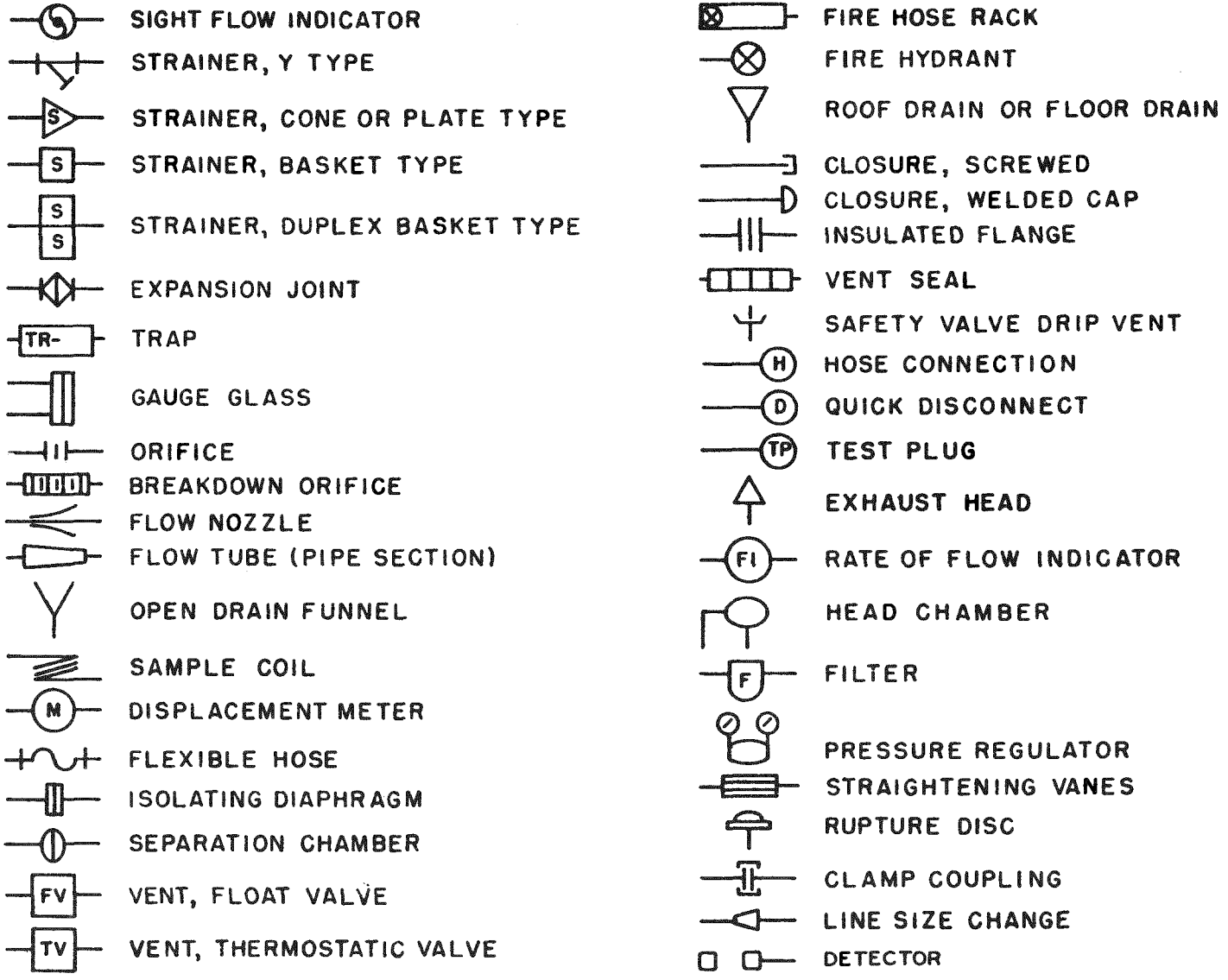
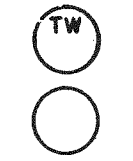


TABLE 7B-4. LEGEND INSTRUMENT SYMBOLS



TEMPERATURE ELEMENT TEST WELL

LOCAL INDICATOR

LOCAL ELECTRONIC DEVICE

LOCAL PNEUMATIC DEVICE

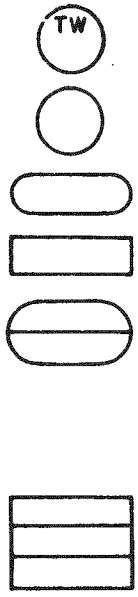
ELECTRONIC TRANSMITTER OR CONTROLLER
- FIRST LINE - SERVICE
- SECOND LINE - TRANSMITTER OR RECEIVER DESIGNATION

PNEUMATIC TRANSMITTER OR CONTROLLER
- FIRST LINE - SERVICE
- SECOND LINE - TRANSMITTER OR RECEIVER DESIGNATION
- THIRD LINE - DESIGN SET POINT

INSTRUMENT FUNCTIONS

- RCD - RECORDER
- CONT - CONTROL
- IND - INDICATOR
- CMP - COMPUTER

TABLE 7B-4. LEGEND INSTRUMENT SYMBOLS (CONCLUDED)



TEMPERATURE ELEMENT TEST WELL

LOCAL INDICATOR

LOCAL ELECTRONIC DEVICE

LOCAL PNEUMATIC DEVICE

ELECTRONIC TRANSMITTER OR CONTROLLER
- FIRST LINE - SERVICE
- SECOND LINE - TRANSMITTER OR RECEIVER DESIGNATION

PNEUMATIC TRANSMITTER OR CONTROLLER
- FIRST LINE - SERVICE
- SECOND LINE - TRANSMITTER OR RECEIVER DESIGNATION
- THIRD LINE - DESIGN SET POINT

INSTRUMENT FUNCTIONS

- RCD - RECORDER
- CONT - CONTROL
- IND - INDICATOR
- CMP - COMPUTER

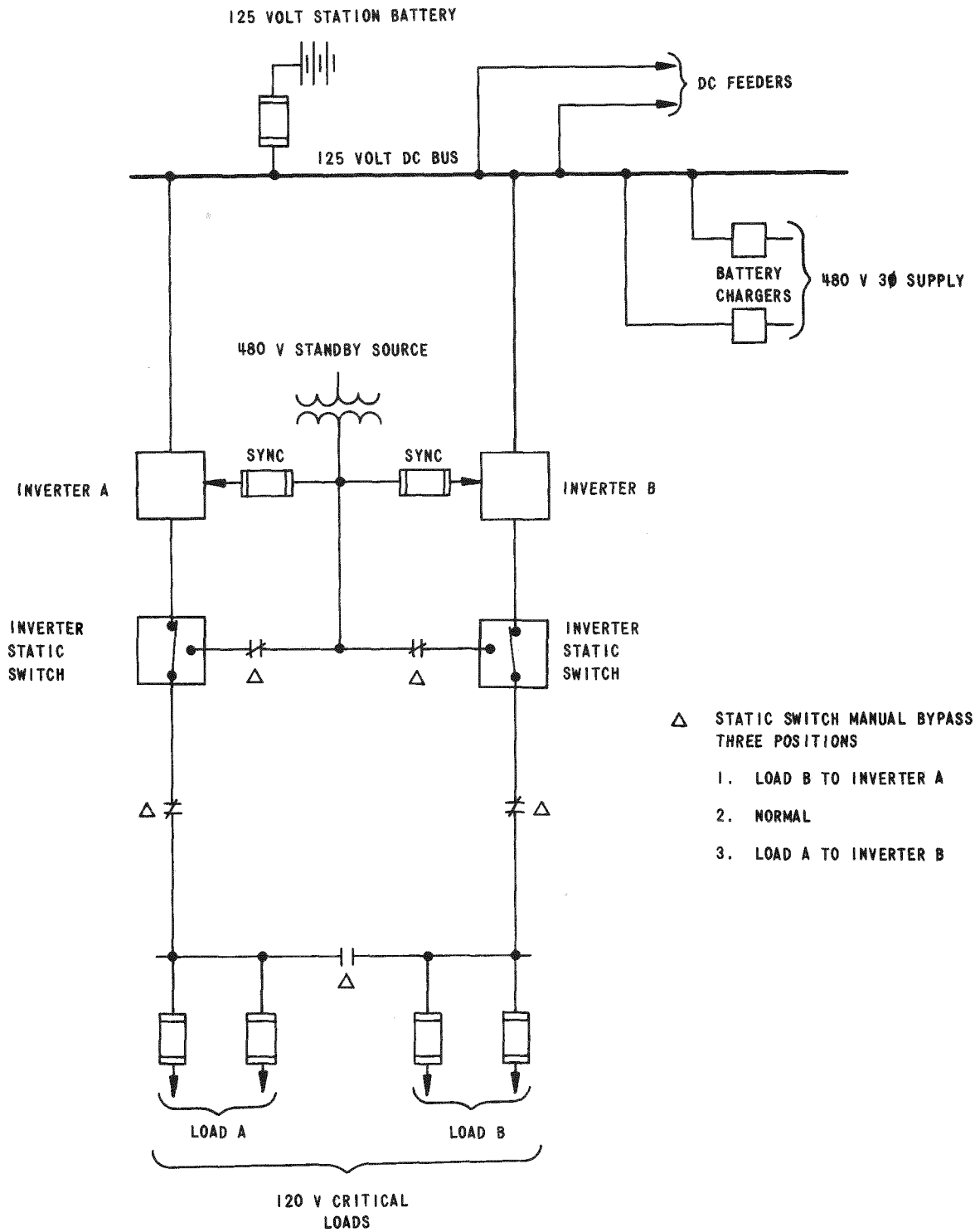


Figure 7B-1. UNINTERRUPTABLE POWER SUPPLY SYSTEM

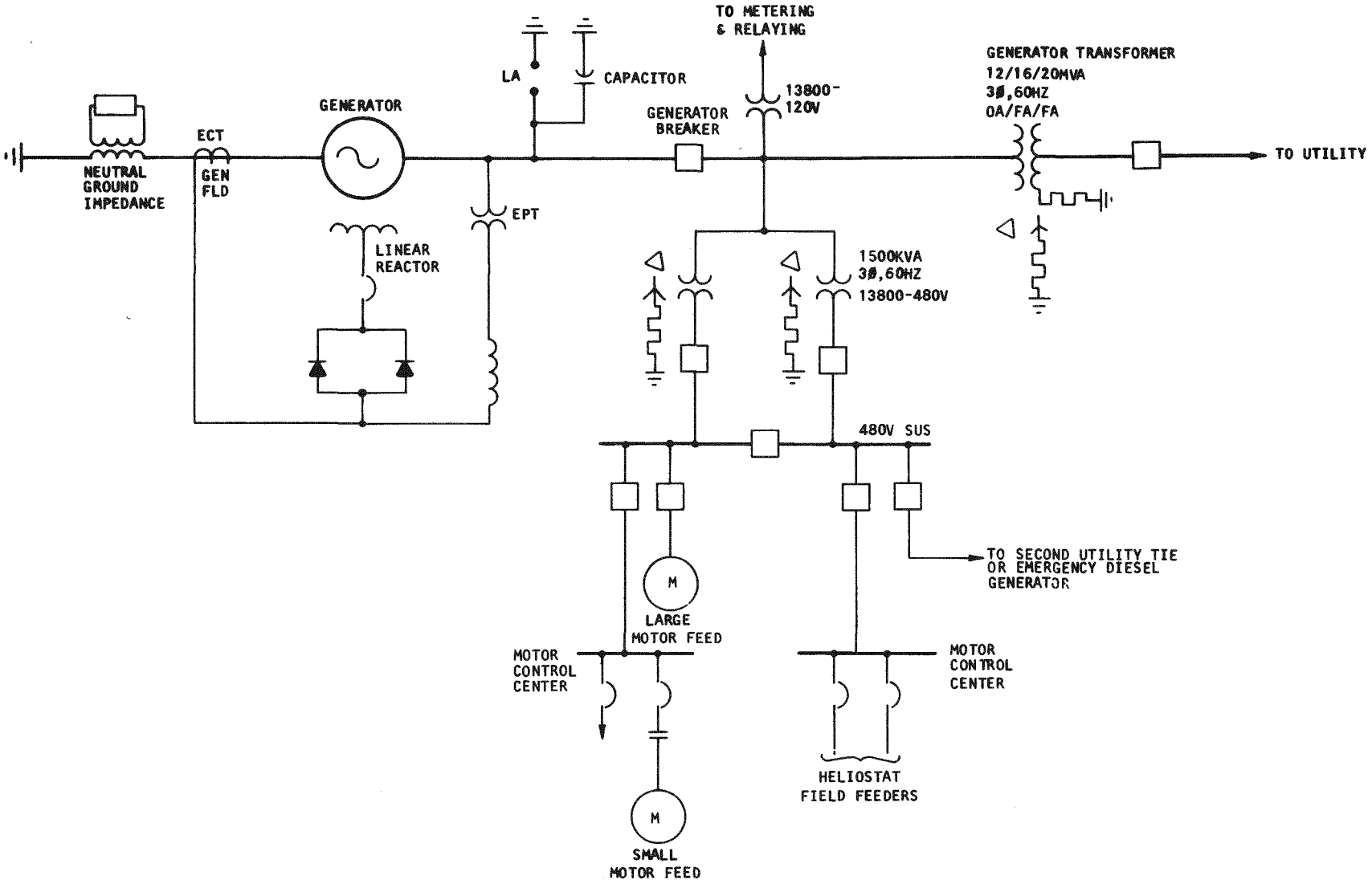


FIGURE 7B-2. ONE LINE DIAGRAM

